[redacted]

22

CLASSIFICATION CHANGED
TO Unclassified
BY DD254 R.E. Godfrey
DATE 16 August 1966
A. Patterson
7-13-67

S-IVB/IB AND S-IVB/V COMMON BATTLESHIP REPORT (U)

N70-76084 (ACCESSION NUMBER) None (THRU)
385 (PAGES) (CODE)
CR-113297 (NASA CR OR TMX OR AD NUMBER) (CATEGORY)
FACILITY FORM 602

FEBRUARY 1966
DOUGLAS REPORT SM-[redacted]
47012

PREPARED BY:
SATURN S-IVB TEST PLANNING
AND EVALUATION COMMITTEE
AND COORDINATED BY: C. VASI
S-IVB/IB TP & E SECTION
SATURN DEVELOPMENT ENGINEERING

PREPARED FOR:
NATIONAL AERONAUTICS AND
SPACE ADMINISTRATION
UNDER NASA CONTRACT NAS7-101

for K. J. Young

APPROVED BY: A. P. O'NEAL
DIRECTOR, SATURN DEVELOPMENT ENGINEERING

[redacted]

DOUGLAS MISSILE & SPACE SYSTEMS DIVISION
SPACE SYSTEMS CENTER — HUNTINGTON BEACH, CALIFORNIA

[redacted]

ABSTRACT

This report presents the evaluation of the Saturn S-IVB Static Firing Test Program that was conducted at the Douglas Aircraft Company, Sacramento, California. The static firing program consisted of a series of short and full-duration engine firings to prove major design parameters of the propulsion system and also to verify the integrity of the hydraulic, pneumatic, and electrical control systems.

This report is a contractual requirement as defined in Douglas Report No. SM-41410: Data Submittal Document, Saturn S-IVB System dated March 1965. It was prepared by the Saturn S-IVB Test Planning and Evaluation Committee for the National Aeronautics and Space Administration under Contract NAS7-101.

DESCRIPTORS

DSV-IVB	Sacramento Test Center
Battleship Vehicle	Test Stand Beta 1
Systems Testing	Beta Complex
Saturn S-IVB	Static Firings

21 February 1966

PREFACE

The purpose of this report is to document the Saturn S-IVB Battleship Static Firing Test Program. The static firing program was conducted at the Douglas Aircraft Company, Sacramento Test Center, Sacramento, California for a period of from 18 September 1964 to 20 August 1965.

This report, prepared in compliance with the National Aeronautics and Space Administration Contract NAS7-101, is published in accordance with Douglas Report No. SM-41410: Data Submittal Document, Saturn S-IVB System dated March 1965.

21 February 1966

TABLE OF CONTENTS

TABLE OF CONTENTS (Continued)

TABLE OF CONTENTS (Continued)

APPENDICES

LIST OF TABLES

LIST OF TABLES (Continued)

LIST OF TABLES (Continued)

LIST OF ILLUSTRATIONS

LIST OF ILLUSTRATIONS (Continued)

LIST OF ILLUSTRATIONS (Continued)

LIST OF ILLUSTRATIONS (Continued)

LIST OF ILLUSTRATIONS (Continued)

LIST OF ILLUSTRATIONS (Continued)

LIST OF ILLUSTRATIONS (Continued)

SECTION 1

INTRODUCTION

1. INTRODUCTION

This report was prepared by the Saturn S-IVB TP&E (Test Planning and Evaluation) Committee for the National Aeronautics and Space Administration under NASA contract NAS7-101. This report presents a detailed evaluation of the S-IVB battleship static firing test program.

The battleship tank was installed on the Beta Complex test stand No. 1 on 18 December 1963. Battleship buildup and checkout activities proceeded concurrently with test stand, Test Control Center, and facility equipment installations and checkout.

The J-2 engine was installed on the battleship tank on 4 June 1964. Checkout of the battleship, GSE, and support systems was completed by mid-September. Saturn S-IVB/IB battleship configuration tests were performed between 18 September 1964 and 14 May 1965. Saturn S-IVB/V battleship configuration testing was performed between 19 June and 20 August 1965.

The S-IVB/IB static firing test program consisted of four full duration and six short duration firings. In addition, 17 other tests (cryogenic loadings, chilldown, and environmental tests) were conducted. The S-IVB/V test program consisted of two full duration and five short duration firings.

The battleship vehicle assembly was removed from the Beta Complex test stand No. 1 on 3 September 1965.

SECTION 2

SUMMARY

2. SUMMARY

This section contains a summary of the battleship test program. The countdowns are discussed briefly and the evaluations are summarized.

Prior to all static firings, leak checks and complete functional tests of the pneumatic, propellant, aft environmental control, electrical power distribution, and sequencer systems were successfully completed. Refer to Appendix 3 for the battleship test history.

2.1 Test Summary

2.1.1 Cold Flow and Childown Testing

The cold flow and childown tests (figure 2-1) consisted of a series of nonfiring tests conducted to establish and evaluate operating procedures for propellant loading, engine purging, venting, and a childown sequence for proper engine start. Four countdowns, CD 614000, 614002, 614003, and 614004, were required for these tests.

2.1.2 Propulsion Development Firings

The propulsion development firings consisted of a series of shakedown firings ranging from a 10-sec firing to a full-duration firing. These firings were performed to establish engine operation, countdown procedures, and engine start procedures. The firings were also used to determine and evaluate the performance of the J-2 engine with the S-IVB stage. Data were obtained to evaluate the performance of the PU, propellant tanks pressurization, and the pneumatic control systems. In addition, data were obtained to evaluate vibration and acoustical effects. Six countdowns (CD 614005 through 614010) were required for these tests.

2.1.3 J-2 Engine Temperature Conditioning Tests

During the J-2 engine temperature conditioning tests (CD 614011 through 614019) which were conducted per Rocketdyne's engine childown procedure, an apparent LH2 pump stall developed. This problem was investigated during the next nine countdowns and upon completion of the tests, DAC had developed a satisfactory childown procedure.

2.1.4 Saturn S-IVB/IB System Development Firings

The system development firings were conducted to evaluate the performance of the engine, hydraulic, pneumatic, pressurization, and PU systems. Data were obtained to finalize all operating procedures, engine parameters, PU parameters, and pressure and chilldown procedures.

These tests consisted of CD 614020 through 614025, 614028, and 614030 through 614032. One ambient and two hot gimbaling tests were also conducted.

2.1.5 Saturn S-IVB/V System Development Firings

The system development firings were conducted to determine engine restart capabilities and to evaluate the propellant repressurization and PU systems. Data were obtained to establish loading and venting procedures for the ambient helium repressurization system, and to verify minimum chilldown requirements for engine restart after simulated orbital coast period shutdown. These tests consisted of seven countdowns: 614033 through 614035, and 614041 through 614044. One ambient and two hot gimbaling tests were also conducted.

2.2 Evaluation Summary

2.2.1 Engine System

Chilldown and loading of the engine start tank and control sphere for both the S-IVB/IB and S-IVB/V were successfully demonstrated. The LOX and LH2 recirculation systems adequately chilled the engine pumps and provided pump inlet conditions well within the required start boxes in both S-IVB/IB and S-IVB/V tests.

Thrust chamber chilldown was adequate to meet Rocketdyne's original engine start requirement for the thrust chamber temperature. However, as shown by the results of an early test (CD 614007), this requirement did not guarantee a satisfactory engine start. Subsequent special chilldown tests demonstrated that additional parameters (lower tube temperatures) should be included in the start requirements when there is a hold period between chilldown and engine start.

The S-IVB battleship program demonstrated the ability of the Rocketdyne J-2 engine to function on the S-IVB stage. The engine performance showed no large or unexplainable deviation from the manufacturer's acceptance data. The four full-duration tests that were used for the S-IVB/IB analysis showed satisfactory engine start, steady state, and cutoff operation of the propulsion system. The engine response to the propellant utilization valve movement was also satisfactory. The S-IVB/V engine conditioning and restart requirements were demonstrated by two tests. The flow integral technique of cryogenic calibration was established and verified during the battleship test program.

2.2.2 Oxidizer System

The originally designed flight pressurization (cold gas) system was changed during the battleship test program because it could not maintain the LOX tank ullage pressure above the desired minimum pressure of 37 psia during the pressurization system start transients. In the new (hot gas) system, the orifices controlling the helium flow through the J-2 heat exchanger are now located downstream of the heat exchanger, producing a significant reduction of LOX tank ullage pressure drop during the engine start transients.

Aside from the start transient problem, the LOX pressurization system functioned adequately and satisfactorily maintained ullage pressure so that NPSH (net positive suction head) requirements were met for all battleship tests.

Cold flow testing had demonstrated that the performance of the LOX recirculation system was adequate for S-IVB/IB type missions. Results of the S-IVB/IB battleship hot firings confirmed cold flow results by showing that, during all tests, the available NPSH at ESC (Engine Start Command) met the start requirements. Results from the S-IVB/V battleship test indicated that the LOX recirculation system is able to satisfactorily accomplish a dry duct chilldown, which is a primary requirement for S-IVB/V type missions.

2.2.3 Fuel System

Throughout all S-IVB/IB and S-IVB/V type battleship tests, the LH2 tank pressurization system performed adequately. The LH2 tank ullage pressure was maintained within acceptable limits which resulted in LH2 tank NPSH requirements being met on all tests.

The LH2 recirculation system proved to be adequate for S-IVB/IB missions during cold flow tests. Results were confirmed during the S-IVB/IB battleship hot firing tests.

The ability of the LH2 recirculation system to successfully accomplish an S-IVB/V type dry duct chilldown was demonstrated during S-IVB/V battleship countdowns when all engine start requirements were met.

2.2.4 Pneumatic Control and Purge Systems

Throughout all battleship testing, pneumatic control was successfully maintained and all purges were successfully accomplished.

During the early cold flow tests, problems developed with the stage pneumatic control module which required rework. Therefore, during the S-IVB/IB tests, pneumatic control and purge supply were maintained from GSE supply.

During S-IVB/V tests, the rework module was reinstalled and the pneumatic system was proved adequate for pneumatic control, purge operations, and leakage makeup.

2.2.5 Environmental Control System

Tests were conducted to verify that the environmental control system could adequately purge the aft skirt and interstage area to an oxygen content level of 4 percent by volume, or less, in a reasonable time. The tests indicated that this level was reached in less than three minutes. This indicated that little mixing occurred during the initial period of the purge and that the GN2 flow was a blanket effect that pushed the air from the interstage. Tests were conducted and verified that the aft skirt and interstage thermo-conditioning and purge system could maintain the temperature of all electronic equipment mounted on the aft skirt within their correct operating ranges. Also verified was that during S-IVB/V operation, the helium bottle used for purging the propellant pumps seal cavities could be controlled adequately with respect to maintaining its enclosure outlet temperature above 77 deg F. During the thermal verification test the APS (auxiliary propulsion system) outlet temperatures were within the design limits of 87 ±5 deg F. The temperature of the APS at finplane I was slightly cooler than that of the APS at finplane III; this lower temperature was typical of most of the temperatures measured on the finplane I side of the manifold.

2.2.6 PU System

The PU system functioned properly on all S-IVB battleship firings. Propellant mass was determined by the PU system, level sensors and a flow integral analysis. Each method of analysis proved good repeatability and had good agreement with the other analyses. The PU mass sensor nonlinearities were similar for the three countdowns considered. The PU valve command and position history simulation was in close agreement with the actual command and position histories indicating good accuracy of the nonlinearity curves.

2.2.7 Data Acquisition System

The data acquisition system for battleship testing consisted of flight-type transducers hardwired to a ground instrumentation system and recorded on magnetic tape. The recording system consisted of digital and constant bandwidth FM. Strip charts were provided for real time display of redline and cutoff parameters. Operation of the instrumentation system was satisfactory as indicated by its 95.9 percent valid data acquisition. No problems were experienced with the battleship stage instrumentation that would affect its use on a flight stage.

2.2.8 Electrical System

The stage electrical control system operated satisfactorily throughout the battleship tests. The sequencer performance was as expected. The electrical systems that were not included in this program were the range safety, ullage rocket ignition and jettison systems, and APS control.

The electrical power system consisted of two forward power supplies, two aft power supplies, two inverters for the LOX and LH2 chilldown motors, and a static inverter/converter. The forward power supply No. 1 was not used.

Forward power supply No. 2 operated satisfactorily supplying 2.7 amps prior to engine ignition and increasing to 3.45 amps after engine start.

Operation of the aft power supply No. 1 was within expectations. The current surged to 28 amps during start sequence and maintained current levels between 8 to 12 amps during engine steady-state operation.

The aft power supply No. 2 which supplied 56 vdc to the chilldown inverters and the auxiliary hydraulic pump, operated successfully. The current increased from 50 amps to 74 amps when the pump started to pressurize the accumulator. The current decreased to approximately 44 amps when the accumulator reached full pressure.

The chilldown inverters were not installed during the early part of the battleship program but they were successfully used in the S-IVB/IB and S-IVB/V tests. The only problem noted was the erratic speed of the LH2 chilldown pump during S-IVB/V chilldown tests.

Inverter phase voltages were nominally 52 vdc and the phase currents indicated 35-40 amps start transients dropping to 10-15 amps during steady-state operations. Phase frequency was 408-410 amps and the inverter temperature varied between 525 and 545 deg R. All data were within the expected range. The static inverter/converter operated satisfactorily and all parameters were within their prescribed tolerances.

2.2.9 Hydraulic System

The hydraulic system was evaluated for four full-duration firings; CD 614025 and 614030 were for the S-IVB/IB; and CD 614043 and 614044, were for the S-IVB/V.

For each of these countdowns the system was serviced using the fill, flush, bleed and fluid sample procedures used for a flight stage. The reservoir fluid level was maintained at 85 ± 2 percent full volume before each firing and did not decrease below 25 percent during hydraulic pump operation.

Pressure data were within the design limits of the pumps and verified compensator pressure settings which had been determined in previous tests. All reservoir pressure readings and fluid temperatures were within design limits. GN2 pressure was acceptable for all firings. CD 614028 was cut

pg 12

off manually after 374 sec of engine operation because of a high hydraulic reservoir oil temperature. The anomaly was caused by a defective high-pressure relief valve.

The hydraulic system successfully positioned and gimbaled the engine in response to simulated guidance commands.

2.2.10 Thrust Vector Control

A vast amount of data pertinent to the engine control system performance was obtained including engine gimbal friction, engine position, phase and gain characteristics at both low frequencies and command amplitudes.

Evaluation of these engine gimbaling tests indicated that all test objectives were fulfilled. The thrust vector control system closed loop response behaved as predicted and satisfied performance requirements.

The results of these gimbaling tests will be utilized to establish an accurate mathematical model of the flight control system for purposes of control system stability studies and flight performance predictions.

2.2.11 Acoustics and Vibration

Fifty-nine acoustic and vibration parameters were monitored during the battleship program. Data from 16 countdowns (18 firings) were reduced for this evaluation.

In general, data obtained over several firings from a particular parameter were very repeatable. The majority of the parameters monitored, both acoustic and vibration, exhibited high levels at ESC and ECO. These levels ranged from 2db to 7db higher than the steady-state levels during mainstage. At engine start, the transients persisted from ESC +2 sec to ESC +7 sec. Engine cutoff transients lasted from 0.5 to 1.5 sec after ECO.

2.2.12 Aero/Thermodynamic Analysis

Temperatures measured during the S-IVB/IB battleship aft interstage environmental tests (CD 614031 and 614032) by sensors located on the J-2 engine thrust chamber were used to verify analytical predictions for the flight stages and to determine whether the temperature of the engine thrust chamber tubes will exceed the maximum allowable starting temperature prior to first ignition. Predicted tube temperatures at liftoff were 210 deg R forward of the manifolds and 170 deg R aft of the manifolds. The predicted temperatures were in good agreement with the actual.

Common bulkhead temperatures measured during these tests could not be used to predict flight temperatures because the battleship used a steel instead of a honeycomb bulkhead.

Temperature gradients across the honeycomb and along the weld seams during the LOX loading phase were generated analytically on the basis of the measured ullage gas temperatures.

2.2.13 Reliability and Human Engineering

Hardware failure summary of all flight critical items were prepared by reliability engineering, and numerous recommendations have been adopted based on human engineering evaluation of Complex Beta and the Saturn S-IVB Battleship Vehicle.

Pg 14

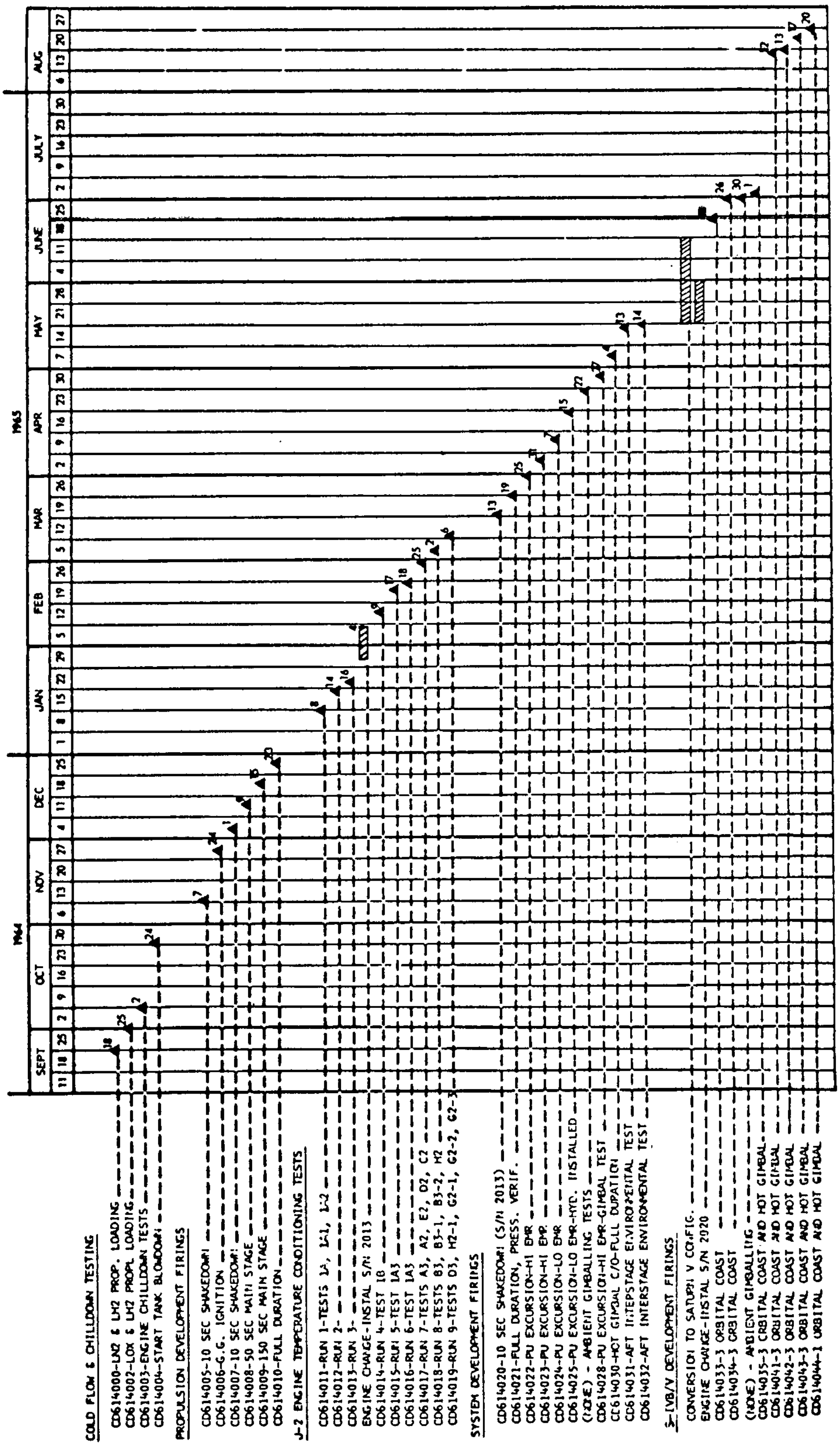

Figure 2-1 S-IVB Battleship Static Test Program

SECTION 3

TEST CONFIGURATION

3. TEST CONFIGURATION

The test configuration consisted of the battleship test vehicle, GSE (ground support equipment) installed on the Beta Complex test stand No. 1, and GSE installed in the test control center (blockhouse) and the Beta Complex test facilities.

3.1 Battleship Test Vehicle Configuration

The battleship test vehicle configuration during most of the static firing tests was basically that of the S-IVB/IB stage. However, the configuration was modified to that of the S-IVB/V stage during the final phase of the tests. This modification primarily consisted of the installation of 10 ambient helium bottles to the thrust structure for LOX and LH2 tank repressurization.

The battleship test vehicle consisted of the battleship tank assembly and flight stage systems. The tank was a heavy-duty stainless steel, cylindrical vessel with hemispherical heads mounted on a dummy aft interstage and the J-2 engine mounted on the thrust structure. The internal configuration of the LOX and LH2 tanks was similar to the S-IVB flight stage except for openings provided for special instrumentation, cameras, lighting, and emergency LOX drain provisions. All flight stage systems were installed using either flight or prototype flight components except for the following:

a. Telemetry system

b. Separation and range safety pyrotechnic systems

c. Electrical power system batteries

d. Ullage and retrorockets

e. Auxiliary propulsion system

3.1.1 Propulsion System

The propulsion systems for both S-IVB/IB and S-IVB/V battleship configurations were the same as the flight stage except for the addition of emergency LOX drain provisions and the domotor valve installation on the LH2 tank.

3.1.2 Electrical Power System

The electrical power system consisted of external power supplied to the vehicle through prototype forward and aft power distribution boxes. Two prototype childown inverters were used for the chilldown pumps and one prototype static inverter-converter supplied power for the propellant utilization system.

3.1.3 Sequencing System

The sequencer used was a prototype version. Command signals to the sequencer are normally received from the switch selector in the stage; however, in the battleship vehicle configuration, the commands were received from the GSE console in the Beta Complex test control center.

3.1.4 Hydraulic Systems

The hydraulic systems were the same as for the flight stages.

3.1.5 Propellant Utilization (PU) System

The PU system consisted of an integrated system using prototype components. These components included the following:

a. Static inverter-converter

b. Propellant utilization electronics assembly

c. LH2 mass probe

d. LOX mass probe

e. Engine mixture-ratio valve

3.1.6 Aft Skirt and Interstage Thermoconditioning and Purge System

The aft skirt and interstage thermoconditioning and purge system was a prototype configuration. The main variations from the flight stage configuration were due to the structural differences between the battleship vehicle and the flight stages.

3.1.7 Instrumentation

Instrumentation consisted of static test and flight-type transducers. All parameters were transmitted to the ground recording system by means of hardwire. A telemetry system was not used. In addition, adequate instrumentation was provided in the Beta Complex facilities to evaluate the performance of the facilities.

3.2 GSE - Beta Complex Test Stand I

The GSE installed on the test stand included manually controlled battleship GSE and electrical equipment to supply control and/or power.

3.2.1 Manually Controlled GSE

Manually controlled GSE used to control propellant and gases were as follows:

a. Pneumatic console A

b. Pneumatic console B

c. Pneumatic console C

d. Gas heat exchanger

e. LOX valve control complex

f. LH2 valve control complex

3.2.2 Electrical GSE

Electrical GSE, with the exception of the test stand cable network and the terminal cable network was located in the aft umbilical room and included the following:

a. Umbilical junction box

b. Control switching rack

c. External power rack

d. Inverter power supply

e. Gimbal power supply

3.3 GSE - Test Control Center

The test control center GSE included the following:

a. Safety officers' console

b. Test conductors' console

c. TV control console

d. Facilities control console

e. Instrumentation control console

The GSE installed in the launch control console included the following:

a. LH2 loading control panel

b. LOX loading control panel

c. Hydraulic and gimbal control panel

d. Helium control panel

e. Vehicle system control panel

f. Chilldown inverter control panel

g. Engine firing control panel

h. Automatic propellant loading set

i. GH2/GN2 control panel

j. PU control panel

k. Engine component checkout panel

The patch panel junction box and test control center cable network were used only for the battleship test.

3.4 Beta Complex Test Facilities

The Beta Complex test facilities included the following:

a. Propellant transfer systems

b. Pneumatic systems

c. Water systems

d. Venting systems

SECTION 4

TEST OPERATIONS

4. TEST OPERATIONS

The countdown procedures developed during the battleship stage programs served two basic functions: (1) to effectively and safely prepare the stage for the test currently being conducted and (2) to develop an overall procedure to be used for conducting the acceptance and launch countdowns of the flight stages.

Typical S-IVB/IB and S-IVB/V battleship countdown procedures are illustrated in figures 4-1 and 4-2. The countdowns were initiated by the usual vehicle systems checks and propellant and pneumatic panel loading and control setups and, as shown, proceeded through propellant and pneumatic system loading and system checks and preparations. At approximately SLO (simulated liftoff) -17 min, the automatic sequence was initiated with the engine start tank chilldown sequence.

The total of approximately 3 hr 15 min were required from the initiation of final countdown to Engine Start Command.

4.1 Purges

Before the firing countdown was initiated, the LH2 tank and engine were purged with GH2 to remove the nitrogen remaining from the previous GN2 purges. When required, the LOX tank was purged with GN2. The remaining system purges were conducted during the firing countdown. The system purges are described in the following paragraphs.

4.1.1 LH2 Tank Purge

Before the LH2 tank was loaded, an initial GN2 purge was accomplished (when required) to remove air and humidity from the LH2 tank, umbilical line, and facility LH2 loading line, and to establish a GN2 blanket. The GN2 was introduced through the LH2 umbilical drain and blanket pressure line into the umbilical nozzle and vented through the LH2 tank vent-relief valve and the GSE LH2 main fill and topping control system vent valve. The purge was continued until the gases contained 1 percent oxygen by volume. The 20-psia GN2 blanket was locked in the tank.

When LH2 was to be loaded, the tank, umbilical line, and facility loading line were purged with GH2 to remove the GN2 blanket and establish a hydrogen atmosphere in all areas that will contain liquid or gaseous hydrogen. This GH2 purge gas was obtained from console C, 2,500 to 1,500 psia ambient GH2 supply. The purge gas flowed from console C through the LH2 tank GH2 purge line to the LH2 tank prepressurization line and into the LH2 tank. The gas flowed out of the tank through the LH2 fill and drain valve and umbilical drain to the burn pond for 40 min while the LH2 tank ullage pressure was monitored and prevented from exceeding 23 psig. After the purge valve was closed, the tank pressure was allowed to decrease to 5 psig, the umbilical drain was closed, and a gas sample was taken from the bottom of the tank. (If the GN2 concentration is more than 1 percent, the purge is continued for 5 min, then resampled and, if necessary, continued until the GN2 concentration is less than 1 percent.) The LH2 tank was then pressurized to 20 ± 1 psig through the LH2 tank purge line, the LH2 tank vents were opened, and the pressure decreased to 3 ± 1 psig. The LH2 prevalve was then opened, the LH2 recirculation valve was closed, and the LH2 tank was pressurized and vented three additional times.

4.1.2 LOX Tank Purge

Before the LOX tank was loaded, an initial GN2 purge was accomplished (when required) to remove air and humidity from the tank, the umbilical line, and the facility LOX loading line, and to establish a GN2 blanket. The GN2 was introduced through the LOX umbilical drain and blanket pressure line into the umbilical nozzle and vented through the tank vent-relief valve and the GSE LOX main fill and topping control system vent valve. The vented purge gases were sampled periodically and analyzed with a gas chromatograph. When the gases contained 1 percent oxygen by volume, the purge was terminated, and the tank was vented to the 22-psia blanket pressure which was maintained in the tank.

4.1.3 LOX Chilldown Pump Purge

The LOX chilldown pump motor container was purged of air and humidity before LOX was loaded. A pressure of 49 to 54 psia was maintained in the container when LOX was present in the LOX tank. The ambient helium used for this purpose was supplied from the stage pneumatic control helium sphere (which was replenished by facility helium as required) through the pneumatic power control module to the LOX chilldown pump purge module which maintained the required pump container pressure.

4.1.4 Engine Turbine Start Tank Purge

The engine turbine start tank, which used cold hydrogen gas for start operations, contained air and moisture and was, therefore, purged with helium at 50 psia for 5 min soon after propellant loading was completed. During the automatic sequence, cold GH2 was used to chill the tank to the required temperature before it was filled. The cold GH2 was supplied from the LH2 vaporizer in the LH2 main fill and topping control system. The purge gas was supplied to the start tank through the start tank fill customer connect point and was vented out of the start tank vent and relief valve through the overboard drain customer connect point and the GH2 vent stack.

4.1.5 Engine Thrust Chamber Jacket Purge

A helium purge of the thrust chamber LH2 jacket is necessary to purge the jacket of air and humidity and, after ground firing, to purge it of hydrogen. The purge was accomplished by flowing helium through the jacket and out the thrust chamber for 5 min at 100 scfm. The helium was ground supplied from pneumatic console C at 50 psia.

4.1.6 Engine Pump Purge

A helium purge of the engine LOX turbine seal cavity, LH2 turbine seal cavity, LH2 pump seal cavity, and gas generator injector was necessary before the propellants were loaded to purge out air and humidity and, after the firing, to purge out propellant vapors. The purge was accomplished by flowing 5 scfm helium for 10 min at 105 to 130 psia from the stage pneumatic control helium sphere.

4.2 Loading and Unloading

The battleship stages were successfully loaded with LOX, LH2, and cold helium during all countdown which required that propellants be on board. The propellant loading rates obtained averaged 2,757 and 804 gpm for LH2 and LOX respectively (table 4-1). The following loading procedures were developed.

4.2.1 LH2 Loading

Prior to loading LH2, the LH2 tank, the LH2 umbilical, and the LH2 transfer line were purged in accordance with the established purging procedures. The

LH2 tank was precooled through the topping valve with the LH2 vents open for approximately 5 min. The main fill valve was placed in the reduced fill position and loading was continued until the mass level reached the 5 percent level. The main fill valve was then opened and the tank was filled to the 98 percent level at the rapid fill rate of approximately 2,600 to 3,000 gpm. At this time, the main fill valve was placed in the reduced fill position until the mass level was at the 99.25 percent level. The modulating valve was then used to replenish and maintain the tank at the 100 percent level.

4.2.2 LOX Loading

The LOX tank was filled in three phases; precool, rapid fill, and topping. The precool phase of approximately 5 to 7 min was conducted at an average flowrate of approximately 500 gpm. During this precool phase, the LOX tank ullage pressure was being increased, which was constantly increasing the precool flowrate. The loading rate attained was 804 gpm until the 98 percent level was attained when the main fill valve was closed to the reduced position and the loading completed in the reduced flow and replenish mode.

4.2.3 LH2 Unloading

The LH2 tank was loaded by pressurizing and maintaining the LH2 tank at approximately 35 psia, opening the main fill and fill and drain valves and the LH2 storage tank vent valve, and draining the LH2 back into the ground storage facility. The unloading rates achieved were between 2,000 and 2,100 gpm.

4.2.4 LOX Unloading

The LOX tank was unloaded by pressurizing and maintaining the LOX tank between 37 to 40 psia, opening the main fill and fill and drain valves and the LOX storage tank vent valve, and draining the LOX back into the ground storage facility. The unloading rates achieved were between 800 and 1,000 gpm.

4.2.5 Cold Helium Loading

There are eight cold helium spheres located in the LH2 tank. These spheres were purged with ambient helium before LH2 transfer by pressurizing to 500 psia and venting to 15 psia. Prior to loading LH2, the spheres were pressurized to and maintained at 750 psia with ambient helium to prevent excessive helium pressure loss from childown of the spheres during loading of the cold LH2. When 50 percent of the LH2 had been loaded, cold helium (from the cold helium ground source) loading into the spheres was started by pressurizing the spheres to a nominal pressure of 3,100 psia and cooling them to 50 deg R. The pressure source remained connected until liftoff with cold helium fill time of approximately 40 min. The spheres were protected from temperature changes by the pressure relief valve and were vented through the solenoid vent valve, both of which are in the vehicle cold helium fill module.

4.2.6 Pneumatic Control Helium Sphere Loading

Prior to loading, the pneumatic control helium sphere and lines were purged by filling to 500 psia and venting to 15 psia. The sphere was then filled to 1,500 psia and allowed to stabilize for an hour, then filled to 3,000 psia. The temperature of the loaded gas was not allowed to exceed 80 deg R during the second loading. Approximately 1 lbm of helium was loaded into the spheres at a maximum rate of 0.003 lbm of helium per sec.

4.2.7 Propulsion GSE Performance

The propulsion GSE (ground support equipment) consisted of pneumatic consoles A, B, and C, a gas heat exchanger, and a LOX and LH2 valve control complex. The GSE installed in the launch control console consisted of an LH2 loading control panel, LOX loading panel, helium loading panel, GH2/GN2 control panel, and engine firing control panel. For ease of organization, the GSE performance will be discussed in order by function rather than by items of equipment.

4.3 Terminal Countdown

The major events of the terminal countdown were engine conditioning; final topping and prepressurization of the propellant tanks; and, if necessary, final addition of helium to the cold helium spheres, the pneumatic control spheres, and, for the S-IVB/V tests, the repressurization spheres. Reviews of the terminal count sequence for the battleship tests indicate that the variations consisted primarily in changes in starting times and in duration of the engine conditioning event. The other events were essentially fixed in the sequence; i.e., the LOX tank was prepressurized at either 3 or 3.5 min before SLO and the LH2 tank prepressurization was always initiated 10 sec later than that of the LOX tank.

During the testing of the J-2003 engine (CD 614005 to 614010), the sequence of engine conditioning events was changed twice as a result of problems encountered (table 4-2). During CD 614005, chilldown of the LOX and LH2 pumps was initiated at SLO -10 min. During this test, the ignition of the gas generator started an uncontrolled combustion which ultimately resulted in damage to several engine components. The violent reaction at ignition occurred because of an oxygen-rich mixture ratio in the gas generator as a result of a very effective chilldown by the LOX recirculation system.

After this test, the LOX and LH2 engine pump chilldown was started at SLO -3 min 30 sec. The gas generator body was equipped with a heater and with temperature skin patches to control and monitor the temperature within the limits suggested by Rocketdyne.

The next change in the terminal count sequence involving engine conditioning was made after CD 614007. During this test, the LH2 pump surged during the engine start transient. Insufficient chilldown of the engine, particularly of the thrust chamber jacket, was believed to have caused this incident. To prevent recurrence, the thrust chamber jacket was extended from 20 to 51 min, starting at SLO -50 min and ending at SLO -1 min, and the engine pump chilldown was initiated at SLO -8 min 45 sec instead of at SLO -3 min 30 sec (CD 614006 and 614007 had shown that the gas generator heater could control the body temperature within the desired limits). These changes eliminated the problem of the final pump surge in the tests discussed in the following paragraphs. (For further discussion of the effect of these sequence changes, see paragraph 6.1.)

During the tests with the J-2003 engine, the sequencing of chilldown and loading of the engine control and start spheres was not changed. The first battleship tests (CD 614014, 614017, 614018, and614019) with the J-2013 engine were the special thrust chamber jacket chilldown and warmup test to investigate the effect of these events on the LH2 pump performance during the engine start transient (start tank blowdown tests; engine was not fired). In some of these tests the pump chilldown period was also varied to examine its effect.

See Section 6 for details of the J-2013 firing tests (CD 614020 and 614030). The thrust chamber jacket chilldown initiation varied from SLO -12 min to SLO -8 min 30 sec. Variations were made to accommodate LOX tank pressurization system chilldown procedures (also using helium) and still provide sufficient thrust chamber chilldown. Thrust chamber chilldown was terminated at approximately SLO +70 to SLO +72 sec. Engine pump chilldown was initiated at SLO -5 min in all these tests.

The start tank loading time was changed after CD 614023 from SLO -4 minutes to SLO -2 min. Also, the sphere was loaded to a lower pressure for CD 614024 and subsequent tests. A change was made to obtain required conditions at ESC without venting the start tank during the period between end of fill and ESC. The engine pneumatic control helium sphere conditioning procedure was changed for the same reason. This sphere was vented to approximately 2,800 psia at SLO -2 min to prevent further venting prior to ESC.

Prior to the S-IVB/V tests, the sequence was not changed except for the time of termination of thrust chamber chilldown. This time was established during the count on the basis of the ambient conditions and the prediction curves of the heatup rate for the given ambient conditions. Thrust chamber chilldown was initiated at SLO -20 min. Because of the S-IVB/V stage mission requirements, the engine pump chilldown was started later in the terminal count (SLO -2 min 30 sec) and the chilldown and fill of the engine start tank and pneumatic control helium sphere were started earlier.

4.4 Propellant Loading GSE

The propellant loading GSE performance was acceptable. The LOX was transferred under pressure (125 psig) from the LOX storage tank, through the LOX valve control complex to the battleship LOX tank. The main fill and replenish flow control was provided by the valves included in the valve control complex which were actuated by electrical signals emanating from the vehicle propellant system. The LH2 was transferred under pressure from the LH2 storage tank, through the LH2 valve control complex to the battleship LH2 tank. The main fill and replenish flow control was provided by the valves in the valve control complex which are actuated by electrical signals emanating from the vehicle propellant system. In addition, the valve complex controlled the transfer of LH2 to the gas heat exchanger. The propellant loading complex consisted of LOX valve control complex DSV-IVB-205 and LH2 valve control complex DSV-IVB-206.

4.4.1 GH2, GN2, and Helium Supply Systems

Pneumatic console A, Model DSV-IVB-201, performed adequately and was acceptable. The console was used for receiving helium gas at 6,000 psig and nitrogen gas at 2,500 psig and reducing and regulating these gases to meet the requirements of purging, blanket pressures, checkout, countdown, and unloading operations. Pneumatic console B, Model DSV-IVB-208, was used for receiving helium gas at 3,000 psig at 60 deg R, nitrogen gas at 2,500 psig, and hydrogen gas at 200 psig, and reducing and regulating these gases to meet the requirements of purging, blanket pressures, checkout, countdown, and unloading operations. Pneumatic console C, Model DSV-IVB-202, was used for receiving hydrogen gas at 2,500 psig, nitrogen gas at 750 psig, and helium gas at 3,000 psig at 210 deg R, and reducing and regulating these gases, as required for purging, blanket pressures, checkout, and countdown and unloading operations. The gas heat exchanger, Model DSV-IVB-207, was used to receive helium gas at 3,000 and 2,700 psig, and hydrogen gas at 800 psig, from the pneumatic consoles. The heat exchanger cooled the ambient temperature helium and hydrogen gases to 60 deg R and 210 deg R respectively, and transferred the cooled gases to the pneumatic consoles B and C for subsequent charging of the stage cold gas spheres during countdown.

4.4.2 LOX Tank Prepressurization

Near the end of the LOX tank fill operations, the LOX tank was prepressurized with ground cold helium. Prepressurization was begun at the 99.25 percent full point and required approximately 30 sec. The tank was prepressurized to 39.5 psia at which pressure the tank prepressurization pressure switch actuated and closed the prepressurized valve in the LOX tank pressurization control module. If tank pressure decreased to 37.5 psia the pressure switch opened the valve to repressurize the tank.

4.4.3 LH2 Tank Prepressurization

Near the end of the LH2 tank fill operations, the LH2 tank was prepressurized with ground-supplied helium which was supplied to the vehicle at 100 deg R and 600 psia. The helium pressure decreased the tank pressure through expansion upon flowing from the pressurization line into the tank. Prepressurization began at the 99 percent LH2 level and required approximately 60 sec to reach 30.5 psia. At this pressure, the tank prepressurization pressure switch actuates and closes the ground prepressurization valve. If the tank pressure decreased to 28.5 psia, the pressure switch opened the valve to repressurize the tank.

TABLE 4-1
PROPELLANT LOADING RATES

COUNTDOWN NO.	LH2 RAPID FILL (gpm)	LH2 ULLAGE PRESSURE MAXIMUM (psia)	LH2 STORAGE TANK PRESSURE (psia)	LH2 LOAD (lbm)	LOX RAPID FILL (gpm)	LOX ULLAGE PRESSURE MAXIMUM (psia)	LOX STORAGE TANK PRESSURE (psia)	LOX LOAD (lbm)
614011	2,800			39,9XX	700			169,9XX
614012	2,730			37,9XX	757			183,9XX
614013	2,890	18.8 to 20.0		39,9XX	765	26.5		183,9XX
614014	2,860			38,5XX	810			188,0XX
614014	3,050		61		860		81	
614015					907		82	188,0XX
614016	2,710			38,5XX	930			150,0XX
614016	3,010		60		963		83	
614017	2,680			38,5XX	770			188,0XX
614018	2,750			39,5XX	820		75	188,0XX
614019	2,680			39,5XX	750			188,0XX
614020	2,660			39,5XX	770			180,0XX
	3,100		82					
614021	2,870			39,5XX	920			188,0XX
614022	2,910			28,1XX	890			188,0XX
614023	2,120			37,9XX	575			189,6XX
614028	2,460			38,2XX	660			192,4XX
614005	2,610		54	37,4XX				192,8XX
614006								
614007								
614008								
614009	2,740			39,9XX	820			169,9XX
614010	2,750			39,XXX	815			183,6XX
Average Rate	2,757				804			
Percent of Design Rate	92				80			

21 February 1966

TABLE 4-2
TERMINAL COUNT PROCEDURES

ITEM	CD 614006 RUN 1	CD 614007	CD 614008	CD 614009	CD 614010	CD 614011 RUN 1A	CD 614014 RUN 1B	CD 614017 RUN A3	CD 614017 RUN A2	CD 614017 RUN E2	CD 614017 RUN D2	CD 614018 RUN B3-1	CD 614018 RUN B3-2	CD 614018 RUN H2	CD 614019 RUN D3	CD 614019 RUN H2-1	CD 614019 RUN G2-1	CD 614019 RUN C-2-3	CD 614020 RUN 2	CD 614021 RUN 1	CD 614023	CD 614028	CD 614030
Close LOX and LH2 Pre-valves	-3:30	-3:45	-8:45	-8:45	-8:45	-20:30	-20:30	-3:15	-20:30	-20:30	-20:30	-2:15	-2:15	-20:30	+0:15	-20:30	-20:30	-20:30	-5:00	-5:00	-5:00	-10:00	-05:00
Turn on Chilldown Pumps	-3:30	-3:45	-8:45	-8:45	-8:26	-20:30	-20:30	-3:15	-23:30	-20:30	-20:30	-2:15	-2:15	-20:30	+0:15			-20:30	-5:00	-5:00			
Initiate Start Tank Chilldown	-16:00	-16:00	-16:00	-16:00	-16:00	-17:30	-17:30		-17:30	-17:30	-17:30	-17:30	-17:30	-17:30	-17:30	-17:30	-17:30	-17:30	-17:30	-17:30	-17:30	-17:30	-17:30
Initiate Engine Control Sphere Chilldown	-9:00	-9:00	-9:00	-9:00	-9:00	-10:30	-10:30	-17:30	-10:30	-10:30	-10:30	-10:30	-10:30	-10:30	-10:30	-10:10	-15:00	-15:00	-10:30	-10:30			-17:30
Gas Generator Heater Off	+01:00	+01:00																					
Thrust Chamber Ambient Purge On			-55:00	-55:00	-55:00	-10:00		-12:00	-12:00	-18:00	-18:00	-12:00	-12:00	-23:00					-13:00	-13:00	-14:30	-17:30	-17:30
Press. Eng Cont Sphere to 3,000 ±5 psia	-7:00	-7:00	-7:00	-7:00	-7:00	-8:30		-3:30	-3:30	-3:30	-3:30	-3:30	-3:30	-3:30	-3:30	-3:30	-3:30	-3:30	-4:30	-4:30	-17:30	-17:30	
Press. Eng Start Sphere to 1,225 ±125 psia	-5:30	-5:30	-5:30	-5:30	-5:30	-7:00	-6:45 +5:10	-3:00	-3:30	-3:30	-3:30	-3:30	-3:30	-3:30	-2:00	-3	-3:00	-3:00	-4:00	-4:00	-4:00	-2:00	-02:00
Initiate T/C Chilldown (Reg at 3,000 ±100 psia)	-20:00	-20:00	-50:00	-50:00 -4:00	-50:00 -00:45	-5	-8:00	-7:00	-8:00	-13:00	-13:00	-7:00	-7:00	-18:00	-9:00	-33:00		-12:00	-8:30	-8:30	-10:00	-12:00	-12:00
Prepress. LOX Tank	-3:00	-3:00	-3:00	-3:00	-3:00	-4:30	-4:30	-4:30	-4:30	-4:30	-4:30	-4:30		-4:30	-3:00	-4:20	-4:30	-4:30	-2:30	-3:30	-3:30	-3:00	-03:00
Prepress. LH2 Tank	-2:50	-2:50	-2:50	-2:50	-2:50	-4:20	-4:20	-4:20	-4:20	-4:20	-4:20	-4:30		-4:20	-2:50	+4:00	-4:20	-4:20	-3:20	-3:20	-3:20	-2:30	-02:30
Hold for T/C to Cool to 210° R						+1:00	0:00																
Sequence Start	+01:20	+01:19	+01:19	+01:19	+01:19	+4:1868	8:00	+0:23	3:42	2:25	10:34	+0:5.6	+0:2.8	+8.51	+2:20	+7:58.7	+3:9.8	+3:05	+01:28	+01:25	+01:20	+1:20	+1:20
T/C Chilldown Off (Target 2.10° R)	0:00 0:00	0:00	+01:00	-08:50 -00:15	-3:15 +01:00	4:24 220° R	+8:02.43 245° R	0:23 280° R	+1:17 260° R	0:00 210° R	+7:14 217° R	-0:30 260° R	-0:11 249° R	+1:17 169° R	+0.07 198° R	+0.13 154° R	-0:8.1 192° R	+0.2.3 206° R	+01:11 227° R	+01:14 289° R	+01:07	+1:12 +1:12	+1:10 +1:10
Sequence Cutoff						4:34.43																	
Engine Start	+00:31	+01:31	+01:30	01:30	+01:30		8:19.1	+0:36	+3:55	2:38	+10:47	+0:24.8	+0:18	+9:05	+2:33	+8:12.7	+3:23.5	+3:19	+01:37	+1:34	+01:33	+1:33	+1:33
Cutoff	01:32	01:45	+2:24	04:04	+08:25		8:20.2	+0:36	+3:55	+2:38	10:47	+0:24.5	+0:18	+9:05	+2:33	+8:12.7	+3:23.5	+3.19	01:51	+2:03	+9:23	+7:48	+09:46

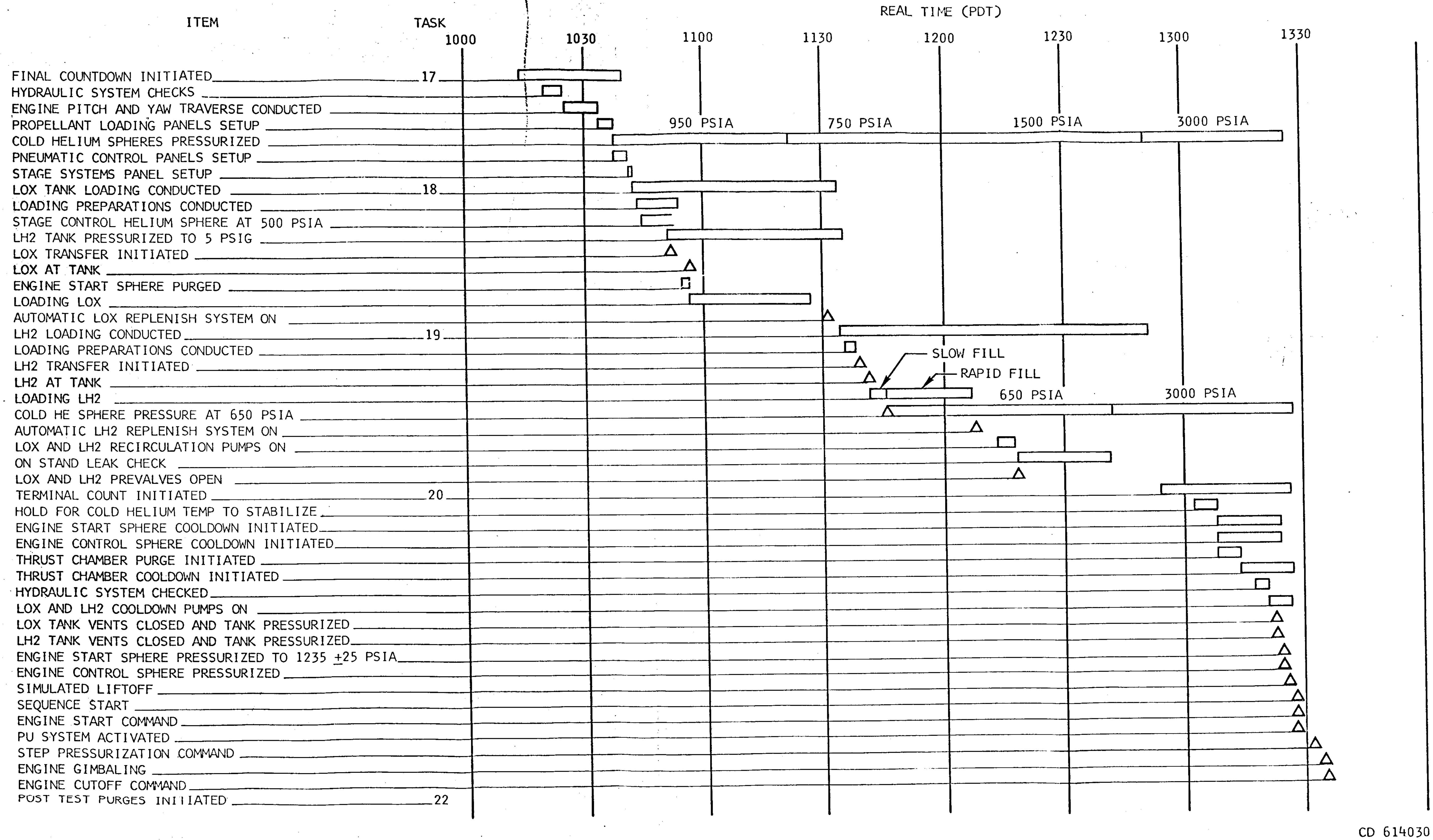

Figure 4-1 S-IVB/IB Battleship Countdown Procedure

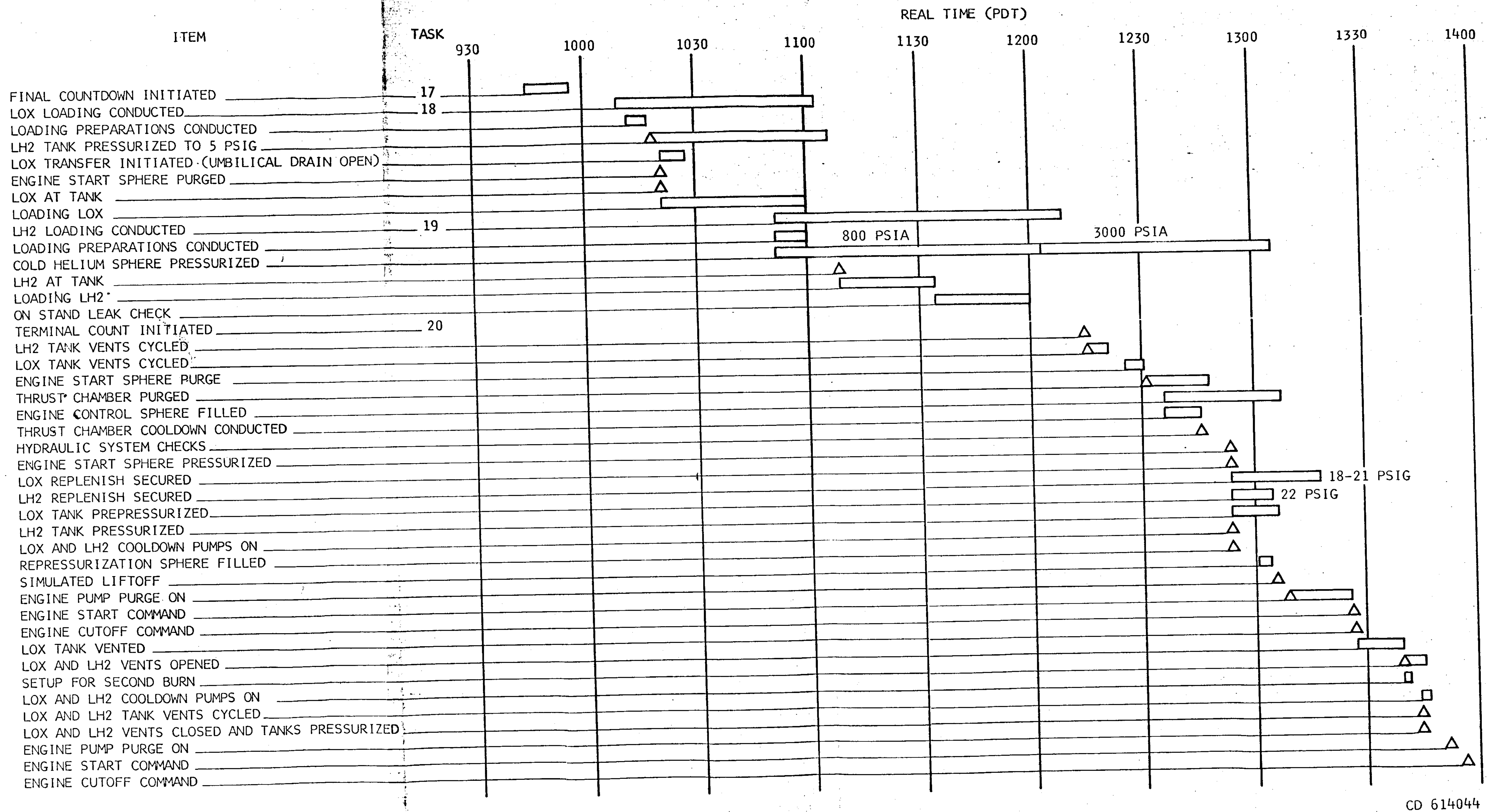

Figure 4-2 S-IVB/V Battleship Countdown Procedure

SECTION 5

SEQUENCE OF EVENTS

TABLE 5-1 (Sheet 1 of 4)
TYPICAL S-IVB/IB BATTLESHIP FIRING SEQUENCE OF EVENTS

FUNCTION	PICKUP/ DROP-OUT	TIME
LOX Recirculation Valve Closed	DO	T -582.3
LH2 Recirculation Valve Closed	DO	T -582.3
LH2 Recirculation Valve Open	PU	T -582.2
LOX Recirculation Valve Open	PU	T -582.2
LOX Chilldown Inverter Energized	PU	T -292.4
LH2 Chilldown Inverter Energized	PU	T -287.0
Engine Ready	PU	T -94.6
Simulated Booster Liftoff		T -0*
LH2 Pre-Valve Closed	DO	T +85.87
LOX Pre-Valve Closed	DO	T +85.96
LH2 Pre-Valve Open	PU	T +87.98
LOX Pre-Valve Open	PU	T +88.40
LOX Chilldown Inverter Energized	DO	T +93.38
LH2 Chilldown Inverter Energized	DO	T +93.48
LOX Recirculation Valve Open	DO	T +93.51
LH2 Recirculation Valve Open	DO	T +93.58
LOX Recirculation Valve Closed	PU	T +93.61
LH2 Recirculation Valve Closed	PU	T +93.65
Start Command (GSE)	PU	T +93.67
LH2 Tank Stop Pressure Control Valve Energized	PU	T +93.68
ASI Spark On	PU	T +93.68
GG Spark On	PU	T +93.68
Engine Ready	DO	T +93.70
Helium Control Solenoid Energized	PU	T +93.70
Ignition Phase Solenoid Energized	PU	T +93.70
ASI LOX Valve Open	PU	T +93.73
Main LH2 Valve Closed	DO	T +93.76
Main LH2 Valve Open	PU	T +93.80
ASI Ignition Detected	PU	T +93.85
ASI Spark No. 2 OK	PU	T +94.16
GG Spark No. 1 OK	PU	T +94.16

* T = time from simulated boost liftoff

TABLE 5-1 (Sheet 2 of 4)
TYPICAL S-IVB/IB BATTLESHIP FIRING SEQUENCE OF EVENTS

FUNCTION	PICKUP/ DROP-OUT	TIME
ASI Spark No. 1 OK	PU	T +94.20
GG Spark No. 2 OK	PU	T +94.21
Start Tank Discharge Valve Control Solenoid Energized	PU	T +94.31
Start Tank Discharge Valve Closed	DO	T +94.47
Start Tank Discharge Valve Open	PU	T +94.54
Start Tank Depressurized	PU	T +94.67
Start Tank Pressurized	DO	T +94.76
Mainstage Control Solenoid Energized	PU	T +94.76
Start Tank Discharge Valve Control Solenoid Energized	DO	T +94.76
GG Valve Open	PU	T +94.86
GG Valve Closed	DO	T +94.86
LOX Turbine Bypass Valve Open	DO	T +94.98
LOX Turbine Bypass Valve Closed	PU	T +95.14
Mainstage OK	PU	T +96.13
Mainstage OK Pressure Switch No. 2 Depressurized	DO	T +96.14
Mainstage OK Pressure Switch No. 1 Depressurized	DO	T +96.14
Main LOX Valve Open	PU	T +97.33
LOX Level, Position 12	DO	T +98.0
ASI Spark On	DO	T +98.01
GG Spark On	DO	T +98.01
ASI Spark No. 2 OK	DO	T +98.14
GG Spark No. 1 OK	DO	T +98.14
ASI Spark No. 1 OK	DO	T +98.21
GG Spark No. 2 OK	DO	T +98.25
LH2 Liquid/Gas Differentiator 4	DO	T +105.6
PU Activated	PU	T +108.24
LOX Level, Position 11	DO	T +116.0
LH2 Liquid/Gas Differentiator 5	DO	T +160.2

TABLE 5-1 (Sheet 3 of 4)
TYPICAL S-IVB/IB BATTLESHIP FIRING SEQUENCE OF EVENTS

FUNCTION	PICKUP/ DROP-OUT	TIME
LOX Level, Position 10	DO	T +200.3
LH2 Liquid/Gas Differentiator 6	DO	T +214.4
LOX Level, Position 9	DO	T +228.3
LH2 Liquid/Gas Differentiator 7	DO	T +268.8
LOX Level, Position 8	DO	T +304.0
LH2 Liquid/Gas Differentiator 8	DO	T +322.4
LOX Level, Position 7	DO	T +348.1
LH2 Liquid/Gas Differentiator 9	DO	T +376.4
LOX Level, Position 6	DO	T +405.5
LH2 Liquid/Gas Differentiator 10	DO	T +423.6
LOX Level, Position 5	DO	T +450.9
LH2 Liquid/Gas Differentiator 11	DO	T +478.0
LOX Level, Position 4	DO	T +492.7
LOX Level, Position 3	DO	T +555.4
LH2 Level, Position 2	DO	T +579.2
LOX Level, Position 2	DO	T +580.4
LOX Level, Position 1	DO	T +601.4
GSE Cutoff Energized	PU	T +602.74
Mainstage Control Solenoid Energized	DO	T +602.75
ASI Ignition Detected	DO	T +602.75
Engine Cutoff Energized (Vehicle)	PU	T +602.76
Engine Cutoff On	PU	T +602.76
Ignition Phase Solenoid Energized	DO	T +602.77
Main LOX Valve Open	DO	T +602.83
GG Valve Open	DO	T +602.83
Main LOX Valve Closed	PU	T +602.87
Mainstage OK	DO	T +602.88
Mainstage OK Pressure Switch No. 2 Depressurized	PU	T +602.89
Mainstage OK Pressure Switch No. 1 Depressurized	PU	T +602.89
Main LH2 Valve Open	DO	T +602.90
GG Valve Closed	PU	T +602.92

21 February 1966

TABLE 5-1 (Sheet 4 of 4)
TYPICAL S-IVB/IB BATTLESHIP FIRING SEQUENCE OF EVENTS

FUNCTION	PICKUP/ DROP-OUT	TIME
Main LH2 Valve Closed	PU	T +603.07
LOX Pre-Valve Open	DO	T +603.58
LH2 Pre-Valve Open	DO	T +603.58
LH2 Level, Position 1	DO	T +603.6
Helium Control Solenoid Energized	DO	T +603.73
LH2 Pre-Valve Closed	PU	T +603.89
LOX Pre-Valve Closed	PU	T +603.89
LOX Turbine Bypass Valve Closed	DO	T +606.88
LOX Turbine Bypass Valve Open	PU	T +607.97

TABLE 5-2 (Sheet 1 of 7)
TYPICAL S-IVB/V BATTLESHIP FIRING SEQUENCE OF EVENTS

FUNCTION	PICKUP/ DROP-OUT	TIME
FIRST BURN		
LH2 Recirculation Valve Closed	DO	T -144.7
LH2 Recirculation Valve Open	PU	T -144.2
LOX Recirculation Valve Closed	DO	T -144.1
LOX Recirculation Valve Open	PU	T -144.0
LH2 Chilldown Inverter Energized	PU	T -137.0
LOX Chilldown Inverter Energized	PU	T -131.0
Simulated Booster Liftoff		T -0
LOX Pre-Valve Open	PU	T +533.79
LH2 Pre-Valve Open	PU	T -534.03
LOX Chilldown Inverter Energized	DO	T +539.04
LH2 Chilldown Inverter Energized	DO	T +539.04
LOX Recirculation Valve Open	DO	T +539.18
LH2 Recirculation Valve Open	DO	T +539.20
LOX Recirculation Valve Closed	PU	T +539.24
LH2 Recirculation Valve Closed	PU	T +539.28
Start Command (GSE) On	PU	T +539.30
Engine Start Mag-Latch On	PU	T +539.30
ASI Spark On	PU	T +539.31
GG Spark On	PU	T +539.31
Helium Control Solenoid Energized	PU	T +539.32
Ignition Phase Solenoid Energized	PU	T +539.33
ASI LOX Valve Open	PU	T +539.36
Main LH2 Valve Closed	DO	T +539.40
Main LH2 Valve Open	PU	T +539.43
ASI Ignition Detected	PU	T +539.45
ASI Spark No. 2 OK	PU	T +539.79
GG Spark No. 1 OK	PU	T +539.79
ASI Spark No. 1 OK	PU	T +539.82
GG Spark No. 2 OK	PU	T +539.84

T = Time from simulated booster liftoff

TABLE 5-2 (Sheet 2 of 7)
TYPICAL S-IVB/V BATTLESHIP FIRING SEQUENCE OF EVENTS

FUNCTION	PICKUP/ DROP-OUT	TIME
LH2 Tank Step Press Cont. Valve Energized	PU	T +541.62
Start Tank Discharge Valve Cont. Sol. Energized	PU	T +542.38
Start Tank Discharge Valve Closed	DO	T +542.55
Start Tank Discharge Valve Open	PU	T +542.63
Start Tank Depressurized	PU	T +542.74
Start Tank Pressurized	DO	T +542.75
Start Tank Discharge Valve Cont. Sol. Energized	DO	T +542.83
Mainstage Control Solenoid Energized	PU	T +542.83
GG Valve Open	PU	T +542.93
GG Valve Closed	DO	T +542.94
Start Tank Discharge Valve Closed	DO	T +542.95
Main LOX Valve Closed	DO	T +542.96
LOX Turbine Bypass Valve Open	DO	T +543.03
Start Tank Discharge Valve Closed	PU	T +543.18
LOX Turbine Bypass Valve Closed	PU	T +543.29
Mainstage Press OK	PU	T +544.02
ASI Spark No. 2 OK	DO	T +544.99
Main LOX Valve Open	PU	T +545.24
ASI Spark On	DO	T +545.46
GG Spark On	DO	T +546.04
GG Spark No. 1 OK	DO	T +546.13
GG Spark No. 2 OK	DO	T +546.13
ASI Spark No. 1 OK	DO	T +546.13
Start Command (GSE) On	DO	T +551.86
Start Tank Pressurized	PU	T +553.95
Start Tank Depressurized	DO	T +553.96
LH2/Gas Differentiator 3	DO	T +551.00
PU Activated	PU	T +554.07

21 February 1966

TABLE 5-2 (Sheet 3 of 7)
TYPICAL S-IVB/V BATTLESHIP FIRING SEQUENCE OF EVENTS

FUNCTION	PICKUP/ DROP-OUT	TIME
LOX Level, Position 11	DO	T +578.5
LH2/Gas Differentiator 4	DO	T +598.7
LH2/Gas Differentiator 5	DO	T +644.7
LOX Level, Position 10	DO	T +649.0
LH2/Gas Differentiator 6	DO	T +693.2
Engine Cutoff Energized (Vehicle)	PU	T +710.42
GSE Cutoff Energized	PU	T +710.43
Engine Cutoff On	PU	T +710.43
PU Activated	DO	T +710.43
Mainstage Control Solenoid Energized	DO	T +710.44
ASI Ignition Detected	DO	T +710.44
Engine Start Mag-Latch On	DO	T +710.44
Ignition Phase Solenoid Energized	DO	T +710.48
ASI LOX Valve Open	DO	T +710.52
GG Valve Open	DO	T +710.54
Main LOX Valve Open	DO	T +710.55
Mainstage Press OK	DO	T +710.59
Main LH2 Valve Open	DO	T +710.60
Main LOX Valve Closed	PU	T +710.62
GG Valve Closed	PU	T +710.64
Main LH2 Valve Closed	PU	T +710.78
LOX Turbine Bypass Valve Open	PU	T +711.01
LOX Pre-Valve Open	DO	T +711.25
LH2 Pre-Valve Open	DO	T +711.27
LH2 Pre-Valve Closed	PU	T +711.59
LOX Pre-Valve Closed	PU	T +711.65
J-2 Engine Ignition Buss (28 VDC)	DO	T +713.8
LH2 Tank Vent Valve Open	PU	T +757.7
LH2 Tank Vent Valve Closed	DO	T +757.7

TABLE 5-2 (Sheet 4 of 7)

TYPICAL S-IVB/V BATTLESHIP FIRING SEQUENCE OF EVENTS

Simulated Coast Period (From 1 to 3 Orbits)

FUNCTION	PICKUP/ DROP-OUT	TIME
SECOND BURN		
LH2 Recirculation Valve Closed	DO	T_1 -590.9
LOX Recirculation Valve Closed	DO	T_1 -590.4
LOX Recirculation Valve Open	PU	T_1 -590.4
LH2 Recirculation Valve Open	PU	T_1 -590.4
LH2 Chilldown Inverter Energized	PU	T_1 -585.4
LOX Chilldown Inverter Energized	PU	T_1 -578.6
Sequence Start		T_1 -13.0
LOX Pre-Valve Closed	DO	T_1 -8.96
LH2 Pre-Valve Closed	DO	T_1 -8.75
LOX Pre-Valve Open	PU	T_1 -6.55
LH2 Pre-Valve Open	PU	T_1 -6.30
LOX Chilldown Inverter Energized	PU	T_1 -1.31
LH2 Chilldown Inverter Energized	PU	T_1 -1.31
LOX Recirculation Valve Open	DO	T_1 -1.17
LH2 Recirculation Valve Open	DO	T_1 -1.14
LOX Recirculation Valve Closed	PU	T_1 -1.11
LH2 Recirculation Valve Closed	PU	T_1 -1.10
Second Engine Burn On Command (GSE)	PU	T_1 -1.05
LH2 Tank Step Pressure Control Valve Energized	PU	T_1 -1.04
Start Command On	PU	T_1 -1.04
Engine Start Mag-Latch On	PU	T_1 -1.04
ASI Spark On	PU	T_1 -1.03
GG Spark On	PU	T_1 -1.03
Helium Control Solenoid Energized	PU	T_1 -1.02
Ignition Phase Solenoid Energized	PU	T_1 -1.01
Engine Ready	DO	T_1 -1.00

T_1 = Time from second burn engine start

TABLE 5-2 (Sheet 5 of 7)
TYPICAL S-IVB/V BATTLESHIP FIRING SEQUENCE OF EVENTS

FUNCTION	PICKUP/ DROP-OUT	TIME
ASI LOX Valve Closed	PU	T_1 -0.98
Main LH2 Valve Closed	DO	T_1 -0.95
Main LH2 Valve Open	PU	T_1 -0.91
ASI Ignition Detected	PU	T_1 -0.86
ASI Spark No. 2 OK	PU	T_1 -0.64
GG Spark No. 1 OK	PU	T_1 -0.64
ASI Spark No. 1 OK	PU	T_1 -0.52
GG Spark No. 2 OK	PU	T_1 -0.50
Second Burn Engine Start		T_1 -0
Start Tank Discharge Valve Control Sol. Energized	PU	T_1 +3.07
Start Tank Discharge Valve Closed	DO	T_1 +3.25
Start Tank Pressurized	DO	T_1 +3.46
Start Tank Depressurized	PU	T_1 +3.45
Mainstage Control Solenoid Energized	PU	T_1 +3.52
Start Tank Discharge Valve Cont. Sol. Energized	DO	T_1 +3.52
GG Valve Closed	DO	T_1 +3.62
GG Valve Open	PU	T_1 +3.63
Main LOX Valve Closed	DO	T_1 +3.65
LOX Turbine Bypass Valve Open	DO	T_1 +3.77
Start Tank Discharge Valve Closed	PU	T_1 +3.88
LOX Turbine Bypass Valve Closed	PU	T_1 +3.98
Mainstage Pressure OK	PU	T_1 +4.69
ASI Spark No. 2 OK	DO	T_1 +5.70
Main LOX Valve Open	PU	T_1 +5.89
GG Spark No. 2 OK	DO	T_1 +5.92
GG Spark No. 2 OK	PU	T_1 +6.14
ASI Spark No. 1 OK	DO	T_1 +6.15
ASI Spark No. 2 OK	PU	T_1 +6.33
ASI Spark No. 2 OK	DO	T_1 +6.39

TABLE 5-2 (Sheet 6 of 7)
TYPICAL S-IVB/V BATTLESHIP FIRING SEQUENCE OF EVENTS

FUNCTION	PICKUP/ DROP-OUT	TIME
ASI Spark No. 1 OK	PU	T_1 +6.47
GG Spark No. 2 OK	DO	T_1 +6.57
GG Spark On	DO	T_1 +6.73
ASI Spark On	DO	T_1 +6.73
GG Spark No. 1 OK	DO	T_1 +6.78
ASI Spark No. 1 OK	DO	T_1 +6.80
Start Tank Pressurized	PU	T_1 +11.55
Start Tank Depressurized	DO	T_1 +11.56
Second Engine Burn On Command (GSE) On	DO	T_1 +14.01
PU Activated	PU	T_1 +14.71
LOX Level, Position 8	DO	T_1 +32.0
LH2/Gas Differentiator 8	DO	T_1 +43.0
LOX Level, Position 7	DO	T_1 +70.5
LH2/Gas Differentiator 9	DO	T_1 +96.0
LOX Level, Position 6	DO	T_1 +127.8
LH2/Gas Differentiator 10	DO	T_1 +144.3
LOX Level, Position 5	DO	T_1 +172.0
LH2/Gas Differentiator 11	DO	T_1 +196.1
LOX Level, Position 4	DO	T_1 +212.0
LH2/Gas Differentiator 12	DO	T_1 +246.2
LOX Level, Position 3	DO	T_1 +271.0
LOX Level, Position 2	DO	T_1 +297.2
LOX Level, Position 2	DO	T_1 +297.2
Observer Cutoff On	PU	T_1 +318.84
GSE Cutoff Energized	PU	T_1 +318.85
Engine Start Mag-Latch On	DO	T_1 +318.85
Engine Cutoff Energized (Vehicle)	PU	T_1 +318.85
PU Activated	DO	T_1 +318.85
Engine Cutoff On	PU	T_1 +318.85
Ignition Phase Solenoid Energized	DO	T_1 +318.87
ASI LOX Valve Open	DO	T_1 +318.92

TABLE 5-2 (Sheet 7 of 7)
TYPICAL S-IVB/V BATTLESHIP FIRING SEQUENCE OF EVENTS

FUNCTION	PICKUP/ DROP-OUT	TIME
Main LOX Valve Open	DO	T_1 +318.95
GG Valve Open	DO	T_1 +318.96
Main LH2 Valve Open	DO	T_1 +319.01
Main LOX Valve Closed	PU	T_1 +319.03
Mainstage Pressure OK	DO	T_1 +319.03
GG Valve Closed	PU	T_1 +319.05
Main LH2 Valve Closed	PU	T_1 +319.18
LOX Pre-Valve Open	DO	T_1 +319.66
LH2 Pre-Valve Closed	PU	T_1 +319.98
LOX Pre-Valve Closed	PU	T_1 +320.05
J-2 Engine Ignition Buss (28 VDC)	DO	T_1 +323.2

SECTION 6

ENGINE SYSTEM

6. ENGINE SYSTEM

Three Rocketdyne J-2 engines, S/N J-2003, J-2013, and J-2020, were used during the battleship test program (figure 6-1). Engine S/N J-2003 was used through CD 614010, J-2013 engine for the subsequent S-IVB/IB tests, and engine J-2020 for the S-IVB/V tests.

Procedures were developed for conditioning and loading the engine control helium sphere and the turbine start tank and for chilling the thrust chamber and the LOX and LH2 pumps. Satisfactory procedures were developed for starting the engines, therefore, engine start, steady-state, and cutoff performance characteristics were established.

The several tests conducted during this program are discussed in the following paragraphs.

6.1 Engine Conditioning

6.1.1 Engine LOX and LH2 Pump Childown

A satisfactory engine pump chilldown procedure was developed so that at ESC, the available NPSH at each of the pump inlets was within the start requirements (paragraphs 7.2 and 8.2).

6.1.2 Thrust Chamber Chilldown

The cryogenic propellants used in the S-IVB J-2 engine require that the engine be conditioned to the low temperatures prior to engine start. This conditioning is necessary in order to prevent thermal shock and gasification of the propellants with attendant start transient problems at engine ignition.

6.1.2.1 S-IVB/IB

During all the S-IVB/IB battleship firing tests, the T/C (thrust chamber) chilldown was adequate to meet the Rocketdyne engine start requirement of 260 $\pm$50 deg R for the T/C temperature C-0199 or C-0645 (tables 6-1 through 6-4). However, after CD 614007, this requirement was discovered to be inadequate to guarantee a satisfactory engine start. During the engine start transient of this countdown, an LH2 pump surge (figure 6-2) occurred which appeared to have been caused by improper T/C conditions at engine start. A review meeting of National Aeronautics and Space Administration, Marshall

Space Flight Center, Rocketdyne Division, North American Aviation, and Douglas Aircraft Company brought out that the Rocketdyne requirement was based on data obtained from tests during which T/C chilldown was continued until engine start. During the battleship tests (CD 614005, 614006, and 614007) the T/C chilldown was terminated at SLO (simulated liftoff), approximately 90 sec before ESC. During the meeting, it was decided that until further investigation had been made, the duration of T/C chilldown would be extended for subsequent tests. Therefore, the T/C chilldown during CD 614008, 614009, and 614010 was initiated at SLO -50 min and continued to SLO +1 min, leaving only 30 sec for warmup. The T/C chilldown parameters from the two chilldown procedures are compared in figure 6-3. The LH2 pump performance during the start transients of these firings was satisfactory as shown in figure 6-2. Chilldown data for CD 614005 through 614009 are shown in table 6-1. These data indicate that a 20-min chilldown duration was more than sufficient to obtain a T/C temperature within the start requirement.

The data also show the effects on the T/C temperature of changes in cold helium supply conditions due to control sphere loading, chilldown orifice size, or propellant tank prepressurization. The effect of wind velocity is also noticeable. The effects of helium supply and ambient conditions are further illustrated in figures 6-4, 6-5, and 6-6 which present T/C chilldown data from other battleship tests. The wind velocity was a significant and erratic factor (figure 6-6) in the T/C conditioning during the testing because the engine was unprotected. (During an actual launch the engine would be covered by the aft interstage.) The effect of wind velocity was demonstrated during CD 614007 which was identical to CD 614006 in all significant respects except wind speed (figure 6-3). The greater warmup during CD 614007 resulting from the 7.8 mph wind caused the LH2 pump surge, whereas the 2 to 3 mph wind of CD 614006 produced no problems. During CD 614010 the T/C temperature could not be sufficiently reduced to meet the start requirement, and the firing had to be postponed. The wind velocity on that day was 20 to 30 mph.

Special tests were conducted with engine J-2013 during CD 614014, 614017, 614018, and 614019. The object of this special program was to determine the LH2 pump performance during depressurization of the engine start tank after the various T/C chilldown tests.

This program consisted of three phases, as outlined in Test Requests 1024, 1025, and 1026. Briefly the phases were as follows:

a. TR 1024

T/C childown tests during which the T/C temperature was reduced to a specific level and engine sequence initiated at the temperature level.

b. TR 1025

T/C childown tests during which the T/C temperature was reduced to a specific level and engine sequence initiated after a preselected hold time.

c. TR 1026

Turbopump and T/C childown tests during which the turbopump childown (recirculation) time was varied while the T/C pressure and hold time were not changed.

During these tests the engine was covered by an enclosure which was purged to reduce the effect of environmental changes. The data are summarized in tables 6-2 and 6-5. Pertinent data gathered during significant tests of this series appear in figures 6-7 through 6-17. Figure 6-7 covers CD 614014; significant tests of CD 614017 are represented by figures 6-8 through 6-11, CD 614018 by figures 6-12 and 6-13, and CD 614019 by figures 6-14 through 6-17. The data on the LH2 pump performance during these tests are shown in figure 6-18.

The results of Phase I tests (figures 6-7, 6-8, and 6-12) indicated that the start requirement of 260 $\pm$50 deg R for measurement C-0199 was adequate when there was essentially no time lag between the termination of T/C childown and the engine start sequence (figure 6-18). However, this requirement did not appear to be a valid criterion when a hold time (warm up) was included before engine start. This inadequacy is shown by the results of test A2 of CD 614017 (figure 6-8) which included a 150 sec hold time. The temperature of C-0199 at engine start was 300 deg R, which was within limits, but a pump stall occurred during this test. However, during test H2 of CD 614018, the engine went through an acceptable start transient although C-0199 indicated

339 deg R at engine start (figure 6-18). The hold time for this test was 450 sec. The unsatisfactory results of tests D2 (CD 614017) and G2-3 (CD 614019) further demonstrated the inadequacy of the start criterion (figure 6-19).

Since flight conditions include a time lag between the end of T/C chilldown and engine start, an attempt was made to find another correlation between the T/C temperatures and engine start. Analysis of the test data, indicated that a correlation existed that was based on the average of the lower-tube temperatures (C-0678 and C-0680). As shown in figure 6-20, the test data indicated that, without exception, a successful start was obtained when the average lower tube temperature was 360 deg R or less, based on an LH2 lead of 1 sec, while a pump stall occurred when the temperature was higher. Rocketdyne test results also agree with this correlation.

Engine firing was resumed after CD 614019. During the following S-IVB/IB tests (CD 612020 through 612030) the approach to T/C chilldown was consistently cautious with respect to warmup before ESC. The warmup was limited to less than 30 sec as it was during CD 614008 through 614010. The duration of T/C chilldown was shorter than it was during earlier tests and varied from 9 to 13 min. The allotted chilldown period was sufficient when the wind velocity was less than approximately 15 mph.

During CD 614025 the wind velocity was 20 mph. In order to obtain sufficient chilldown, during the countdown, the normally used helium supply orifice was replaced by a larger one, thus allowing a larger flowrate. The data of the special chilldown test prior to the terminal count showed that sufficient chilldown could be obtained by the increased cold helium flow.

The LH2 pump performance during all these tests was satisfactory as shown by the LH2 pump performance plots in figures 6-21 and 6-22. Chilldown data are summarized in table 6-3.

Three tests incorporating aft interstage environmental control in combination with sequenced operation of the T/C preconditioning system were conducted during CD 614031 and 614032 (figure 6-23). The environmental system consisted of a cylindrical bag-type enclosure of the same shape and volume as the aft interstage. It was planned to condition this enclosure with 3,500 scfm of GN2 introduced through the environmental manifold located near the umbilical outlet. The gas in the enclosure was to be vented through openings near the simulated interstage bottom. At SLO, the GN2 purge would be terminated.

During CD 614031-1, several deviations occurred. After LOX loading the GN2 flow stopped because the GN2 vaporizer malfunctioned. Consequently, the pressure inside the bag decreased to ambient, and since the wind was blowing, the bag started to collapse. To keep the bag under control the purge was continued with air, and as a result, frost formed on the LOX tank aft dome, the thrust cone structure, and other components. During CD 614031-2, the purge was also maintained after SLO because of the wind condition. Because of these deviations, the environmental tests were repeated for CD 614032, but ambient helium was used for tank prepressurization instead of cold helium.

The effects of the deviations in the environmental conditioning during CD 614031 are difficult to assess, but from the data of CD 614031-2 and 614032, it appears that these effects did not cause any significant variations in the results of the T/C conditioning. The rate of chilldown during CD 614032 was approximately the same as during CD 614031-2, and the heatup rate during the simulated boost period was the same (according to the T/C temperature) or even lower (according to the lower tube temperature) during CD 614032 which more closely simulated flight conditions.

The effect of using cold helium for prepressurization can be seen by comparing the data of CD 614031-2 with those of CD 614032. In CD 614031-2 and 614032, the gas heat exchanger cross-over valve, which connects the two sets of helium coils in the heat exchanger, was open. Data of CD 614031-2 show the adverse effect of an increase cold helium demand for prepressurization on T/C chilldown. Data of CD 614032 do not show any change in the T/C temperature profile because ambient helium was used for prepressurization. In CD 614031-1 the cross-over valve was closed; therefore, prepressurization had no effect. Comparison of the data of the three tests shows that the chilldown rate was somewhat higher during CD 614031-2 and 614032 than it was during CD 614031-1, in which only four heat exchanger coils were employed (figure 6-23). The helium supply orifice temperatures also indicate the difference.

Although the use of 12 heat exchanger coils enhanced the rate of T/C chilldown, much of this advantage over the four-coil operation appears to have been offset by the negative effect of prepressurization. At the end of chilldown, the T/C and lower tube temperatures (C-0678 and C-0680) were somewhat lower during CD 614031-2 as compared with CD 614031-1; but at engine ignition the tube temperatures were practically the same and the T/C temperatures differed by only 10 deg R. Since all these temperatures were well within the requirements for engine start, the difference in the operation of the T/C chilldown system seems minor.

The results of this chilldown program (table 6-5) did not indicate that other variables affected engine start. For instance, the time for engine pump chilldown recirculation was varied from approximately 2.5 to 30 min but these changes did not seem to affect the engine start of test D3 and G2-1 of CD 614019 (table 6-2 and figure 6-18). The effect of engine start tank conditions could not be established because these conditions were essentially constant from test to test.

6.1.2.2 S-IVB/V

The S-IVB/V tests were conducted during CD 614033 through CD 614035 and CD 614041 through CD 614044. The major differences, as compared to the S-IVB/IB tests, were the longer boost period (540 sec vs 90 sec for S-IVB/IB) and the longer LH2 lead times (3 sec vs 1 for S-IVB/IB). The longer LH2 lead was included to compensate for warmup that will occur during the 9-min boost. The chilldown was initiated at SLO -20 min. Termination time was determined during the test on the basis of the prevailing wind conditions and prediction curves for warmup as a function of wind velocity.

During this series of tests, the lower tube temperatures (C-0678 and C-0680) were used as a criterion for T/C conditioning. The redline value was 460 deg R. During the final test (CD 614044) the average of the lower temperatures exceeded the redline by approximately 30 deg and the T/C temperature (C-0199) exceeded its redline of 310 deg R by approximately 60 deg R, but the LH2 pump performance was still satisfactory.

Figure 6-6 also presents C-0199 and lower tube temperature profiles for CD 614044 in this series of tests. During several of the tests, wind speed and direction readings at the test stand were collected at increments of 1 min or less so that the specific effect of wind speed on T/C temperatures might be observed. This reveals an obvious and pronounced effect of momentary wind speed variation on T/C temperatures. Specifically, temperature redlines were exceeded at ESC (CD 614044) because of the momentary increase in wind speed after T/C chilldown termination and before ESC. The warmup rate at the average wind speed during T/C chilldown would have precluded the excessive temperature rise that occurred. Table 6-5 is a summary of countdowns in this series.

The LH2 lead of several seconds during start sequence for both burns in S-IVB/V tests is excellent conditioning for successful engine starts. Figure 6-24 illustrates that a stall was not approached during tests under such conditions.

6.2 Engine Start Tank and Control Sphere Conditioning

The engine start tank and control sphere are supplied and conditioned by the GSE pneumatic systems. GH2 is supplied at 1,500 psia, cooled in the gas heat exchanger, and delivered through console C to the engine start tank. The control sphere helium is cooled in the heat exchanger and delivered through console C at 3,000 psia.

6.2.1 S-IVB/IB

The objectives of the S-IVB/IB engine control sphere and start tank testing were to develop procedures for conditioning the sphere and tank to demonstrate that the required temperatures and pressures could be provided at ESC (Engine Start Command).

The engine start requirements for the engine start tank and control sphere were as follows:

	Pressure (psia)	Temperature (deg R)
Start Tank	1,250 $\pm$50	210 $\pm$50
Control Sphere	1,800 to 3,000	210 $\pm$50

Prior to the initiation of start tank chilldown, the control sphere was pressurized to approximately 1,000 psia to prevent it from collapsing as it was cooled down by the temperature decrease in the start tank. The engine start tank loading (figure 6-25) was accomplished by flowing cold GH2 through the tank and out the vent valve until the required temperature was reached. At this time, the vent valve was closed and the tank was pressurized.

During the testing of the J-2003 engine (CD 614005 through CD 614010), the engine start tank chilldown was initiated at SLO -16 min and continued until loading was initiated at SLO -5.5 min. The control sphere was loaded (pressurized to 3,000 psia) at SLO -9 min. The start tank requirements were met during all tests, although venting the sphere and tank in the period between the end of fill and ESC was usually required to attain proper pressure. The loading procedure was changed during the J-2013 engine tests (CD 614020 to CD 614030). Prior to CD 614025 the start tank chilldown was initiated at SLO -17.5 min and continued until SLO -4 min when start tank loading was initiated. The control sphere was pressurized to 1,000 psia prior to the initiation of start tank chilldown, and loading was completed at SLO -4.5 min. Starting with CD 614025, the chilldown procedure was altered to avoid the necessity of venting the sphere and tank. This was accomplished by reducing the supply pressures and extending the start tank chilldown period an additional 2 min until SLO -2 min. The control sphere was pressurized to 3,000 psia before the initiation of start tank chilldown.

The engine start tank and control sphere configurations used with the J-2013 engine differed from those used with the J-2003 engine in that the control sphere vent was located within the engine pneumatic package. As shown in figure 6-25, this vent was located at the inlet to the pneumatic package on the J-2003 engine. This change in vent location resulted in a reduction of the control sphere flow during chilldown venting. Table 6-6 is a summary of the test results shown in figures 6-26, 6-27, and 6-28. Items shown in table 6-6 that are of particular interest include: (1) the degree of compliance with required temperatures and pressures at ESC, (2) the temperature and pressure changes due to warmup and venting between end of fill and ESC, and (3) gas consumption during start and cutoff transients.

Differences in sphere temperatures and pressures both before and after fill are due to variations in GSE gas heat exchanger performance, heat transfer between control sphere and start tank, and chilldown duration and sequence. Warmup rates for the start tank during the hold period between fill and ESC were found to be approximately 3 deg/min as shown by the data presented in the following table:

Countdown	Time (sec)	SLO (deg R)	Warmup Rate (deg/min)
614025	150	208 to 216	3.12
614030	150	218 to 230	4.04

Compliance with Rocketdyne-specified requirements for start tank and control sphere temperatures and pressures at ESC was successfully demonstrated throughout the battleship test program. This is shown by a comparison of the Rocketdyne requirements with lines 6 and 11 of table 6-6. The GSE supply system for preconditioning and filling the start tank and control sphere was proved to be acceptable during the test program. Typical GSE performance data, such as GH2 supply orifice and heat exchanger temperatures and pressures are shown in figures 6-29 and 6-30. Start tank and control sphere loading was acceptable. Table 6-6 shows that the start tank GH2 mass at ESC varied from 4.04 to 5.19 lbm. Line 18 of the table shows that start tank usage during the engine start sequence was 3.13 to 4.12 lbm of GH2. Start tank temperature differential during depressurization at engine start averaged 60 deg R.

The mass consumed from the control sphere during propellant valve operation at ESC and ECO is shown on lines 18 and 19 of the table. Values ranged from 0.03 to 0.23 lbm of helium. Because of data inaccuracy, the calculated consumptions should be considered as approximate.

6.2.2 S-IVB/V

The objective of the S-IVB/V tests was to obtain the required pressures and temperatures in the engine start tank and control sphere at engine start for both first and second burn. These start requirements (figure 6-31) were met for both burns during the three S-IVB/V countdowns that were evaluated.

The chilldown procedure was the same for all three tests evaluated (CD 614034, CD 614043, and CD 614044). Chilldown was started at ESC -34 min and continued until ESC -20 min. The control sphere was pressurized to 3,000 psia at ESC -33.5 min. Both the start tank and control sphere were chilled by flowing cold GH2 through the start tank. The supply was regulated to 940 to 980 psia for these tests, which resulted in a chilldown flowrate of 3 lbm/sec. At the end of the 14-min chilldowns, the start tank temperatures ranged from 109 to

122 deg R for the three tests. When chilldown was terminated, the start tank temperature was still decreasing, indicating that a lower temperature would have been obtained if chilldown had been continued.

Chilldown was terminated and start tank fill was initiated at ESC -20 min by closing the start tank vent valve. The start tank was filled in approximately 15 min to a pressure that was 350 psi less than that desired at ESC to allow the pressure to increase to the start requirement by ambient warmup of the GH2 (figures 6-32 and 6-33). This procedure was followed in an attempt to avoid venting the start tank prior to ESC. However, venting was necessary as the temperature at the end of fill was lower than predicted because of the low GSE supply temperature (figure 6-34). The temperature rise after fill (2.7 deg R/min) agreed with that predicted, but the percentage of temperature change was larger and resulted in a pressure increase that was greater than expected.

At ESC, the start tank was reduced to 200 psia. Recharging of the tank began immediately after blowdown. At first burn engine cutoff, the start tank had been recharged to 1,195 to 1,330 psia or to 6.4 to 7.5 lbm (table 6-7) which was more than sufficient for second burn engine start. During the simulated coast period, the start tank temperature increased with time due to heat input. The pressure was maintained relatively constant during this time by continuously venting the tank. At the time of second burn engine start, the mass in the start tank had been decreased to 3.9 to 4.6 lbm.

The start tank pressure and temperature (figure 6-35) were well within the restart requirements. Second burn engine start depleted the tank to 215 to 245 psia. During second burn, the start tank was again recharged to 5.2 to 5.5 lbm. The mass recharged during second burn was less than first burn because of the higher temperature during second burn.

The control sphere conditions were within the start requirement for both first and second burn for all three countdowns (figures 6-34 and 6-35). During start tank chilldown the control sphere was also being chilled. The control sphere temperature was considerably higher than the start tank temperature, but was decreasing at a faster rate and the temperatures were converging. At the end of chilldown, the control sphere temperature was

175 to 185 deg R which was 65 deg warmer than the start tank. After the start tank was filled, its temperature increased while the control sphere temperature continued to decrease, steadied out, and then started increasing slightly. The sphere temperatures continued to converge until, at ESC -7 min, they were the same. From then until engine start, both the sphere and tank heated up at the same rate.

During these S-IVB/V battleship tests, the average helium consumption from the control sphere was 0.32 lbm during engine start and 0.06 lbm during engine cutoff. Data from these tests are summarized in table 6-7.

6.3 Engine Performance

Six countdowns, 614023, 614025, 614028, 614030, 614043, and 614044 formed the basis of analysis of the J-2 engine performance during the S-IVB battleship test program. These tests were selected because they most clearly demonstrated the battleship engine performance program test objectives. The first four tests were performed on the S-IVB/IB configuration and utilized engine S/N J-2013, while the latter two tests were performed on the S-IVB/V configuration and utilized engine J-2020.

The test objectives of the S-IVB battleship program for the engine were as follows:

a. Establish the engine circulation chilldown procedure and evaluate the operation of the chilldown system

b. Determine flow and pressure characteristics in the low pressure propellant ducts

c. Determine engine thrust buildup, rated operation, and shutdown characteristics

d. Evaluate engine start and mainstage firing under simulated orbital conditions

e. Evaluate LOX depletion cutoff

f. Determine the cryogenic calibration of the PU system by the propellant "flow integral" method.

All of these objectives were met satisfactorily before the conclusion of the battleship program.

6.3.1 Engine Analysis

The engine performance was analyzed by reconstructing the various tests from Engine Start Command to cutoff. The engine performance level in the form of "Tag Values" and other pertinent coefficients, as well as the engine acceptance data, were provided by Rocketdyne in the engine log book. Several computer programs were developed which utilized the log book relationships to convert measured data into performance values. The AA89 program was the most advanced of these at the time of the battleship tests; therefore, the majority of the reconstruction of each test was performed by this program. Future analyses will employ statistical averages of the reconstructions of all available programs. Such a technique of relating the engine and stage performance will be the basis of the "flow integral" method of cryogenic calibration of the propellant tanks. Sophistication of this technique was developed during these tests.

6.3.1.1 Start Transients

A computer program, F839, which was used to analyze start and cutoff transients for the S-IV stages, was modified for the S-IVB stage. The start impulse (I start) was determined from the equation

$$I_{Start} = \int_{T_1}^{T_2} F = A_t \, P_c \, C_f$$

WHERE T_1 = Time of Engine Start Command

T_2 = Time 90 percent thrust was reached

F = Thrust

A_t = Thrust Chamber Throat Area

P_c = Thrust Chamber Combustion Pressure

C_f = Thrust Coefficient

C_f as a function of chamber pressure was determined during the battleship program from flowmeter data. A plot of the relationship is shown in figure 6-36. This function was used for the transient portions of the tests.

[redacted]

Figure 6-37 shows the chamber pressure start transient for the four tests of the S-IVB/IB system. As can be seen, all starts are practically identical in shape with the exception of that for CD 614023, which as shown in the data and the table below had a lower P_c (thrust chamber pressure) rise rate during the final portion of the approach to mainstage.

The 90 percent of steady-state level for the engine operation was defined as a P_c level of 618 psia.

The time from Engine Start Command to the time of 90 percent steady-state (T_2 - T_1), the start impulse, and the time from the first chamber pressure rise to T_2 are as follows:

Time	CD 614023	CD 614025	CD 614028	CD 614030
T_1 to T_2 (sec)	3.22	2.96	2.95	2.90
Impulse (lbf-sec)	202,176	133,710	133,026	138,150
Rise Time (sec)	2.22	1.75	1.77	1.75

CD 614043 and CD 614044 were conducted under simulated orbital conditions. The test included a simulated S-IVB/V boost phase, a first burn of the S-IVB/V, simulated orbital coast period, and a second S-IVB/V burn. The second burn of CD 614043 and CD 614044 occurred after simulated three-orbit and one-orbit coast periods. Figure 6-38 shows the chamber pressure start transients of CD 614044. An analysis was made of the available data with the following results:

Time	CD 614043		CD 614044	
	1st Burn	2nd Burn	1st Burn	2nd Burn
T_1 to T_2 (sec)	5.22	6.26	5.22	6.38
Impulse (lbf-sec from T_1 to T_2)	141,295	141,305	141,280	141,292
Time from first pressure rise to 90% thrust (sec)	1.61	1.62	1.6	1.63

21 February 1966

[redacted]

[redacted]

The first burn (T_1 to T_2) was longer on the S-IVB/V tests because an additional 375-sec hold was inserted after SLO to account for the S-II stage burn time. The second burn (T_1 to T_2) was longer because of the hold simulating orbital conditions. However, the times from the initial pressure rise to 90 percent chamber pressure on all transients compare very well.

There was no measurable impulse prior to the initial pressure rise on the S-IVB/IB tests, whereas the long hydrogen leads for chilldown purposes on the S-IVB/V tests contributed an average 2,000 lb-sec additional start impulse.

As expected, considerable sideloading occurred during the start transients (figure 6-39); therefore, when stable operation was reached (approximately ESC +12 sec), restraining arms were used to restrict the entire motion until the sideloads ceased. The battleship program demonstrated that the engine start characteristics were not adversely affected by any S-IVB operating conditions.

6.3.1.2 Steady-State Operation

The battleship tests were conducted under a range of conditions simulating the probable conditions that might occur for the flight. The J-2 engine operated satisfactorily during all tests. Two tests (CD 614023 and CD 614028) were conducted with an overload of LOX to cause a positive PU valve excursion during the initial portion of the test. One test (CD 614025) was conducted with an overload of LH2 to cause a negative PU valve excursion during the initial portion of the test. A nominal loading was attempted for one S-IVB/IB test (CD 614030) and for both S-IVB/V tests. The loading values for the six tests were as follows:

	S-IVB/IB					S-IVB/V		
Countdown	614023	614025	614028	614030	Nominal Load	614043	614044	Nominal Load
LOX (lbm)	189,800	184,115	192,556	187,650	188,053	195,768	193,200	193,227
LH2 (lbm)	36,980	39,125	38,180	38,487	38,469	44,917	42,800	42,793

The S-IVB/V values included an excess 3,250 lbm LH2 which was to be boiled off during a three-orbit simulated coast period. The LOX boiloff during this same period was predicted to be 375 lbm and was included in the load.

The PU system was biased so that there would be no reaction to the excess propellants. The boiloff bias was removed after the first burn.

The normal open loop operation time (PU system not active) is 6 sec, but the time was extended because of the uncertainty of the first movement of the PU valve and subsequent uncertainty of the initial mixture ratio. Rocketdyne data indicate that a low mixture ratio increases the side loads during the start transient. A condition was established whereby the test would be terminated if the side loads did not subside below 3,000 lbf within 10 sec of ESC. In order that a normal subsidence be assured, the PU system was not activated until well after the limiting side load conditions had been met. The times from Engine Start Command to PU activate for the six tests discussed here are as follows:

CD 614023	15.002 sec
CD 614025	14.569 sec
CD 614028	15.162 sec
CD 614030	13.839 sec
CD 614043	
(1st Burn)	14.7 sec
(2nd Burn)	15.75 sec
CD 614044	
(1st Burn)	14.679 sec
(2nd Burn)	15.82 sec

The S-IVB battleship tests demonstrated that there was no problem and all subsequent tests had or will have the normal open loop time.

When the PU system was activated, almost identical performance response was noted for CD 614023 and CD 614028. Typical performance data are presented in figure 6-40. In both instances the PU valve went to the stop in the LOX rich position which was approximately +30 deg. The valve remained in this position until the condition of LOX overload was eliminated. During this period the average engine performance was as follows:

	CD 614023	CD 614028
Thrust (lbf)	227,970	227,790
$\dot{W}$t (lbm/sec)	540.88	540.4
Isp (sec)	421.48	421.52
EMR	5.643	5.640

In CD 614025 (figure 6-41) the performance response was opposite in direction but approximately equal in amount at PU activate, as compared to CD 614023 and CD 614028. The PU valve went to the stop in the low mixture ratio position and remained there until the LH2 overload condition was eliminated. During this period, engine performance was as follows:

Thrust (lbf)	172,610
$\dot{W}$t (lbm/sec)	411.1
Isp (sec)	427.17
EMR	4.56

A near nominal loading was achieved for CD 614030. It was predicted that normal operation for a nominal load would be a short low-mixture ratio excursion by the PU valve. The validity of this prediction can be seen in figure 6-42, which shows that the PU valve and engine performed as predicted. Performance during the period of correction for initial mass error was as follows:

Thrust (lbf)	172,800
Wt (lbm/sec)	399.43
Isp (sec)	432.61
EMR	4.40

A performance comparison of open loop operation to the steady-state conditions during closed loop operation prior to PU cutback for the tests showed the following:

	CD 614023	CD 614025	CD 614028	CD 614030
Thrust (lbf)	+24,660.6	-27,565	+25,231	-30,512
$\dot{W}t$ (lbm/sec)	+63.17	-65.239	+64.705	-78,309
Isp (sec)	-4.12	+0.635	-4.297	+7.038
EMR	+0.539	-0.509	+0.556	-0.707

The evaluation of CD 614025 revealed a discrepancy in the influence coefficients. The positive specific impulse change as a function of the negative EMR change was not in agreement with the engine log values or the manufacturer's acceptance test. The necessary corrections were made as can be seen in the values for CD 614030.

Study of the available data indicates near-nominal operation of the PU system during both "burns" of CD 614043 which simulated a three-orbit coast period. The values given for loaded propellants on this test were PU indicated values with no flow integral verification. There was nothing during either burn to indicate anything other than normal engine system performance.

The performance was also quite normal for the first burn of CD 614044. The PU system indicated near nominal loads for a one-orbit coast simulation. Near the end of the coast period, an attempt was made to adjust the LOX load to the desired 126,000 lbm for start of second burn; 2,000 lbm LOX were mistakingly dumped causing a very large equivalent LH2 overload. At PU activate, the PU valve traveled to the stop in the LH2 rich position and remained there for the duration of the test. The performance of the engine responded accordingly giving low EMR (4.631), low thrust (185,500 lbf) and high specific impulse (428.2 sec). The chamber pressure, which is a good indication of the engine performance, is shown for both burns of CD 614044 in figure 6-43.

The flight function of the S-IVB/V vehicle is very precise and delicate. An exact evaluation of ground test and correlation to a flight vehicle would at best be difficult. The data available for the battleship tests were not conducive to this type analysis. A quantitative system evaluation was considered satisfactory for the battleship tests and demonstrated the stage capability of responding to a given command.

6.3.1.3 Cutoff Transients

A depletion test involving either propellant, in the sense that the tank was empty at cutoff, was not possible with the J-2 engine. Cutoff on all the tests discussed herein was initiated manually either when LH2 pump NPSH was below the specified minimum or the LOX volume reached the 1 percent level in the tank. Either of these conditions was defined as depletion. Evaluation of engine performance at these conditions showed that the transients were normal and consistent with the manufacturer's acceptance tests. Typical cutoff transients of the thrust chamber pressure are shown in figure 6-44. The perturbations seen at the end of the engine thrust chamber decay period do not represent a detriment to the performance. The perturbations were also noted on the manufacturer's data. Analysis of the cutoff transient was aided by the F839 computer program. Cutoff impulse was determined to 5 percent of the chamber pressure value at the cutoff signal. Cutoff transient values are shown in the following table.

CD	614023	614025	614028	614030	614043		614044	
					1st Burn	2nd Burn	1st Burn	2nd Burn
T*	0.963	0.663	0.670	0.630	0.910	0.85	0.829	0.890
I**	89,330	351,945	38,159	32,868	55,200	53,960	52,010	55,141

*Time from cutoff command to 5% thrust (sec)

**Cutoff impulse from cutoff command to 5% thrust (lbf-sec)

The data problems noted in paragraph 6.3.1.1 handicapped the cutoff analysis also. Definitions which would eliminate factors contributing to the wide range of values had not been made at the time of this report. The analysis is expected to be satisfactory for the production tests.

6.3.2 Gas Generator Performance

With one exception (CD 614005), there were no failures directly attributable to the gas generator.

The gas generator failure on CD 614005 occurred just after mainstage signal. There was an extremely sharp pressure rise in the gas generator combustor and the LH2 injector manifold. A similar rise in pressure was noted at the gas generator LOX poppet valve immediately thereafter. The LOX poppet valve was destroyed, the number 2 spark plug was blown from its threaded shell, and the LOX injector sense line was burned through and partially consumed. The LOX poppet was blown through the LH2 turbine inlet manifold, coming to rest in the start tank discharge line. Two turbine blades in the LH2 turbine were destroyed.

The data indicated that failure occurred as a result of overcooling of the gas generator during recirculation chilldown. Corrective measures have been taken to insure that overcooling does not recur. Four tests were selected as representative of the battleship test program: CD 614010, CD 614025, CD 614030, and CD 614043. Typical data from these tests (figures 6-45 and 6-46) indicate that the gas generator operated normally during engine operation. In all cases, the gas generator exhaust gas temperature remained within desired operating limits and did not exceed the following redline temperature values. The gas generator exhaust gas temperatures were above 710 deg R within 0.5 sec after mainstage control signal. The maximum temperature limits of 2,460 deg R between 0.5 and 3.5 sec after mainstage control signal, and 1,910 deg R for the remainder of the test, were not exceeded.

A method of obtaining the gas generator propellant flowrates as a function of time was supplied by the engine manufacturer and used in calculating all mass flowrate data.

The exhaust gas temperatures, pressures, and propellant mass flowrates all passed through a transient period which approached steady-state operation within 5 sec of engine start. The steady-state values vary slightly, but were close to the mean values listed by the engine manufacturer.

Table 6-1
Thrust Chamber Childown (Engine J-2003)

	MEAS.(1) NO.	614005 RUN 3	CD 614006	CD 614007	CD 614008	CD 614009	CD 614010 RUN 1	CD 614010 RUN 2
T/C Temperatures at End of Chilldown (°R)	C0199	217	210	216	212	226	370	250
	C0676						314	229
	C0678			NOT INSTALLED			215	234
	C0680						215	212
Initiation of Chilldown, (sec)		(4) SLO-1190	SLO-1189	SLO-1191	SLO-2991	SLO-2993	(5) 1449:31	SLO-3050
Chilldown Duration (sec)		1190	1190	1191	2717/159	2466/244	1543	2865/111
Wind Speed (mph)		5	2-3	7.8	5	Calm	17	5
Ambient Temp. (°R)		515	516	522	521	510	521	524
Cold Helium Supply: Avg. Flowrate (lb/min)		11.0	11.4	11.6	9.7	11.9	13.2	9.7
Cold Helium Supply: C0707 (°R)		80	80	80	55	55	75	65
Crossover Valve Position (sec)		Closed	Closed	Closed	Opened @ SLO-376	Opened @ SLO-380	Opened @ 1459:06	Opened @ SLO-367
Propellant Prepressurization Initiation (sec)		SLO-177	SLO-174	SLO-178	SLO-177	SLO-175	(5) 1456:34	SLO-172
Warmup Time Prior to ESC (sec)		90	90	90	174/35	273/30	(2)	142/25
T/C Temperatures at ESC (°R)	C0199	247	238	270	220	230		264
	C0645							(3)
	C0676						(2)	235
	C0678			NOT INSTALLED				(3)
	C0680							(3)
LH2 Pump Surge		No	No	Yes	No	No	(2)	No

Notes: (1) Refer to Figure 6-1 for instrumentation locations
(2) No Engine Start Command
(3) Data missing or otherwise unreadable
(4) SLO = simulated liftoff
(5) Real time

Table 6-2
Thrust Chamber Childown (Engine J-2013)
CD 614011 Thru 614019

	MEAS.(1) No.	614011 TEST 1A1(2)	614014	614017 TEST A3	614017 TEST A2	614017 TEST E2	614017 TEST D2	614018 TEST B3-1	614018 TEST B3-2	614018 TEST H2	614019 TEST D3	614019 TEST H2-1	614019 TEST G2-[illegible]	614019 TEST G2-3
T/C Temperatures at End of Chilldown (°R)	C0199*	220	246	278	254	208	214	243	260	170	207	163	200	208
	C0645*	253	241	Avg.	Avg.	Avg.	Avg.	247	Avg.	Avg.	Avg.	Avg.	Avg.	Avg.
	C0676*	164	196	187	180	Off Scale Low	Off Scale Low**	Off Scale Low**	Off Scale Low**	Off Scale Low**	Off Scale Low**	Off Scale Low**	Off Scale Low**	162
	C0678*	160	207	187	190	180	Off Scale Low**	Off Scale Low**	Off Scale Low**	Off Scale Low**	Off Scale Low**	Off Scale Low**	Off Scale Low**	173
	C0680*	170	233	214	218	172	168	177	166	Off Scale Low**	160	Off Scale Low**	Off Scale Low**	164
Initiation of Chilldown, (sec)		SLO-266	SLO-951	SLO-415	SLO-473	SLO-774	SLO-775	SLO-412	SLO-412	SLO-1071	SLO-532	SLO-1966	SLO-531	SLO-717
Chilldown Duration (sec)		526	954	441	551	778	1214	445	403	1180	539	1980	540	720
Wind Speed (mph)		1-4	15-25	Calm	0-2	Calm	0-2	3	3	6	0-4	0-4	0-5	6
Ambient Temp. (°R)		511	506	519	525	528	529	518	518	526	515	520	518	515
Cold Helium Supply Avg. Flowrate (lb/sec)		14.6	14.2	12.6	13.1	14.0	14.1	23.2	20.1	23.4	22.8	23.0	21.4	20.4
Cold Helium Supply Avg. C0681* (°R)		79	84	90	85	80	80	79	80	70	70	70	75	80
Crossover Valve Position		OPEN	OPEN	OPEN	OPEN	OPEN	OPEN	OPEN	OPEN	OPEN	OPEN	OPEN	OPEN	OPEN
Propellant Prepressurization Initiation (sec)		SLO-241	SLO-748	SLO-267	SLO-266	SLO-266	SLO-263	SLO-267	SLO-268	SLO-258	SLO-176	SLO-260	SLO-267	SLO-275
Warmup Time Prior to ESC (sec)		142(1)	15	5	150	150	200	180	30	450	150	500	200	200
T/C Temperatures at ESC (°R)	C0199*	304	246	260 Avg.	300 Avg.	250 Avg.	300 Avg.	259	260 Avg.	339 Avg.	283 Avg.	244 Avg.	268 Avg.	264 Avg.
	C0645*	327	241	260 Avg.	300 Avg.	250 Avg.	300 Avg.	262	260 Avg.	339 Avg.	283 Avg.	244 Avg.	268 Avg.	264 Avg.
	C0676*	281	227	278 Avg.	362 Avg.	323 Avg.	363 Avg.	242	250 Avg.	360 Avg.	340 Avg.	380 Avg.	338 Avg.	408 Avg.
	C0678*	304	232	278 Avg.	362 Avg.	323 Avg.	363 Avg.	217	250 Avg.	360 Avg.	340 Avg.	380 Avg.	338 Avg.	408 Avg.
	C0680*	272	263	278 Avg.	362 Avg.	323 Avg.	363 Avg.	295	250 Avg.	360 Avg.	340 Avg.	380 Avg.	338 Avg.	408 Avg.
LH2 Pump Surge			No	No	Yes	No	Yes		No	No	No	Yes	No	Yes

Notes: (1) No Engine Start Command
(2) CD 614011 Utilized Engine J-2003
* Refer to figure 6-1 for instrumentation locations
** Less than 160°R
SLO Simulated liftoff

Table 6-3
Thrust Chamber Chilldown (Engine J-2013)
CD 614020 Thru 614032

COUNTDOWN	MEASUREMENT NO.	614020 RUN 2	614021	614022 RUN 1	614022 RUN 2	614022 RUN 3	614023	614024 RUN 1	61[illegible]	614025 SPECIAL CHILL	614025	614028	614030	614031 RUN 1	614031 RUN 2	614032
T/C Temperature at End of Chilldown (°R)	C0355	231	(1)	273	27[illegible]	275	234	2[illegible]2	(1)	(1)	(1)	264	285	(1)	199	(1)
	C0645*	230	277	270	278	272	235	284	295	245	217	259	279	206	194	186
	C0676*	200	238	217	230	248	179	(1)	(1)	(1)	(1)	(1)	255	200	186	177
	C0678*	232	(1)	(1)	(1)	(1)	NOT REQUESTED									
	C0680*	210	(1)	212	235	230	180	260	(1)	(1)	(1)	(1)	(1)	(1)	(1)	(1)
Initiation of Chill-down, (sec)		SLO-597	SLO-593	SLO-599	SLO-6[illegible]	SLO-717	SLO-600	SLO-599	SLO-720	SLO-600	SLO-716	SLO-710	SLO-710	SLO-1197	SLO-1200	SLO-1196
Childown Duration (sec)		673	590	667	670	788	667	75[illegible]	792	1050	786	783	782	1190	1195	1188
Wind Speed (mph)		2 to 5	4 to 6	6 to 10	10	9 to 10	0 to 3	10 to 20	14+	20	7	3	8 to 10	Simulated Aft Interstage		
Ambient Temperature (°R)		519	521	520	517	515	519	514	514	520	520	526	530	526	526	525
Cold Helium Supply Avg Flowrate (lb/sec) Avg Temp C0681* (°R)		14.6 90	11.9 95	13.3 95	11.7 95	12.6 95	13.1 85	14.0 100	13.1 100	23.2 75	23.2 69	11.6 100	11.6 90	11.5 105	13.0 80	13.2 77
Crossover Valve Position (sec)		Opened @ SLO-262	Opened @ SLO-260	Opened @ SLO-270	Opened @ SLO-270	Opened @ SLO-270	Opened @ SLO-267	Opened @ SLO-234	Opened @ SLO-269	Opened @ SLO-225	Open	Opened @ SLO-253	Opened @ SL[illegible]335	Closed	Open	Open
Propellant Prepressurization Initiation (sec)		SLO-205	SLO-207	SLO-207	SLO-207	SLO-208	SLO-207	SLO-171	SLO-207	No Pre-press.	SLO-179	SLO-178	SLO-171	SLO-598	SLO-180	SLO-177
Warmup Time Prior to ESC (sec)		22	23	300(2)	23	23	25	200(2)	22	60(2)	24	20	22	300(2)	200(2)	150(2)
T/C Temperatures at ESC (°R)	C0199*	235	(1)	338	(1)	(1)	(1)	351	289	(1)	(1)	(1)	(1)	(1)	(1)	(1)
	C0645*	(1)	282	350	280	280	239	352	299	276	223	264	233	266	243	230
	C0676*	248	310	461	293	298	211	(1)	393	(1)	(1)	(1)	310	380	3[illegible]	280
	C0678*	260	(1)	(1)	(1)	(1)	NOT REQUESTED									
	C0680*	230	(1)	428	292	(1)	215	446	(1)	(1)	(1)	(1)	(1)	(1)	(1)	(1)
LH2 Pump Surge		No	No	----	----	----	No	----	No	----	No	No	No	----	----	----

Notes: (1) Data missing or otherwise unreadable

(2) No Engine Start Command

* Refer to figure 6-1 for instrumentation locations

SLO = Simulated liftoff

21 February 1966

Table 6-4
Thrust Chamber Childown Countdowns

COUNTDOWN	MEAS.(1) NO.	614034 RUN 1	614034 RUN 2	614035 RUN 1	614035 RUN 2	614042	614043	614014
T/C Temperatures at End of Childown (°R)	C0199/C0645	215	205	215	235	245	215	227
	C0676*			NOT	REQUESTED			
	C0678*	178	179	213	209	220	195	211
	C0680*	160	156	201	198	213	181	182
Initiation of Chill-down, (sec)		SLO-1192	SLO-1192	SLO-1195	SLO-596	SLO-1192	SLO-1193	SLO-1194
Childown Duration (sec)		1538	1257	1620	924	1455	1317	1257
Wind Speed (mph)		4	2	5-10	5-10	7.5	4	5
Ambient Temperature (°R)			NOT	RECORDED			84	79
Cold Helium Supply Avg. Flowrate (lb/sec) C0681 (°R)		13.9 76	11.4 79	14.2 80	13.8 85	11.4 78	13.9 75	13.9 75
Crossover Valve Position (sec)		Closed @ SLO-187	Closed @ SLO-190	Closed @ SLO-190	Closed @ SLO-190	Closed @ SLO-187	Closed @ SLO-188	Closed @ SLO-186
		Opened @ SLO-105	Closed @ SLO-190	Closed @ SLO-190	Closed @ SLO-190	Closed @ SLO-187	Closed @ SLO-183	Closed @ SLO-186
Propellant Prepressurization Initiation (sec)		SLO-174	SLO-176	SLO-177	SLO-177	SLO-175	SLO-175	SLO-177
Warmup Time Prior to ESC (sec)		195	475	115	212	177	420	477
T/C Temperatures at ESC (°R)	C0199/C0645	257	328	247	295	280	310	370
	C0676*			NOT	REQUESTED			
	C0678*	323	442	308	403	381	434	487
	C0680*	333	439	313	388	389	464	495
LH2 Pump Surge		----	----	----	----	----	No	No

Notes: (1) Data missing or otherwise unreadable

* Refer to figure 6-1 for instrumentation locations

SLO Simulated liftoff

TABLE 6-5
SUMMARY OF T/C CHILLDOWN TESTS

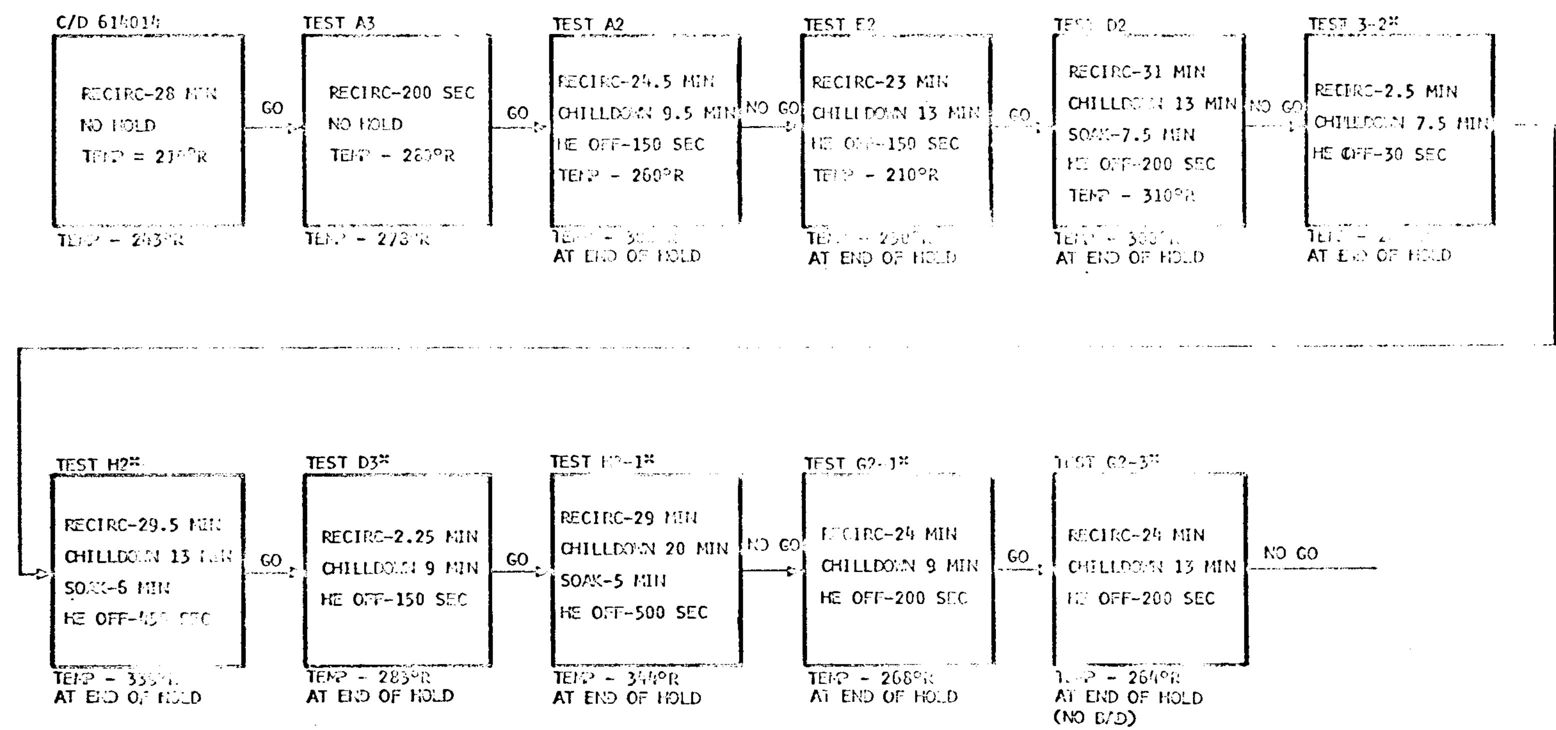

NOTE: CONDITIONS FOR TEST ARE INSIDE BOXES. CONDITIONS MET ARE UNDER BOXES.

*LARGER ORIFICE INSTALLED

21 February 1966

TABLE 6-6
TEST RESULTS SUMMARY

ITEM	TURBINE START TANK DATA							HELIUM CONTROL SPHERE DATA						
	J-2003 ENGINE		J-2013 ENGINE					J-2003 ENGINE		J-2013 ENGINE				
	614005-3	614006	514017-A3	614020	614021	614025	614030	614005	614006	614017-A3	614020 RUN 2	614021	614025	614030
Start of Childown (sec)	ESC - 1044	ESC - 1043	ESC - 1170	ESC - 1145	ESC - 1145	ESC - 1145	ESC - 1145							
Avg. Flowrate at Fill (lbm/min)		4.0												
Start of Fill (sec)	ESC - 417	ESC - 415	ESC - 212	ESC - 335	ESC - 335	ESC - 215	ESC - 215	ESC - 515	ESC - 515	ESC - 305	ESC - 365	ESC - 365	ESC - 215	ESC - 230
Temperature at Start of Fill (°R)	160	175	190	164	132	155	175	142	171	399	204	524	511	513
Temperature at End of Fill (°R)	205	212	208	200	174	206	218	226	270	394	370	592	565	601
Temperature at ESC (°R)	215	225	216	216	180	217	228	205	220	237	230	200	204	213
Temperature after Start Tank Blowdown (°R)*	165	166	110	169	118	156	169	200	215	228	212	192	198	206
Temperature at ECO (°R)	NR	NR	NR	NR	NR	NR	NR	202	217	NR	231	196	224	238
Temperature after ECO (°R)	NR	NR	NR	NR	NR	NR	NR	194	209	232	220	191	221	232
Pressure at Start of Fill (psia)	220	270	210	225	200	225	240	151	249	450	650	1,150	800	995
Pressure at End of Fill (psia)	1,155	1,250	1,202	1,210	1,245	1,140	1,170	2,840	2,900	2,990	3,030	3,100	2,025	3,025
Pressure at ESC (psia)	1,260	1,250	1,230	1,275	1,298	1,225	1,225	2,800	2,520	2,870	3,020	3,060	3,160	2,990
Pressure After STDV Opens (psia)*	110	145	15	165	200	175	190	2,520	2,265	2,460	2,670	2,700	2,845	2,710
Pressure at ECO (psia)	NR	NR	NR	NR	NR	NR	NR	2,520	2,265	--	3,025	2,890	2,785	2,490
Pressure After ECO (psia)	NR	NR	NR	NR	NR	NR	NR	2,350	2,130	2,455	2,675	2,530	2,675	2,477
Gas Mass at ESC (lbm)	4.34	4.12	4.22	4.17	5.19	4.26	4.04	2.34	2.03	2.14	2.27	2.64	2.65	2.45
Gas Mass After Start Tank Blowdown (lbm)	0.53	0.70	0.11	0.77	1.42	0.90	0.91	2.25	1.93	1.94	2.21	2.43	2.48	2.31
Gas Mass at ECO -10 sec (lbm)	NR	NR	NR	NR	NR	NR	NR	2.21	1.78	--	2.32	2.55	2.17	1.93
Gas Mass After ECO (lbm)	NR	NR	NR	NR	NR	NR	NR	1.98	1.73	1.90	2.17	2.42	2.14	1.89
ΔM Used at Start (lbm)	3.81	3.42	4.12	3.40	3.77	3.36	3.13	0.09	0.10	0.20	0.06	0.21	0.17	0.14
ΔM Used at Cutoff (lbm)	NR	NR	NR	NR	NR	NR	NR	0.23	0.05	—	0.15	0.13	0.03	0.04

NR = Not Required

* For control sphere, temperature and pressure were taken at ESC +10

TABLE 6-7
ENGINE START TANK AND CONTROL SPHERE CHILLDOWN AND LOADING DATA

ITEM	TURBINE START TANK DATA 614034 RUN 1	TURBINE START TANK DATA 614043 RUN 1	TURBINE START TANK DATA 614044 RUN 1	HELIUM CONTROL SPHERE DATA 614034 RUN 1	HELIUM CONTROL SPHERE DATA 614043 RUN 1	HELIUM CONTROL SPHERE DATA 614044 RUN 1
Start of Childdown (sec)	ESC* -2,025	ESC -2,025	ESC -2,025	--	--	--
End of Childdown (sec)	ESC -1,200	ESC -1,200	ESC -1,200	--	--	--
Avg Childdown Flowrate (lb/min)	2.95	2.99	3.10	--	--	--
Temperature at Start of Fill (°R)	109	119	122	486	525	
Temperature at End of Fill (°R)	132	143	150	O/S HIGH	O/S HIGH	
Temperature at ESC (R) - First Burn	180(3)	191(3)	200(3)	179	189	200
Temperature After STDV (°R) First Burn(1)	128	133	144	171	180	193
Temperature at ECO (°R) First Burn	141	144	150	154	156	167
Temperature After ECO (°R) First Burn (2)	--	--	--	152	155	164
Temperature at ESC (°R) Second Burn	251	271	215	244	266	
Temperature After STDV (°R) Second Burn (1)	181	200	149	229	232	
Temperature at ECO (°R) Second Burn	181(6)	193	172	229	204	
Temperature After ECO (°R) Second Burn (2)	--	--	--	227	201	
ΔT Coast (9-8) (°R) Second Burn	110	81	65	92	111	
Pressure at Start of Fill (psia)	265	262	282	1,155	755	
Pressure at End of Fill (psia)	940	938	929	3,110	3,100	
Pressure at ESC (psia) First Burn	1,300(3)	1,188(3)	1,276(3)	3,450	3,350	3,570
Pressure After STDV (psia) First Burn(1)	198	197	215	2,940	2,755	3,051
Pressure at ECO (psia) First Burn	1,329	1,316	495	2,380	2,255	2,396
Pressure After ECO (psia)(2)	--	--	--	2,290	2,200	2,319
Pressure at ESC (psia) Second Burn	1,294	1,285	1,285	3,950	3,950	3,290
Pressure After STDV (psia) Second Burn(1)	216	224	245	3,140	3,200	2,674
Pressure at ECO (psia) Second Burn	690(6)	1,322	1,215	3,140	2,250	
Pressure After ECO (psia) Second Burn(2)	--	-	--	3,010	2,145	
ΔT Coast (min)	95	82	41	95	82	
ΔM Coast (24-26) (lbs)	3.67	2.82	1.72	--	--	
Gas Mass at ESC (lbm) First Burn	5.51	4.74	4.87	3.14	2.97	2.99
Gas Mass After STDV (lbm) First Burn	1.27	1.21	1.21	2.88	2.64	2.71
Gas Mass at ECO (lbm) First Burn	7.53	7.25	6.35	2.67(5)	2.54(5)	2.50(5)
Gas Mass After ECO (lbm) First Burn(2)	--	--	--	2.60	2.49	2.46
Gas Mass at ESC (lbm) Second Burn	3.86	4.32	4.63	2.74(4)	2.57(4)	
Gas Mass After STDV (lbm) Second Burn(1)	0.95	0.78	1.34	2.40	2.24	
Gas Mass at ECO (lbm) Second Burn	3.01(6)	5.20	5.47	2.40	2.00	
Gas Mass After ECO (lbm) Second Burn(2)	--	--	--	2.33	1.94	
ΔM During Start - First Burn	4.24	3.53	3.66	0.26	0.33	0.28
ΔM During Cutoff - First Burn	--	--	--	0.07	0.05	0.04
ΔM During Start - Second Burn	2.91	3.54	3.29	0.34	0.33	
ΔM During Cutoff - Second Burn	--	--	--	0.07	0.06	

*Control sphere pressurized at ESC -2,000 sec and continuously maintained at pressure until engine start.

NOTES:
(1) Start tank pressure or temperature obtained at end of start tank blowdown. Control sphere pressure or temperature which existed after completion of helium usage during engine start.
(2) This pressure or temperature was not desired for the start tank. Control sphere pressure or temperature which existed after the completion of helium usage during engine cutoff.
(3) Start tank was vented during the time interval from end of fill to engine start.
(4) The control sphere mass calculated at second burn engine start was greater than that calculated at first burn cutoff. This was due to either inaccuracies in instrumentation and compressibility factor or to a leakage from the ground supply to the sphere during the simulated coast period.
(5) Similar as for footnote 4. The differences between these values at ECO and those after STDV are due to either leakage from the control sphere or to inaccuracies in the data and compressibility factor.
(6) Countdown 614034 second burn lasted only 4 sec. This was the reason for the low recharge pressure and mass at ECO. It also accounts for the lack of temperature variation during the firing.

21 February 1966

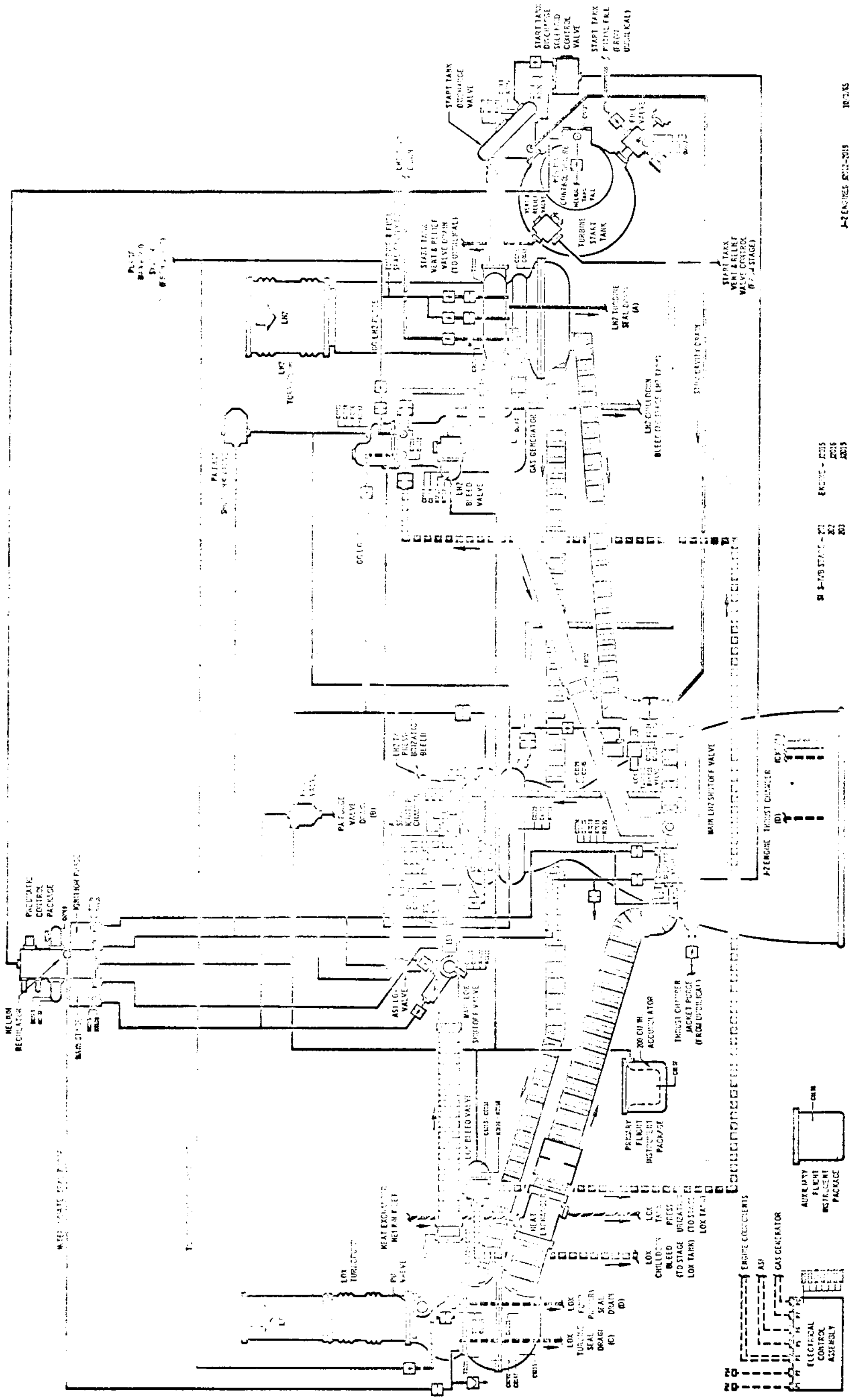

Figure 6-1 J-2 Engine Configuration and I[illegible] Schematic

21 February 1966

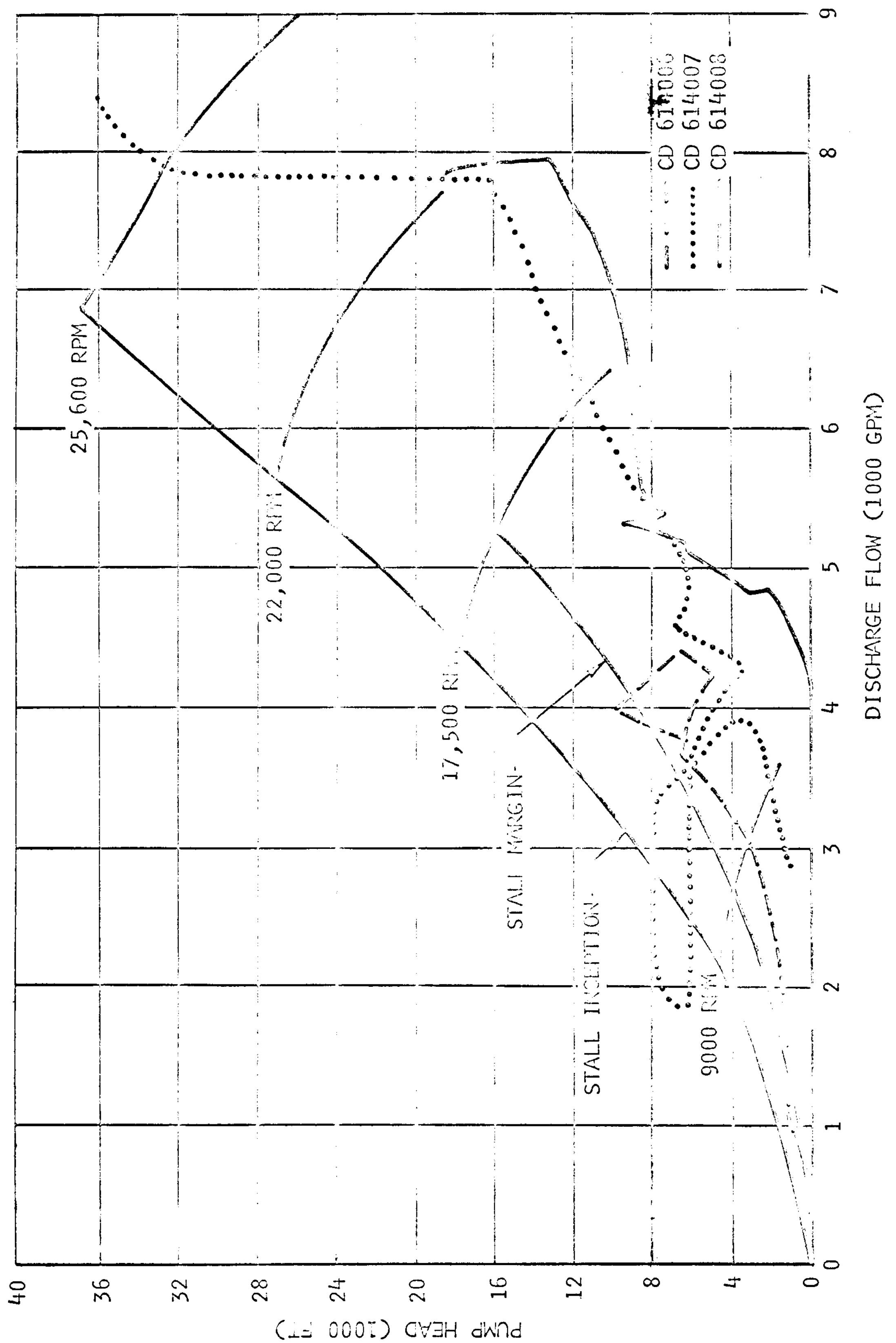

Figure 6-2 LH2 Pump Performance (Engine J-2003)

21 February 1966

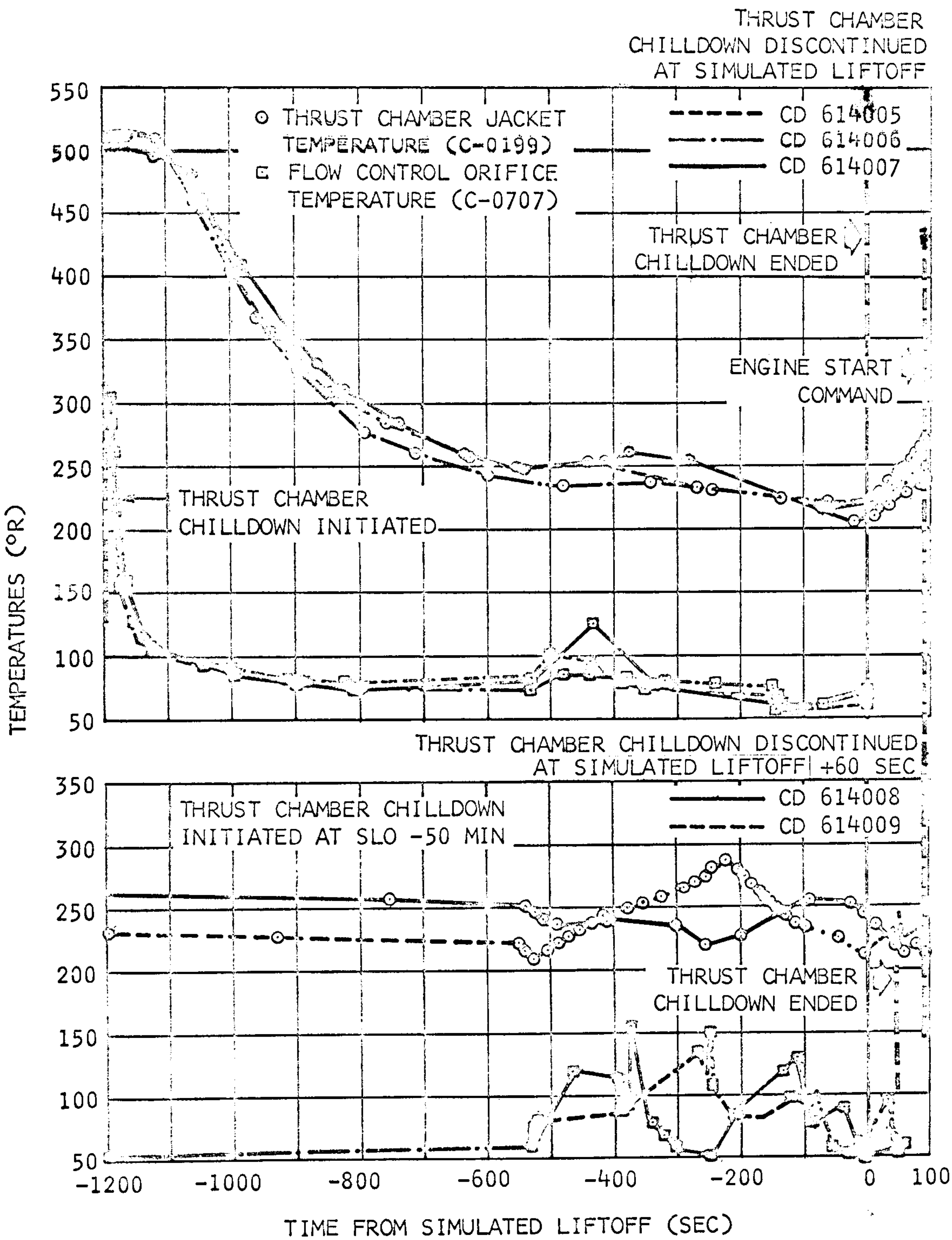

Figure 6-3 Effect of Changing Thrust Chamber Chilldown Procedures

21 February 1966

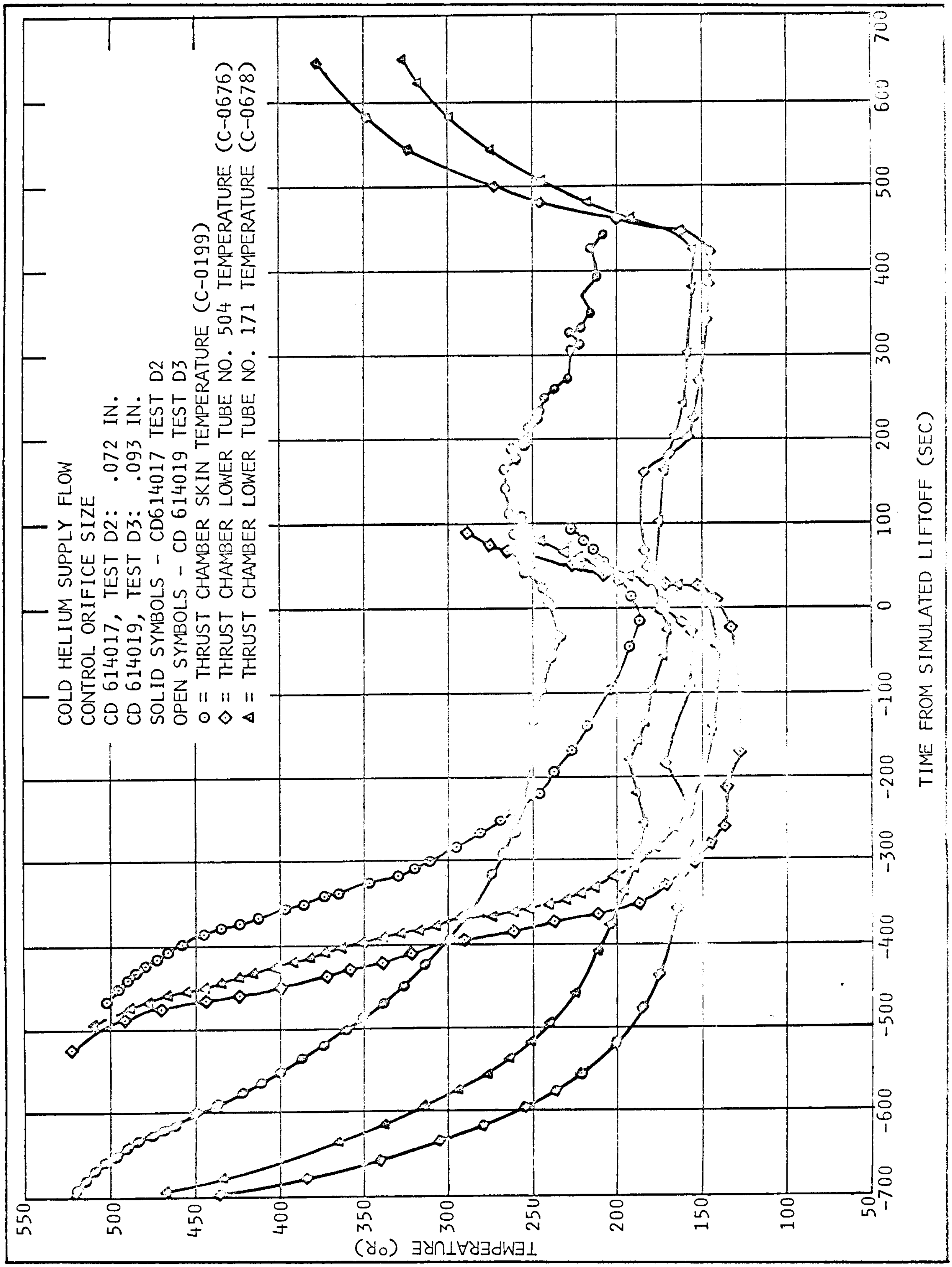

Figure 6-4 Cold Helium Supply Flow Control Orifice Size Effect on T/C Childown Temperature Profile

21 February 1966

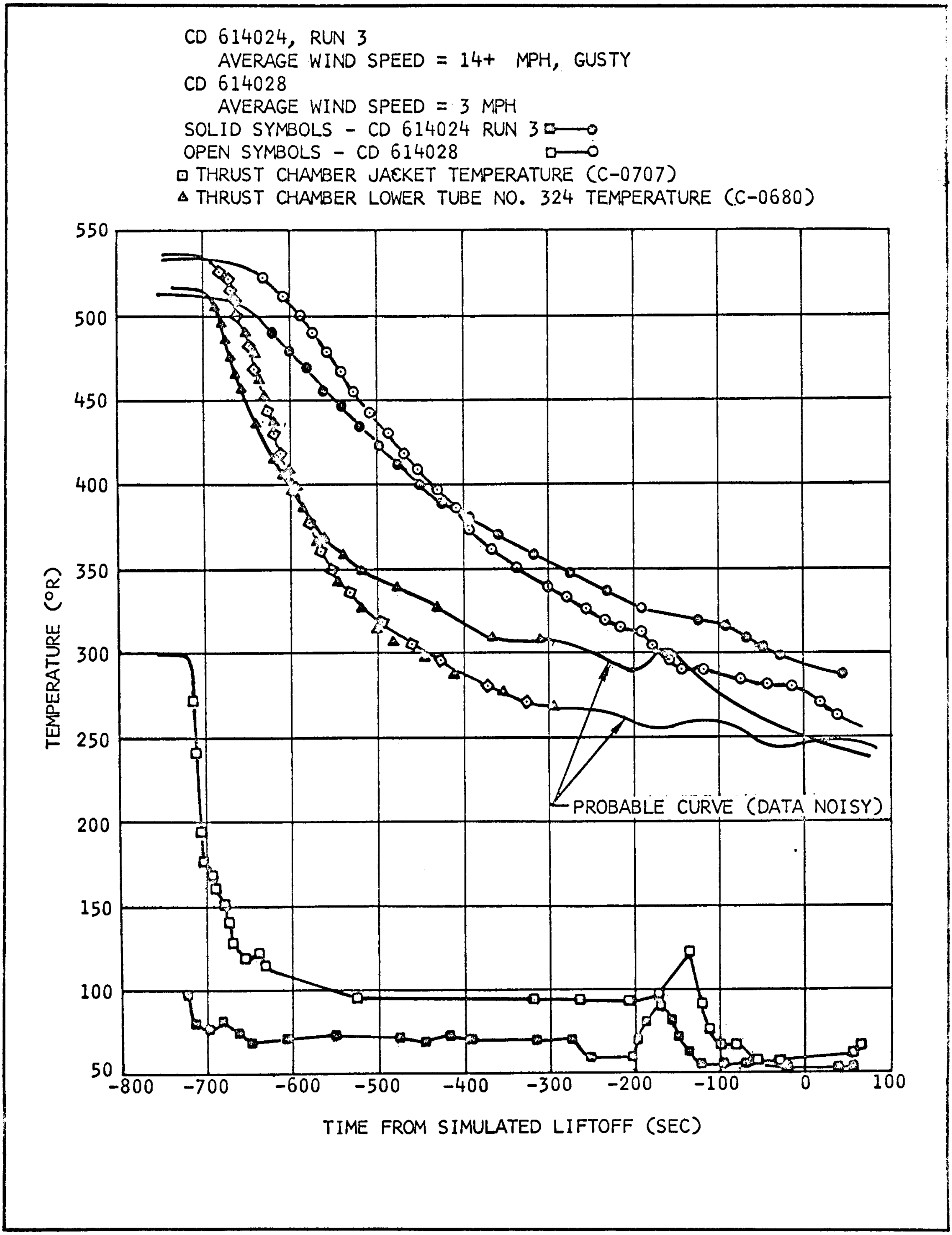

Figure 6-5 Wind Effect on T/C Chilldown Temperature Profile

21 February 1966

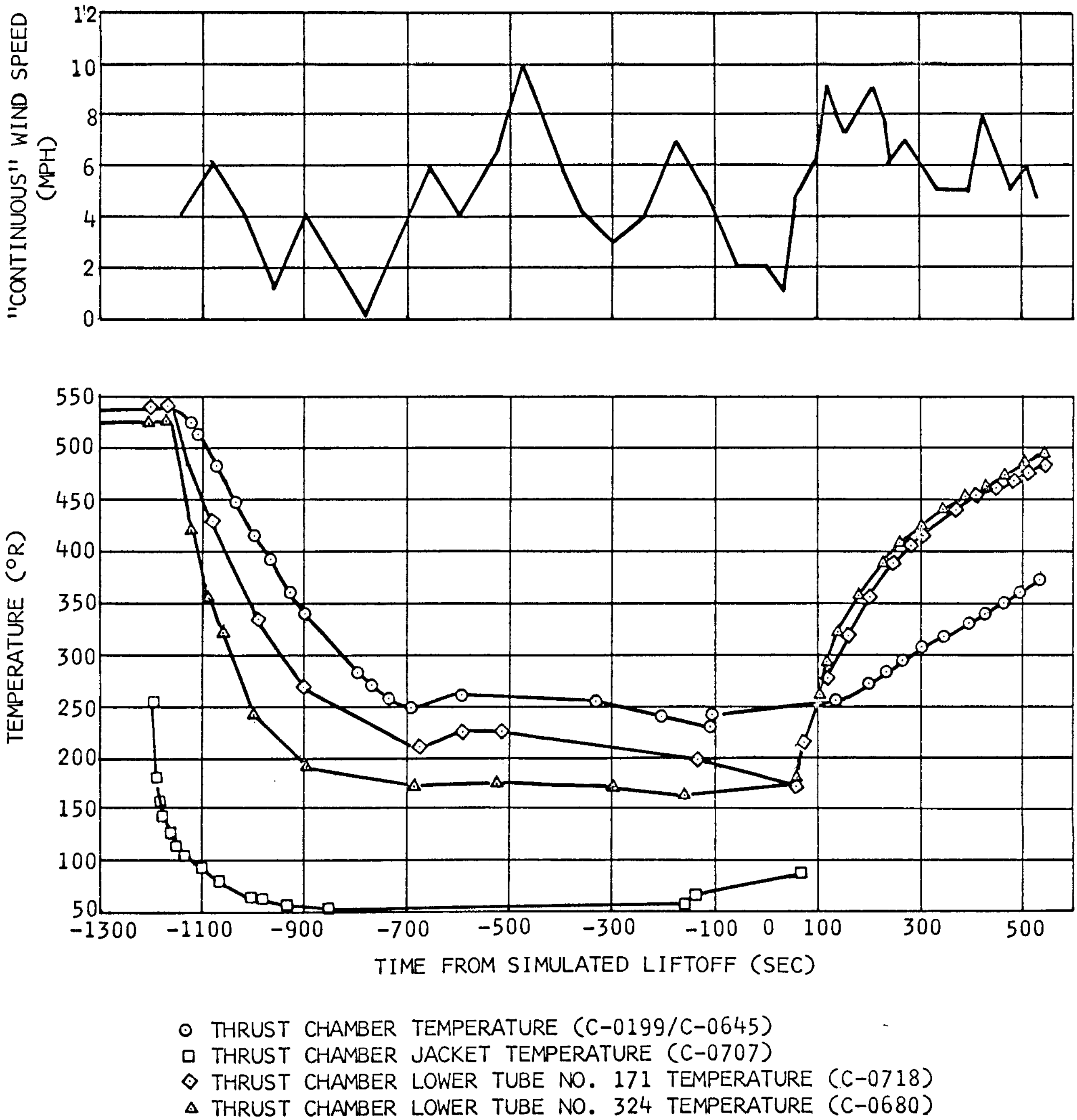

Figure 6-6 Wind Effect on T/C Chilldown Temperature Profile - CD 614044

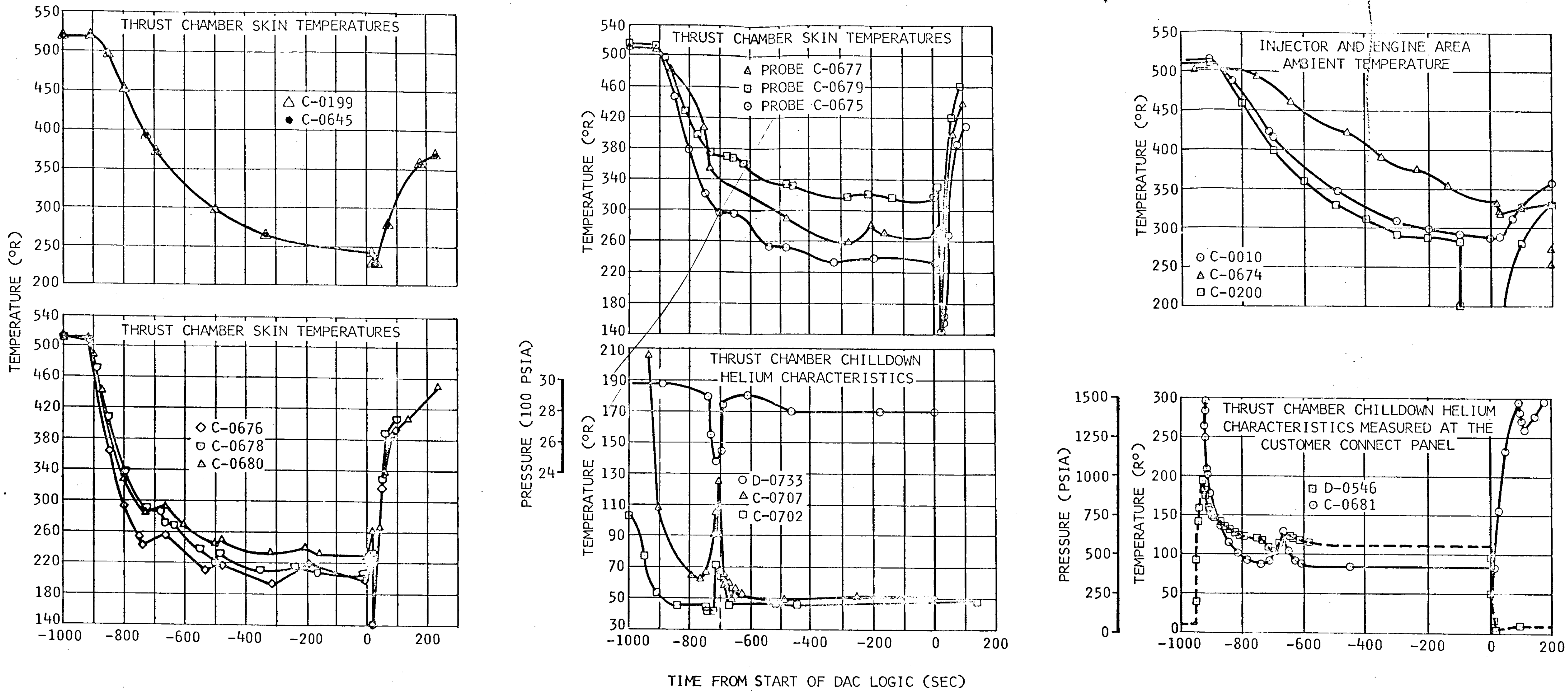

NOTE:

THRUST CHAMBER SKIN TEMPERATURES (C-0199/C-0645)
THRUST CHAMBER LOWER TUBE NO. 504 TEMPERATURE (C-0676)
THRUST CHAMBER LOWER TUBE NO. 171 TEMPERATURE (C-0678)
THRUST CHAMBER LOWER TUBE NO. 324 TEMPERATURE (C-0680)
THRUST CHAMBER UPPER TUBE NO. 144 TEMPERATURE (C-0577)
THRUST CHAMBER UPPER TUBE NO. 324 TEMPERATURE (C-0679)
THRUST CHAMBER UPPER TUBE NO. 504 TEMPERATURE (C-0675)

HELIUM HEAT EXCHANGER OUTLET TEMPERATURE (C-0702)
CHILLDOWN ORIFICE E04B TEMPERATURE (C-0707)
ENGINE AREA AMBIENT TEMPERATURE (C-0010)
CHILLDOWN MEDIUM TEMPERATURE AT CUSTOMER CONNECT PANEL (C-0681)
GAS GENERATOR INJECTOR NO. 2 TEMPERATURE (C-0674)
GAS GENERATOR GH2 TEMPERATURE (C-0200)
CHILLDOWN ORIFICE E04B PRESSURE (D-0773)
CHILLDOWN HELIUM PRESSURE AT CUSTOMER CONNECT PANEL (D-0546)

Figure 6-7 Engine Temperature Conditioning Test (CD 614014)

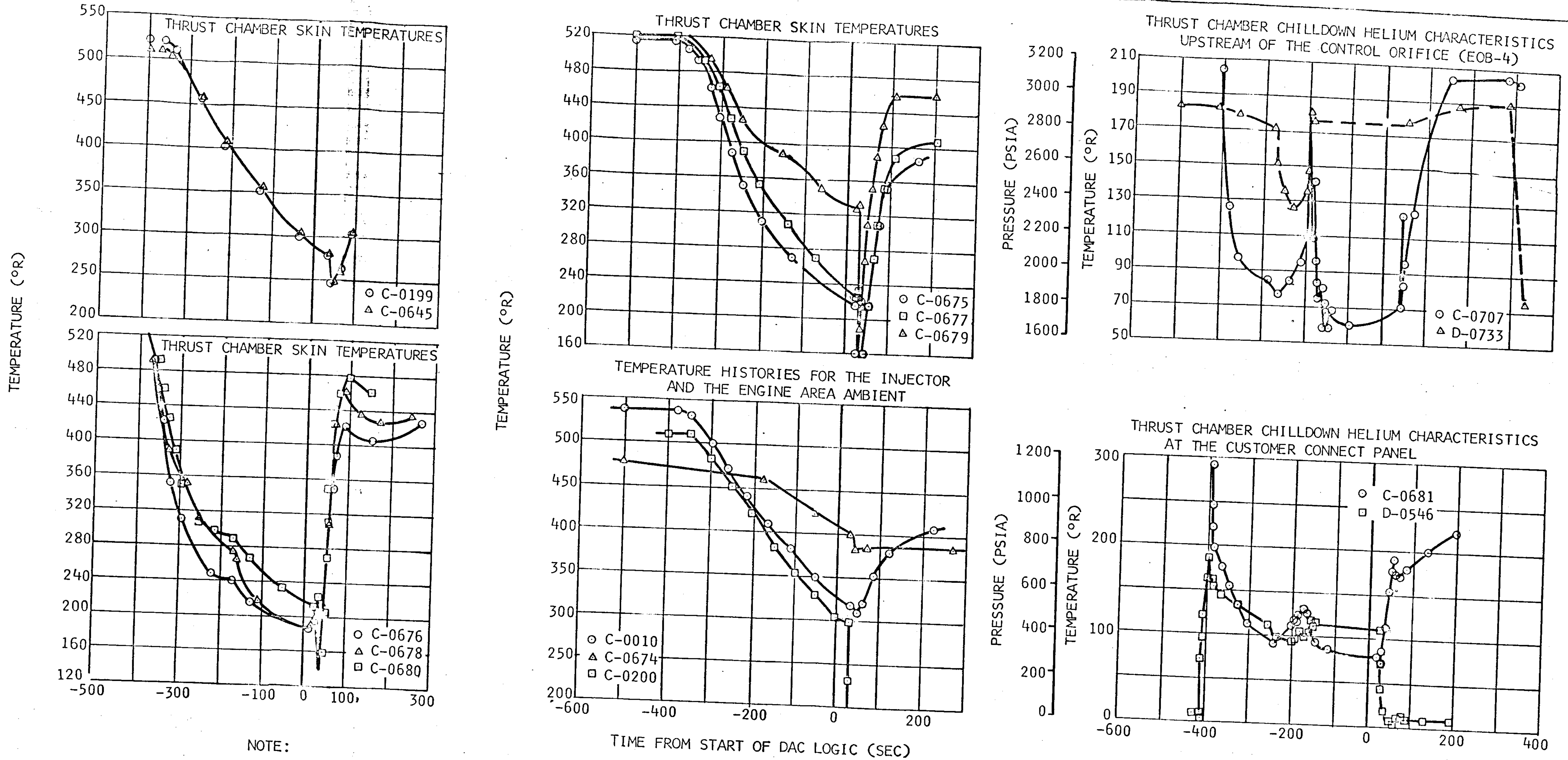

NOTE:

THRUST CHAMBER SKIN TEMPERATURE (C-0199/C-0645)
THRUST CHAMBER LOWER TUBE NO. 504 TEMPERATURE (C-0676)
THRUST CHAMBER LOWER TUBE NO. 171 TEMPERATURE (C-0678)
THRUST CHAMBER LOWER TUBE NO. 324 TEMPERATURE (C-0680)
THRUST CHAMBER UPPER TUBE NO. 144 TEMPERATURE (C-0677)
THRUST CHAMBER UPPER TUBE NO. 324 TEMPERATURE (C-0679)
THRUST CHAMBER UPPER TUBE NO. 504 TEMPERATURE (C-0675)

HELIUM HEAT EXCHANGER OUTLET TEMPERATURE (C-0702)
CHILLDOWN ORIFICE E04B TEMPERATURE (C-0707)
ENGINE AREA AMBIENT TEMPERATURE (C-0010)
CHILLDOWN MEDIUM TEMPERATURE AT CUSTOMER CONNECT PANEL (C-0681)
GAS GENERATOR INJECTOR NO. 2 TEMPERATURE (C-0674)
GAS GENERATOR GH2 TEMPERATURE (C-0200)
CHILLDOWN ORIFICE E04B PRESSURE (D-0773)
CHILLDOWN HELIUM PRESSURE AT CUSTOMER CONNECT PANEL (D-0546)

Figure 6-8 Engine Temperature Conditioning Test - A3

CD 614017

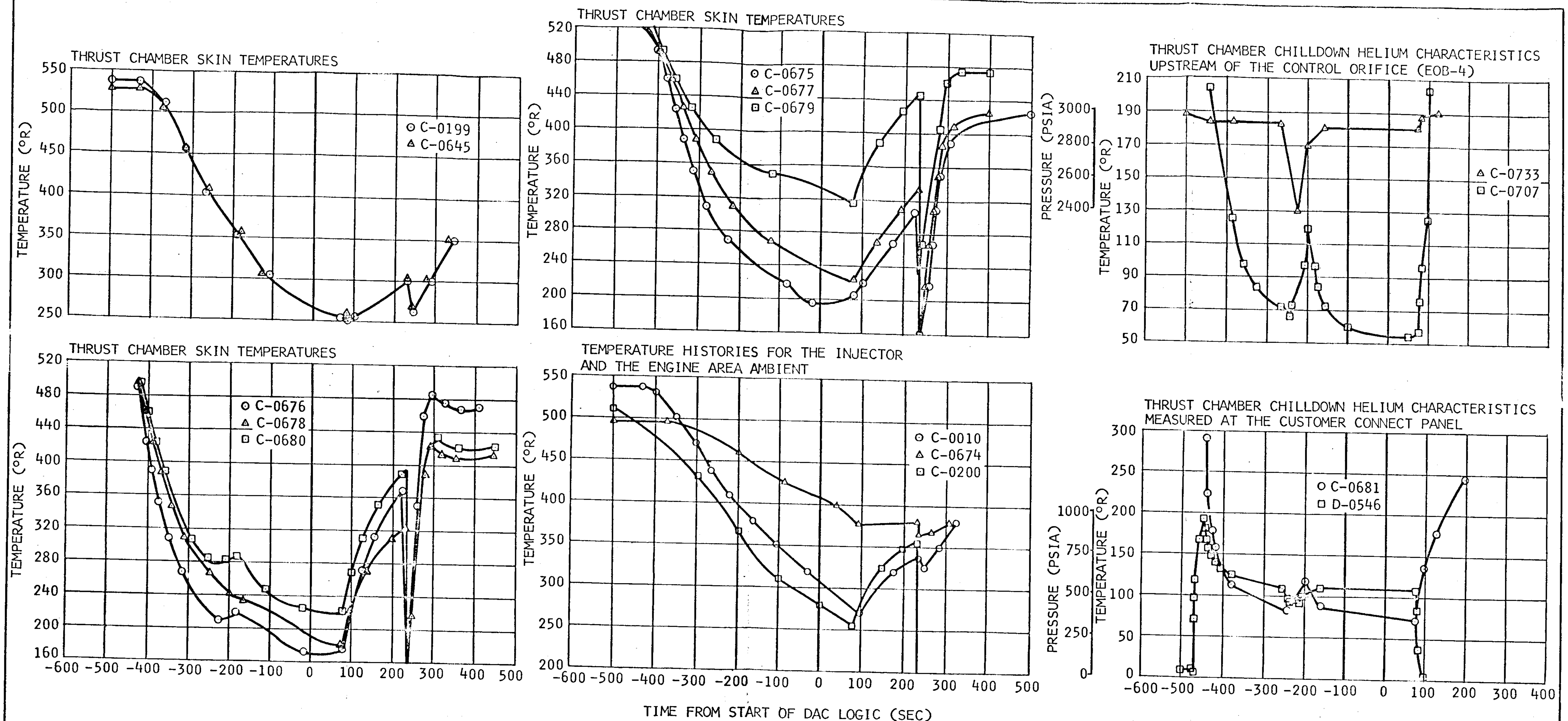

NOTE:

THRUST CHAMBER SKIN TEMPERATURE (C-0199/C-0645)
THRUST CHAMBER LOWER TUBE NO. 504 TEMPERATURE (C-0676)
THRUST CHAMBER LOWER TUBE NO. 171 TEMPERATURE (C-0678)
THRUST CHAMBER LOWER TUBE NO. 324 TEMPERATURE (C-0680)
THRUST CHAMBER UPPER TUBE NO. 144 TEMPERATURE (C-0677)
THRUST CHAMBER UPPER TUBE NO. 324 TEMPERATURE (C-0679)
THRUST CHAMBER UPPER TUBE NO. 504 TEMPERATURE (C-0675)

HELIUM HEAT EXCHANGER OUTLET TEMPERATURE (C-0702)
CHILLDOWN ORIFICE E04B TEMPERATURE (C-0707)
ENGINE AREA AMBIENT TEMPERATURE (C-0010)
CHILLDOWN MEDIUM TEMPERATURE AT CUSTOMER CONNECT PANEL (C-0681)
GAS GENERATOR INJECTOR NO. 2 TEMPERATURE (C-0674)
GAS GENERATOR GH2 TEMPERATURE (C-0200)
CHILLDOWN ORIFICE E04B PRESSURE (D-0773)
CHILLDOWN HELIUM PRESSURE AT CUSTOMER CONNECT PANEL (D-0546)

CD 614017

Figure 6-9 Engine Temperature Conditioning Test - A2

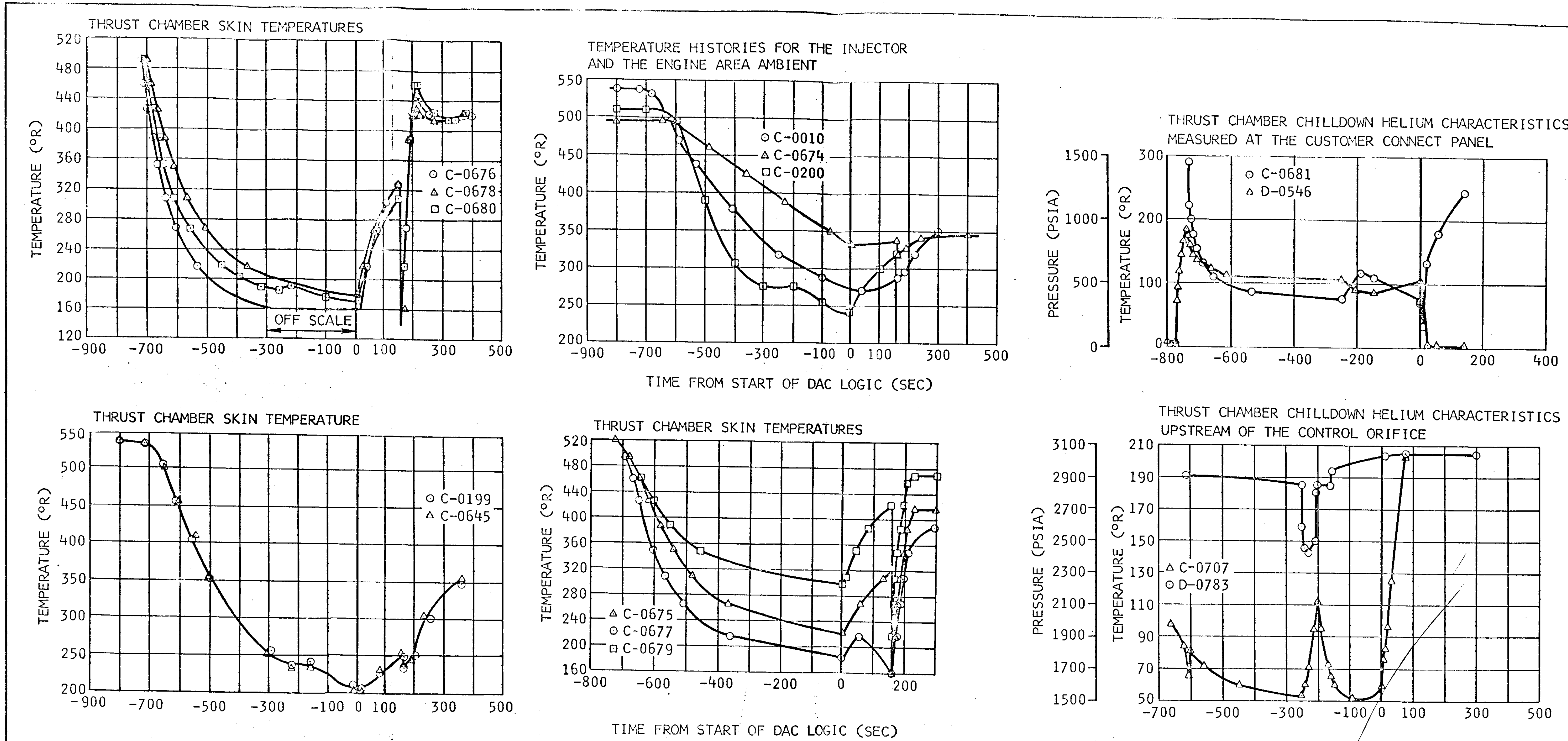

NOTE:

THRUST CHAMBER SKIN TEMPERATURE (C-0199/C-0645)
THRUST CHAMBER LOWER TUBE NO. 504 TEMPERATURE (C-0676)
THRUST CHAMBER LOWER TUBE NO. 171 TEMPERATURE (C-0678)
THRUST CHAMBER LOWER TUBE NO. 324 TEMPERATURE (C-0680)
THRUST CHAMBER UPPER TUBE NO. 114 TEMPERATURE (C-0677)
THRUST CHAMBER UPPER TUBE NO. 324 TEMPERATURE (C-0679)
THRUST CHAMBER UPPER TUBE NO. 504 TEMPERATURE (C-0675)

HELIUM HEAT EXCHANGER OUTLET TEMPERATURE (C-0702)
CHILLDOWN ORIFICE E04B TEMPERATURE (C-0707)
ENGINE AREA AMBIENT TEMPERATURE (C-0010)
CHILLDOWN MEDIUM TEMPERATURE AT CUSTOMER CONNECT PANEL (C-0681)
GAS GENERATOR INJECTOR NO. 2 TEMPERATURE (C-0674)
GAS GENERATOR GH2 TEMPERATURE (C-0200)
CHILLDOWN ORIFICE E04B PRESSURE (D-0773)
CHILLDOWN HELIUM PRESSURE AT CUSTOMER CONNECT PANEL (D-0546)

CD 614017

Figure 6-10 Engine Temperature Conditioning Test - E2

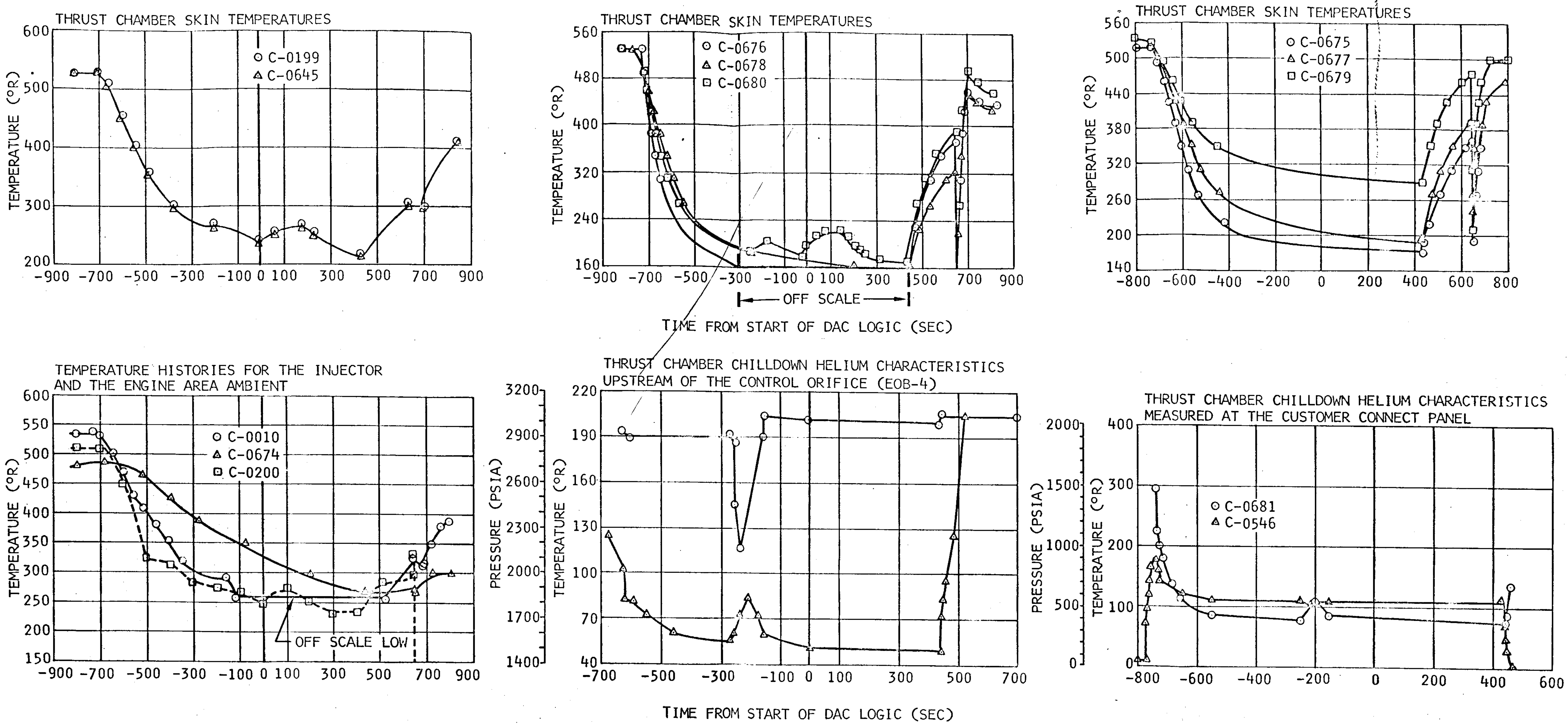

NOTE:

THRUST CHAMBER SKIN TEMPERATURE (C-0199/C-0645)
THRUST CHAMBER LOWER TUBE NO. 504 TEMPERATURE (C-0676)
THRUST CHAMBER LOWER TUBE NO. 171 TEMPERATURE (C-0678)
THRUST CHAMBER LOWER TUBE NO. 324 TEMPERATURE (C-0680)
THRUST CHAMBER UPPER TUBE NO. 144 TEMPERATURE (C-0677)
THRUST CHAMBER UPPER TUBE NO. 324 TEMPERATURE (C-0679)
THRUST CHAMBER UPPER TUBE NO. 504 TEMPERATURE (C-0675)

HELIUM HEAT EXCHANGER OUTLET TEMPERATURE (C-0702)
CHILLDOWN ORIFICE E04B TEMPERATURE (C-0707)
ENGINE AREA AMBIENT TEMPERATURE (C-0010)
CHILLDOWN MEDIUM TEMPERATURE AT CUSTOMER CONNECT PANEL (C-0681)
GAS GENERATOR INJECTOR NO. 2 TEMPERATURE (C-0674)
GAS GENERATOR GH2 TEMPERATURE (C-0200)
CHILLDOWN ORIFICE E04B PRESSURE (D-0773)
CHILLDOWN HELIUM PRESSURE AT CUSTOMER CONNECT PANEL (D-0546)

CD 614017

Figure 6-11 Engine Temperature Conditioning Test - D2

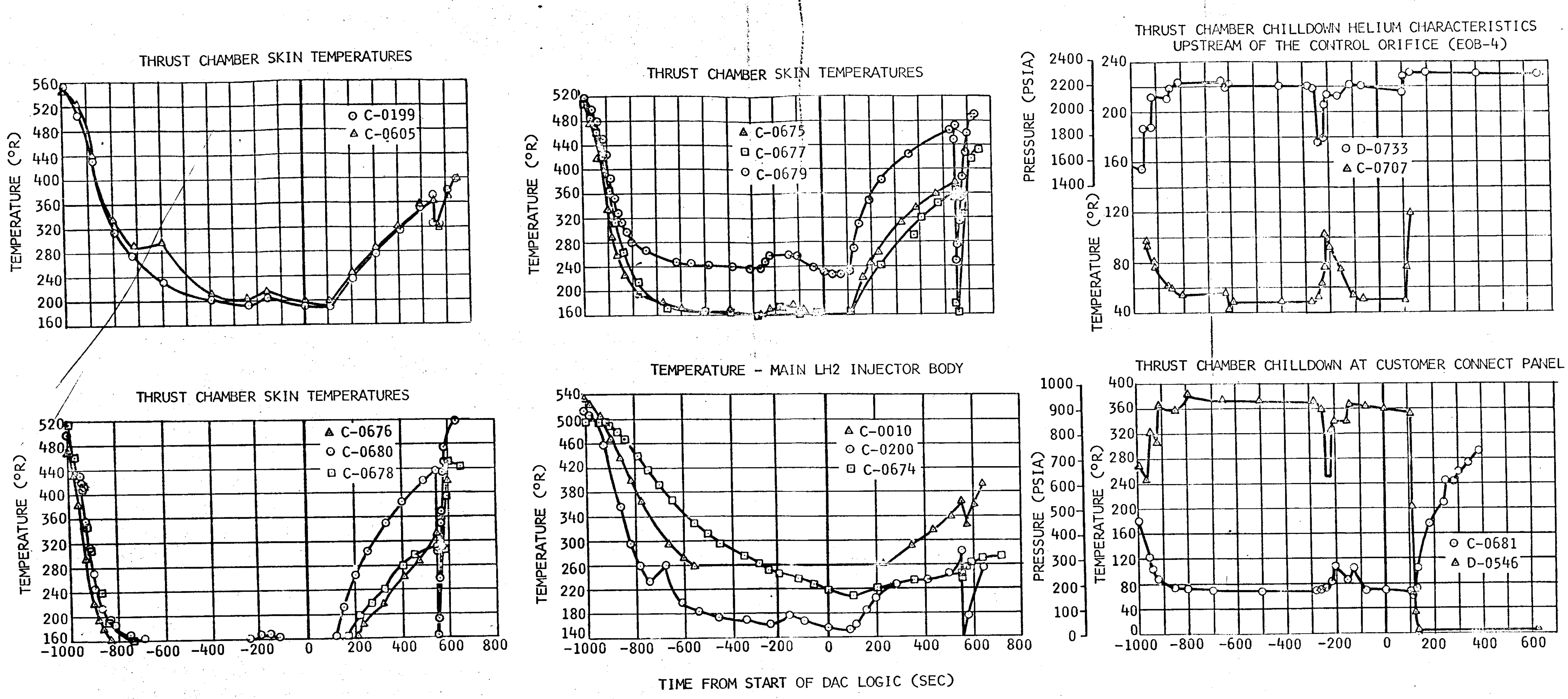

NOTE:

THRUST CHAMBER SKIN TEMPERATURES (C-0199/C-0645)
THRUST CHAMBER LOWER TUBE NO. 504 TEMPERATURE (C-0676)
THRUST CHAMBER LOWER TUBE NO. 171 TEMPERATUER (C-0678)
THRUST CHAMBER LOWER TUBE NO. 324 TEMPERATURE (C-0680)
THRUST CHAMBER UPPER TUBE NO. 144 TEMPERATURE (C-0677)
THRUST CHAMBER UPPER TUBE NO. 324 TEMPERATURE (C-0679)
THRUST CHAMBER UPPER TUBE NO. 504 TEMPERATURE (C-0675)

HELIUM HEAT EXCHANGER OUTLET TEMPERATURE (C-0702)
CHILLDOWN ORIFICE E04B TEMPERATURE (C-0707)
ENGINE AREA AMBIENT TEMPERATURE (C-0010)
CHILLDOWN MEDIUM TEMPERATURE AT CUSTOMER CONNECT PANEL (C-0681)
GAS GENERATOR INJECTOR NO. 2 TEMPERATURE (C-0674)
GAS GENERATOR GH2 TEMPERATURE (C-0200)
CHILLDOWN ORIFICE E04B PRESSURE (D-0773)
CHILLDOWN HELIUM PRESSURE AT CUSTOMER CONNECT PANEL (D-0546)

CD 614018

Figure 6-13 Engine Temperature Conditioning Test - H2

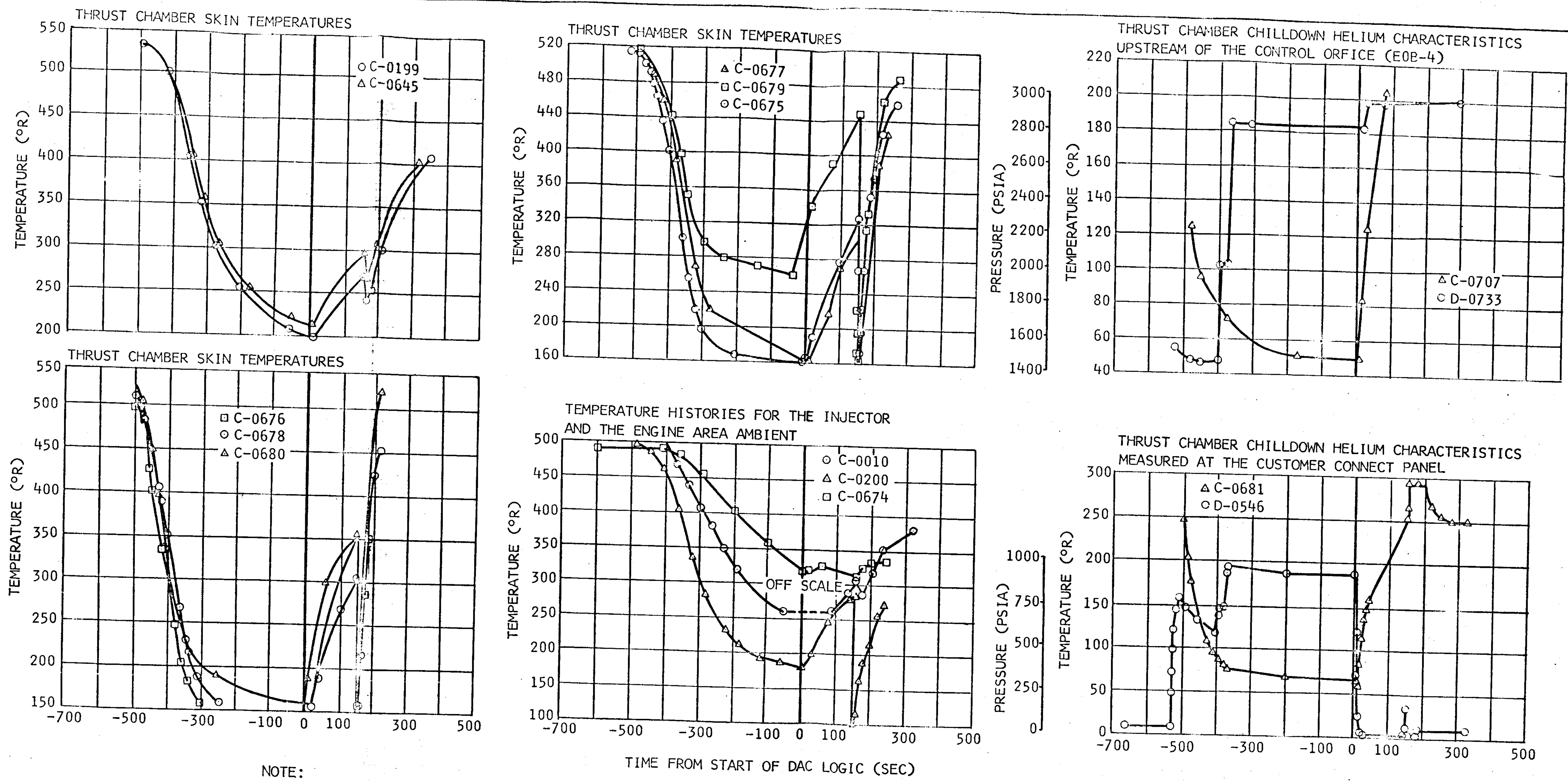

NOTE:

THRUST CHAMBER SKIN TEMPERATURES (C-0199/C-0645)
THRUST CHAMBER LOWER TUBE NO. 504 TEMPERATURE (C-0676)
THRUST CHAMBER LOWER TUBE NO. 171 TEMPERATURE (C-0678)
THRUST CHAMBER LOWER TUBE NO. 324 TEMPERATURE (C-0680)
THRUST CHAMBER UPPER TUBE NO. 144 TEMPERATURE (C-0677)
THRUST CHAMBER UPPER TUBE NO. 324 TEMPERATURE (C-0679)
THRUST CHAMBER UPPER TUBE NO. 504 TEMPERATURE (C-0675)

HELIUM HEAT EXCHANGER OUTLET TEMPERATURE (C-0702)
CHILLDOWN ORIFICE E04B TEMPERATURE (C-0707)
ENGINE AREA AMBIENT TEMPERATURE (C-0010)
CHILLDOWN MEDIUM TEMPERATURE AT CUSTOMER CONNECT PANEL (C-0681)
GAS GENERATOR INJECTOR NO. 2 TEMPERATURE (C-0674)
GAS GENERATOR GH2 TEMPERATURE (C-0200)
CHILLDOWN ORIFICE E04B PRESSURE (D0773)
CHILLDOWN HELIUM PRESSURE AT CUSTOMER CONNECT PANEL (D-0546)

CD E14019

Figure 6-14 Engine Temperature Conditioning Test - D3

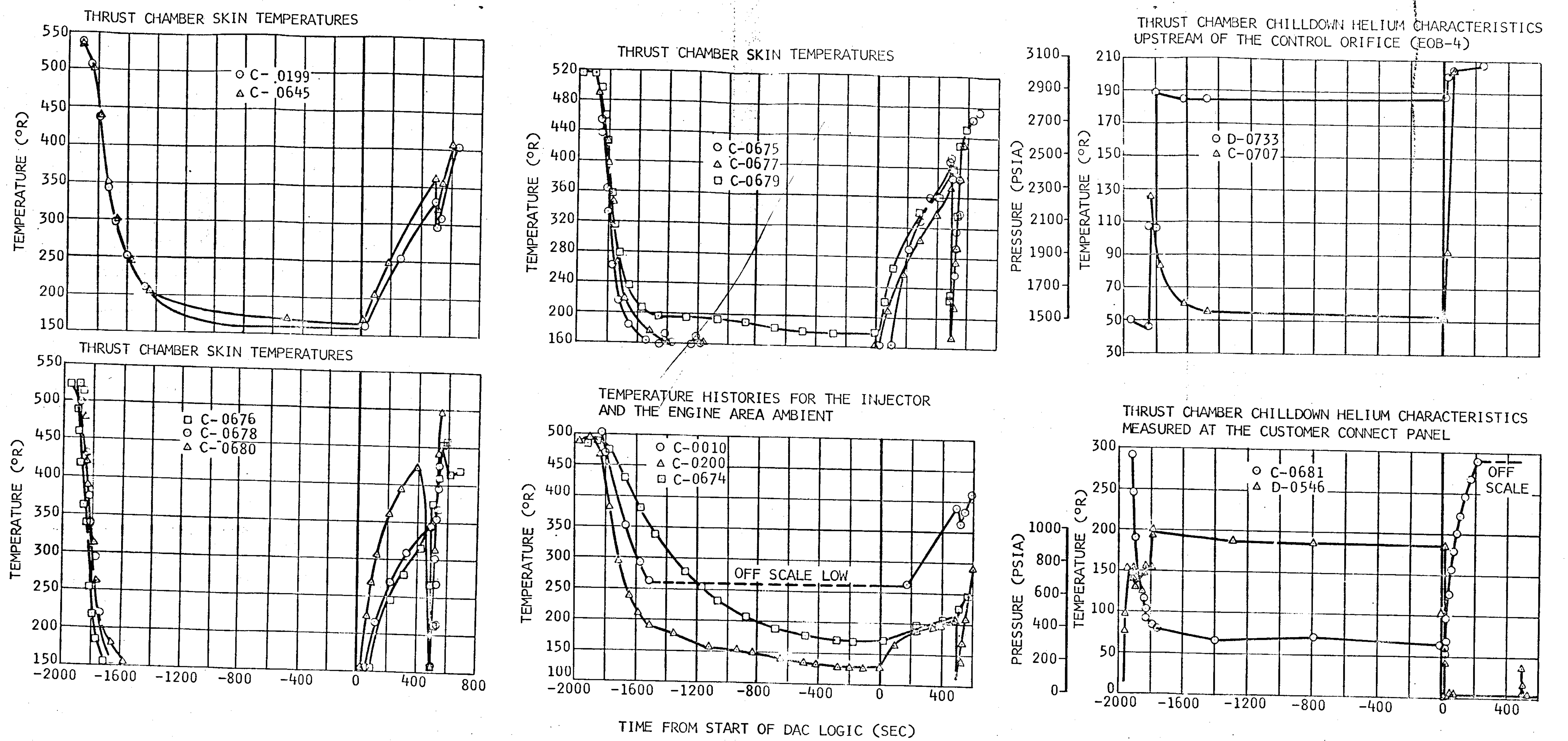

NOTE:

THRUST CHAMBER SKIN TEMPERATURES (C-0199/C-0645)
THRUST CHAMBER LOWER TUBE NO. 504 TEMPERATURE (C-0676)
THRUST CHAMBER LOWER TUBE NO. 171 TEMPERATURE (C-0678)
THRUST CHAMBER LOWER TUBE NO. 324 TEMPERATURE (C-0680)
THRUST CHAMBER UPPER TUBE NO. 144 TEMPERATURE (C-0677)
THRUST CHAMBER UPPER TUBE NO. 324 TEMPERATURE (C-0679)
THRUST CHAMBER UPPER TUBE NO. 504 TEMPERATURE (C-0675)

HELIUM HEAT EXCHANGER OUTLET TEMPERATURE (C-0702)
CHILLDOWN ORIFICE E04B TEMPERATURE (C-0707)
ENGINE AREA AMBIENT TEMPERATURE (C-0010)
CHILLDOWN MEDIUM TEMPERATURE AT CUSTOMER CONNECT PANEL (C-0681)
GAS GENERATOR INJECTOR NO. 2 TEMPERATURE (C-0674)
GAS GENERATOR GH2 TEMPERATURE (C-0200)
CHILLDOWN ORIFICE E04B PRESSURE (D0773)
CHILLDOWN HELIUM PRESSURE AT CUSTOMER CONNECT PANEL (D-0546)

CD 614019

Figure 6-15 Engine Temperature Conditioning Test - H2-1

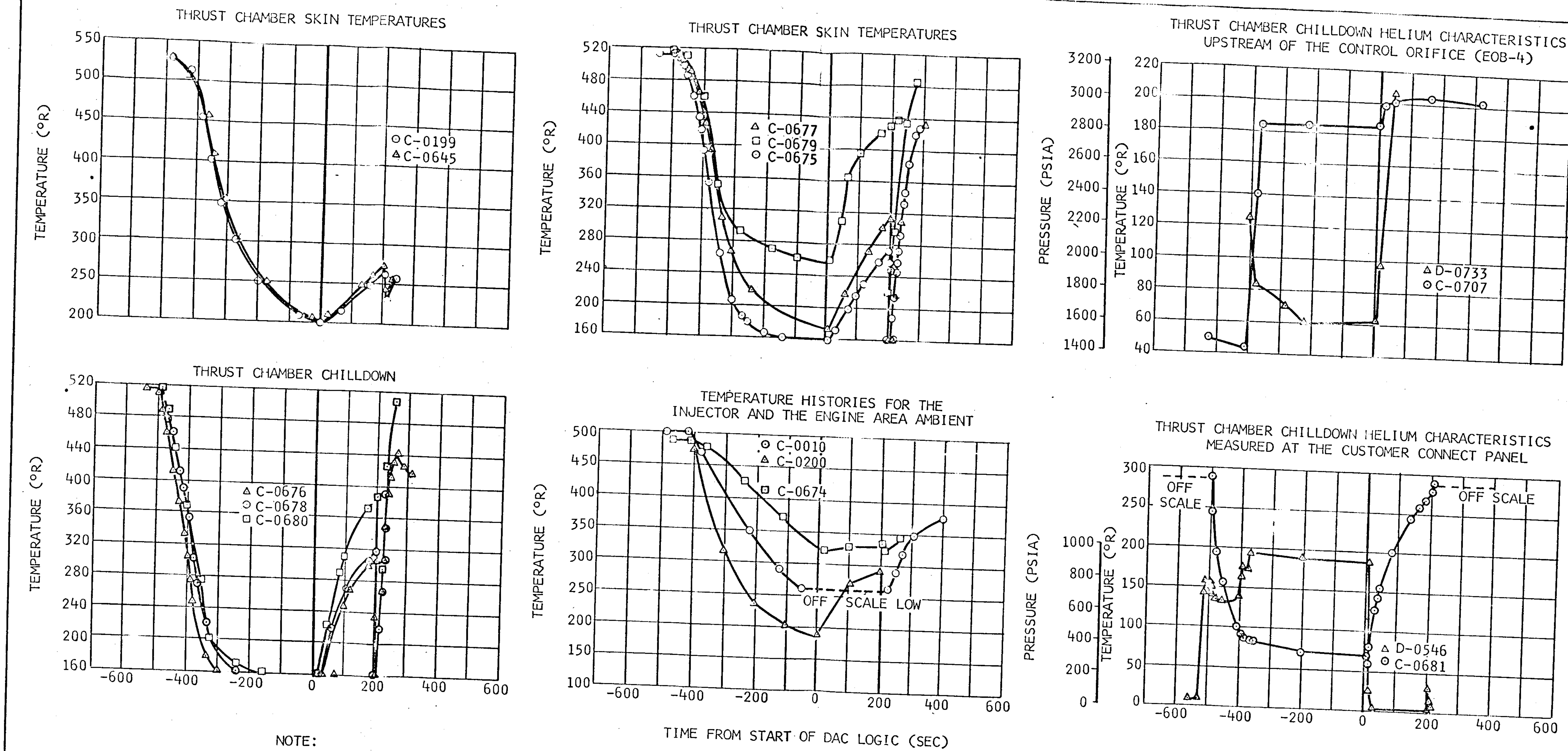

NOTE:

THRUST CHAMBER SKIN TEMPERATURES (C-0199/C-0645)
THRUST CHAMBER LOWER TUBE NO. 504 TEMPERATURE (C-0676)
THRUST CHAMBER LOWER TUBE NO. 171 TEMPERATURE (C-0678)
THRUST CHAMBER LOWER TUBE NO. 324 TEMPERATURE (C-0680)
THRUST CHAMBER UPPER TUBE NO. 144 TEMPERATURE (C-0677)
THRUST CHAMBER UPPER TUBE NO. 324 TEMPERATURE (C-0679)
THRUST CHAMBER UPPER TUBE NO. 504 TEMPERATURE (C-0675)

HELIUM HEAT EXCHANGER OUTLET TEMPERATURE (C-0702)
CHILLDOWN ORIFICE E04B TEMPERATURE (C-0707)
ENGINE AREA AMBIENT TEMPERATURE (C-0010)
CHILLDOWN MEDIUM TEMPERATURE AT CUSTOMER CONNECT PANEL (C-0681)
GAS GENERATOR INJECTOR NO. 2 TEMPERATURE (C-0674)
GAS GENERATOR GH2 TEMPERATURE (C-0200)
CHILLDOWN ORIFICE E04B PRESSURE (D0773)
CHILLDOWN HELIUM PRESSURE AT CUSTOMER CONNECT PANEL (D-0546)

Figure 6-16 Engine Temperature Conditioning Test - G2-1

CD 614019

21 February 1966

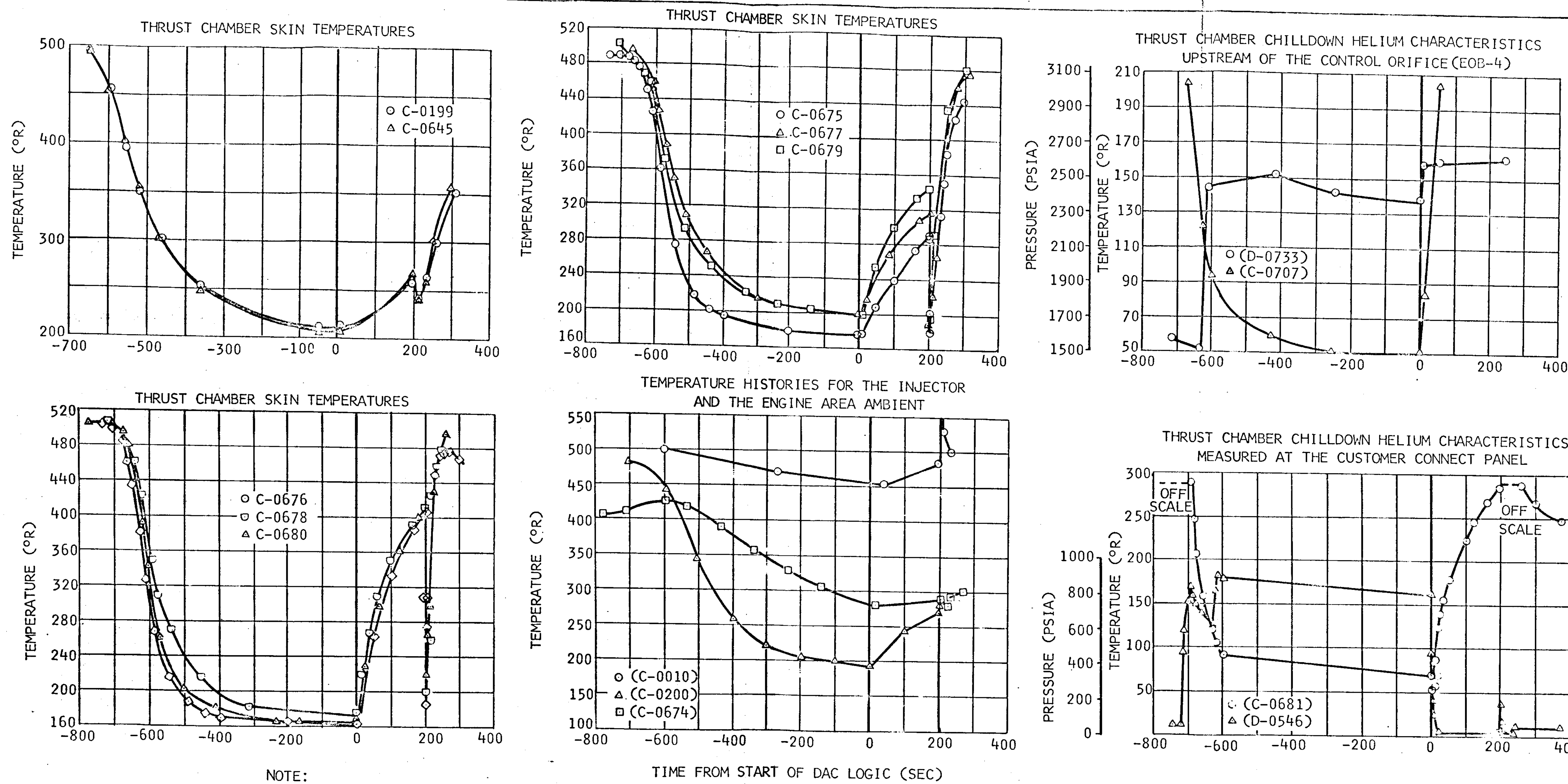

NOTE:

THRUST CHAMBER SKIN TEMPERATURE (C-0199/C-0645)
THRUST CHAMBER LOWER TUBE NO. 504 TEMPERATURE (C-0676)
THRUST CHAMBER LOWER TUBE NO. 171 TEMPERATURE (C-0678)
THRUST CHAMBER LOWER TUBE NO. 324 TEMPERATURE (C-0680)
THRUST CHAMBER UPPER TUBE NO. 144 TEMPERATURE (C-0677)
THRUST CHAMBER UPPER TUBE NO. 324 TEMPERATURE (C-0679)
THRUST CHAMBER UPPER TUBE NO. 504 TEMPERATURE (C-0675)
HELIUM HEAT EXCHANGER OUTLET TEMPERATURE (C-0702)
CHILLDOWN ORIFICE E04B TEMPERATURE (C-0707)
ENGINE AREA AMBIENT TEMPERATURE (C-0010)
CHILLDOWN MEDIUM TEMPERATURE AT CUSTOMER CONNECT PANEL (C-0681)
GAS GENERATOR INJECTOR NO. 2 TEMPERATURE (C0674)
GAS GENERATOR GH2 TEMPERATURE (C-0200)
CHILLDOWN ORIFICE E04B PRESSURE (D-0773)
CHILLDOWN HELIUM PRESSURE AT CUSTOMER CONNECT PANEL (D-0546)

CD 614019

Figure 6-17 Engine Temperature Conditioning Test - G2-3

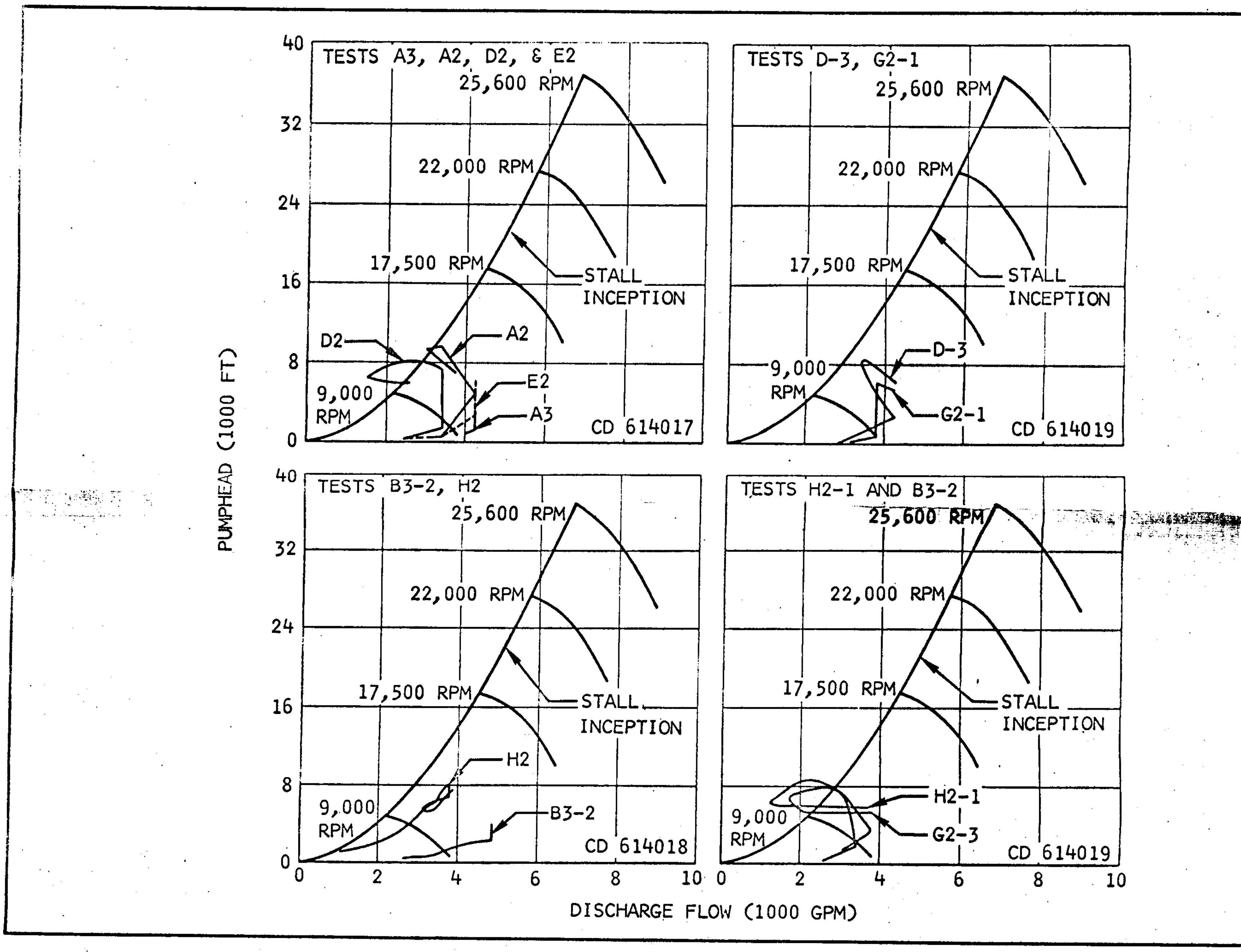

Figure 6-18 LH2 Pump Performance (Engine 2013)

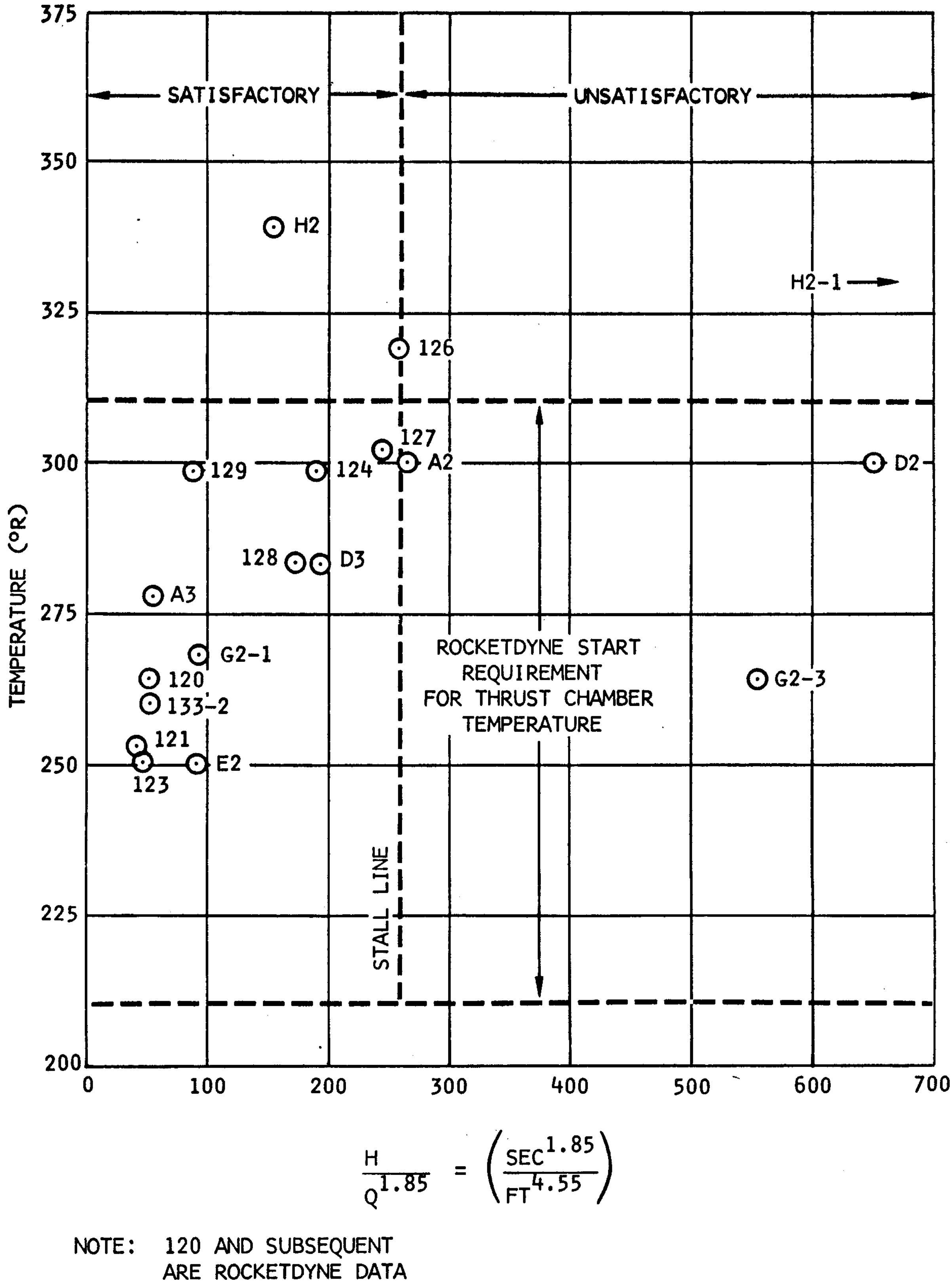

Figure 6-19 Effect of Average Thrust Chamber Temperature on Engine LH2 Pump Stall

21 February 1966

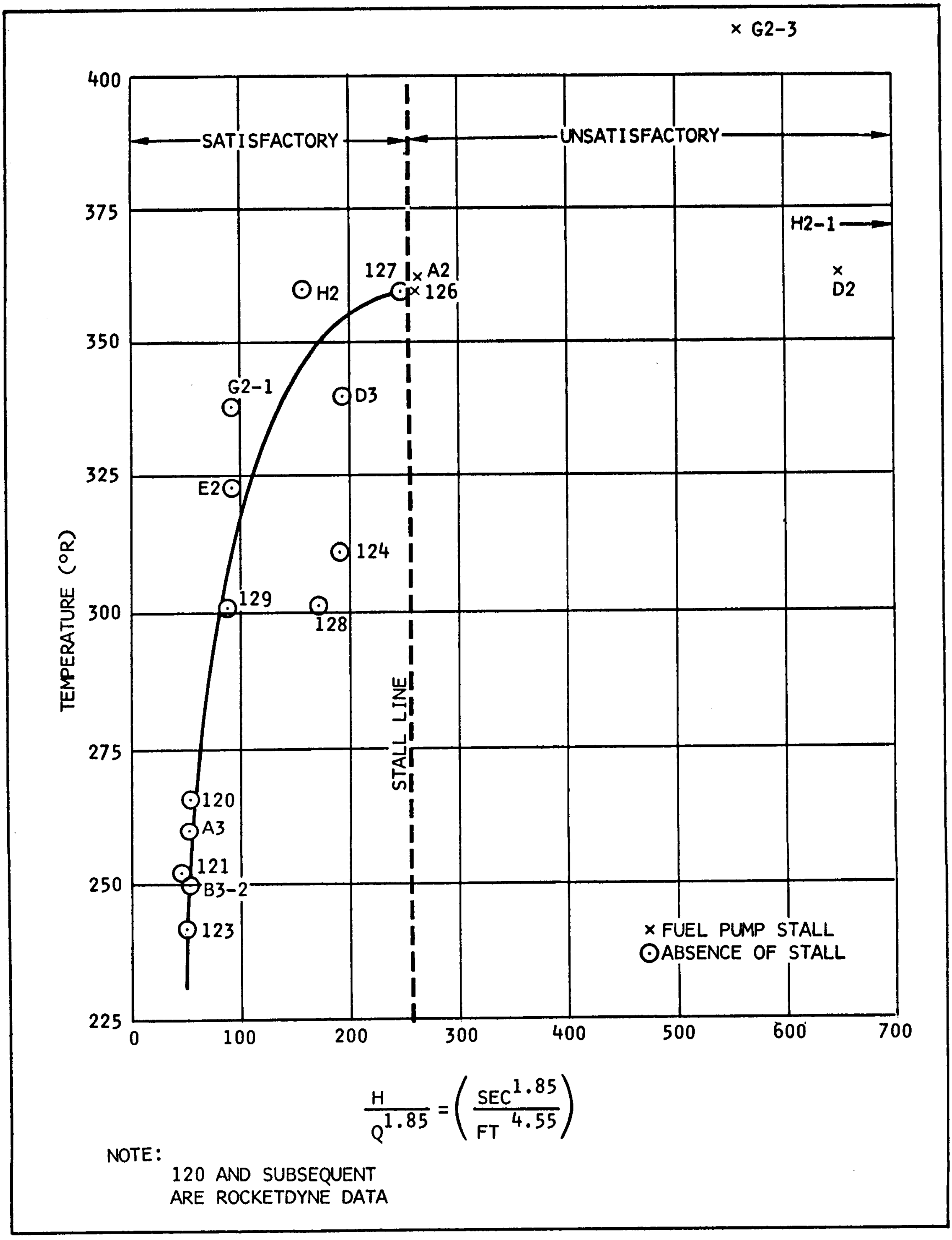

Figure 6-20 Effect of Average Lower Tube Temperature on LH2 Pump Stall

21 February 1966

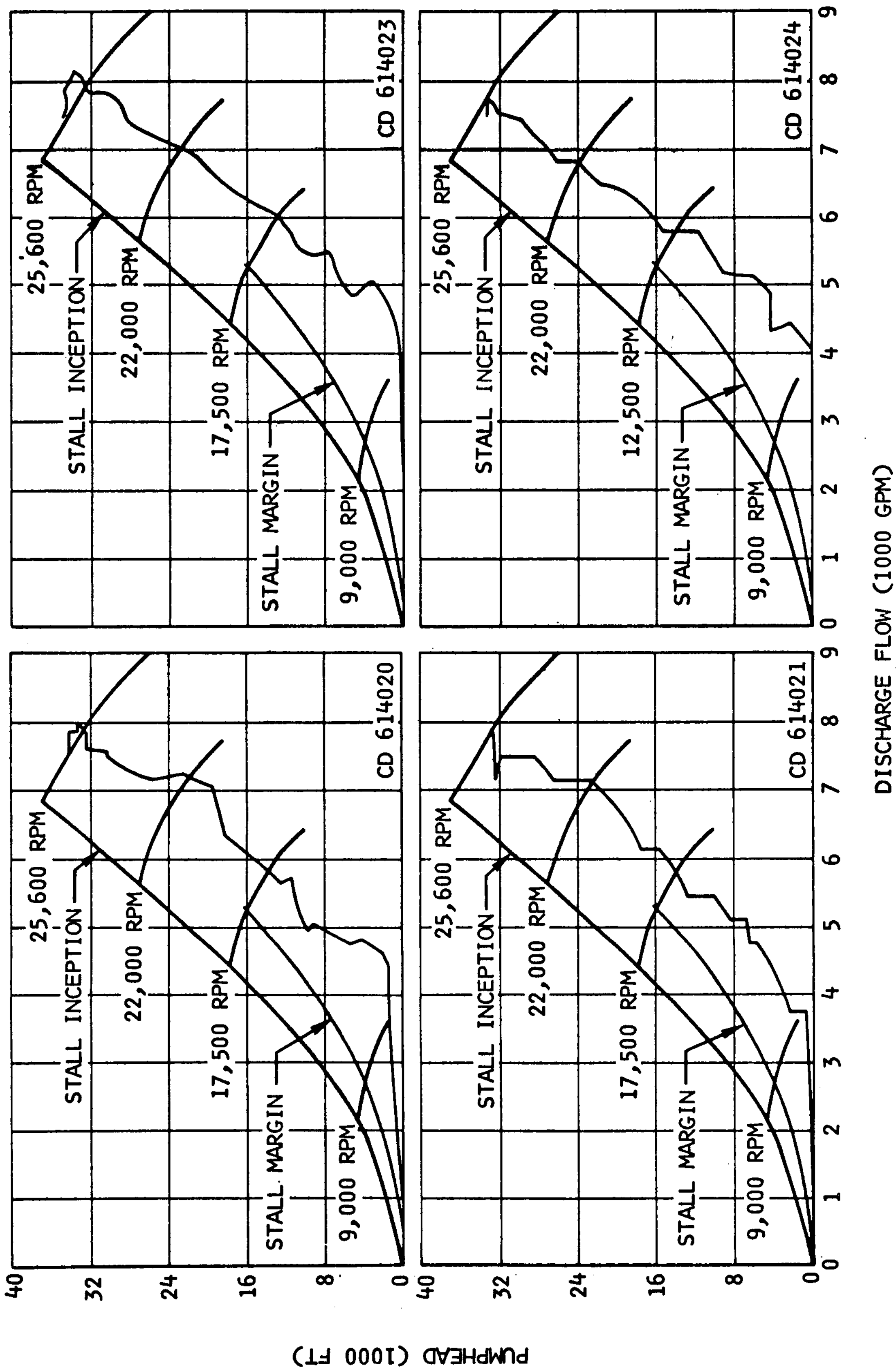

Figure 6-21 LH2 Pump Performance (Engine 2013) - CD 614020 Thru 614024

21 February 1966

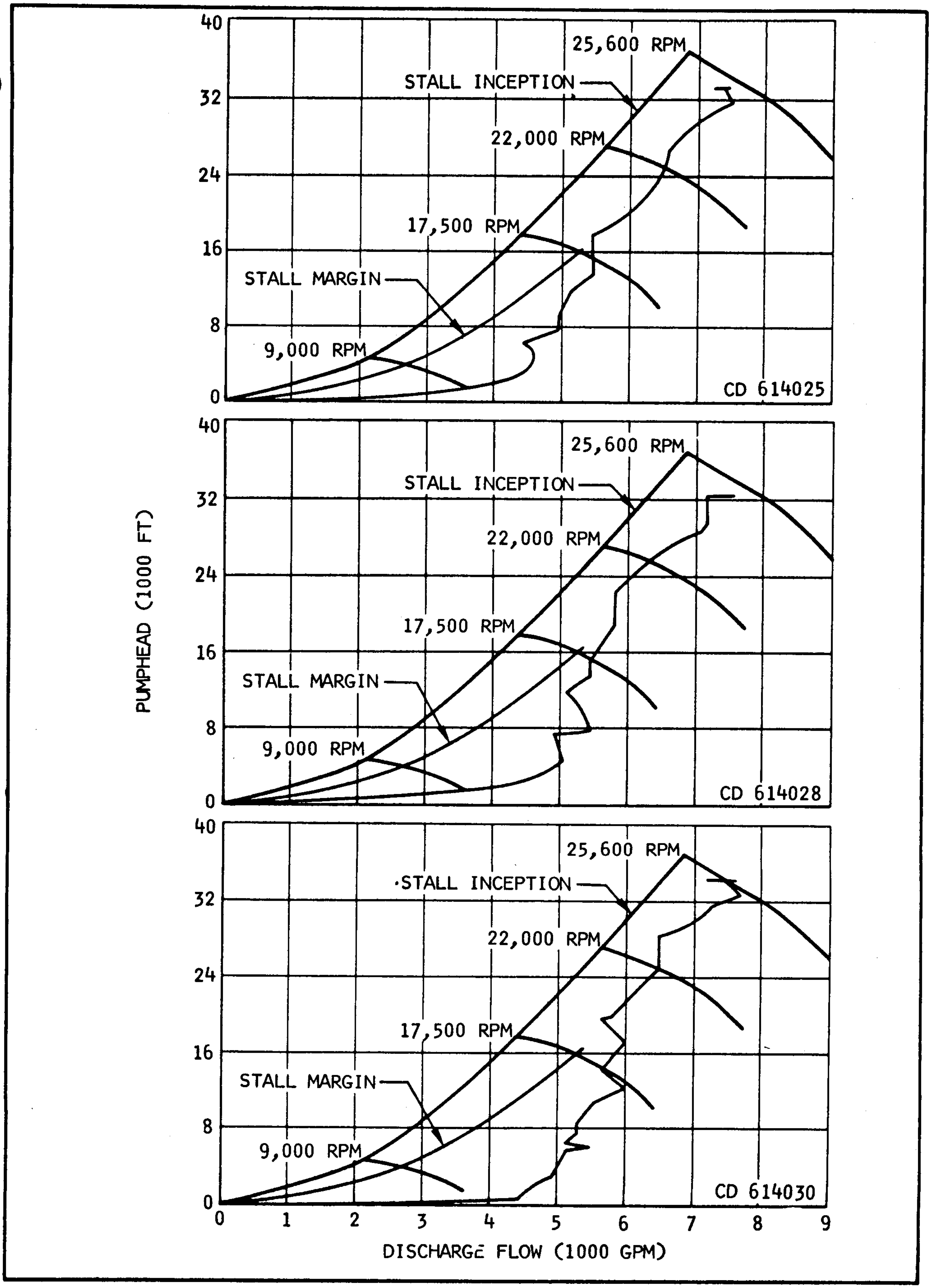

Figure 6-22 LH2 Pump Performance (Engine 2013) - CD 614025 Thru 614030

21 February 1966

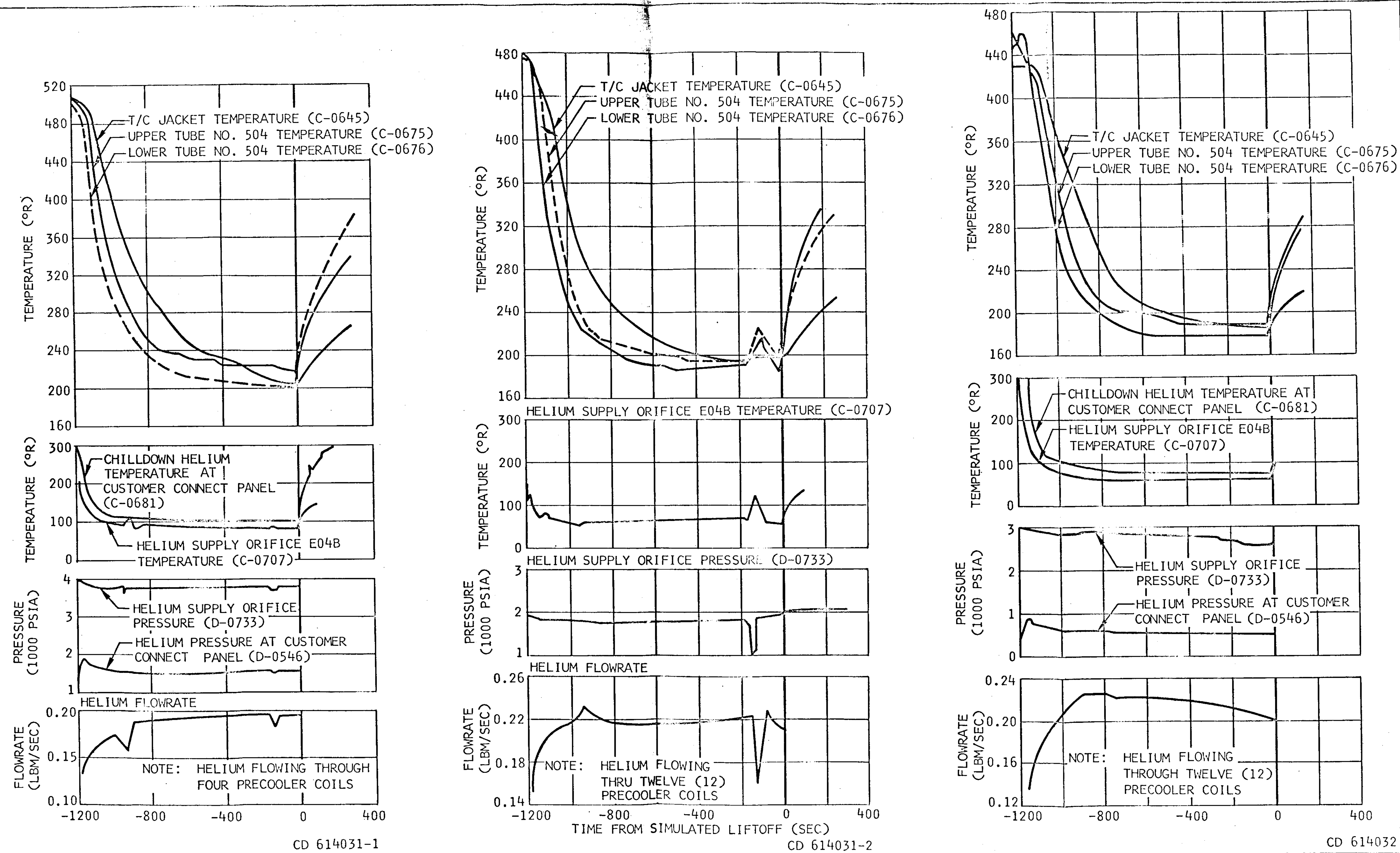

Figure 6-23 Thrust Chamber Childown With Aft Interstage Inclosed

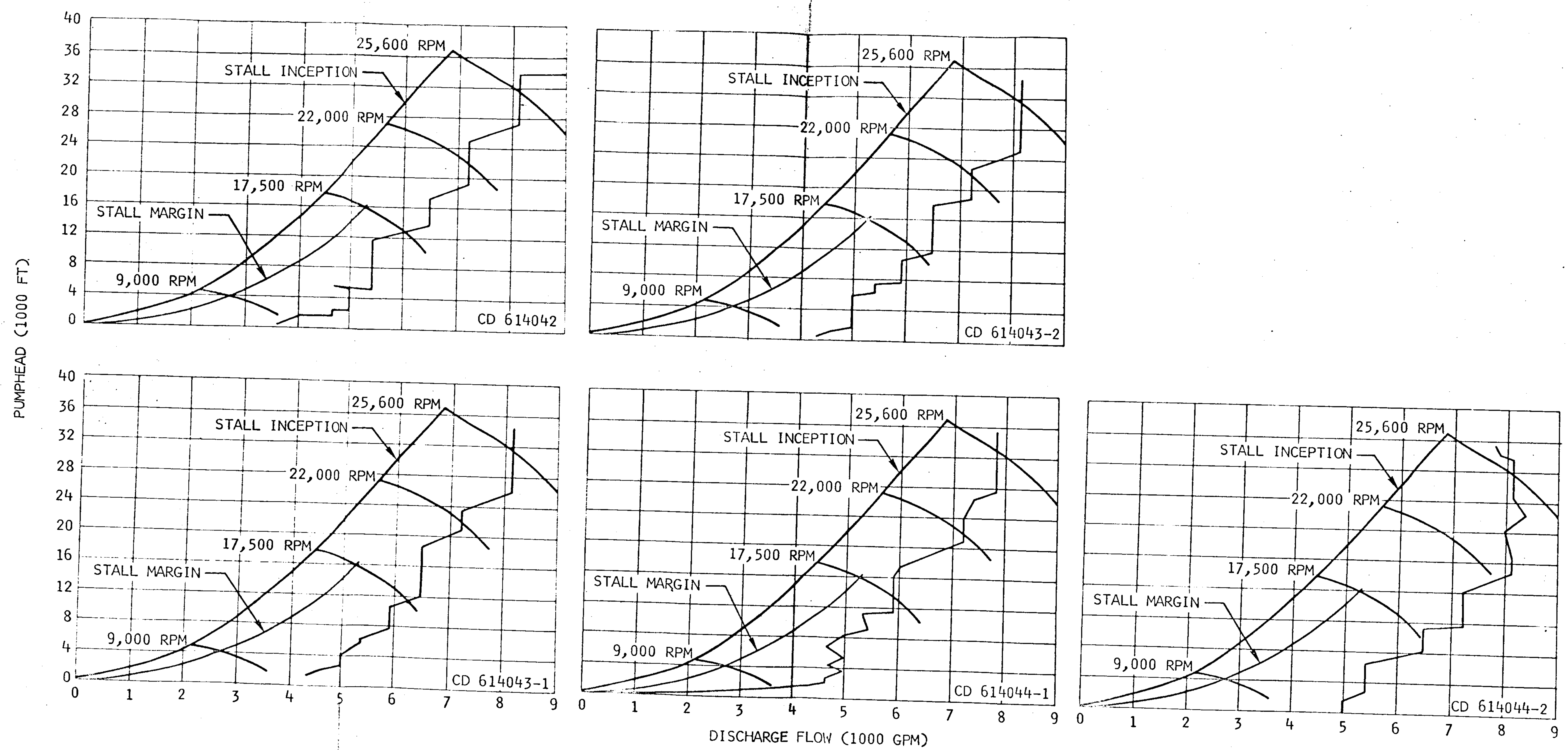

Figure 6-24 LH2 Pump Performance (Engine J-2020)

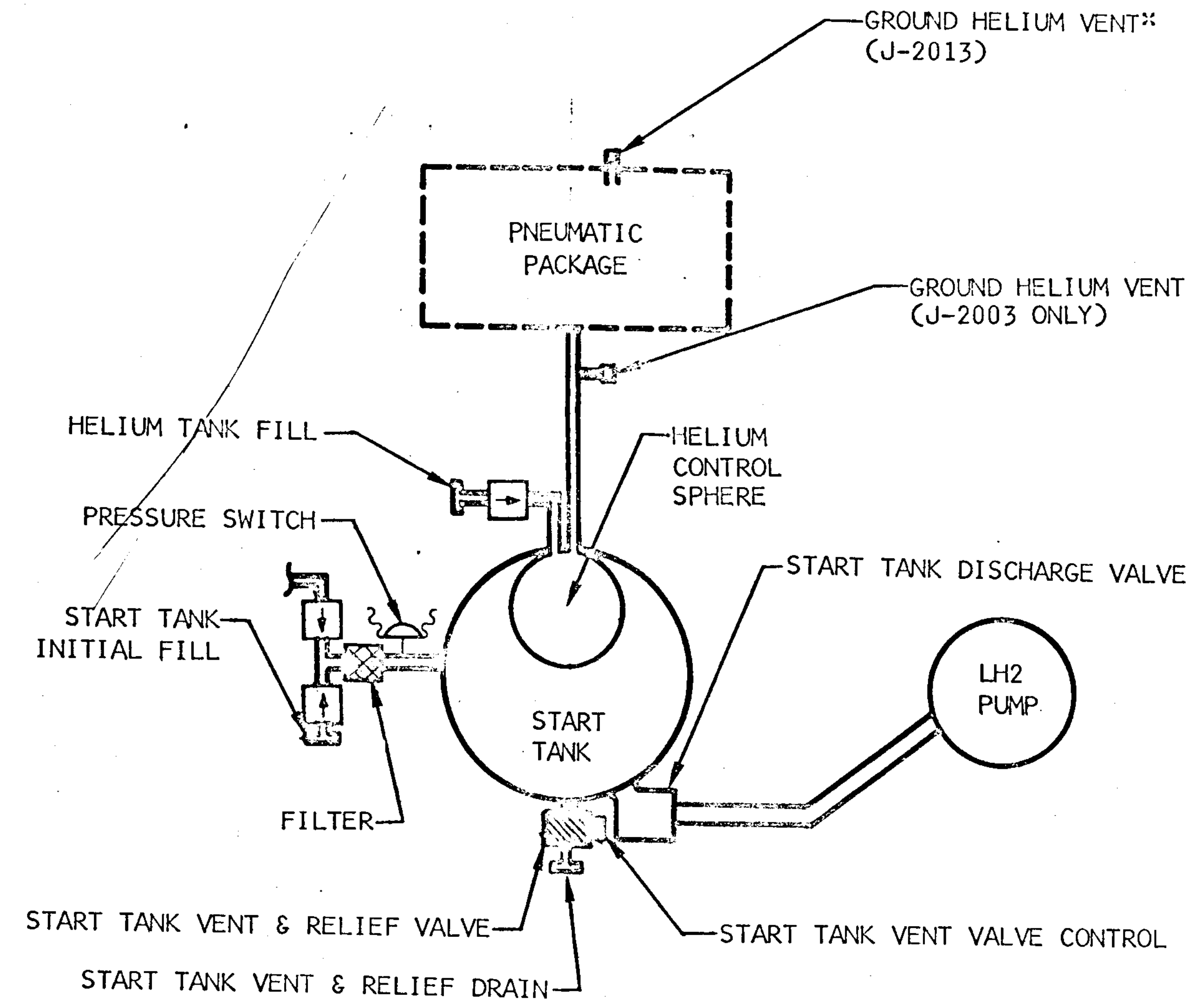

*THE GROUND HELIUM VENT IS NOW LOCATED IN THE PNEUMATIC PACKAGE ON J-2013 ENGINE. PREVIOUSLY, THIS VENT WAS LOCATED ON A TEE AT THE INLET TO THE PNEUMATIC PACKAGE ON J-2003 ENGINE.

Figure 6-25 Helium Control Sphere and Start Tank (Engine J-2013)

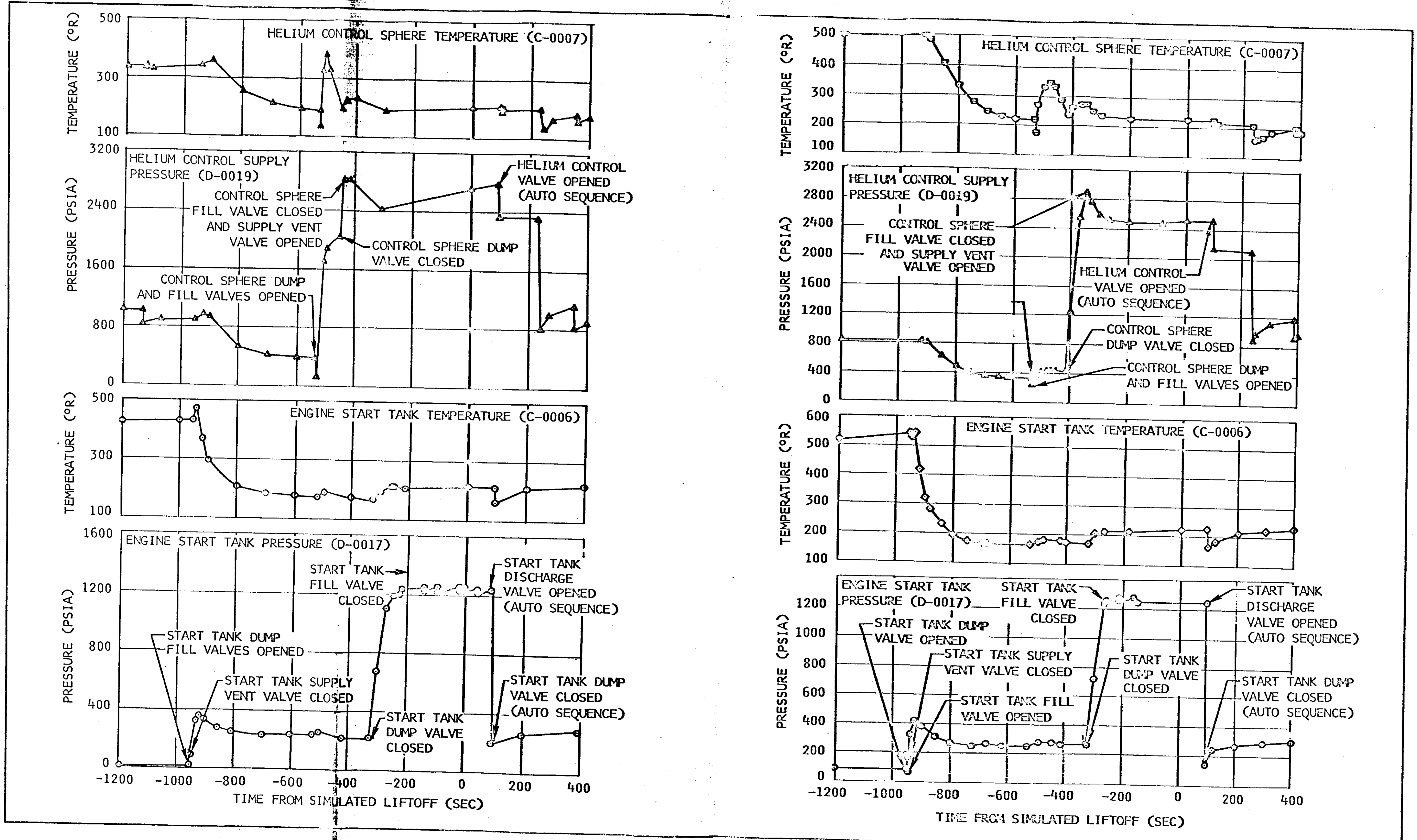

Figure 6-26 Engine Helium Control Sphere and Start Tank Results - CD 614005

21 February 1966

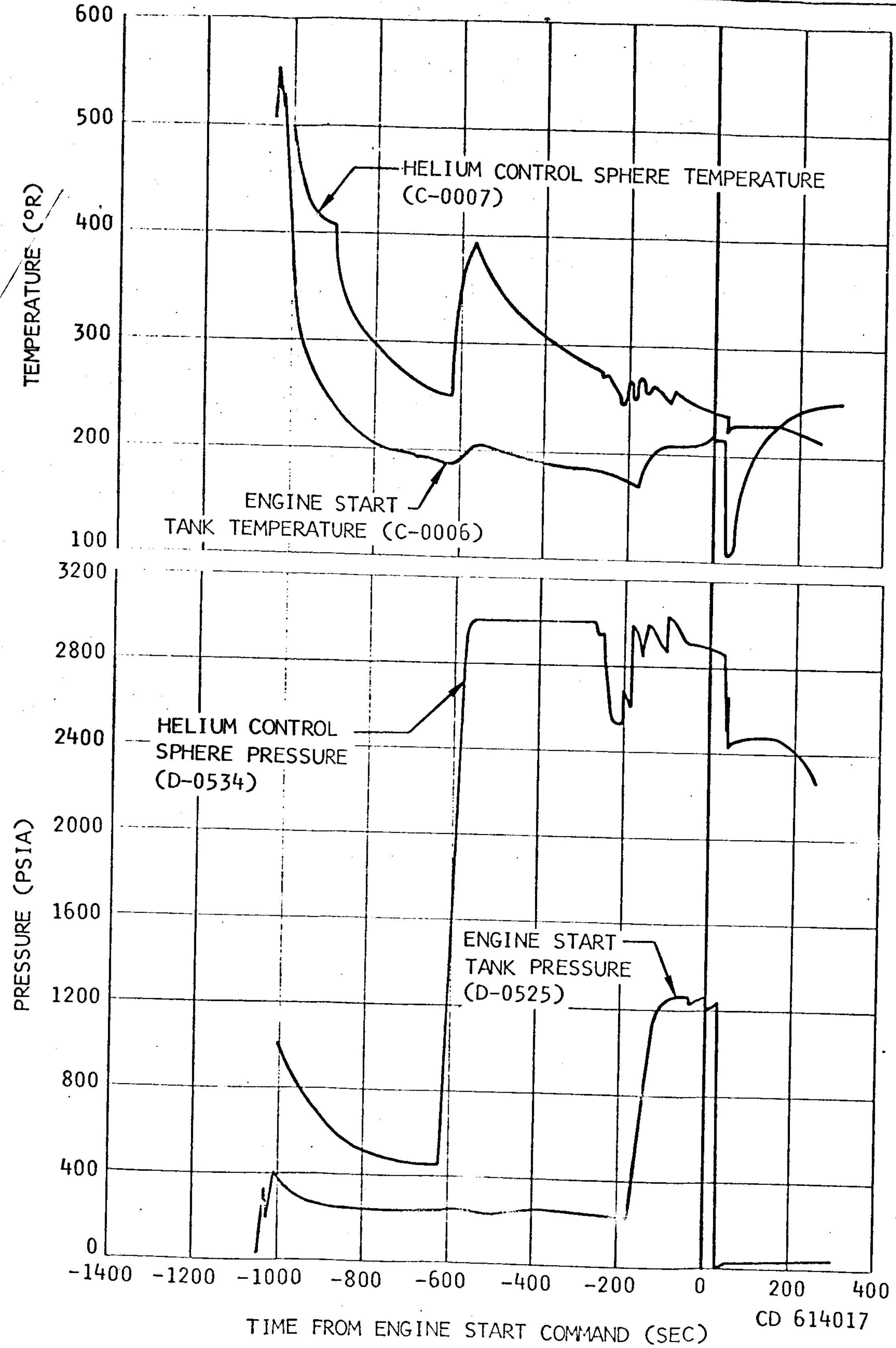

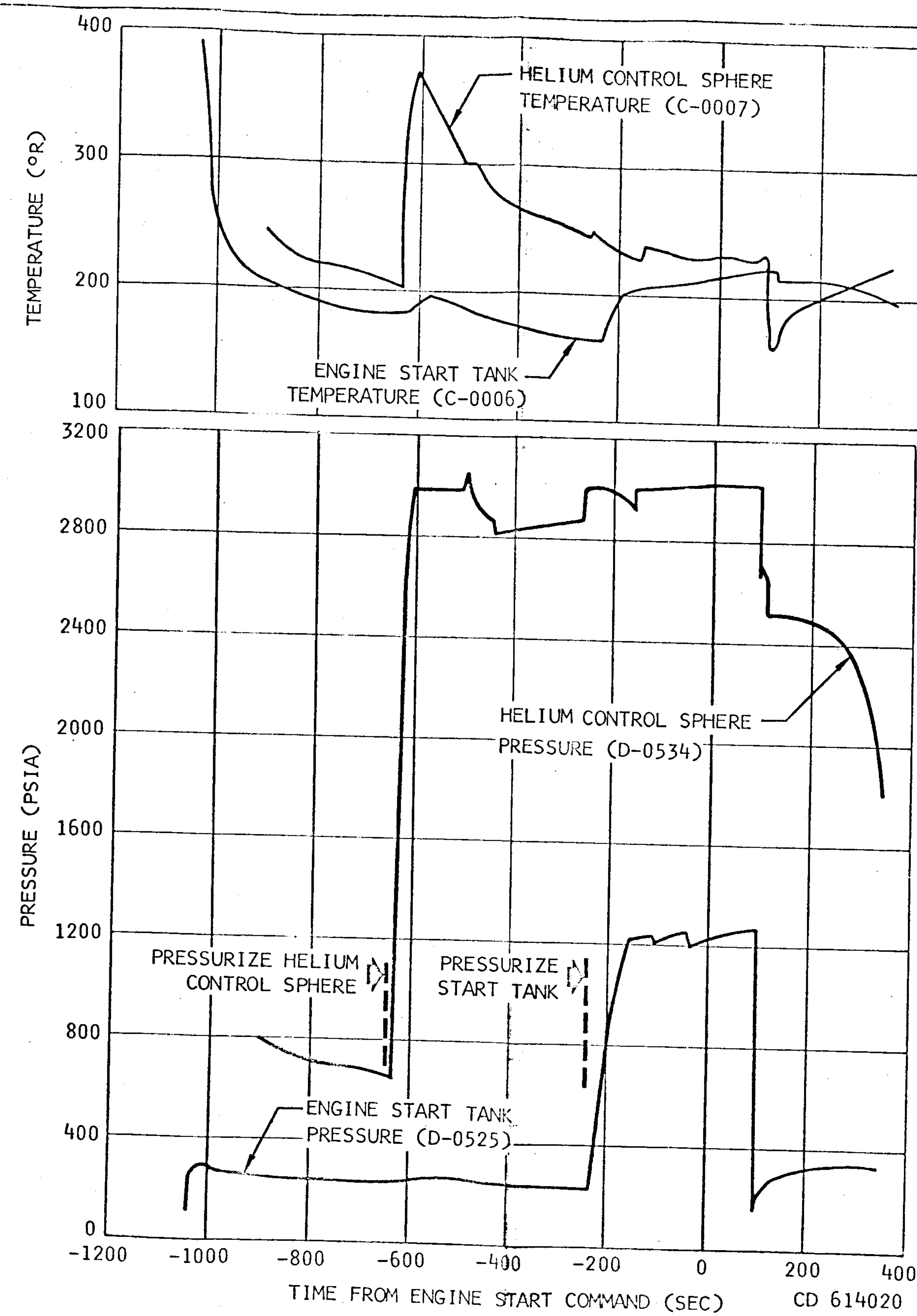

Figure 6-27 Engine Helium Control Sphere and Start Tank Operation

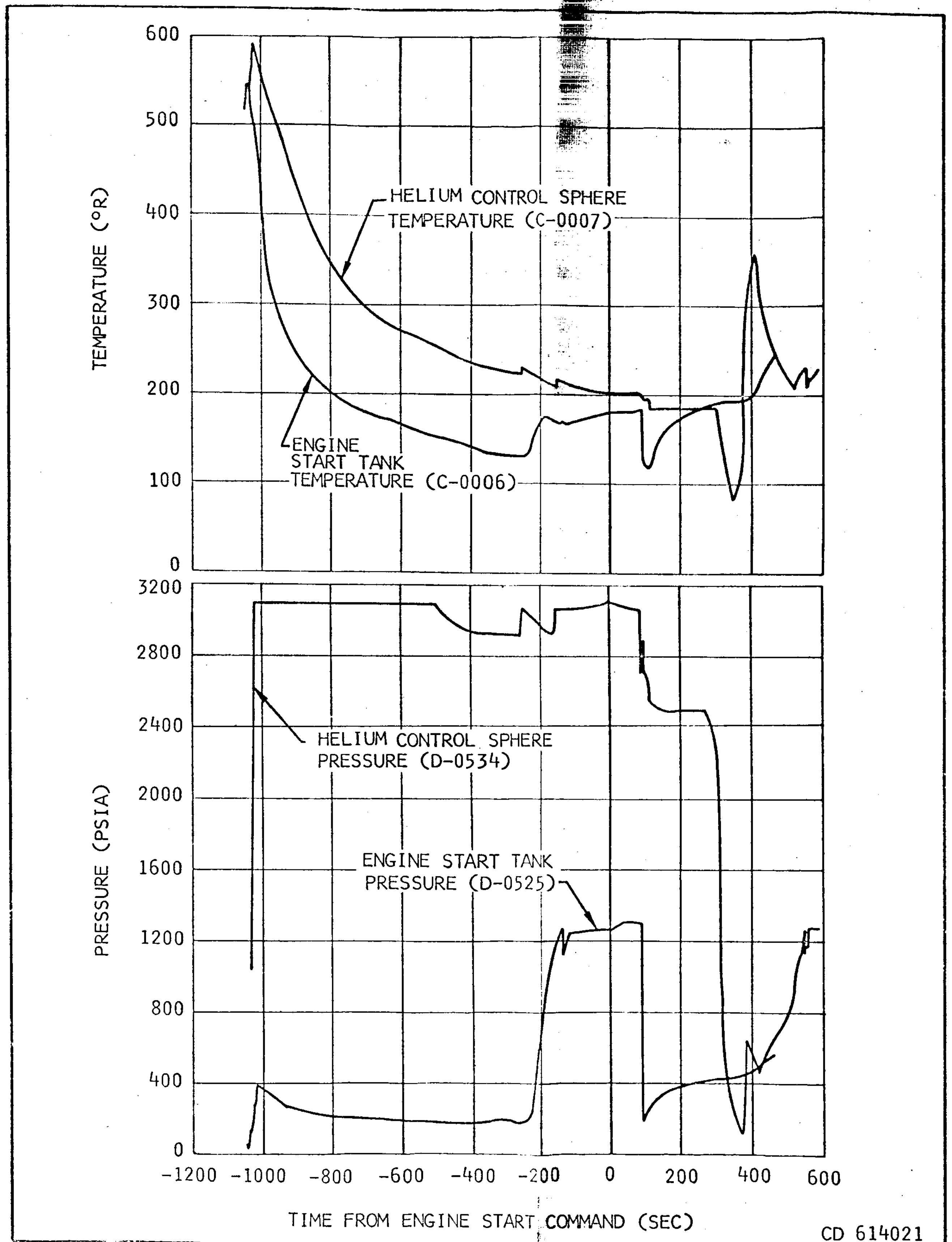

Figure 6-28 Engine Helium Control Sphere and Start Tank Performance

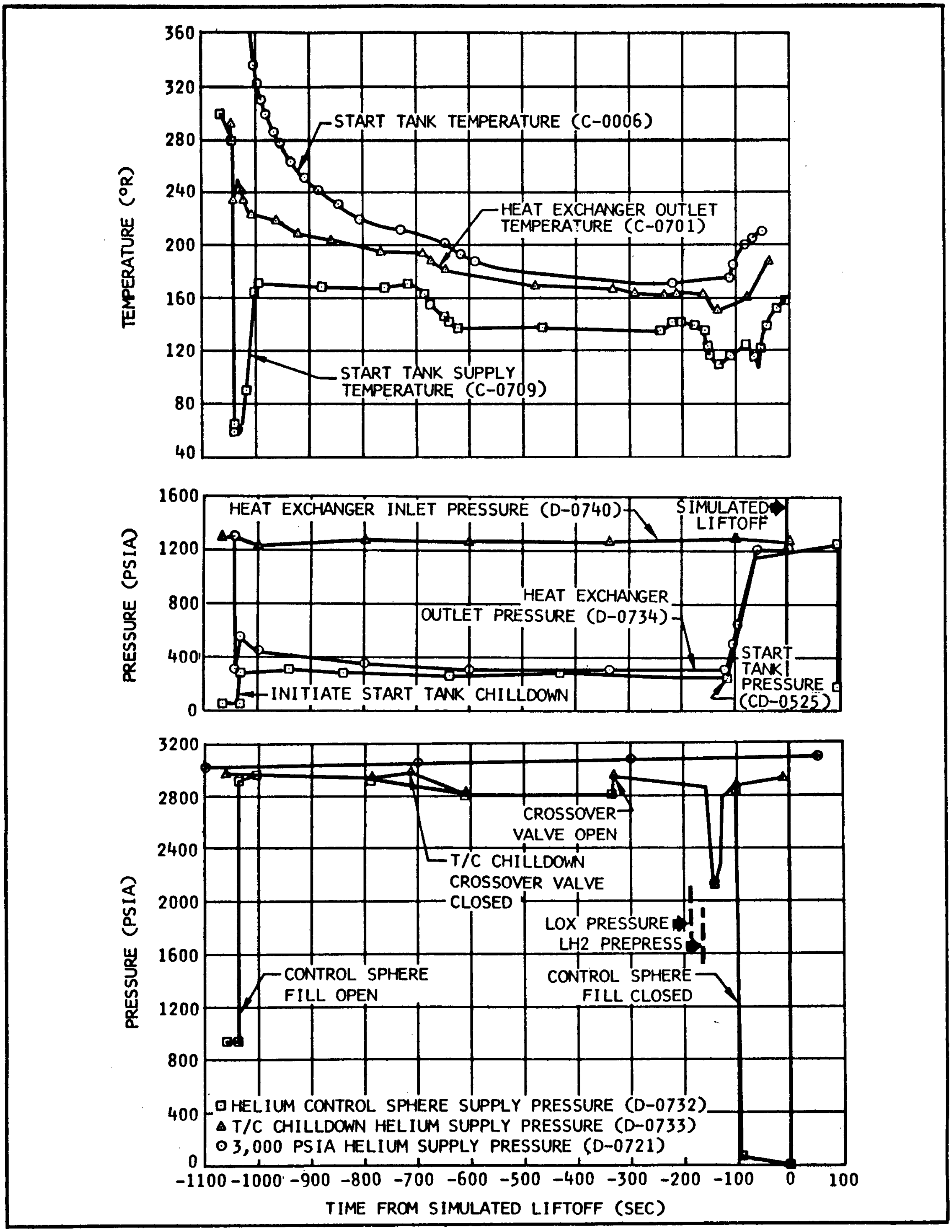

Figure 6-29 Gas Heat Exchanger Performance - CD 614030

21 February 1966

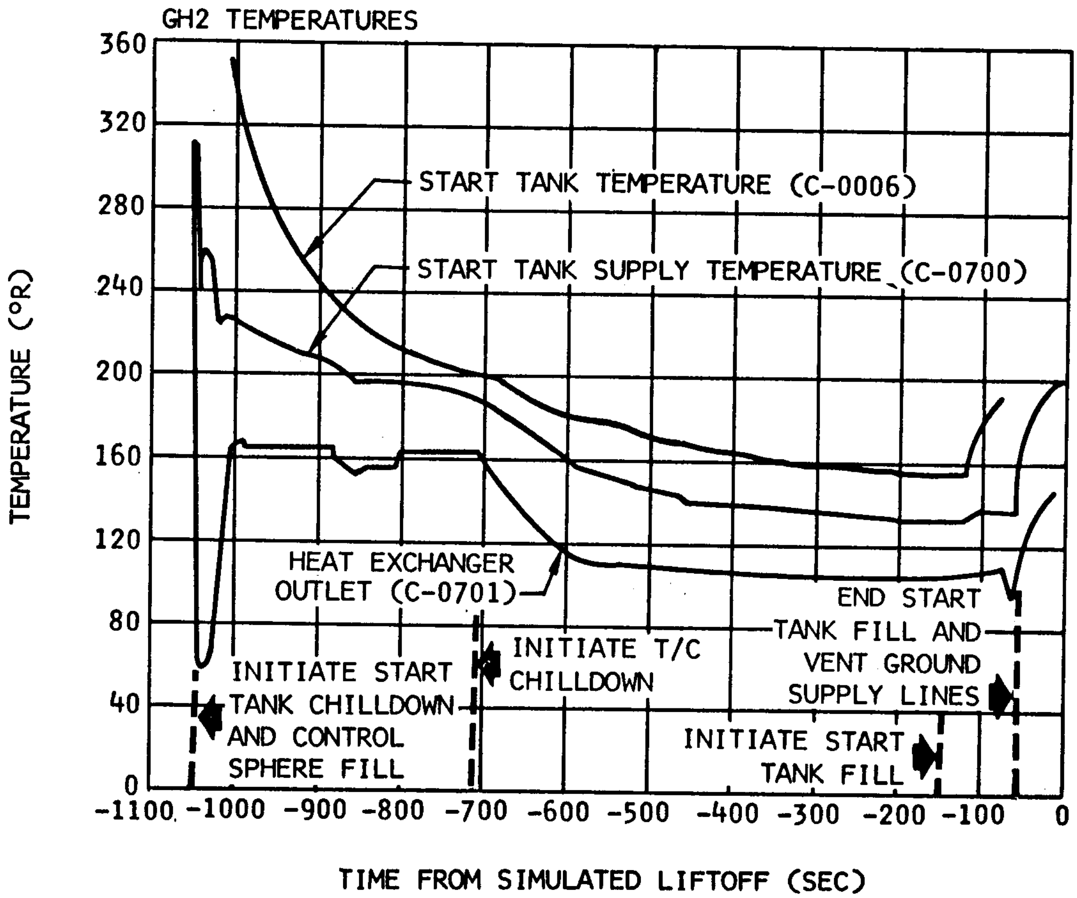

Figure 6-30 Gas Heat Exchanger Performance - CD 614025

21 February 1966

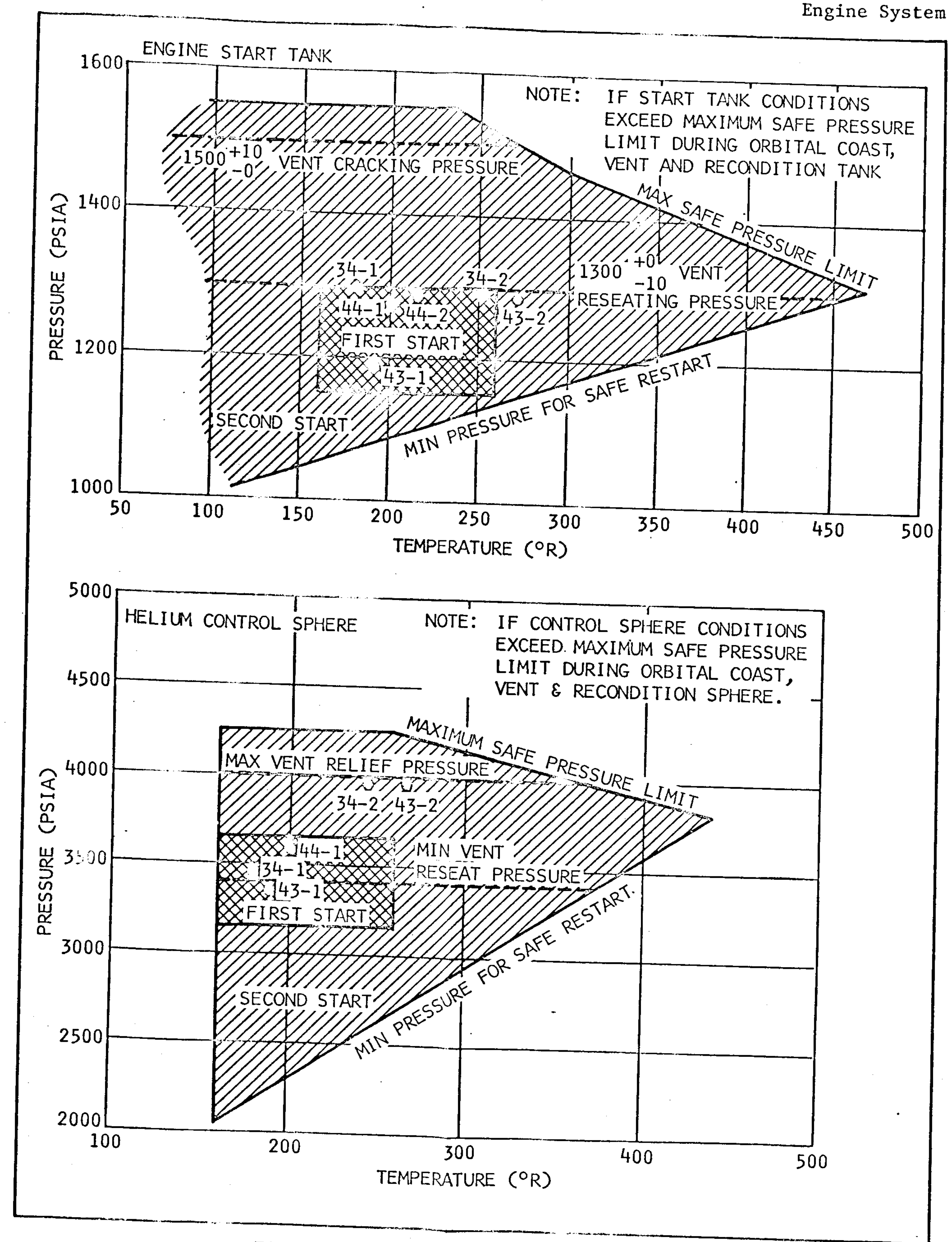

Figure 6-31 Engine Start Requirements

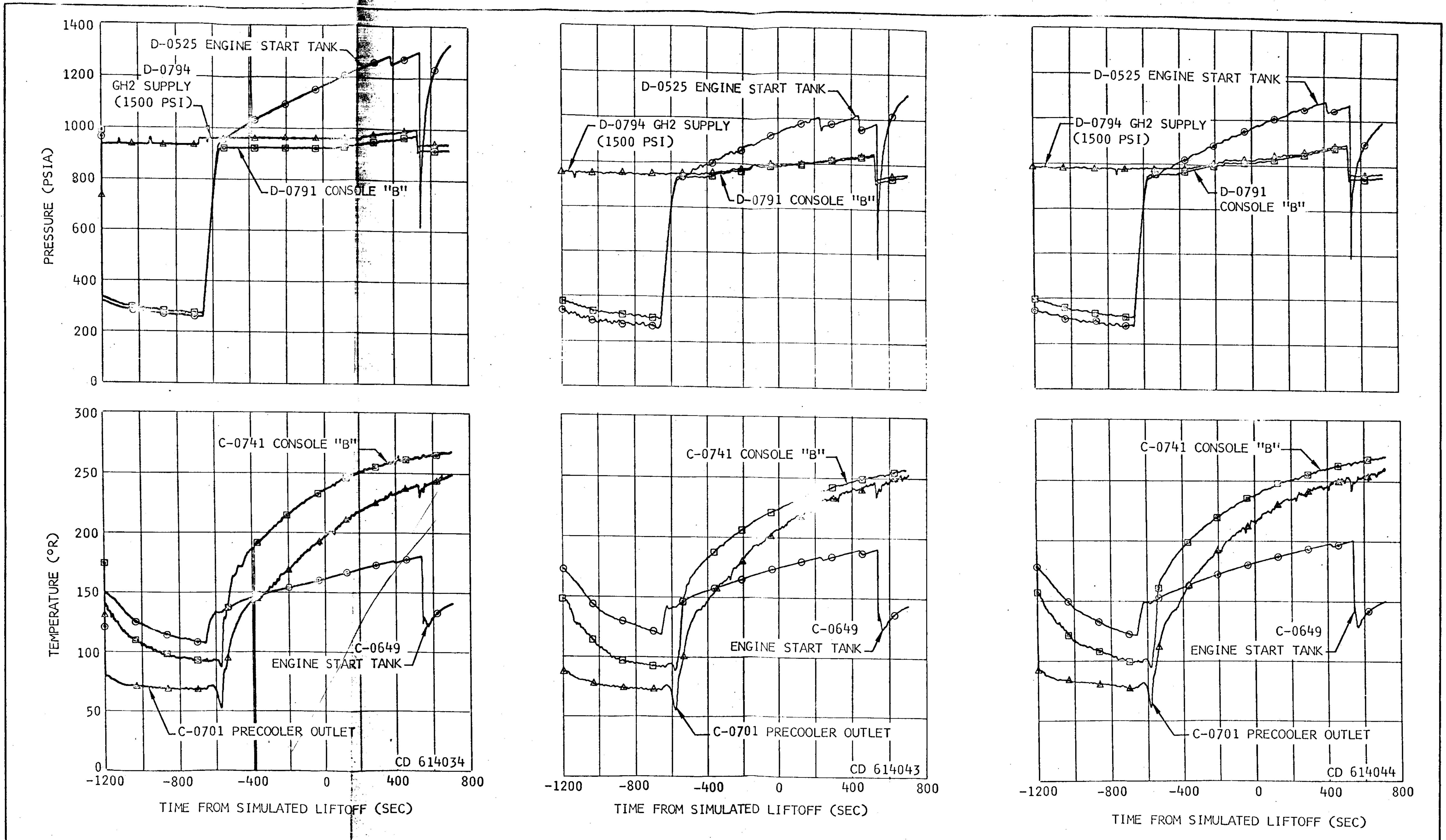

Figure 6-32 Engine Start Tank Performance

21 February 1966

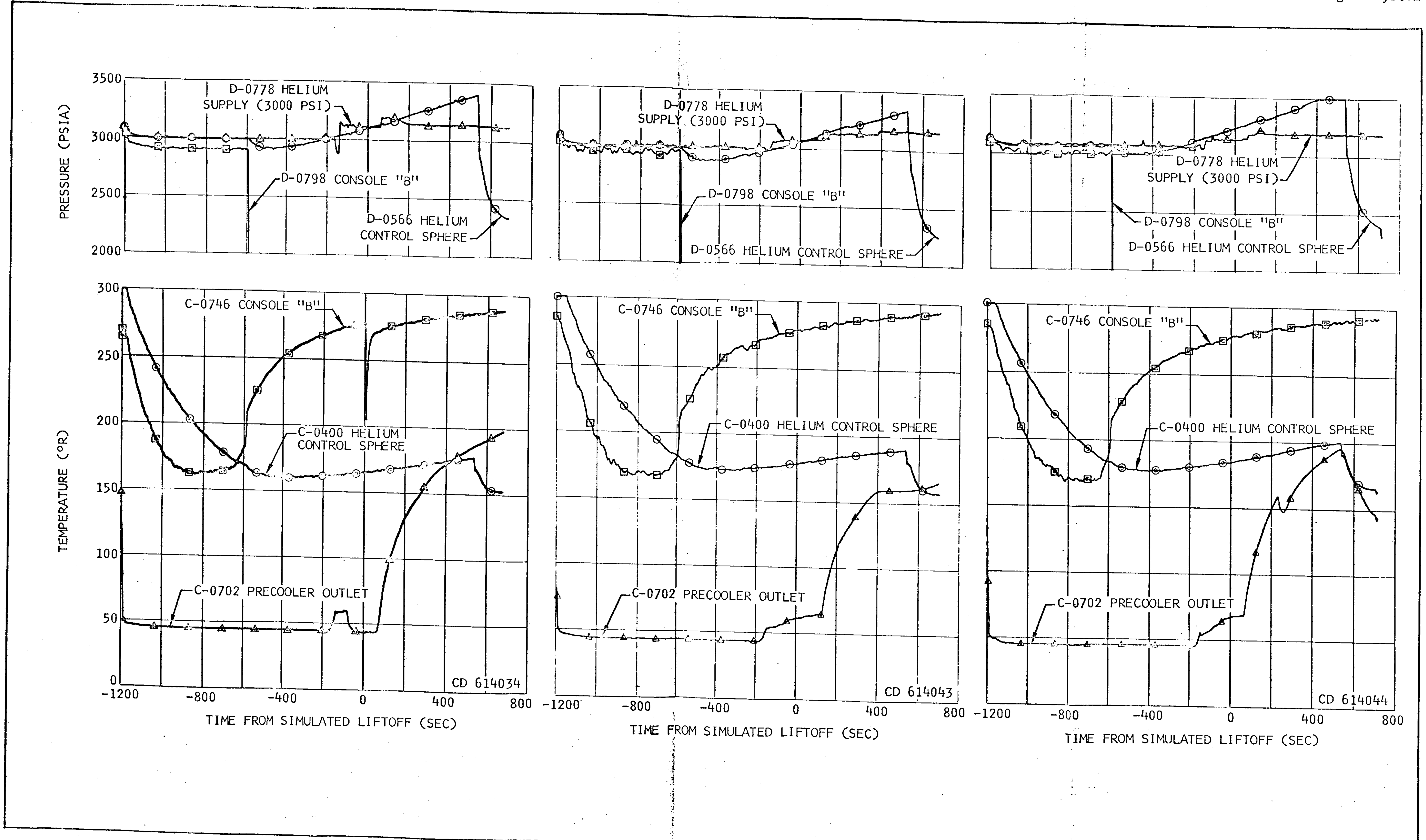

Figure 6-33 Engine Helium Control Sphere Data

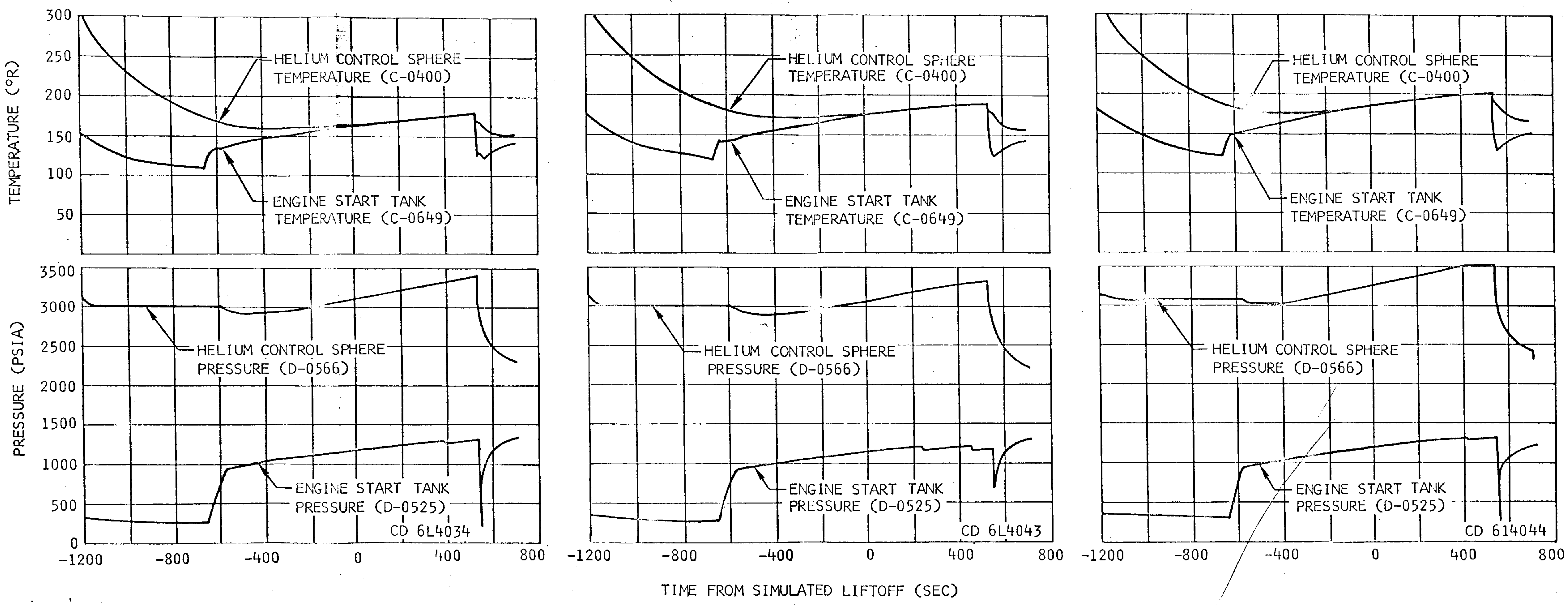

Figure 6-34 Engine Helium Control Sphere and Start Tank Performance - 1st Burn

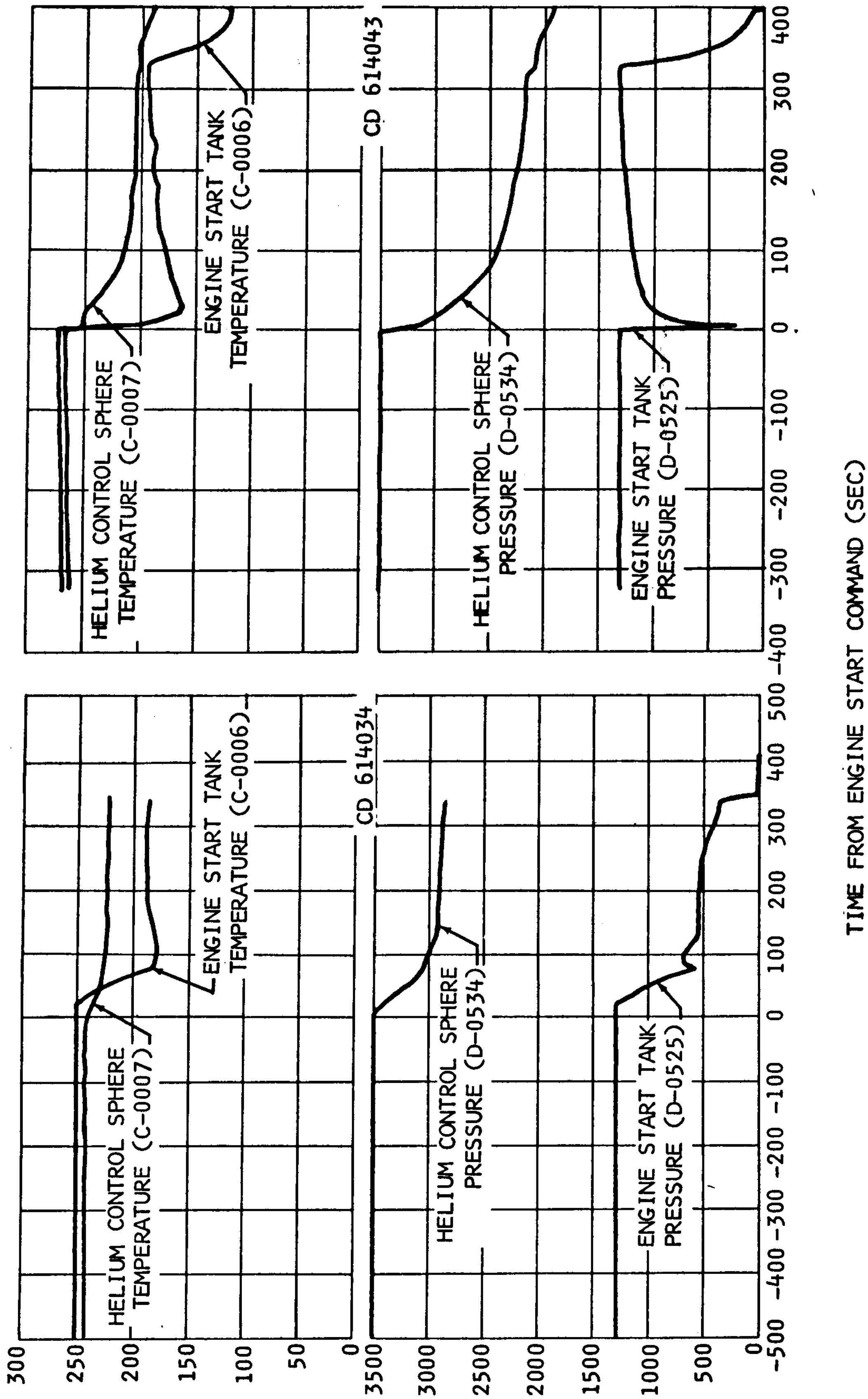

Figure 6-35 Engine Helium Control Sphere and Start Tank Performance - 2nd Burn

21 February 1966

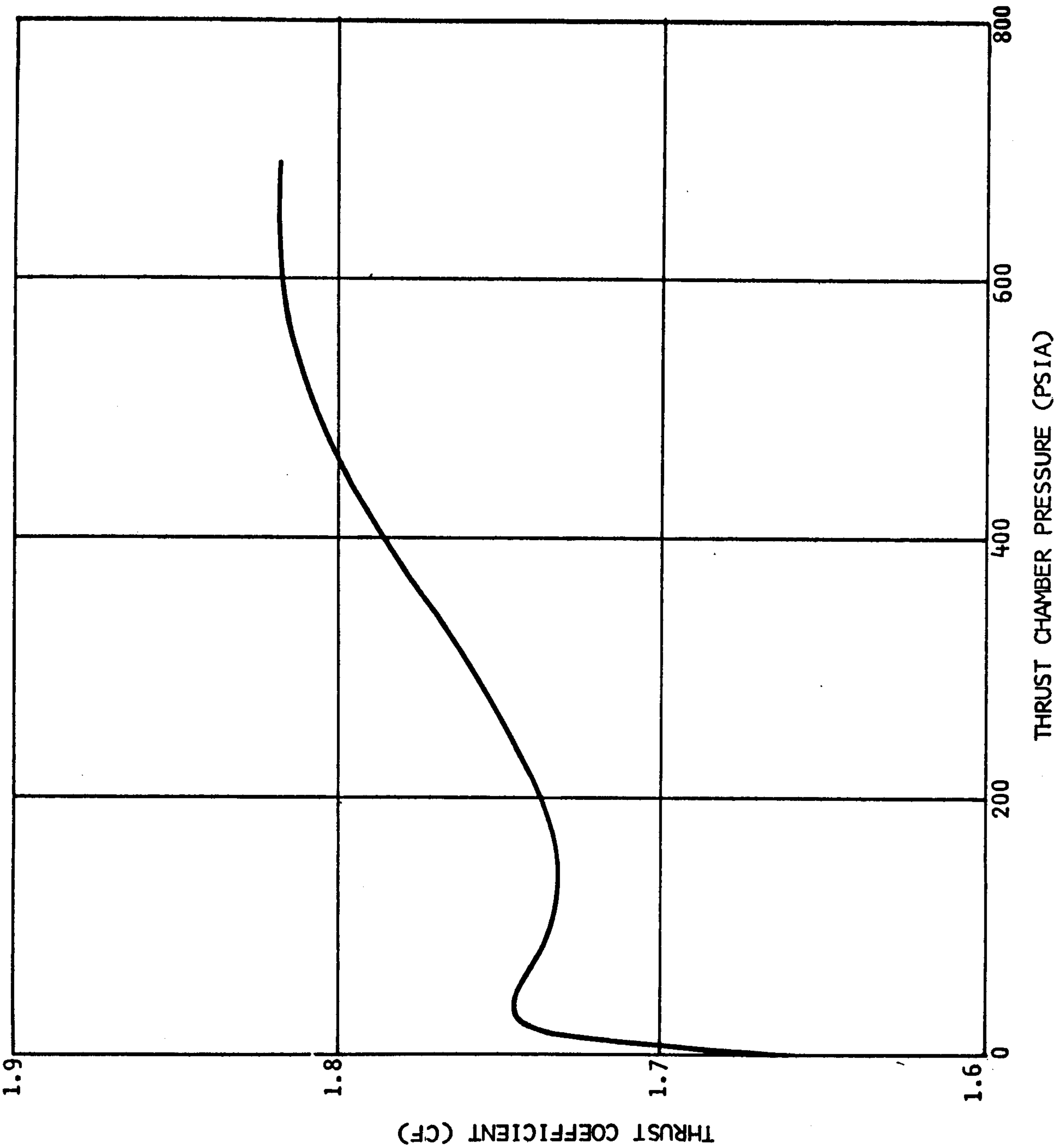

Figure 6-36 Thrust Coefficient as Affected By Thrust Chamber Pressure

21 February 1966

[redacted]

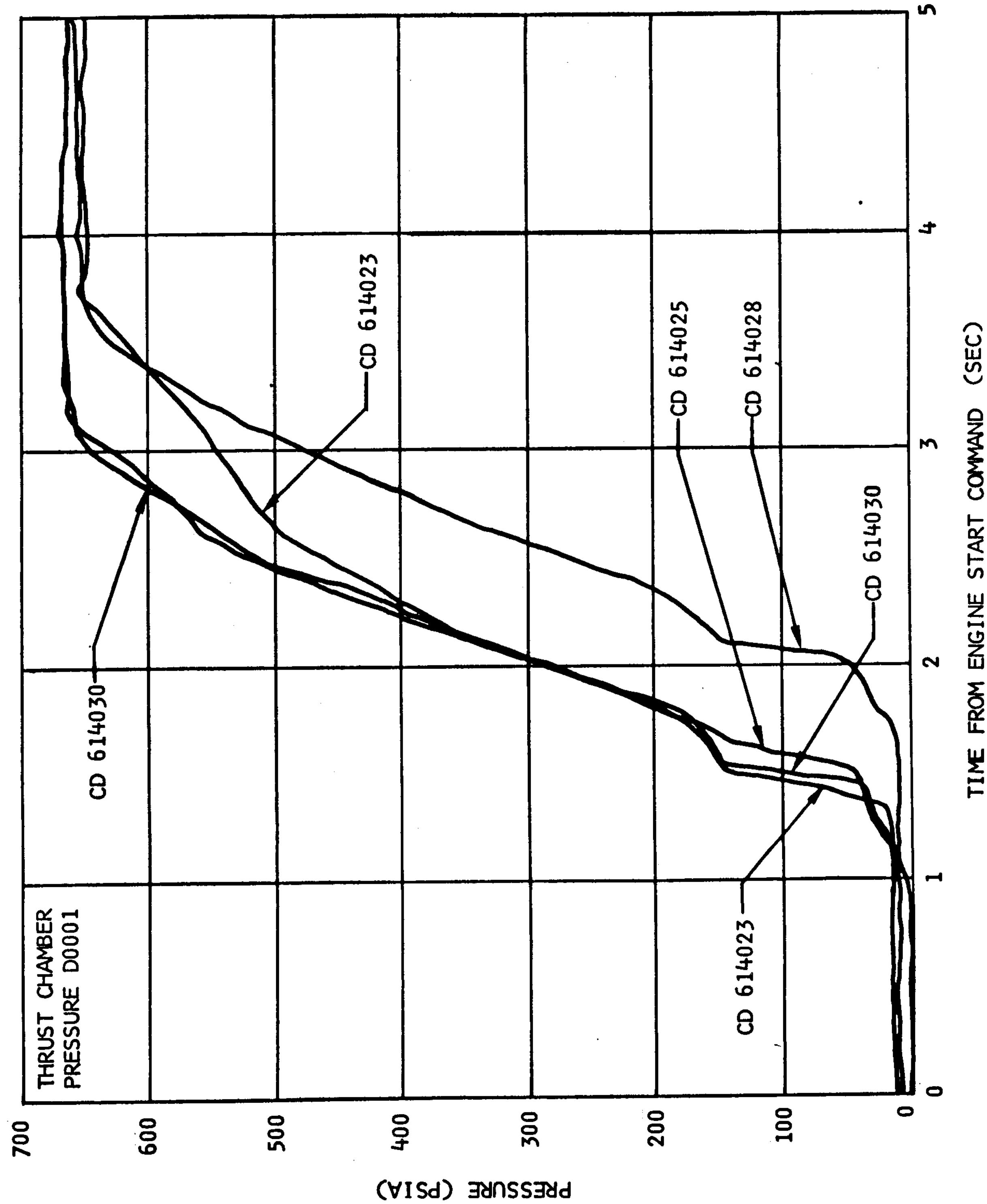

Figure 6-37 Thrust Chamber Pressure During Start Transients

[redacted]

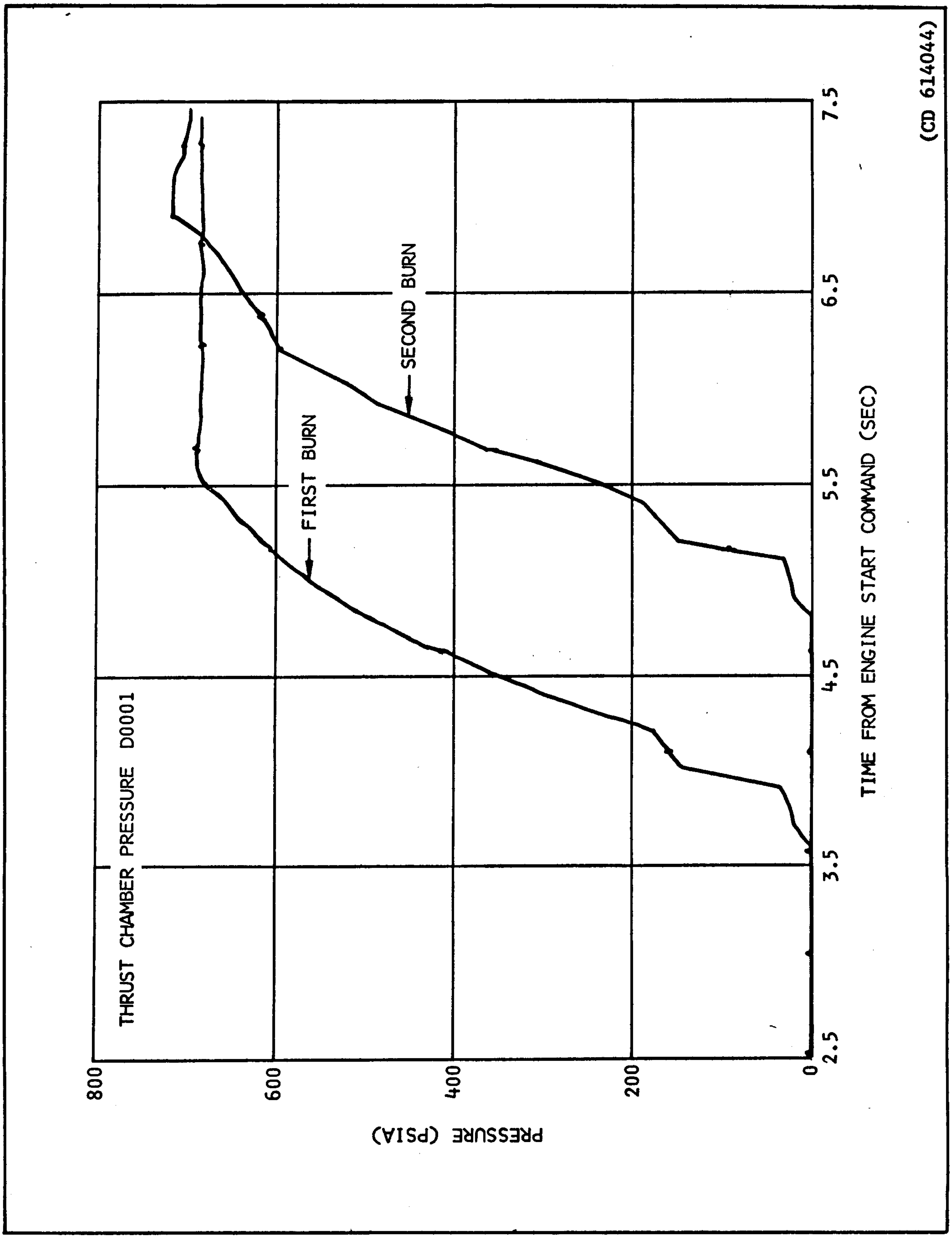

Figure 6-38 Thrust Chamber Pressure Start Transients

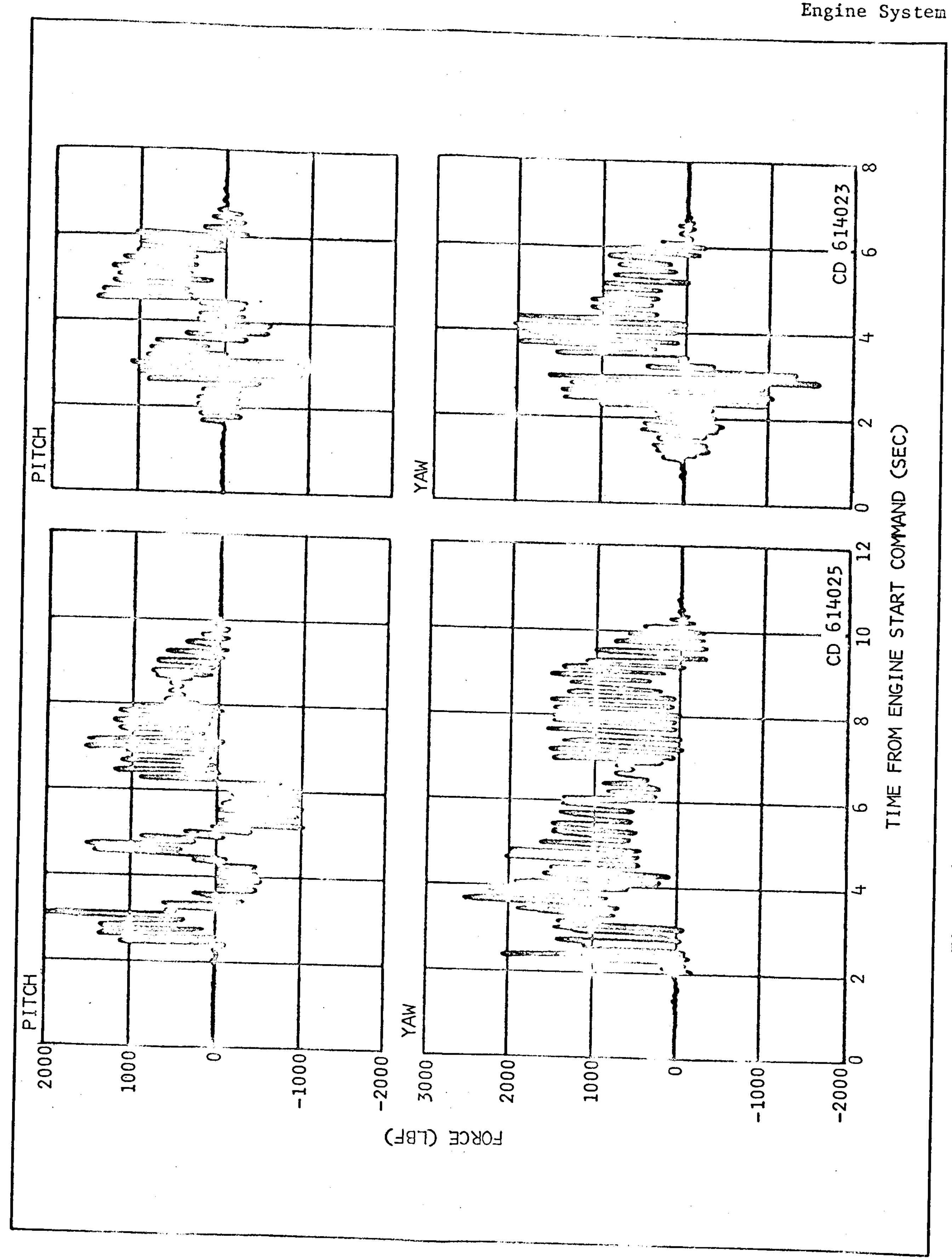

Figure 6-39 Engine Side Loads During Start Transients

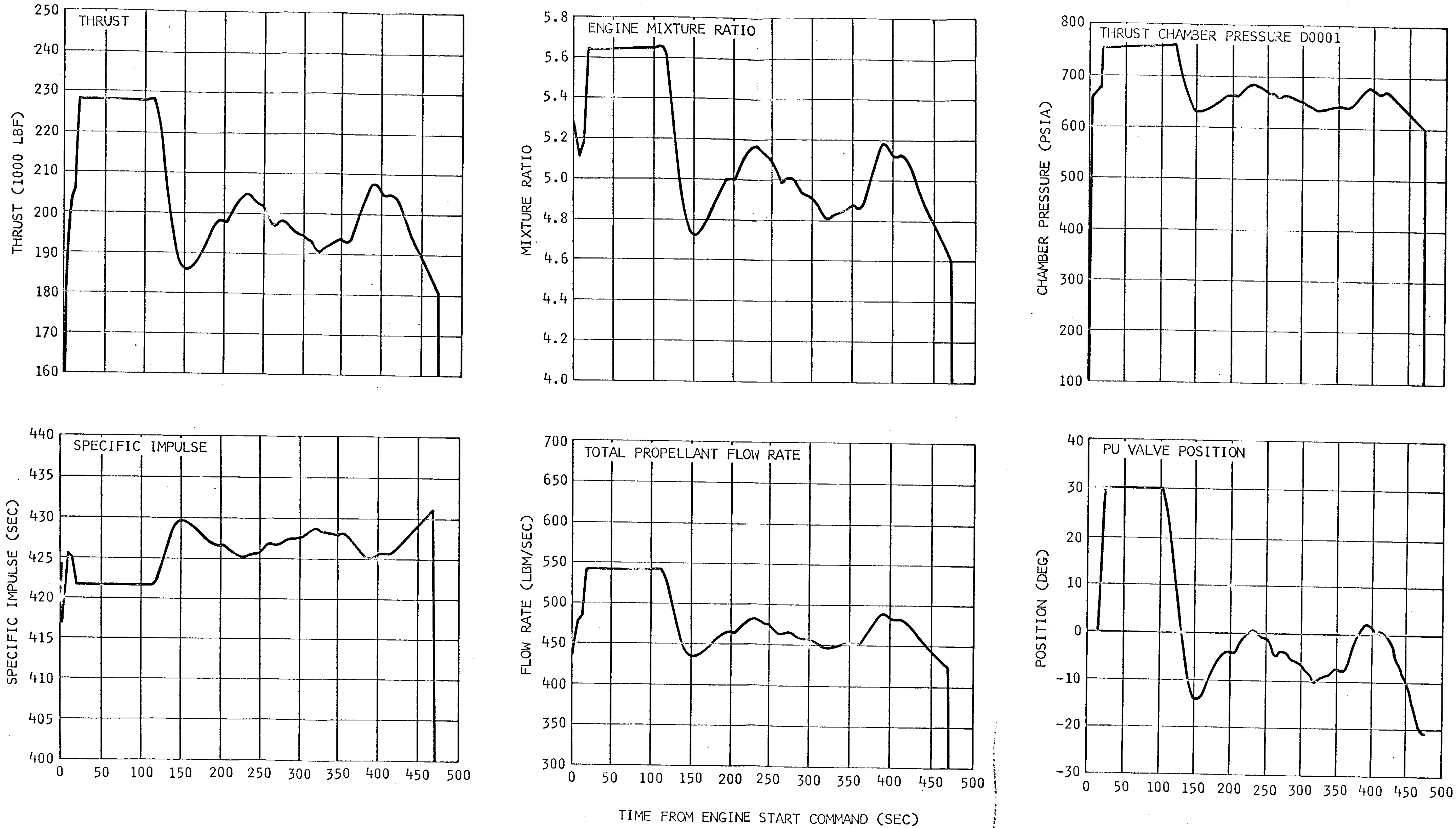

Figure 6-40 Steady State Engine Performance - CD 614023

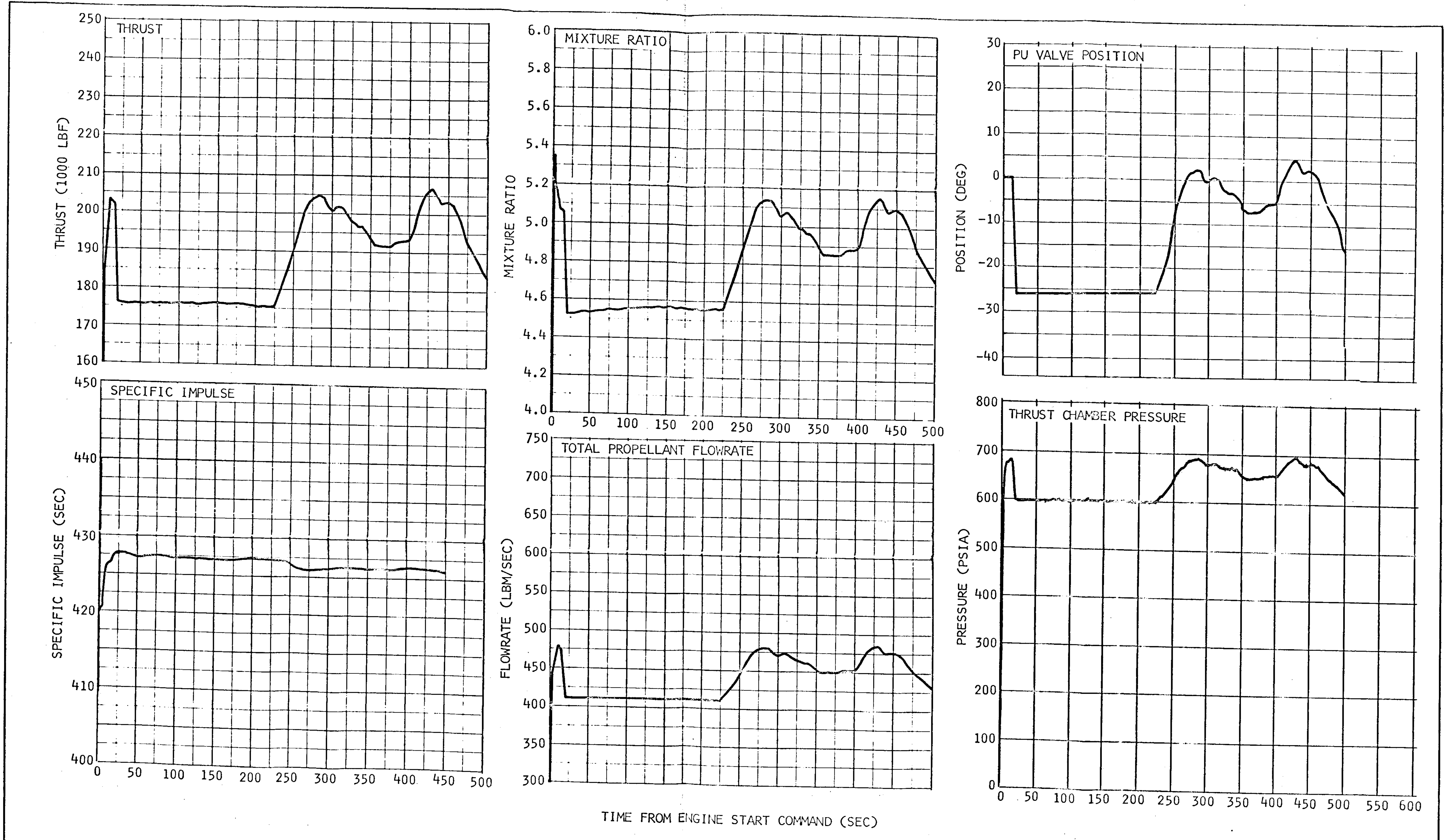

Figure 6-41 Steady State Engine Performance - CD 614025

[redacted]

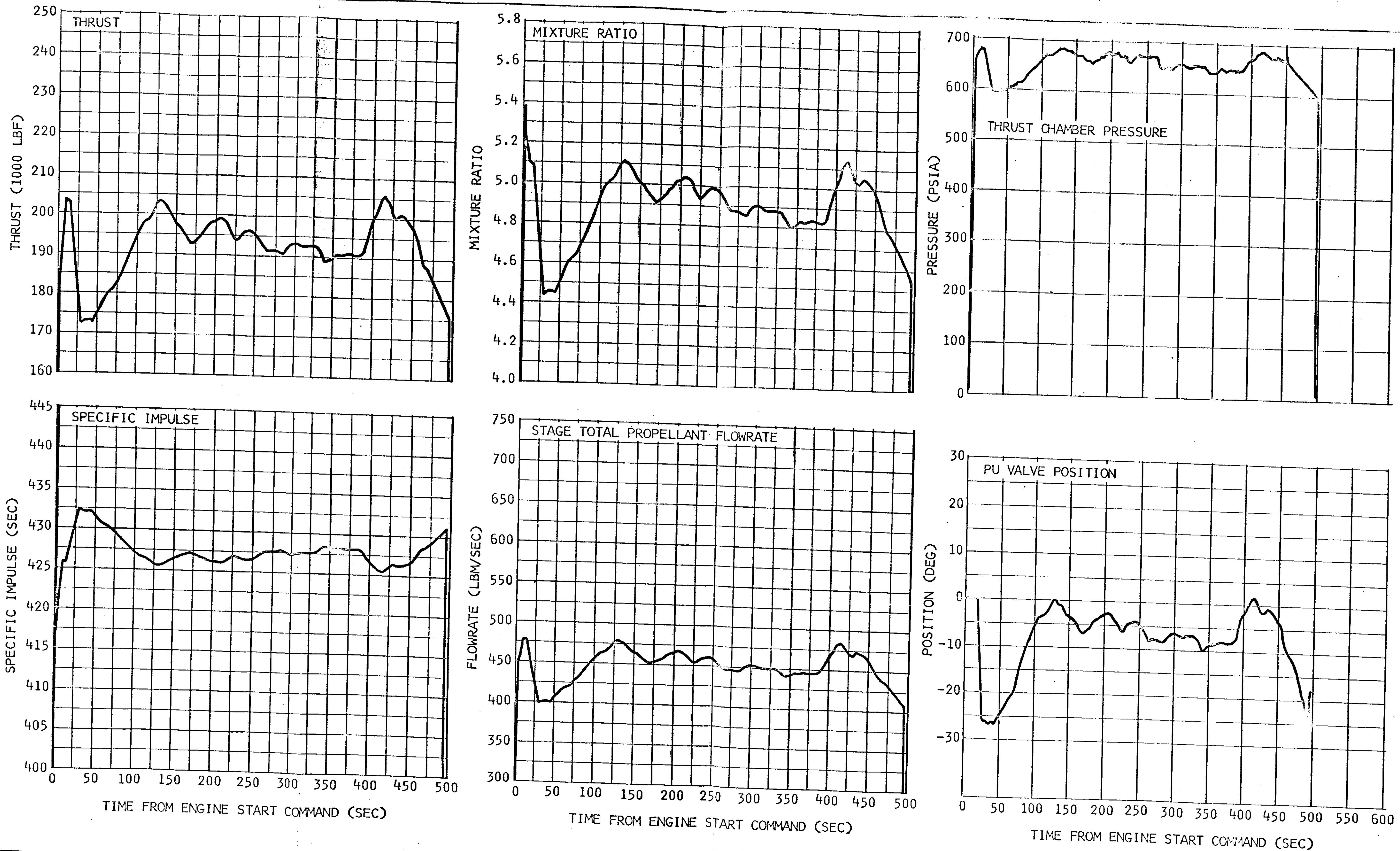

Figure 6-42 Steady State Engine Performance - CD 614030

[redacted]

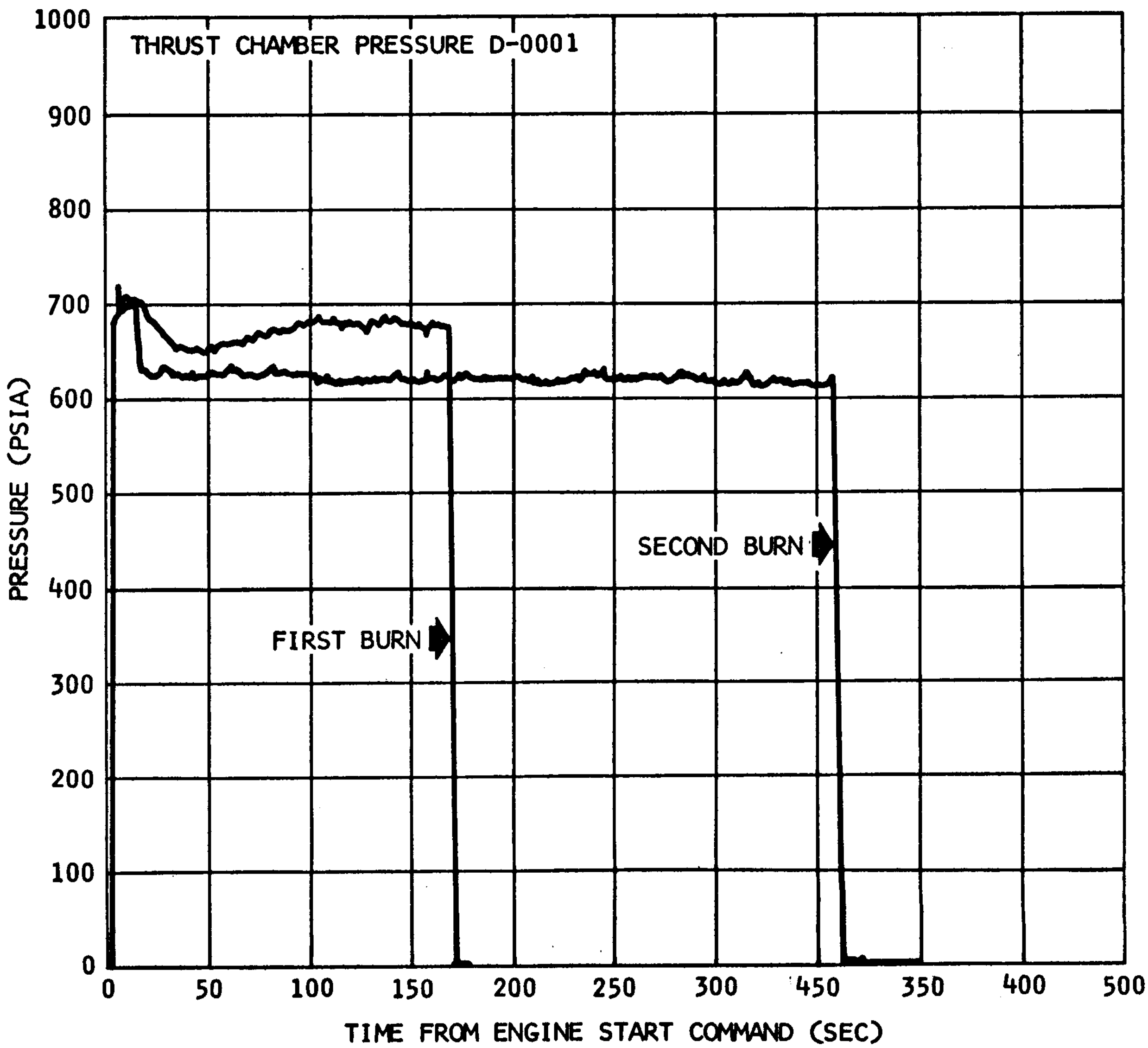

Figure 6-43 Thrust Chamber Pressure During Steady State Operation - CD 614044

21 February 1966

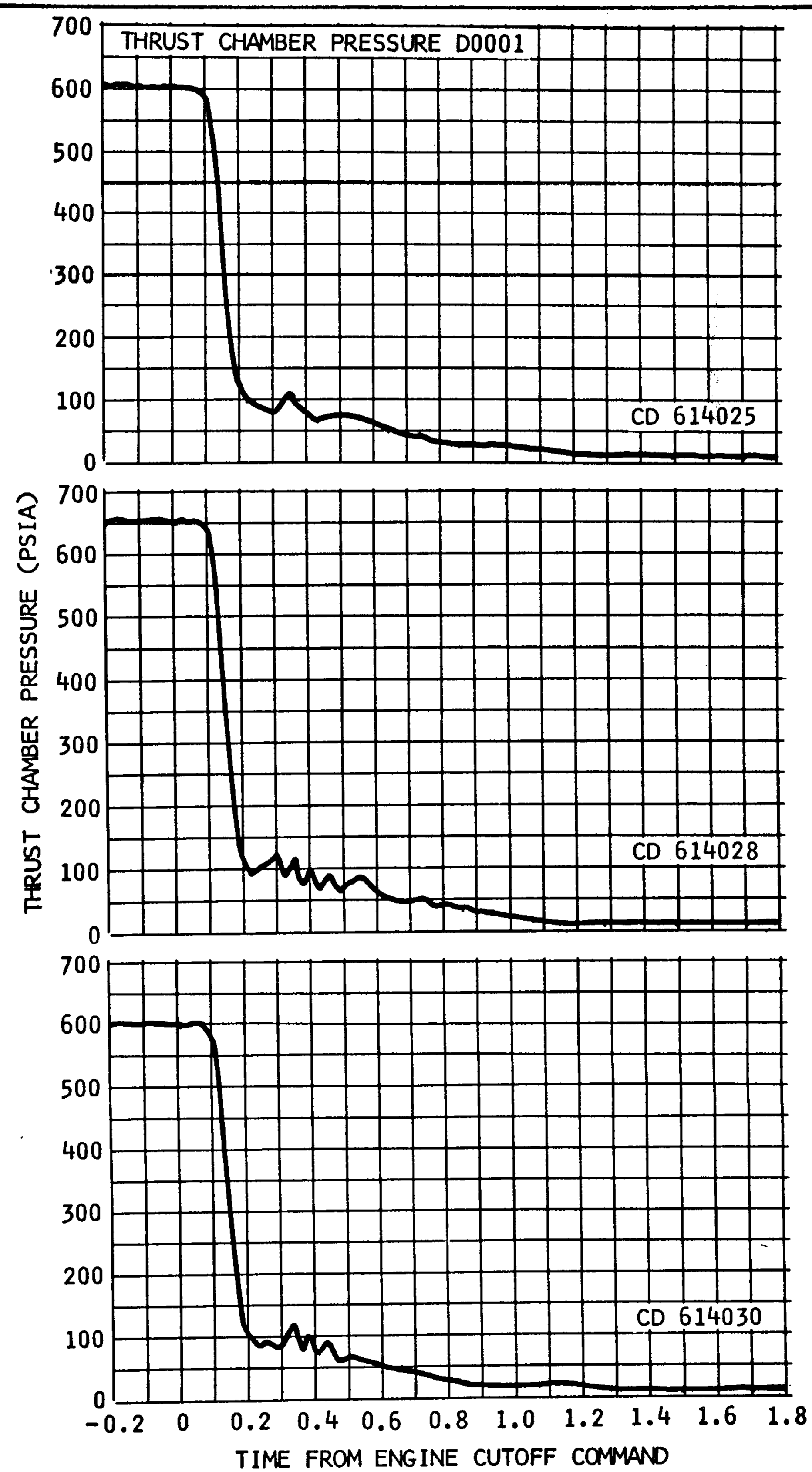

Figure 6-44 Thrust Chamber Pressure Cutoff Transients

21 February 1966

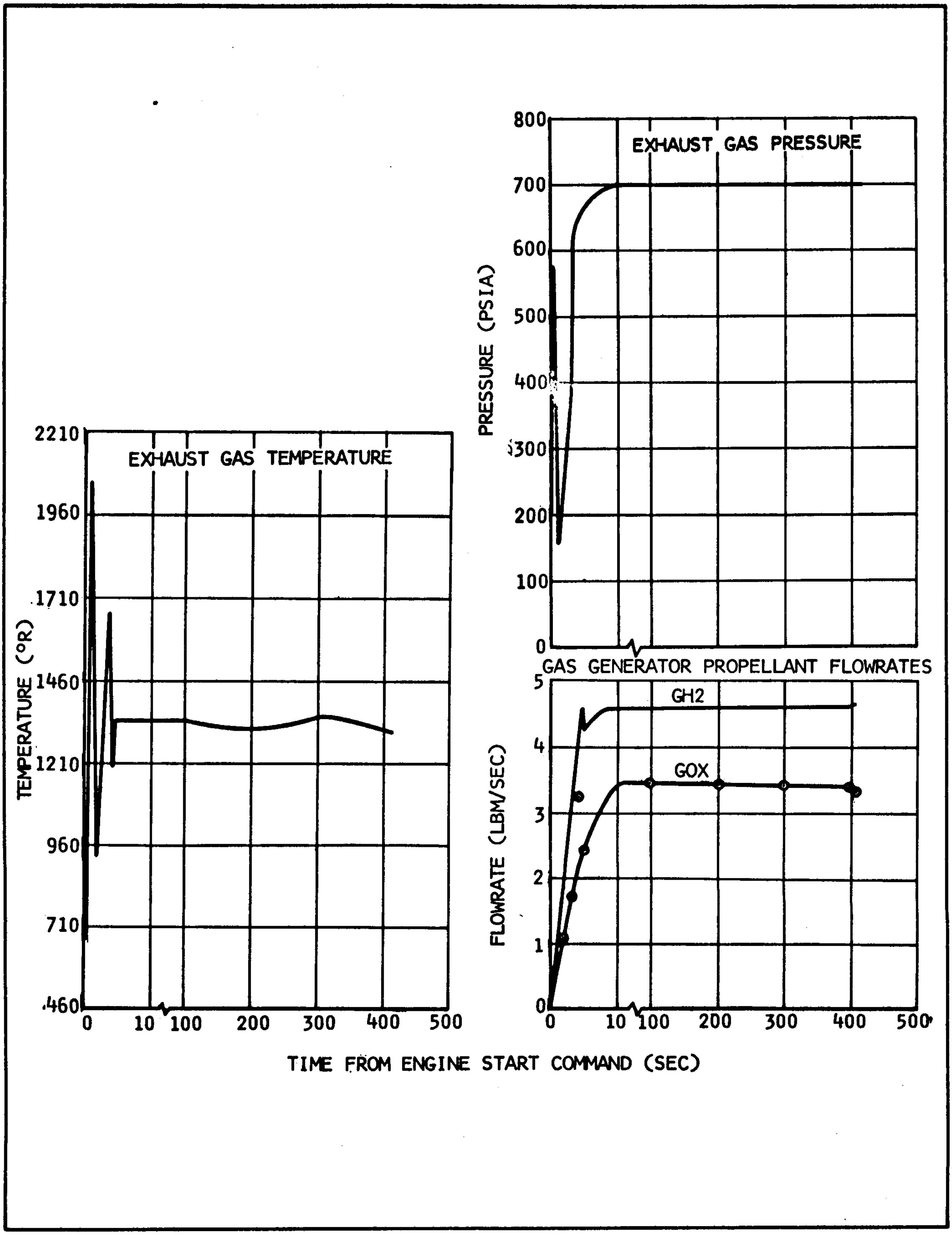

Figure 6-45 Gas Generator Performance - CD 614010

21 February 1966

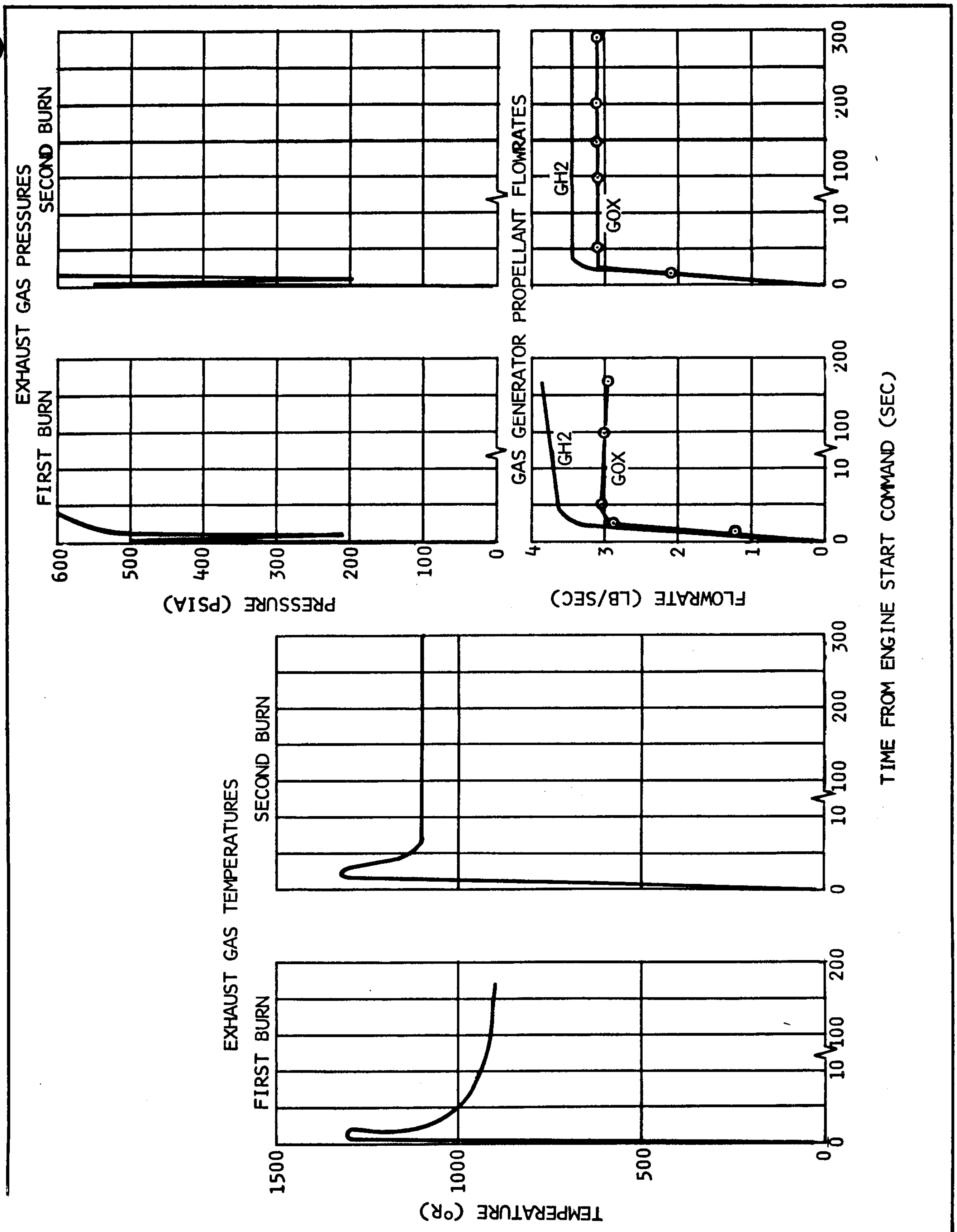

Figure 6-46 Gas Generator Performance - CD 614043

21 February 1966

SECTION 7

OXIDIZER SYSTEM

7. OXIDIZER SYSTEM

The battleship program of the oxidizer system covered developmental testing of the LOX tank pressurization system, the LOX chilldown recirculation system, and the engine LOX supply, all of which demonstrated a satisfactory performance during the course of the testing. Several pressurization system test configurations were utilized due to problems with components availability and inadequate original design before the final configuration was settled upon. The chilldown and supply systems operated satisfactorily at all times.

7.1 LOX Tank Pressurization Systems

The LOX tank pressurization system produced satisfactory operating results in prepressurizing the LOX tank ullage and maintaining pressure during engine firing, although several configurations and a minor redesign were tried before acceptable results were attained with operational hardware.

7.1.1 Configuration Deviation

The configuration of the LOX tank pressurization system was changed several times during battleship testing. The system was originally designed as a cold gas system (figure 7-1), but could not be tested until CD 614024 because the flight pressurization control module was not available. Therefore, during the first battleship tests (CD 614000 through 614009), the LOX tank was pressurized with ambient helium from the GSE supply through an auxiliary system (figure 7-2). Prepressurization with cold helium was accomplished by installing a valve replacing the module in the flight pressurization system (figure 7-3). A "breadboard" LOX tank pressurization control assembly (figure 7-2) was installed prior to the 415-sec firing test on the J-2003 engine (CD 614010). The "breadboard" system was schematically the same as the cold gas flight pressurization system except for the two orifices replacing the regulator. (It should be noted that in some tests one or two regulators were used instead of the orifices.)

The originally designed flight pressurization system (figure 7-1) was tested during CD 614024, 614025, and 614028. This configuration was changed prior to CD 614030 because it could not maintain minimum LOX tank ullage pressure

(37 psia) during the start transient unless the flow-controlling orifices were oversized. The original and the redesigned flight pressurization systems are referred to as cold gas and hot gas systems, respectively, to indicate the principle factor in design change. In the hot gas system (figure 7-1) the orifices controlling the flow through the J-2 heat exchanger are located downstream of the exchanger as opposed to the upstream location in the cold gas system. The effect of this change could not be observed on the S-IVB/IB configuration because the regulator failed during the initial phase of the last firing of this configuration (CD 614030). However, as indicated by the S-IVB/V configuration tests, the change produced a satisfactory improvement in the pressurization system start transient response.

Aside from the start transient problems, the LOX pressurization system functioned adequately in maintaining the tank ullage pressure within design limits of 37 to 40 psia throughout the engine firing in all battleship tests. However, the cold helium regulator used in these tests was designed to maintain plenum chamber pressure at 385 $\pm$25 psig. Its performance record was poor (table 7-1) and further testing on the S-IVB-202 stage indicated that the probable cause was an inlet temperature higher than that for which the regulator was designed. However, its operation did not adversely affect system performance, and no changes are contemplated.

7.1.2 S-IVB/IB

7.1.2.1 Prepressurization

The prepressurization system proved to be completely satisfactory. In general, the LOX tank was prepressurized with cold helium from the GSE supply through the gas heat exchanger and console B to the tank (figure 7-3); however, for some tests (CD 614010, 614023, and 614025) this procedure was modified. Ambient helium from the GSE was supplied through the auxiliary system for CD 614010 and 614023 because the "breadboard" assembly could not lock up the cold helium regulator during ground prepressurization.

During CD 614025, the LOX tank was prepressurized with helium from the cold helium spheres. This was part of the pressurization system conditioning procedure that was attempted in order to reduce the effect of start transients on tank ullage pressures (paragraph 7.1.2.2).

Prepressurization data indicate (figure 7-4 and table 7-2) that the ullage temperatures were consistently at 163 deg R at the start of prepressurization. The ullage pressure prior to prepressurization was 15.3 to 15.5 psia in CD 614008, 614009, and 614010 and 14.9 in subsequent tests. The difference was the result of replacing the original ullage pressure transducer with another model. The LOX saturation pressure at 163 deg R was 15.2 psia, falling between the two sets of ullage pressure data.

The LOX tank prepressurization was initially approximately 3 min prior to simulated liftoff and, depending on ullage volume and the method used for prepressurization, required from 10 to 55 sec. Prepressurization was terminated by the prepressurization control pressure switch or by manual control when the pressure reached 36 to 41 psia and was followed by a decrease in tank ullage pressure because of cooling of the ullage gas.

Several makeup cycles were usually required before the ullage conditions stabilized. The ullage temperature increased during prepressurization to 248 to 330 deg R because the helium entering the LOX tank was near ambient temperature due to heat transfer in the lines. The temperature then decreased to 245 to 278 deg R at Engine Start Command.

7.1.2.2 Pressurization

LOX tank pressurization data obtained during the battleship tests are summarized in table 7-1. As shown, the ullage pressure at engine start varied from 37.1 to 39.4 psia, thus was within the design range of 38.5 $\pm$1.5 psia.

In general, the LOX pressurization system, in its various configurations, maintained the ullage pressure within the design range of 37 to 40 psia throughout all engine firings. Notable exceptions were the ullage pressure decreases during the system's start transients during CD 614024, 614025, 614028, and 614030; the pressure increases during CD 614010 and 614023; and the pressure decay near the end of engine firing during CD 614025 (figure 7-5). The latter was the result of undersizing of the flow controlling orifices. These orifices were sized for a helium flow at 40 deg R, but the actual steady-state temperature at the orifices varied between 50 to 60 deg R due to heat transfer in the line between the cold helium spheres and the LOX tank pressurization control module (paragraph 7.1.1). Heat transfer in this line also reduced the helium flowrate in the cold gas system during its start transient, thus causing a decrease of ullage pressure during this period. A good illustration of the heat transfer is shown by the LOX pressurization module outlet temperature (figure 7-10). Approximately 25 to 35 sec of flow were required before this temperature decreased to 80 deg R. During CD 614028, to compensate for the initial heating of the helium flow, the pressurization lines were pre-chilled by venting helium from the cold helium spheres out through the cold helium module vent valve at simulated liftoff. However, the effect of this line childown could not be determined because the regulator failed during the start transient period. As mentioned in paragraph 7.1.1, the system was subsequently redesigned to reduce the effect of initial high temperatures on the flowrate. During the first test with the hot gas system (CD 614030), the regulator failed again. As this test was the last firing in the S-IVB/IB test series, the hot gas system performance could not be fully evaluated until S-IVB/V test data became available (paragraph 7.1.3).

The start transient did not occur during tests in which the "breadboard" system was employed. In this system, two parallel orifices replaced the regulator. Since the orifices were sized to simulate a regulator failing in the fully open position, the system operated in a bang-bang mode, and the plenum chamber pressure data of CD 614023 (figure 7-9) indicate that the average value was approximately 550 psia. This is considerably higher than the value (400 psia) which was used for flow control orifice sizing. The higher pressure, therefore, compensated for the temperature effect on the flowrate.

The tank ullage pressure increased over its maximum operating limit of 40 psia in CD 614010 and 014023. Because the "breadboard" system was employed, when one (or both) of the shutoff valves failed open, the helium flowrate increased excessively, causing the ullage pressure to rise. During CD 614010, the tank ullage pressure increased to the vent relief setting in approximately 3 sec. As shown in table 7-1, the ullage pressure reached a maximum of 45.6 psia, which is above the upper relief setting. It appears that the relief valve could not immediately handle the large flow increase. The shutoff valve failure occurred at ESC +25 sec. The ullage volume was still small and the cold helium sphere pressure was still high. During CD 614023 the failure occurred at ESC +165 sec, and the ullage pressure again increased to the vent relief setting, but at a slower rate. The relief setting of 43.6 psia was reached in 27 sec.

The LOX tank ullage temperature stratification is shown in table 7-1 and figure 7-6 which indicates that the ullage temperature profile is quite consistent.

The temperature data from the vent inlet to the LOX tank are shown in figure 7-12. The data, in conjunction with the pressure and the effective area of the inlet, were used to estimate prepressurization flowrates as other means were not readily available (paragraph 7.1.2.1). The helium inlet temperature was also compared with the theoretical mixture temperature of the helium flow through the heat exchanger and its bypass. Good agreement was obtained during steady-state operations, but 30 to 50 sec were required after a change from overcontrol to undercontrol and vice versa before reasonable agreement was obtained.

The diffuser inlet temperature cycles were similar to those of the vent inlet temperature. The heat lost by the helium gas to the LOX bulk was greater during overcontrol than undercontrol and decreased as the liquid level dropped.

The calculated collapse factors (figure 7-7) were slightly lower than expected (1.5 to 1.6) for the battleship firings.

The collapse factor was calculated from the following equation:

$$C_F = \frac{\Sigma \dot{W} \Delta t \; T \; R}{P \; \dot{V} \; 144 \; t}$$

$\dot{W}$ = total pressurant flowrate (lb/sec)

Δt = time increment (sec)

T = temperature of gas entering the LOX tank (deg R)

P = ullage pressure (psia)

$\dot{V}$ = volumetric rate of change of ullage volume (ft^3/sec)

R = gas constant of pressurant $\frac{ft - 1lb}{lbm - R}$

t = time from ESC (sec)

Note that this collapse factor definition uses the diffuser inlet temperature instead of the control orifice temperature used in the S-IV collapse factor definition.

7.1.2.3 LOX Tank Pressurization Control Module

The LOX tank pressurization control module performed adequately during the S-IVB/IB testing, although some regulator anomalies were encountered. All problems and deviations from predictions were satisfactorily explained.

Figure 7-10 shows the history of the control module outlet temperature during engine firing. The effect of this temperature transient on the helium flowrate was noted earlier. During steady-state operation, the module outlet temperature was 15 to 20 deg R higher than that of the cold helium sphere because of line heat transfer. A comparison of the observed temperature differences with predicted values is shown in figure 7-14. The actual and predicted temperature changes in the line agree in trend, but actual heating was greater than predicted in all cases. The data indicate that better agreement would have been obtained if predicted values had been 20 percent higher. However, agreement was still within the accuracy limits of the generalized empirical correlations used in prediction and of the uncertainty in instantaneous wind velocity near the helium lines. The scattering of the data was probably partly caused by wind velocity fluctuations.

The module pressure, measured at the plenum chamber, was approximately 400 psia (as required) most of the time during firing tests in which the module was available (figure 7-5). However, during CD 614028 and 614030, the module pressure decreased sharply immediately after its initial rise at ESC, indicating a regulator failure. The module was returned to Calmec after battleship testing. Examination showed that the ring gaps on the regulator piston had lined up, allowing leakage into the regulator pilot area. This leakage upset the pressure forces necessary to open the regulator and caused the failure. Later in the firing, the helium gas in the regulator stabilized at cold temperatures, allowing the existing bleed ports to remove the excessive leakage so that the regulator could open and operate normally.

Table 7-3 presents the data on the module orifices used in the various tests. The helium flowrates are shown in table 7-1 and figures 7-8 and 7-10. As noted earlier, (paragraph 7.1.2.2) the orifice sizes were increased after the test results of CD 614025 showed that, although the pressurization system had almost continuously operated in the overcontrol mode, the ullage pressure could not be maintained above the minimum limit of 37 psia toward the end of firing. Satisfactory results were obtained with the larger orifices.

7.1.2.4 Cold Helium Supply

The cold helium sphere data are summarized in table 7-4. At engine start, the average sphere temperature varied from 38 to 43 deg R, which was well below the maximum allowable temperature of 50 deg R. The sphere pressure at engine start was approximately the required 3,000 psia during CD 614010, 614023, and 614030 (figure 7-13). During CD 614025 and 614028 the pressure was several hundred psi lower because of sphere blowdowns prior to ignition. These blowdowns were part of the pressurization system conditioning procedures that were performed in an attempt to eliminate the start transient problem. There was approximately 320 lbm of helium in the spheres at engine start during all tests.

The sphere temperature and pressure histories during engine firing are illustrated in figure 7-13. Both the temperature and pressure decreased initially and after reaching a minimum value, began to increase because of heat transfer from the relatively warmer LH2 tank ullage. Because of the variation in time of exposure to the LH2 tank ullage, the sphere temperatures reached different minimum values which were dependent on sphere position.

Table 7-4 also shows the helium mass consumptions for several tests. The consumption depended primarily on the burn time and to a lesser extent on engine EMR and the sizes of the flow controlling orifices. Shutoff valve failures as in CD 614010 and 614023 also affected the consumption. The helium mass consumption calculated from sphere conditions at ESC and ECO agreed very well with the results obtained from integration of the helium flowrate.

7.1.2.5 Helium Heat Exchanger

The J-2 helium heat exchanger performed with satisfactory results and, after predictions were adjusted for actual operating conditions, appeared to operate within satisfactory agreement with the predictions. The heat exchanger inlet temperature history is shown in figures 7-8 through 7-10. After the initial hardware chilldown period, this temperature was consistently 15 to 25 deg R higher than the LOX tank pressurization control module outlet temperature. This condition had not been considered in the predictions.

Data on the heat exchanger pressure drop in the cold gas and hot gas system are shown in figure 7-15. The pressure drop data obtained from the cold gas system tests agreed reasonably well with the Rocketdyne prediction curves; however, the heat exchanger pressure drop data from the hot gas system test were higher than the predictions.

The J-2003 heat exchanger performance data from CD 614010 are shown in figure 7-8, which also shows the Rocketdyne predicted heat exchanger outlet temperatures for an engine with a 1,460 deg R gas generator temperature. In this test the gas generator operated at 1,390 deg R so that the difference between actual performance and the prediction shown here appears to be reasonable.

Performance data on the J-2013 heat exchanger are shown in tables 7-5 and 7-6 and figures 7-9 and 7-11. Table 7-6 compares the test results, the J-2013 engine log book data, and the conditions which NASA used for the curves in figure 7-16 for prediction of the heat exchanger helium outlet temperature.

Comparison of the data shows that the helium inlet temperature was higher than the values assumed by NASA. It shows further that the hot gas (gas generator combustion products) temperatures were in good agreement except for the value at low EMR. The effect of the latter difference shows up in figure 7-16 in which the helium outlet temperature data fall below the predicted curve. The helium outlet temperature data for EMRs of 5.0 and 5.6 agree reasonably well with the corresponding prediction curves, except that the trend of the data as a function of the helium flowrate has a different slope than the prediction.

Analysis, based on generalized heat transfer coefficient correlations, showed that: (1) the data were not consistent with the correlations, which explained the trend difference with respect to the effect of helium flowrate, and (2) the prediction curve for minimum PU was inconsistent with the other two curves for nominal and maximum PU, if the three PU valve positions are assumed to represent EMR values of 4.5, 5.0, and 5.6. The prediction curve for an EMR of 4.5 falls below the NASA curve and is in reasonable agreement with the data. The accuracy of the data and of the correlations used for prediction indicated that the differences between data and predictions were within acceptable limits. It can therefore be concluded that the heat exchanger performance was adequate.

The heat exchanger helium outlet temperature data (figures 7-8, 7-9, and 7-11) used here were obtained from measurement C-0228 at the heat exchanger outlet. Another measurement (C-0009) was also called heat exchanger outlet temperature, and was located at the stage side of the engine interface, approximately 10 feet downstream of the heat exchanger but, since this 10-foot line was uninsulated, the temperature indications were lower than those of C-0228. During steady-state conditions the temperature difference was strictly caused by heat transfer to the ambient environment, as has been verified by analysis of the data. However, during transients, the heat transfer to the hardware of the line becomes an additional factor which complicates the relation between C-0009 data and the heat exchanger outlet temperature. Since measurement C-0228 has been deleted from flight stages, it will be necessary to use C-0009 data plus a rather questionable correction factor for the heat exchanger performance evaluation.

7.1.3 S-IVB/V

A thorough analysis of S-IVB/V pressurization system test data has not yet been completed. The data from CD 614043 (typical of S-IVB/V configuration testing) and a preliminary evaluation are presented in the following paragraphs.

7.1.3.1 Prepressurization

LOX tank prepressurization data are shown in figure 7-17. Prepressurization was initiated 12 min prior to engine start and required only 10 sec. Makeup cycles were not required to maintain tank pressure as the pressure was increasing due to the continuous helium purge flow to the vent valve. The tank was vented several times to ensure that the LOX pump inlet pressure would not exceed 48 psia at engine start. Both the rapid prepressurization and the continuously increasing ullage pressure were a result of the small ullage volume.

7.1.3.2 Pressurization During First Burn

The LOX tank pressurization system maintained ullage pressure above 37 psia during the start transient (figure 7.18), in favorable comparison to the results with the cold gas system used in the S-IVB/IB battleship testing. The pressurization system cycled seven times in maintaining ullage pressure within the operating range of 37 to 40 psia during engine firing. The LOX tank ullage temperature data (figure 7-18) shows the usual stratified temperature profile.

The cold helium sphere pressure was 3,030 psia at engine start and decreased to 1,600 psia at ECO (figure 7-19). The sphere temperatures shown in figure 7-19 ranged from 38 to 41 deg R at engine start and decreased to 27 to 33 deg R at ECO. The helium consumption was 55 lbm.

The plenum chamber pressure (cold helium regulator outlet pressure) history shown (figure 7-19) was typical of all the battleship test results obtained after the regulator had been reworked. The pressure was drifting upward during the firing and cycling as the system alternated between undercontrol and overcontrol operation. The plenum chamber pressure displayed neither of these characteristics during tests that were performed before the regulator had been reworked. Later testing performed in conjunction with S-IVB-202 acceptance firing indicated that the hot gas system, with its greater flow capabilities, in conjunction with the higher than expected module inlet temperature (paragraph 7.1.1) imposed a greater demand in the overcontrol mode than the regulator was capable of handling.

The following table presents the minimum and maximum plenum chamber pressures obtained during the S-IVB/V tests.

	CD 614034	CD 614043		CD 614044	
		1st Burn	2nd Burn	1st Burn	2nd Burn
Maximum Pressure, (psia)	440	455	465	475	475
Minimum Pressure, (psia)	330	370	350	370	370

The LOX tank pressurization module inlet and outlet temperature and the temperature increase of the helium flowing from the cold helium spheres to the module are presented in figure 7-19. Both the temperature increase and the module outlet temperature were somewhat higher than normal.

The heat exchanger performance was normal. The helium outlet temperature (C-0009) was in agreement with the prediction after correction was made for the heat loss in the 10-foot uninsulated line. The pressure drop and the heat transfer through the heat exchanger during undercontrol and overcontrol operation are shown in figure 7-19.

The primary orifice pressure and temperature data are presented in figure 7-20. Comparison of these data with the heat exchanger outlet data showed that the differences were negligible.

The overcontrol valve inlet pressure (figure 7-20) was 30 to 40 psia lower than the heat exchanger outlet pressure during overcontrol (when the valve was open). This pressure drop was expected because the line to the valve was smaller than that to the primary orifice and the flowrate was larger. Figure 7-20 shows the pressures downstream of the overcontrol valve and downstream of the hot-cold gas junction. These data confirmed that the flow in the orifices and overcontrol valve was choked.

The LOX vent helium inlet parameters are shown in figure 7-20. The vent temperature did not exceed the redline value of 560 deg R during first burn. Comparison of this temperature with the theoretical mixture temperature of the hot and cold gas showed poor agreement. The differences were the result of line heat transfer transients caused by the overcontrol and undercontrol cycles. The helium flowrate data are shown in figure 7-20. The overcontrol flowrate data should be considered as preliminary because the effective area of the overcontrol valve was not determined by calibration but was estimated by balancing flowrates through the orifices and LOX vent helium inlet during overcontrol and undercontrol. Additional system data are also presented in figure 7-20. The LOX tank collapse factor for this time period is presented in figure 7-18.

7.1.3.3 LOX Tank Repressurization

LOX tank ullage repressurization prior to engine second burn appeared to be satisfactory, although use of the auxiliary pressurization system was necessary to bring ullage pressure up to minimum engine start conditions. This situation occurred because the ullage pressure was approximately 16.5 psia at the initiation of repressurization, rather than the nominal 30-psia orbital pressure; and the repressurization spheres did not contain sufficient mass to compensate for this difference.

Repressurization sphere temperature and pressure were approximately 515 deg R and 2,700 psia (figure 7-21) at the initiation of repressurization which occurred approximately 290 sec before second burn Engine Start Command (2ESC). Tank ullage pressure increased to a maximum of 28.5 psia by 2ESC -260 sec, at which time the repressurization spheres were depleted to approximately 100 psia. The ullage pressure collapsed to 25 psia in 85 sec at which time the auxiliary system was utilized to bring tank ullage pressure up to 38 psia. Two makeup cycles from the auxiliary system were required prior to 2ESC to maintain the ullage pressure at satisfactory levels.

The LOX tank ullage temperature was approximately 160 to 175 deg R prior to repressurization and, depending on location, increased to a maximum of 270 deg R during repressurization. The temperature increased from 245 deg R to 340 deg R under auxiliary pressurization (ambient helium) and was at 275 deg R at 2ESC. These temperatures were measured at the LOX tank 100 percent level.

7.1.3.4 Pressurization During Second Burn

After engine start, the LOX tank ullage pressure increased from 35 to 40.5 psia then cycled within the design range of 37 to 40 psia during the remainder of engine firing. The initial pressure increase was momentarily interrupted at ESC +10 sec (figure 7-22) because the pressurization system was still going through its start transient. The cold helium sphere pressure and temperature data are shown in figure 7-23. The pressure decreased continuously from 2,400 psia at ESC to 1,060 psia at ECO. The sphere temperatures also decreased initially but then increased after reaching minimum values at approximately 140 to 150 sec after Engine Start Command. The temperature increase and the differences in sphere temperatures were caused by heat transfer from the LH2 tank ullage as the LH2 level decreased and the spheres became uncovered. The helium consumption during second burn was 115 lb. The total consumption for the two firings was 170 lb.

The plenum pressure history (figure 7-23) shows the same cycling and upward drift exhibited during first burn pressurization (paragraph 7.1.3.2). During the last two undercontrol cycles, the pressure increased sufficiently to activate the regulator backup switch, and the system went into backup operation. This figure shows only part of the pressure fluctuations during this mode of operation because the sampling rate for this plot was only one per sec.

The rest of the LOX pressurization data, with the exception of diffuser inlet temperature (figure 7-24) and collapse factor (figure 7-22), were quite similar to the results obtained during first burn. Both the diffuser inlet temperature and collapse factor were higher than during first burn.

7.2 LOX Childown System

The LOX chilldown system is shown schematically in figure 7-25. Three engines were used during battleship testing. An experimental engine, J-2003, was used for CD 614000 through 614013; flight engines J-2013 and J-2020 were used in the subsequent S-IVB/IB and S-IVB/V tests respectively. The differences between them with respect to LOX chilldown was that the flight engines were equipped with 1.5-in. bleed valves while the J-2003 engine was equipped with a 5/8-in. bleed valve. The engine return line was also routed differently. These two differences affected the chilldown flowrates considerably (table 7-8).

The childdown operation was the same for all tests, but initial conditions, duration, and the start time in the terminal count sequence were varied. The variations in the initial conditions and duration of childdown resulted from differences in the countdown procedure prior to childdown. The normal procedure for S-IVB/IB testing was to load the LOX tank with the prevalve and bleed valve open* and start the childdown (several hours later) with an unpressurized tank. The variations in S-IVB/IB testing were (a) opening the bleed valve at initiation of childdown (CD 614006) and (b) starting childdown with a pressurized tank (CD 614017-A3). The normal procedure for S-IVB/V testing was to load the LOX tank with the prevalves closed and pressurize the tank prior to the childdown that preceeded first engine burn. After the first firing, the prevalves were closed again, and the LOX was purged out of the feed duct with ambient helium. The childdown prior to second burn started while the tank was still unpressurized. The effects of these variations on the recirculation system performance are shown in table 7-8 and are discussed in the following paragraphs.

7.2.1 S-IVB/IB

Cold flow testing had already demonstrated that the LOX childdown system performance was adequate. The S-IVB/IB hot firing test results confirmed this. As shown in table 7-8, the available NPSH at ESC, which is the prime criterion, exceeded the minimum requirement by a considerable margin. Since steady-state conditions were achieved at the LOX pump inlet during all tests, the childdown duration did not affect the temperature obtained there at the end of childdown. The effect of childdown duration is clearly illustrated in figures 7-26, 7-27, and 7-28, which show the temperature histories at the pump inlet and gas generator bleed valve. The childdown flowrate noticeably affected the LOX pump inlet temperature, as shown by the values obtained at the end of childdown in the tests with the J-2003 and J-2013 engines (table 7-8). The flowrate data (figures 7-26 and 7-27) indicate that the flow resistance in the J-2013 engine was considerably lower than that in the J-2003 engine because of the difference in the bleed valve sizing (5/8 and 1-1/2 in.). In order to express the flow resistance quantitatively, a flow coefficient (C) was defined by using the Darcy

*During the J-2003 engine tests, the bleed valve was opened at the time that the 50 percent load level in the LH2 tank was reached.

equation $P = \frac{K \dot{W}^2}{A^2 2g}$. The flow coefficient (C) corresponds to the term $\frac{K}{A^2 2g}$ in the equation and depends only on the geometry of the system.

Values of C are also shown in table 7-8. The flowrate during CD 614005 was higher than it was during subsequent tests with the J-2003 engine. The decrease in flow was the result of replacing the bleed valve, which was destroyed in the uncontrolled gas generator combustion during CD 614005.

The temperature and flowrate data were used to calculate the ambient heat input to the various sections of the system. The results, shown in table 7-9 indicate that the heat inputs to the J-2003 and J-2013 engine were approximately the same (within the data accuracy). This was expected as the major resistance to the heat transfer would be the outside film coefficient, which depends on the ambient conditions.

7.2.2 S-IVB/V

During S-IVB/V battleship tests, the LOX tank was loaded with the prevalve closed in order to obtain more severe initial conditions for chilldown than are expected during orbital coast. The chilldown data from these tests therefore, are very significant with regard to prediction of the recirculation system performance and the time required for orbital chilldown prior to restart in S-IVB/V flights.

The results from these tests are shown in figures 7-29 through 7-35 and are summarized in table 7-10. These data indicate that the recirculation system performance was adequate and also show that a 10-min chilldown period was more than sufficient to obtain engine interface conditions that were within the engine start requirements (figure 7-29). These data also indicate that steady-state conditions were reached or closely approached after 5 min of chilldown. Analysis of the data is still in progress; however, based on these data and a preliminary comparison of the test conditions with those expected to be encountered while in orbit, the 5-min period allowed in the flight sequence prior to engine restart appears to be adequate to meet start requirements.

As noted in paragraph 7.1, the test conditions for S-IVB/V tests prior to first and second burn differ in two respects from each other:

a. First burn chilldown was initiated when the tank was already pressurized; for the second burn chilldown tests, the tank was pressurized approximately 5 min after initiation of chilldown.

b. During both tests, the suction ducts were intended to be "dry" at the start of chilldown, but this condition was accomplished in a different manner (tank loading with a closed prevalve versus helium purging to remove LOX from the suction duct).

The effect of the latter difference is particularly hard to assess because of a small leakage in the LOX prevalve which allowed some LOX into the suction duct.

Because of the LOX leak and the test condition differences, steady-state conditions were obtained much sooner during the first burn tests than during the second burn tests.

7.2.3 Engine LOX Supply

The engine LOX supply system performed well. The available NPSH at the LOX pump inlet remained well above requirements throughout all engine firings.

7.2.3.1 S-IVB/IB

LOX pump inlet pressure and temperature data for several tests are shown in figure 7-36. Figures 7-37 through 7-44 present histories of these tests. The pump inlet pressure decreased after engine start and then cycled with ullage pressure while generally decreasing due to the decrease in liquid head in the LOX tank. The pump inlet temperature decreased during the start transient, steadied out, and then began to increase at a rate which became faster as the firing continued.

The NPSH at the LOX pump inlet during firing was calculated from the pump inlet pressure and temperature data by a Fortran computer program. A constant term was used in the program for dynamic pressure. This was necessary since a program which calculates dynamic pressure from data was not yet available. Hand calculations were made to verify the results of the program. As seen in figures 7-26, 7-27, 7-39 and 7-41, the hand calculated values of NPSH and the program results were in close agreement. Differences were due to differences in pressure and temperature data and to the effect of dynamic pressure variations. The pressure and temperature data differences were the result of using different data sources (strip charts and the digital data acquisition system).

Five tests were used for evaluating NPSH during firing and confirmed satisfactory system operation. Two of these tests (CD 614008 and CD 614009) were conducted with engine J-2003. The other three tests (CD 614025, 614028, and 614030) were made with engine J-2013. The NPSH cycled with ullage pressure while generally decreasing with time due to a decrease in liquid head and an increase in fluid temperature at the pump inlet. The NPSH data are shown in figures 7-37 through 7-41 and summarized in table 7-9.

The frictional pressure drop in the LOX suction duct was computed from ullage pressure, pump inlet pressure and temperature, PU probe mass, engine flowrate, and pump discharge pressure and temperature data. The suction duct pressure drop was calculated for CD 614008, 614009, 614010, 614023, 614025, 614028, and 614030 (figure 7-42). The average pressure drop from all these tests was determined to be 1.23 psi; the predicted pressure drop was 2.58 psi at nominal flowrate.

LOX pump inlet temperature data and PU probe mass data were plotted for CD 614010, 614020, 614023, 614024, 614025, 614028, and 614030 (figure 7-44). The pump inlet temperatures were normalized by shifting the data so that each of the tests had the same initial steady-state temperature. This normalizing eliminated such test-to-test variations as instrumentation error, and bulk heating prior to engine start. The normalized temperatures were then plotted as a function of the mass remaining in the LOX tank (figure 7-43). This temperature-mass plot shows that all the tests except CD 614030 fall very close to the same curve, indicating that the heat input into the LOX was very nearly the same for all these tests. There are very small differences between the test results due to the EMR variations.

The CD 614030 data indicate that heat input to the LOX in the tank during engine firing was greater than in the previous tests, possibly because the LOX pressurization system hardware was changed and resulted in a warmer pressurization gas during the initial phase of burn. This could have been responsible for the warmer liquid temperature observed during this countdown.

7.2.3.2 S-IVB/V

The LOX was supplied to the engine in a satisfactory condition throughout both first and second firings of the engine during the three S-IVB/V tests which were evaluated. This was demonstrated by the NPSH at the engine interface during engine firing (table 7-10). In all tests, the available NPSH never decreased below the allowable minimum.

During engine firing, the NPSH followed the ullage pressure while generally decreasing with time due to the decrease in liquid head pressure, as the LOX was drained from the tank, and the increase in liquid temperature. NPSH data and histories of LOX temperatures in the tank and at the engine interface are shown in figures 7-45 through 7-49.

TABLE 7-1
BATTLESHIP LOX TANK PRESSURIZATION DATA

ITEM	CD 614008	CD 614009	CD 614010	CD 614023	CD 614024 (1)	CD 614025 (1)	CD 614028 (1)	CD 614030
Type of Pressurization Control System	Aux. Amb. He From GSE	Aux. Amb. He From GSE	"Breadboard" System Cold He Bang-Bang Cold Gas Config.	"Breadboard" System Cold He Bang-Bang Cold Gas Config.	Calmec Module Cold Helium Cold Gas Configuration	Calmec Module Cold Helium Cold Gas Configuration	Calmec Module Cold Helium Hot Gas Configuration	Calmec Module Cold Helium Hot Gas Configuration
Burn Time (sec)	54	154	415	472	44	509	376	496
Ullage Press. at Start (psia)	39.4	39.0	38.4	37.4	37.2	37.1	38.3	37.95
Ullage Temp at Start 100% (°R)	267	255	278	262	-	245	252	262
Control Cycles During Burn	9	11	0	3	0 (2)	1 (3)	8	5
Flight Control Pressure Switch Control Bank	Controlled Manually	Controlled Manually	No Data	39.7/37.8	No Data	40.2/37.9	39.6/37.5	39.6/37.6
Minimum Ullage Pressure (psia)	38.5	38.0	38.4	37.4	36.1	34.0	30.7	30.4
Maximum Ullage Pressure (psia)	41.0	40.5	45.6 (4)	43.6 (5)	38.0	40.2	39.95	40.2
Ullage Pressure at ECO (psia)	39.75	39.1	38.5	42.5	36.95	35.3	37.7	39.2
Ullage Temperature at ECO								
C0059 100% Level (°R)	313	352	253	287	251	330	310	338
C0526 90% Level (°R)	228	276	252	259	199	268	267	278
C0058 80% Level (°R)	—	—	247	253		260	258	268
C0057 50% Level (°R)	—	—	207	223		212	205	227
Flowrates (7)								
Overcontrol (lbm/sec)			0.1 to .22		0.20 to 0.25	0.25 to 0.36	0.25 to 0.59	0.35 to 0.42
Undercontrol (lbm/sec)			0.8 to 0.24 after valve failure		0.135 to 0.19	0.25 to 0.26	0.26 to 0.33	0.29 to 0.32
Plenum Chamber Press (psia) Max	—	—	—	—	400	450	450	420
Plenum Chamber Press (psia) Min	—	—	—	—	400	390	25	130
Total Helium Usage During Firing (lbm) (6)	No Data	No Data	176	188	—	162	128	147
Significant Problems or Failures	None	None	Shutoff valve failure occurred at ESC +25 sec causing flowrate to increase to 0.88 lbm/sec. The valve when operating in relief mode was not able to control this increase.	Shutoff valve failure similar to CD 614010 occurred at SLO +258 sec.	Low ullage press. and flow rates after start due to temp. transients. System went to overcontrol until CD. Aux. He used.	Large initial ullage press. drop due to temp. transients. Orifices were undersized causing system to operate almost continuously in overcontrol. OK for low EMR run; therefore, no aux. He required.	Cold Helium Reg. failed to fully open until 20 sec. after start. Aux. helium used. Reg. recovered and worked O.K.	Cold Helium Reg. Failure. Press. dropped but not low enough to require aux. helium again. Reg. recovered and worked O.K.

(1) The following are special procedures for conditioning of the LOX pressurization system to eliminate start transient effect on ullage pressure are listed below:

CD 614024	CD 614025		CD 614028
SLO -14 min 30 sec	SLO -3 min 35 sec	SLO -3 min	SLO
Initiate cold helium flow from GSE prepressurization supply through LOX tank vent for 2 min to chill vehicle pressurization lines.	Open dump valve in cold helium fill module and dump helium overboard for 35 sec.	Close helium dump valve and LOX tank vent valve. Prepressurize LOX tank from cold helium spheres. (Dump valve did not open during countdown.)	Blow cold helium spheres down through fill module dump valve from 3,000 to 2,300 psia.

(2) Ullage pressure started to drop immediately after engine start due to cold gas configuration temperature transients. System went to overcontrol and remained in this mode until the CD of this short run.

(3) Flow controlling orifices were undersized. Therefore the pressurization system operated almost continually in the overcontrol mode.

(4) The ullage pressure exceeded 44 psia (the upper vent setting) when the shutoff valve failure occurred 25 sec after ESC. The flowrate in the LOX tank reached 0.88 lbm/sec immediately after valve failure. It appears that the vent and relief valve when operating in the relief mode, was not able to flow this amount of helium. The pressure increased to 45.6 psia before decreasing.

(5) The high ullage pressure was the result of a shutoff valve failure similar to that of CD 614010. The ullage pressure increased to the vent setting due to the high pressurization flowrates.

(6) The variations in helium mass consumed during the individual runs is primarily dependent on burn time. However, the orifice sizes and number of control cycles also affect the consumption.

(7) The variations in flowrate from test to test were the result of changes in orifices inlet temperatures, an example of which is the bypass orifice. The temperature decreased rapidly from ambient as the line chilled down then reached a minimum when the cold helium sphere temperature reached a minimum. The orifice inlet temperature then warmed up as the sphere temperature increased. The flowrate changed in response to these temperature variations.

TABLE 7-2 (Sheet 1 of 2)
LOX TANK PREPRESSURIZATION

COUNTDOWN	614008	614009	614010	614023	614024	614025	614028	614030
Type of Prepressurization	Cold Helium	Cold Helium	Ambient Helium	Ambient Helium	Cold Helium with Auxiliary Helium Makeup	Cold Helium	Cold Heli-um	Cold Helium
Prepressurization Supply	Normal GSE	Normal GSE	Automatic Auxiliary	Automatic Auxiliary	Normal GSE & Auxiliary	Cold Helium Spheres in LH2 Tank	Normal GSE	Normal GSE
Initial Ullage Pressurization, (psia)	15.5	15.25	15.5	14.95	14.95	14.95	14.87	14.95
Final Ullage Pressurization, (psia)	41.0	40.25	42.0	36.8	37.95	38.1	37.7	36.45
Prepressurization initiated (sec)	SLO -180	SLO -177	SLO -179	SLO -208	SLO -208	SLO -177	SLO -179	SLO -173
Time for Prepressurization (sec)	27	53	31	10	37	55	15	19
Makeup Cycles after Initial Prepressurization	8	5	6	16	15	11	9	12
Ullage Pressurization at ESC (psia)	39.4	39.0	38.4	37.4	37.2	37.1	38.3	37.95
Ullage Temperature at Start of Prepressurization 100% Level (°R)	163	163	163	163	163	163	163	163
Ullage Temperature at ESC (°R)	267	255	278	262	---	245	252	262

SLO = Simulated liftoff

TABLE 7-2 (Sheet 2 of 2)
LOX TANK PREPRESSURIZATION

COUNTDOWN	614008	614009	614010	614023	614024	614025	614028	614030
Ullage Temperature at End of Main Prepressurization, (°R) 100% Level	288	255	330	262	---	248	253	262
Ullage Volume (ft^3)	*	*	*	148	233	230	118	178

*Ullage volume could not be determined due to inoperative PU probe.

TABLE 7-3
LOX TANK PRESSURIZATION MODULE ORIFICES

COUNTDOWN	ORIFICE	ACTUAL DIAMETER (IN.)	ACTUAL AREA (IN^2)	C_D	EFFECTIVE AREA (IN^2)
	COLD GAS CONTROL SYSTEM				
614010	Secondary	0.0995	0.00776	*0.85	0.0066
	Primary	0.0995	0.00776	*0.85	0.0066
	Bypass	0.1610	0.02035	0.86	0.0149
	Secondary	0.0995	0.00777	0.87	0.00676
614020,	Primary	0.0995	0.00777	1.00	0.00776
	Bypass	0.1610	0.02035	0.86	0.0149
	Secondary	0.089	0.00622	0.976	0.00607
614021,	Primary	0.109	0.00933	0.896	0.00836
	Bypass	0.159	0.01985	0.849	0.01685
	Secondary	0.089	0.00622	0.976	0.00607
614022, Run No. 1	Primary	0.109	0.00933	0.896	0.00836
	Bypass	0.159	0.01985	0.849	0.01685
	Secondary	0.089	0.00622	0.976	0.00607
614023, Run No. 2	Primary	0.109	0.00933	0.896	0.00836
	Bypass	0.159	0.01985	0.849	0.01685
	Secondary	0.109	0.00933	0.896	0.00836
614024, Run No. 1	Primary	0.089	0.00622	0.976	0.00607
	Bypass	0.159	0.01985	0.849	0.01685
	Secondary	0.109	0.00933	0.896	0.00836
614025, Run No. 2	Primary	0.089	0.00622	0.976	0.00607
	Bypass	0.159	0.01985	0.849	0.01685
	Secondary	0.158	0.0196	0.90	0.01765
614028,	Primary	0.100	0.00785	0.97	0.007615
	Bypass	0.164	0.0211	0.88	0.0186
	HOT GAS CONTROL SYSTEM				
	Secondary	Removed	**	**	0.0332
614030,	Primary	0.242	0.04595	0.836	0.0384
	Bypass	0.161	0.02035	0.904	0.0184

* = Assumed
** = Effective area of valve

TABLE 7-4
COLD HELIUM SPHERE DATA

COUNTDOWN	614010*	614023*	614025	614028	614030
Temperature at ESC (°R)	42	43	38	39	43
Pressure at ESC (psia)	3,020	2,970	2,500	2,320	3,000
Mass in Spheres at ESC (lbm)	326	321	320	317	324
Burn time (sec)	414.6	471.9	509.1	375.8	495.9
Upper Sphere Minimum Temperature (°R)	30	33	33.0	32.6	35
Lower Sphere Minimum Temperature (°R)	27.8	29	29	29	30
Minimum Sphere Pressure (psia) Corresponding to Minimum Temperature	750	985	1,140	1,035	1,320
Time after ESC when Minimum Pressure Occurred, (sec)	235	254	260	262	251
Sphere Pressure at ECO	750	900	1,230	1,160	1,250
Temperature in Spheres at ECO (°R)					
Spheres 1 & 8	40	52	51	42	51
Spheres 2 & 7	44	55	57	47	56
Spheres 3 & 6	47	59	58	49	58
Spheres 4 & 5	47	60	59	50.4	60
LH_2 Ullage Temperature at ECO (°R)	126	151	150	153	152
Mass Remaining in Spheres at ECO (lbm)	150	139	175	193	177
Mass Consumed During Firing (lbm)	176	182	145	124	147

*Shutoff valve failure during engine firing.

TABLE 7-5
J-2013 ENGINE HEAT EXCHANGER PERFORMANCE DATA

CD	TIME FROM ESC (sec)	EMR	HELIUM FLOW (lbm/sec)	OUTLET TEMPERATURE (°R) C-0228	OUTLET TEMPERATURE (c/c) (°R) C-0009	LOX TURBINE OUTLET TEMPERATURE (°R) C-0215	INLET TEMPERATURE (°R) C-0008	INLET PRESSURE (psia) D-0056	OUTLET PRESSURE (psia) D-0161
614030	130	5.0	0.20	895	856	989	78	383	367
614030	40	4.5	0.190	805	775	901	107	361	343
614030	200	4.93	0.194	890	864	980	67	394	376
614030	250	4.9	0.106	925	873	980	72	391	389
614030	320	4.86	0.107	910	860	958	76	399	390
614028	60	5.59	0.24	966	920	1,070	---	170	100
614028	80	5.59	0.076	1,016	932	1,068	---	88	65
614028	100	5.59	0.270	948	924	1,066	---	191	111
614028	110	5.59	0.079	1,015	932	1,065	---	89	66
614028	125	5.59	0.290	949	923	1,060	---	185	109
614028	240	5.0	0.094	942	887	986	---	96	70
614028	265	4.95	0.336	850	832	976	---	188	114
614025	160	4.5	0.165	821	797	890	---	130	81
614025	187	4.5	0.068	851	797	890	---	77	58
614025	225	4.5	0.163	821	797	890	---	124	78
614025	290	5.0	0.163	912	867	977	---	124	78
614025	360	4.83	0.150	882	860	935	---	124	77

TABLE 7-6
COMPARISON OF J-2013 ENGINE HEAT EXCHANGER DATA

	NASA CONDITIONS			TEST DATA			J-2013 ENGINE LOG BOOK
PU	HOT GAS INLET TEMPERATURE (°R)	GAS GENERATOR FLOW (lbm/sec)	HELIUM INLET TEMPERATURE (°R)	EMR	LOX TURBINE OUTLET TEMPERATURE (°R)	AVERAGE HELIUM INLET TEMPERATURE (°R)	GAS GENERATOR FLOW (lbm/sec)
Maximum	1,060	7.1	31	5.6	1,065	75	7.0
Nominal	990	6.5	31	5.0	985	75	6.5
Minimum	950	6.1	31	4.5	895	75	5.8

Data presented in this table were used to analyze differences between data and predictions on heat exchanger performance (paragraph 7.1.2.5) and to develop the prediction curves (figure 7-14).

21 February 1966

TABLE 7-7
S-IVB/IB LOX PUMP CHILLDOWN

Countdown		614005-3	614006	614007	614008	614009	614010-2	614014	614017-A3	614017-E2	614025	614030
Engine No.		J-2003	J-2003	J-2003	J-2003	J-2003	J-2003	J-2013	J-2013	J-2013	J-2013	J-2013
Chilldown Time (min)		10	5	5	10	10	10	28	3.5	23	6	6
Initiation of Chilldown (sec)		SLO -580	SLO -190	SLO -215	SLO -500	SLO -500	SLO -500	SLO -1,680	SLO -185	SLO -1,220	SLO -280	SLO -275
Gas Generator Bleed Valve Open		50% LH2 Load	Start of Chilldown	50% LH2 Load	50% LH2 Load	50% LH2 Load	50% LH2 Load	Start of LOX Load	Start of LOX Load	Start of LOX Load	Start of LOX Load	Start of LOX Load
Initiation of Prepressurization (sec)		SLO -180	SLO -180	SLO -180	SLO -180	SLO -180	SLO -180	SLO -750	SLO -270	SLO -270	SLO -180	SLO -175
Prevalve Open (End of Chilldown) (sec)		ESC -6.5	ESC -6.5	ESC -6.5	ESC -6.5	ESC -6.5	ESC -6.5	ESC -7.5	ESC -7.5	ESC -7.5	ESC -7.5	ESC -7.5
Available NPSH at ESC (psia)		28.8	27.4	28.1	27.1	27.1	25.2	32.9	29.6	28.3	27.8	28.8
Minimum Required NPSH at ESC (psi)		16	16	16	16	16	16	16.3	16.3	16.3	16.3	16.3
Available NPSH at Engine Inlet (psi)	UC	45	—	—	46	46	46	13.3	—	13.0	13.2	13.7
	PC	67	69	70	70	70	70	42.5	39.3	39.7	36.7	37.6
Chilldown Flowrate (gpm)	UC	23	—	—	16.8	17	16	39.4	—	38.7	38.8	38.1
	PC	24	17	17.5	17	17	17	44	43	43.3	42.8	42
Engine Interface Pressure (psia)	UC	62	—	—	65	64	64	29.6	—	28.9	29.4	30.0
	PC	84	86.5	88	88.5	88	87.5	58.9	55.5	55.8	53	54.2
System Pressure Drop (psid)	UC	41.1	41.6	—	43.3	42.6	43.1	8.9	—	8.0	8.5	9.0
	PC	45.7	42.1	45.1	42.8	42.6	44.6	10.8	10.4	9.7	9.7	9.9
Flow Coefficient C ($sec^2/in.^2/ft^3$)	UC	222	—	—	433	435	477	16.28	—	15.12	14.5	16.0
	PC	225	412	417	419	435	437	16.40	15.68	14.38	15.0	16.0
Engine Interface Temperature (°R)	UC	164.8	—	—	166.1	165.7	166.0	164.3	—	163.9	164.2	164.3
	PC	164.8	165.5	165.9	166.0	165.7	166.0	164.5	164.2	164.1	164.3	164.7
Gas Generator Bleed Valve Temperature (°R)	UC	168	—	—	170	168.5	170.1	166.0	—	165.4	166.0	166.3
	PC	167	173	170	169	168.5	170.1	166.2	165.8	165.4	166.1	166.5
Return Line Temperature (°R)	UC	—	—	—	169	168	169	167.5	—	168.0	166.8	167.1
	PC	—	—	174	170	168.5	170.1	167.9	167.0	168.0	166.5	166.9
Heat Input Section 1 (Btu/hr) (Tank - LOX Pump Inlet)*	UC	8,300	—	—	10,900	9,500	10,600	9,100	—	5,400	8,100	8,800
	PC	8,300	8,700	10,600	10,600	9,500	10,600	12,200	9,000	8,000	9,000	13,600
Heat Input Section 2 (Btu/hr) (LOX Pump Inlet - Gas Generator)	UC	17,000	—	—	15,100	7,100	16,000	15,500	—	13,500	16,600	18,200
	PC	12,200	29,500	16,600	11,800	7,100	16,100	17,300	15,900	13,000	17,800	17,500
Heat Input Section 3 (Btu/hr) (Gas Generator - Tank Return)	UC	—	—	—	—	—	—	13,800	—	23,400	6,800	6,300
	PC	—	—	16,200	3,900	—	—	17,300	12,000	26,100	4,000	3,900
Total System Heat Input (Btu/hr)	UC	—	—	—	—	—	—	38,400	—	42,300	31,500	33,300
	PC	—	—	43,400	26,400	—	—	46,800	36,900	47,100	31,700	35,000
LOX Pump Inlet Temperature Rise Rate from End of Chilldown (°R/min to ESC)		1.2	0	2.9	3.0	1.2	1.9	—	3.3	3.4	3.8	3.4
Wind Speed (mph)		5	2-3	7-8	5	0-3	5	20-25	0-2	0-2	10	3

NOTES:
SLO = Simulated Liftoff Time
ESC = Engine Start Command
UC = Chilldown Period when LOX Tank is Unpressurized
PC = Chilldown Period when LOX Tank is Pressurized
*LOX Temperature in Tank 163.3° R

TABLE 7-8
S-IVB/V LOX PUMP CHILLDOWN

COUNTDOWN	614034		614043		614044	
	1st BURN	2nd BURN	1st BURN	2nd BURN	1st BURN	2nd BURN
Length of Chilldown (min)	11	10	11	10	11	10
Start of Chilldown at ESC (sec)	-654	-581	-670	-579	-675	-592
Start Prepressurization at ESC (sec)	-720	-295	-720	-295	-720	-295
Maximum Engine Interface Pressure During Transient Surges (psia)	----	55	----	52	----	49
Engine Interface Pressure at ESC (psia)	45.4	43.6	46.6	40.3	44.7	43.0
Engine Interface Temperature at ESC (°R)	165.1	----	164.7	165.5	165.4	165.5
Available NPSH at ESC (psi)	28.4	----	30.0	22.9	27.4	25.6
Required NPSH at ESC (psi)	16.7	16.7	16.7	16.7	16.7	16.7
Time from start of childown until saturated temperature reached at childown return line (sec)	8	13	23	13	25	23
Heat-up rate at engine interface at end of chilldown (°R/min)	3.9	----	2.2	5.8	4.0	3.8

TABLE 7-9
S-IVB/IB LOX NPSH

COUNTDOWN	614009	614010	614025	614028	614030
Maximum Available NPSH (psi)	33.8	34.5	32.5	29	35
Minimum Available NPSH (psi)	26.3	22	19.8	22	21
Required Minimum NPSH (psi)	15	15	20.0 (EMR=5.5:1) 14.0 (EMR=5.0:1)	20.0 (EMR=5.5:1) 14.0 (EMR=5.0:1)	20.0 (EMR=5.5:1) 14.0 (EMR=5.0:1)
Pressurization Cycles	11	—	—	7	5

TABLE 7-10
S-IVB/V LOX NPSH

COUNTDOWN	614034-1	614043-1	614043-2	614044-1	614044-2
Maximum available NPSH (psi)	33	33.8	—	33.3	29.3
Minimum available NPSH (psi)	26.1	25.2	—	26.2	21.2
Minimum required NPSH (psi)	14.0 (EMR=5.0:1) 20.0 (EMR=5.5:1)	14.0 (EMR=5.0:1) 20.0 (EMR=5.5:1)	14.0 (EMR=5.0:1) 20.0 (EMR=5.5:1)	14.0 (EMR=5.0:1) 20.0 (EMR=5.5:1)	14.0 (EMR=5.0:1) 20.0 (EMR=5.5:1)
Pressurization Cycles	6	6	—	5	3 1/2

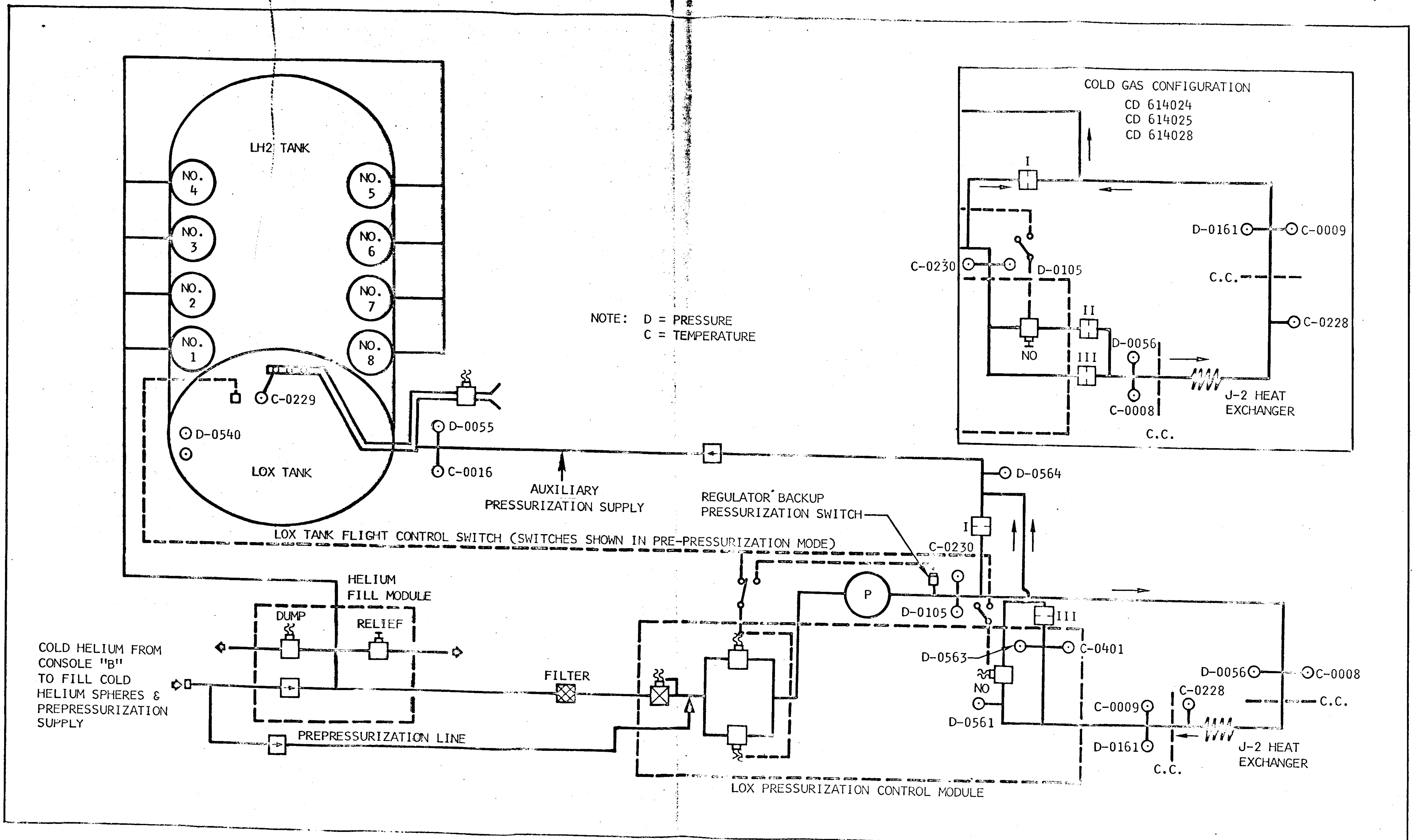

Figure 7-1 LOX Tank Pressurization System (Hot Gas Configuration - CD 614030 thru CD 614044)

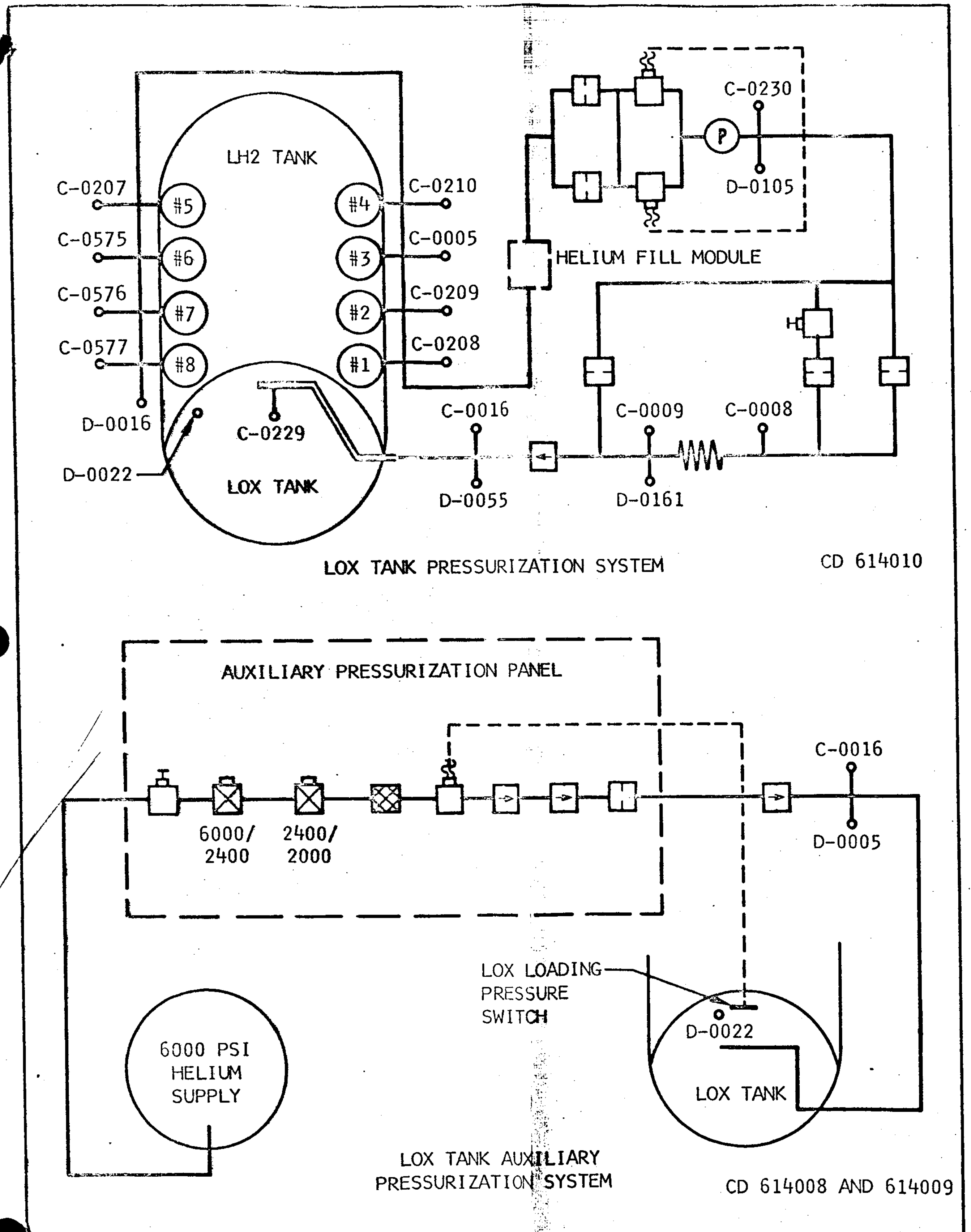

Figure 7-2 LOX Tank Temporary Pressurization Systems

21 February 1966

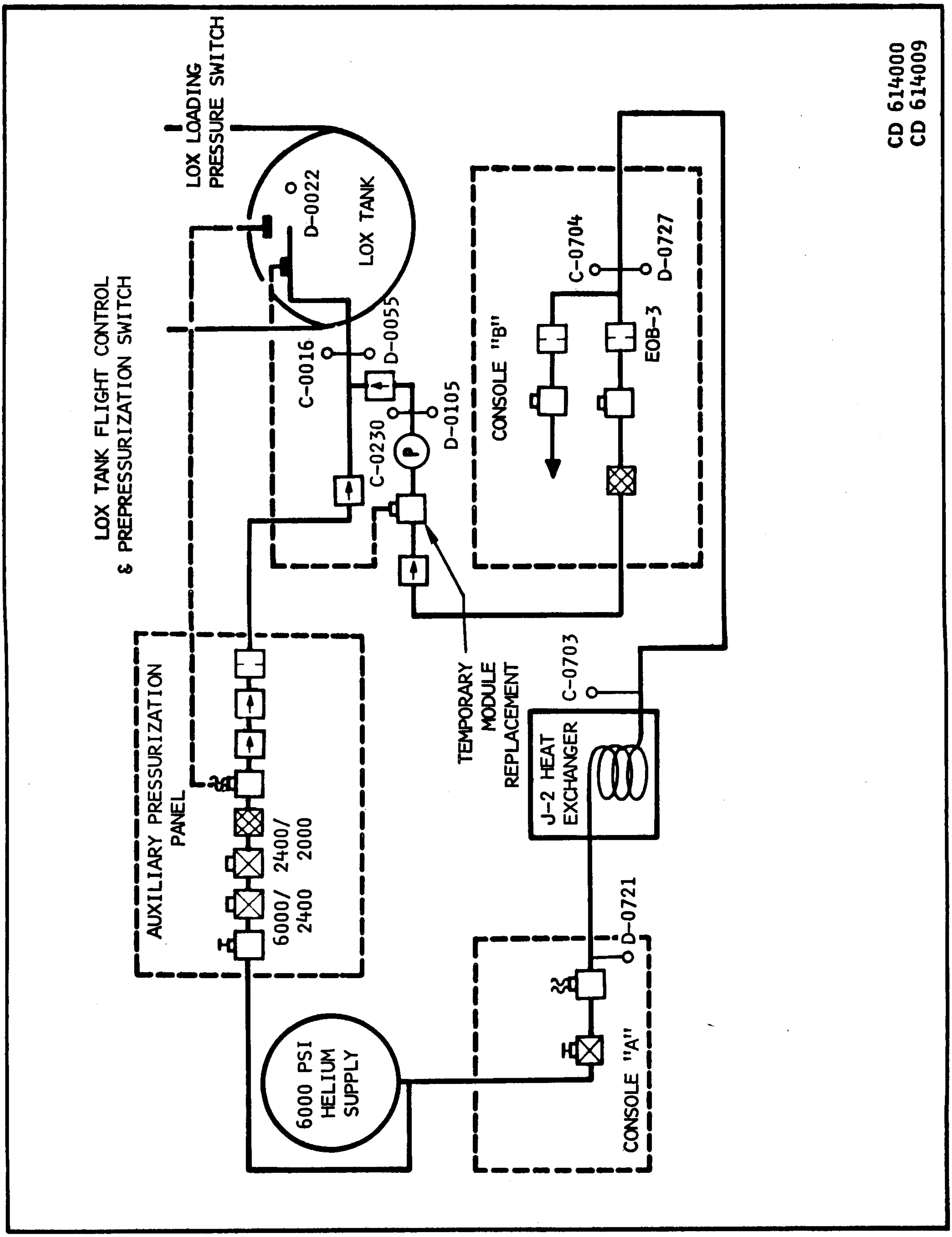

Figure 7-3 LOX Tank Pressurization System

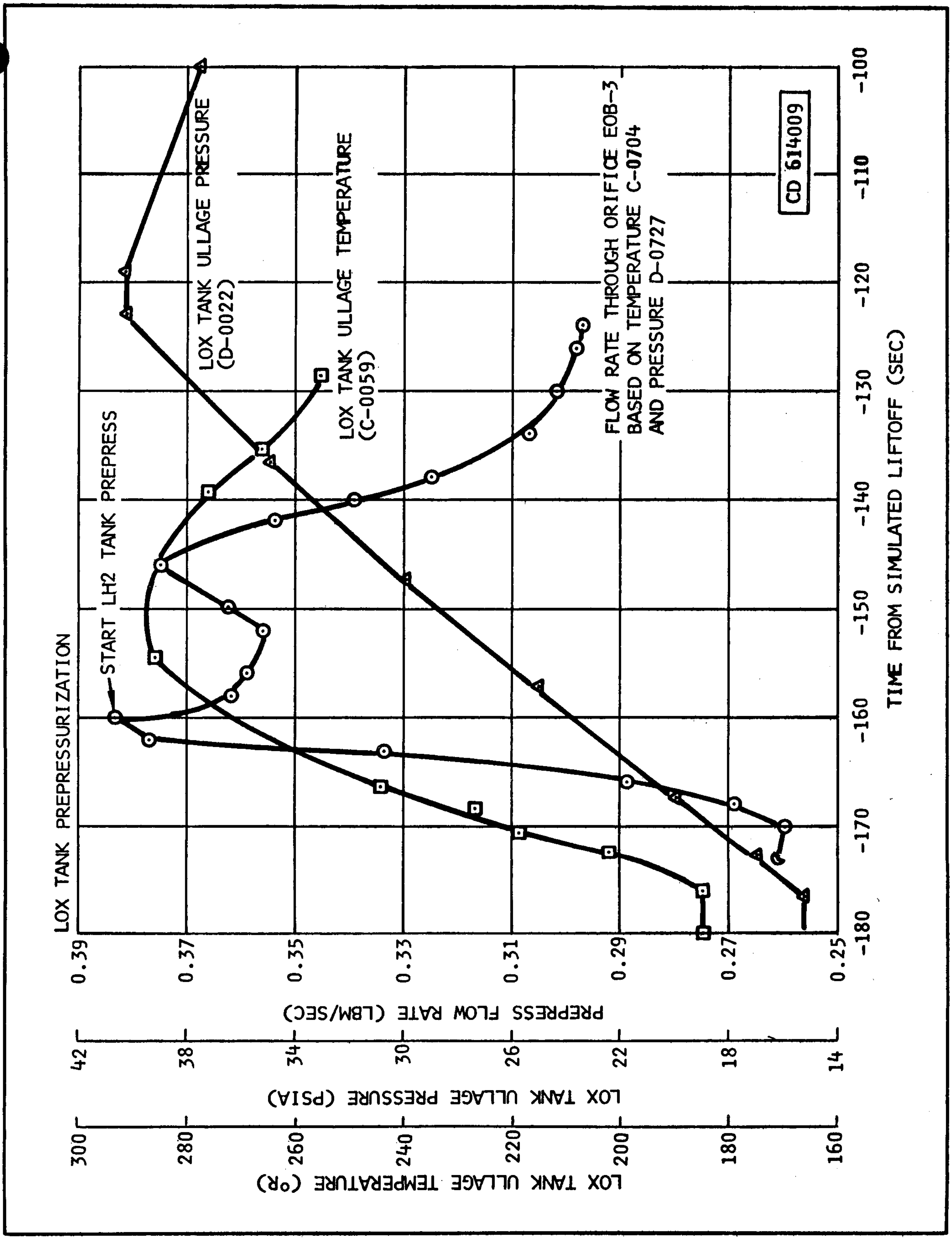

Figure 7-4 LOX Tank Prepressurization Performance

21 February 1966

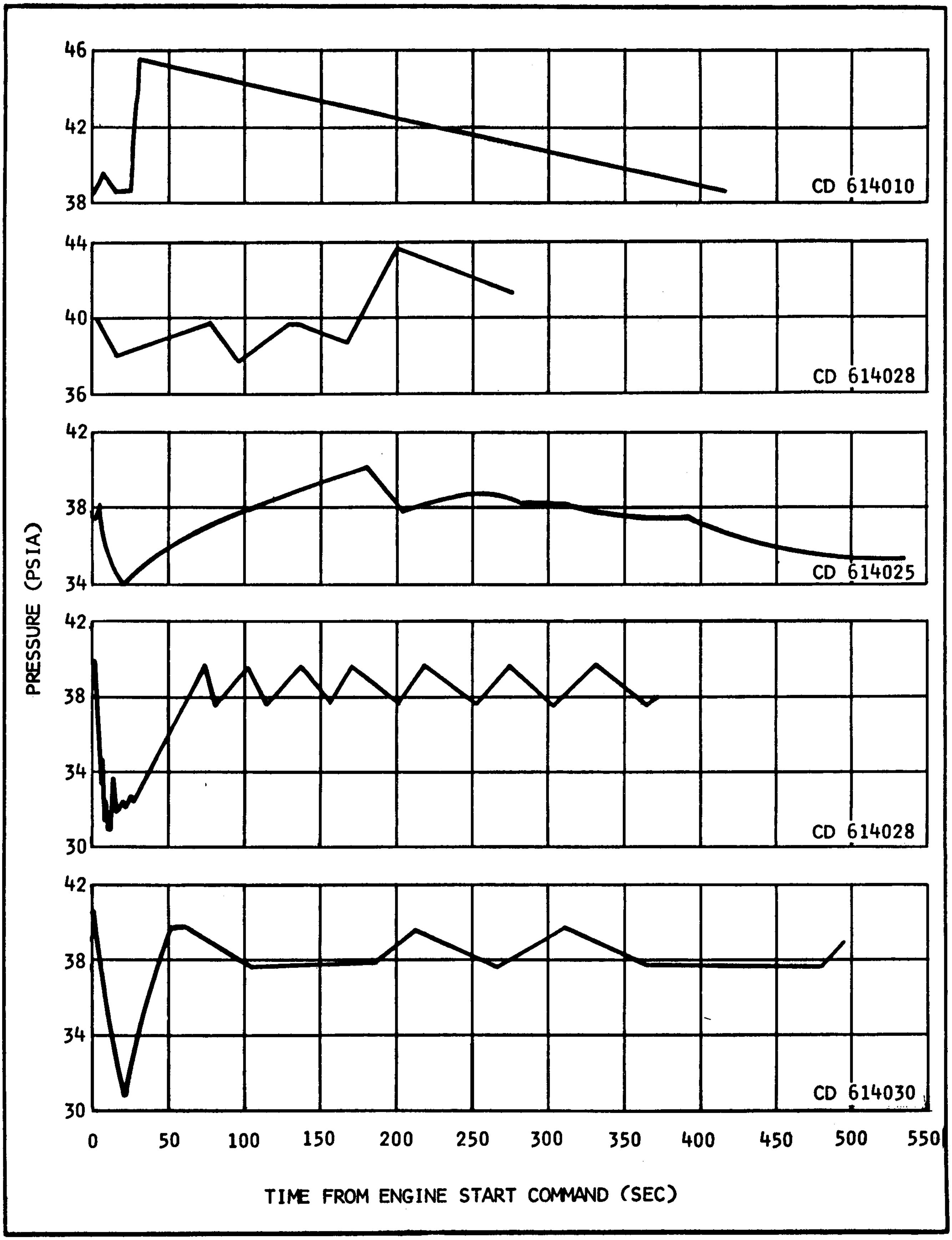

Figure 7-5 LOX Tank Ullage Pressure History

21 February 1966

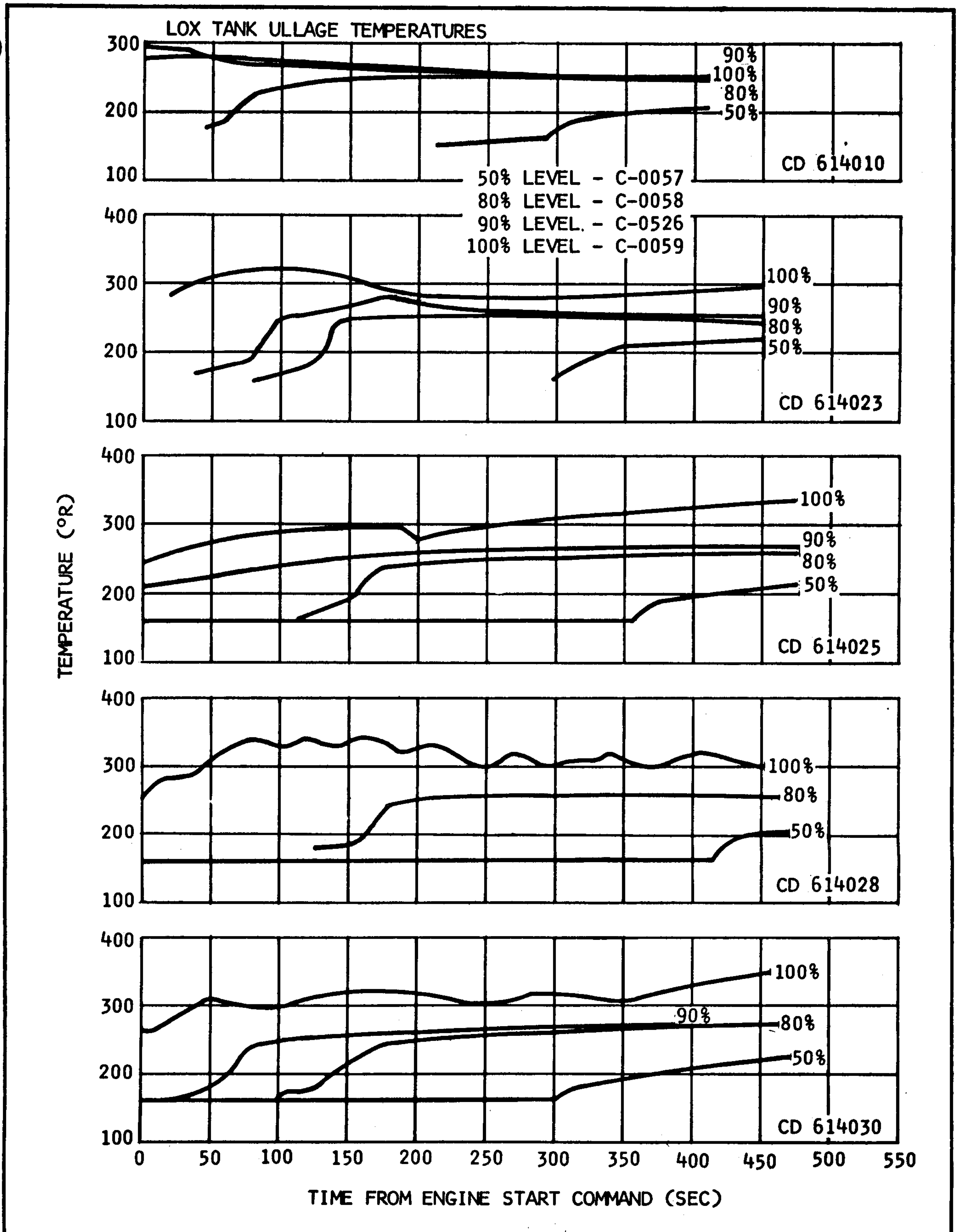

Figure 7-6 LOX Tank Ullage Temperature History

21 February 1966

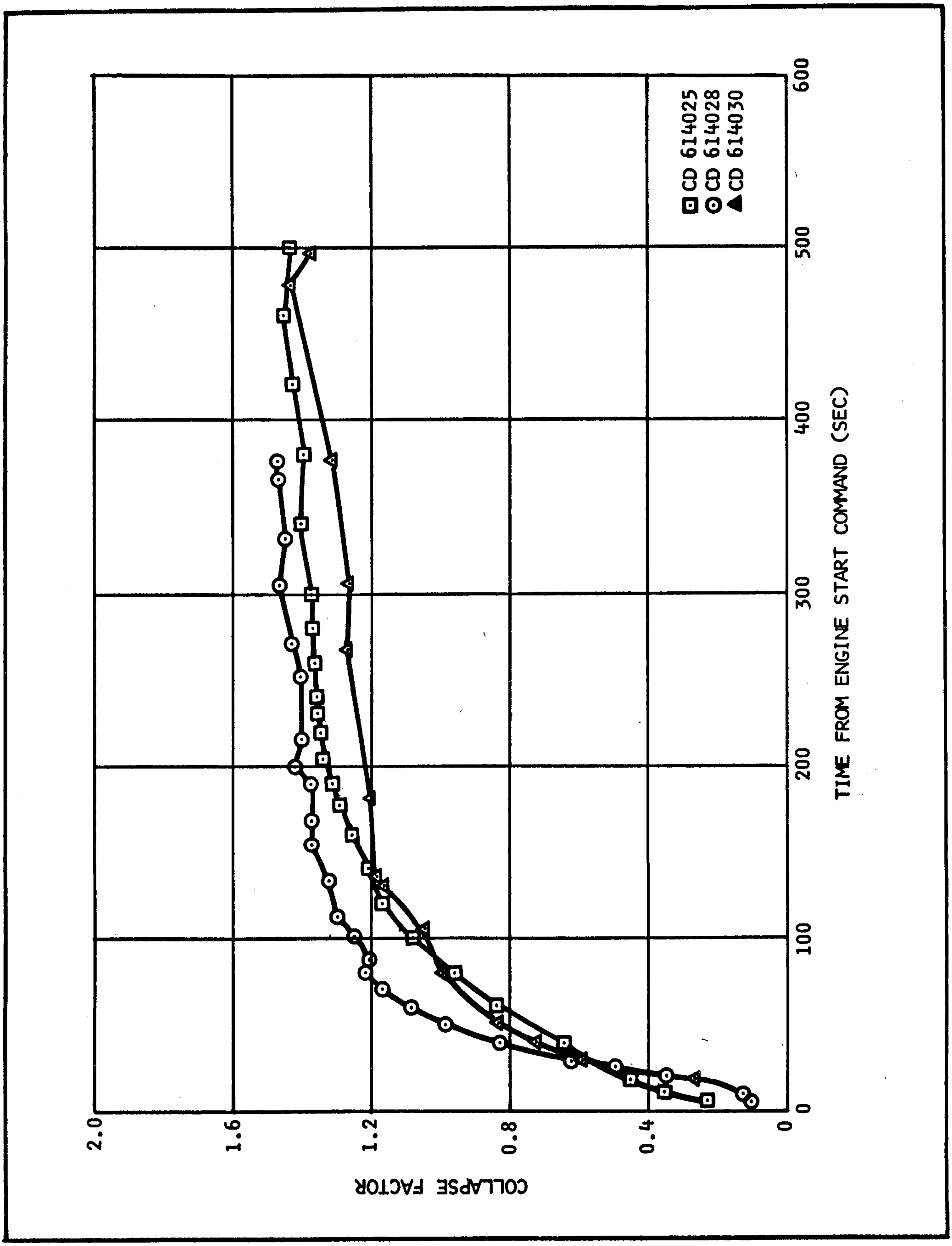

Figure 7-7 Collapse Factor History

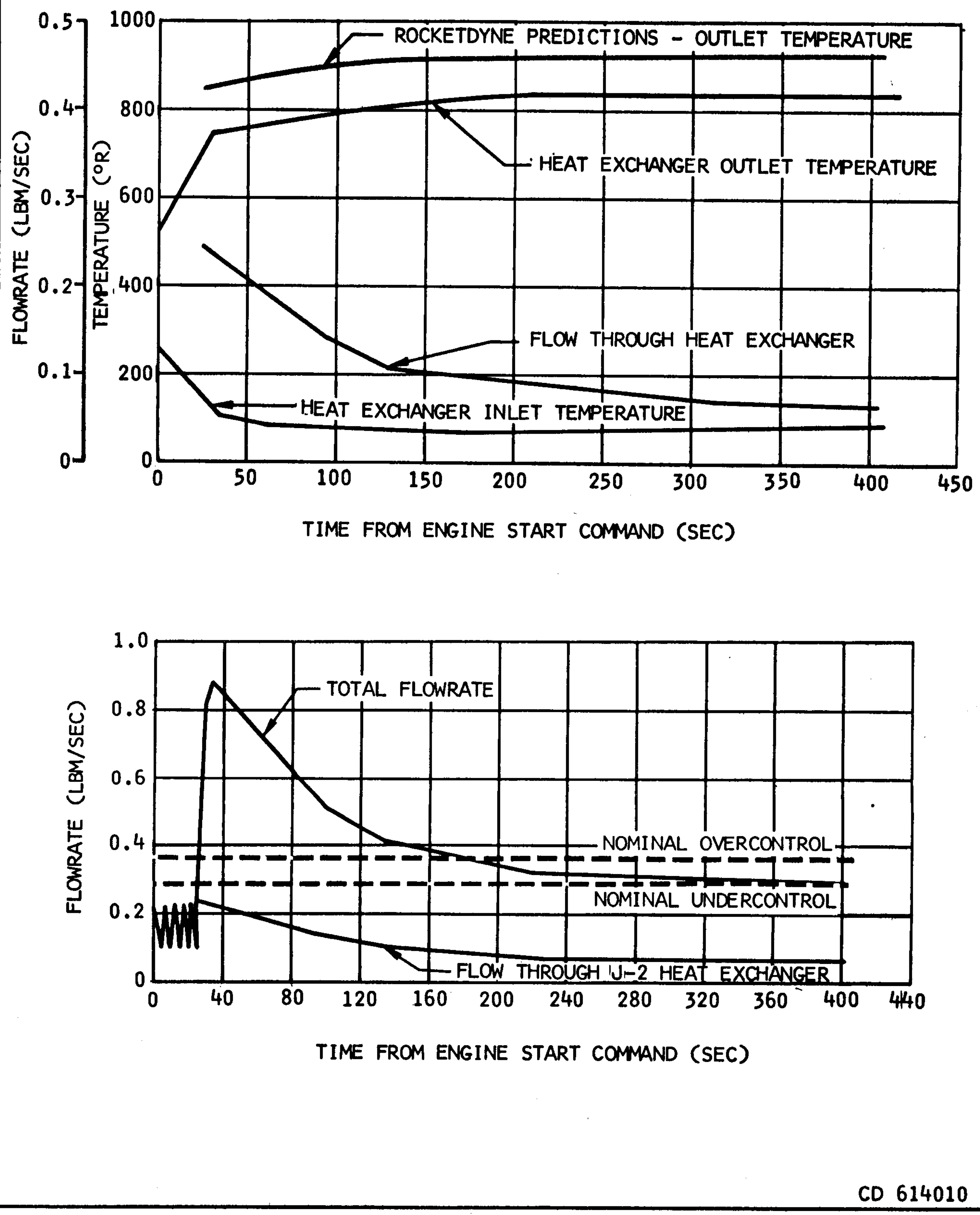

Figure 7-8 J-2 Heat Exchanger Parameters

21 February 1966

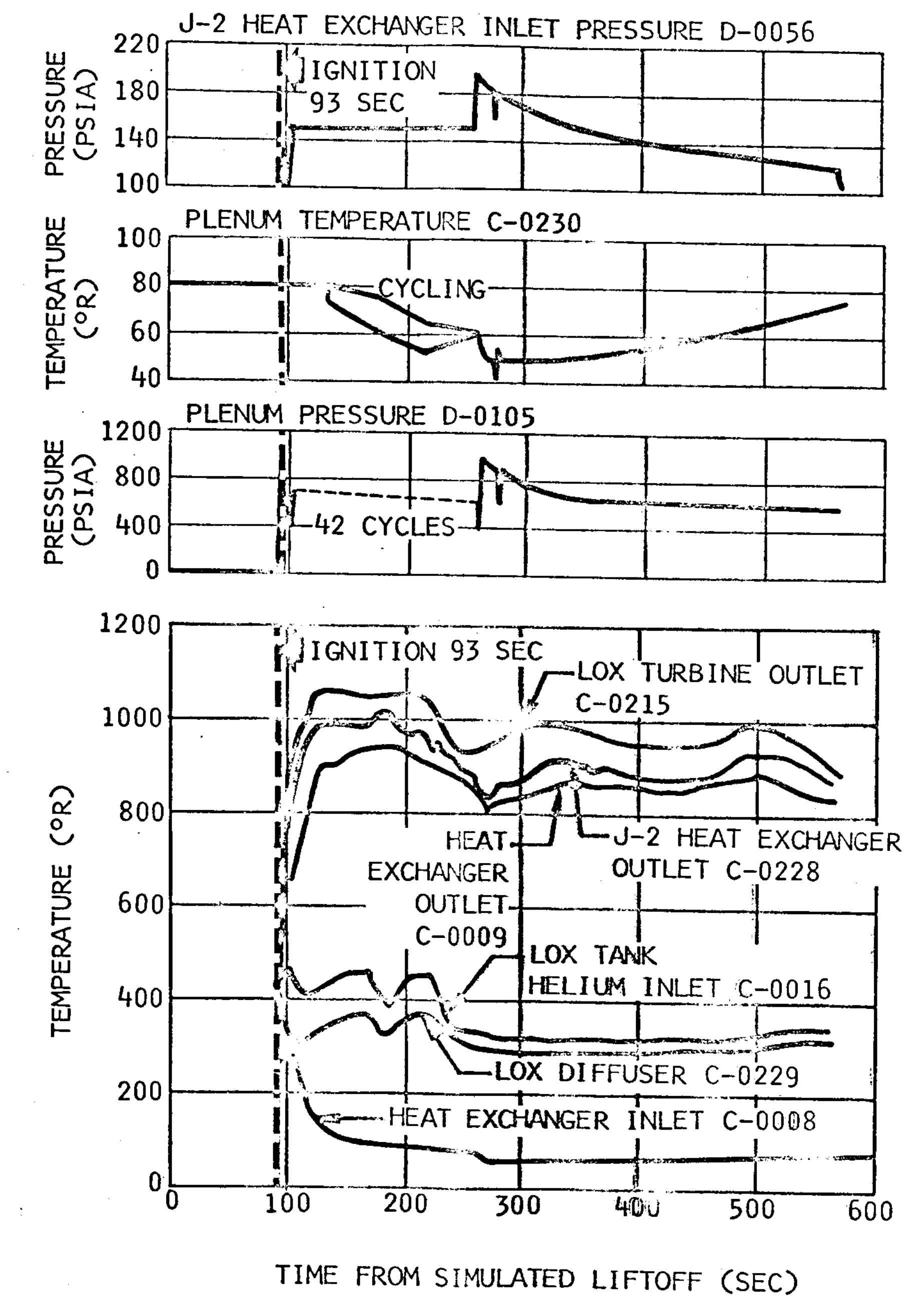

Figure 7-9 Heat Exchanger Operating Conditions

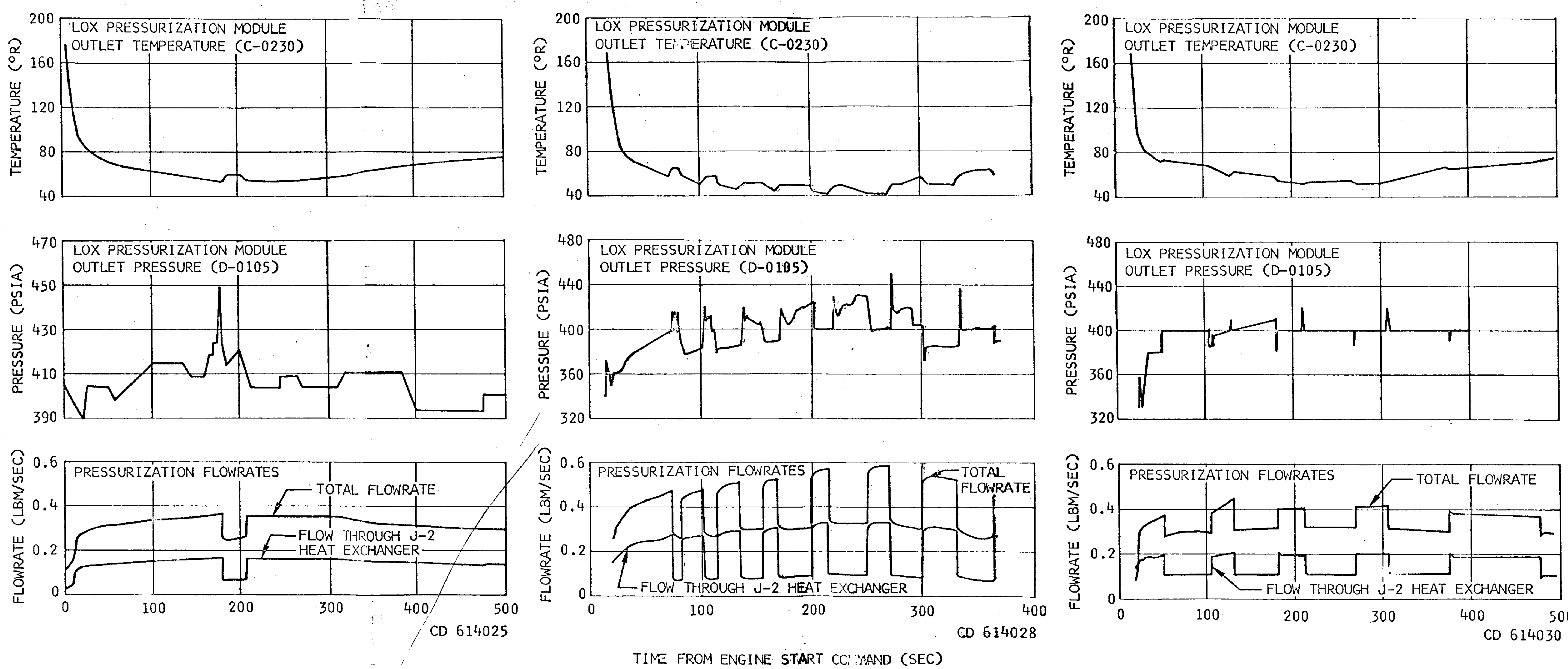

Figure 7-10 Pressurization Module Outlet Conditions

21 February 1966

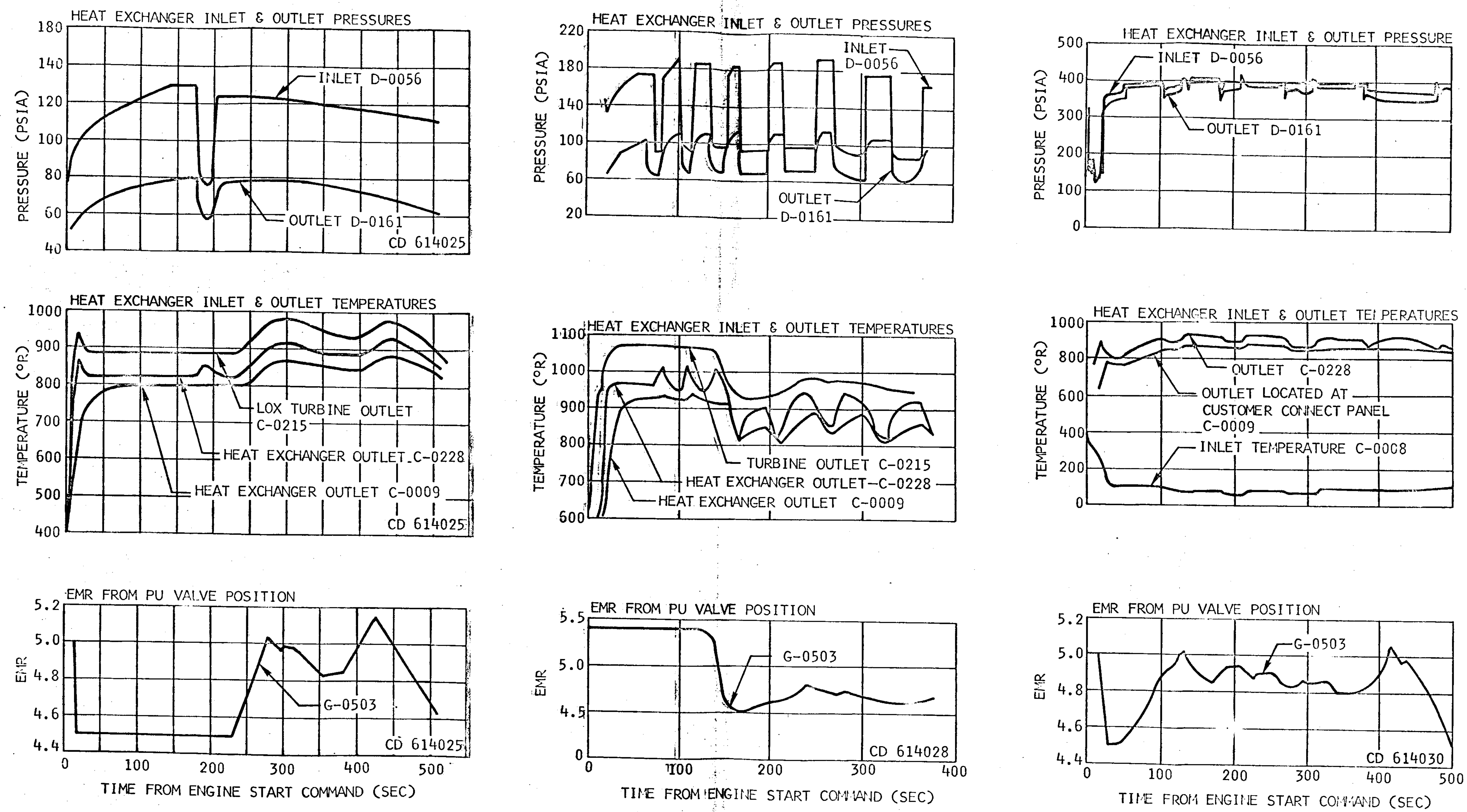

Figure 7-11 Heat Exchanger Conditions

21 February 1966

Figure 7-11

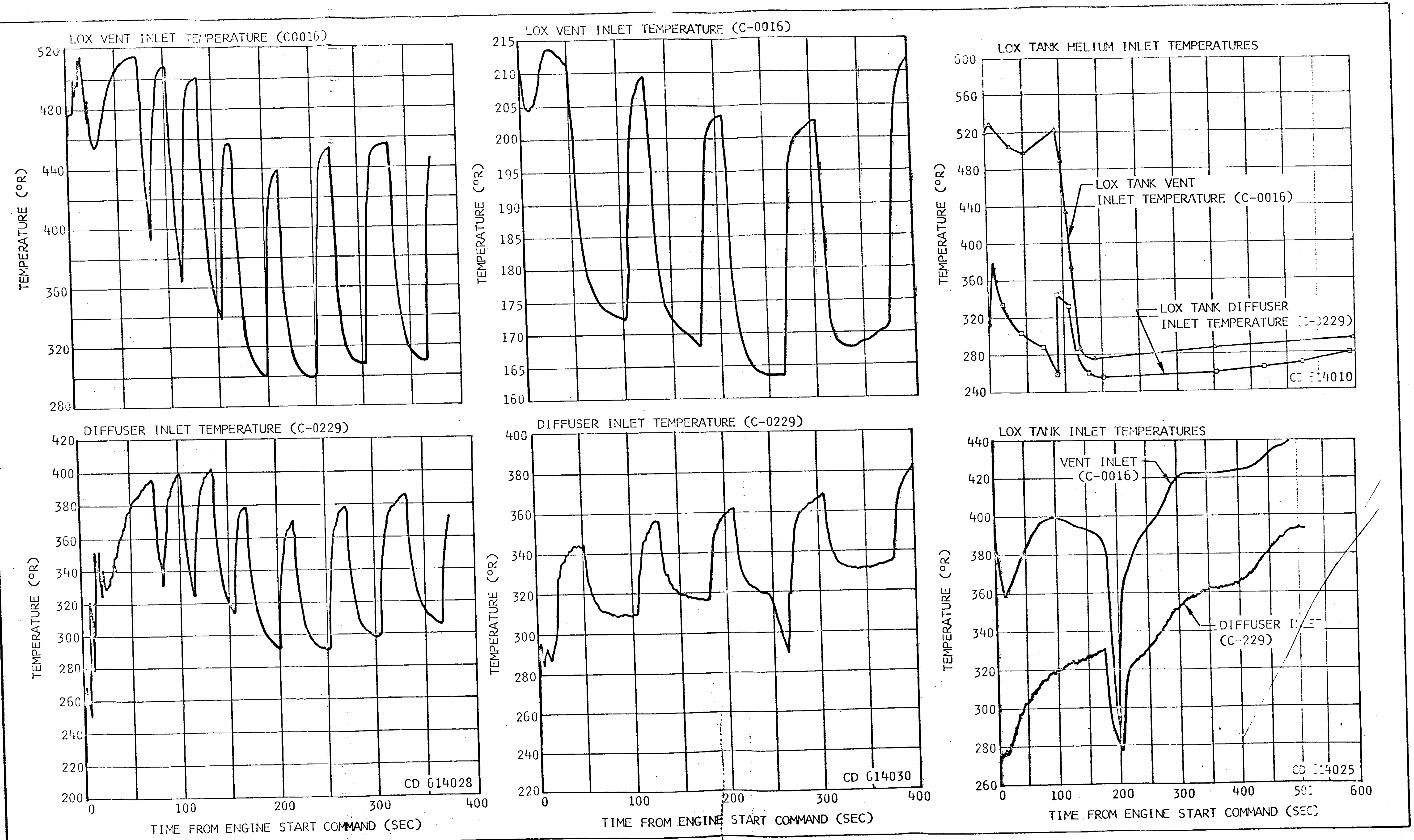

Figure 7-12 LOX Tank Pressurant Supply Temperature History

21 February 1966

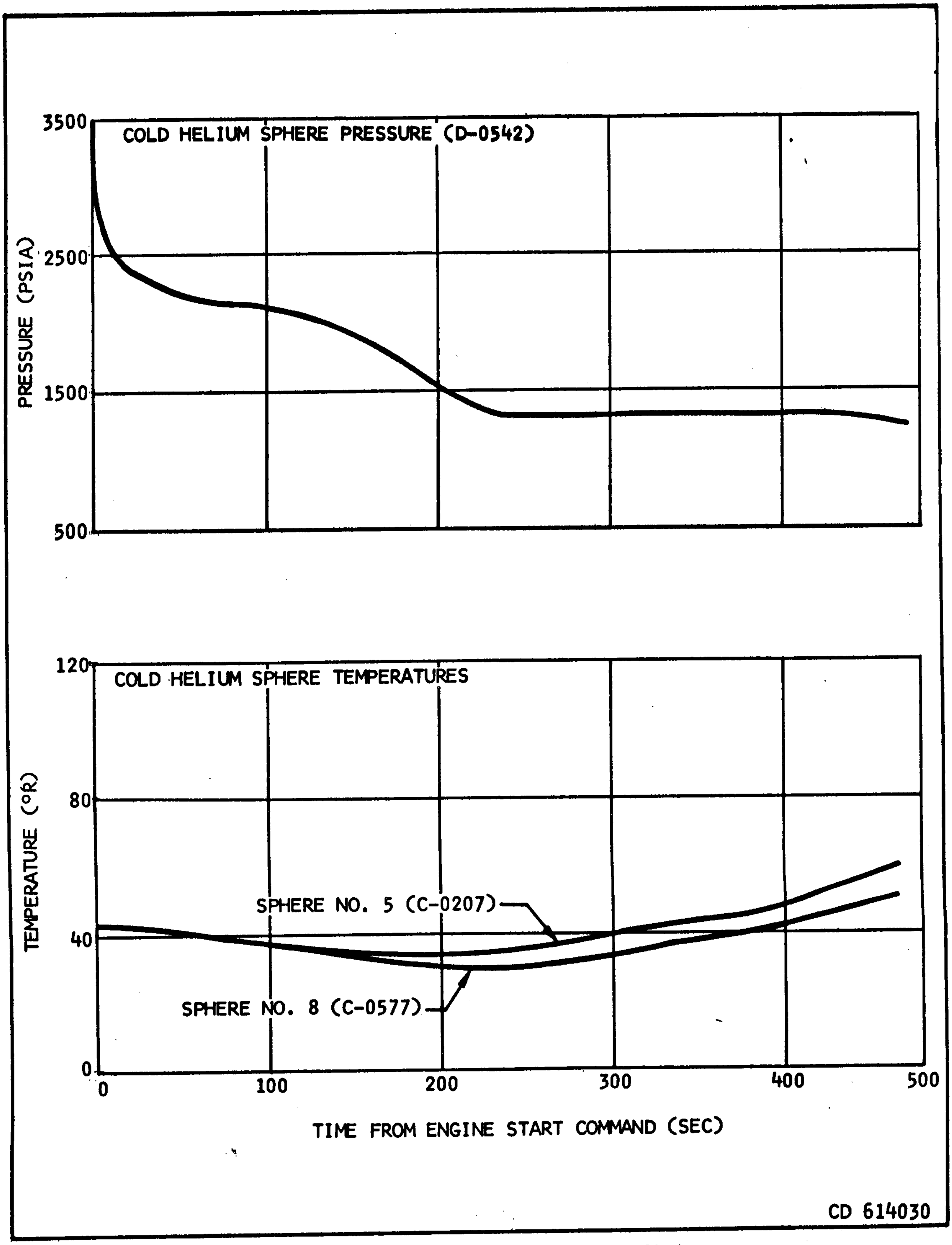

Figure 7-13 Cold Helium Sphere Conditions

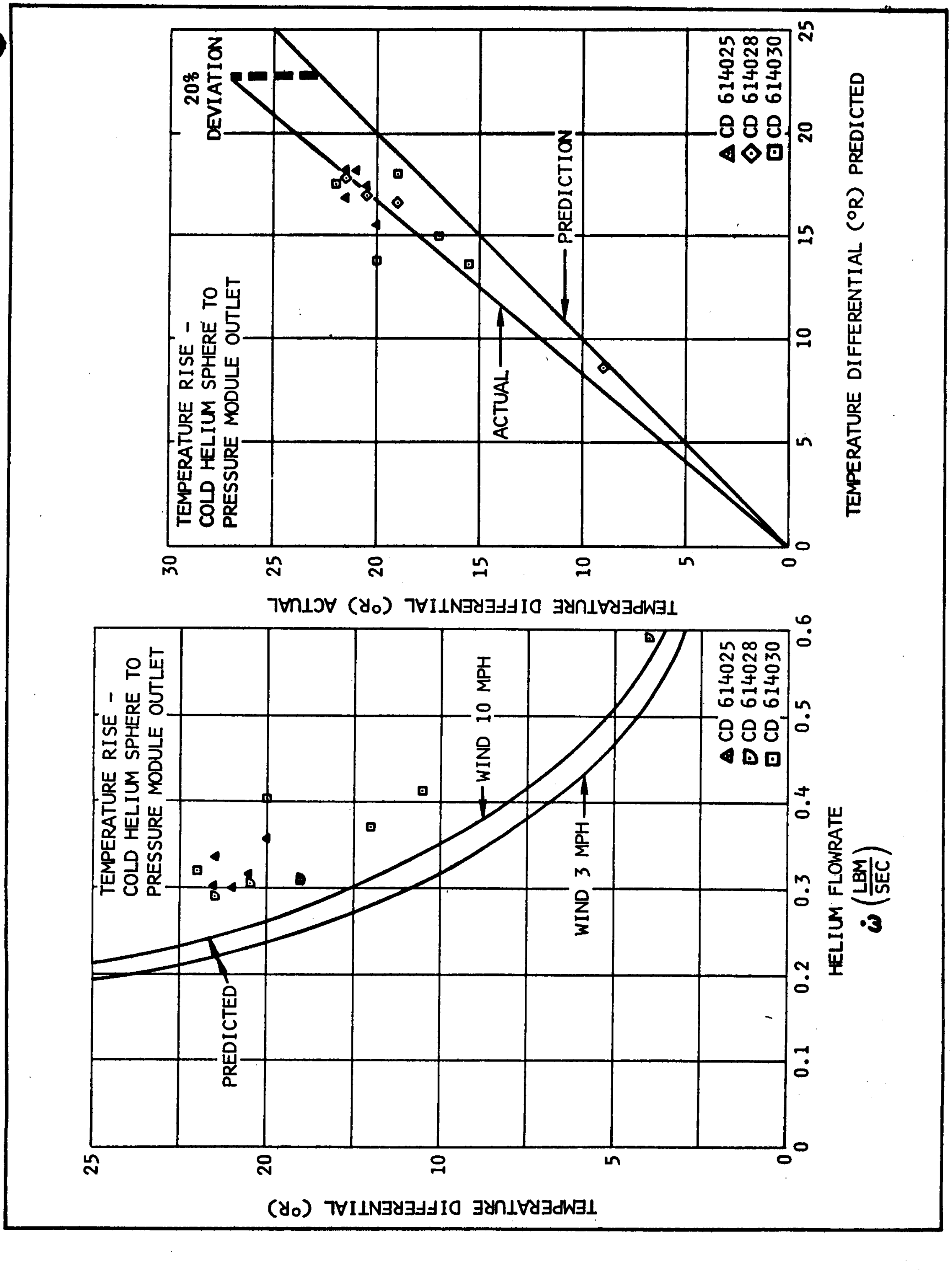

Figure 7-14 Pressurization Module Inlet Line Temperature Pickup

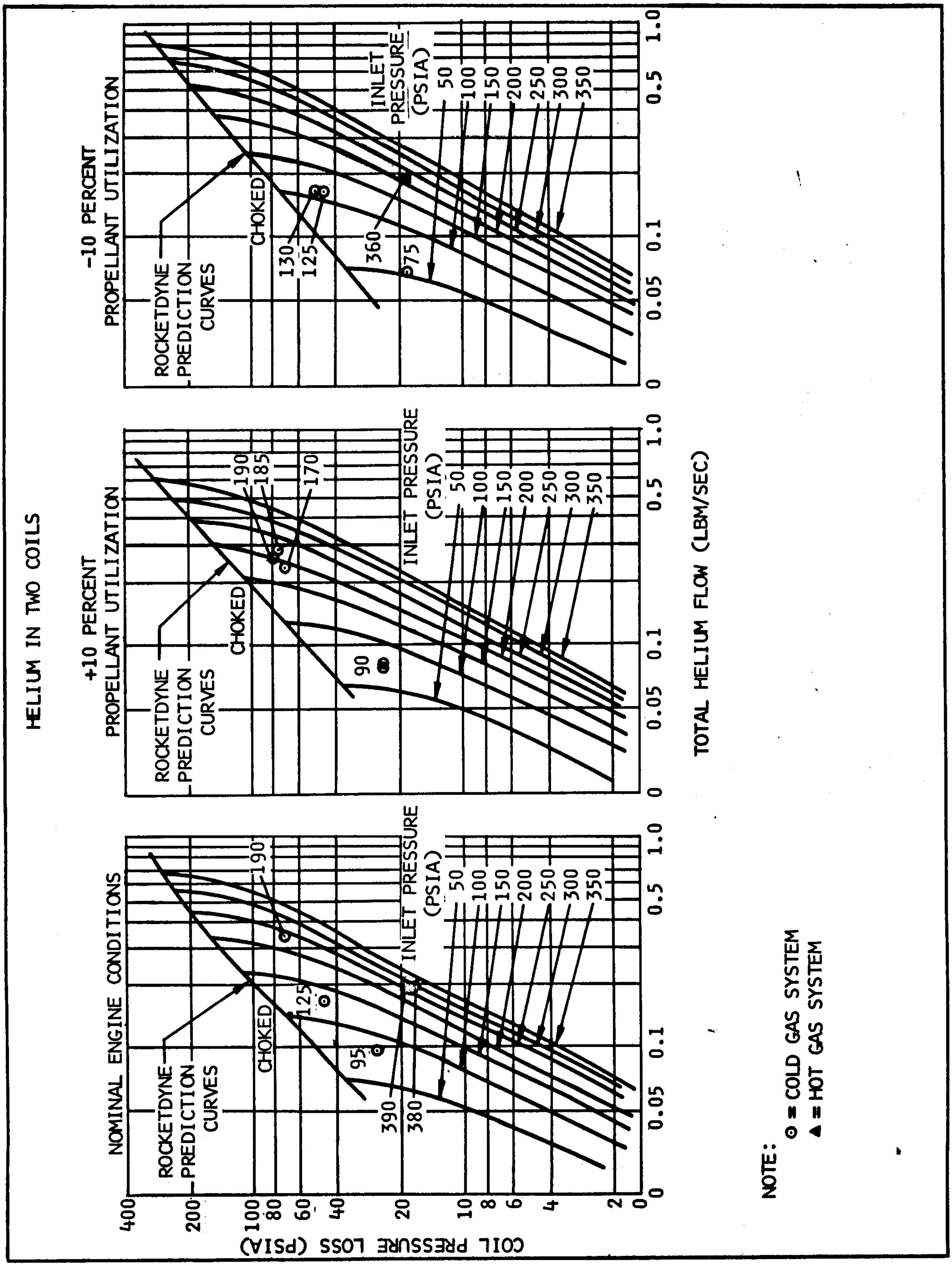

Figure 7-15 Heat Exchanger Pressure Drop

21 February 1966

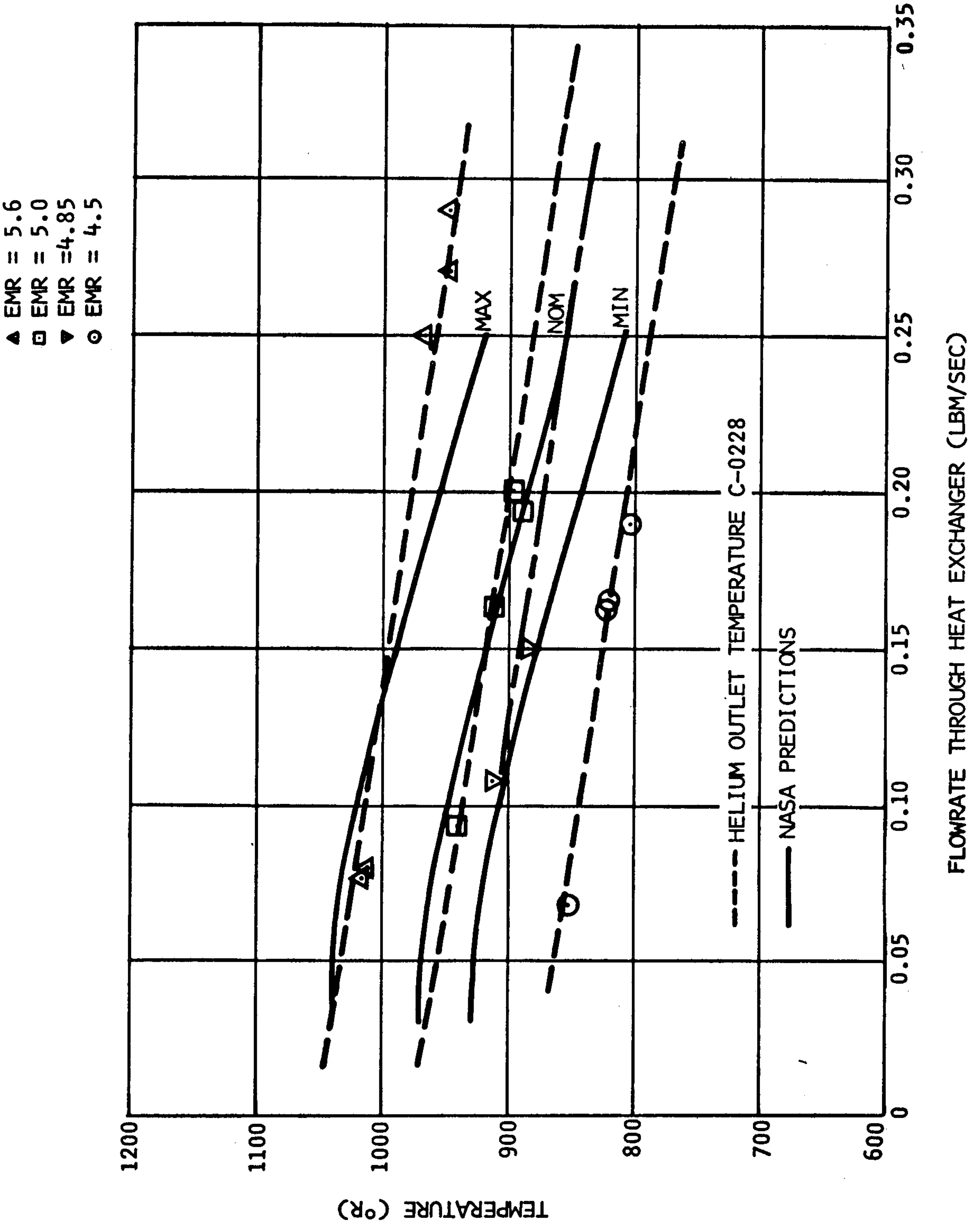

Figure 7-16 J-2 Heat Exchanger Performance

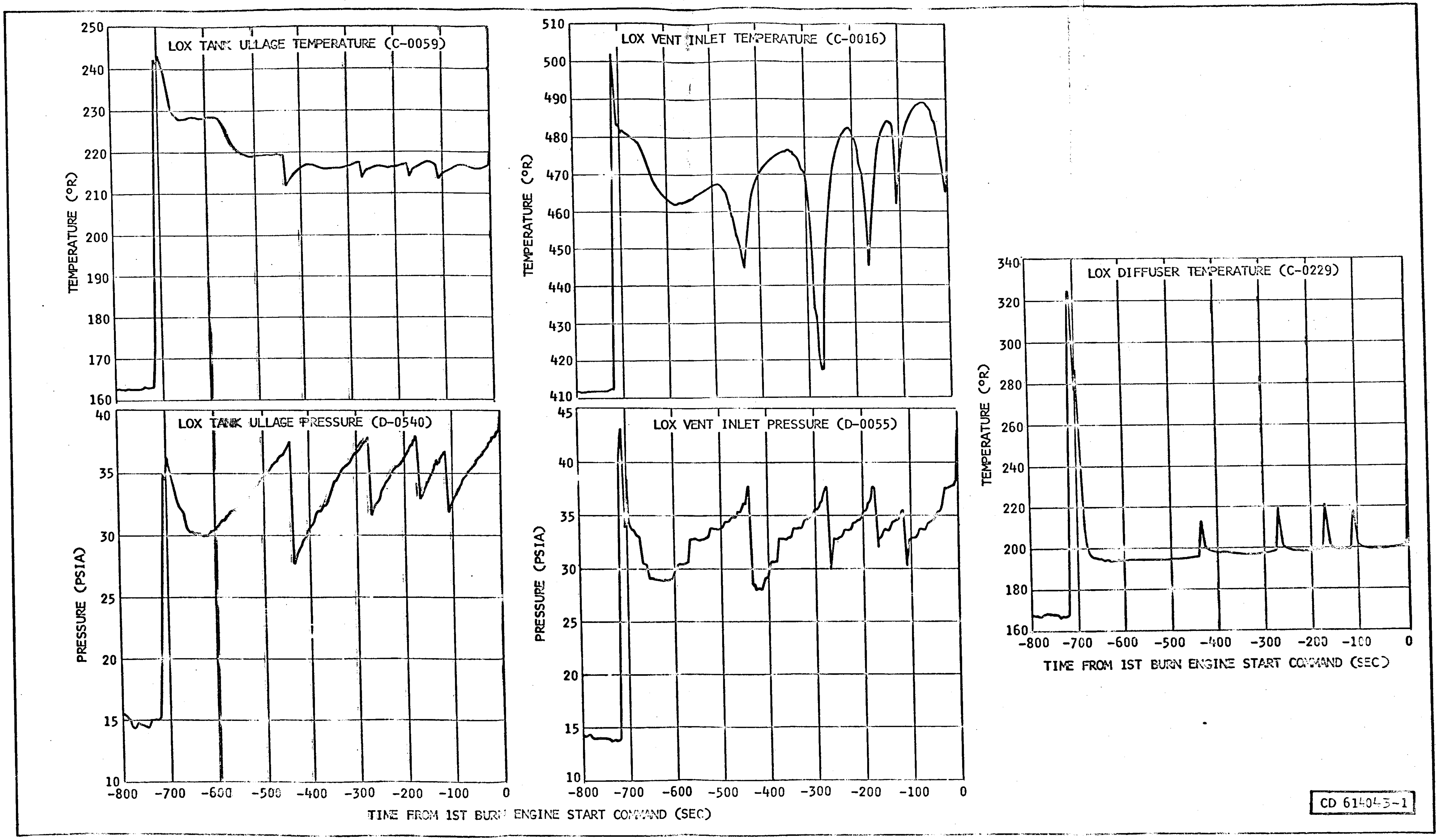

Figure 7-17 LOX Tank Conditions During Prepressurization

21 February 1966

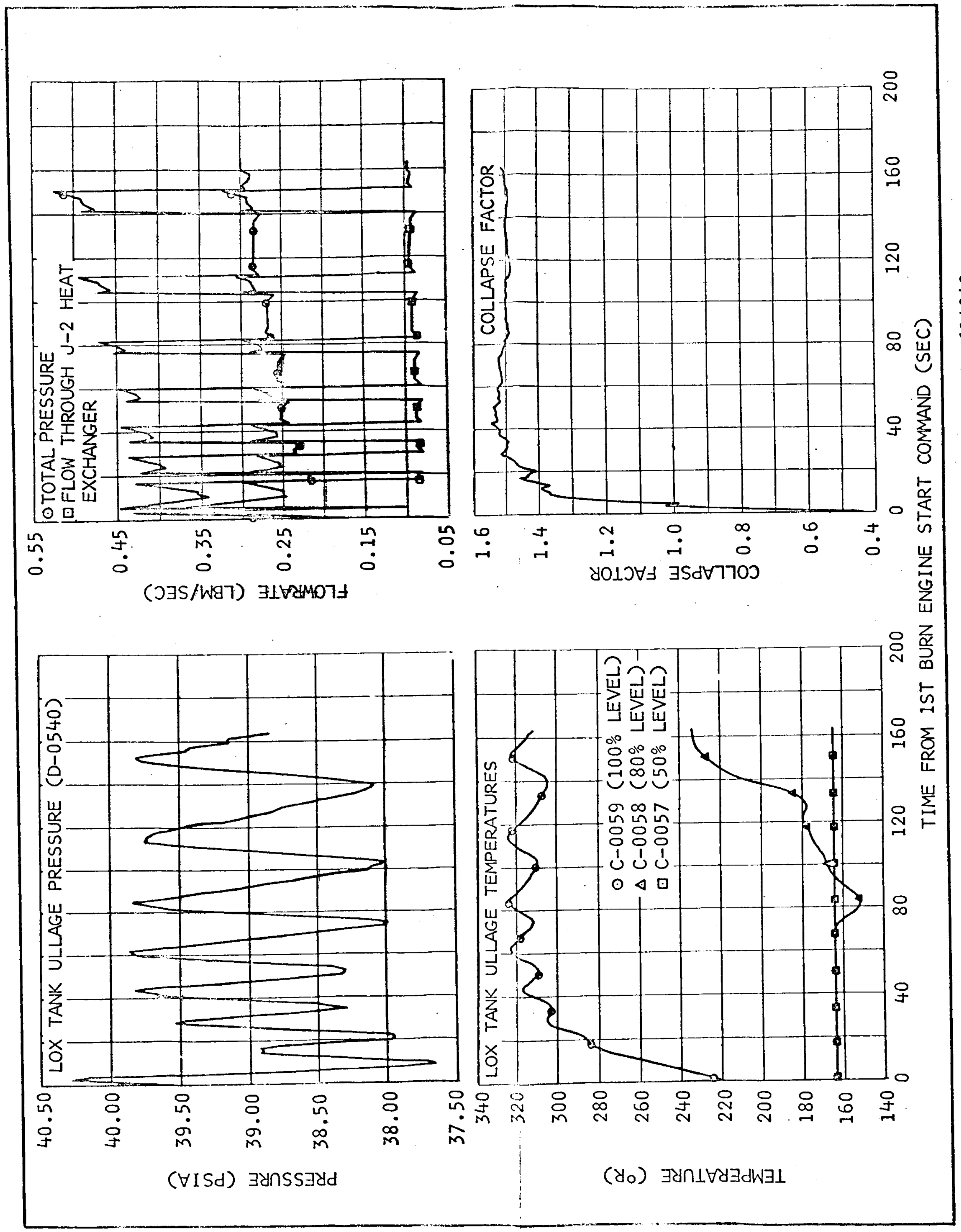

Figure 7-18 LOX Tank Conditions During 1st Burn - CD 614043

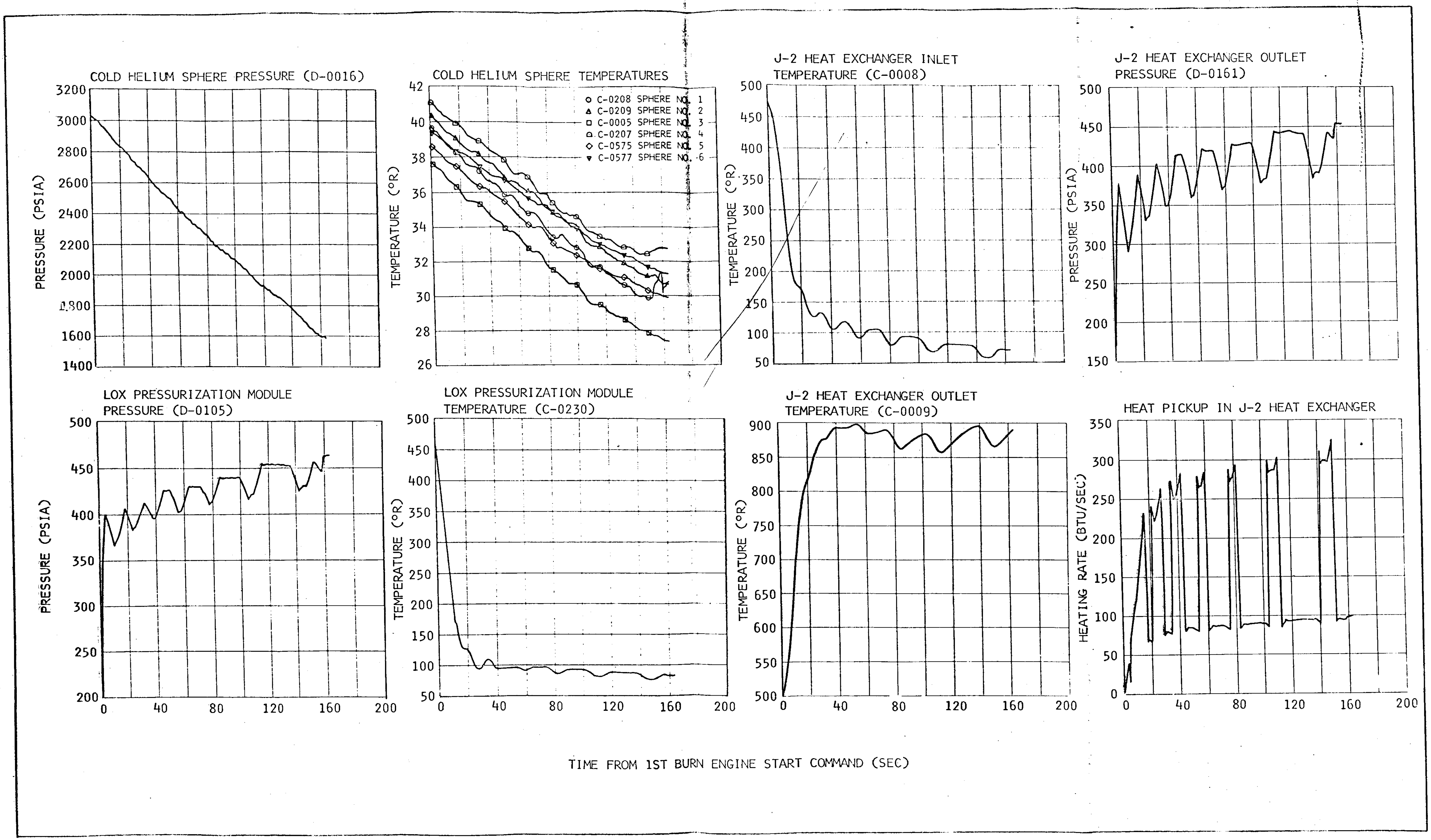

Figure 7-19 LOX Tank Pressurant Supply Conditions During 1st Burn - CD 614043

21 February 1966

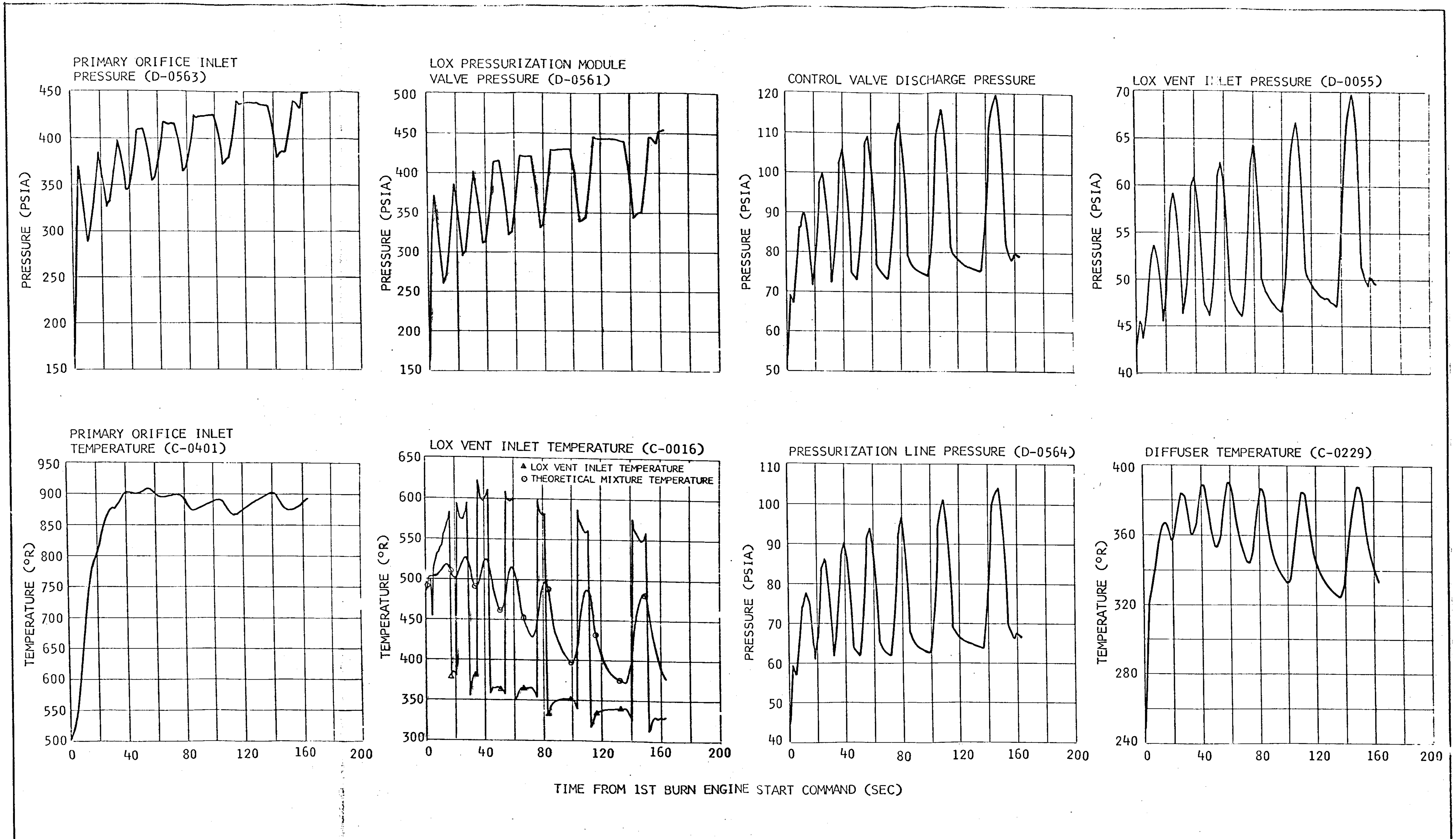

Figure 7-20 LOX Tank Pressurant Delivery During 1st Burn - CD 614043

21 February 1966

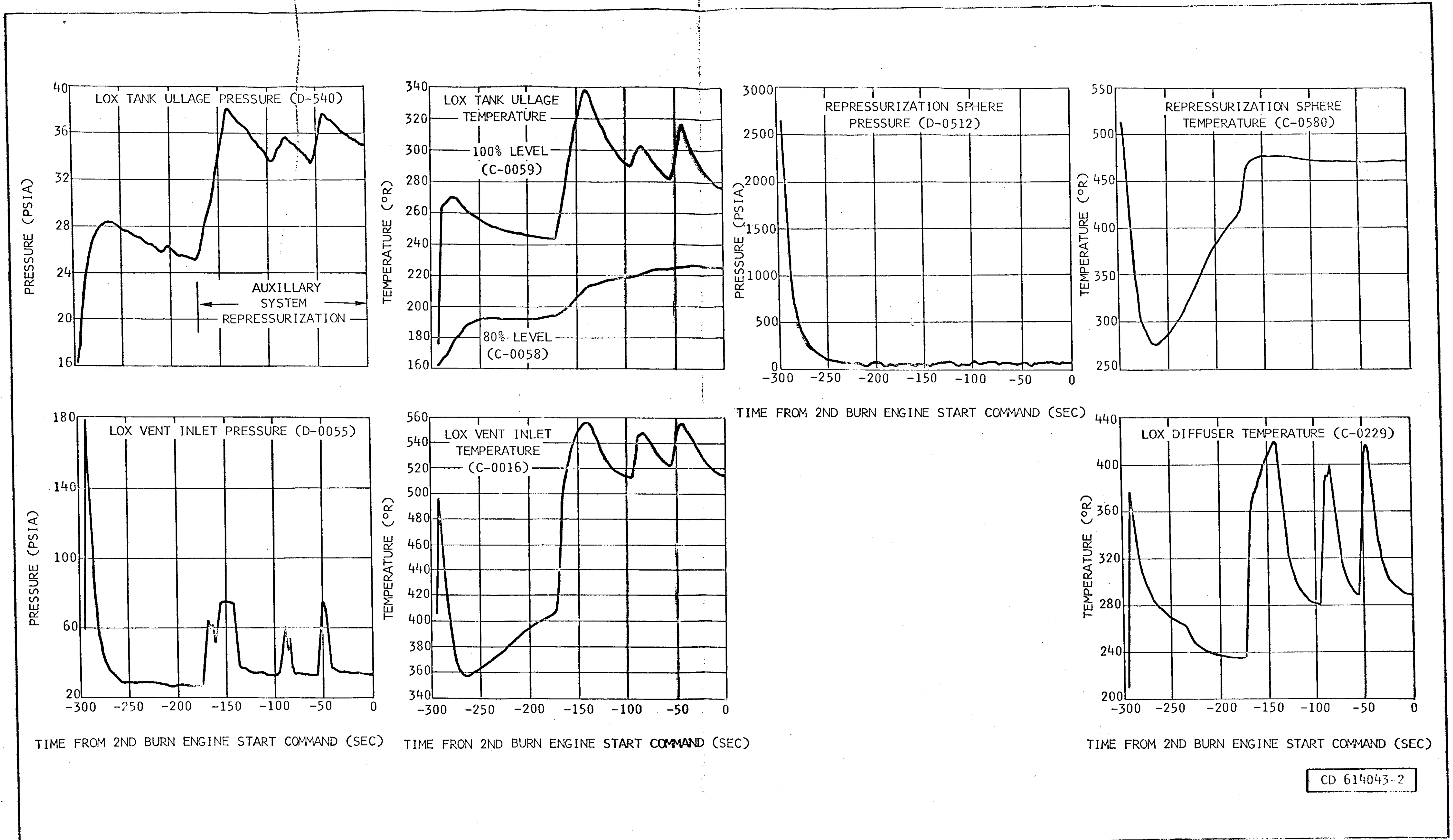

Figure 7-21 Repressurization Performance

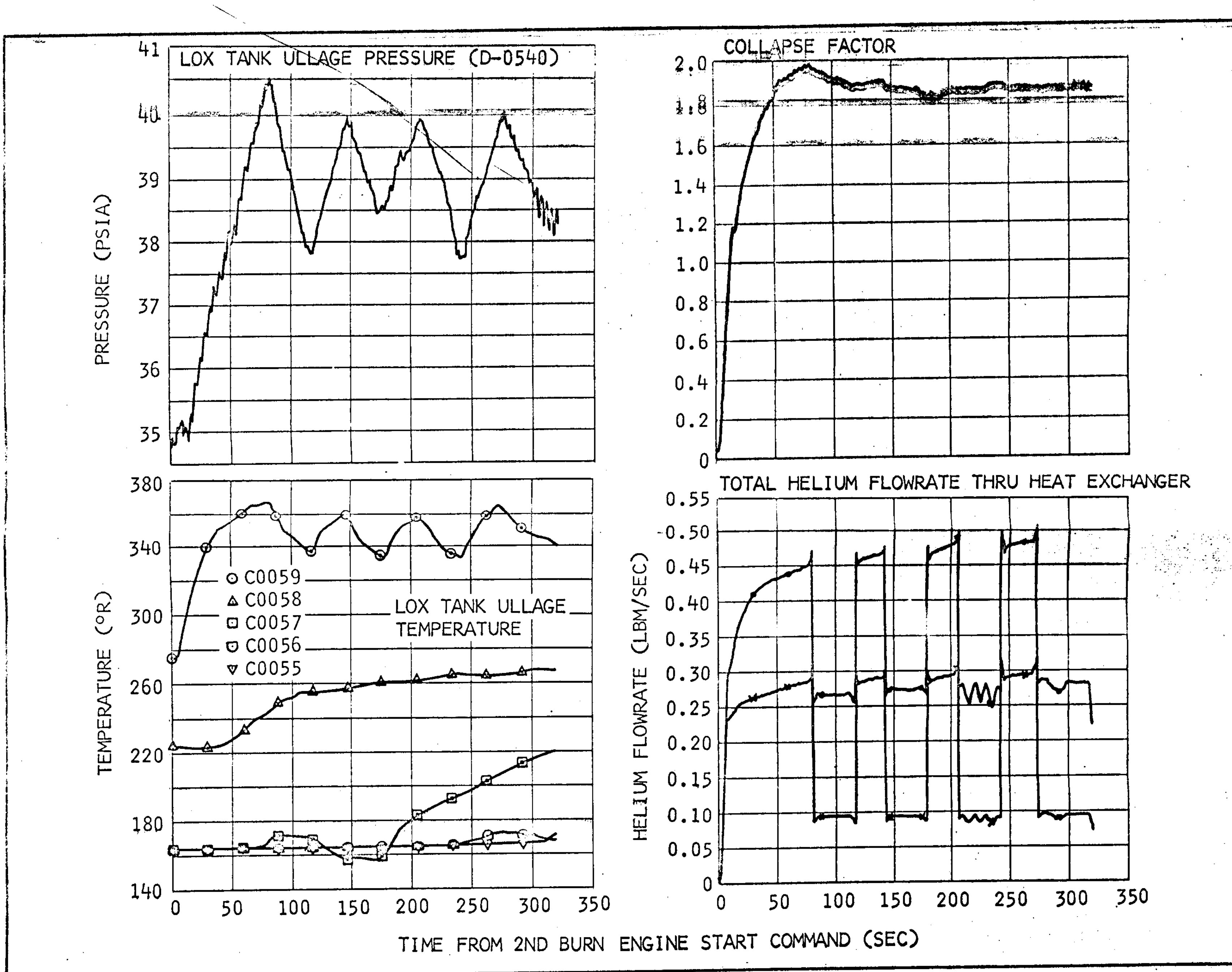

Figure 7-22 LOX Tank Conditions During 2nd Burn - CD 614043

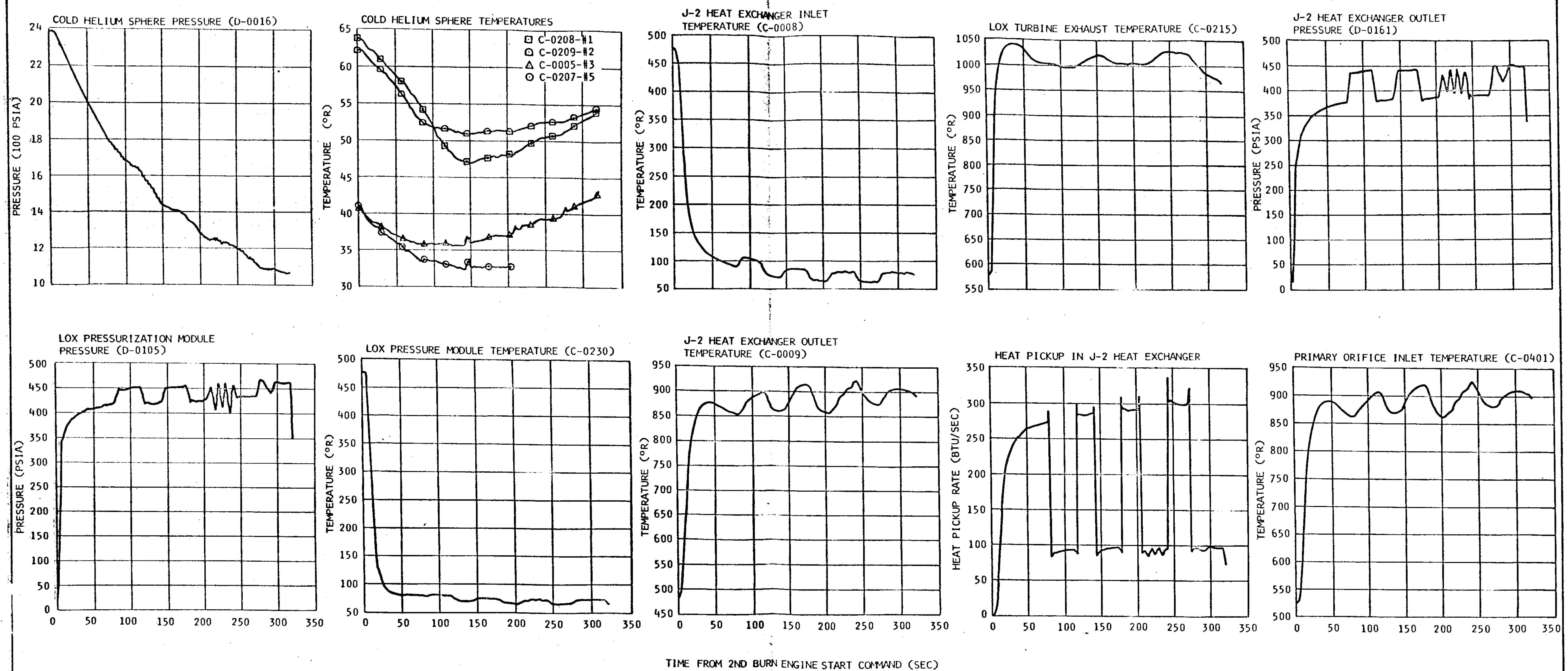

Figure 7-23 LOX Tank Pressurant Supply Performance During 2nd Burn - CD 614043

21 February 1966

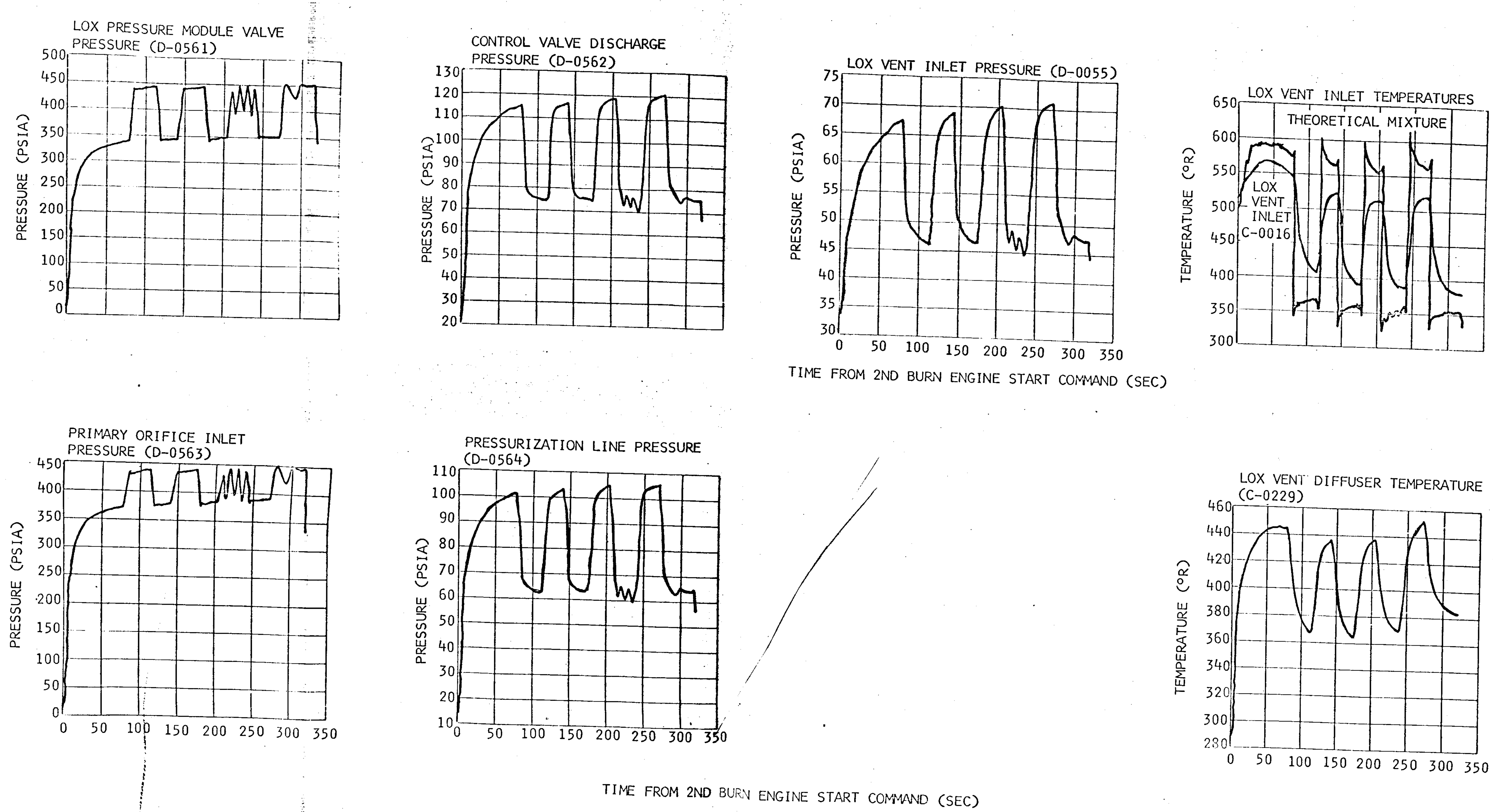

Figure 7-24 LOX Tank Pressurant Delivery During 2nd Burn - CD 614043

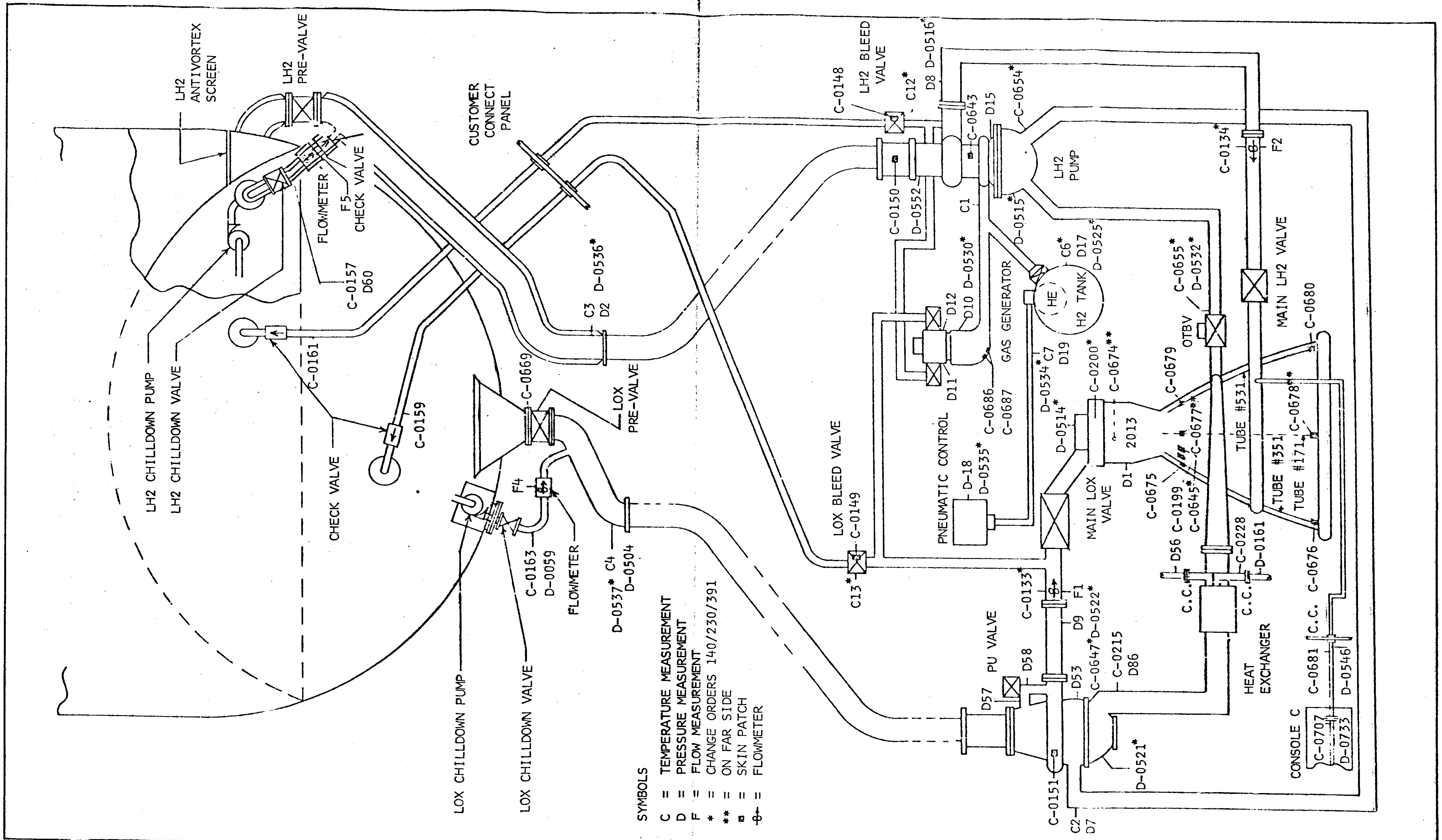

Figure 7-25 LH2 and LOX Recirculation Chilldown Systems Schematic

21 February 1966

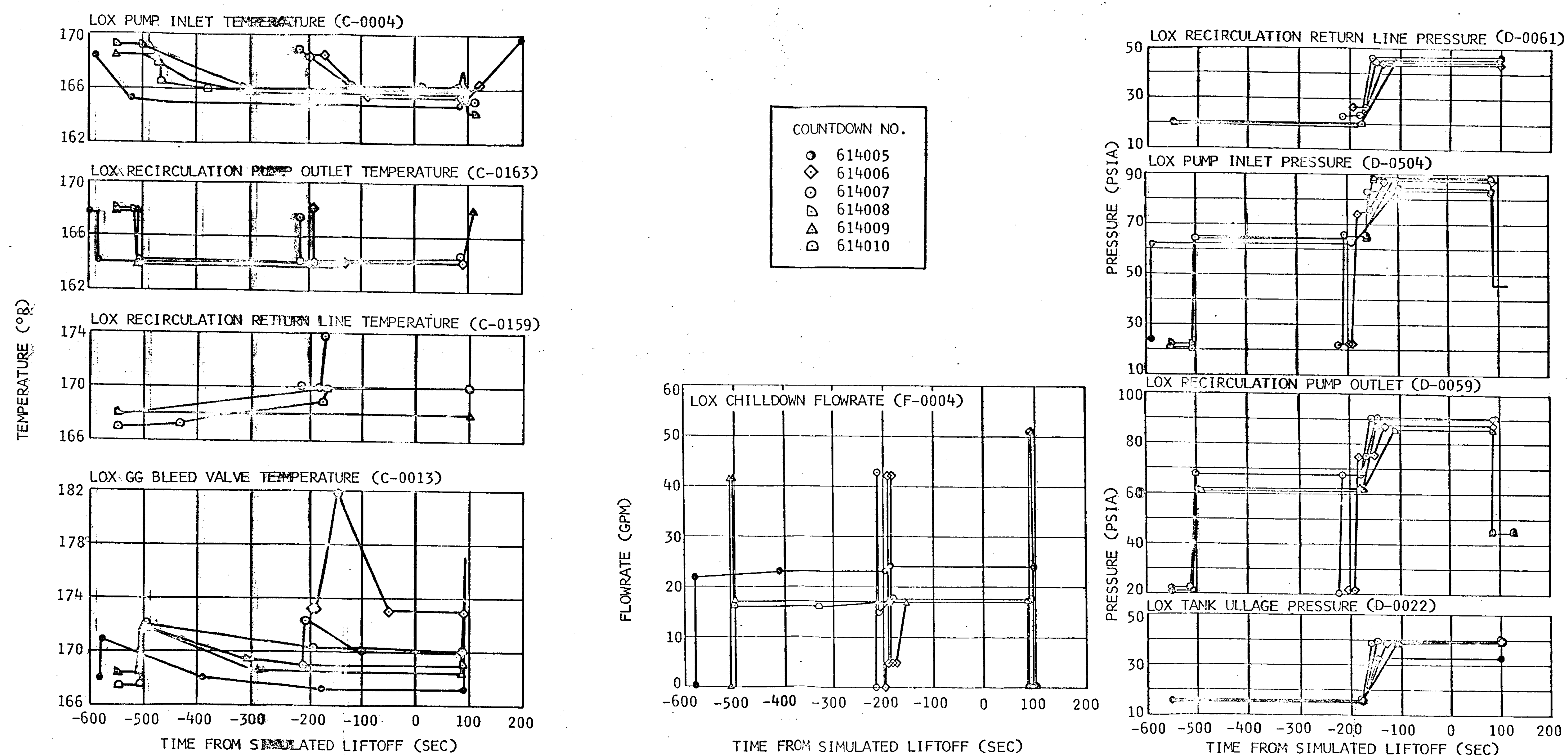

Figure 7-26 Chilldown Performance History

21 February 1966

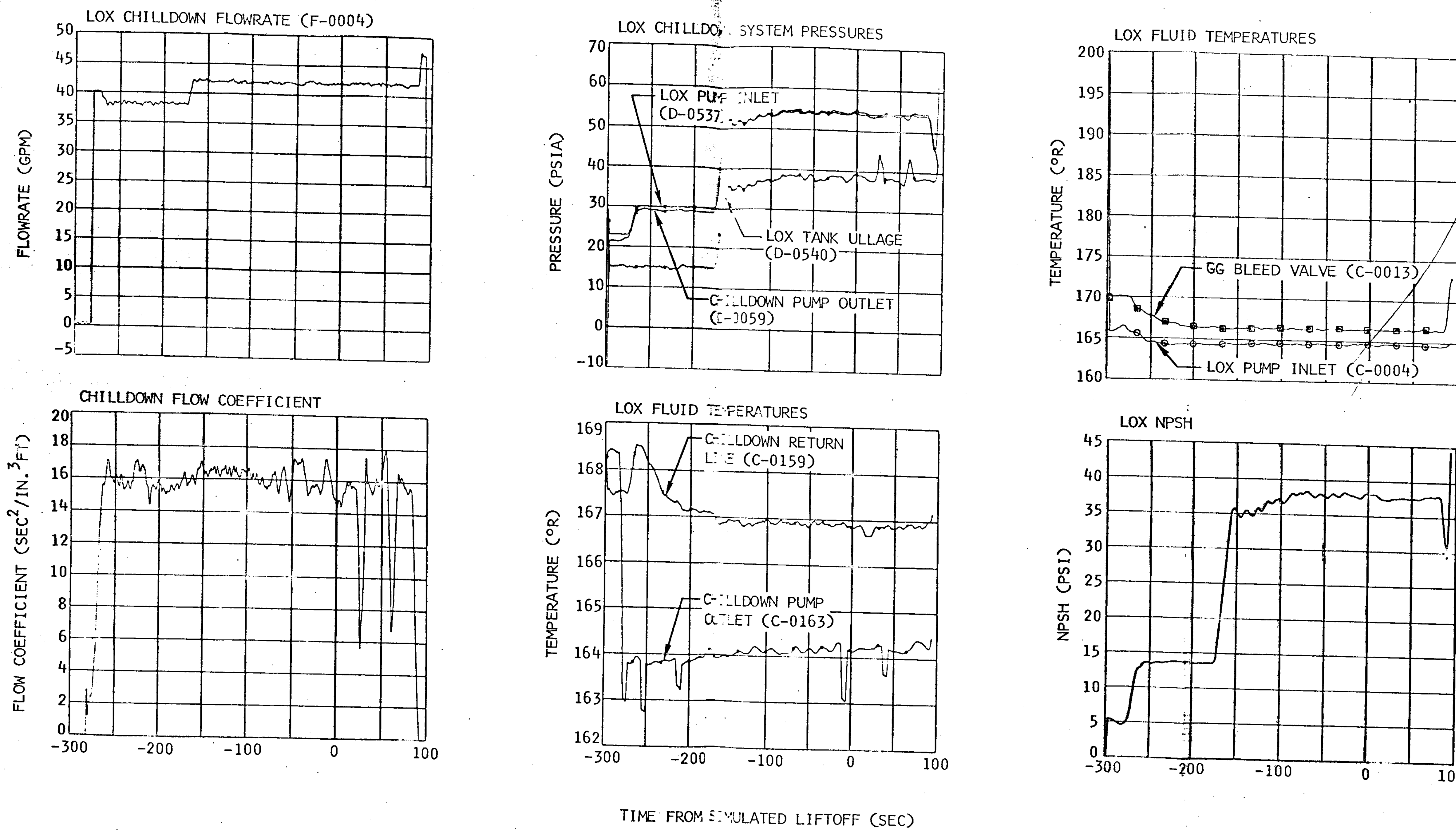

Figure 7-27 Chilldown Performance - CD 614030

21 February 1966

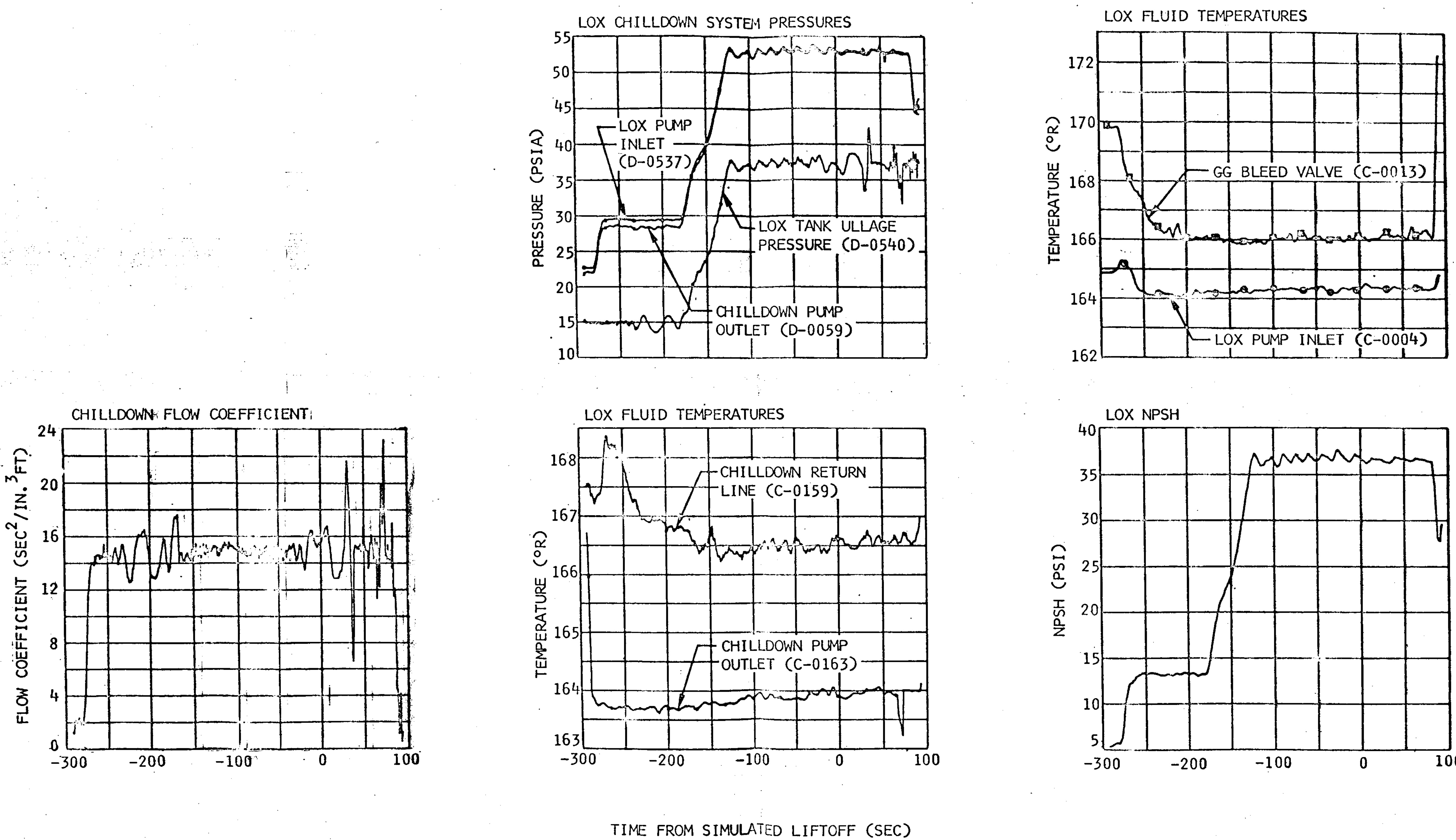

Figure 7-28 Chilldown Performance - CD 614025

21 February 1966

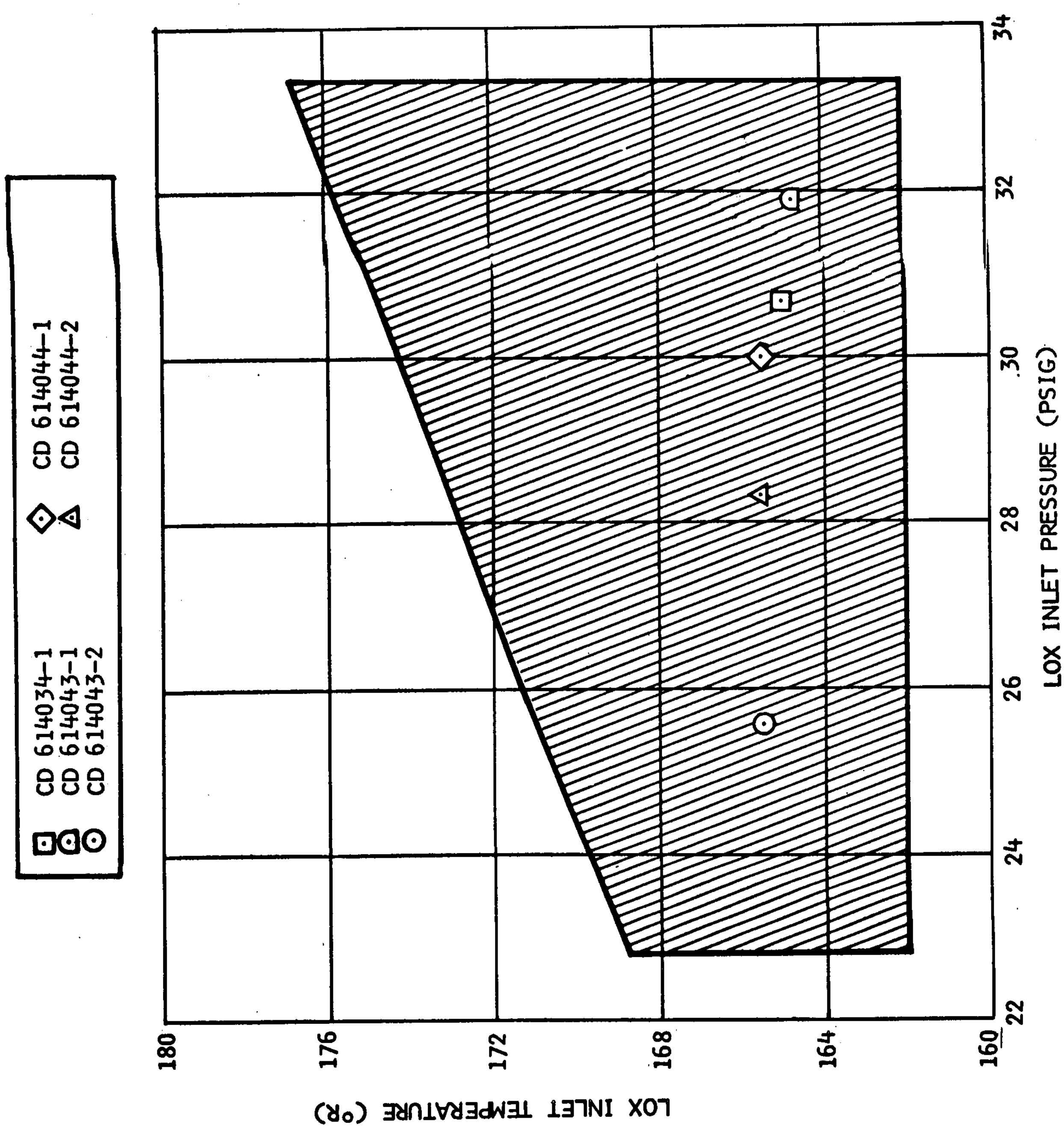

Figure 7-29 LOX Pump Inlet Prestart Conditions

21 February 1966

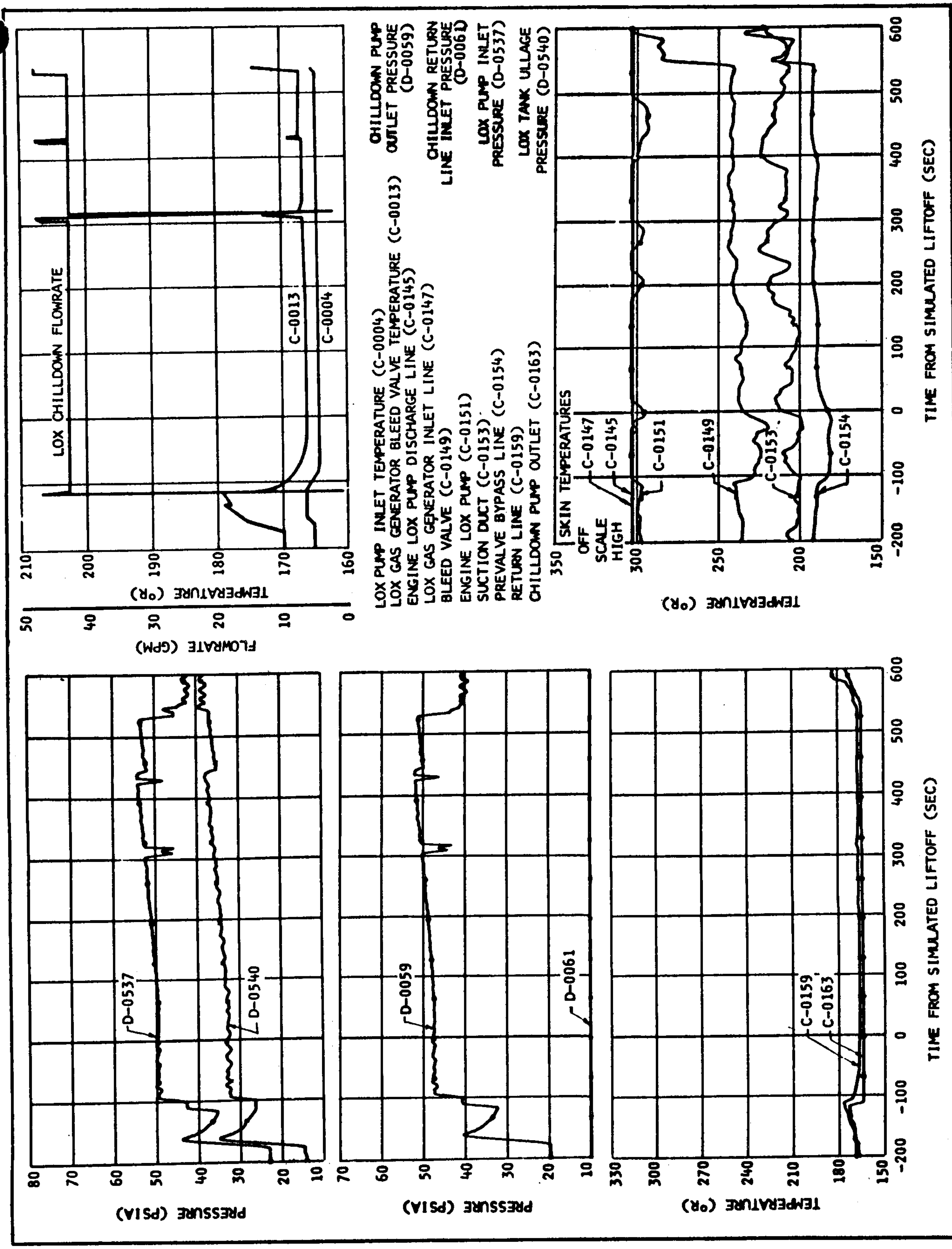

Figure 7-30 Chilldown Performance During 1st Burn - CD 614034

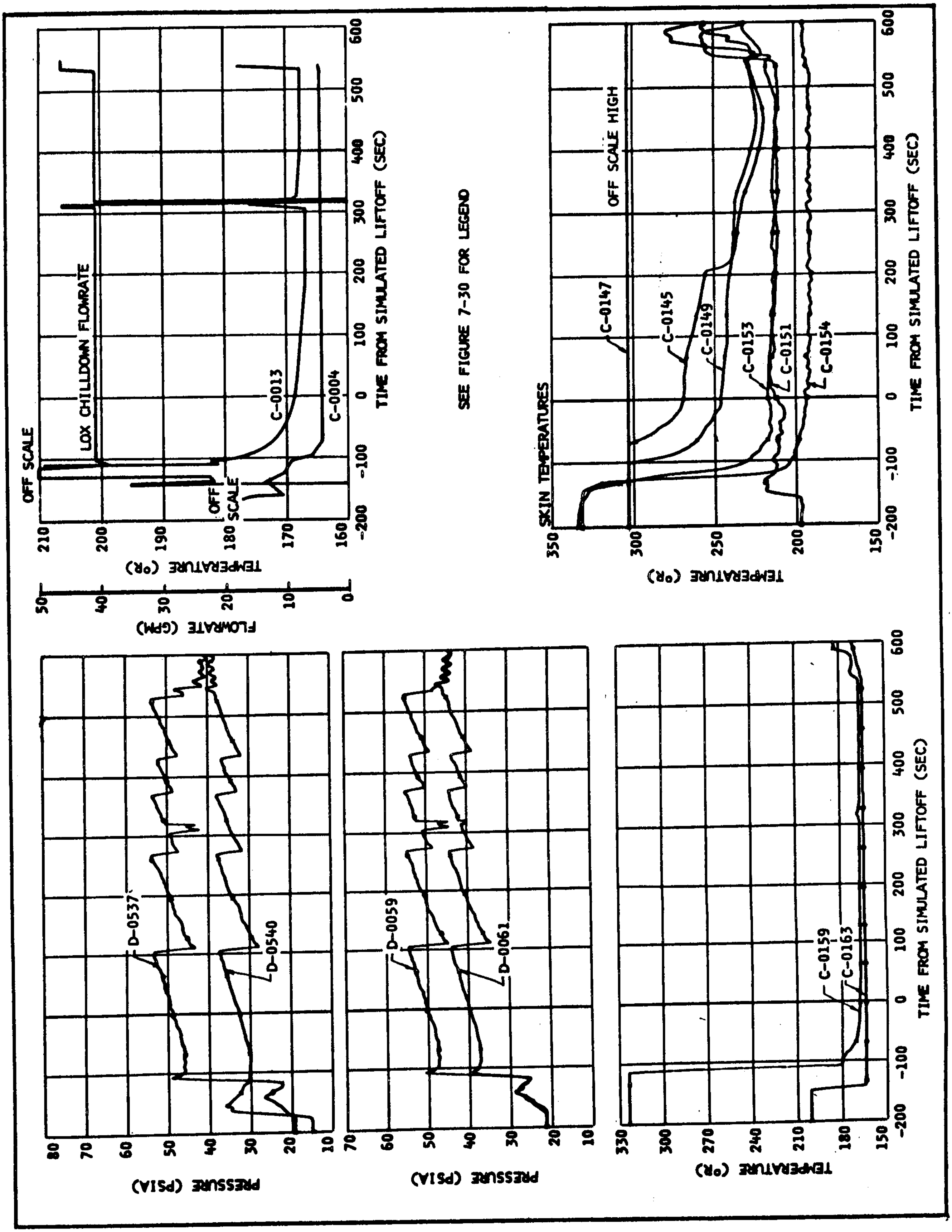

Figure 7-31 Chilldown Performance During 1st Burn - CD 614043

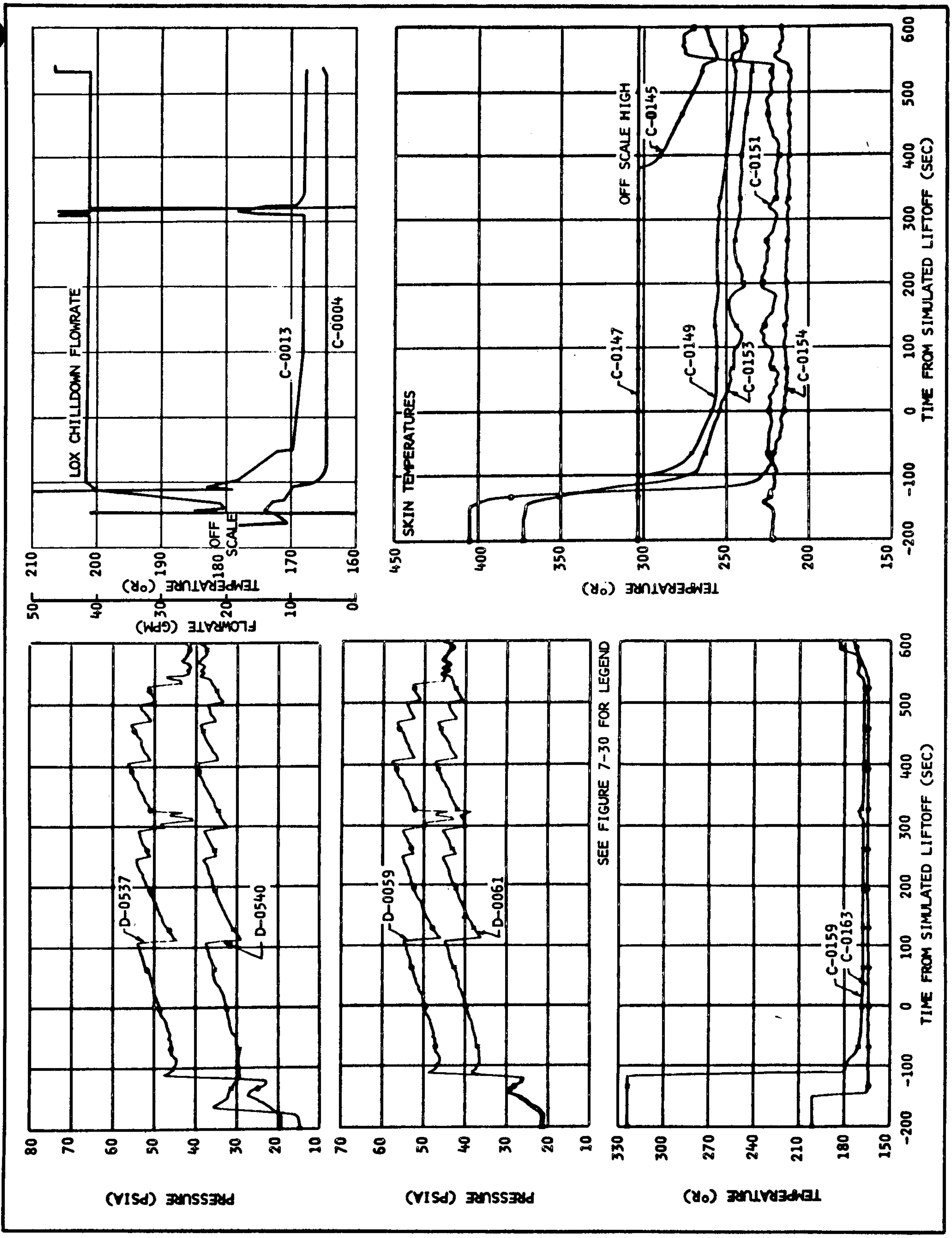

Figure 7-32 Childown Performance During 1st Burn - CD 614044

21 February 1966

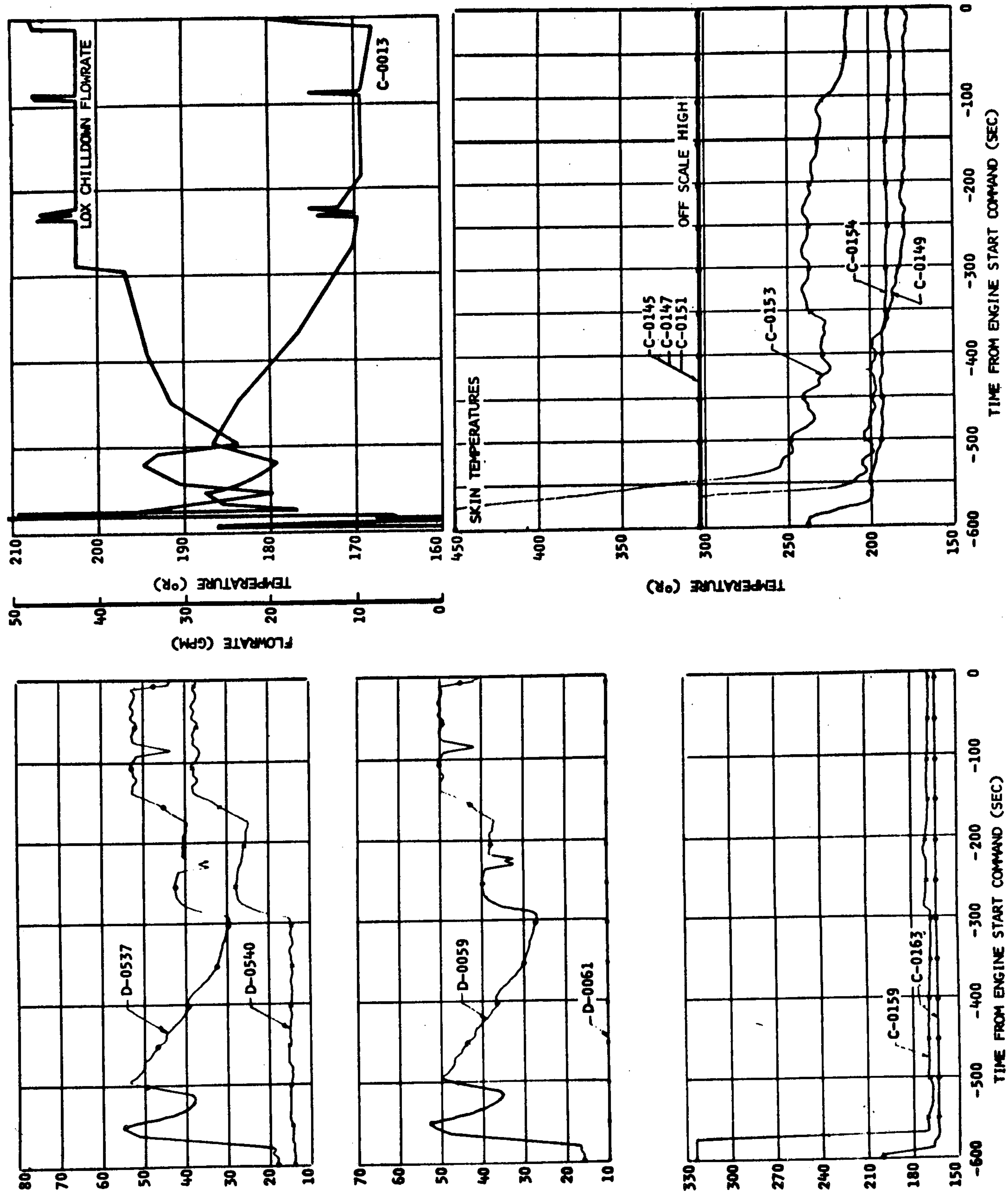

Figure 7-33 Chilldown Performance During 2nd Burn - CD 614034

21 February 1966

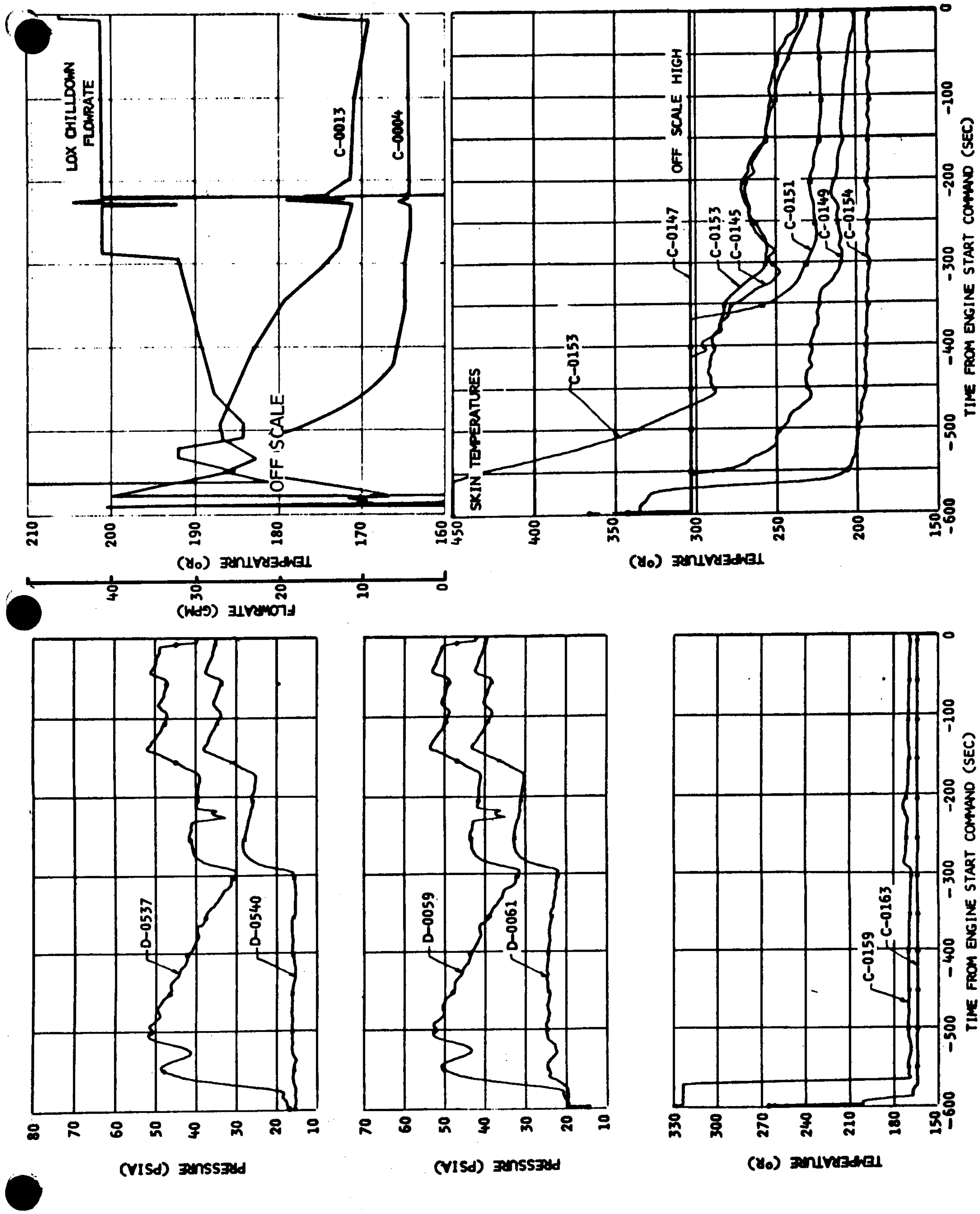

Figure 7-34 Chilldown Performance During 2nd Burn - CD 614043

21 February 1966

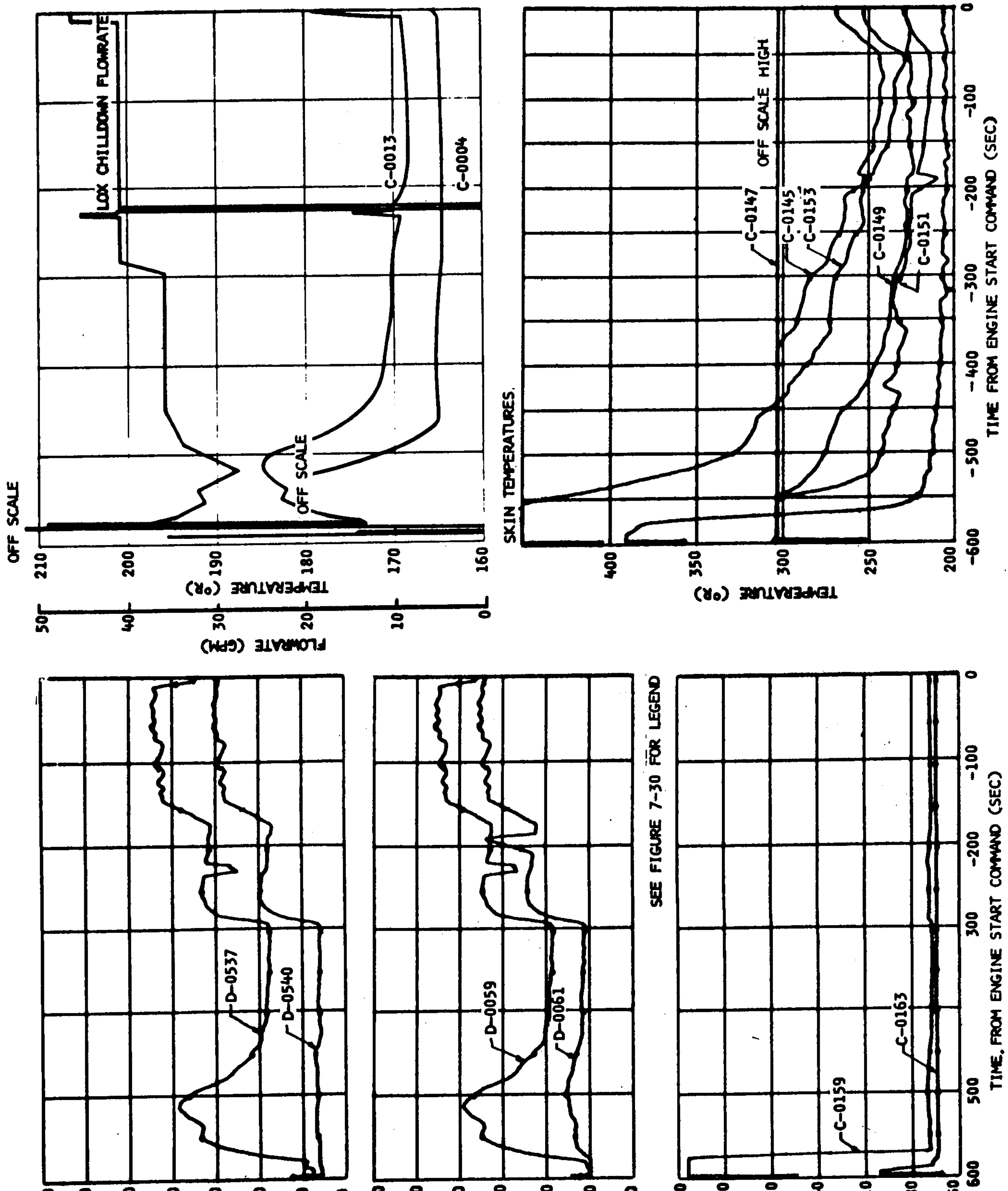

Figure 7-35 Childown Performance During 2nd Burn - CD 614044

21 February 1966

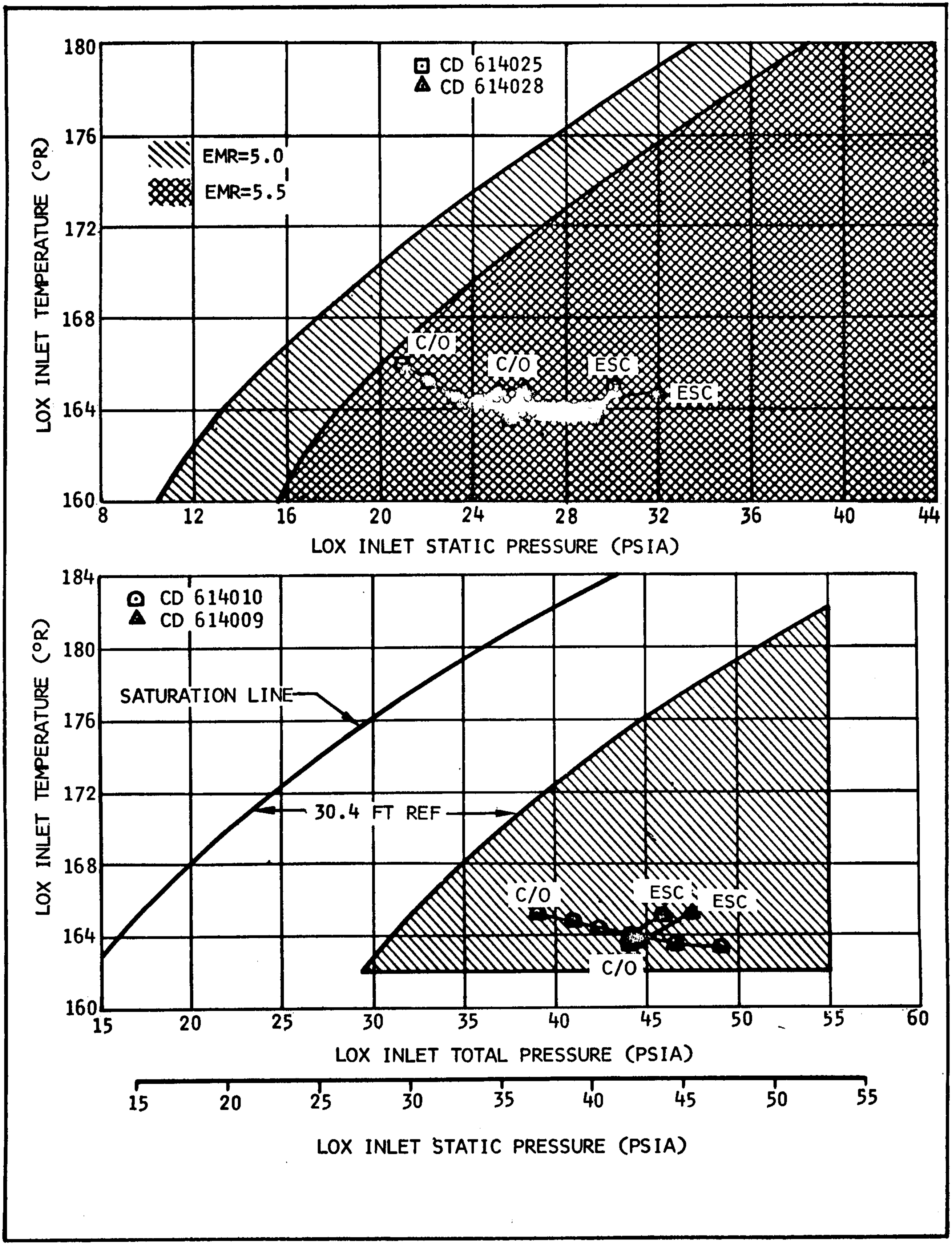

Figure 7-36 LOX Pump Inlet Conditions

21 February 1966

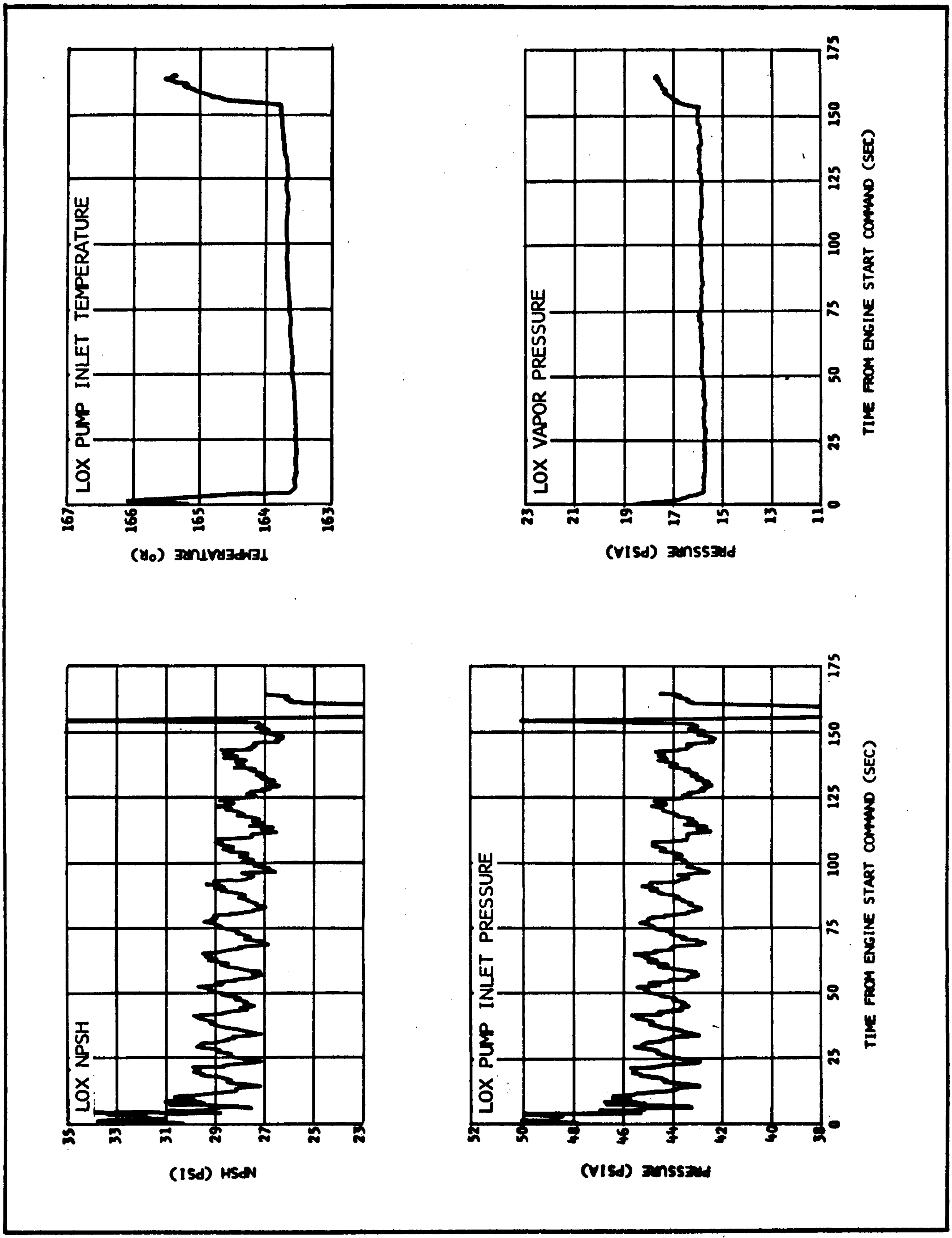

Figure 7-37 LOX Supply Conditions - CD 614009

21 February 1966

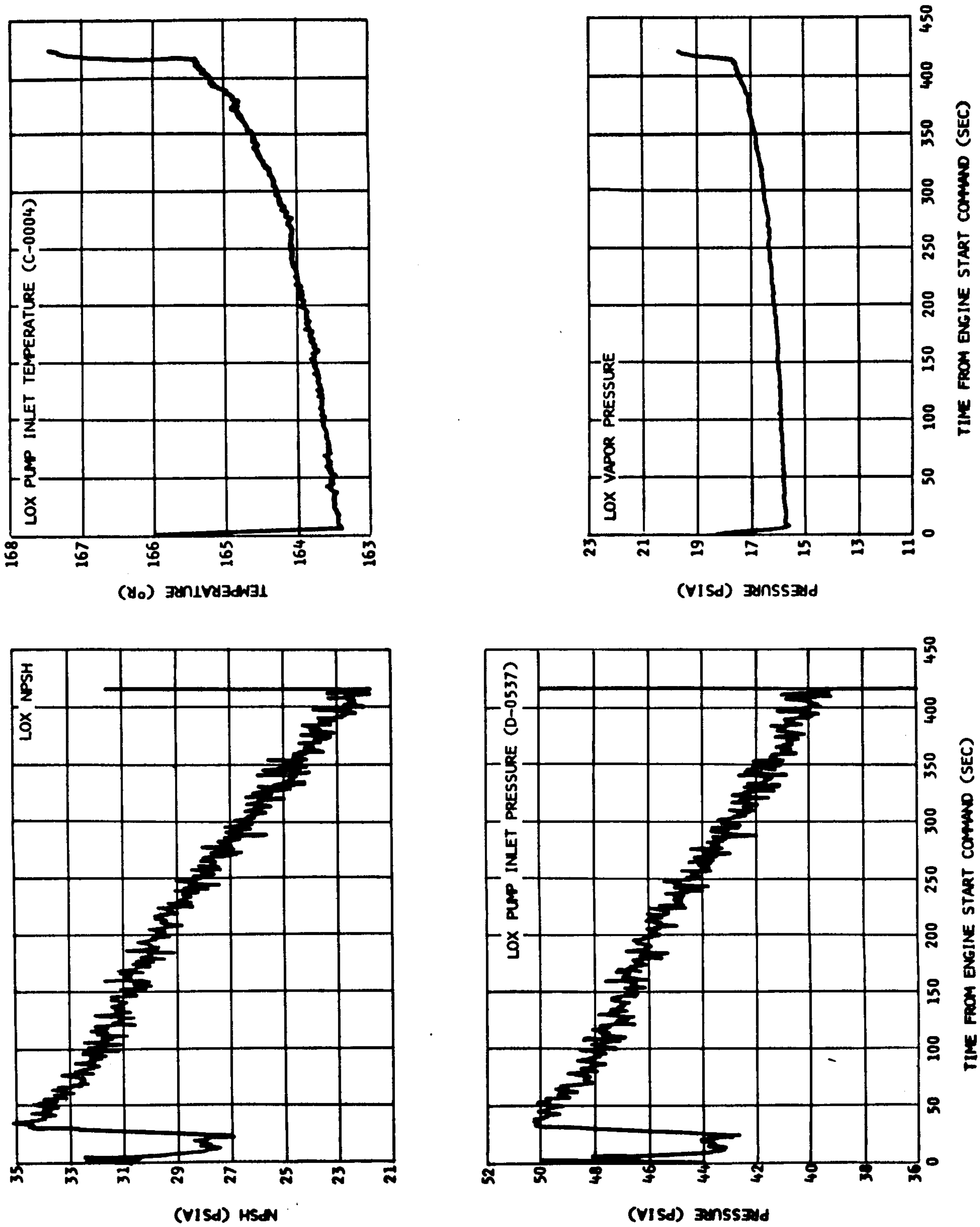

Figure 7-38 LOX Supply Conditions - CD 614010

21 February 1966

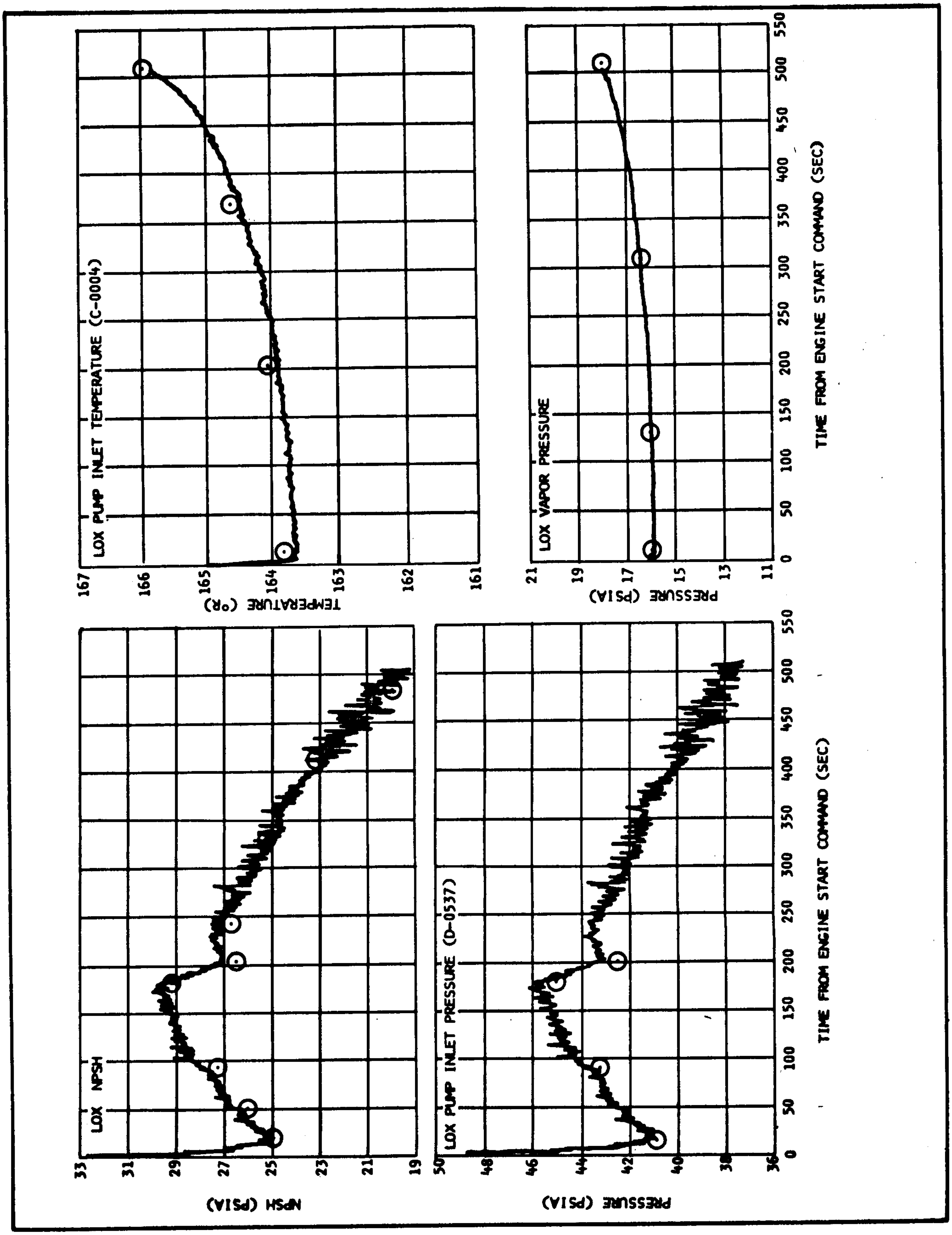

Figure 7-39 LOX Supply Conditions - CD 614025

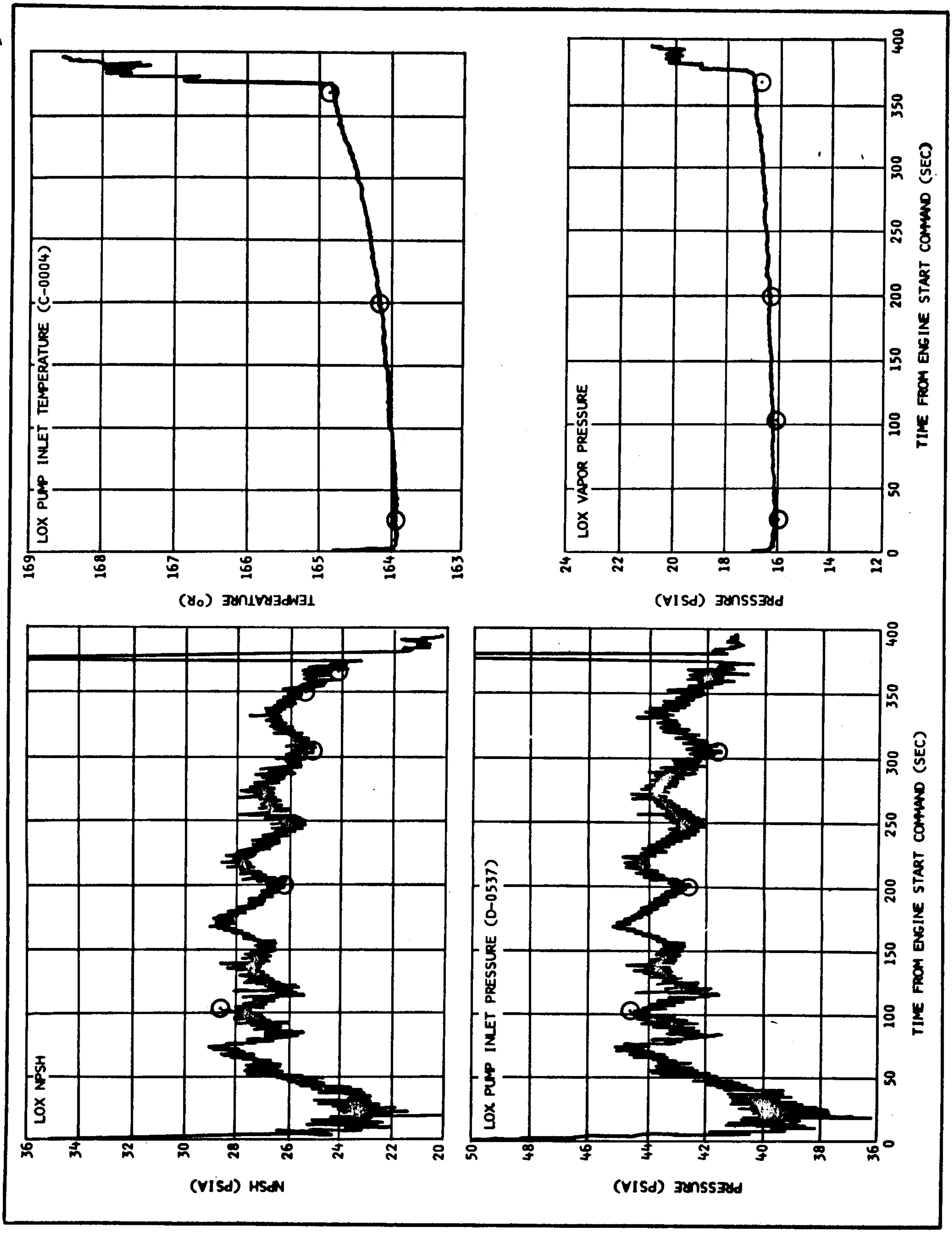

Figure 7-40 LOX Supply Conditions - CD 614028

21 February 1966

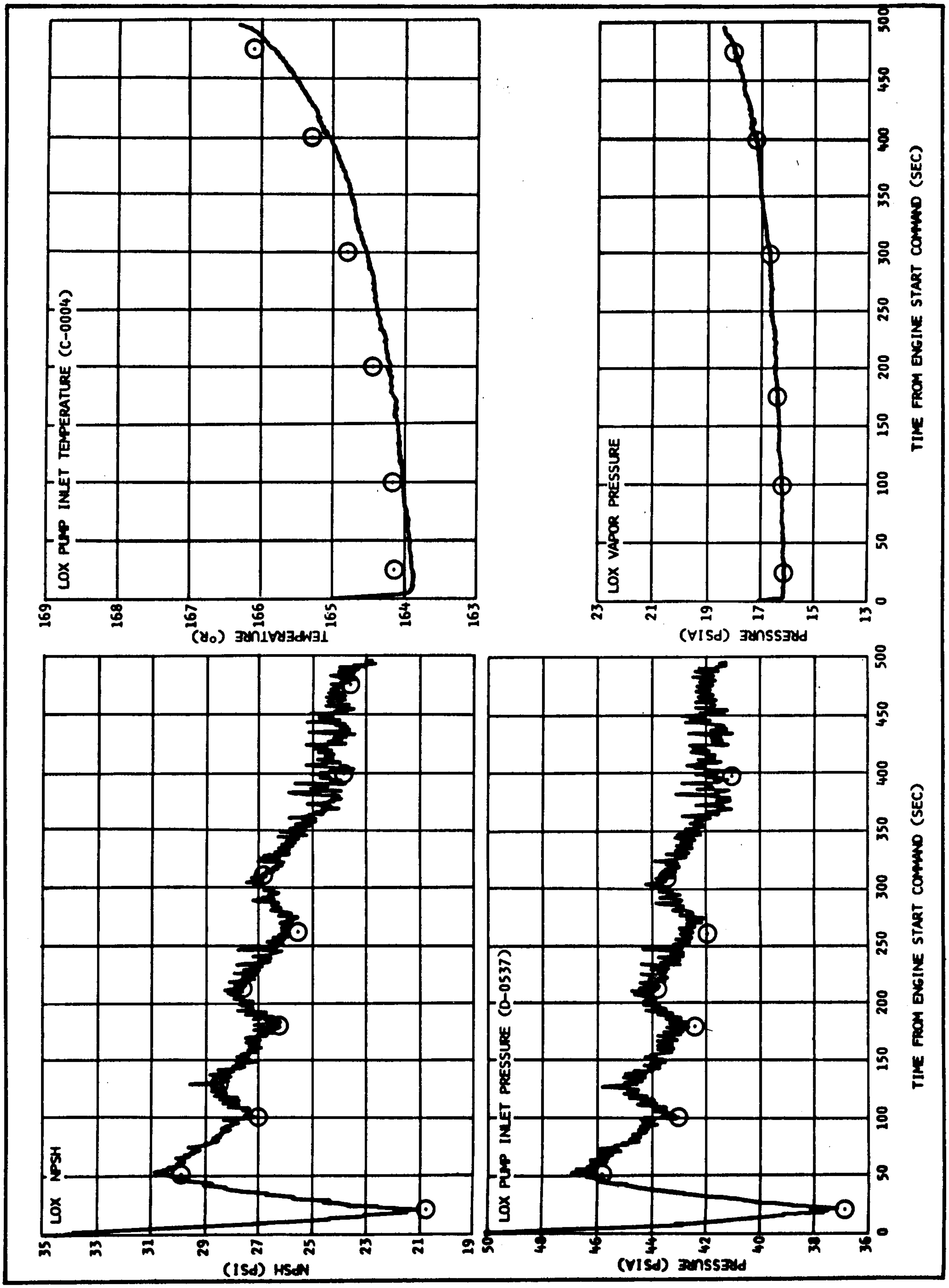

Figure 7-41 LOX Supply Conditions - CD 614030

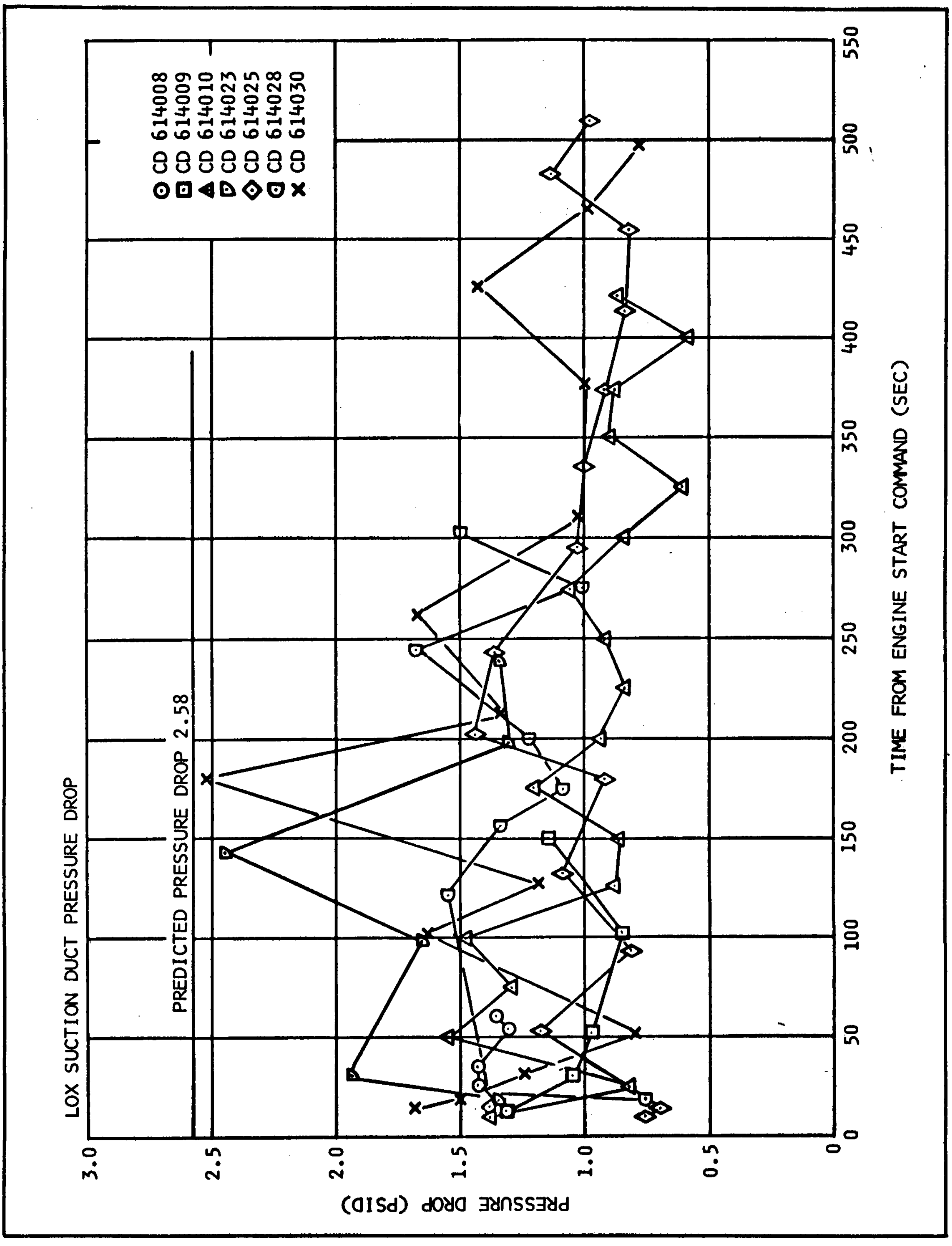

Figure 7-42 Suction Duct Pressure Drop History

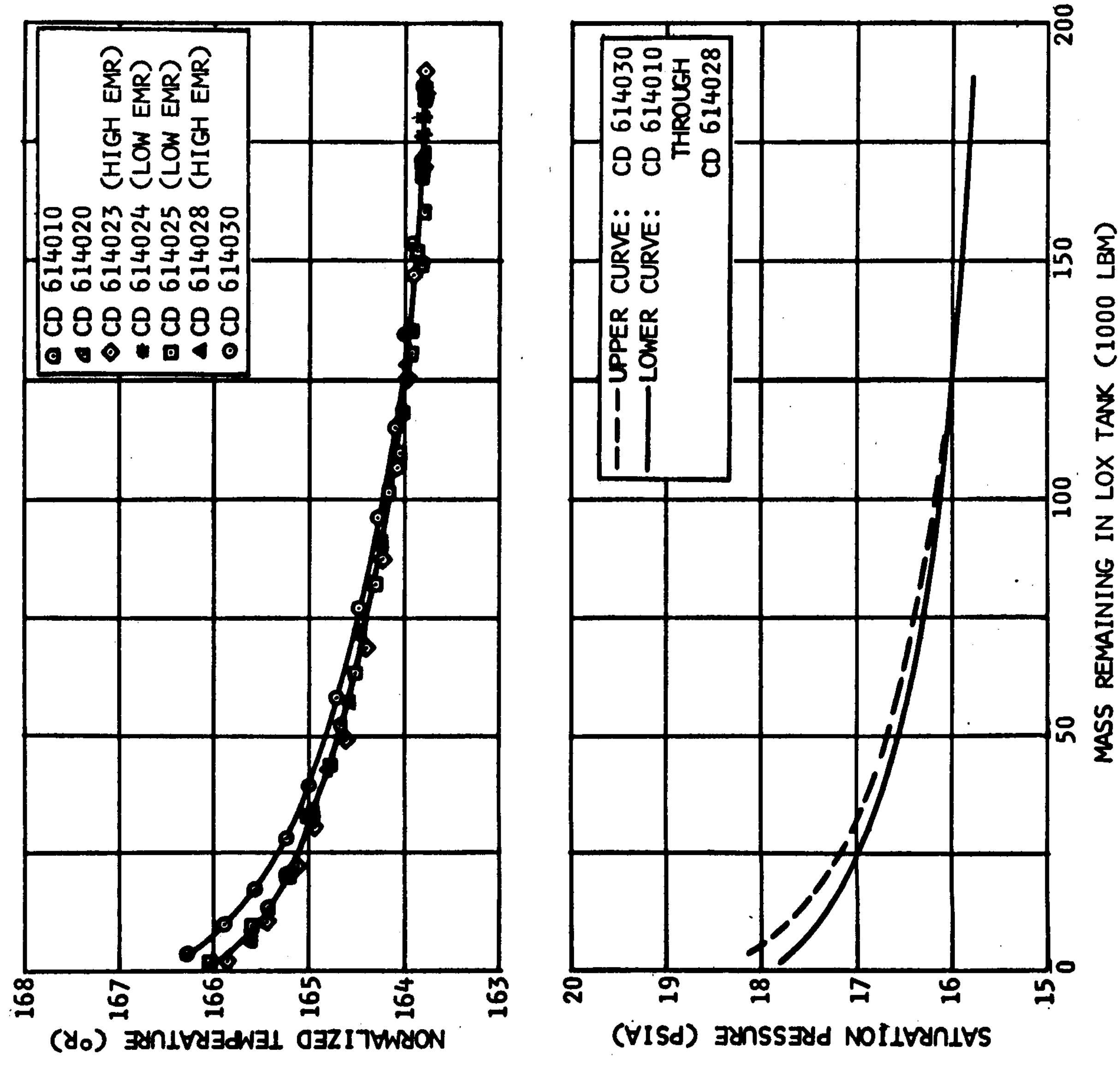

Figure 7-43 Normalized LOX Temperature and Pressure History

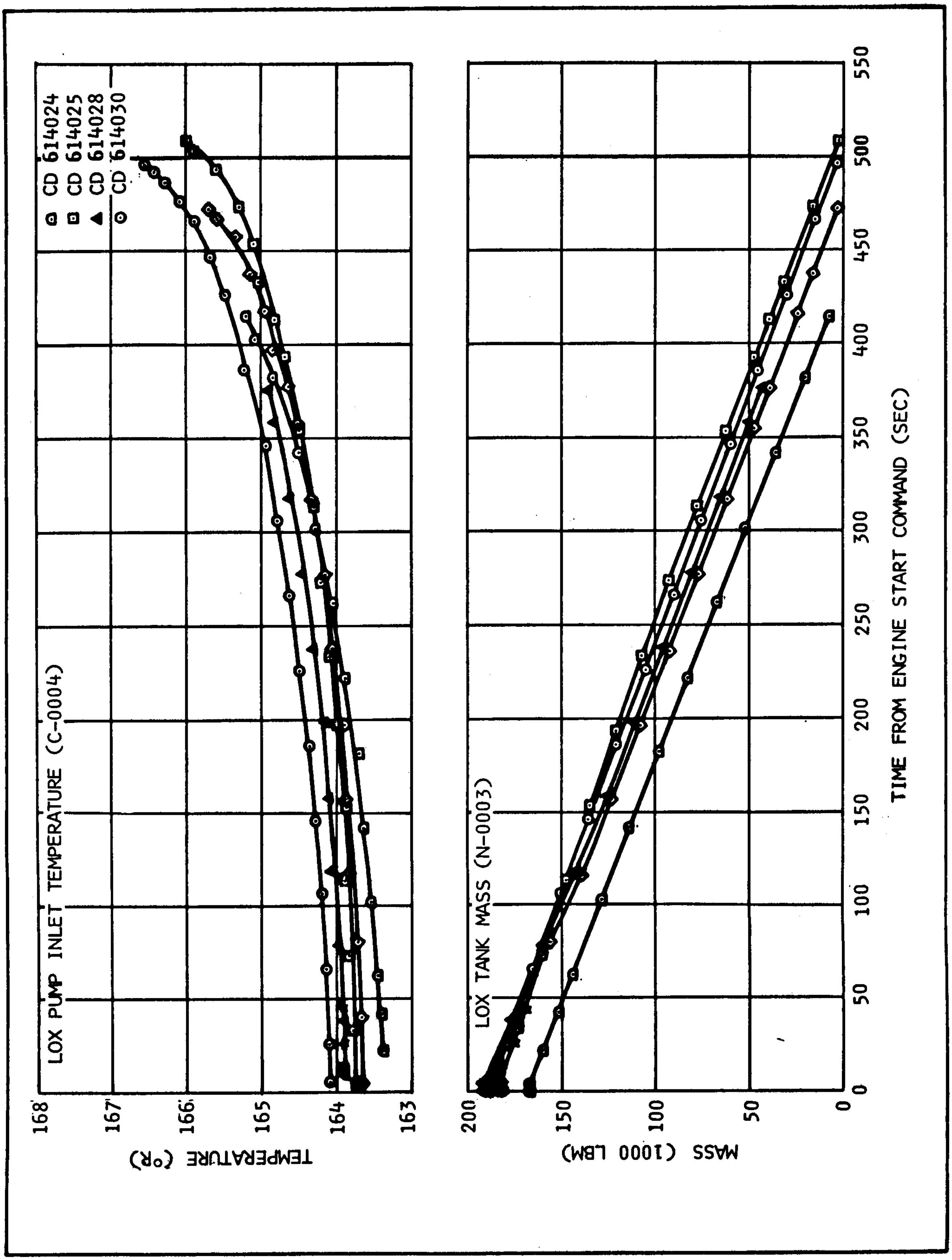

Figure 7-44 LOX Pump Inlet Temperature and Tank Mass History

21 February 1966

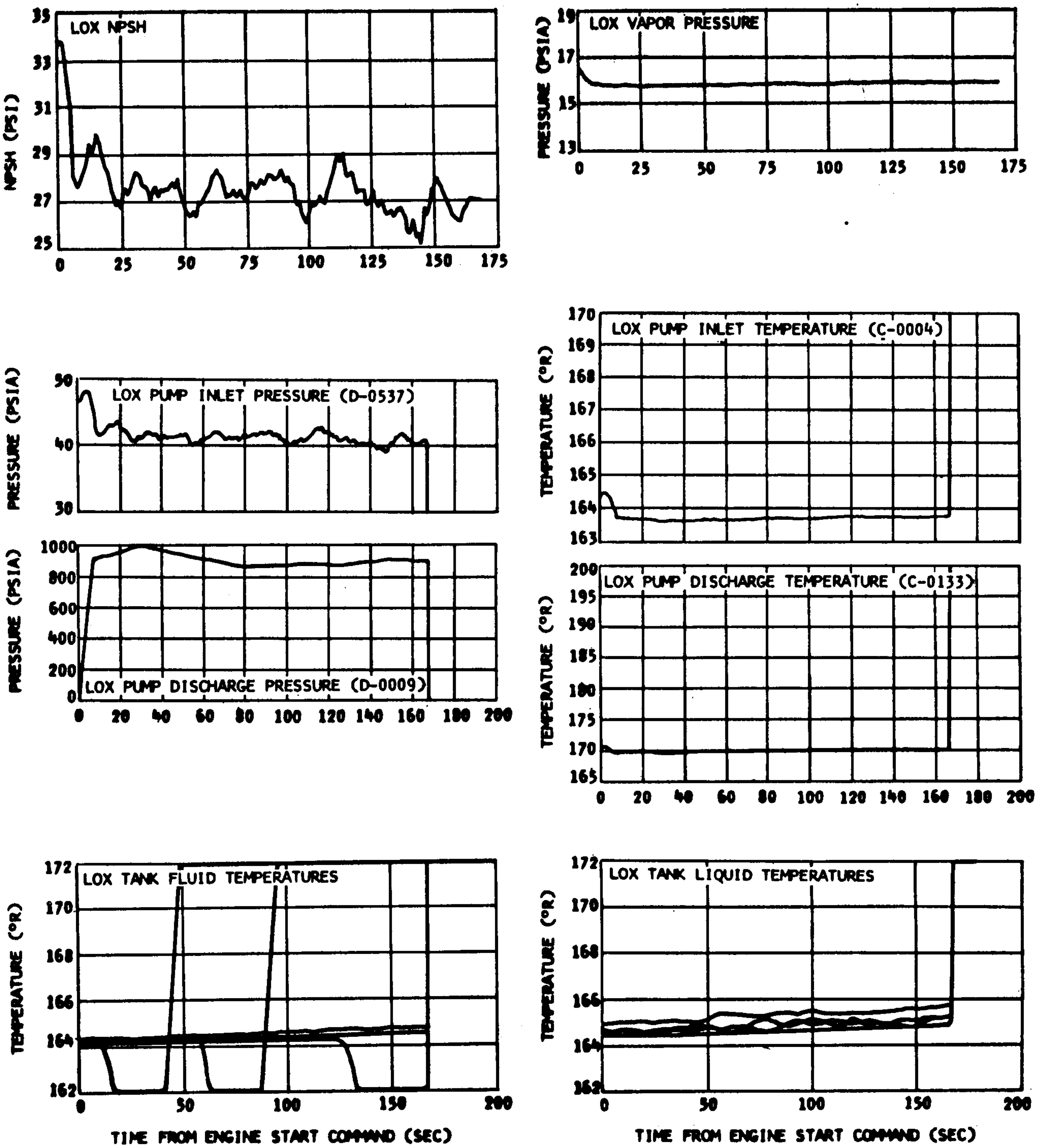

Figure 7-45 LOX Supply Conditions During 1st Burn - CD 614034

21 February 1966

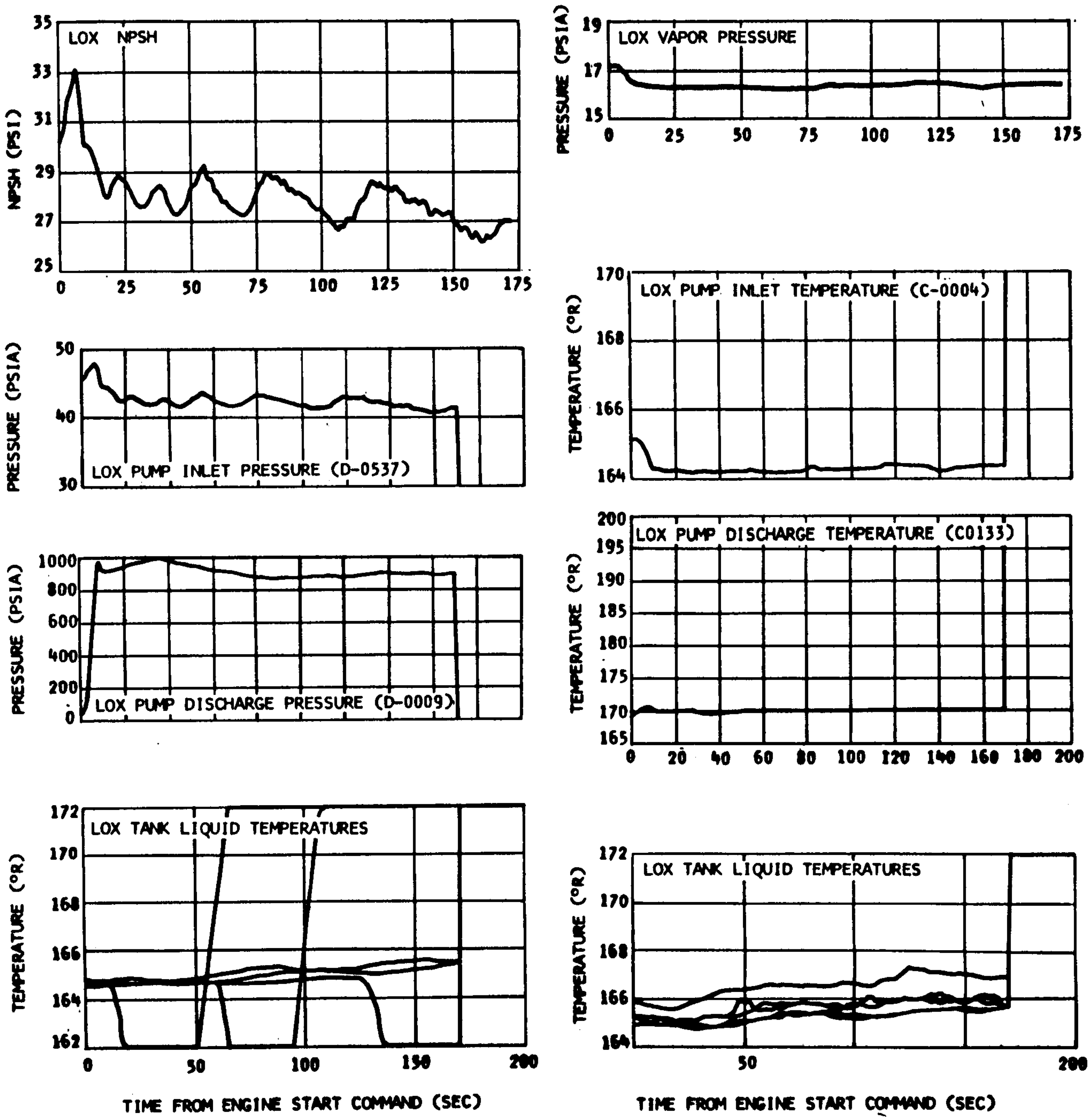

Figure 7-46 LOX Supply Conditions During 1st Burn - CD 614043

21 February 1966

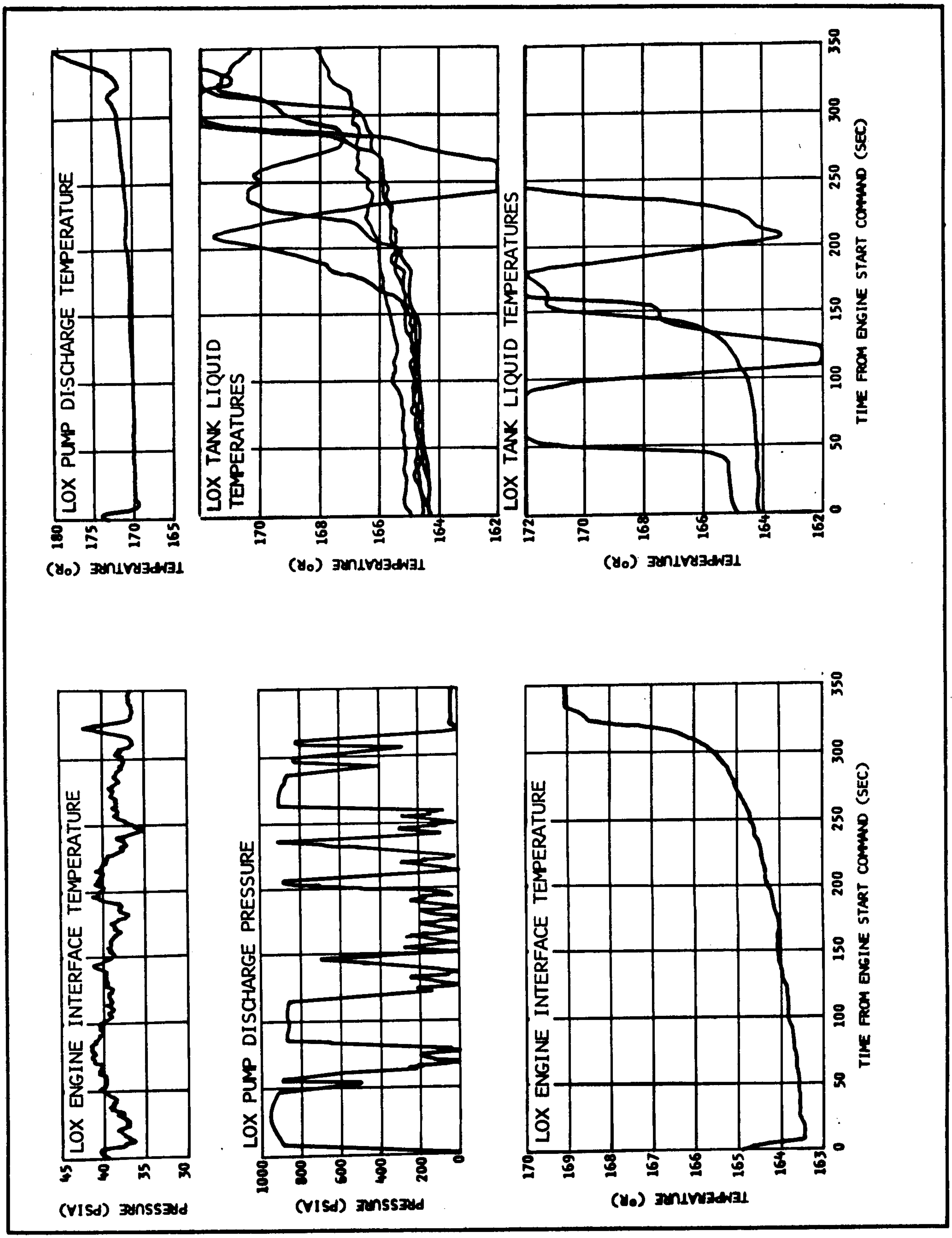

Figure 7-47 LOX Supply Conditions During 2nd Burn - CD 614043

21 February 1966

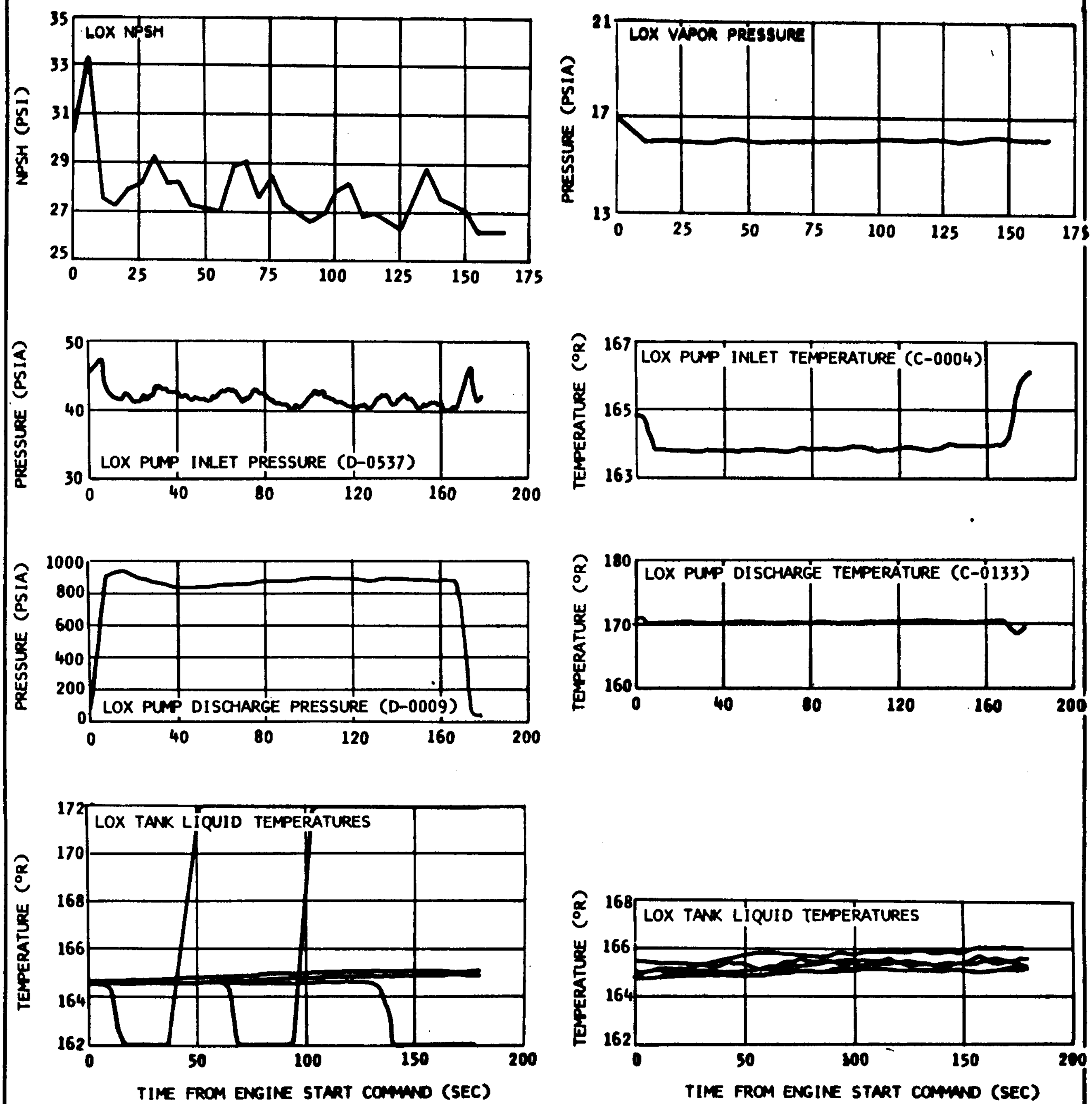

Figure 7-48 LOX Supply Conditions During 1st Burn - CD 614044

21 February 1966

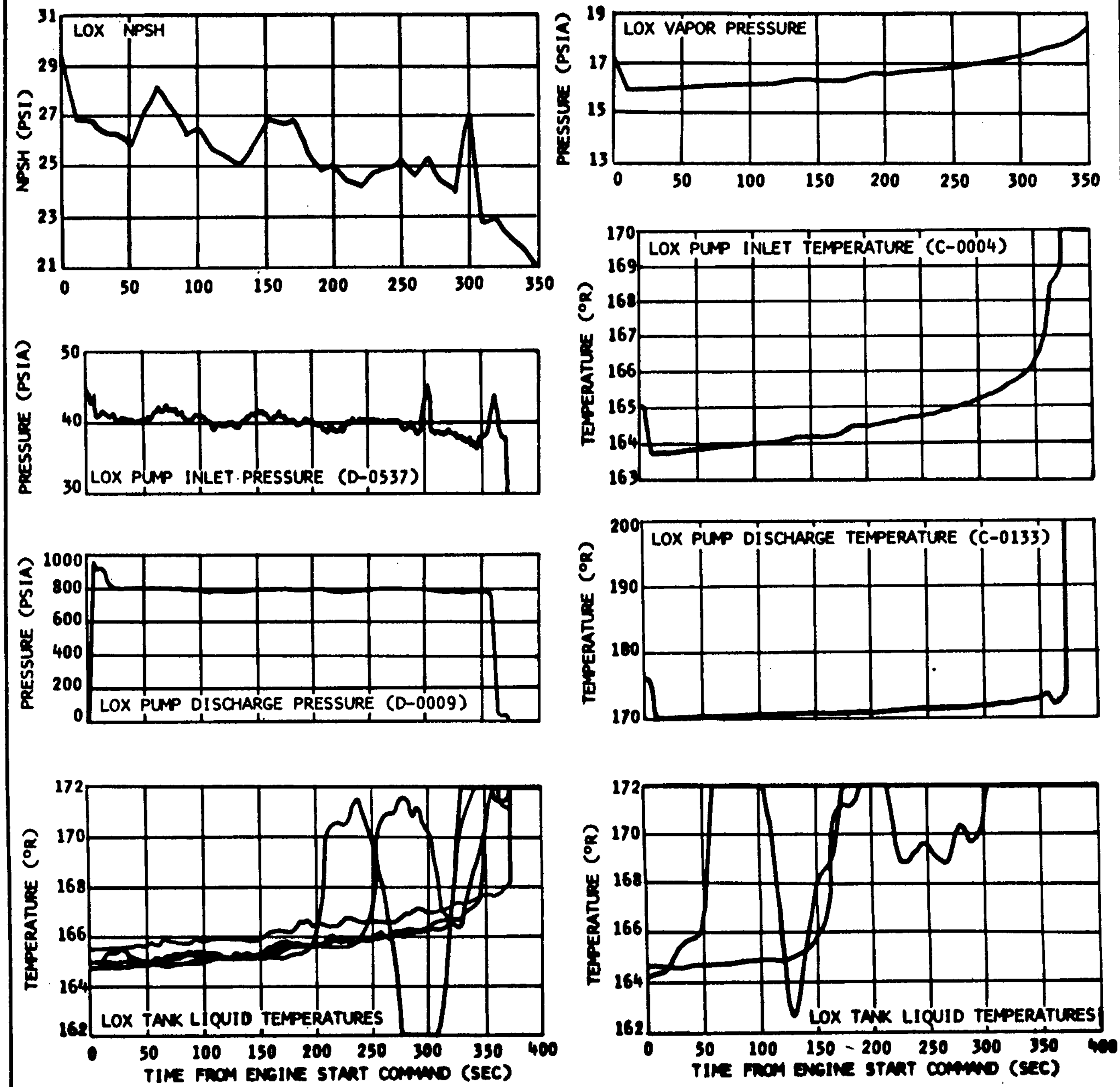

Figure 7-49 LOX Supply Conditions During 2nd Burn - CD 614044

21 February 1966

SECTION 8

FUEL SYSTEM

8. FUEL SYSTEM

The LH2 tank pressurization system, the LH2 recirculation system, and the engine supply system performed satisfactorily during the developmental testing of the battleship program. The fuel system data are presented and discussed in the following paragraphs.

8.1 LH2 Tank Pressurization System

The LH2 tank pressurization system satisfactorily prepressurized the LH2 tank and maintained the tank ullage pressure during engine operation. The configuration of the pressurization system was the same during all tests, but the pressurant gas was supplied by three different engines (S/N J-2003, J-2013, and J-2020) during various phases of the battleship program.

8.1.1 S-IVB/IB

8.1.1.1 Prepressurization

The prepressurization of the LH2 tank was satisfactorily accomplished during all battleship tests. The cold helium was supplied from the GSE prepressurization system as shown in figure 8-1. A typical prepressurization history of the LH2 tank ullage and inlet temperature, pressure, and flow during CD 614010 is shown in figure 8-2. Prepressurization flowrate was low initially because of warm gas in the supply line and then increased rapidly and stabilized at 0.97 lbm/sec as the GH2 temperature decreased. After the prepressurization was completed, the ullage pressure continued to increase due to the temperature rise of the ullage. The ullage temperature rise during prepressurization was acceptable and amounted to approximately 25 deg R. Prepressurization data from CD 614023, 614028, and 614030 are summarized in table 8-1 and indicate that the temperature of the pressurant gas from the GSE heat exchanger was in the range of 71 to 115 deg R. The LH2 tank inlet temperatures were initially high due to heat transferred from the lines to the gas.

8.1.1.2 Pressurization

During the initial S-IVB battleship tests, the LH2 tank was pressurized from the GSE supply because the flight pressurization control module was not available. The flight configuration LH2 tank pressurization system was first tested during CD 614009. This 150-sec engine firing was followed by CD 614010, a full duration test with the same engine (S/N J-2003). A schematic of the LH2 tank pressurization system is shown in figure 8-1. LH2 tank pressurization system data from these countdowns are presented in table 8-2 and figures 8-3 and 8-4.

The operation of the pressurization system was satisfactory. Although GH2 flowrates were lower than predicted (table 8-3), ullage pressure was maintained within the desired limits varying between 40.7 and 28.8 psia from engine start to step pressurization (table 8-2). Acceptable limits were 42 (vent setting) to 28 psia. Pressurization module cycling from undercontrol to overcontrol occurred twice during CD 614010. Design requirements for upper and lower pressure cycling limits were satisfactorily met.

Step pressurization during CD 614010 was initiated at ESC (Engine Start Command) +250 sec and required 148 sec to increase the ullage pressure to a reference pressure of 39 psia. During subsequent tests with the S/N J-2013 engine, 70 to 96 sec were usually required to reach 39 psia (table 8-4). The relatively slow pressurization rate during the step pressurization mode was caused by a lower than expected step pressurization flowrate. The LH2 tank pressurization module had not been flow-calibrated prior to the test.

The ullage temperatures were lower than predicted because the temperature of the GH2 supply from the J-2003 engine was lower than anticipated. The initial and final ullage temperatures were 70 deg R and 125 deg R (table 8-2). The LH2 tank ullage temperature profiles are also shown in figure 8-4 and indicate that the ullage temperature gradients were negligible (good mixing) throughout the firing of CD 614010. The 101 percent temperature probe was not a valid indicator of ullage temperature at engine start due to its location.

During CD 614010, when corrected for the predicted temperature of 200 deg R, the nominal flowrate was higher than predicted, control was slightly lower, and the step pressurization flowrate was much lower as indicated in table 8-2. During later tests, the step orifice was removed to increase the step pressurization flowrate.

The full duration S-IVB/IB battleship tests with the J-2013 engine are listed in table 8-5 (CD 614023 to 614030). LH2 tank pressurization system test results for these countdowns are summarized in table 8-6.

During the first 30 sec of engine operation, the LH2 tank ullage pressures were usually observed to increase and then start to decrease as shown in figures 8-5 and 8-6.

The increase in ullage pressure was neither large (0.8 to 1.7 psia) nor significant from the standpoint of performance, since tank pressures up to vent pressure (42 psia) are acceptable. However, the ullage pressure change was of interest because it resulted from the simultaneous interaction of several LH2 pressurization system variables. Test data reveal that the following occurred during the first 10 sec of engine burn.

a. The LH2 tank pressurization module inlet pressure increased to 750 psia in 4 sec and to 780 psia in 10 sec.

b. The LH2 tank pressurization module inlet temperature decreased from approximately 257 $\pm$25 deg R to 205 $\pm$5 deg R as engine burn progressed from start to cutoff. Nearly all of the temperature differential occurred during the start transient.

c. Module effective flow area remained constant at the value given in table 8-7 for undercontrol.

d. The calculated GH2 flowrates increased to 0.38 lbm/sec in 4 sec and to 0.41 $\pm$0.01 lbm/sec in 10 sec as a result of the combined influence of paragraphs a, b, and c.

e. GH2 pressurant gas initially received heat energy from the pressurization line that connects the module outlet with the LH2 tank inlet. A comparison of module inlet temperatures with LH2 tank inlet temperatures reveals that the tank inlet temperatures were higher from 0 to +10 sec after start due to the hot line.

f. The LH2 tank ullage pressure at engine start increased at a varying rate which was dependent on the combined influence of paragraphs d and e. After 10 sec of J-2 engine operation, an additional variable, engine mixture ratio (EMR) exerted strong influence on the LH2 pressurization system performance.

g. The EMR was constant at 5.0 for the first 10 sec of all four full duration tests, then changed to either a high or a low EMR (table 8-5 and figures 8-5 and 8-6).

h. Pressures and temperatures throughout the LH2 pressurization system were found to increase or decrease directly with EMR during these countdowns. The approximate influence of EMR on module inlet pressure and temperature is shown graphically in figure 8-7. Predicted values of pressure and temperature variation with EMR and GH2 flow are plotted for reference as solid lines. Rocketdyne report R-3825-1: J-2 Engine Manual is the source of predicted pressure, temperature, and flow variations with EMR. Figure 8-7 also shows actual test results plotted as individual data points.

The pressurant flowrates (figures 8-5 and 8-6) reflected the EMR changes as they occurred.

In addition to the influences noted, ullage pressure was increased by commanding the pressurization module to change either to overcontrol or to the step mode of flow control. These modes of flow control are discussed by countdown in the following paragraphs.

During CD 614025, the LH2 tank ullage pressure decreased to 29.1 psia at 153 sec after engine start (figure 8-5). The ullage pressure then cycled as noted until ESC +250 sec when step pressurization was commanded. The LH2 tank inlet pressure reflected the changes in pressure control mode. As shown by the ullage pressure data in table 8-6, the overcontrol valve (in the module) opened at 29.1 psia and closed at 30.7 psia. Valve operation was within specified limits of 28 to 31 psia and thus was acceptable.

During CD 614023, 614028, and 614030, module overcontrol valve cycling did not occur. This may be confirmed by noting that, prior to ESC +250 sec, there are no step changes to the LH2 tank inlet pressures. During the engine burn intervals of start to +250 sec, the ullage pressure gradually decayed but remained above the LH2 tank pressure switch actuation level of 29 psia. This performance is acceptable.

For each test, the Step Pressurization Command was sent to the module by a sequence timer at ESC +250 sec. The command increased module flow area as shown in table 8-7. As noted in reference symbol E of table 8-4, ullage pressure during all four countdowns increased to 39 psia (or higher) as required. The time interval from step command to 39 psia varied from 70 to 96 sec and was acceptable. Measured LH2 tank pressurization system characteristics are listed in table 8-6.

From ESC +400 sec to cutoff, all LH2 tank pressurization system pressures and temperatures except LH2 tank ullage decreased until engine shutdown. Typical examples are pressurization module inlet temperature and inlet pressure. The EMR* decrease is responsible for the decrease in the LH2 tank pressurization system temperatures and pressures.

The LH2 tank ullage gas temperatures at the 90 percent level averaged 70 deg R at engine start and 152 deg R at engine cutoff. Plots of ullage gas temperatures at various levels are presented in figure 8-8, which shows that there was little or no ullage gas temperature stratification.

The temperature probe (C-0039) located at the 101 percent level in the LH2 tank was found to indicate a higher temperature than the other probes at engine start. The probe is physically mounted on the LH2 tank upper dome wall as shown in figure 8-9 and this location apparently is responsible for its higher indicated temperature. At engine start, incoming GH2 flow enters the tank and is deflected toward the upper dome by the inlet diffuser. This relatively warm gas at temperatures between 180 and 300 deg R (figures 8-5 and 8-6) is believed to flow along the upper dome wall and produce a local environment that is warmer than the ullage volume average temperature. Therefore, the 90 percent level probe was used in lieu of the 101 percent probe in estimating ullage gas temperatures.

The data in figures 8-5 and 8-6 indicate that temperature differences between the J-2 engine injector and the LH2 tank inlet vary from 3 to 21 deg R during engine burn. In some cases, cooling of GH2 flow between the injector tapoff port and the LH2 tank inlet port is indicated by the data. This is unlikely since much of the system hardware is exposed to an ambient (approximately 530 deg R) environment. Expansion cooling of GH2 when throttled through the

*EMR was calculated from PU valve position module orifices is negligible (less than 3 deg). Therefore, it is believed that the indicated cooling of GH2 flow was actually an instrumentation and data processing error.

Test data indicate that actual GH2 flow compares acceptably with predicted values of 0.4 lbm/sec (undercontrol), 0.8 lbm/sec (overcontrol), and 1.2 lbm/sec (step). Predictions were based on an inlet pressure of 750 psia and inlet temperature of 200 deg R.

GH2 flow through the LH2 pressurization system lines was found to be adiabatic. Test data evaluation has verified the validity of the initial design concept which assumed adiabatic flow from the J-2 engine tapoff port to the LH2 tank pressurization port.

Both the measured and calculated static tank inlet temperatures (CD 614030) are compared in figure 8-6. This figure is significant because it shows that calculated static temperature (assuming adiabatic flow) is nearly equal to measured temperature during undercontrol when the probability of non-adiabatic flow theoretically should be greatest. The larger deviation between calculated and measured static temperature during step pressurization is fictitious and is due to the location of the probe. Test data indicate that at low flowrates the probe gives nearly a true static temperature reading. As flow increases, the measured temperature approaches the total temperature and records a higher than actual tank inlet static temperature.

Collapse factors (C_f) obtained from the data of CD 614023, 614025, 614028, and 614040 are shown in figure 8-10. The collapse factors were calculated from the following equation:

$$C_f = \frac{\Sigma \dot{W} \ \Delta t \qquad T}{\frac{(P \ \dot{V} 144) t}{R}}$$

Where:

$\dot{W}$ = Total pressurant flowrate (lbm/sec)

Δt = Calculation time increment (sec)

T = Temperature of gas entering tank (deg R)

P = Ullage pressure (psia)

$\dot{V}$ = Volumetric rate of change in ullage volume (ft^3/sec)

R = Gas constant of pressurant (ft-lbf/lbm-deg R)

t = Time from engine start (sec)

Note that this collapse factor definition employs the diffuser inlet temperature instead of the control orifice temperature used in the Saturn IV definition. The tendency for C_f to vary during engine firing in a random manner is due primarily to instantaneous changes in the GH2 flowrate into the tank. The changes in flowrate, in turn, are caused principally by EMR and module flow area changes. Module inlet pressure and GH2 flowrate vary directly with EMR as explained earlier. The values of C_f are judged acceptable and in agreement with predicted performance.

8.1.2 S-IVB/V

The test data from three countdowns (CD 614034, 614043, and 614044) were used to evaluate the S-IVB/V pressurization and repressurization systems. The results obtained from these tests are discussed in the following paragraphs.

8.1.2.1 Prepressurization

The LH2 tank prepressurization time for CD 614043 was 23 sec (figure 8-11) which was less than that required for the S-IVB/IB battleship because of the smaller S-IVB/V ullage volume. The 37 deg R ullage temperature increase, noted during prepressurization, was typical of values observed during S-IVB/IB tests. Operation of the prepressurization system was satisfactory.

8.1.2.2 Pressurization During First Burn

The S-IVB/V battleship ullage pressure remained above the lower limit of 28 psia, and all ullage pressures and temperatures were acceptable. Typical data from CD 614043 are presented in figure 8-12.

At ESC, all three pressurization flow paths (normal, control, and step) were open until ESC +2.8 sec, when the ullage pressure control was transferred to the LH2 tank pressure switch. This caused the usual ullage pressure increase just after ESC. During first burn pressurization of the three countdowns evaluated, cycling of the module in overcontrol occurred as shown in the following table.

Countdown No.	No. of Overcontrol Cycles	Overcontrol "On" Pressure (psia)	Overcontrol "Off" Pressure (psia)
614034	1	28.7	30.7
614043	2	28.7 28.3	30.3 Cutoff
614044	2	29.2 29.2	31.0 31.0

The ullage temperatures were in the range of 120 to 130 deg R during the latter half of first engine burn for CD 614043. Temperatures at the various tank levels differed by less than 10 deg indicating good mixing of the ullage gas.

8.1.2.3 Repressurization Prior to Second Burn

Repressurization of the LH2 tank was successfully accomplished for all tests. The ullage pressure was increased from ambient (15 psia) to 33 psia in approximately 55 sec. Typical data are presented in figure 8-13. Repressurization was terminated by the LH2 tank pressure switch at 33 psia which was acceptable. The repressurization helium supply was adequate as shown by the 550 psia pressure remaining at the termination of the prepressurization operation.

8.1.2.4 Pressurization During Second Burn

LH2 tank pressurization during second burn was performed satisfactorily. Typical second burn LH2 tank pressurization system operations are shown in figure 8-14. The ullage pressure ranges for three countdowns are shown in the following table.

Countdown	Ullage Pressure Range (psia)	No. of Overcontrol Cycles
614034	40 to 41.1	0
614043	38.3 to 32.0	0
614044	38.1 to 31.8	1 (at 31.8 psia)

Overcontrol during second burn was accomplished by opening the step flow path.

8.2 LH2 Recirculation

The LH2 recirculation system is shown schematically in figure 7-25.

8.2.1 S-IVB/IB

For the S-IVB/IB battleship tests, the LH2 tank was loaded with the prevalve open* which exposed the LH2 pump and other hardware to LH2 for a long period of time before the chilldown pump was started. Because of this, the hardware was largely chilled before LH2 pump chilldown, and fluid conditions throughout the chilldown system reached their steady-state values within 1 or 2 min after the chilldown pump was started.

Countdowns 614005-3 through 6140010-2 were used for evaluating the performance of the chilldown system with the J-2003 engine (table 8-8). Four of these tests consisted of approximately 10-min chilldowns; the other two were 5-min chilldowns.

During all these tests, the chilldown pump was started before the LH2 tank was pressurized and was shut down at engine start. The LH2 tank was pressurized while chilldown was in progress and markedly affected chilldown. Chilldown was ended at ESC -6.5 sec, when the prevalve was opened to remove any bubbles that may have collected beneath it. Essentially all the chilldown flow then returned to the tank through the open prevalve, and the LH2 at the engine interface started to increase in temperature because there was no appreciable chilldown flow through the engine from that time until engine start.

When the chilldown pump was started, the liquid in the tank was saturated. The LH2 was subcooled just downstream of the chilldown pump, since the chilldown pump developed a head of 10 psi while only slightly heating the LH2 passing through it. Because of a decrease in pressure (resulting from the flow resistance) and an increase in temperature (from heat input), the LH2 became less subcooled as it proceeded through the system. For four of the tests, the NPSH at the engine LH2 pump inlet was 5 to 6.5 psi during unpressurized

---

*The bleed valve was also open in the J-2013 engine tests. During the J-2003 engine tests, the bleed valve was generally opened when LH2 tank loading had reached the 50 percent point (table 8-8).

chilldown, and the LH2 was saturated between the engine LH2 pump inlet and the GG bleed valve. This was indicated by the GG bleed valve temperature which was approximately the same or lower than the engine interface temperature during this time. The heat input to this portion of the system caused the LH2 to vaporize. Therefore, during unpressurized chilldown, subcooled liquid flow existed from the chilldown pump to slightly beyond the engine LH2 pump inlet where the LH2 became saturated, and two-phase flow existed from there to the exit of the chilldown system.

After the LH2 tank was pressurized to 40.4 to 42.7 psia, the NPSH at the engine LH2 pump inlet increased to 29 to 32 psi, and the LH2 became subcooled throughout the remaining portion of the system so that subcooled LH2 existed throughout the entire chilldown system. The change from two-phase flow to subcooled liquid flow throughout the chilldown system caused the flowrate to increase from 55 to 95 gpm when the tank was pressurized. The mass flowrate increased due to the higher density of subcooled liquid flow.

The chilldown tests in CD 614006 and 614007 (figures 8-15 and 8-16) were conducted for 5 min rather than 10 min. Countdown 614006 also differed in that the GG bleed valve was not opened until the start of chilldown, while in all the other tests, it was opened when the LH2 tank load reached the 50 percent level. As a result, the hardware downstream of the GG bleed valve was warm and dry prior to the start of chilldown, and the LH2 at the LH2 pump inlet remained saturated for the first 30 sec of chilldown (until the tank was pressurized). The GG bleed valve temperature cycled on and off scale indicating slugging flow. During the 10-min chilldowns, when the bleed valve was opened long before chilldown started, the LH2 at the LH2 pump inlet was subcooled by 6 psi. In the tests where the bleed valve was opened early, the bleed valve temperature was saturated during this early part of chilldown. Also during CD 614006, the bleed valve temperature was still decreasing at the end of pressurized chilldown, indicating that chilldown had not been as complete as it had been during the tests where the bleed valve was opened during loading, which demonstrates the advantage of having the bleed valve open during loading. However, it should be noted that the engine LH2 pump inlet temperature stabilized at a value similar to that of the other tests and that start requirements were easily met.

During CD 614007 (figure 8-16) the GG bleed valve was opened during loading, but chilldown was not started until ESC -5 min. Data from this test indicate that temperatures were slightly higher than those of the 10-min chilldowns, but otherwise were very similar.

During CD 614010-2, there was a larger-than-normal heat input to the chilldown system. This resulted in an NPSH at the engine interface of only 1.5 psi and a flowrate of only 44 gpm during unpressurized chilldown as opposed to typical values of 5 to 6.5 psi and 55 gpm respectively. However, when the tank was pressurized, the flowrate increased to a normal 95 gpm and the NPSH increased to a normal 30 psi at the engine interface.

In spite of the variations in chilldown times, procedures, and heat inputs, start conditions were easily obtained during all of these tests. The available NPSH at engine start was 18.2 to 22.9 psi compared to a required minimum of 9.4 psi. Figure 8-17 presents typical data from the 10-min chilldown tests.

A flow coefficient was defined by $\Delta P = \frac{CW^2}{\rho}$ where $C = \frac{K}{A^2 \, 2_g}$ in the Darcy equation. Therefore, this flow coefficient depends only on the geometry of this system. It is a measure of the flow resistance of a system and is directly proportional to the pressure drop in the system.

The flow coefficient could only be determined during pressurized chilldown when the LH2 in the system was all liquid. For the six tests with the J-2003 engine, the pressure drop moved between 7.4 and 10.0 psi. The corresponding flow coefficients were 41.8 to 49.8 $sec^2/in^2 \, ft^3$ (table 8-8). It should be noted that in the J-2003 engine the LH2 bleed valve was 1 in. in diameter instead of 1.5 in. as in the flight engines.

Since the flow coefficient was dependent only on the system geometry, its value was the same during both pressurized and unpressurized chilldown. With the flow coefficient and flowrate, pressure, and temperature data during unpressurized chilldown, it was possible to estimate an average fluid quality in the two-phase flow region of the chilldown system during unpressurized chilldown. For purposes of calculation, two-phase flow was considered to exist from the engine interface to the exit of the chilldown system. The average fluid quality was defined as mass vapor/mass mixture and varied from a low of 0.067 during CD614008 to a high of 0.143 during CD 614010. The quality during CD 614010 was very high because of high heat input which resulted in the LH2 being nearly saturated at the engine interface. The short (5-min) tests during CD 614006 and 614007 were of higher qualities than the 10-min tests (CD 614008 and 614009), which was expected since the hardware was not well chilled. Also the average quality of CD 614006 (test where GG bleed valve was opened at start of childown) was higher than that of the other short test (CD 614007) where the GG bleed valve was opened during loading.

The heat input rates to the various sections of the chilldown system were calculated from flowrate and temperature data during pressurized chilldown. The heat input rate in section 1 (tank 1 percent level to engine interface) ranged from a low of 6,400 Btu/hr during CD 614008 to a high of 8,500 Btu/hr during CD 614010. The heat input rate in section 2 (engine interface to GG bleed valve) ranged from 22,200 Btu/hr during CD 614008 to 33,400 Btu/hr during CD 614006. Since it was not possible to calculate the heat input rate in section 3 (GG bleed valve to exit of chilldown system) because of insufficient data accuracy, the total heat input to the system could not be determined.

During unpressurized chilldown, the heat input rate in section 1 was calculated the same way as it was for pressurized chilldown since the LH2 was still subcooled in this section. The calculated heat input ranged from a low of 7,000 Btu/hr during CD 614008 to a high of 16,900 Btu/hr during CD 614006. The heat input rate in sections 2 and 3 during unpressurized chilldown was determined from the average fluid quality. Since no pressure transducer was located at the GG bleed valve, it was not possible to separate the heat inputs in sections 2 and 3. The heat input rate in sections 2 and 3 ranged from a low of 24,600 Btu/hr during CD 614008 to a high of 41,900 Btu/hr during CD 614010. The total heat inputs to the chilldown system during unpressurized chilldown ranged from 31,600 Btu/hr during CD 614008 to 53,000 Btu/hr during CD 614010.

The heat up rate at the engine interface, from the end of chilldown (opening the prevalve) to Engine Start Command, ranged from 2.5 deg R/min during CD 614005 to 9.9 deg R/min during CD 614010. The average value for these six tests was 5.9 deg R/min.

The LH2 bleed valve of the J-2013 engine was larger (1.5 in.) than the valve in the J-2003 engine (1 in.), and the chilldown system through the engine was routed differently. The stage portion of the chilldown system was the same for both engines. The chilldown procedure was basically the same, with the tank loaded with the prevalves opened as before. With the J-2013 engine, the bleed valve was open from the start of loading.

Five tests were used for evaluation of the chilldown system with the J-2013 engine. These tests consisted of a 28 min, 21 min, 3.5 min, and two 6-min chilldowns. Test data are summarized in table 8-8. In the 3.5-min test of CD 614017-A3 (figure 8-18) chilldown was started after the LH2 tank was pressurized. In the other four tests, chilldown was started before the tank was pressurized which is the normal procedure (figure 8-19).

During unpressurized chilldown, the LH2 was subcooled from the tank to the engine interface and saturated at the bleed valve. From the bleed valve to the exit of the chilldown system, two-phase flow existed. When the LH2 tank was pressurized, the LH2 became subcooled liquid throughout the entire chilldown system. When the LH2 tank was pressurized to 31.0 to 35.1 psia, the flowrate increased from 101.4 -130 gpm to 138.2 -157 gpm because of the higher density of subcooled liquid flow.

During CD 614017-A3 (figure 8-18) chilldown was started after the LH2 tank was pressurized, and the test was very short (3.5 min). Steady-state flowrate and fluid temperatures were the same as for the other four chilldown tests during pressurized chilldown. About the only difference was that steady-state conditions were reached sooner.

In tests with the J-2013 engine, the available NPSH at the engine interface during unpressurized chilldown was 5.1 to 7.8 psi; during pressurized chilldown this increased to 20.0 to 23.8 psi. The prevalve was opened at ESC -7.8 sec. When this occurred, the flow resistance was greatly reduced which caused a drop in the chilldown pump developed head to near zero, and a loss in NPSH at the engine interface. During the 8 sec of essentially no flow through the engine chilldown system, the LH2 at the engine interface heated up and caused a further decrease in NPSH. As a consequence of these decreases, the NPSH at engine start was 12.0 to 14.7 psi. However, the available NPSH was still greater than the required minimum of 10.5 psi.

During unpressurized chilldown, the system pressure drop was 9.0 to 9.5 psi. After the tank was pressurized, the pressure drop was 6.1 to 8.4 psi. The flow coefficient was determined from pressure drop and flowrate data during pressurized chilldown when subcooled liquid flow existed throughout the chilldown system. The calculated flow coefficients were 13.5 to 16.0 $sec^2/in.^2ft^3$. The flow coefficient is directly proportional to the system pressure drop.

The average fluid quality during unpressurized chilldown was calculated from the flow coefficient and flowrate, pressure, and temperature data. Since there was no pressure transducer at the bleed valve, it was necessary to compute the average fluid quality for the portion of the system from the engine interface to the exit of the system. This quality was defined as mass vapor/mass mixture and, for the different tests, ranged from a low of 0.019 in CD 614017-E2 to a high of 0.036 in CD 614030 (figure 8-19).

During pressurized chilldown the heat input rate for all sections of the system was calculated from flowrate and temperature data. The heat input rate in section 1 ranged from 6,600 Btu/hr during CD 614017-E2 to 13,300 Btu/hr during CD 614030. In section 2 the heat input rate ranged from 16,200 Btu/hr during CD 614017-E2 to 24,300 Btu/hr during CD 614030. In section 3 the heat input rate ranged from 7,500 Btu/hr during CD 614025 to 27,000 Btu/hr during CD 614017-E2. The total heat input rates for pressurized chilldown were 42,500 Btu/hr during CD 614025 to 56,000 Btu/hr during CD 614030.

During unpressurized chilldown, the heat input rate was calculated the same way as during pressurized chilldown for section 1 where subcooled liquid existed. This same method was used for section 2, although the LH2 became saturated in this section. Because the bleed valve temperature was higher than the engine interface temperature, it was assumed that the saturation point was near the downstream end of the section. The heat input to section 3 went entirely toward vaporizing the LH2 and was calculated from the average quality.

During unpressurized chilldown, the heat input rate to section 1 ranged from 8,800 Btu/hr during CD 614017-E2 to 13,600 Btu/hr during CD 614030. The heat input rate in section 2 ranged from 6,200 Btu/hr during CD 614030 to 12,450 Btu/hr during CD 614017-E2. The heat input rate in section 3 ranged from 16,700 Btu/hr during CD 614017-E2 to 24,200 Btu/hr during CD 614030. The total heat input rates during unpressurized chilldown ranged from a low of 37,800 Btu/hr during CD 614014 to a high of 44,000 Btu/hr during CD 614030.

The heat up rate at the engine interface from the end of chilldown (opening of the prevalve) to engine start varied from 4.6 deg R/min during CD 614025 to 6.0 deg R/min during CD 614017-E2. The average value was 5.2 deg R/min.

8.2.2 S-IVB/V

The S-IVB/V chilldown tests (CD 614034 to 614044) were initiated with the ducts and hardware warm and dry. For the first burn chilldown tests, the LH2 tank was loaded with the prevalve closed. For the second burn chilldown tests, the suction duct was purged with ambient helium during the simulated coast period to warmup the hardware. For first burn the LH2 tank was pressurized before the chilldown pump was started. For second burn chilldown, the chilldown pump was started and the tank was pressurized 5 min later. During the first and second burn tests, the initial chill period was marked by pressure and flow surges caused by vaporization of the LH2, except during the first burn of CD 614034 when the LH2 duct was filled prior to the start of chilldown. The vapor formation caused the pressure in the suction duct to increase rapidly and forced the check valve in the bypass line to close, thus halting the flow. After the pressure was relieved through the return line to the tank, the flowmeter registered off-scale at 160 gpm and the flow once again proceeded through the system.

For the first burn tests during which chilldown was started after the tank was pressurized, the engine LH2 pump inlet pressure and temperature and the bleed valve temperature cycled for 1.5 to 2 min and then steadied out at a saturated condition (figure 8-20). The LH2 became subcooled at the engine interface 3 to 3.5 min after the start of chilldown and at the bleed valve 1.5 min later. Shortly after the LH2 at the engine interface became subcooled, the engine interface pressure and temperature were within the engine start requirements. At engine start, the available NPSH at the engine interface was well above the minimum requirement. The 11-min chilldown used for the first burn was more than adequate for reaching start requirements under ground conditions, which were more severe than the conditions that will be encountered during orbital chilldown. Therefore, it appears that orbital chilldown can be successfully accomplished within the 5-min period allotted in the present flight sequence.

The advantage of starting chilldown with the LH2 tank pressurized is apparent when the second burn chilldown tests are compared with those of first burn. During the second burn chilldown tests, the engine pump inlet and bleed valve temperatures and engine interface pressure cycled throughout the unpressurized portion of chilldown with the temperatures continually decreasing. Shortly before prepressurization, both the engine interface and bleed valve conditions were saturated. At the completion of prepressurization, the fluid at the engine interface became subcooled, and the fluid at the bleed valve became subcooled a short time later. Engine interface start requirements were met very soon after prepressurization (figure 8-21). The 10-min second burn chilldown was more than adequate under the conditions which existed at the time of the test.

Table 8-9 presents a summary of the fuel system chilldown tests.

8.3 Engine LH2 Supply

The LH2 was supplied to the engine in a satisfactory condition during all the firings of the S-IVB/IB and S-IVB/V battleship test programs. During these tests, the engine interface pressure and temperature were such that the available NPSH exceeded the minimum requirement throughout engine firing.

8.3.1 S-IVB/IB

During firing, the engine interface pressure followed the ullage pressure while generally decreasing with respect to the ullage pressure due to decrease of liquid head as the LH2 was consumed. The engine interface temperature decreased during the start transient, steadied out, then increased with time due to heating of the LH2 in the tank.

The engine interface pressure and temperature data were used in a Fortran computer program to calculate the available NPSH during engine firing. A constant term was used for the dynamic pressure since the program was not yet able to calculate dynamic pressure from engine flowrate and pump discharge conditions. The available NPSH was calculated for CD 614009, 614010, 614025, 614028, and 614030. Typical results are shown in figures 8-23 and 8-24 and are briefly summarized in table 8-10. It can be seen that the available NPSH at the engine interface was above the required minimum throughout the firings. The pressure drop (figure 8-24) in the suction duct was calculated from ullage pressure, engine interface pressure and temperature, PU probe mass, pump discharge pressure and temperature, and engine flowrate. The pressure drop was calculated for CD 61400, 614009, 614010, 614023, 614025, 614028, and 614030 and averaged 1.13 psi as compared with the originally predicted value of 1.76 psi.

The engine interface temperatures during CD 614010, 614020, 614023, 614024, 614025, 614028, and 614030 were normalized by shifting them so that their initial steady-state temperatures were the same. These normalized temperatures were then plotted against the mass remaining in the LH2 tank. This plot (figure 8-25) shows that the data from all seven tests agree very closely, which indicates that the heat input to the tank and the LH2 stratification pattern during engine firing were very similar during the different tests.

Figure 8-26 presents the engine inlet parameters for both engines plotted within their respective operating regions and shows satisfactory operation of the LH2 supply systems.

8.3.2 S-IVB/V

The LH2 was supplied to the engine in a satisfactory condition throughout first and second burn for all three of the S-IVB/V countdowns evaluated (CD 614034, 614043, and 614044). The first burn tests consisted of 170-sec firings with planned cutoff. The second burn tests ran until cutoff was necessitated by propellant depletion (approximately the 1 percent level). The duration of second burn varied with EMR and mass remaining in the tanks at second burn engine start.

During these tests, the engine pump inlet pressure followed the ullage pressure while decreasing slightly due to loss of liquid head as the LH2 was consumed. The engine interface temperatures decreased during the start transient, stabilized, and then increased with time due to the heating of the LH2 in the tank. (Figures 8-27 and 8-28 present typical S-IVB/V operating data.)

The available NPSH at the engine interface exceeded the minimum required value throughout both first and second burns of all three countdowns (table 8-11). The NPSH increased just after engine start mainly due to the decrease in temperature at the engine interface during this time. The NPSH then followed the ullage pressure while generally decreasing with time due to the decrease in liquid head and the increase in engine interface temperature which resulted from the heat input to the LH2 tank during firing.

TABLE 8-1
S-IVB/IB LH2 TANK PREPRESSURIZATION

COUNTDOWN	614023	614028	614030
Type of Prepress.	Cold Helium	Cold Helium	Cold Helium
Prepress. Supply	Normal GSE Supply	Normal GSE Supply	Normal GSE Supply
Initial Ullage Press. (psia)	16.2	17.2	17.2
Final Ullage Press. (psia)	32.8	34.2	33.7
Time Before Sim. Liftoff When Prepress. was Initiated (sec)	SLO -200	SLO -170	SLO -170
Time to Prepress (sec)	33	30	30
Ullage Press. at Engine Start (psia)	33.4	36.4	34.7
Ullage Temperature at Start of Prepress. 101% Level (°R)	44	49	58
Ullage Temperature at End of Prepress. 101% Level (°R)	65	77	75
Ullage Temp. at ESC (°R)	104	126	119
Ullage Vol. (ft^3)	1,719	1,609	1,519
Max. GSE Prepress. Orifice Inlet Temp (°R)	115	99	102
Min. GSE Prepress. Orifice Inlet Temp (°R)	71	71	71
Max. Helium Flowrate (lbm/sec)	0.88	0.85	0.85
Min. Helium Flowrate (lbm/sec)	0.77	0.73	0.73
Total Helium Flow (lbm)	29	24.4	22.8

NOTE: Data from CD 614025 was omitted since the GSE hydrogen purge system of ambient GH2 was used instead of helium to prepressurize the LH2 tank.

TABLE 8-2
S-IVB/IB LH2 TANK PRESSURIZATION SYSTEM PERFORMANCE DATA
(ENGINE J-2003)

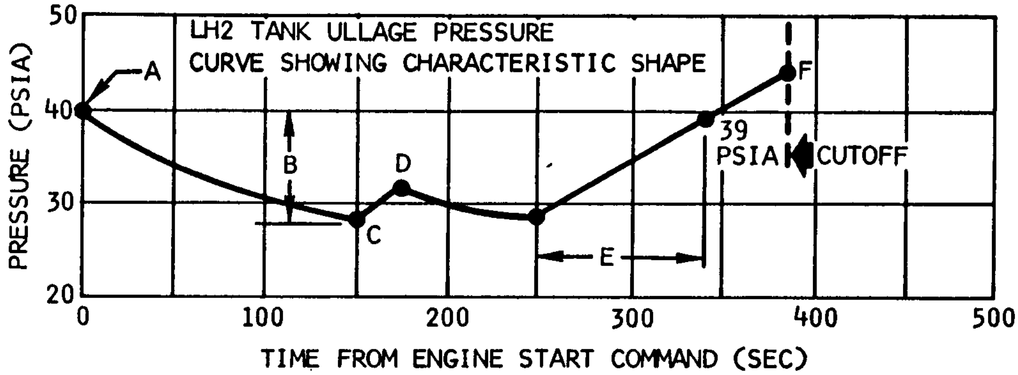

DESCRIPTION	REFERENCE SYMBOL	CD 614010	CD 614009
Pressure Range to "Start" Command (psia)	A	40.7	40.5
Ullage Pressure Range from "Start" to "Step" Command (psia)	B	40.7 to 28.8	40.0 to 30.2
Pressurization Module "Control Mode" Valve Opens (psia)	C	28.8	28
Control Mode Valve Closes (psia)	D	30.6, 30.3	
Time to Reach 39 psi from Step Command (sec)	E	148	Run Cutoff Before Reaching 39 psia
Ullage Pressure at Engine Cutoff (psia)	F	70	N/A
Average Ullage Gas Temperature at Start (°R)		70	-
Average Ullage Gas Temperature at Cutoff (°R)		125	N/A
"Undercontrol" GH2 Flow (lbm/sec)		0.5	
"Overcontrol" GH2 Flow (lbm/sec)		0.98	
"Step" GH2 Flow (lbm/sec)		1.25	

TABLE 8-3
S-IVB/IB GH2 FLOWRATES

PARAMETER	CALCULATED FROM TEST DATA - CD 614010		PREDICTED FOR
	AT ACTUAL T_{gas} = 130° R	AT T_{gas} = 200° R (for comparison)	T_{gas} = 200° R
Undercontrol	0.5 lbm/sec	0.4 lbm/sec	0.35 lbm/sec
Overcontrol	0.98 lbm/sec	0.79 lbm/sec	0.8 lbm/sec
Step	1.29 lbm/sec	0.96 lbm/sec	1.2 lbm/sec

TABLE 8-4
S-IVB/IB LH2 TANK PRESSURIZATION SYSTEM PERFORMANCE DATA
(ENGINE J-2013)

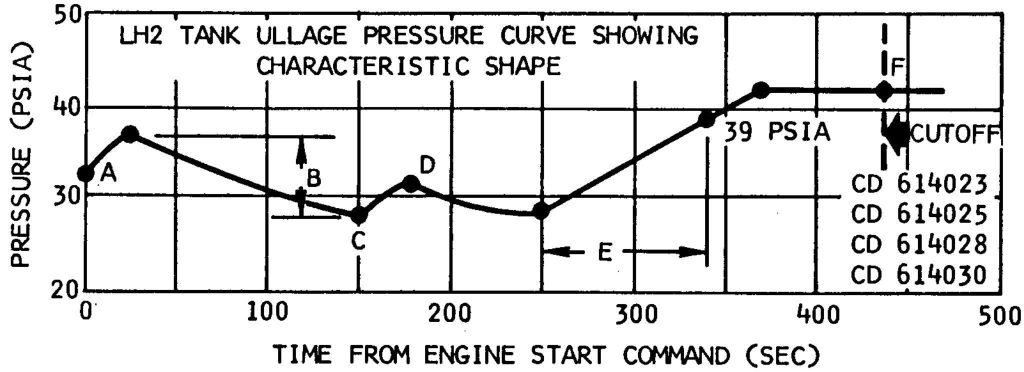

DESCRIPTION	REFERENCE SYMBOL	PERFORMANCE DATA
Pressure Range to "Start" Command	A	33.4 to 37.0 psia
Ullage Pressure Range from "Start" to "Step" Command	B	29.1 to 38.7 psia
Pressurization Module "Overcontrol" Valve Opens	C	29.5 psia
Overcontrol Mode Valve Closes	D	30.7 psia
Time to Reach 39 psia from Step Command	E	70 to 96 sec
Ullage Pressure at Engine Cutoff	F	41.7 to 43.2 psia
Average Ullage Gas Temp at Start		70° R
Average Ullage Gas Temp at Cutoff		152° R
"Undercontrol" GH2 Flow		0.40 to 0.46 lbm/sec
"Overcontrol" GH2 Flow		0.86 (constant) lbm/sec
"Step Mode" GH2 Flow		1.09 to 1.22 lbm/sec

TABLE 8-5
S-IVB/IB ENGINE MIXTURE RATIO DATA

COUNTDOWN	ENGINE BURNTIME	ENGINE MIXTURE RATIO
614023	472 sec	High EMR for 100 sec
614025	509 sec	Low EMR for 100 sec
614028	374 sec	High EMR for 100 sec
614030	495 sec	Low EMR for 25 to 50 sec

TABLE 8-6
S-IVB/IB MEASURED LH2 PRESSURIZATION SYSTEM CHARACTERISTICS

PARAMETER	CD 614023	CD 614025	CD 614028	CD 614030	AVERAGE	DESIGN OBJECTIVES	
						MAXIMUM	MINIMUM
Ullage Pressure at ESC (psia)	33.4	37	36.4	34.7	35.4	Up to Vent	32
Ullage Pressure Range from "Start" to "Stop" Command (psia)	34.3 29.7	38.7 29.1	37.2 31.3	36.1 29.7	36.6 30.0	Vent	28
Pressurization Module "Overcontrol" Valve Opens (psia)	*	29.5	-	-	29.5	-	28
Overcontrol Valve Closes (psia)	-	30.7	-	-	30.7	31	-
Time to Reach 39 psia from "Step" Command (sec)**	96	79	70	86		Not Specified	
Ullage Pressure at Cutoff (psia)	43.2	42.1	42.2	41.7	42.3	-	39.0
Average Ullage Gas Temperatures at Start (°R)	-	+135	-	138	136	Not Specified	
Average Ullage Gas Temperatures at Cutoff (°R)	-	150	-	154	152	Not Specified	

*Indicates no data or not applicable
**Value is influenced by ullage pressure at time that command is given

TABLE 8-7
S-IVB/IB LH2 PRESSURIZATION MODULE DATA

	MODULE EFFECTIVE AREA (in.^{2})			ORIFICE AREA (in.^{2})			
COUNTDOWN	UNDER CONTROL	OVER CONTROL	STEP	UNDER CONTROL	OVER CONTROL	STEP	ENGINE (REF)
614009	-	-	-	-	-	-	J2003
614010	-	-	-	-	-	-	J2003
614023	0.054	0.114	0.146	0.057	0.141	0.149	J2013
614025	0.054	0.114	0.146	0.057	0.141	0.149	J2013
614028	0.054	0.114	0.146	0.057	0.141	0.149	J2013
614030	0.054	0.114	0.146	0.057	0.141	0.149	J2013

TABLE 8-8
S-IVB/IB ENGINE LH2 PUMP CHILLDOWN DATA

COUNTDOWN		614005-3	614006	614007	614008	614009	614010-2	614014	614017-A3	614017-E2	614025	614030
ENGINE		J-2003						J-2013				
Chilldown Time (min)		11	5	5	10	10	10	28	3 1/2	23	6	6
Initiation of Chilldown T(1) (sec)		-580	-190	-220	-510	-510	-500	-1,670	-185	-1,220	-280	-275
Gas Generator Bleed Valve Open at		50% of LH2 Load	Start of Chilldown	50% of LH2 Load	50% of LH2 Load	50% of LH2 Load	50% of LH2 Load	Start of Loading	Start of Loading	Start of Loading	Start of Loading	Start of Loading
Initiation of Prepressurization T (sec)		-170	-160	-160	-160	-170	-160	-750	-270	-270	-170	-175
Prevalve Open at ESC(2) (sec) (End of Chilldown)		6.1	6.4	6.4	6.3	6.4	6.4	7.8	7.8	7.8	7.8	7.8
Available NPSH at ESC (psi)		19.1	20.5	18.5	22.9	21.6	18.2	—	14.4	14.6	14.7	12.0
Minimum Required NPSH at ESC (psi)					9.4					10.5		
Chilldown Flowrate (gpm)	UC(3)	—	56	55	55	53	44	123	—	130	118.3	101.4
	PC(4)	—	94	94.5	95	95	95	155	157	155	152.3	138.2
Engine Interface Pressure (psia)	UC	25.9	28.5	28.0	27.6	26.0	27.6	25.7	—	25.6	26.2	26.8
	PC	48.6	52.2	50.5	51.2	50.0	50.0	39.7	42.0	41.9	43.3	41.0
System Pressure Drop (psid)	UC	8.6	10.9	10.6	10.4	9.1	10.4	9.1	—	9.5	9.0	9.0
	PC	7.4	8.7	8.7	10.0	8.4	9.2	8.4	7.6	7.8	7.4	6.1
Flow Coefficient, C ($sec^2/in.^2ft^3$)	UC	—	—	—	—	—	—	—	—	—	—	—
	PC	—	44.3	43.8	49.8	41.8	45.8	15.56	13.50	14.28	15.4	16.0
Engine Interface Temperature (°R)	UC	38.6	40.9	39.3	38.8	38.5	40.2	—	—	37.7	38.5	39.0
	PC	38.2	38.7	38.7	38.2	37.95	38.65	—	38.0	37.8	38.6	38.7
Available NPSH at Engine Inlet (psi)	UC	5	0	5.3	6.5	6	1.5	—	—	7.8	6.0	5.1
	PC	29	32	29.7	31.5	31	30	—	23.3	23.8	22.5	20.0
Gas Generator Bleed Valve Temperature (°R)	UC	38.6	—	—	37.8	—	37.5	38.9	—	38.8	39.5	39.6
	PC	40.9	42.5	42.0	40.8	—	41.8	39.9	39.7	39.0	40.3	40.7
Return Line Temperature (°R)	UC	37.5	37.6	37.4	37.5	37.5	37.5	38	—	38.0	38.6	39.5
	PC	—	—	—	—	—	—	40.9	41.0	40.9	40.8	42.2
Heat Input (Btu/hr) Tank to Engine Interface	UC	—	16,900	8,300	7,000	7,100	11,100	—	—	8,800	11,000	13,600
	PC	—	7,200	7,700	6,400	6,700	8,500	—	10,600	6,600	13,000	13,300
Heat Input (Btu/hr) Engine Interface to Bleed valve	UC	—	—	—	—	—	—	—	—	12,450	11,000	6,200
	PC	—	33,400	28,800	22,200	—	27,600	—	23,700	16,200	22,000	24,300
Heat Input (Btu/hr) Bleed valve to Tank	UC	—	—	—	—	—	—	18,700	—	16,700	20,000	24,200
	PC	—	—	—	—	—	—	14,300	19,000	27,000	7,500	18,400
Unpressurized Heat Input - Tank to Engine Interface, Engine Interface to Bleed Valve (Btu/hr)		—	34,100	32,400	24,600	27,700	41,900	—	—	29,150	31,000	30,400
Total System Heat Input (Btu/hr)	UC	—	51,000	40,700	31,600	34,800	53,000	37,800	—	37,950	42,000	44,000
	PC	—	—	—	—	—	—	42,000	53,300	49,800	42,500	56,000
Engine Inlet Temperature Rise Rate from End of Chilldown to ESC (°R/min)		2.5	4.7	9.4	5.3	3.7	9.9	—	4.7	6.0	4.6	5.4
Wind Speed (mph)		5	2-3	7-8	5	0-3	5	20-25	0-2	0-2	10	3
Average Fluid Quality, Unpressurized Condition $\left(\frac{\text{lb gas}}{\text{lb mix}}\right)$		—	0.0920	0.0884	0.0670	0.0782	0.1431	0.0224	—	0.0188	0.025	0.036
Tank 1 Percent Level Temperature (°R)	UC	37.4	37.5	37.55	37.3	36.9	37.3	37.1	—	36.9	37.4	37.4
	PC	37.5	37.8	37.75	37.4	37.1	37.6	37.85	37.2	37.2	37.6	37.6
Tank Ullage Pressure (psia)	UC	16.5	16.8	16.5	16.4	16.1	16.4	15.8	—	15.6	16.4	17.0
	PC	40.4	42.7	40.5	40.4	40.8	40.0	31.0	33.6	32.8	35.1	34.1

(1) T = Time from Simulated Liftoff
(2) ESC = Engine Start Command
(3) UC = Unpressurized Chilldown
(4) PC = Pressurized Chilldown

21 February 1966

TABLE 8-9
S-IVB/V LH2 PUMP CHILLDOWN DATA

PARAMETER	CD 614034	CD 614043		CD 614044	
	2nd Burn	1st Burn	2nd Burn	1st Burn	2nd Burn
Length of Childown (min)	10	11	10	11	10
Start Childown Pump at ESC (sec)	-590	-680	-585	-680	-585
Start Pressurization at ESC (sec)	-280	-705	-280	-705	-285
Maximum Engine Interface Pressurization During Transient Surges (psia)	57	80	55	80	52
Engine Interface Pressurization at ESC (psia)	40.4	39.6	39.2	39.6	38.2
Engine Interface Temperature at ESC (°R)	39.55	39.5	39.3	39.7	39.0
Available NPSH at ESC (psi)	16.8	16.2	16.5	15.5	16.5
Required NPSH at ESC (psi)	8.6	8.6	8.6	8.6	8.6
Heat Up Rate at Engine Interface at End of Chilldown (°R/min)	8.0	8.5	15.4	12.9	15.0

TABLE 8-10
S-IVB/IB LH2 NPSH

PARAMETER	CD 614009	CD 614010	CD 614025	CD 614028	CD 614030
Maximum Available NPSH (psi)	23.0	25.0	21.0	20.2	20.5
Minimum Available NPSH (psi)	10.4	9.0	10.3	11.3	10.4
Minimum Required NPSH (psi)	8	8	6 at EMR = 5.0:1 7 at EMR = 5.5:1		
Number of Cycles	1	3	2	1	1

TABLE 8-11
S-IVB/V LH2 NPSH

PARAMETER	CD 614034	CD 614043		CD 614044	
	1st Burn	1st Burn	2nd Burn	1st Burn	2nd Burn
Maximum Available NPSH (psi)	21.7	26	26	25	25
Minimum Available NPSH (psi)	9.3	12.5	15.8	13.8	15
Minimum Required NPSH (psi)	6 psi at EMR = 5.0:0 7 psi at EMR = 5.5:0				
No. of Cycles	1	2	0	0	1

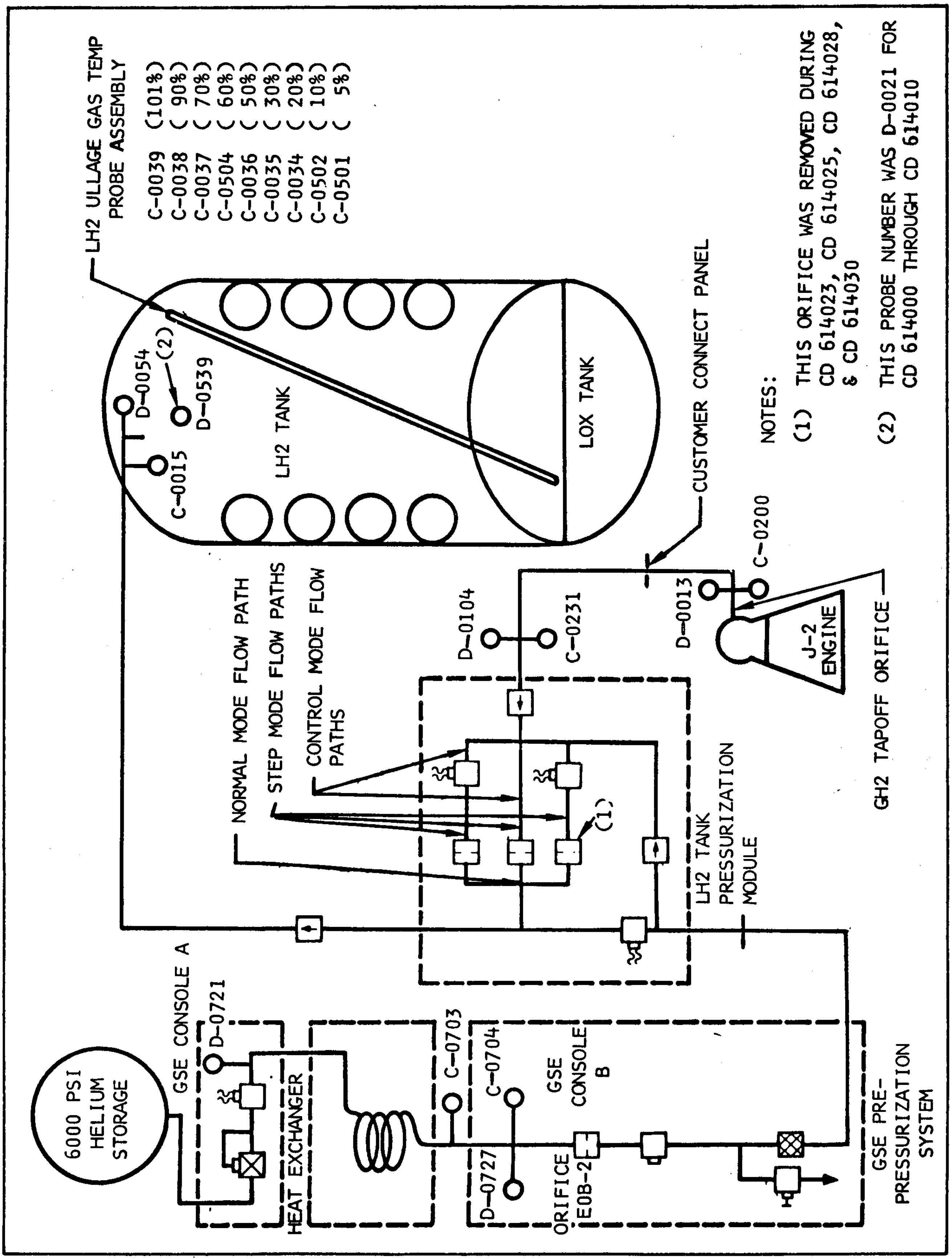

Figure 8-1 LH2 Tank Pressurization System and Instrumentation

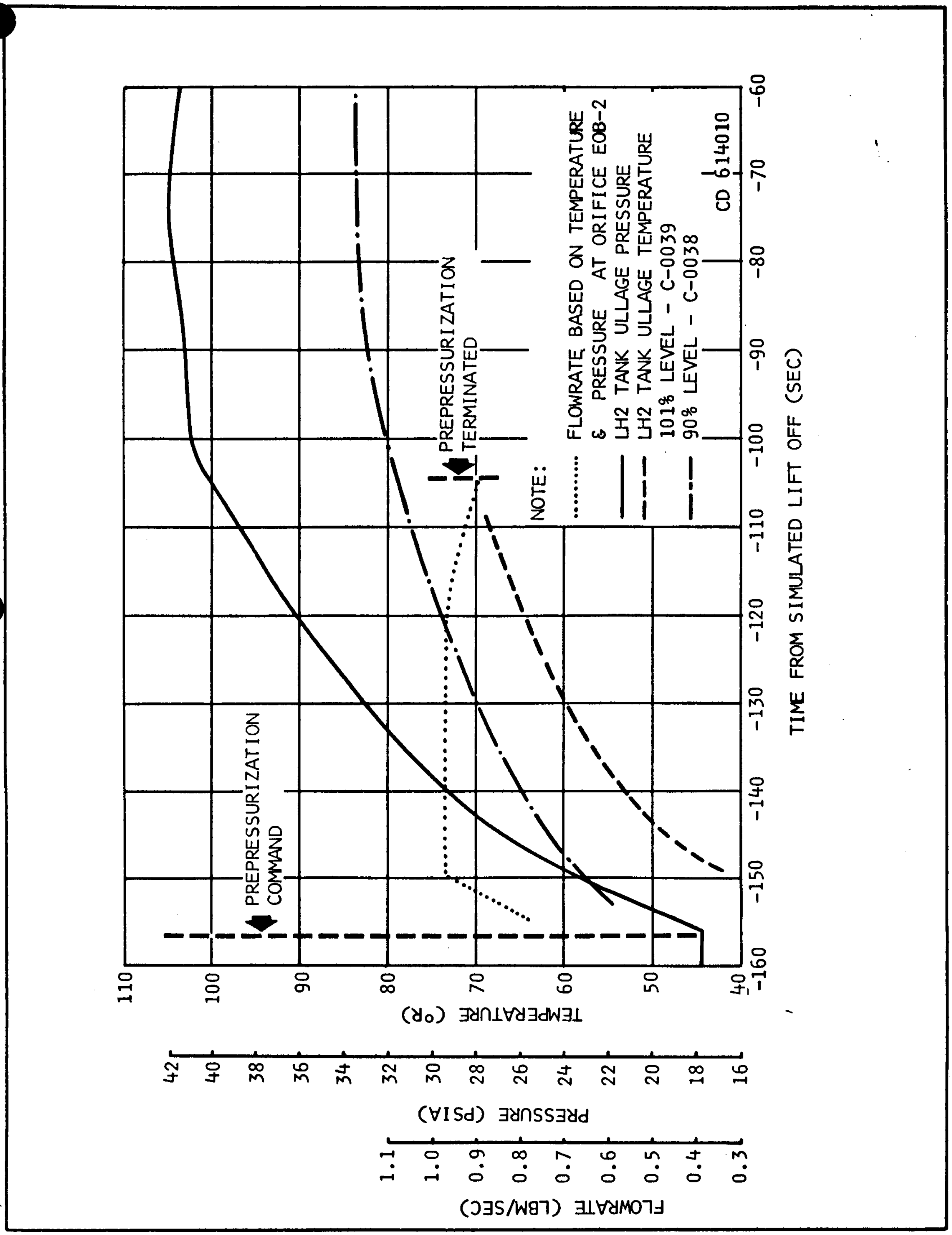

Figure 8-2 LH2 Tank Prepressurization History

21 February 1966

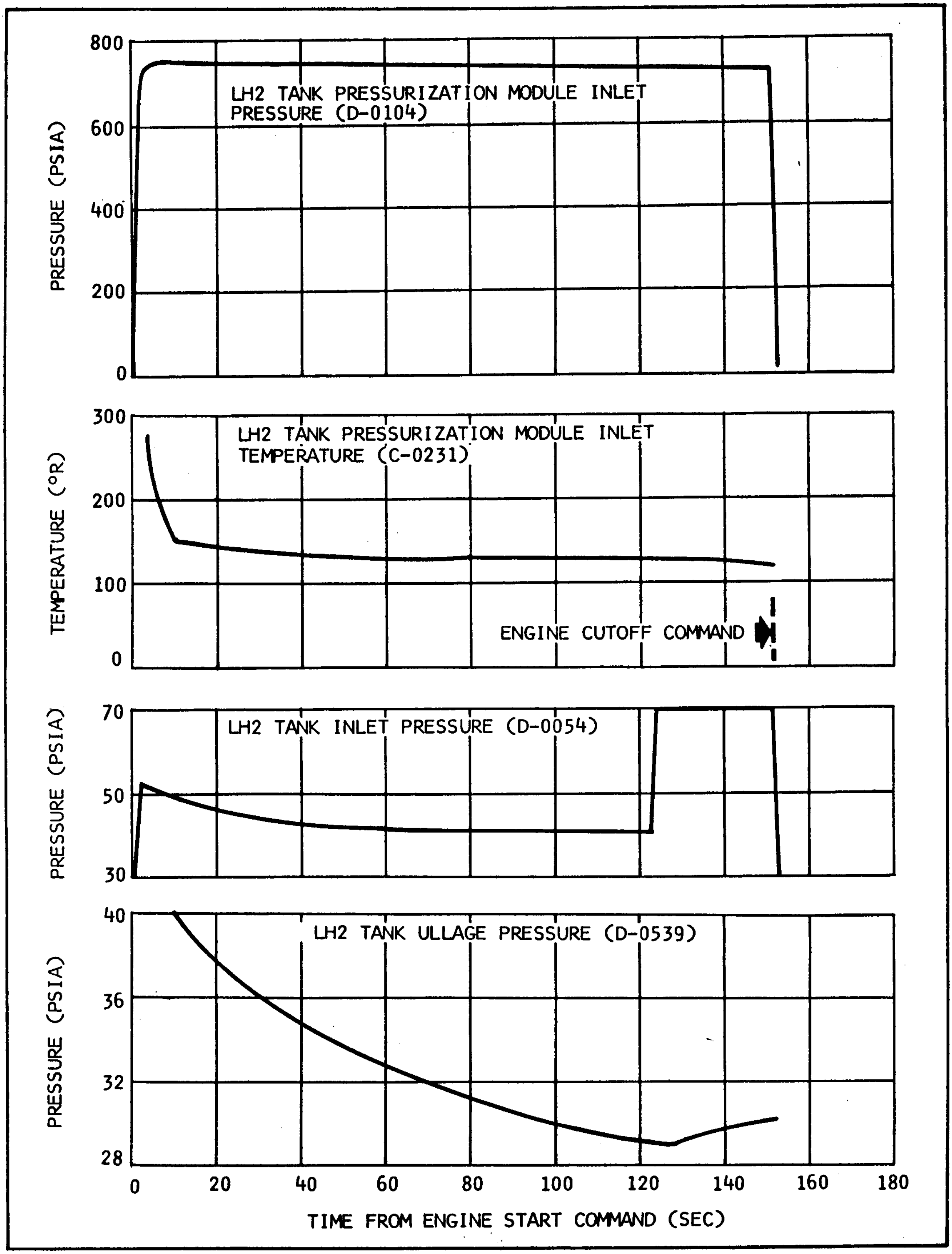

Figure 8-3 LH2 Tank Pressurization System Performance - CD 614009

21 February 1966

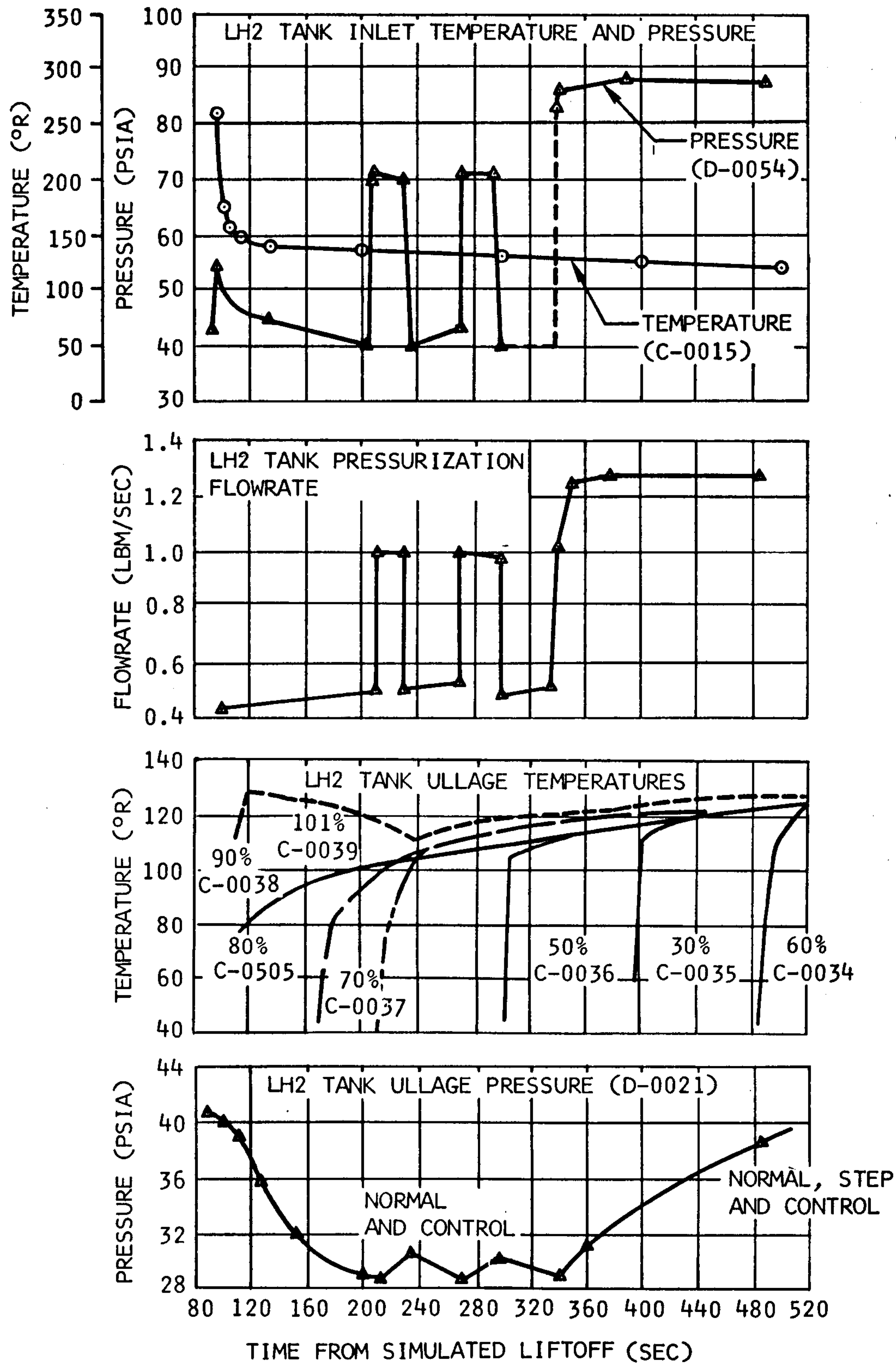

Figure 8-4 LH2 Tank Pressurization System Performance - CD 614010

21 February 1966

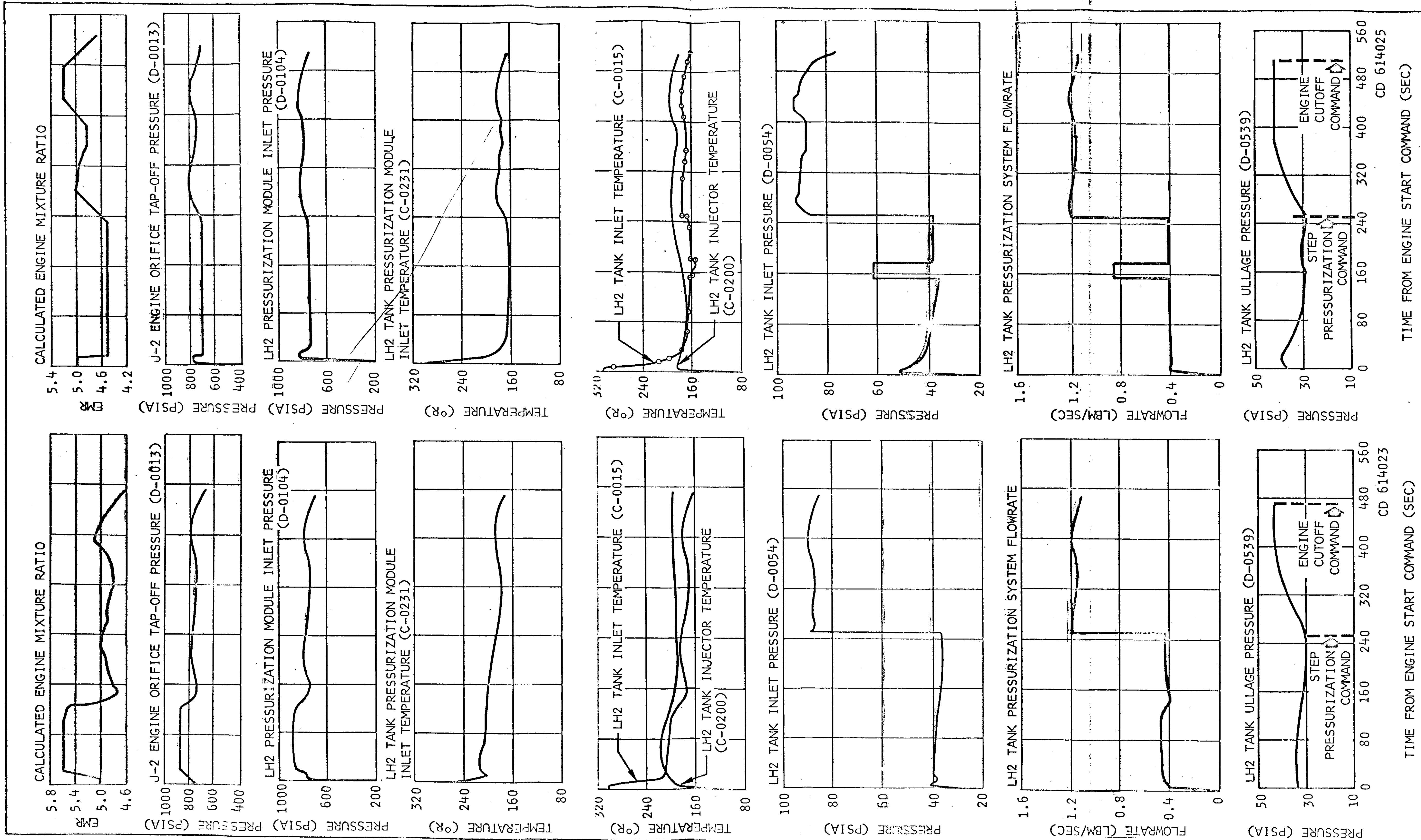

Figure 8-5 LH2 Tank Pressurization System Performance - CD 614023 and CD 614025

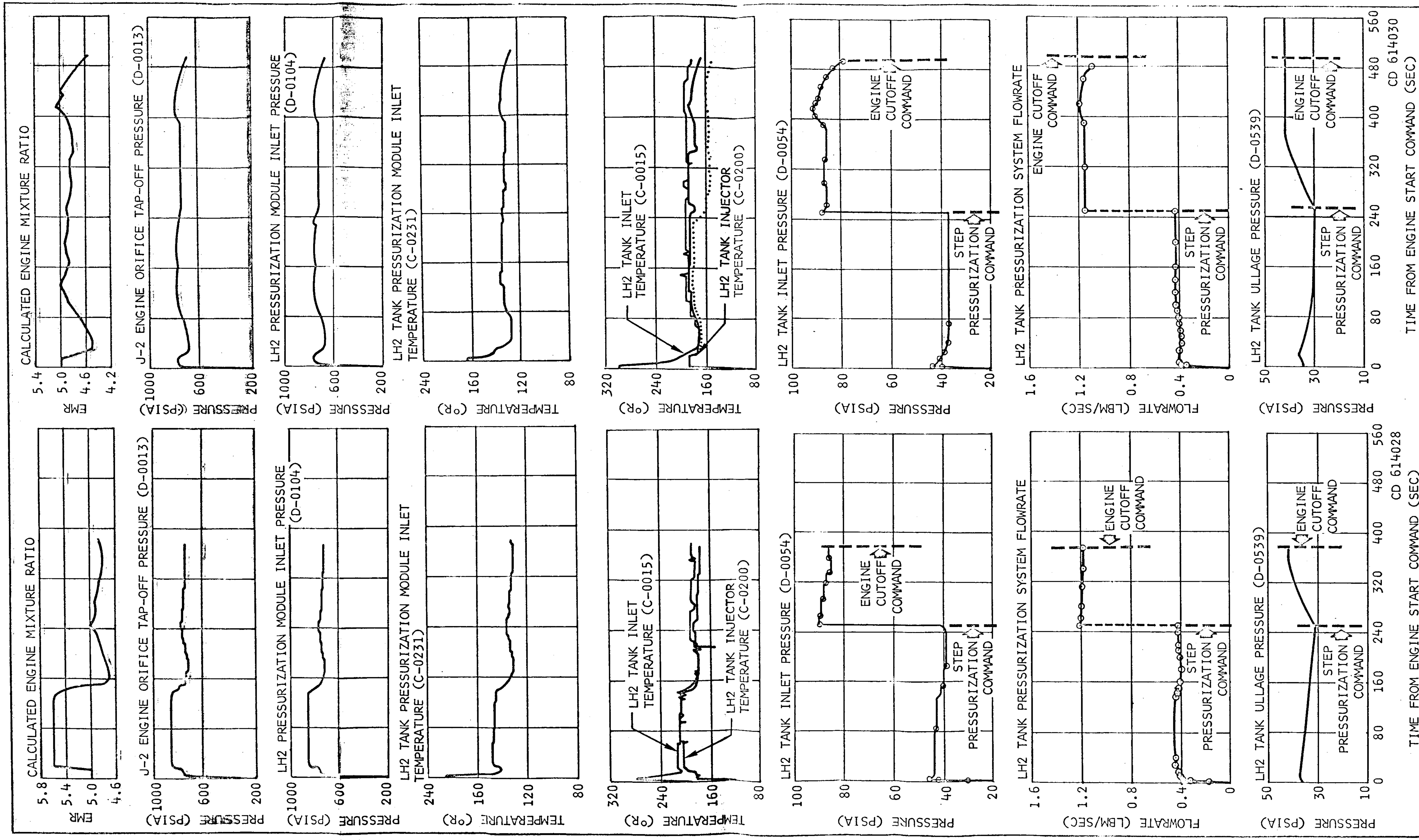

Figure 8-6 LH2 Tank Pressurization System Performance - CD 614028 and CD 614030

21 February 1966

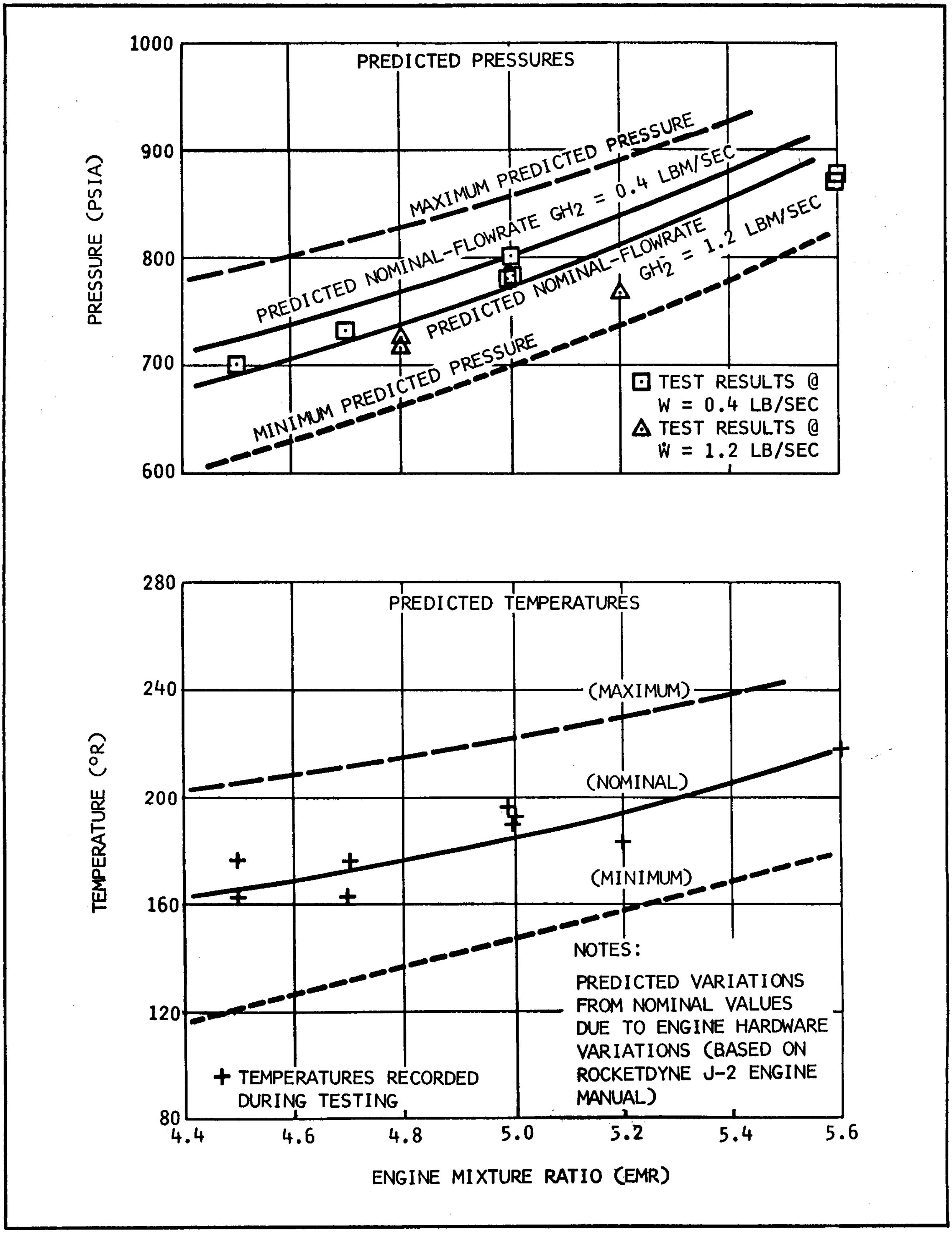

Figure 8-7 Predicted and Actual LH2 Pressurization Module Inlet Pressure and Temperature

21 February 1966

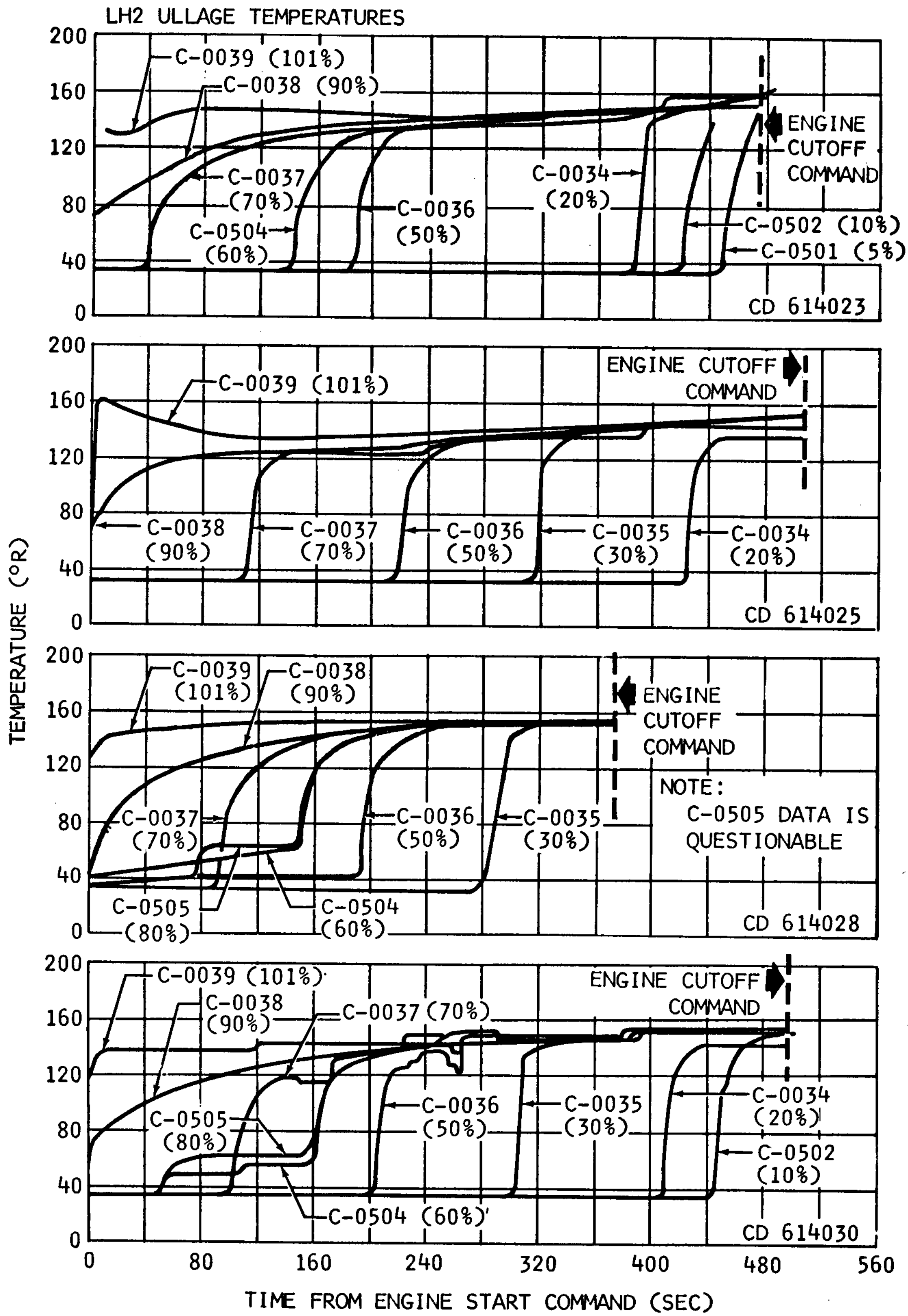

Figure 8-8 LH2 Tank Ullage Gas Temperature Histories

21 February 1966

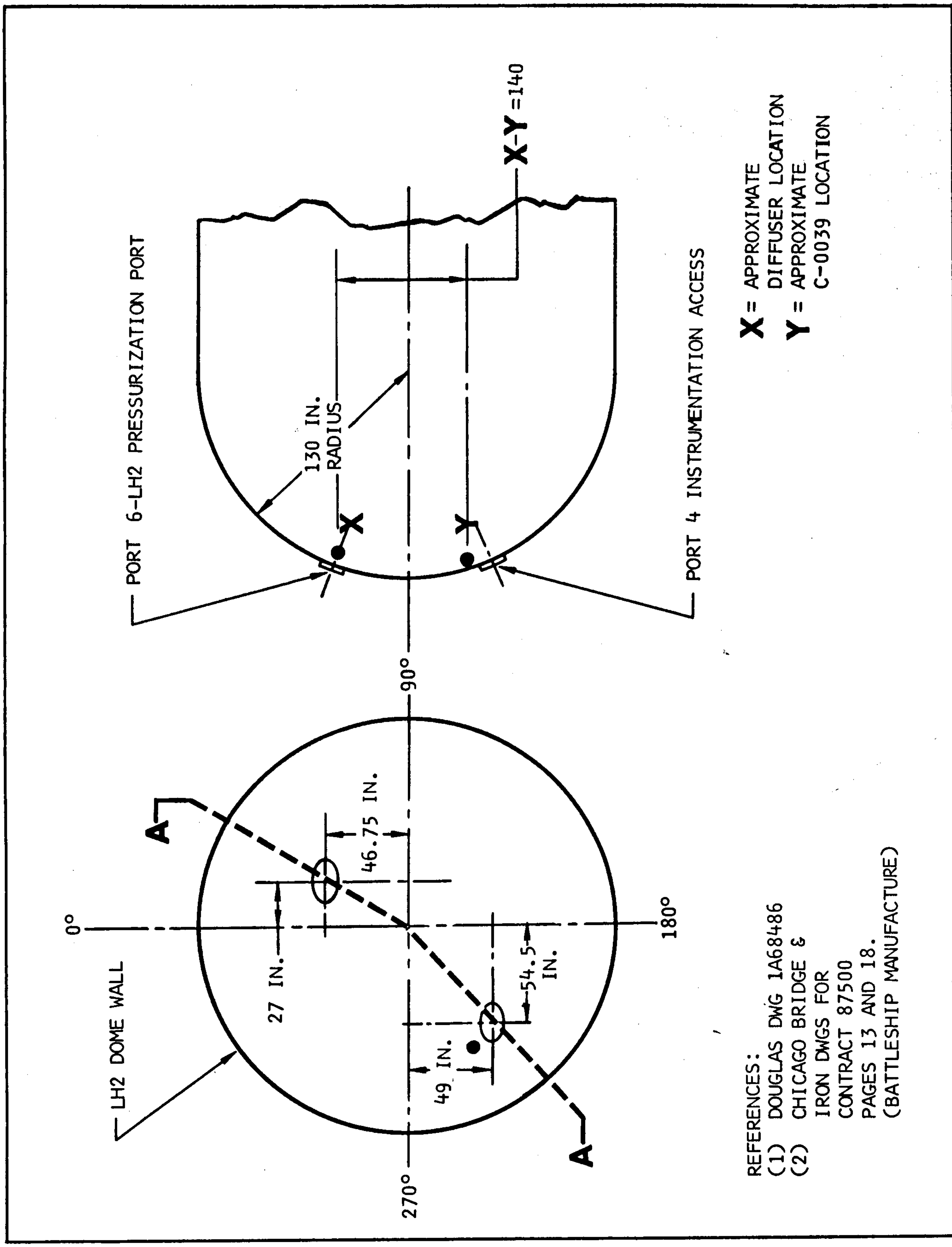

Figure 8-9 Location of LH2 Ullage Gas Temperature Probe C-0039

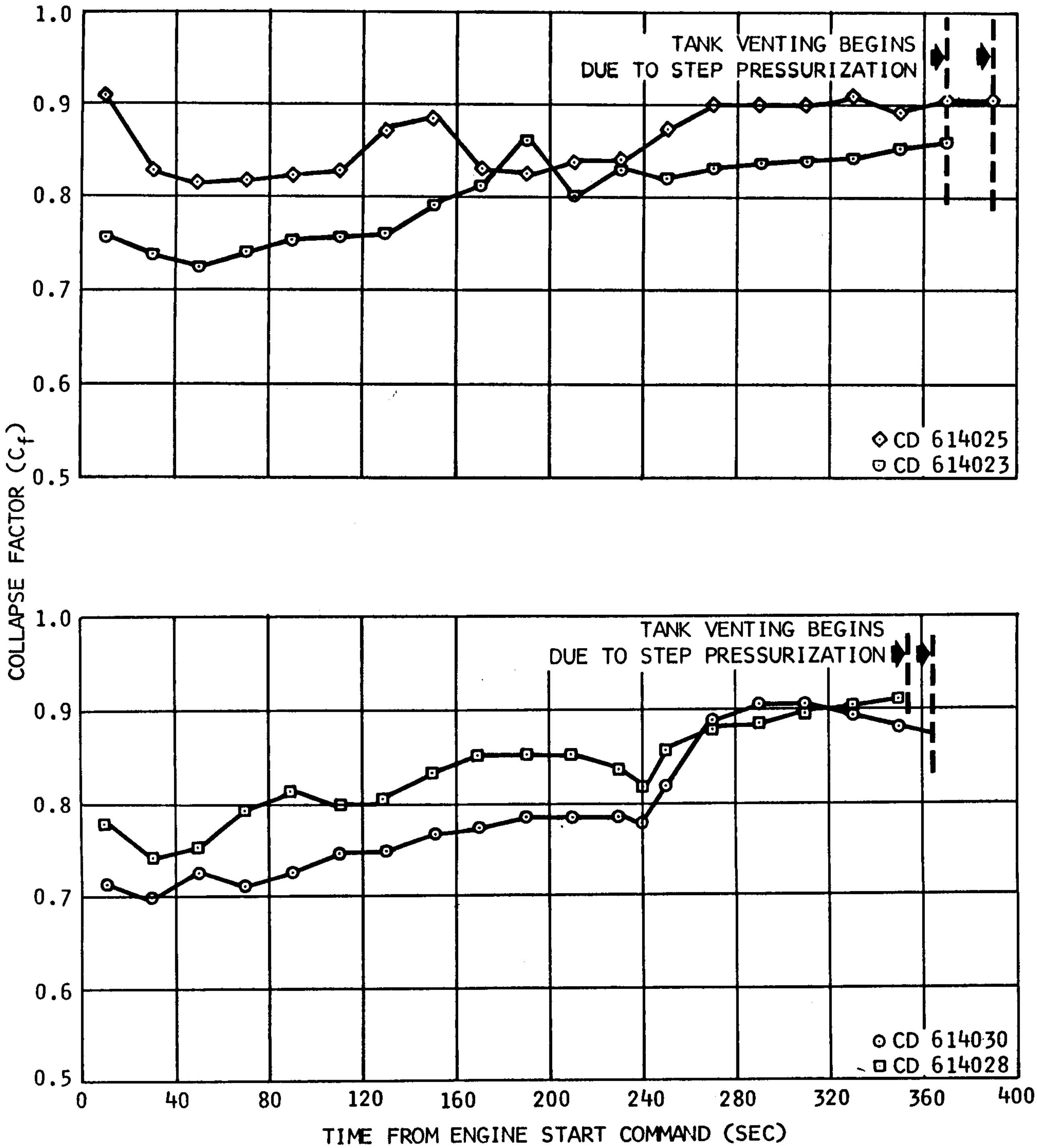

Figure 8-10 Collapse Factors

21 February 1966

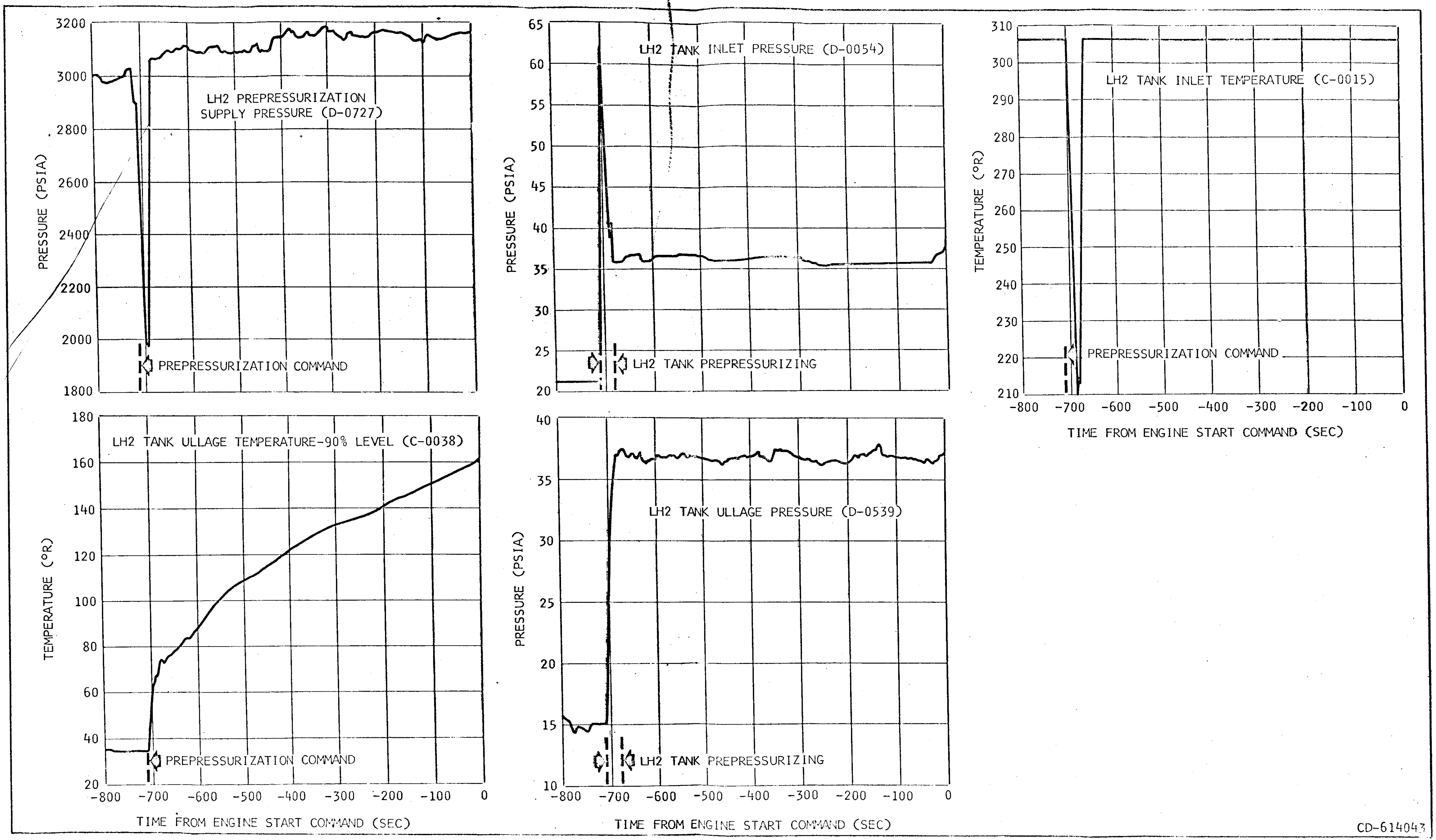

Figure 8-11 LH2 Tank Prepressurization

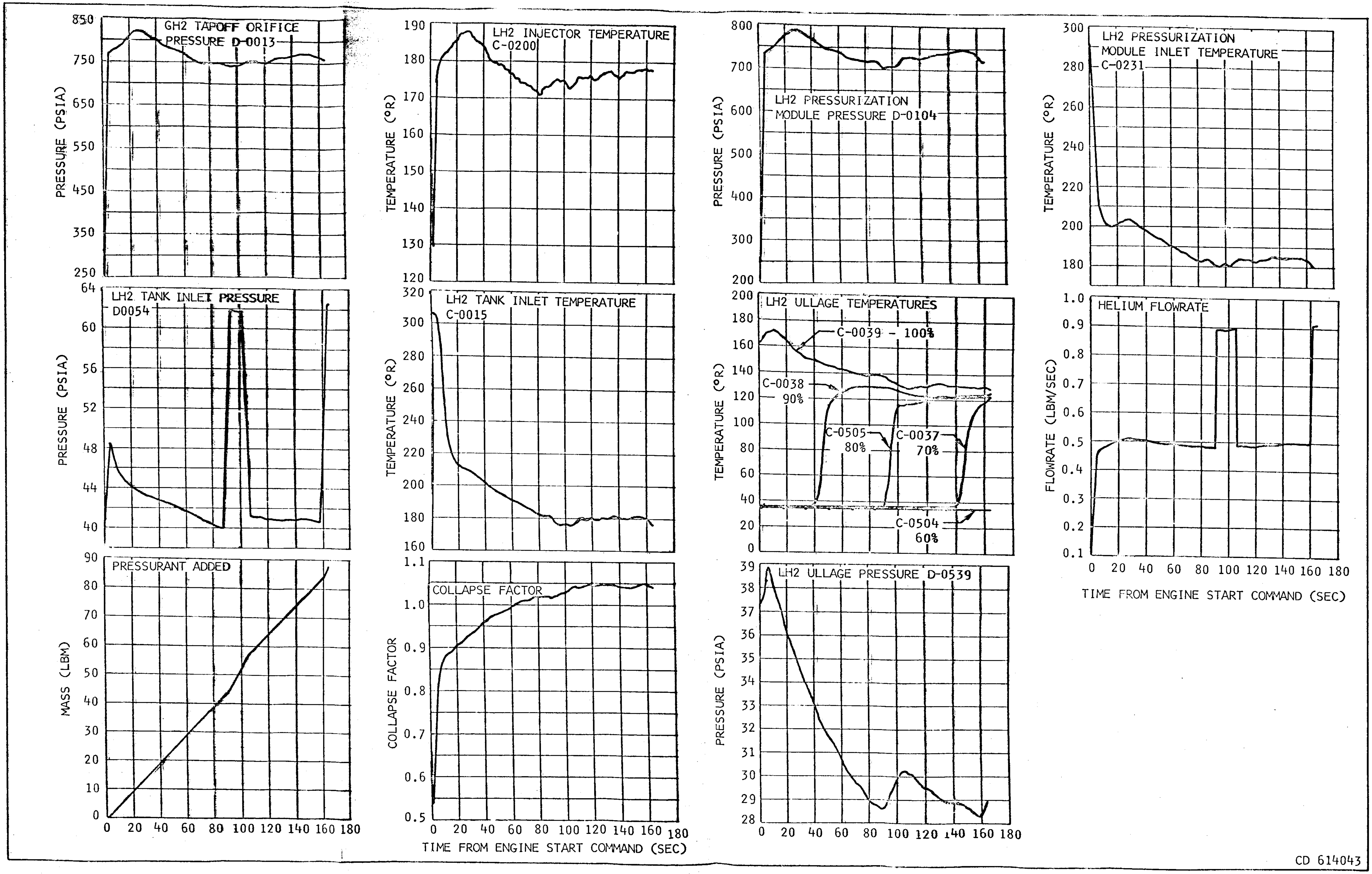

Figure 8-12 LH2 Tank Pressurization System Performance During 1st Burn
21 February 1966

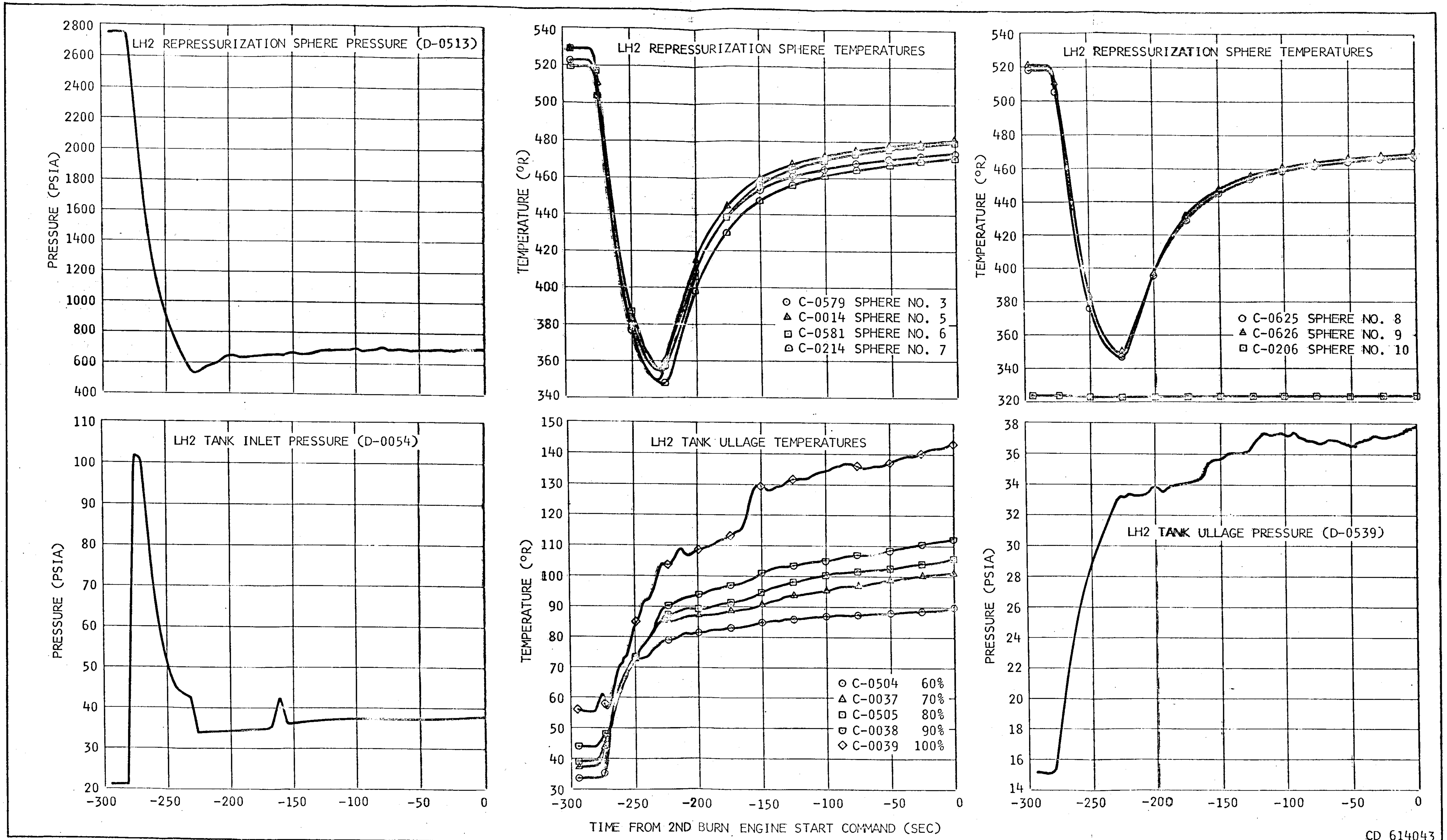

Figure 8-13 LH2 Tank Repressurization Prior to 2nd Burn

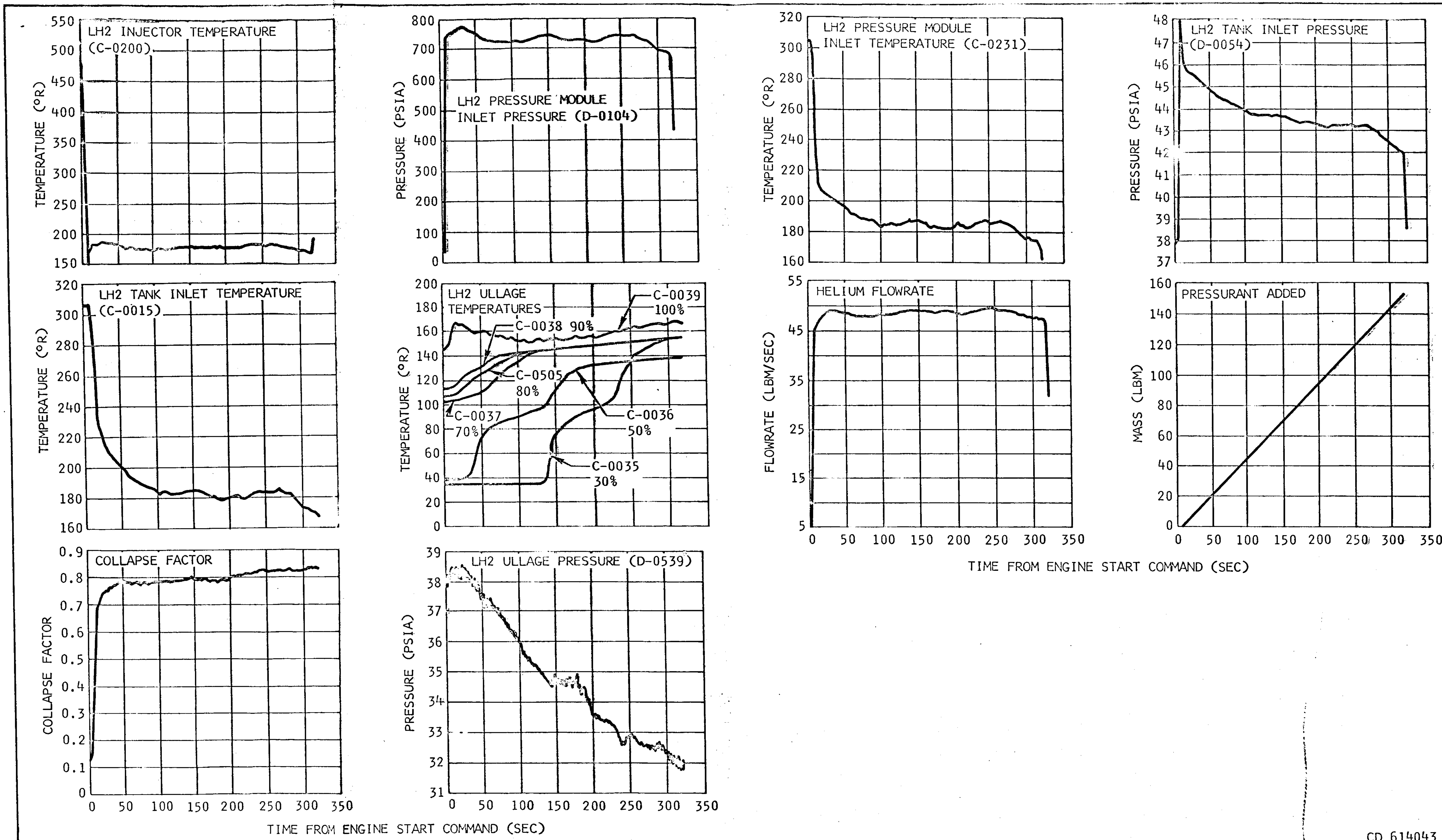

Figure 8-14 LH2 Tank Pressurization System Performance During 2nd Burn

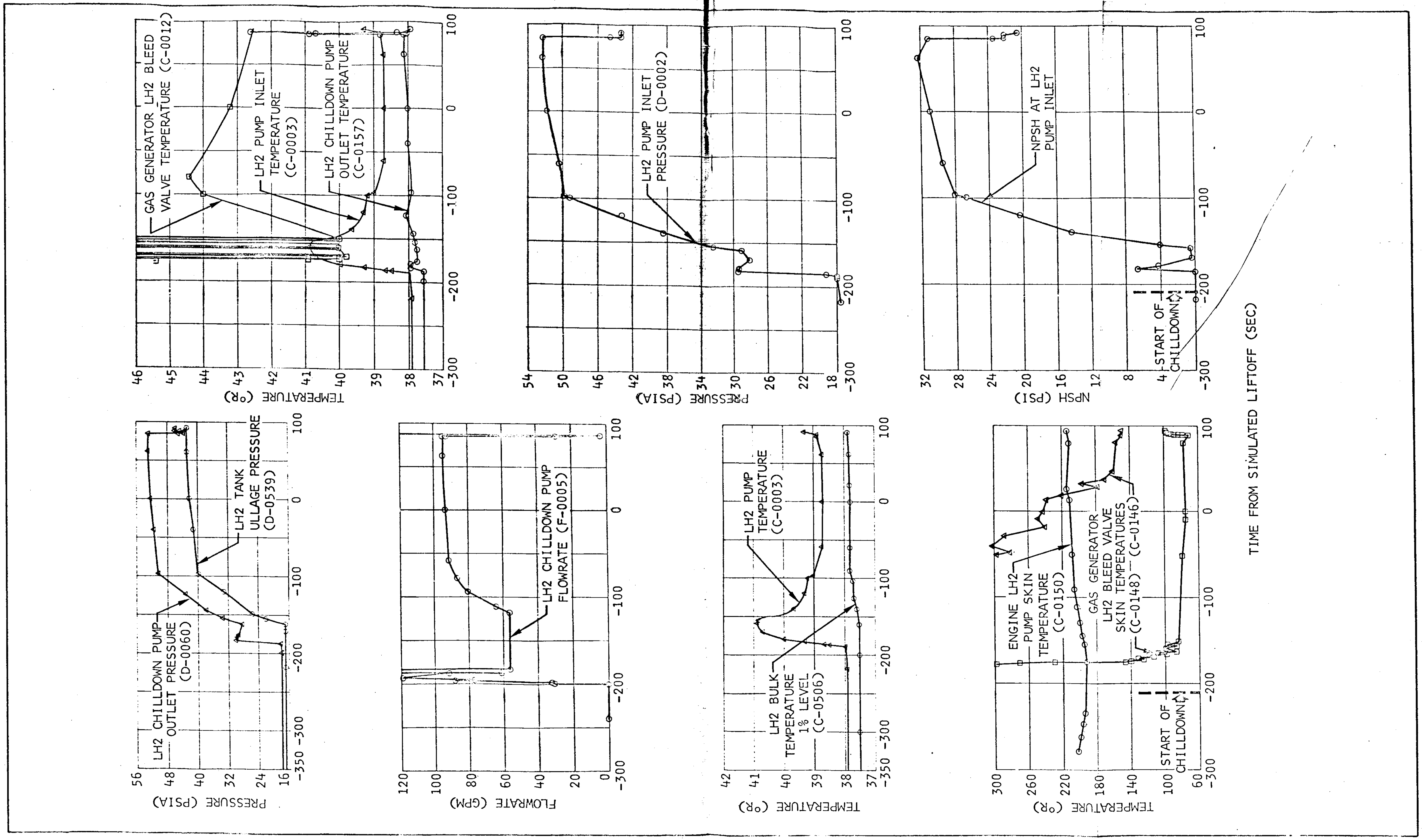

Figure 8-15 LH2 Pump Childdown System Operation During 5-Minute Childdown - CD 614006

21 February 1966

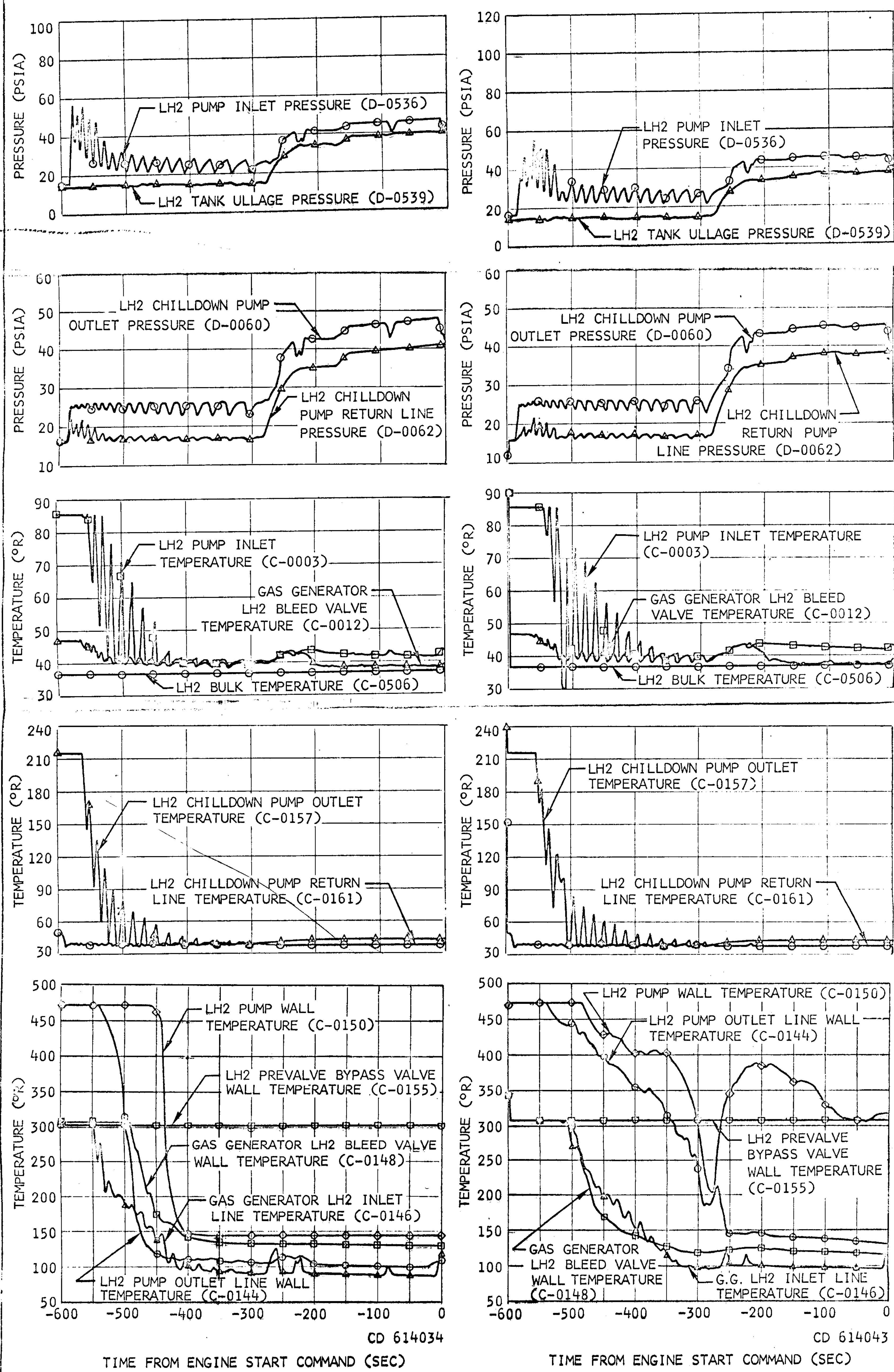

Figure 8-21 LH2 Chilldown System Operation During 2nd Burn

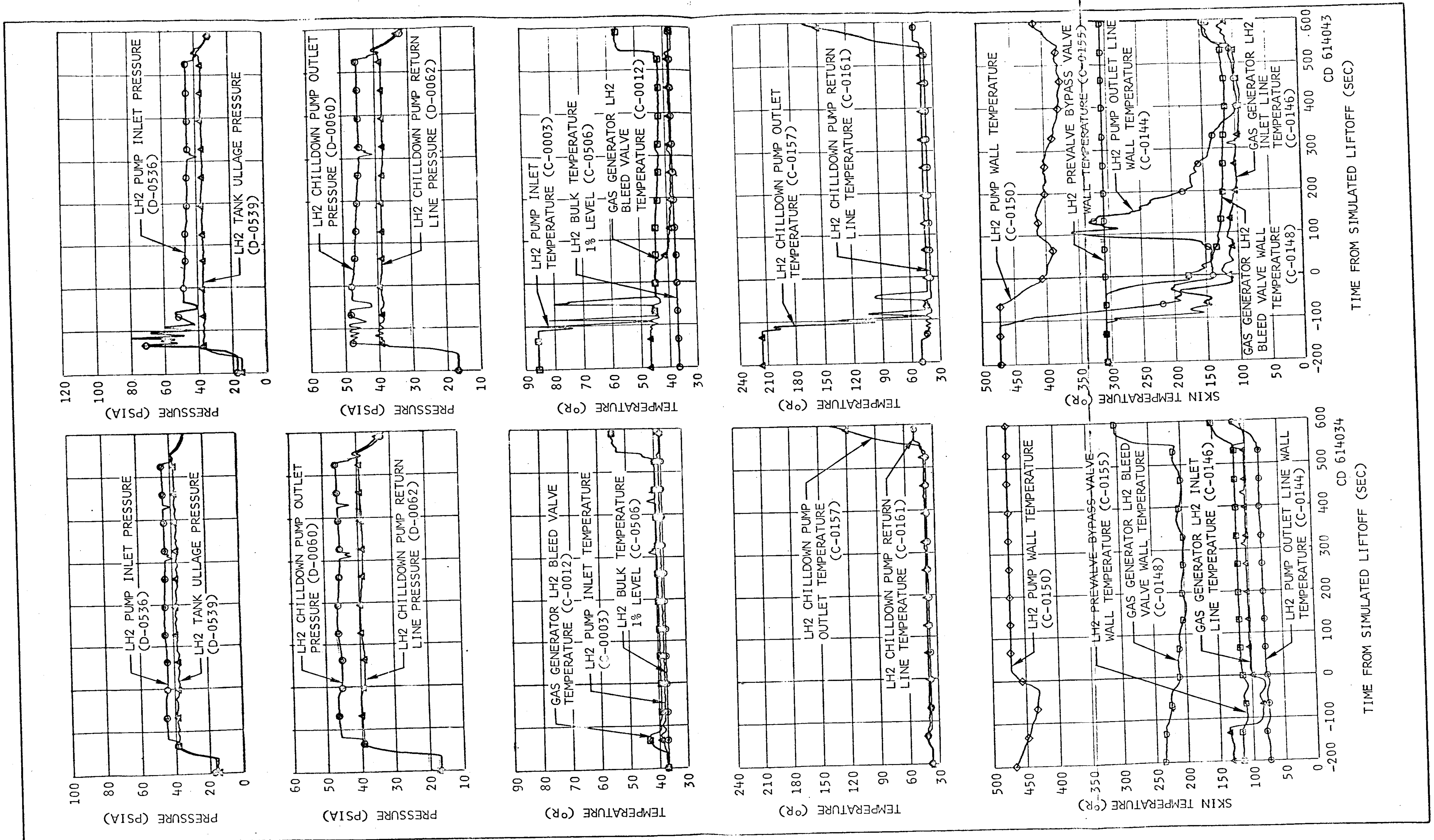

Figure 8-20 LH2 Childown System Operation During 1st Burn

21 February 1966

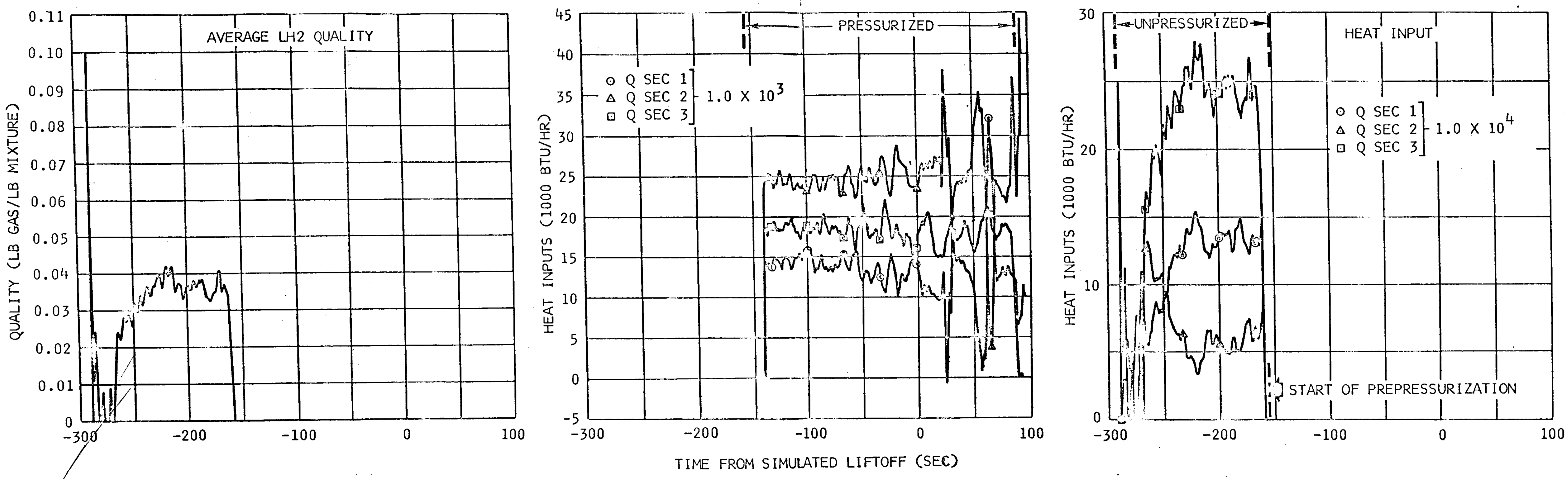

Figure 8-19 LH2 Pump Chilldown System Operation (Sheet 2 of 2)

21 February 1966

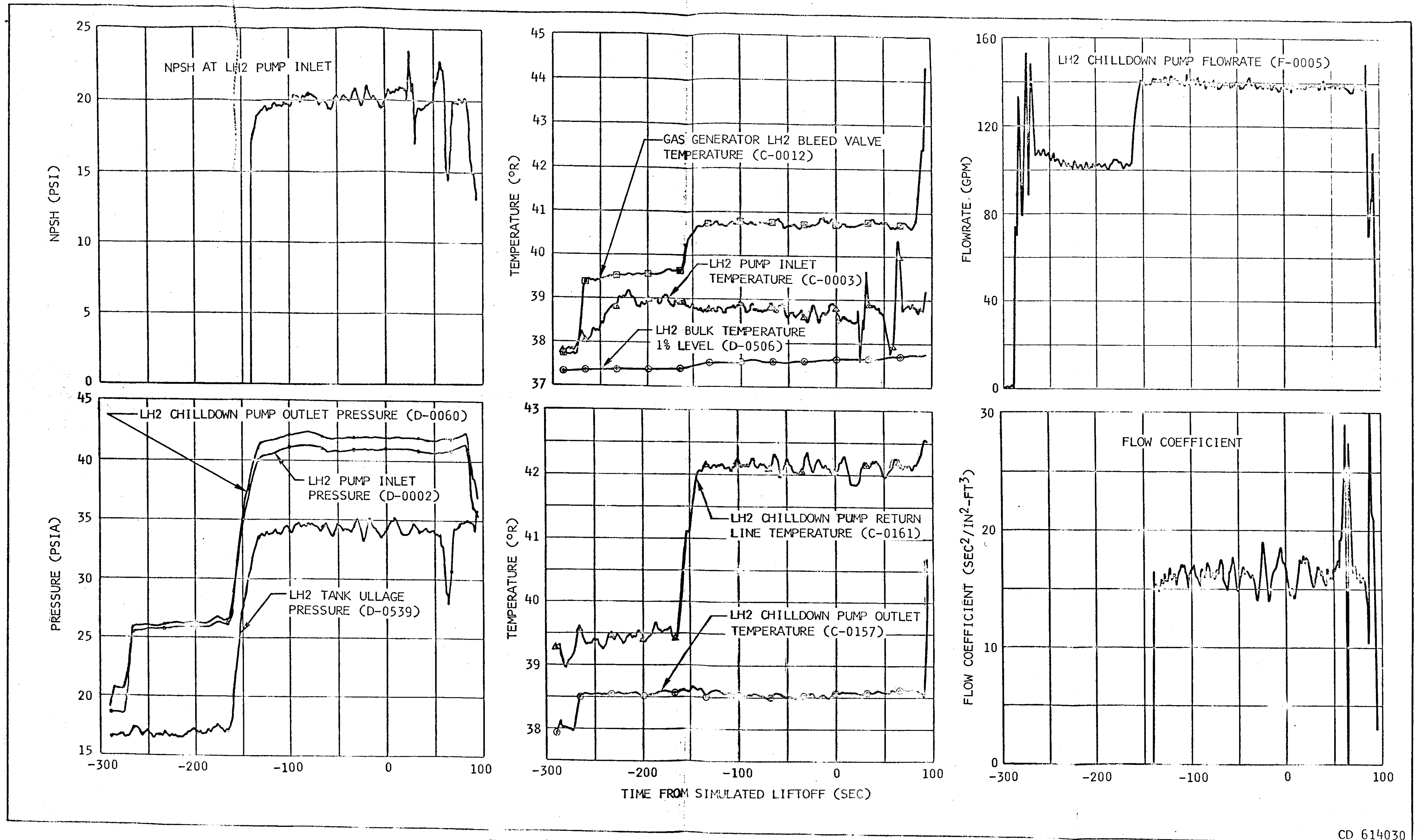

Figure 8-19 LH2 Pump Chilldown System Operation (Sheet 1 of 2)

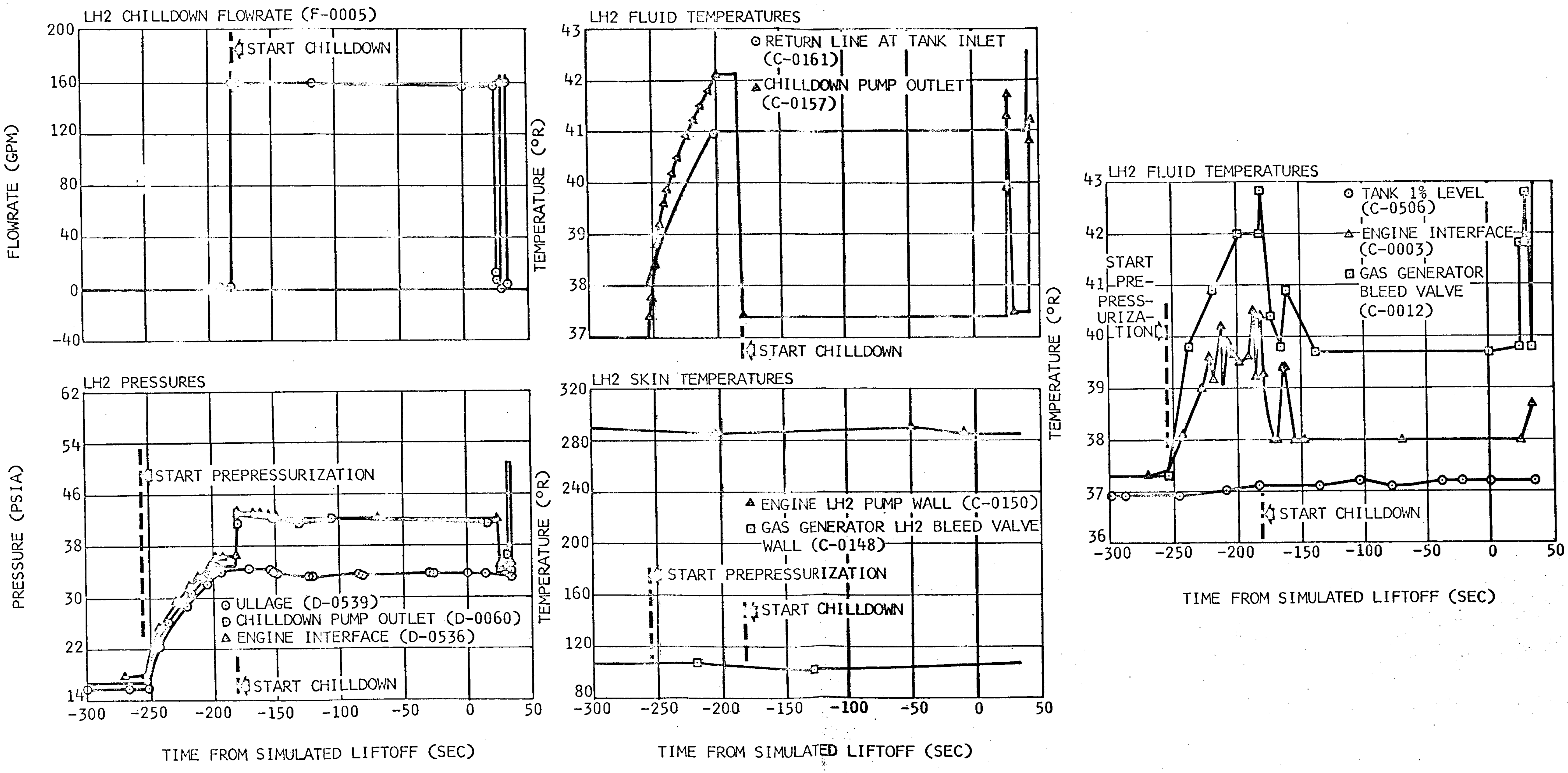

Figure 8-18 LH2 Pump Chilldown System Operation During 3.5 Minute Chilldown

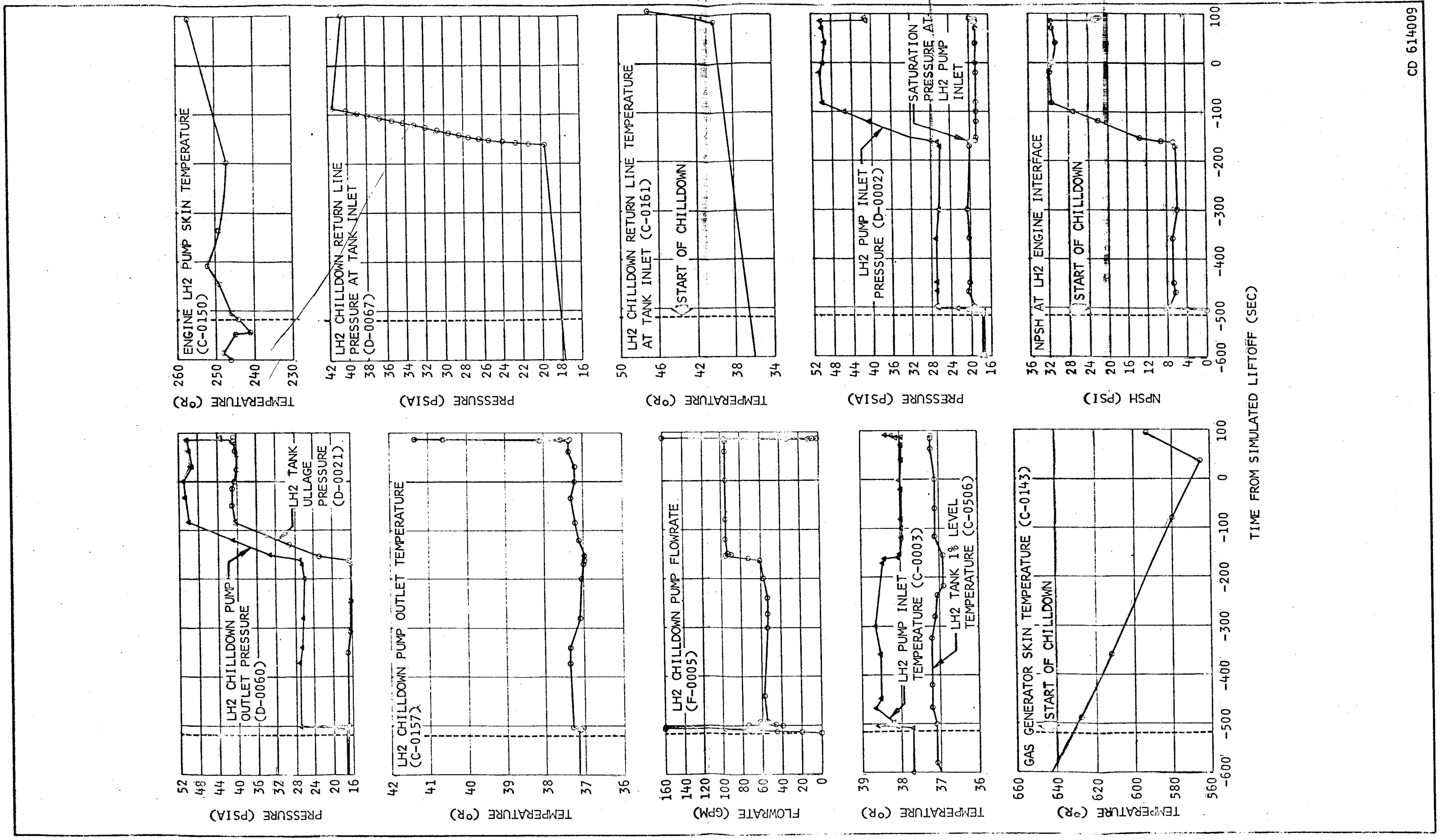

Figure 8-17 LH2 Pump Chilldown System Operation During 10-Minute Childown

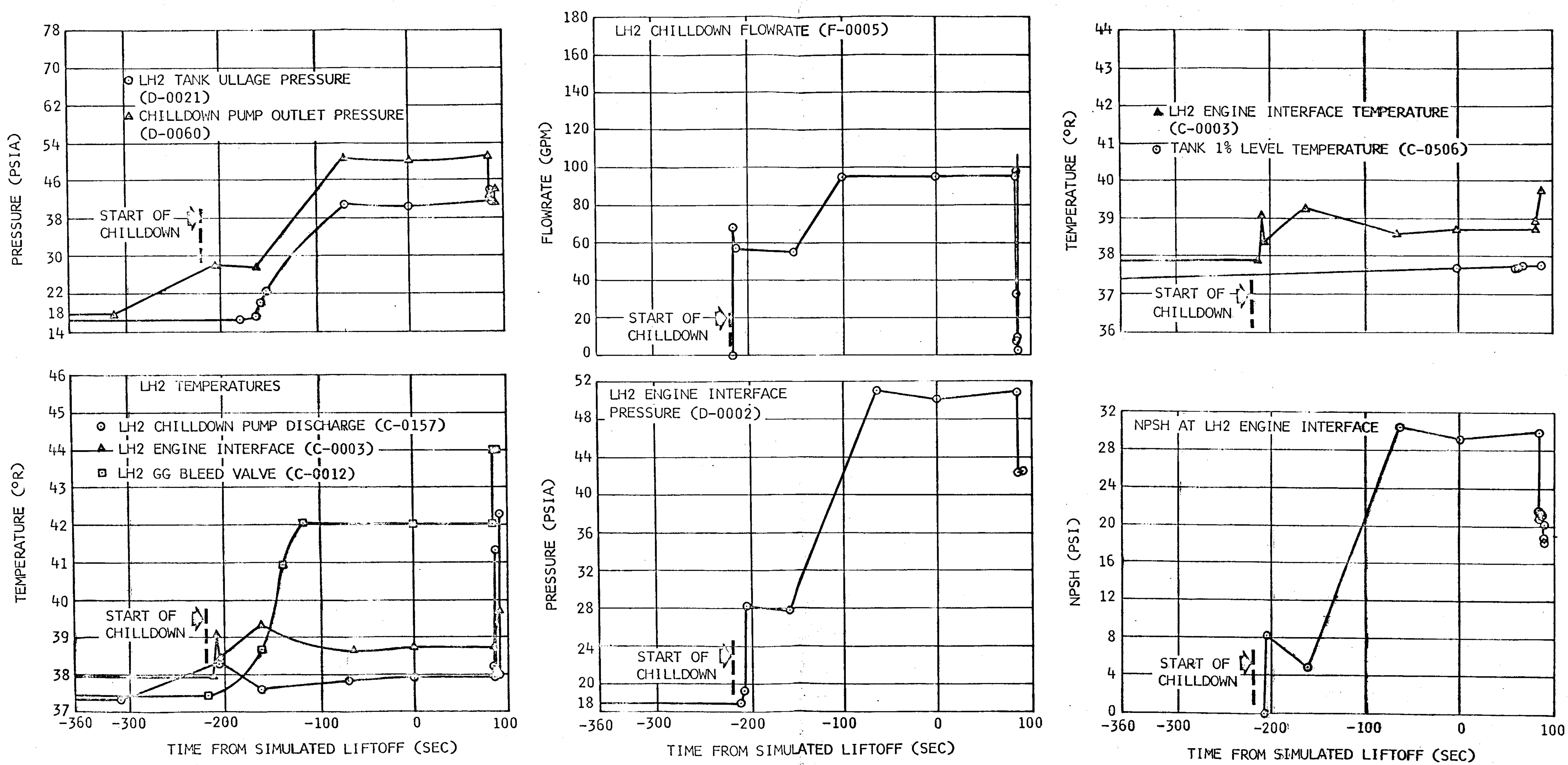

Figure 8-16 LH2 Pump Chilldown System Operation During 5-Minute Chilldown - CD 614007

21 February 1966

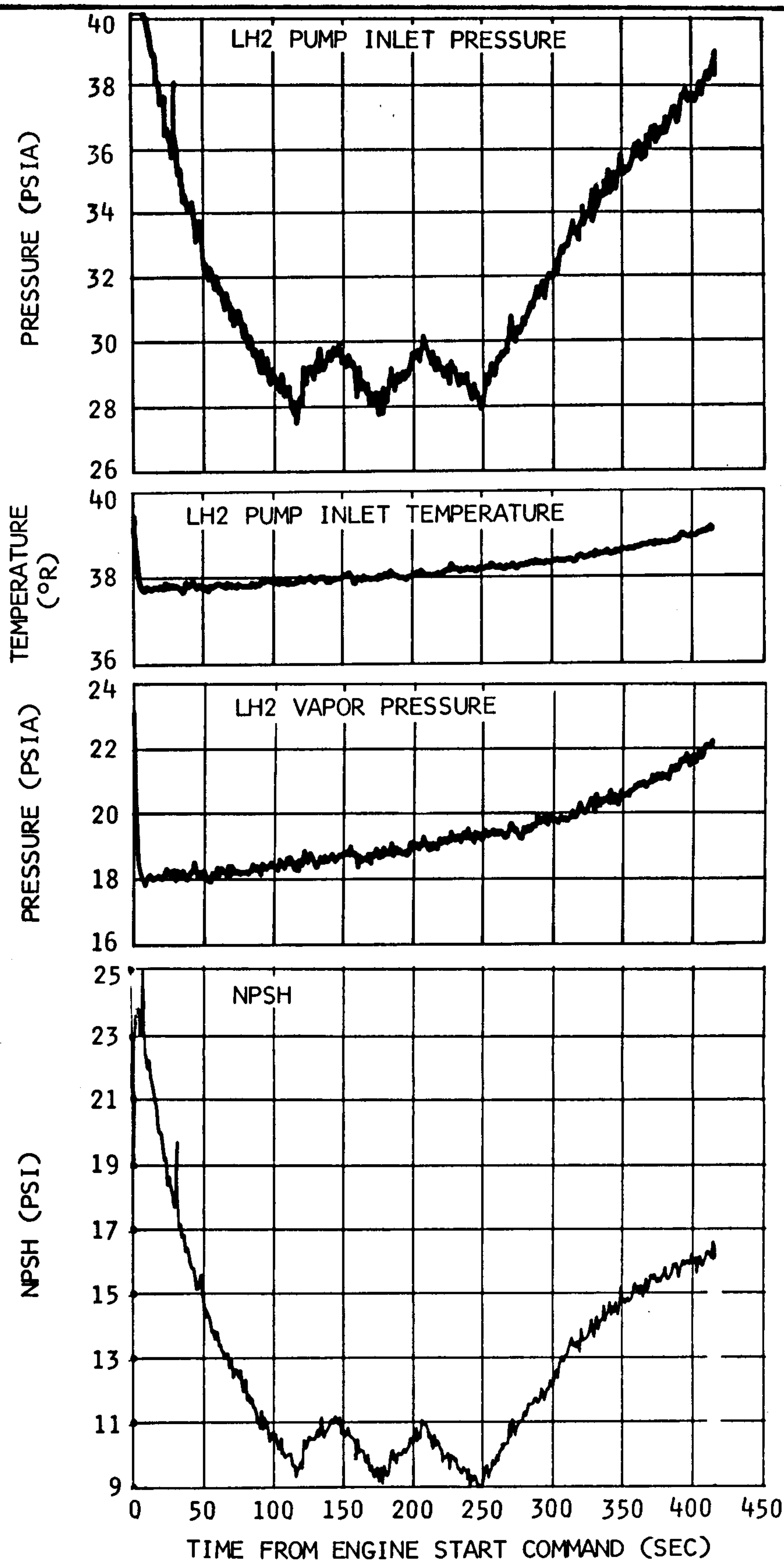

Figure 8-22 Engine LH2 Supply Conditions - CD 614010

21 February 1966

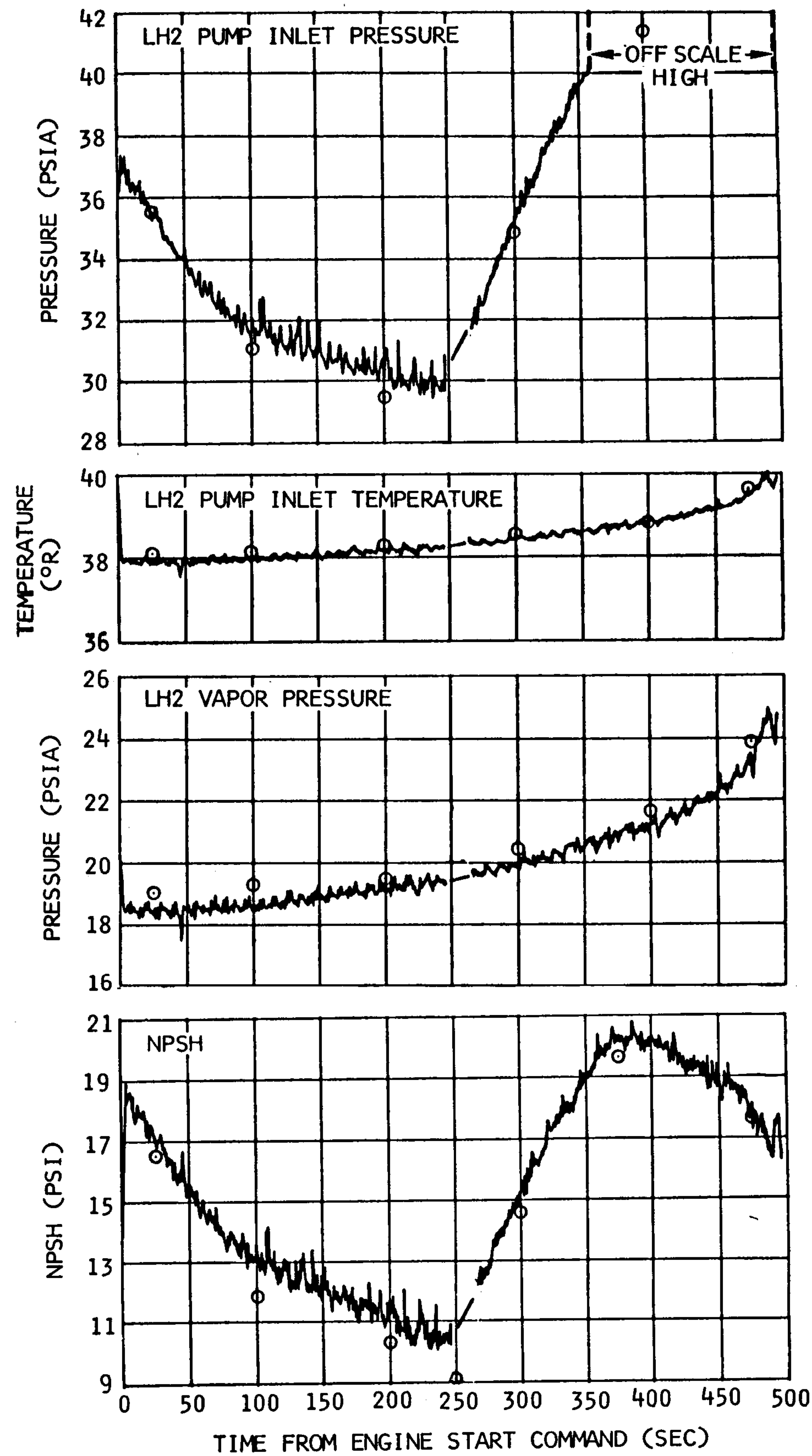

Figure 8-23 Engine LH2 Supply Conditions - CD 614030

21 February 1966

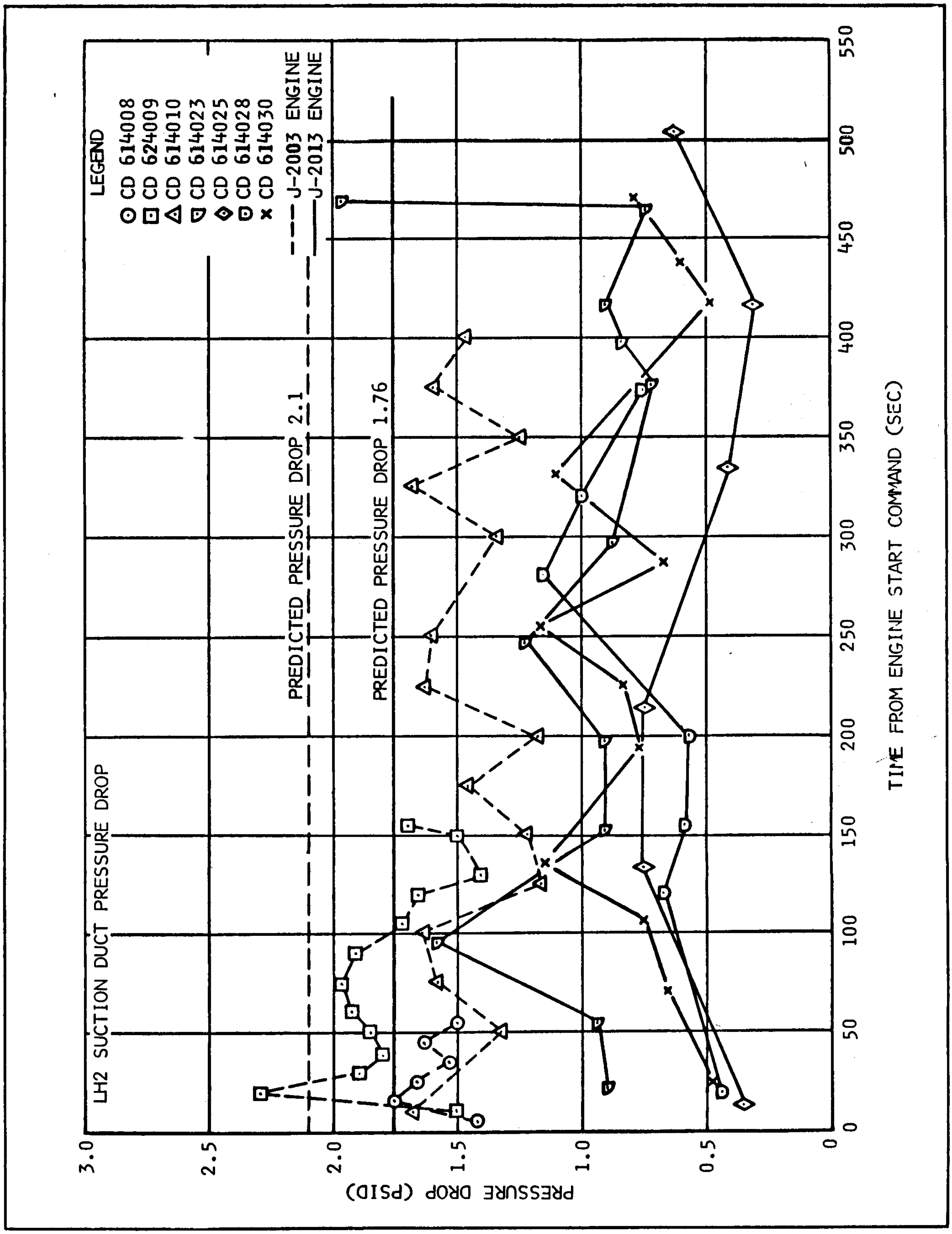

Figure 8-24 LH2 Suction Duct Pressure Drop History

21 February 1966

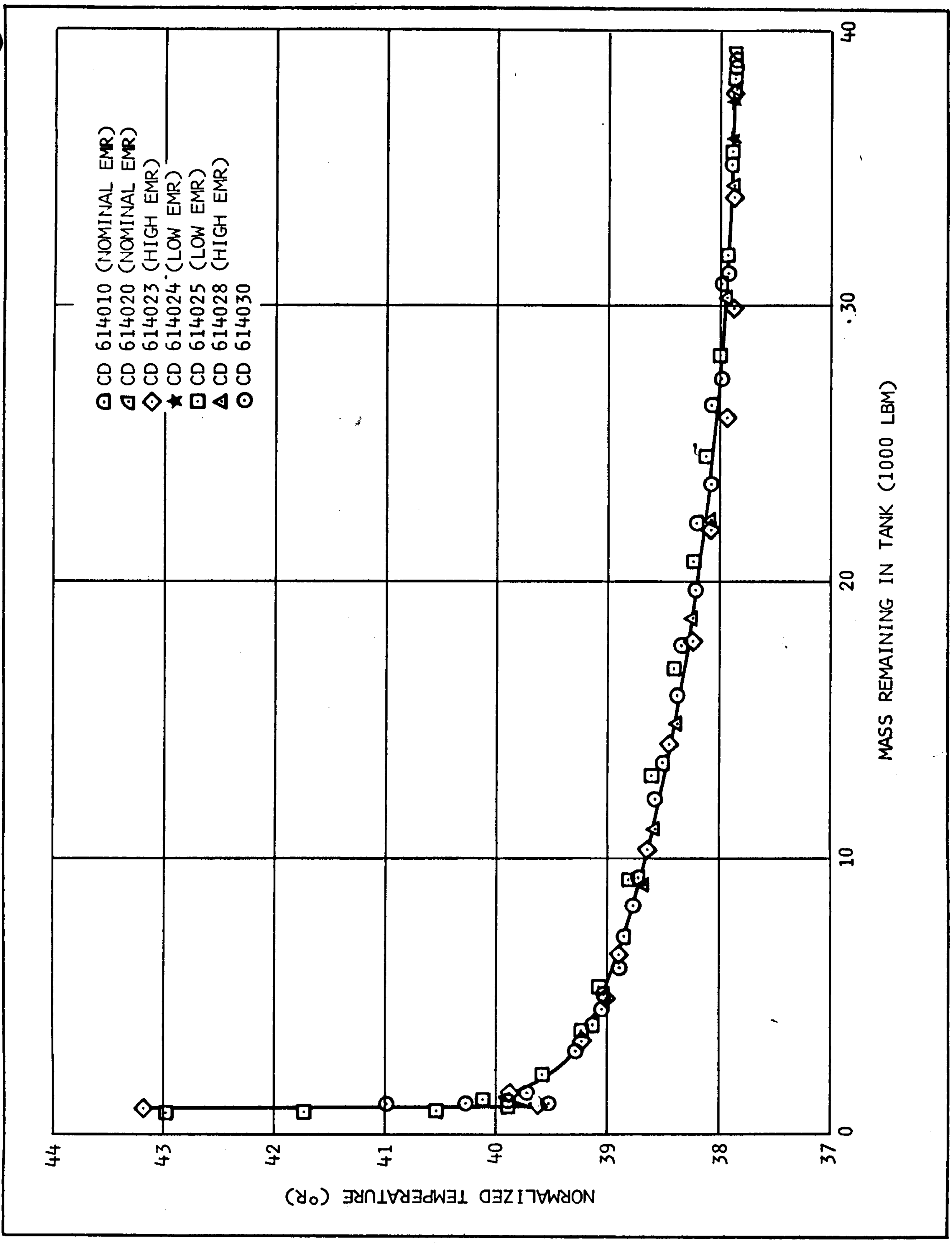

Figure 8-25 LH2 Engine Interface Temperature

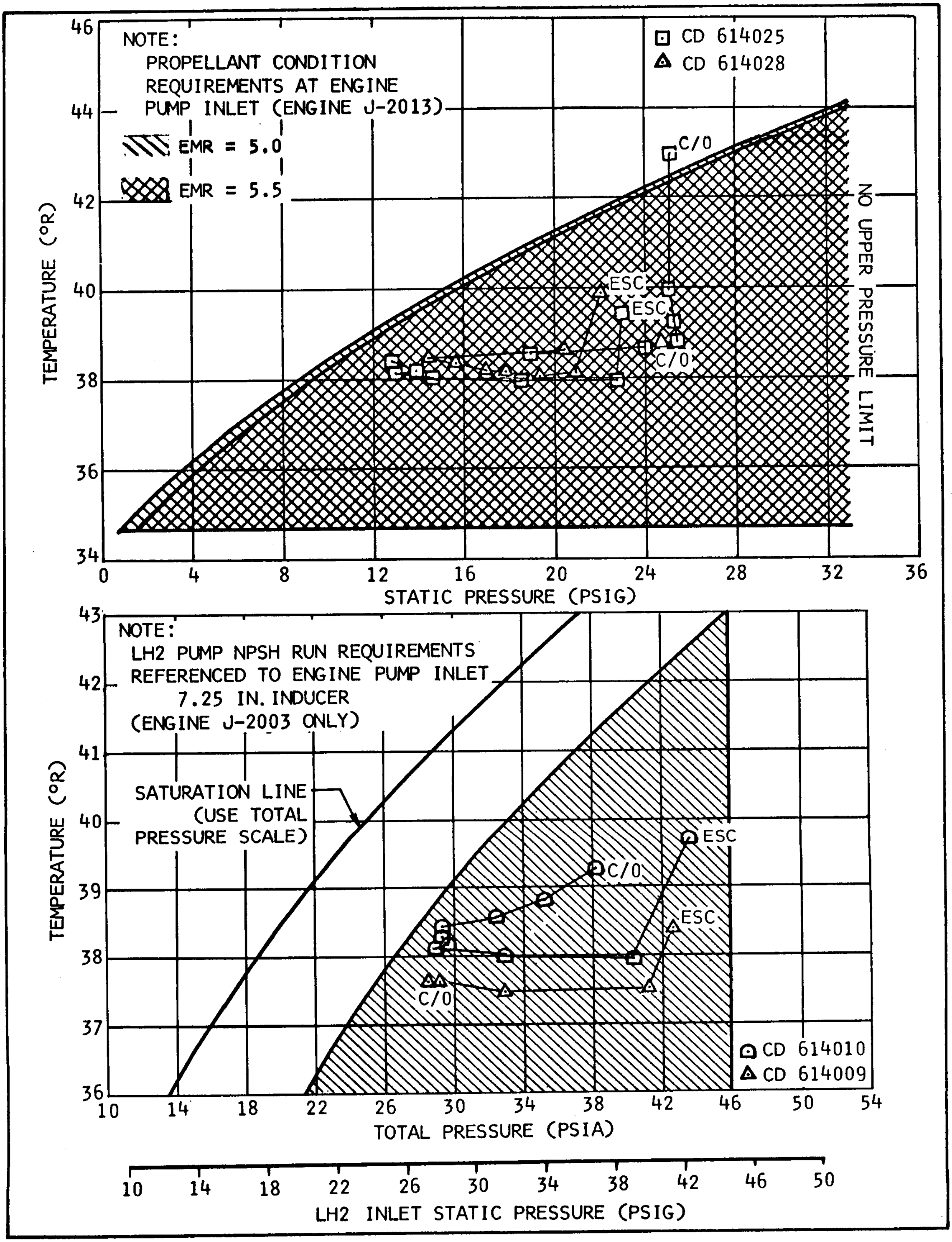

Figure 8-26 Engine LH2 Pump Inlet Conditions

21 February 1966

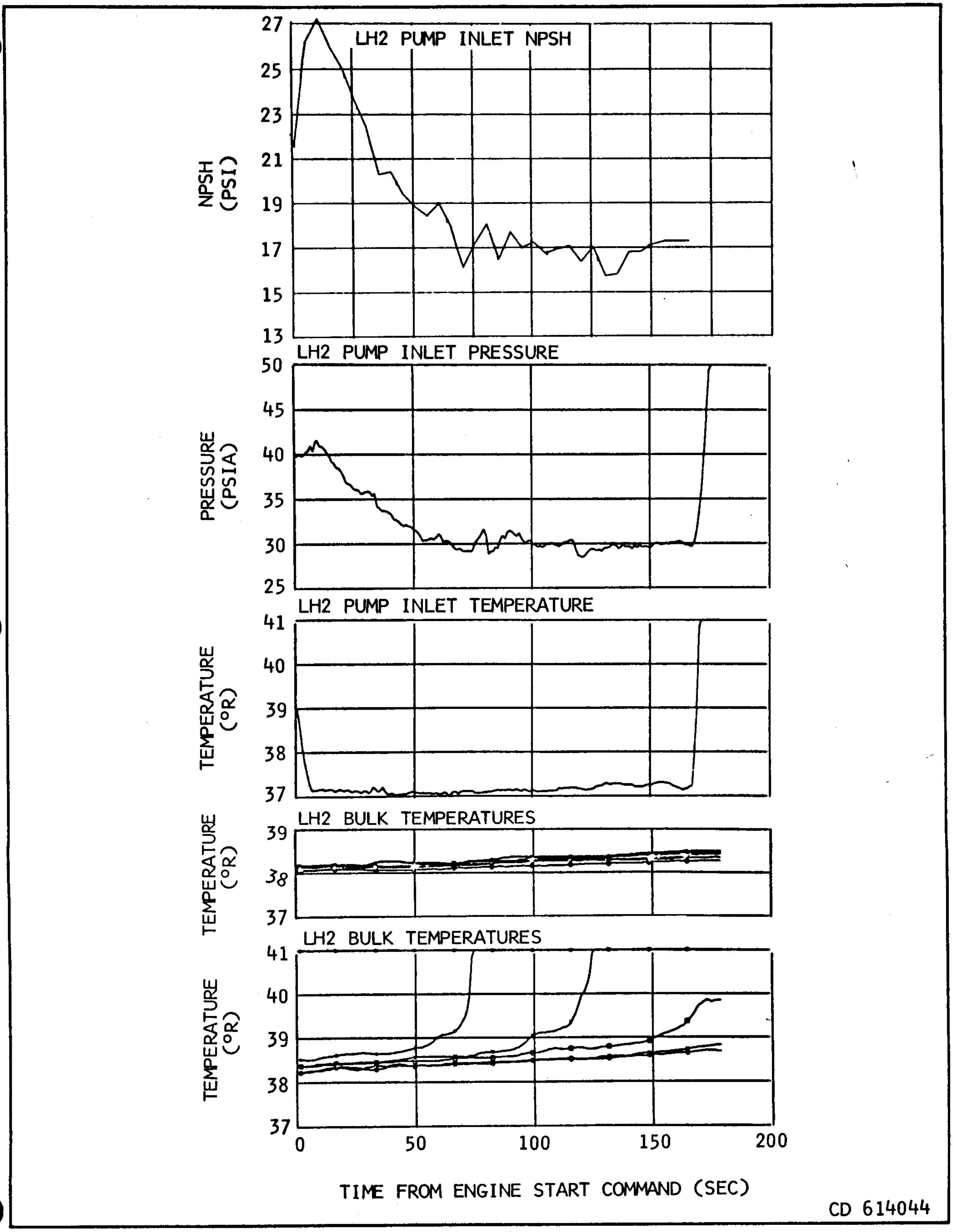

Figure 8-27 LH2 Supply System Performance During 1st Burn

21 February 1966

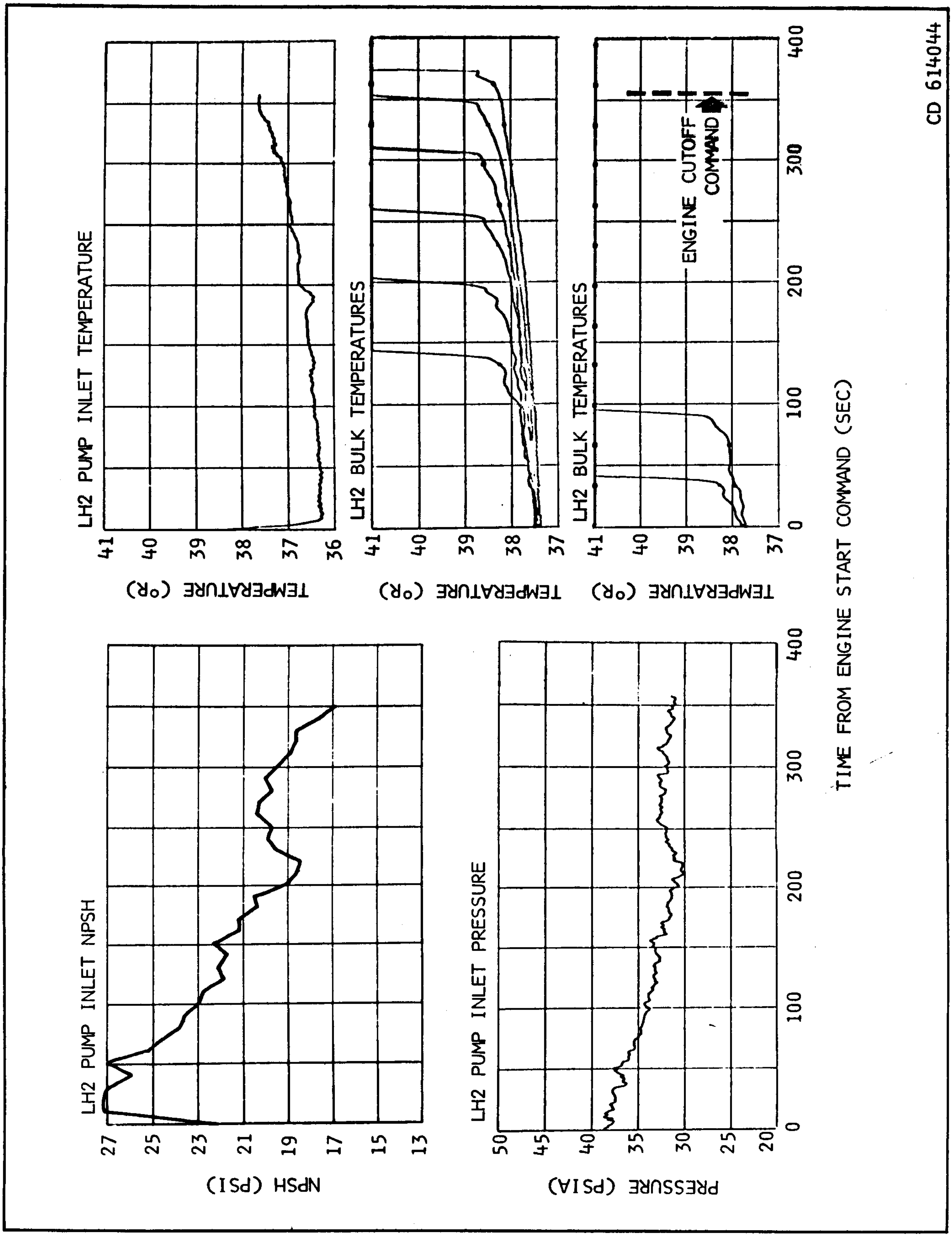

Figure 8-28 LH2 Supply System Performance During 2nd Burn

21 February 1966

SECTION 9

PNEUMATIC CONTROL AND PURGE SYSTEM

9. PNEUMATIC CONTROL AND PURGE SYSTEM

The pneumatic control and purge system performed satisfactorily, and provided the helium required to operate the stage pneumatic power control valves and to accomplish purging operations and leakage makeup.

9.1 S-IVB/IB

Because of regulator problems in the pneumatic power control module during the early cold flow tests, the module was removed for rework and was not available during the S-IVB/IB tests. For these tests the pneumatic control system was supplied with ambient helium at 500 psia from the GSE (ground support equipment). The pneumatic power control sphere pressure was maintained at 500 psia throughout a test by continually supplied helium from the GSE. The LOX chilldown recirculation motor container purge and the turbopump purge were adequate.

9.2 S-IVB/V

Prior to the initiation of the S-IVB/V battleship tests, the pneumatic power control module rework was completed and it was reinstalled. The pneumatic system, and the pneumatic power control module in particular, performed satisfactorily throughout the S-IVB/V test program. Table 9-1 presents the pneumatic control and purge system data that were obtained from CD 614044, which is typical of the data obtained during all S-IVB/V battleship tests.

9.2.1 Ambient Helium Supply

For CD 614044, the pneumatic power control sphere pressure was 2,937 psia at first burn ESC (Engine Start Command), and the pressure decreased to 2,866 psia by ECO (Engine Cutoff). The corresponding second burn sphere pressures were 2,343 psia at ESC and 2,273 psia at ECO. The sphere temperatures were constant at 556 and 536 deg R during first and second burns, respectively.

Table 9-1 indicates that the mass of helium used during the 360 sec duration second burn was approximately the same as that used during the 171 sec duration first burn. This apparent discrepancy is attributable to instrumentation inaccuracies which did not allow accurate caluclation of the small changes in helium mass which occurred during the firings. However, these data show the expected small usage of helium.

9.2.2 Pneumatic Control and Regulation

The pneumatic power control regulator operation was satisfactory, and it exhibited a normal output of 474 to 478 psia. A momentary pressure decrease to 429 psia occurred in the pneumatic system when the chilldown shutoff valves were closed at engine start. When the chilldown shutoff valves are closed, the momentary drain on the pneumatic system reduces the pneumatic line pressure below the minimum requirement of 465 psia. However, since the system recovers within 2 to 3 sec, this operation was acceptable.

A similar pressure decrease occurred on the S-IV stage during periods of high demand and was considered to be normal.

9.2.3 Ambient Helium Purges

The pneumatic power control sphere supplied helium to pressurize and purge the LOX chilldown recirculation motor container. The LOX chilldown motor purge control module operation was completely satisfactory during all firings.

The turbopump purge supply pressure was 6 psi below the allowable minimum of 82 psia because the control orifice in the turbopump purge control module was slightly undersized. This condition had no serious effect on the turbopump purge, and it can be corrected by a properly sized control orifice.

TABLE 9-1
PNEUMATIC CONTROL AND PURGE SYSTEM DATA (S-IVB/V)

PARAMETER	CD 614004		
	DESIGN	FIRST BURN	SECOND BURN
Pneumatic Control Sphere Pressure at ESC (psia)		2,937	2,343
Pneumatic Control Sphere Temperature at ESC (°R)		556	536
Helium Mass in Sphere at ESC (lbm)		7.85	7.06
Pneumatic Power Control Regulator Output Pressure Band (psia)	475 ±25 psig*	474 to 476	474 to 478
Pneumatic Power Control Regulator Minimum Transient Pressure at Time of Closing Chilldown Shutoff Valve (psia)		429**	429**
LOX Chilldown Recirculation Motor Container Pressure (psia)	51 ±2	53	51
Engine Turbopump Purge Supply Pressure (psia)	87 ±5	76	---
Pneumatic Control Sphere Pressure at ECO (psia)		2,866	2,273
Pneumatic Control Sphere Temperature at ECO (°R)		556	536
Helium Mass in Sphere at ECO (lbm)		7.66	6.85
Helium Mass Used (lbm)		0.19	0.21
Burn Time (sec)		171	360

*490 ±25 psia at sea level
**Pressure recovered within 2 sec (acceptable)

SECTION 10

ENVIRONMENTAL CONTROL SYSTEM

10. Environmental Control System

10.1 General Performance

The only ECS (environmental control system) that was operated during the battleship test was the aft purge and thermal conditioning system. The absence of the forward skirt assembly prevented the evaluation of the forward skirt thermal conditioning panels or the forward purge system which will be used during acceptance firings.

The object of the aft ECS was to purge the aft skirt and thrust cone areas, while maintaining an environment that was compatible with design requirements of the components installed in the areas. Design analysis established a flow of 16,000 lb/hr of air or GN2 and a temperature at the umbilical inlet of 150 deg F maximum.

ECS model 326 is used to supply gas to the aft skirt ECS and has the capability of delivering either heated air or GN2 to the interstage depending on the mode of operation for each test phase.

During battleship testing, several changes were made in the routing of air or GN2. Most of the changes were peculiar only to the Sacramento Test Center, and were made because the tests were performed without the aft interstage. Because of the absence of the aft interstage, the components in the aft skirt and aft interstage area were not in an inert atmosphere during either cryogenic loading or static firing. Also, some of the components were not flight configurated and consequently were unable to withstand the cold temperatures experienced in the thrust cone area.

Throughout battleship testing, the performance of the Model 326 system was trouble free, except for the fact that the thermo-switches in the heaters overheated. The thermo-switches gave no further problems after the set point was re-adjusted.

The aft skirt environmental control sensors are the control instrumentation for the environmental control system. The specified control temperature range was 87 ± 5 deg F. The ECS Model 326 does not have the capability of cooling the air/GH2. Therefore, in order to successfully complete a static firing with ambient temperatures in excess of 100 deg F, the sensors control limits were changed to a minimum of 82 deg F and a maximum of 125 deg F.

The aft skirt and interstage was instrumented to evaluate the objectives of the test. The locations of the temperature sensors are indicated on the individual graphs that illustrate the test results (figures 10-1 and 10-2). The oxygen content was determined by oxygen analyzers. Sampling tubes were installed in the purged area at the location shown in figure 10-3. Fifteen sample tubes were used for direct readout by the Model 778 Beckman Oxygen Analyzers; two sample tubes were used for the remote block house readout by the Model F3 Beckman Oxygen Analyzers.

Prior to conducting the purge test, a duct flow balance test was performed. Excessive leakage around the manifold, made it necessary to seal fifteen of the manifold orifices to achieve proper flow through the APS ducts and the thrust structure duct. Flow balances were then established, and were as shown in table 10-1.

10.2.2 Aft Interstage Test

The first attempt to perform the purge test of CD 614031 was aborted when it was noted that the oxygen analyzer meter was being read incorrectly. The test was recycled by flowing air into the environmental enclosure, bringing the oxygen content to 20.5 percent.

The first run was a full duration run of 30 min. The aft interstage area was purged to the 4 percent oxygen content level in approximately 2.5 min, except for the area inside the engine thrust chamber which took approximately 4 min. During the evacuation portion of this test it was noted that air did not disperse the GN2 from the engine thrust chamber area very rapidly. A portable blower was used to evacuate the GN2 and bring the oxygen content level back to 20.5 percent. Because the portable blower was not used in the engine thrust chamber after the aborted run, all of the GN2 was not evacuated from this area before starting run 1. This accounts for the difference in the evacuation rate of air in the engine thrust chamber area between run 1 and runs 2 and 3. During the run, the differential pressure instrumentation malfunctioned and it was impossible to determine the flow used for this run. However, the pressure inside the environmental enclosure was maintained at 1.1 in. of water during the entire cycle of air to GN2 and back to air.

During the second attempt at a static firing (CD 614035) of the S-IVB/V configurated battleship, a fire occurred in the thrust cone area. Combustible gases drifted into the thrust cone and were eventually set aflame. Corrective action was to seal all openings in the thrust cone, and to install an additional purge line to provide more flow to the thrust cone. This was done to insure an inert atmosphere, and a positive pressure in the thrust cone. An impingement curtain was also installed from the aft skirt/aft interstage interface across to the LOX tank/thrust cone junction point and went 360 deg around the vehicle. This installation enclosed the electrical equipment and provided the capability of maintaining a positive pressure and an inert environment in this area. By insuring an inert atmosphere, the chances of fire in the thrust cone and electrical equipment areas were greatly decreased. Later static firings were conducted without incidents.

10.2 Aft Interstage Environmental Tests

10.2.1 History

The aft interstage environmental tests were conducted to verify three objectives and satisfy the qualification requirements for the system. The three test objectives were: (1) verify that the system could adequately purge the aft skirt and interstage area to an oxygen content level of 4 percent by volume, or less, in a reasonable time, (2) verify that the aft skirt and interstage thermo-conditioning and purge system could maintain the temperature of all electronic equipment mounted on the aft skirt within their correct operating ranges, and (3) verify that during S-IVB/V operation, the environment of the helium sphere, used for purging the propellant pumps seal cavities, could be controlled adequately with respect to maintaining its enclosure outlet temperature above 77 deg F.

The aft interstage environmental tests were authorized by Test Request 1034 and were performed in countdowns 614031 and 614032 from May 11, 1965 through May 14, 1965.

The battleship vehicle was used in the S-IVB/IB configuration and was modified to the S-IVB/V configuration by adding the ambient helium sphere. A flame impingement curtain was installed. The model 541 environmental enclosure was installed to simulate the S-IVB/IB aft interstage.

The second run was made after an effort was made to correct the differential pressure instrumentation problems. GN2 flow during this run varied from 15,800 to 16,700 lbm/hr. Environmental enclosure pressure was maintained between 1.0 to 1.1 in. water. From data obtained during the first run, the length of the second run was shortened to 10 min for GN2 purge and 10 min for air purge. The environmental enclosure was purged to the 4 percent oxygen content level in approximately 2 min and 45 sec, except for the sample port located inside the environmental enclosure between fin plane III and IV, at DAC station 42.00, which required approximately 3 min and 10 sec to reach the critical 4 percent oxygen content level. The second exception was again the engine thrust chamber area, which required 4 min and 20 sec to reach the 4 percent oxygen content level. Within the 10 min of air purge all analyzers returned to the 20.5 percent oxygen content, except for the engine thrust chamber area, which again required using the portable blower to evacuate the GN2.

The third run was made with approximately the same conditions that existed during run 2. The time required to purge the environmental enclosure was 2 min and 55 sec to the critical 4 percent oxygen content level, except for the engine thrust chamber area which required 4 min and 30 sec to reach the 4 percent oxygen content level. Within the 10 min of air purge, all analyzers again returned to 20.5 percent oxygen content, except for the engine thrust chamber area.

10.2.3 Thermal Verification and Helium Sphere Conditioning Tests

After the purge test, the helium sphere shroud duct was installed and another flow distribution check was run. To bring the flow to the helium sphere up to required flow it was necessary to change a 1.75 in. hole to a 1.1 in. hole by installing an orifice plate (see table 10-1 for balances). The thermal verification test and helium sphere conditioning test were performed simultaneously.

Countdown 614031 was continued on May 13, 1965. The model 326 environmental blower was flowing approximately 17,200 lbm/hr of air into the environmental enclosure, and maintaining approximately 0.98 in. of water pressure. The flow was switched from air to GN2. Instrumentation noise made it impossible to determine the exact flow of GN2 into the aft interstage, however, the dome regulator pressure was maintained to give approximately 16,000 lbm/hr flow. Fifteen minutes later, LOX transfer was initiated. Shortly thereafter, trouble began to develop in the GN2 system and it became necessary to switch from GN2 back to air. With some LOX on board, the moisture in the air immediately began forming frost on the LOX tank, which invalidated the data taken during the thermal portion of the countdown, making it necessary to rerun the test.

After repairs were made to the GN2 system, the test was rerun on May 14, 1965, and designated CD 614032. This test was performed with strict adherence to the requirements of the thermal verification objectives, which consisted of a GN2 purge of the aft interstage for approximately 30 min prior to loading LOX, a minimum requirement of 60 percent LOX and 20 percent LH2, and a temperature stabilization period of approximately 1 hr after loading, before starting a normal engine chilldown test. GN2 flow varied between 15,000 and 16,200 lbm/hr throughout the test. The APS outlet temperatures, the controlling temperatures for the test, were maintained at 87 ± 5 deg F.

At the conclusion of engine chilldown, the GN2 flow was shut off for 2 min and 9 sec. The flow was then resumed and maintained until after vehicle de-tanking. After de-tanking, air was substituted for GN2 during the balance of securing operations.

10.2.4 Test Results

The data of the purge test taken during the third run are similar to the data taken during the other two runs. This data are shown in figure 10-4.

The calculated evacuation rate of air was made assuming (1) perfect gas mixing (2) zero leakage of air into the interstage and (3) a GN2 flowrate of 16,000 lbm/hr. The calculated rate indicated the 4 percent oxygen content level would be obtained in 3 min. Test results showed the level was reached in less than 3 min. This indicated that (1) little mixing occurred during the initial period of the purge and (2) the GN2 flow was a blanket effect that pushed the air from the interstage.

The results of the helium sphere conditioning test are shown in figure 10-1. The outlet temperature of the helium sphere enclosure remained above the design minimum of 77 deg F until chilldown was initiated at 11:20 A.M., when it decreased to 72 deg F. The 5 deg F below design minimum would not hinder the function of the helium sphere.

The results of the thermal verification test are shown in figures 10-1 and 10-2. Throughout the test, the APS outlet temperatures were within the design limits of 87 $\pm$5 deg F. The temperature of APS I was slightly cooler than that of APS III. This lower temperature was typical of most of the temperatures measured on the fin plane I side of the manifold.

The baffle opposite the umbilical separated the manifold into two sides. The minimum gas temperatures at the electronic equipment of the fin plane III side of the manifold varied from 64 deg F nearest the umbilical inlet to 37 deg F nearest the baffle; the manifold gas temperature throughout the test varied between 87 and 105 deg F for this side. The minimum gas temperature at the electronic equipment on the fin plane I side of the manifold was between 40 and 43 deg F. The manifold gas temperature throughout the test varied between 85 and 105 deg F for this side.

Although no critical temperature was reached near the electronic equipment, a more balanced temperature around the manifold would have been obtained if it was not necessary to seal the fifteen manifold orifices and the manifold was free from leakage.

Figure 10-2 shows the typical temperature observed during the thermal verification test. Gas temperature denoted by measurement number C-0563 was the temperature near the electronic equipment that reflects the 37 deg F noted. The temperature of the gas at the enclosure vents was measurement number C-0765. As the data indicated, the critical period of the test occurred during engine chilldown which occurred at 11:20 A.M. The lowest gas temperature recorded was -125 deg F. The sensor was located at the bottom of the enclosure directly below the edge of the engine thrust chamber.

TABLE 10-1
FLOW DISTRIBUTION TESTS

Item	Run No.	S-IVB/IB Pre-Purge Test Actual (lbm/hr)	S-IVB/IB Pre-Purge Test Flow (scfm)	S-IVB/IB Pre-Purge Test Target (lbm/hr)	S-IVB/IB Pre-Purge Test Flow (scfm)	S-IVB/V Pre-Thermal Verification Test Actual (lbm/hr)	S-IVB/V Pre-Thermal Verification Test Flow (scfm)	S-IVB/V Pre-Thermal Verification Test Target (lbm/hr)	S-IVB/V Pre-Thermal Verification Test Flow (scfm)
Total Flow	1	17,200	3,620			16,750	3,580		
	2	15,800	3,345			16,200	3,475		
	3	13,900	2,980			13,850	3,005		
	4	11,750	2,540			11,700	2,560		
	5	8,450	1,842			7,450	1,645		
APS Fin Plane No. 1	1	1,875	407	1,910	414	1,770	391	1,860	397
	2	1,790	389	1,757	381	1,680	371	1,798	386
	3	1,570	342	1,546	337	1,495	330	1,538	334
	4	1,325	289	1,308	286	1,230	272	1,300	284
	5	960	210	938	205	850	188	827	183
APS Fin Plane No. III	1	1,810	394	1,910	415	1,750	386	1,860	397
	2	1,720	376	1,757	384	1,675	370	1,798	386
	3	1,540	337	1,546	338	1,470	325	1,538	334
	4	1,295	284	1,308	287	1,230	272	1,300	284
	5	1,035	247	938	206	870	192	827	188
Thrust Structure	1	925	201	955	208	879	193	930	206
	2	880	192	877	192	835	184	898	198
	3	775	170	772	169	730	161	769	170
	4	660	145	652	143	620	137	649	143
	5	475	104	468	103	440	97	413	91
Helium Sphere	1					1,350	298	1,397	308
	2					1,280	282	1,350	298
	3					1,125	249	1,155	255
	4					950	210	975	215
	5					645	142	622	137

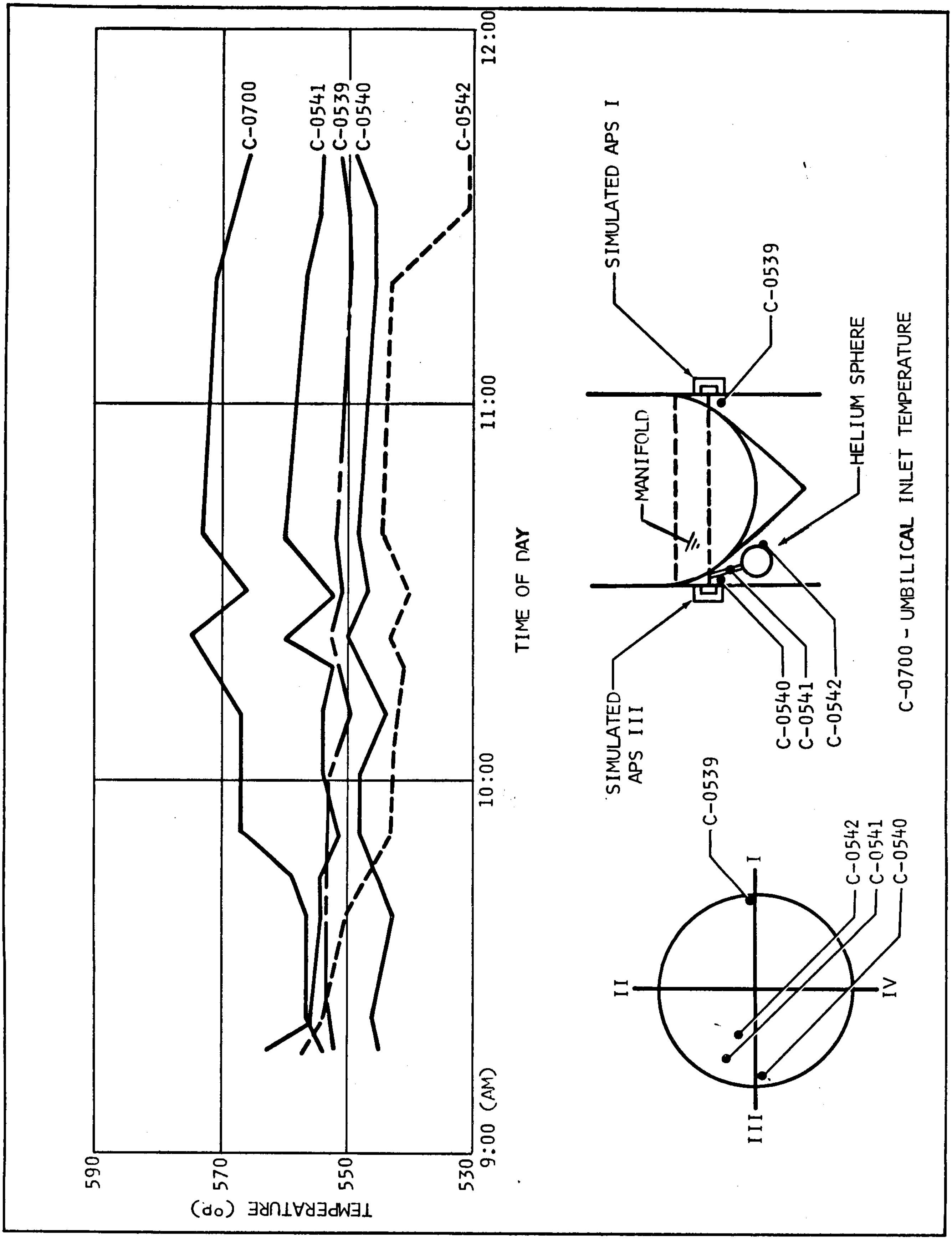

Figure 10-1 Helium Sphere Conditioning Test Results

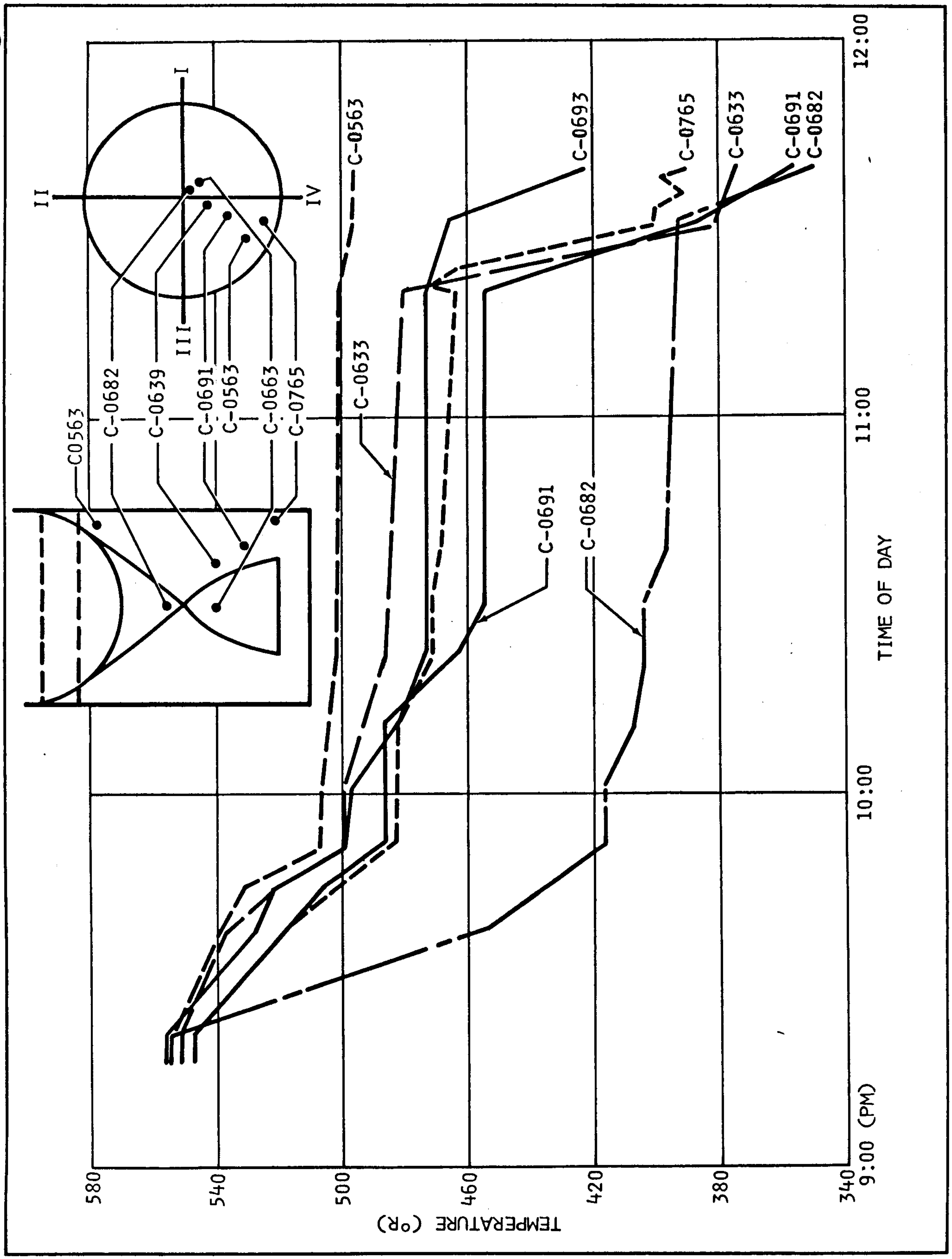

Figure 10-2 Thermal Verification Test Results

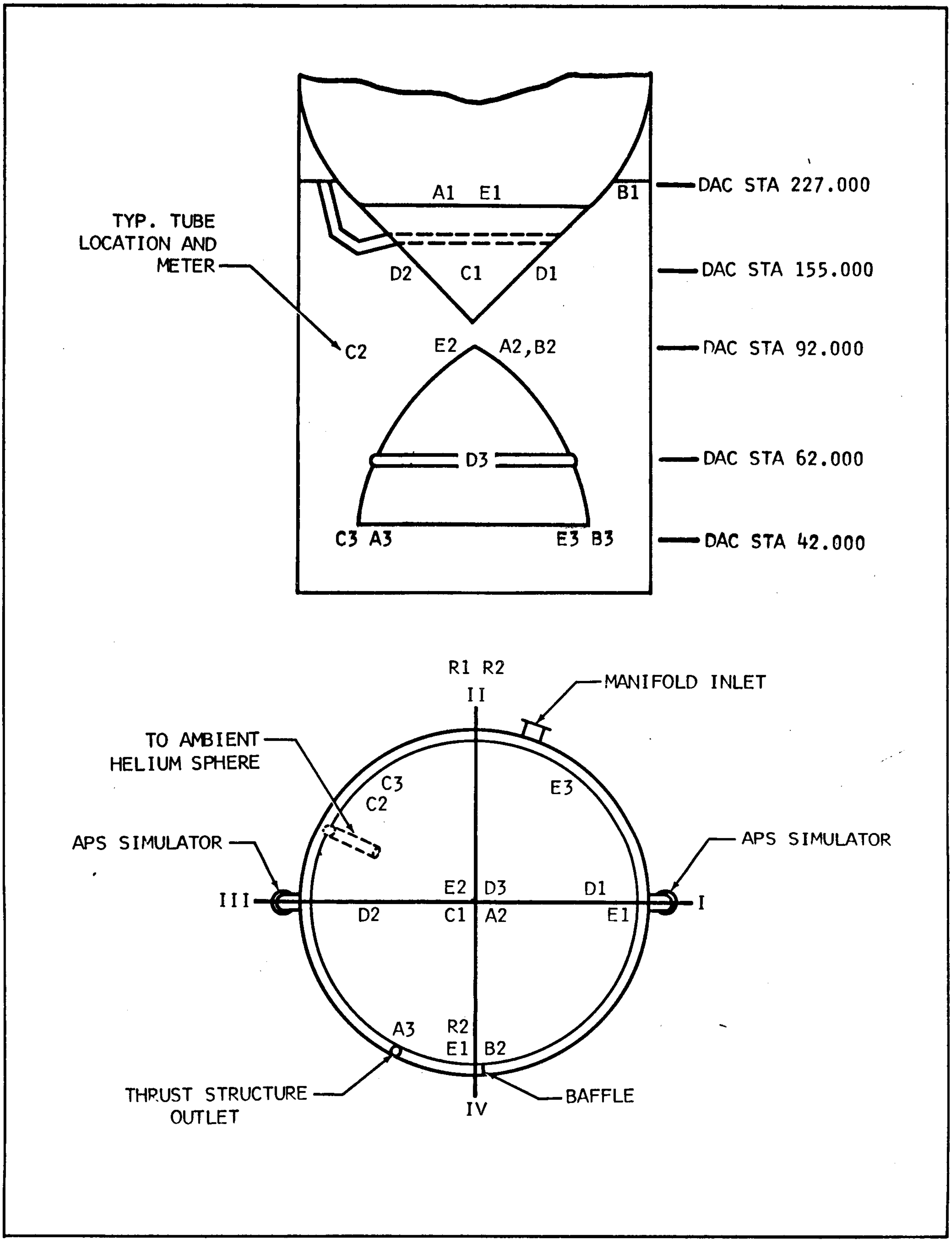

Figure 10-3 Purge Test Sample Tube Locations

21 February 1966

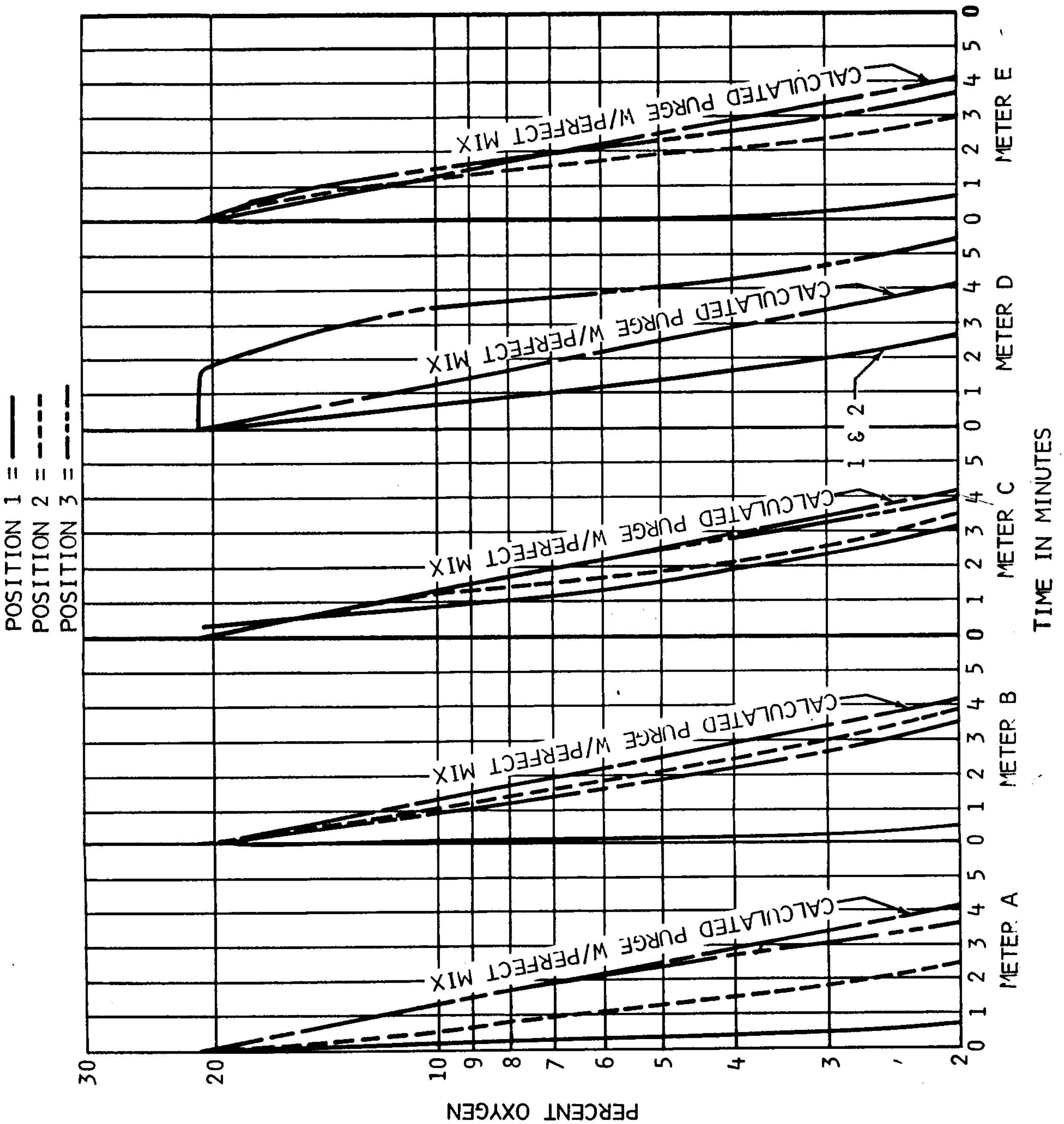

Figure 10-4 Purge Test Data

SECTION 11

PROPELLANT UTILIZATION SYSTEM

11. PROPELLANT UTILIZATION SYSTEM

The PU system functioned properly on all battleship firings. For the most part, the propellant mass as determined from the PU system, level sensors, and flow integral analyses showed good repeatability and was within the accuracies of the analysis involved. The countdowns analyzed were 614023, 614025, and 614030, which were all S-IVB/IB firings. Results of S-IVB/V firings are not presented because of insufficient data.

11.1 Propellant Mass History

The propellant mass values presented in table 11-1 are a comparison between flow integral, level sensors, and the indicated PU system mass. The PU system calibration was not changed for the three countdowns; however, it was apparent that a calibration shift may have occurred for CD 614030. The other two countdowns showed excellent agreement with the level sensors. The LOX residuals as determined from the PU system agree well with those determined by the level sensors; however, the LH2 residuals differed significantly from the level sensor residuals. The possible reasons for these deviations are that the empty capacitance could not be determined accurately for the battleship firings, the tank-to-sensor mismatch at the lower end of the LH2 mass sensor was severe, and the possible inaccuracy of the level sensors. The tank-to-sensor mismatch can be seen by the reaction of the PU valve at the end of the firings (figure 11-1).

A comparison of the three analysis for the battleship countdowns evaluated indicated that the maximum full load deviation between the flow integral results and the PU and point level sensor analysis was 1.1 percent for LOX (CD 614025) and 1.2 percent for LH2 (CD 614030). The maximum deviation of flow integral results from either PU or point level sensor analysis for the remaining two test results was 0.5 percent for the LOX and 0.8 percent for LH2. Applying the full load accuracies of the PU (1.0 percent) and point level sensor (0.3 percent) analysis to the deviations, the flow integral results are approximately the desired 1.0 percent accuracy for the battleship evaluation. This is particularly noteworthy in that the battleship flow integral evaluation was based entirely upon the influence coefficient technique. For flight stages, the total flow integral evaluation is based upon the combined results of engine influence coefficient analysis, injector differential pressure computer program, and flowmeter data evaluation. However, the battleship flow integral evaluation was limited by the unavailability of usable flowmeter data and the noncompletion of the injector differential pressure computer program at the time of evaluation.

The level sensors demonstrated good repeatability from firing to firing; however, the mass values determined from two of the LOX level sensors (L-0500 and L-0010) were evidently in error. This could be caused by inaccurate measurement of the level sensor position. Table 11-2 presents the level sensor analysis with calculated repeatability and accuracy.

11.2 Closed Loop System Performance

11.2.1 Mass Sensor Non-Linearities

The mass sensor non-linearities were determined by comparing the PU system mass to the flow integral mass. The LOX mass sensor non-linearity (figure 11-2) trends and magnitudes were repeatable within the accuracies of the analyses for all three tests. However, the LH2 mass sensor non-linearity (figure 11-3) for one of the tests differed in magnitude but was similar in trend with the other two.

11.2.2 Dynamic Response

The actual PU valve time histories for countdowns 614023, 614025, and 614030 are shown in figure 11-1. The valve oscillations after cutback are due to sensor non-linearities. The sensor non-linearities are a combination of manufacturing non-linearities and sensor-to-tank mismatch; the sum of these is shown in figure 11-2 for LOX and figure 11-3 for LH2. The low frequency valve oscillations are due to sensor-to-tank mismatch, while the higher frequency oscillations are due to sensor manufacturing non-linearities.

The repeatability of the valve oscillations and the derived sensor non-linearities verifies system repeatability.

Simulation PU valve time histories shown in figure 11-1 utilize the derived sensor non-linearities, actual loadings, and actual calibration and are compared with the actual time histories. The simulated summing point error time histories are compared with the actual time histories in figure 11-4. The simulated valve position time histories and error signal time histories closely approximate the actual response.

11.2.3 PU Efficiency

The PU efficiency and the propellants remaining at depletion for the three tests analyzed are presented in the following table. These are based upon the residuals of each test and the propellant flowrates at engine cutoff to the depletion of either propellant.

PU EFFICIENCY

Item	CD 614023	CD 614025	CD 614030
PU Efficiency (Percent)	99.85	99.79	99.79
Propellant Residual at Depletion (lbm)	337 (LOX)	447 (LOX)	452 (LOX)

TABLE 11-1
PROPELLANT MASS HISTORY

ITEM	CD 614023						CD 614025						CD 614030					
	FLOW INTEGRAL (lbm)	PU SYSTEM (lbm)	Δ(1) FI-PU (lbm)	LEVEL SENSOR (lbm)	Δ(2) FI-LS (lbm)	Δ(3) PU-LS (lbm)	FLOW INTEGRAL (lbm)	PU SYSTEM (lbm)	Δ(1) FI-PU (lbm)	LEVEL SENSOR (lbm)	Δ(2) FI-LS (lbm)	Δ(3) PU-LS (lbm)	FLOW INTEGRAL (lbm)	PU SYSTEM (lbm)	Δ(1) FI-PU (lbm)	LEVEL SENSOR (lbm)	Δ(2) FI-LS (lbm)	Δ(3) PU-LS (lbm)
LOX																		
Ignition	190,741	189,967	+774	189,722	+1,019	+245	186,682	184,511	+2,105	184,543	+2,139	+34	187,640	188,099	-454	186,983	+657	+1,111
PU Activate	185,683	184,922	+761	184,669	+1,014	+253	181,817	179,820	+1,997	179,710	+2,107	+110	183,042	182,948	+94	181,734	+1,308	+1,214
L0012	178,015	177,563	+452	176,729	+1,286	+834	179,067	177,251	+1,816	176,605	+2,462	+646	177,195	177,861	-666	176,481	+714	+1,380
L0011	149,438	149,345	+92	148,888	+549	+457	150,578	149,273	+1,305	148,825	+1,753	+448	149,329	149,806	-477	148,700	+629	+1,160
L0502	140,045	140,050	-5	139,252	+793	+798	141,179	140,093	+1,086	139,232	+1,947	+861	139,625	140,327	-702	139,076	+549	+1,251
L0010	--	--	--	--	--	--	115,529	114,875	+654	113,511	+2,018	+1,364	114,543	115,352	-809	113,415	+1,128	+1,937
L00501	99,837	99,856	-19	98,943	-1,894	+913	100,120	99,758	+362	98,915	+1,205	+843	99,372	100,195	-823	98,832	+540	+1,363
L0009	77,309	77,603	-294	76,656	+653	+947	77,515	77,470	+45	76,613	+902	+857	77,189	77,993	-804	76,570	+619	+1,423
L0500	59,853	60,083	-230	58,764	1,089	+1,319	59,892	59,925	-33	58,698	1,194	+1,227	59,736	60,465	-729	58,656	+1,080	+1,809
L0008	44,329	44,410	-81	43,967	+362	+447	44,417	44,404	+13	43,924	493	+480	44,186	44,655	-469	43,905	+281	+750
L0006	19,510	20,007	-497	19,513	+3	+494	19,545	19,884	-339	19,492	+53	+392	19,383	20,218	-835	19,470	-87	+748
L0005	10,191	10,247	-56	10,172	+19	+75	10,126	10,412	-286	10,164	-38	+248	10,243	10,840	-597	10,151	+92	+689
Residuals	2,548	2,401	+147	2,548	0	-147	2,080	2,060	+20	2,080	0	-20	3,132	3,229	-97	3,132	0	+97
LH2																		
Ignition	37,717	37,872	-155	37,672	+45	+200	39,448	39,127	+321	39,119	+329	+8	38,815	38,540	+275	38,345	+470	+195
N0024	--	--	--	--	--	--	35,651	38,090	+561	38,325	+326	-235	--	--	--	--	--	--
PU Activate	36,684	36,799	-115	36,641	+43	+158	38,444	38,298	+146	38,123	+321	+175	37,872	37,448	+424	37,275	+597	+173
N0025	34,326	34,439	-113	34,314	+12	+125	34,507	34,232	+275	34,244	+263	-12	34,701	34,554	+147	34,244	+457	+310
N0026	30,331	30,432	-101	30,357	-26	+75	30,461	30,236	+225	30,288	+173	-52	30,650	30,552	+98	30,288	+362	+264
N0027	26,303	26,348	-45	26,312	-9	+36	26,389	26,196	+193	26,270	+119	-74	26,506	26,458	+48	26,246	+260	+212
N0028	22,347	22,374	-27	22,348	-1	+26	22,380	22,218	+162	22,317	+63	-99	22,540	22,494	+46	22,297	+243	+194
N0029	18,287	18,273	+14	18,300	+13	-27	18,206	18,091	+115	18,296	-90	-205	18,416	18,409	+7	18,263	+153	+146
N0030	14,417	14,453	-36	14,401	+16	+52	14,429	14,401	+28	14,407	+22	-6	14,432	14,520	-88	14,368	+64	+152
N0031	10,263	10,388	-125	10,298	-35	+90	10,270	10,311	-41	10,291	+21	+20	10,303	10,493	-190	10,257	+46	+236
L0002	2,377	2,584	-207	2,331	+46	+253	2,324	2,475	-151	2,329	-5	+146	2,314	2,664	-350	2,322	-8	+42
Residuals	563	857	-294	563	0	+294	541	759	-218	541	0	+218	601	1,011	-410	601	0	+410

NOTES: (1) Flow integral propellant mass minus PU system propellant mass.
(2) Flow integral propellant mass minus level sensor propellant mass.
(3) PU system propellant mass minus level sensor propellant mass.

TABLE 11-2
LEVEL SENSOR PROPELLANT MASS ANALYSIS

LEVEL SENSOR	CD 614023	CD 614025	CD 614030	ACCURACY	REPEATABILITY	
LOX						
L0012	176,729	176,605	176,481	±635	±310	
L0011	148,888	148,825	148,700	±630	±392	
L0502	139,232	139,232	139,076	±625	±410	
L00501	98,943	98,915	98,832	±595	±470	
L0009	76,656	76,613	76,570	±555	±437	
L0500	58,764	58,698	58,656	±505	±396	
L0008	43,967	43,924	43,905	±440	±352	
L0006	19,513	19,492	19,470	±270	±250	
L0005	10,172	10,164	10,151	±200	±185	
LH2						
N0025	34,314	34,244	34,244	±104	±45	
N0026	30,357	30,288	30,288	±95	±42	
N0027	26,312	26,270	26,246	±89	±39	
N0028	22,348	22,317	22,297	±82	±37	
N0029	18,300	18,296	18,263	±71	±36	
N0030	14,401	14,407	14,368	±62	±36	
N0031	10,298	10,291	10,257	±52	±35	
L0002	2,331	2,329	2,322	±33	±24	
LEVEL SENSOR	**CD 614023**	**ACCURACY**	**CD 614025**	**ACCURACY**	**CD 614030**	**ACCURACY**
LOX						
Ignition	189,722	±484	184,543	±415	186,983	±478
Residual	2,548	±180	2,080	±186	3,132	±178
LH2						
Ignition	37,728	±81	39,151	±82	38,407	±83
Residual	563	±36	541	±36	601	±36

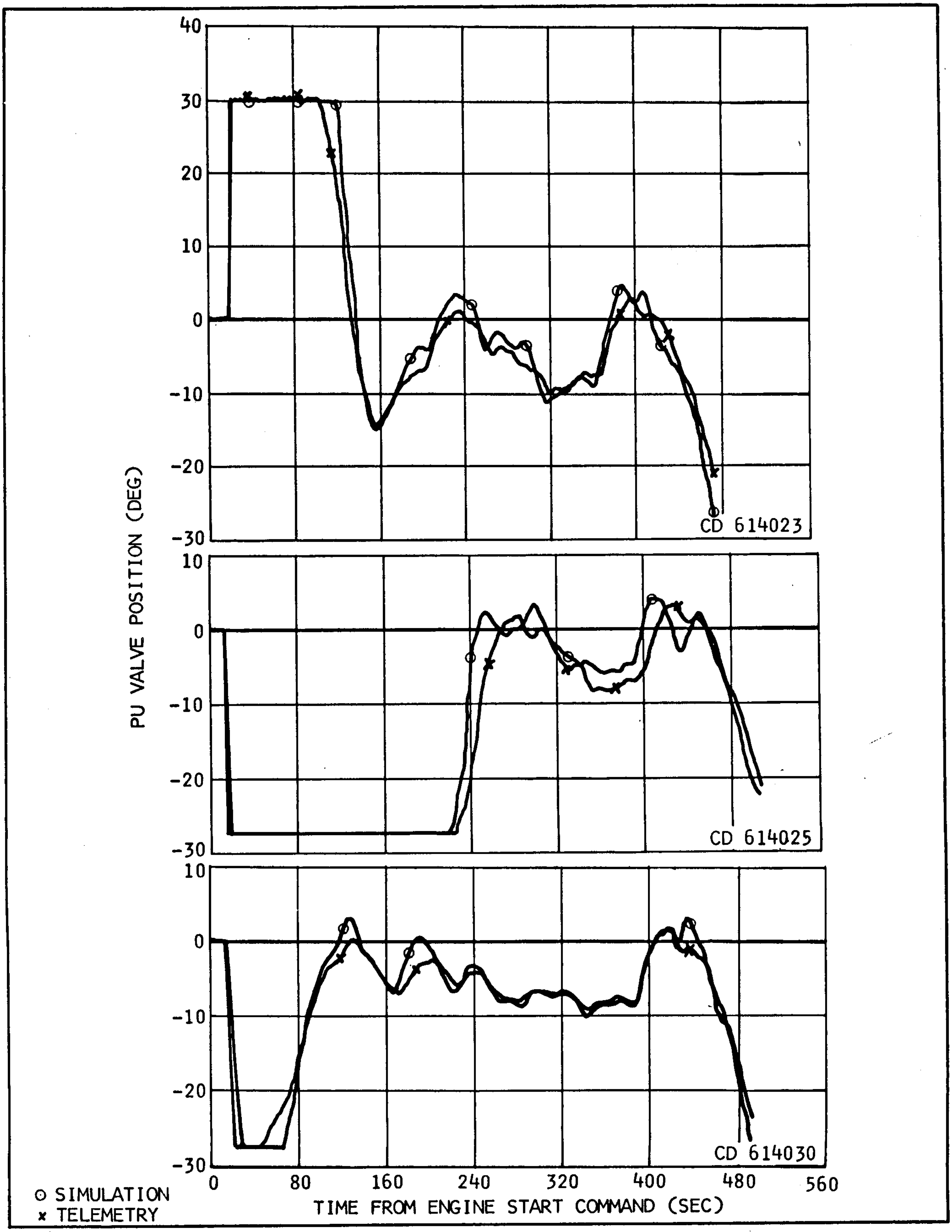

Figure 11-1 PU Valve Time Histories

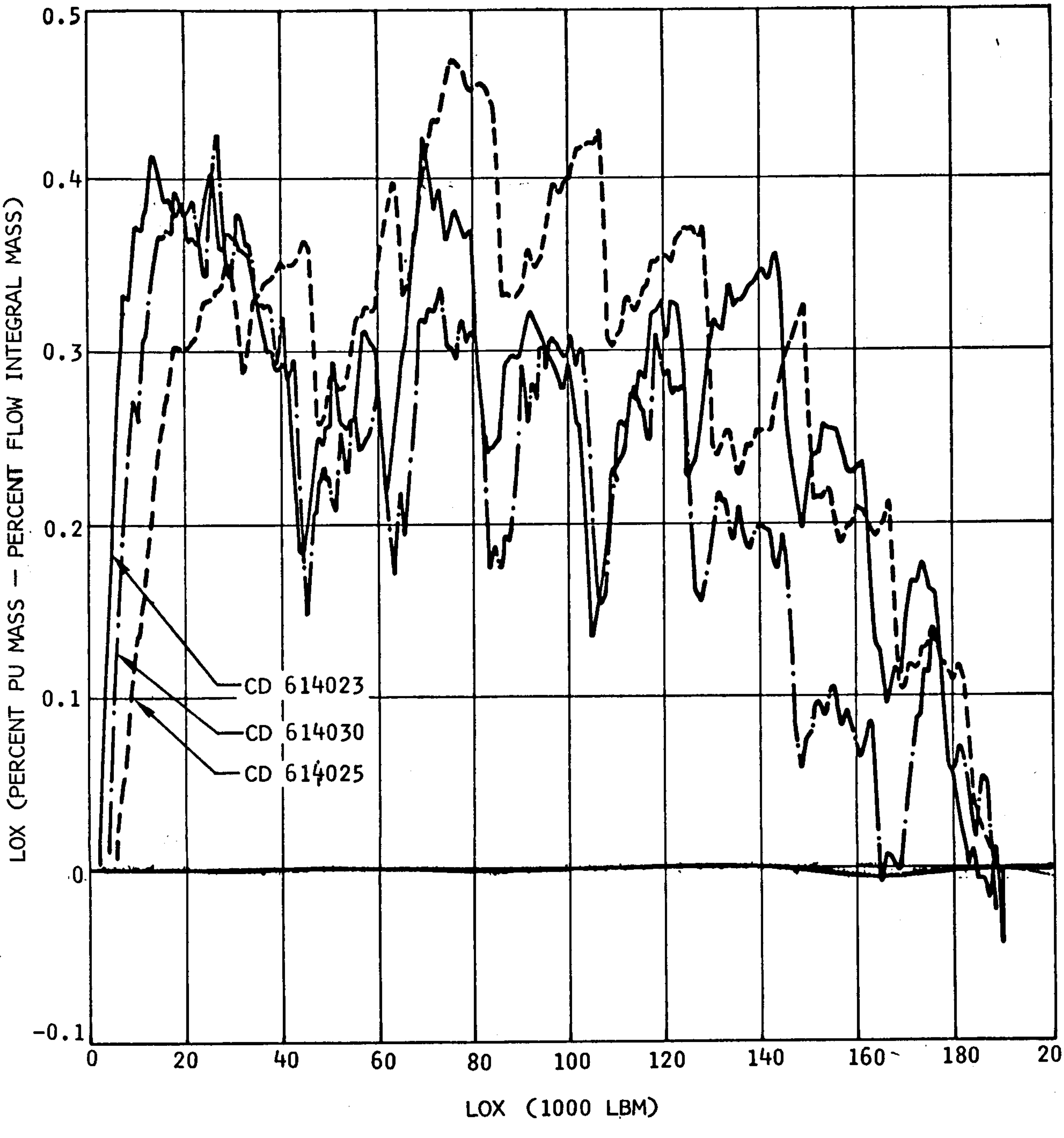

Figure 11-2 LOX Mass Sensor Non-Linearity

21 February 1966

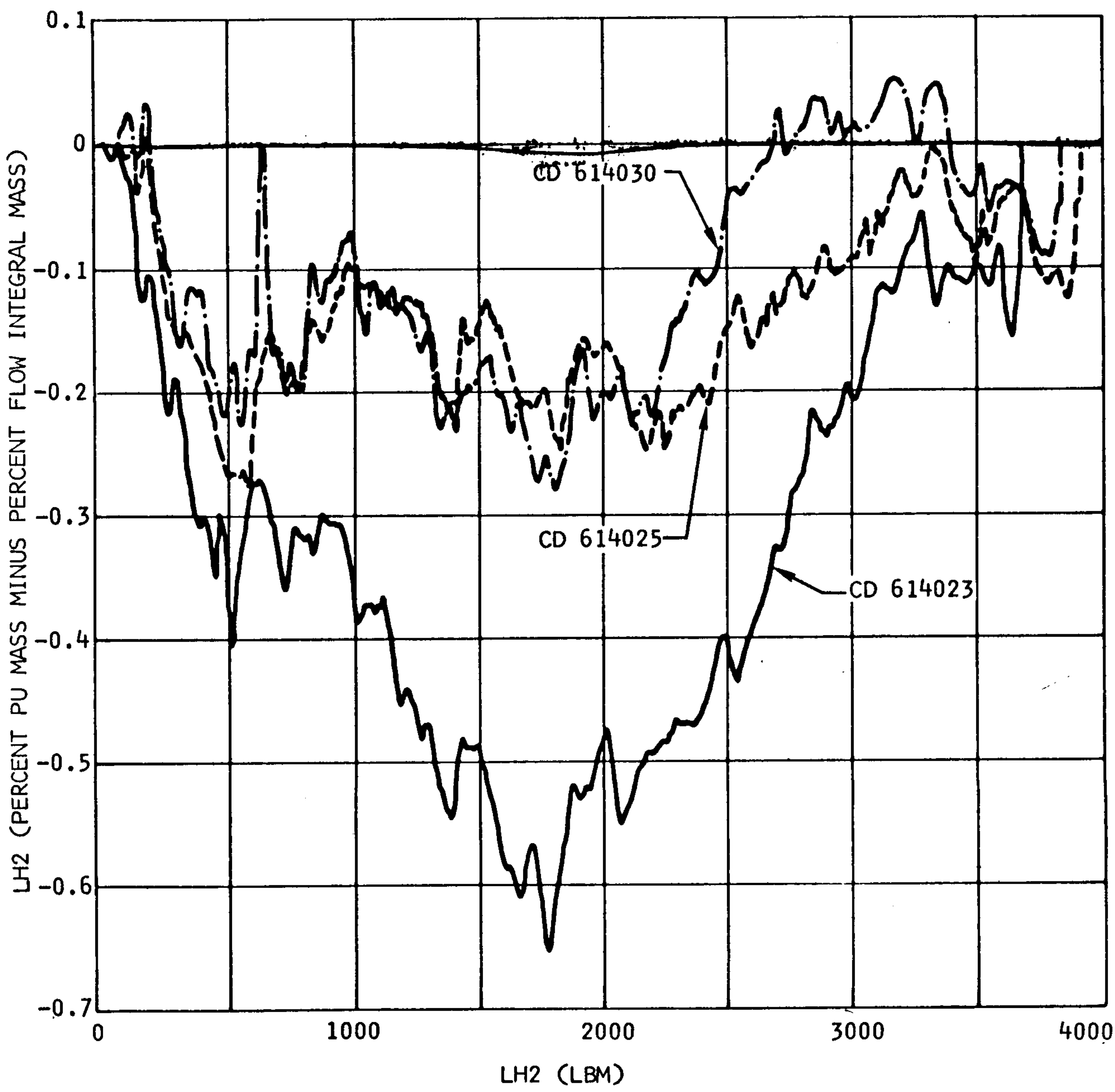

Figure 11-3 LH2 Mass Sensor Non-Linearity

21 February 1966

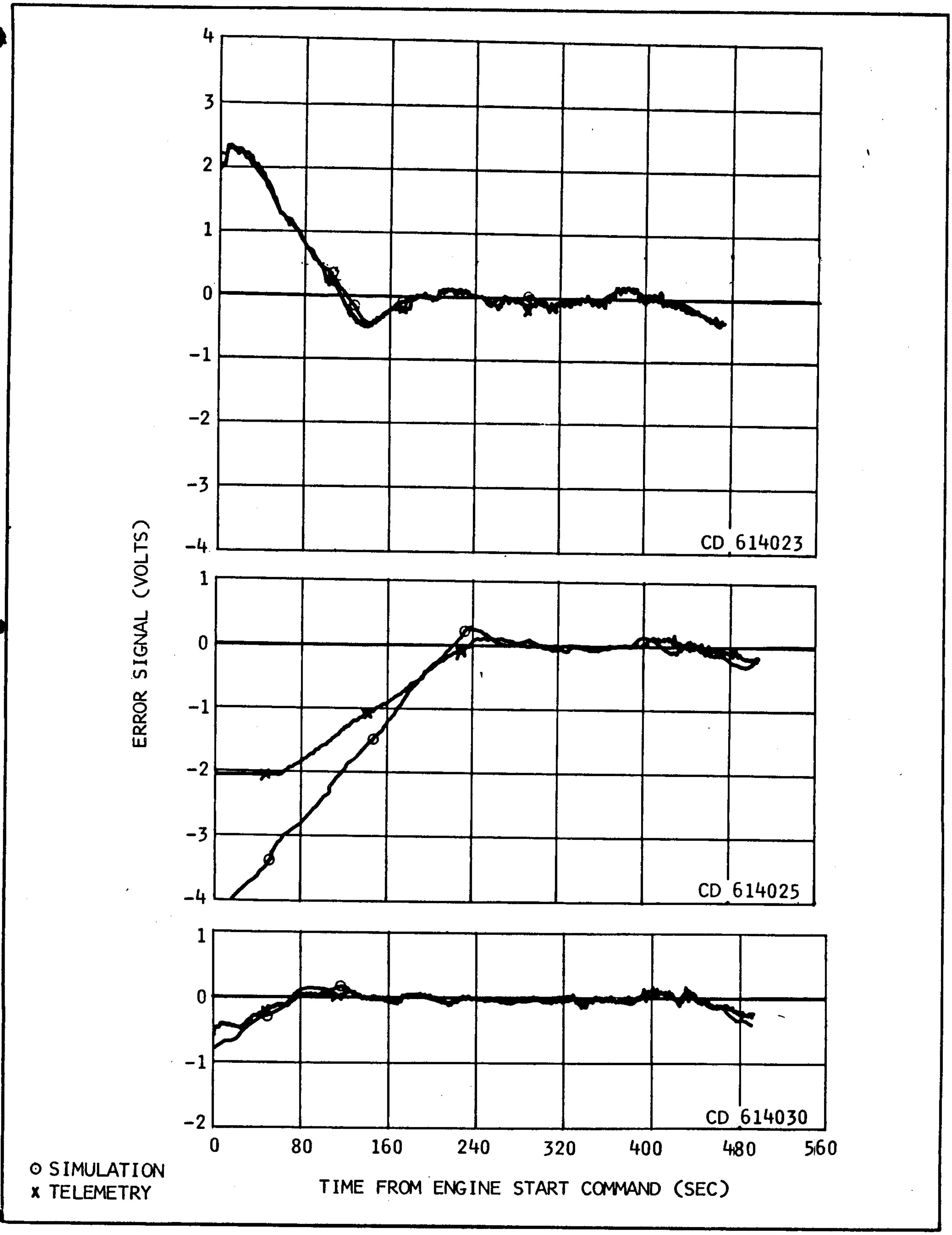

Figure 11-4 PU System Error Signal

21 February 1966

SECTION 12

DATA ACQUISITION SYSTEM

12. DATA ACQUISITION SYSTEM

12.1 Instrumentation Performance

The data acquisition system for battleship testing consisted of all parameters hardwired to a GIS (ground instrumentation system) where the signals were conditioned, when required, and recorded on magnetic tape. The recording system consisted of digital and constant bandwidth FM. Strip charts were provided for real time display of redline and cutoff parameters. No telemetry system was utilized on the battleship program.

Operation of the GIS was satisfactory, as shown by the 95.5 percent valid data acquisition presented in table 12-1. The information in this table is for the last countdown of the chilldown tests and all S-IVB/IB and S-IVB/V system development firings. Minor problems were experienced with patching and set-up of the GIS, however, these were considerably reduced as testing progressed.

The only major problem associated with the instrumentation was in the case of some pressure transducers in the ground support and facility equipment that were replaced with new designs for the following reasons:

a. Case burst pressure inadequate for all ranges above 1,000 psia.

b. Contamination due to the possibility of the silicone oil, which is used as a damping fluid, getting into the measured media in the case of a ruptured diaphram. An explosion could result if the oil combined with liquid oxygen.

c. Freezing of silicone oil temperatures less than -100 deg F making the transducer inoperative.

The only instrumentation used on the battleship stage that is common to flight stages are the transducers, since all signal conditioning was done in the ground equipment and there was no telemetering. No problems were experienced with the battleship stage instrumentation that would affect intended usage on the flight stages.

TABLE 12-1
GROUND INSTRUMENTATION SYSTEM PERFORMANCE

PARAMETER	RECORDED	BAD	PARTIALLY SUCCESSFUL	PERCENT GOOD
Pressures	2,098	63	63	96.9
Temperatures	2,158	97	87	95.5
Stress	69	0	0	100.0
Flows	93	7	2	92.5
Acoustics	109	14	12	87.2
Positions	187	4	1	97.9
Voltage/Currents	556	29	62	94.8
Accelerations	99	7	8	92.9
Events/Switches	5,984	--	--	--
Vibration	240	29	30	87.9
Miscellaneous	230	5	15	97.8
Totals	11,823	255	280	--
FM/FM	1,721	106	108	93.8
Strip Chart	773	6	30	99.3
Digital	3,345	143	142	95.7
Grand Total	5,839	255*	280*	95.5

NOTES:

(1) All events were recorded only on a scratch pen event recorder.

(2) Some parameters were recorded on more than one recording system.

(3) Partially successful measurements are not included in calculation of the "percent good."

*Less events

SECTION 13

ELECTRICAL SYSTEM

13. ELECTRICAL SYSTEM

13.1 Control System

Operation of the vehicle control system was entirely satisfactory throughout the battleship testing. The sequencer performance was as expected and typical times of significant commands and talkbacks are presented in tables 5-1 and 5-2 for the S-IVB/IB and S-IVB/V tests. It should be noted that the given times are for sequencial references only, and should never be used for the actual times for any one test.

The S-IVB/IB sequence of events used simulated booster liftoff time (T) as did the S-IVB/V for first burn. A simulated boost period of approximately 150 sec was used for S-IVB/IB and approximately 540 sec for S-IVB/V. The S-IVB/V tests then simulated three and one orbits, depending on the test, before second burn. The reference time for second burn was 13.0 sec after second burn engine sequence start. The 13.0 sec figure is a nominal time between engine sequence start and Engine Start Command.

The electrical systems that were not included in the battleship program and therefore could not be evaluated were the Range Safety, Ullage Rocket Ignition and Jettison Systems, and APS controls.

13.2 Power System

The electrical power system for the battleship testing consisted of two forward power supplies, two aft power supplies, two inverters for supplying power to the LOX and LH2 chilldown motors, and a static inverter/converter. Forward power supply No. 1 will provide telemetry system power for flight stages. Since all instrumentation was hardwired to the GIS, as discussed in paragraph 12.1, an evaluation of the performance of this power supply could not be accomplished.

The power supply load profiles shown in figure 13-1 are typical performance curves and are not to be used as specific values for any one test. The profile trend is similar for S-IVB/IB and both burns of S-IVB/V testing, therefore, only one set of curves is presented. Following is a discussion of the operation of the power subsystems.

13.2.1 Forward Power Supply No. 2

This unit supplies 28 vdc to the PU (propellant utilization) system and the static inverter/converter. Operation of the power supply was satisfactory, supplying 2.7 amps prior to engine ignition increasing to 3.45 amps after engine start due to the increased loading when the mass bridge servo-systems are in operation. While the PU valve was against its stop, the load was 3.6 amps.

13.2.2 Aft Power Supply No. 1

This unit supplies 28 vdc to the J-2 engine, sequencer, and various valves and pressure switches. Operation of this power supply was within expectations. The current surge to 28 amps at T +90 sec is due to the demands of the J-2 engine during the start sequence. Current levels during engine steady-state operation vary between 8 and 12 amps upon the operation of various valves.

13.2.3 Aft Power Supply No. 2

This unit supplies 56 vdc to the two chilldown inverters and the auxiliary hydraulic pump. When the auxiliary hydraulic pump is turned on, a transient of 270 amps is experienced for approximately 100 ms. An increase in current from 50 amps to 74 amps occurring after the turn-on transient is due to the pump pressurizing the accumulator. As the accumulator reaches full pressure, the flowrate of the pump is reduced and the current drops to 44 amps. When the chilldown inverters are turned on, the load increases to 78 amps dropping to 38 amps when the inverters are turned off just prior to engine ignition.

13.2.4 Chilldown Inverters

The chilldown inverters were not installed for much of the early battleship program. However, the successful performance of the inverters was demonstrated during both S-IVB/IB and S-IVB/V testing. The only problem noted was erratic speed indications of the LH2 chilldown pump during special S-IVB/V chilldown tests. Fluctuations between 5,000 and 15,000 rpm were further indicated by the chilldown flowrates and pump motor currents. Analysis showed this not to be in the electrical system, but was caused by backflow of gases to the pump, resulting from the LH2 vaporizing after being pumped into a nonchilled line. Check valves were installed in the childown valves to prevent the backflow and no further problems in this area were experienced.

The inverter phase voltages were nominally 52 volts and the phase currents indicated 35 - 40 amps start transients dropping to 10 - 15 amps during steady-state operations. The phase frequency was 408 - 410 cps and the inverter temperature varies between 65 and 85 deg R. All data were within the expected range.

13.2.5 Static Inverter/Converter

This unit which provides the servo motor reference phase voltage, the bridge and capacitor reference oven supply voltage and the fine and coarse mass potentiometer supply voltage, operated satisfactorily as all parameters were within their prescribed tolerances.

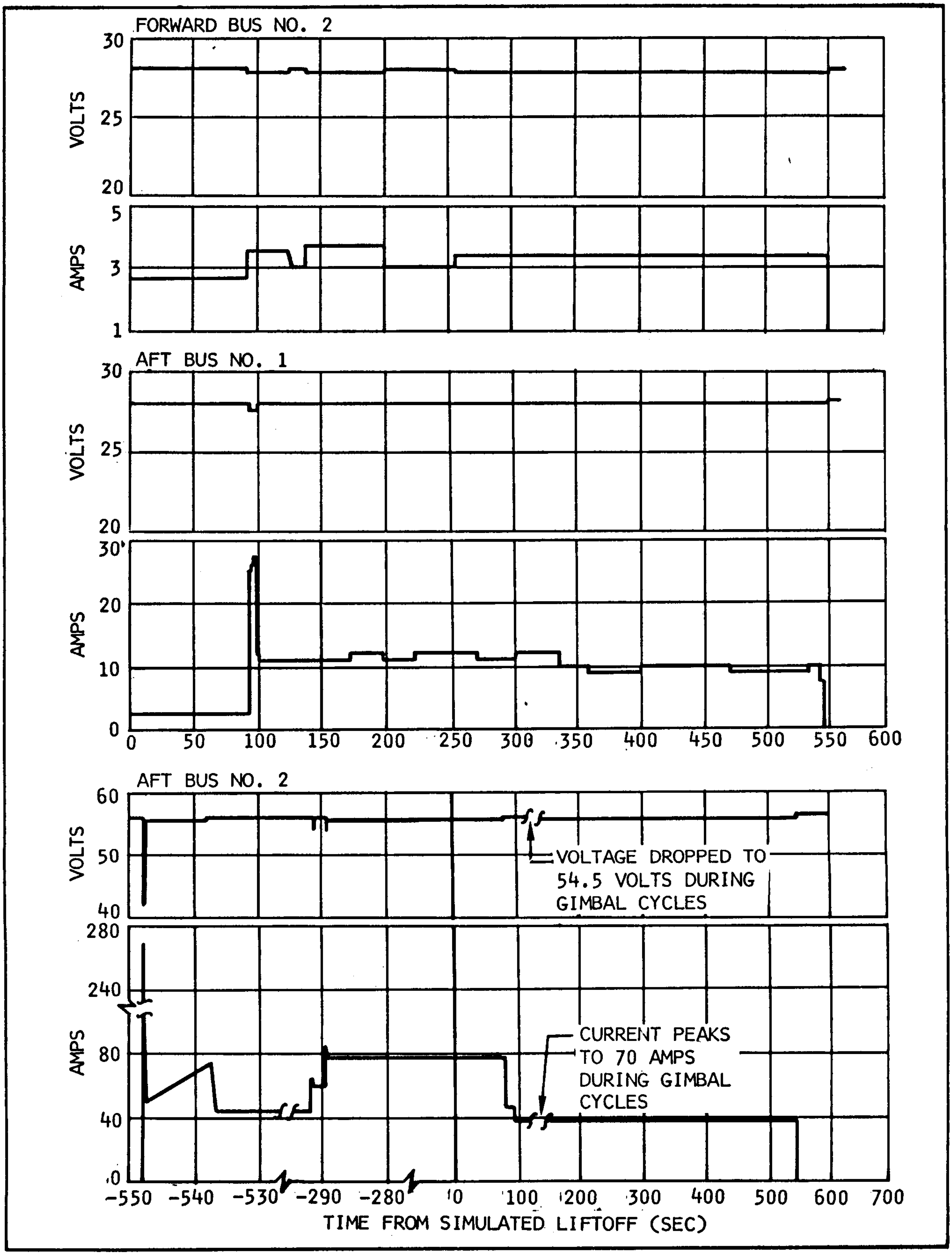

Figure 13-1 Power Supply Load Profiles

SECTION 14

HYDRAULIC SYSTEM

14. HYDRAULIC SYSTEM

The performance evaluation of the S-IVB hydraulic system installation during the battleship firing program is based on system operation during full duration firings. Of these firings, two were during the S-IVB/IB development firing and were designated countdowns 614025 and 614030; two were during the S-IVB/V development firings and were CD 614043 and CD 614044. The only hydraulic system failure of the program occurred during CD 614028 and was the cause of a firing cutoff. An analysis of this failure is discussed in this section.

14.1 General Performance

The hydraulic system was serviced in accordance with a fill, flush, bleed, and fluid samples procedure that was similar to the procedure used for flight stage servicing. The reservoir fluid level was maintained at 85 ± 2 percent of full volume prior to each of the firings and did not decrease below 25 percent during hydraulic pump operation.

The single most important hydraulic variable is the system pressure which was observed both during the prestart period when only the auxiliary pump was operating and during the main stage firing when both auxiliary and engine-driven pumps were operating. All system pressure data were within the design limits of the pumps and verified compensator pressure settings previously determined from tests of the pumps.

The reservoir fluid pressure is a 21.6:1 bootstrap ratio of the system pressure. The reservoir pressure data reflect both this bootstrap ratio and the friction losses (approximately ± 10 psi) of the differential piston seal. All reservoir pressure readings were within design limits.

The accumulator GN2 pressure was acceptable for all firings even though a low precharge value (2,255 psia) was noted during CD 614043. This condition was observed prior to the initiation of the hydraulic system operation but not being critical was not corrected due to the delay it would produce. Development tests have indicated satisfactory system operation with pre-charges of less than 1,800 psia.

A tabulation of nominal pressure measurements obtained during the successful system operation firings is presented in table 14-1.

All fluid temperatures were within the design limits. Rise rates were greater, as expected, during periods of engine gimbaling because of the increased flow and attendant friction losses. During pump operation, the hydraulic pump inlet fluid temperature exceeded the reservoir fluid temperature by a few degrees because the reservoir fluid tended to stratify near the top of the reservoir due to the larger mass at the top providing a better heat sink. The reservoir temperature transducer is located at the top of the reservoir.

A tabulation of temperatures obtained during the successful system operation firings is presented in table 14-2.

14.2 Malfunction Analysis and Supporting Information

The hydraulic system operation anomaly that occurred during CD 614028 has been attributed to a failure in the high pressure relief valve. The disassembly and examination of this valve revealed that (1) the poppet spring had a permanent set and (2) the spring cavity adjusting nut had backed off. The data indicated (1) the poppet was seated during auxiliary pump operation at 3585 psia (2) the poppet was unseated at engine start with the engine-driven pump at a higher compensator setting and (3) the unseated poppet provided a full flow demand in the pumps with system pressure between 3,235 and 3,465 psia.

It is not certain whether unseating of the poppet was caused by the higher engine-driven pump compensator setting or by the main stage induced vibration. The important factors are that the spring had a set, the firing was cutoff at 374 sec and if the firing had been allowed to continue to a full 474 sec the temperature of the fluid would have reached a temperature of 375 deg F. Corrective action to this failure is in process. The temperatures obtained during this failure are included in table 14-2.

14.3 Contamination Analysis

Contamination generation and control was deemed adequate by sampling the pre and post-fire fluid. There was no indication of contamination build-up by system operation during the battleship program. The program and development tests have indicated contamination not to be a problem in this hydraulic system. In fact, the hydraulic system was not flushed or sampled between CD 614043 and CD 614044. The sample following the CD 614044 firing showed no contamination increase over the sample prior to CD 614043. The contamination particle count limits during the battleship program were specified in MSFC-PROC-166. Based on the observations and data presented, the hydraulic system installation successfully met the requirement of positioning and gimbaling the engine in response to simulated guidance commands. The one anomaly in CD 614028, was the result of a material failure, not concept or design.

14.4 Hydraulic Servo Actuator Gimbaling Tests

A series of transient response and frequency tests were performed on the S-IVB servo actuators (refer to Section 15) during hot firing and nonfiring conditions.

The hydraulic system was installed per the flight configuration with the exception of a series "wishbone type" spring installed between the actuators and the thrust structure. The spring assemblies were used to simulate the flight vehicle structure spring rate. This was required since the battleship thrust structure was of steel construction and therefore a more rigid assembly than the vehicle. The J-2 engine was per the S-IVB/IB configuration for CD 614030 and per the S-IVB/V engine configuration for CD 614043. CD 614030 was a full duration firing lasting 493.5 sec during which time the engine was gimbaled for 379 sec commencing 26 sec after engine start. CD 614043, Run No. 4, was a full duration firing consisting of a 170-sec first burn, a 92-minute coast, and a final 319-sec burn. The engine was gimbaled 265 sec during the second burn, commencing 35 sec after engine start.

The method of driving the servo actuators consisted of preprogramming the servo-command signs on magnetic tape at the desired sinusoidal frequencies, steps and ramps. A second signal on the command tape was used as a data timing signal to function as a computer processing indicator to allow time for the changing command frequencies to settle out between data points. Command signals and response signals from position, pressure and acceleration transducers were recorded on a second magnetic tape and reduced with the aid of Production Computer Program No. K097.

Phase and gain data for the pitch and yaw actuator positions with respect to the actuator servo signals were plotted in figures 14-1 and 14-2 for input signals equal to ±1/2 and ±1 deg of engine displacement. The anti-resonance point indicates the average servo structural resonant frequency, exclusive of the piston position feedback load path, occurred at 4.57 cps in the pitch plane and 4.75 cps in the yaw plane. The natural undamped system frequency was calculated to be 4.07 cps in the pitch plane and 4.23 cps in the yaw plane. The following table presents the servo structural resonant frequency for each test reported herein.

	CD 614030		CD 614043	
	PITCH (CPS)	YAW (CPS)	PITCH (CPS)	YAW (CPS)
±1/2 deg	4.7	5.0	4.5	4.6
±1 deg	4.5	4.7	4.6	4.7

The response frequency of 4.57 cps corresponds to a single degree-of-freedom equivalent spring rate of 101,000 lbf/in. This resonant frequency was lower than the measured flight vehicle resonant frequency which for S-IVB-201 stage was approximately 5.2 cps. The wishbone springs were set to give as high a spring rate as possible to approach the flight vehicle dynamics. The ambient spring rate verification tests produced a resonant frequency of 5.8 cps. Data has thus been obtained on the high and low side of the data obtained from production vehicles. Even though the battleship servo structural resonant frequency was on the low side, the results of the tests were valid.

Actuator specification control drawing No. 1A66248 allows the closed-loop frequency response amplitude peaking to be equal to or less than 50 percent or 3.5 db above the nominal amplitude ratio obtained with command signals equal to or greater than ±1/2 deg of engine displacement for all driving frequencies. Thus, the engine response data demonstrate that the differential pressure feedback network built into the servo valves was designed properly and that it was operating satisfactorily during gimbaling. The specification control drawing also allows for a phase lag equal to or less than 35 deg up to and including 1 cps for input signals equal to or greater than command signals of ±1/4 deg of engine displacement. Phase lag data could not be obtained from the accelerometer engine position data at these lower frequencies because of the above-stated reason. However, the phase lag using the actuator position data which is very close to the engine position data at the lower frequencies measured approximately -31 deg for the S-IVB/IB engine configuration and -26 deg for the S-IVB/V engine configuration.

The following table presents the phase lag measurements taken at or near 1 cps for each test reported herein.

	CD 614030				CD 614032			
	PITCH		YAW		PITCH		YAW	
	FREQ (CPS)	PHASE (DEG)	FREQ (CPS)	PHASE (DEG)	FREQ (CPS)	PHASE (DEG)	FREQ (CPS)	PHASE (DEG)
±1/2 deg	1.000	-30.9	1.000	-32.1	1.000	-24.9	.977	-27.7
±1 deg	0.979	-30.6	1.002	-30.9	.969	-24.5	.987	-27.5

Pitch and yaw vehicle mounted position transducers revealed the relative movement of the vehicle with respect to the Beta 1 test stand. Two resonant frequencies are readily apparent at approximately 4.1 and 6.9 cps measured at the forward and at the aft vehicle skirts. The maximum movement occurred through resonance and is tabulated in the following table for CD 614043.

	FORWARD SKIRT				AFT SKIRT			
	±1/2 deg SIGNAL		±1 deg SIGNAL		±1/2 deg SIGNAL		±1 deg SIGNAL	
	FREQ (cps)	PEAK AMPL (in. O-P)	FREQ (cps)	PEAK AMPL (in. O-P)	FREQ (cps)	PEAK AMPL (in. O-P)	FREQ (cps)	PEAK AMPL (in. O-P)
Pitch	4.1	.075	4.2	.153	4.0	.026	4.1	.049
Pitch	7.0	.082	6.9	.159	7.1	.020	7.0	.045
Yaw	4.0	.083	4.2	.121	4.0	.034	4.1	.043
Yaw	6.9	.064	6.8	.123	6.9	.020	6.8	.047

The structural resonant frequencies are due to the coupling effects between the vehicle when mounted on a relatively light aft dummy interstage and the test stand.

The servo actuator differential pressure response curves are plotted in figure 14-3 for CD 614030 and CD 614043. Pitch data for CD 614043 are not available due to a malfunction in the ΔP transducer. Maximum generated differential pressures were produced through the resonant frequency regions averaging 2,005 psi at 4.0 cps, 2,144 psi at 4.4 cps, and 1,103 psi at 7.3 cps for a 1 deg engine command signal.

The series of battleship hydraulic actuator engine gimbaling tests verified that the servo control system was functioning properly with adequate response and with sufficient damping to reduce the closed loop system gain at the resonant frequencies to acceptance values.

TABLE 14-1
HYDRAULIC SYSTEM PRESSURES

Countdown No.	System Pressure (psia)		Reservoir Pressure (psia)	Accumulator*
	Aux Pump Only	Aux & Main Pump		GN2 Pressure (psia) at GN2 Temperature (°F)
614025	3,585	3,585	No Data	2,335 at 59
614030	3,590	3,650	175	2,325 at 76
614043 (Burn 1)	3,685	3,685	173	2,255 at 69
(Burn 2)	3,700	3,650	170	-
614044 (Burn 1)	3,680	3,680	169	No Data
(Burn 2)	3,665	3,665	172	-
Nominal Limit	3,550 to 3,700	3,550 to 3,700	154 to 181	2350 ± 50 at 70

* GN2 conditions prior to pump operation

TABLE 14-2
HYDRAULIC SYSTEM TEMPERATURES

Countdown No.	Firing Duration (Sec)	Reservoir Fluid Temperature (°F)				Pump Inlet Fluid Temperature (°F)			
		Aux Pump "On"	Engine Start	Engine Cutoff	Rise Rate °F/Min	Aux Pump "On"	Engine Start	Engine Cutoff	Rise Rate °F/Min
614025	507	60	80	90	1.2	56	90	128	4.5
614030*	493	63	83	128	5.5	62	92	150	7.1
614043 (Burn 1)	167	63	116	118	0.7	70	123	126	1.1
(Burn 2)*	319	-	108	159	9.6	-	119	165	8.7
614044 (Burn 1)	170	-	95	93	-	-	86	98	4.2
(Burn 2)*	360	-	110	127	2.8	-	119	133	2.3
Nominal Limit	-	-35 min	0 min	275 max	-	-35 min	0 min	275 max	-
614028	374	73	112	318	33.1	70	128	322	31.1

* Indicates gimbal program run

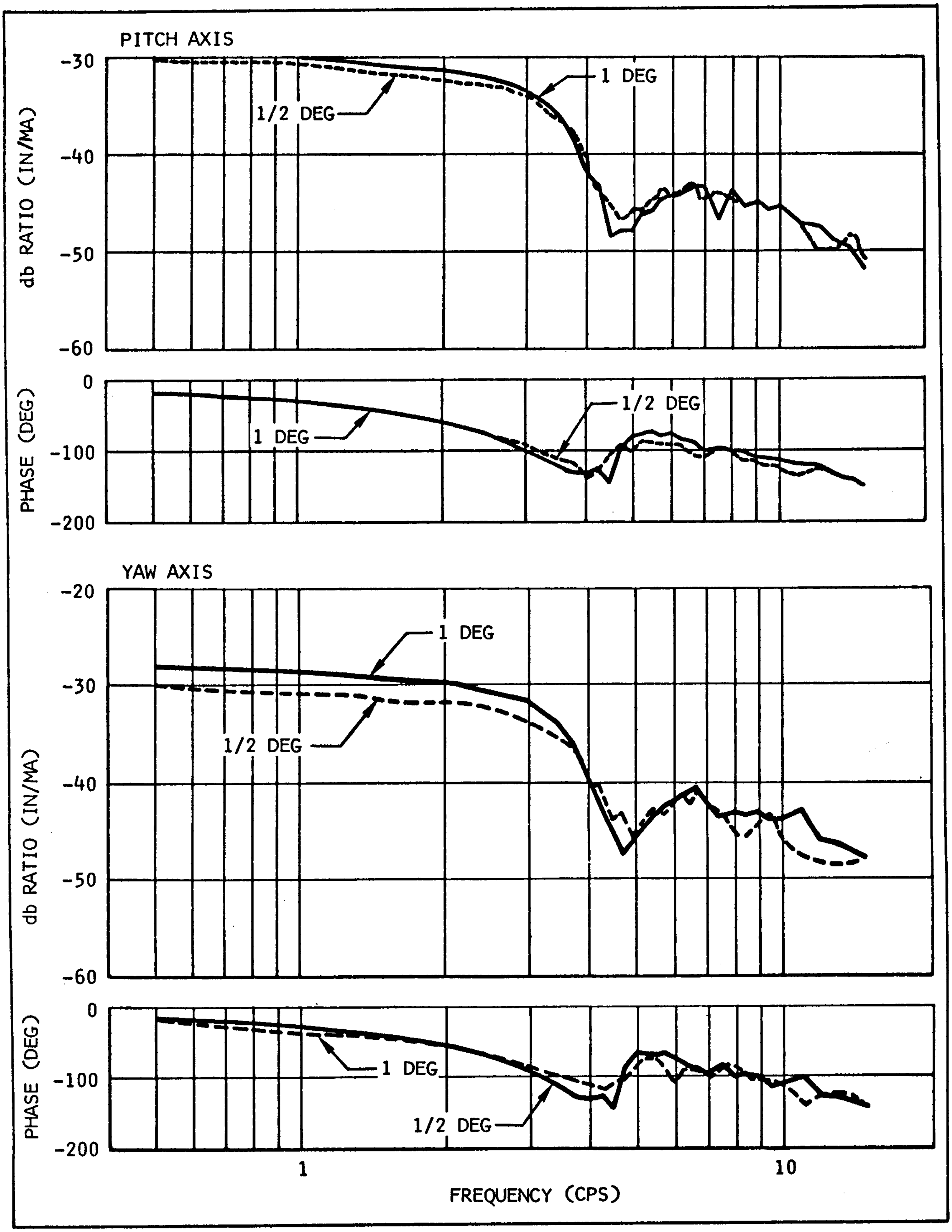

Figure 14-1 Actuator Position Response (CD 614030)

21 February 1966

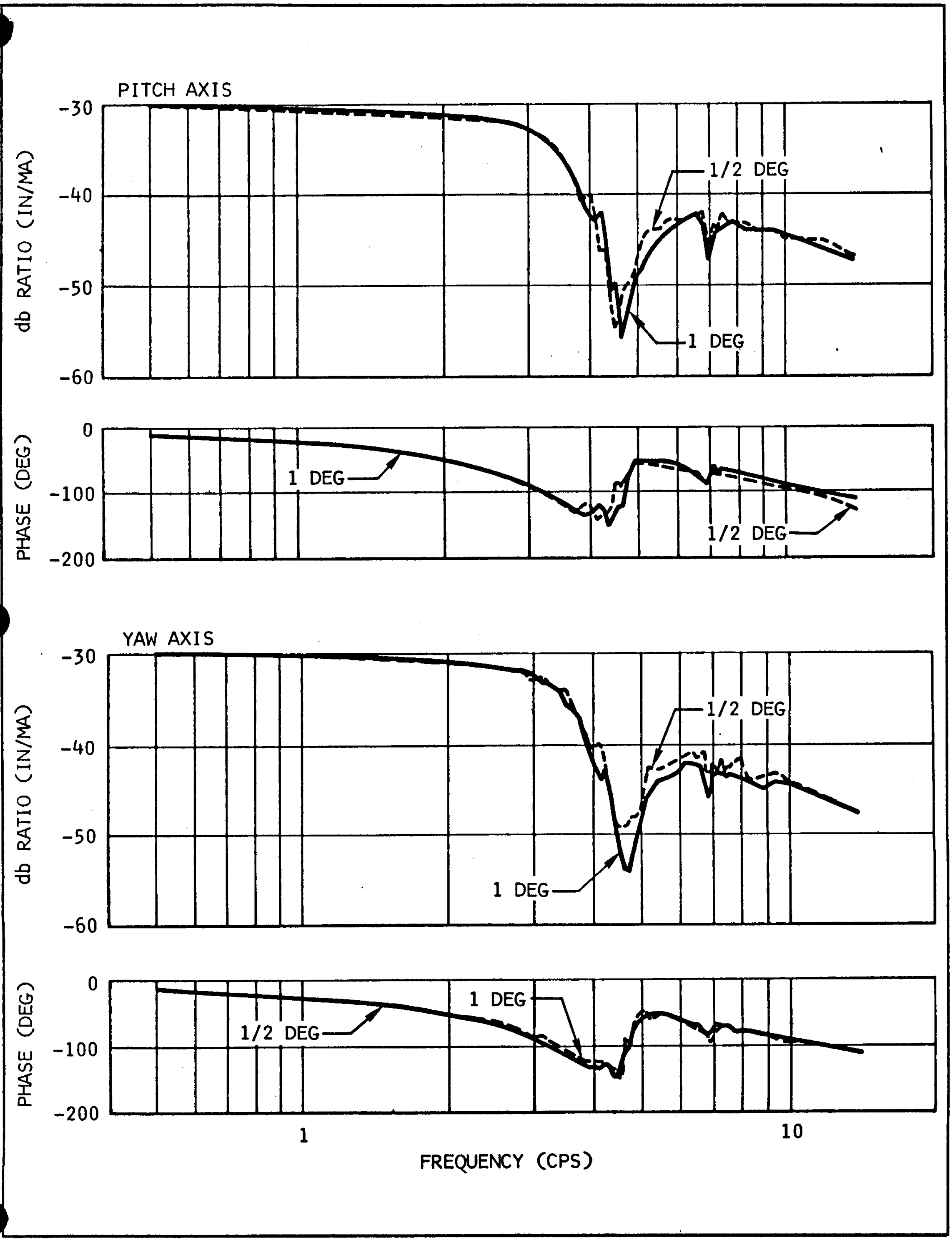

Figure 14-2 Actuator Position Response (CD 614043)

21 February 1966

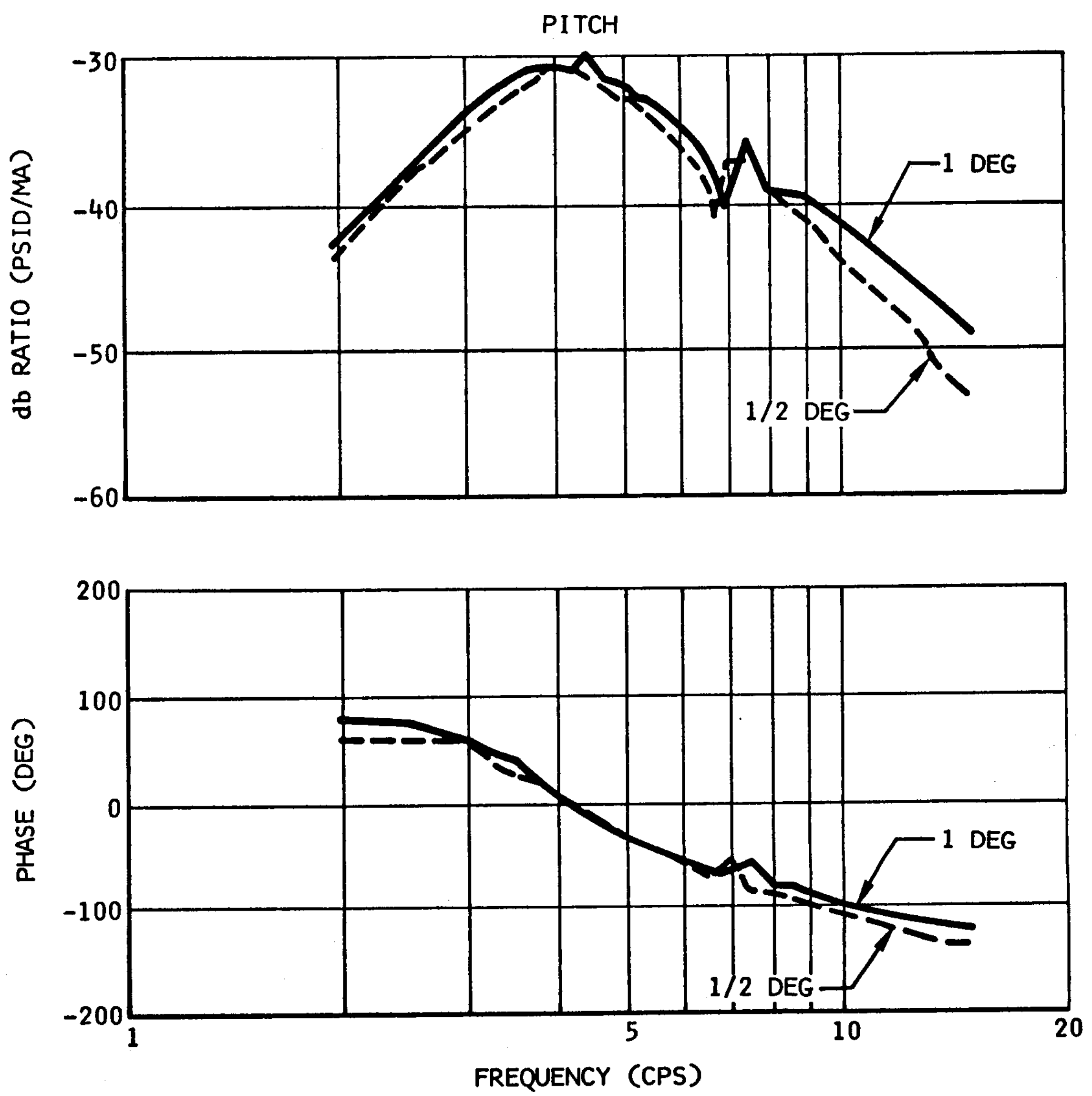

Figure 14-3 Actuator Differential Pressure Response (Sheet 1 of 2)

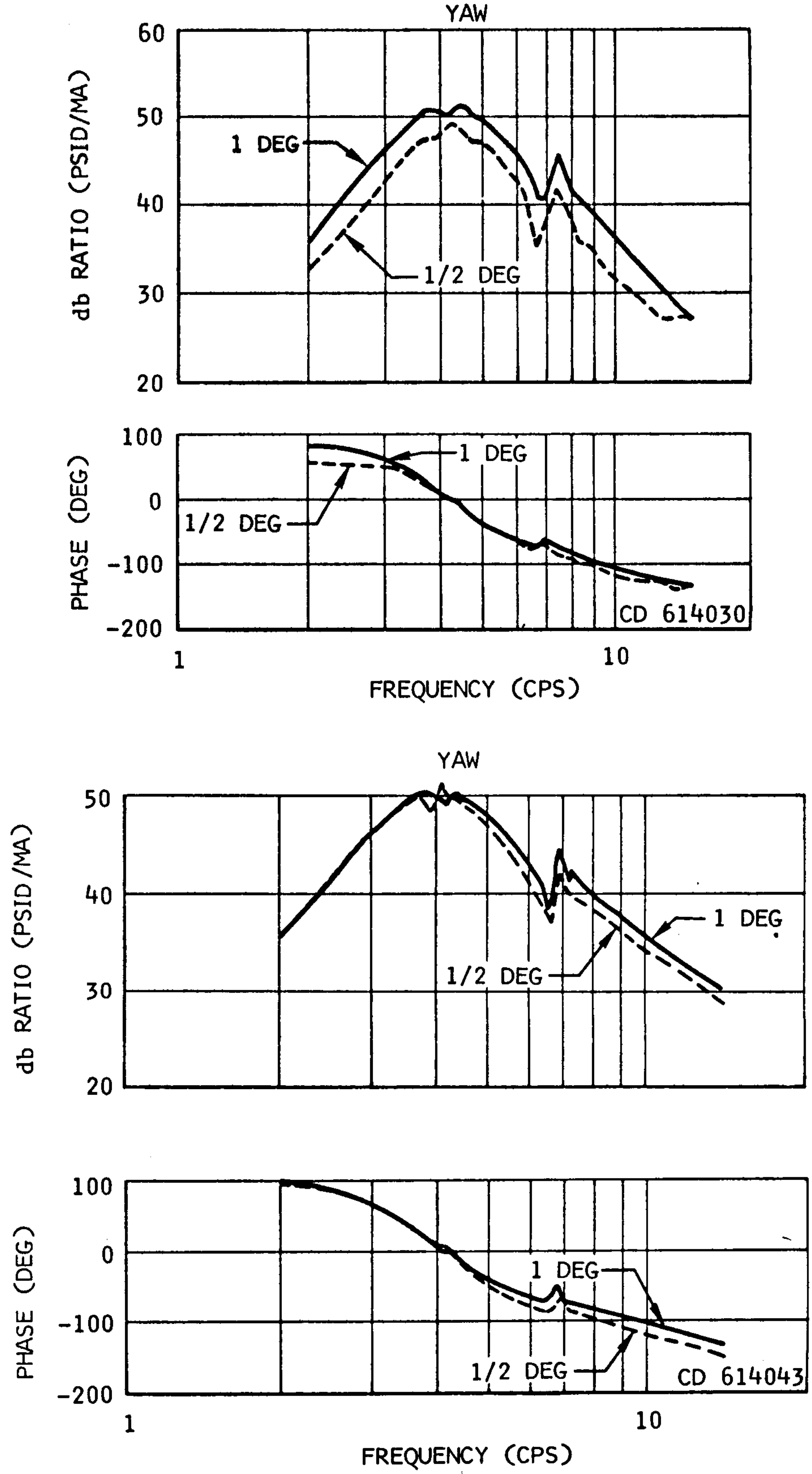

Figure 14-3 Actuator Differential Pressure Response (Sheet 2 of 2)

21 February 1966

SECTION 15

THRUST VECTOR CONTROL

15. THRUST VECTOR CONTROL

15.1 General

Engine thrust vector control system tests were conducted on both the battleship S-IVB/IB and S-IVB/V configurations during ambient and hot firing conditions. These tests were conducted in order to obtain information to accurately define the values of the thrust vector control system parameters and verify satisfactory performance of the thrust vector control system under engine firing conditions. The values of control system parameters are necessary for use in an analytical model which has been developed for flight control system stability studies and flight performance predictions.

The parameter values obtained did not accurately represent those to be expected during flight. Several nonflight conditions existed which altered the control system response. The more significant of these conditions were the use of a nonproduction thrust structure, dynamic compliance of the test stand, the low (sea level) thrust, and the high temperature environment of the engine gimbal bearing. As a result of these conditions, analysis is necessary to extrapolate the thrust vector control system test results to flight conditions such that accurate system parameters can be established for inclusion into the flight control system mathematical model.

15.2 S-IVB/IB

Individual engine gimbaling tests conducted on the S-IVB/IB battleship vehicles are described in the following paragraphs.

15.2.1 Ambient Spring Rate Verification Test

This test was conducted to verify correct setting of the thrust structure spring simulators.

15.2.2 Ambient Engine Gimbaling Test

This test was conducted to checkout test procedures and instrumentation, and to obtain ambient gimbaling data for comparison with hot gimbaling data.

15.2.3 Hot Firing Engine Gimbaling Test

This test was conducted to determine engine operational effects on the thrust vector control system.

15.3 S-IVB/V

15.3.1 Ambient Checkout

This test was conducted to checkout instrumentation and obtain ambient gimbaling data for comparison with hot gimbaling data.

15.3.2 Hot Gimbal Test

This test was conducted utilizing a finely incremented frequency response command tape to enable more accurate definition of control system and test stand resonances.

15.3.3 Ambient and Hot Gimbal Test

This test was conducted primarily to obtain information on low frequency and amplitude phase and gain characteristics of the engine control system.

15.4 Test Objectives

The general objective of the battleship engine gimbaling tests was to determine the response of the thrust vector control system to various commands for both ambient and hot gimbaling environments. Specific major test objectives are as follows:

a. Determine control system closed loop frequency response characteristics.

b. Determine engine actuator control system non-linearities with low frequency, low amplitude commands.

c. Determine the effect of gimbal friction on the engine control system.

d. Determine control system dynamic response to a step command.

e. Determine engine cross-axis coupling effects in the non-gimbaling plane.

15.5 Test Results

The thrust vector control system test parameters of interest consisted of the engine position, actuator piston position, the actuator differential pressure, and the input current to the actuator servo-valve. Typical frequency response plots are presented in figure 15-1.

As previously noted, a nonflight condition which existed during the battleship gimbal tests was the dynamic compliance of the test stand. The test stand dynamic compliance was coupled into the control system responses as evidence in figure 15-1. The test stand resonant frequencies were observed at approximately 4.4 and 7.0 cps.

Results of the frequency response tests (S-IVB/IB and S-IVB/V configurations) are summarized in table 15-1. Special low frequency phase and gain results obtained from camera data during CD 614044 are presented in table 15-2. The phase lag tends to increase and the gain tends to decrease as the command amplitude is reduced. This indicates the existence of nonlinearities, primarily, gimbal friction effects in the control system loop.

Since gimbal friction effects appear in a critical control system frequency range, analyses were performed to determine the value of gimbal friction experienced during the battleship gimbaling tests. This value was obtained through analysis of the engine response to triangular wave inputs during an engine firing.

From the triangular wave data during hot gimbaling, gimbal friction was obtained as shown in figure 15-2. By a straight line approximation of the data points, an evaluation of both coulomb and viscous friction was obtained. Viscous friction values ranging from 180 to 220 lbf-sec/deg were obtained. Coulomb friction values ranging from 720 to 1,040 lbf at the actuator were obtained. It is significant to note that friction values for both positive and negative velocities were not equal. This fact indicates the presence of thrust offset effects or moments on the engine induced by bellows and inlet lines. These ground test results were then extrapolated to the estimated flight conditions.

Figure 15-3 is a plot of NAA/Rocketdyne data and is presented as gimbal bearing dynamic coulomb coefficient of friction for the temperature range of -160 to 60 deg F. The friction values obtained from the battleship test triangular wave analysis are included at the ground test temperature of 40 deg F. Also shown is an extrapolation of battleship test gimbal friction results over the entire temperature range.

Table 15-3 is a summary of the battleship test viscous and coulomb gimbal friction results and includes extrapolated values of coulomb friction for the expected S-IVB/IB and S-IVB/V flight conditions.

Additional information on the control system response was derived from transient response results. Figure 15-4 presents transient response results for actuator position and actuator differential pressure obtained during a square wave step pattern which extended the engine to full deflection. Actuator rates and corresponding actuator load pressure responses are included. The minimum actuator rate of 1.72 in./sec is acceptable for vehicle control during flight. Transient response results for engine position obtained from camera data are presented in figure 15-5.

Engine cross-axis coupling during battleship gimbaling was analyzed during a thrusting condition utilizing the camera film data. Based on this data cross-axis coupling was considered negligible.

15.6 Conclusion

Evaluation of the battleship engine gimbaling test data indicated that all test objectives were fulfilled. The thrust vector control system closed loop response behaved as predicted and satisfied performance requirements. The effect of gimbal friction in the thrust vector position control loop was demonstrated from the test data. Preliminary values of gimbal friction have been obtained for battleship testing conditions and these values have been extrapolated to flight conditions for the S-IVB/IB and S-IVB/V stage. The battleship test gimbal friction results lie within the range but at the lower level predicted by NAA/Rocketdyne. Additional analyses, based on battleship frequency response results, are being conducted to verify the gimbal friction values. The thrust vector control system flight operation is critical at low frequencies from the aspect of stage stability. In order to accurately evaluate the control system stability during flight, the extent and effect of engine gimbal bearing friction are being pursued further.

TABLE 15-1
SUMMARY OF FREQUENCY RESPONSE RESULTS

COMMAND / VARIABLE	MAXIMUM GAIN (db) (INDICATED VARIABLE/INPUT CURRENT) ±1/4 DEG (1.66 ma)	±1/2 DEG (3.32 ma)	±1 DEG (6.64 ma)	RESONANT FREQUENCY (CPS) ±1/4 DEG (1.66 ma)	±1/2 DEG (3.32 ma)	±1 DEG (6.64 ma)	PHASE LAG AT 1.0 CPS (DEG) ±1/4 DEG (1.66 ma)	±1/2 DEG (3.32 ma)	±1 DEG (6.64 ma)
SPRING RATE VERIFICATION (S-IVB/IB) CD 614026 RUN 1									
ΔPθ	---	51.0 psi/ma	---	---	3.35	---	---		---
ΔPψ	---	52.1 psi/ma	---	---	3.58	---	---		---
δAθ	---	-30.4 in./ma	---	---	4.06	---	---	-27.0	---
δAψ	---	-30.2 in./ma	---	---	4.06	---	---	*	---
δMθ	---	-11.9 deg/ma	---	---	3.25	---	---	*	---
δMψ	---	*	---	---	*	---	---	*	---
AMBIENT GIMBAL TEST (S-IVB/IB) CD 614026 RUN 2									
ΔPθ	50.4 psi/ma	50.8 psi/ma	51.2 psi/ma	3.2	3.45	3.45			
ΔPψ	51.7 psi/ma	51.9 psi/ma	52.4 psi/ma	3.2	3.72	3.96			
δAθ	*	*	*	*	*	*	*	*	*
δAψ	*	*	*	*	*	*	*	*	*
δMθ	*	-11.9 deg/ma	-13.3 deg/ma	*	3.2	3.2	*	*	*
δMψ	*	*	*	*	*	*	*	*	*
HOT GIMBAL TEST (S-IVB/IB) CD 614030									
ΔPθ	45.4 psi/ma	49.4 psi/ma	49.2 psi/ma	4.22	3.97	3.97			
ΔPψ	44.0 psi/ma	49.3 psi/ma	49.5 psi/ma	4.21	4.22	3.97			
δAθ	-32.3 in./ma	-30.2 in./ma	-29.6 in./ma	5.69	4.70	4.46	-35.8	-30.9	-30.6
δAψ	-31.0 in./ma	-29.9 in./ma	-29.5 in./ma	5.69	4.96	4.71	-31.0	*	-31.0
δMθ	*	-16.8 deg/ma	-16.2 deg/ma	*	3.20	3.45	*	*	*
δMψ	*	-16.6 deg/ma	-15.5 deg/ma	*	3.45	3.45	*	*	*
HOT GIMBAL TEST (S-IVB/V) CD 614043									
ΔPθ	---	49.8 psi/ma	50.2 psi/ma	---	3.98	3.87	---		
ΔPψ	---	50.7 psi/ma	50.4 psi/ma	---	3.75	3.85	---		
δAθ	---	-30.15 in./ma	-29.8 in./ma	---	4.50	4.55	---	-25.5	-25.0
δAψ	---	-29.7 in./ma	-29.6 in./ma	---	4.65	4.70	---	-27.7	-27.5
δMθ	---	*	-14.7 deg/ma	---	*	3.2	---	*	-31.0

ΔPθ = Actuator Differential Pressure - Pitch Plane
ΔPψ = Actuator Differential Pressure - Yaw Plane
δAθ = Actuator Piston Position - Pitch Plane
δAψ = Actuator Piston Position - Yaw Plane
δMθ = Engine position - Pitch Plane
δMψ = Engine Position - Yaw Plane

*Invalid Data

--- = Not Conducted

TABLE 15-2
Engine Position Phase And Gain Results

COMMAND \ FREQUENCY	PHASE LAG (DEG)		GAIN (DEG/MA) db	
	0.5 (CPS)	1.0 (CPS)	0.5 (CPS)	1.0 (CPS)
±3/4 Deg	-22 ±2	-31 ±2	-17.8	-17.8
±1/2 Deg	-22 ±2	-31 ±2	-18.0	-18.0
±1/4 Deg	-30 ±2	-41 ±2	-18.5	-18.5
±1/8 Deg	-44 ±2	-54 ±2	-18.5	-18.5

TABLE 15-3
Gimbal Bearing Friction-Battleship And Flight Extrapolation

CONDITION	MAXIMUM	MINIMUM
Viscous Friction During Battleship Tests (S-IVB/IB)	220 lb-sec/deg	180 lb-sec/deg
Coulomb Friction During Battleship Tests (S-IVB/IB)	1,040 lb	720 lb
Coulomb Friction During Engine Start (S-IVB/IB)	3,600 lb	2,190 lb
Coulomb Friction During S-IVB/IB Burn	3,510 lb	3,100 lb
Coulomb Friction During S-IVB/V First Burn	4,140 lb	3,000 lb
Coulomb Friction During S-IVB/V Second Burn	4,250 lb	3,200 lb

NOTE: Values presented represent equivalent friction forces seen at the actuator.

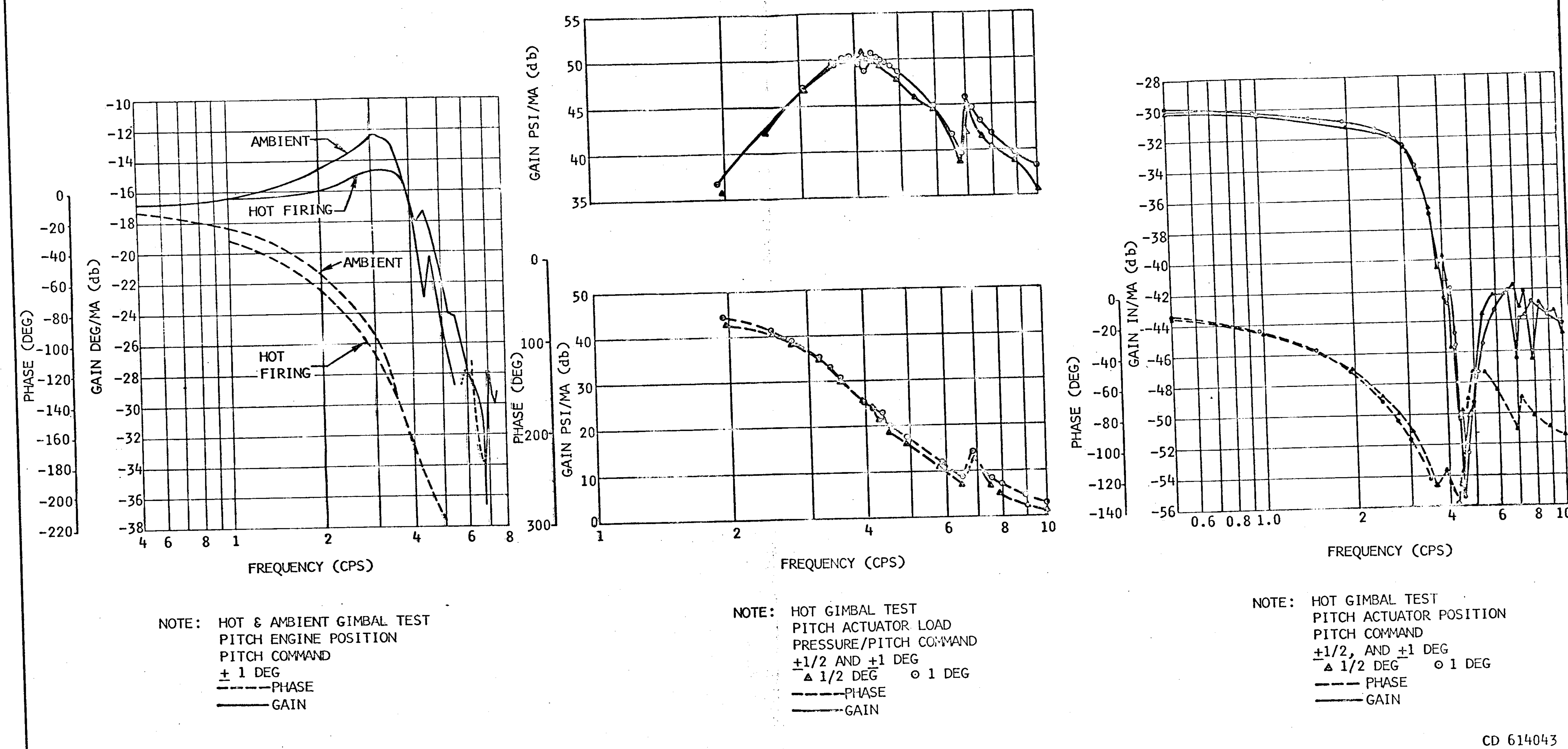

Figure 15-1 Frequency Response

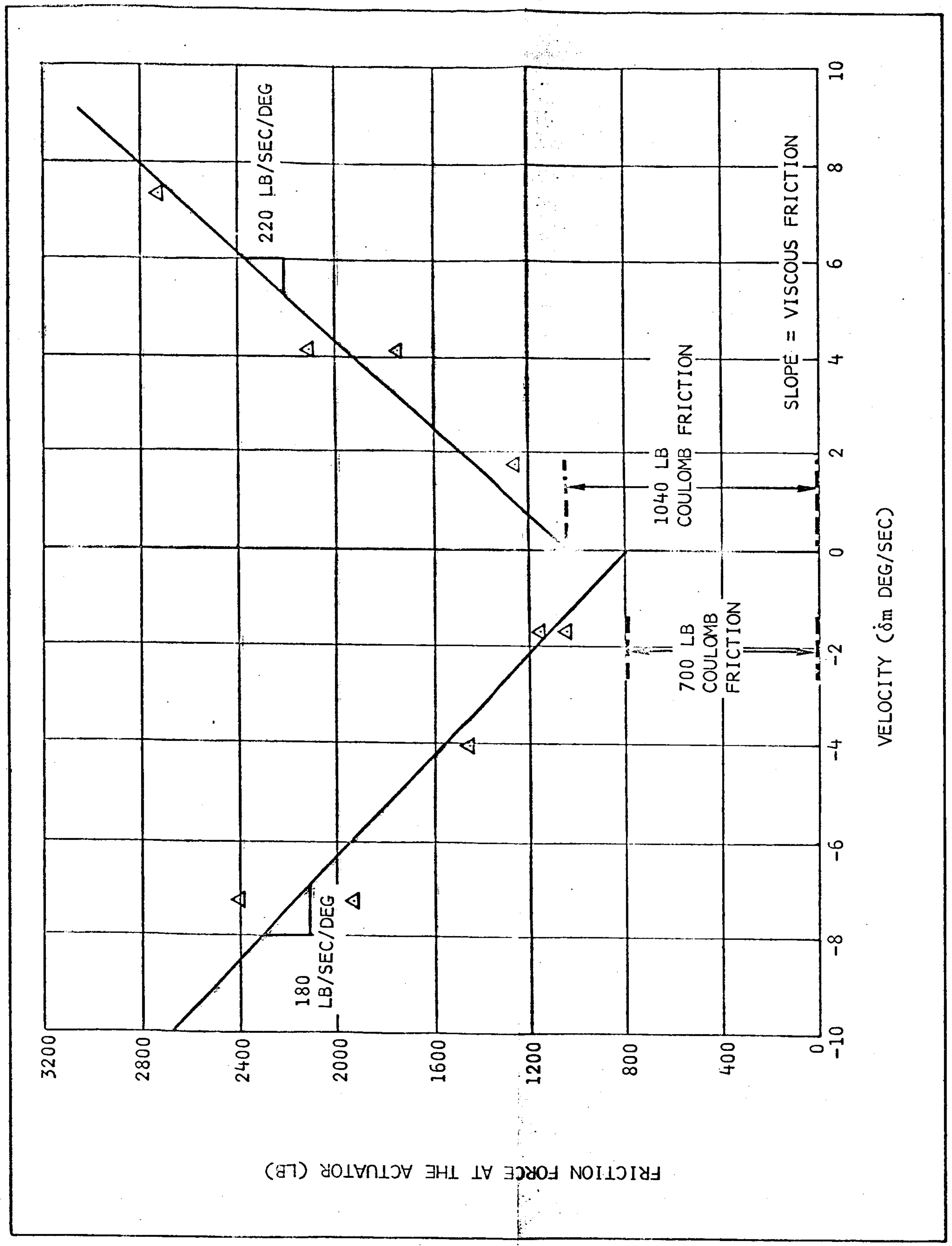

Figure 15-2 Gimbal Friction

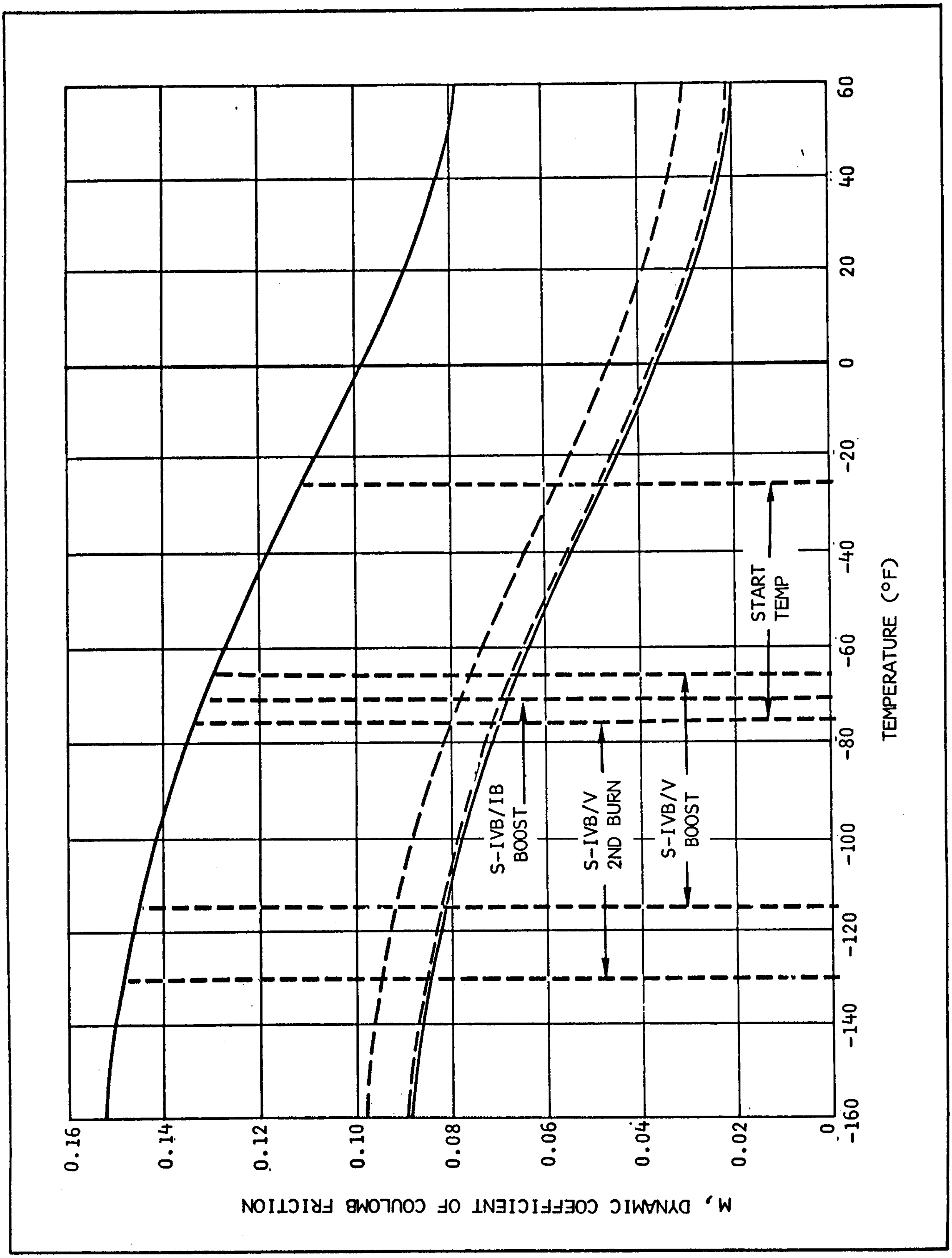

Figure 15-3 Gimbal Bearing Dynamic Coulomb Coefficient of Friction

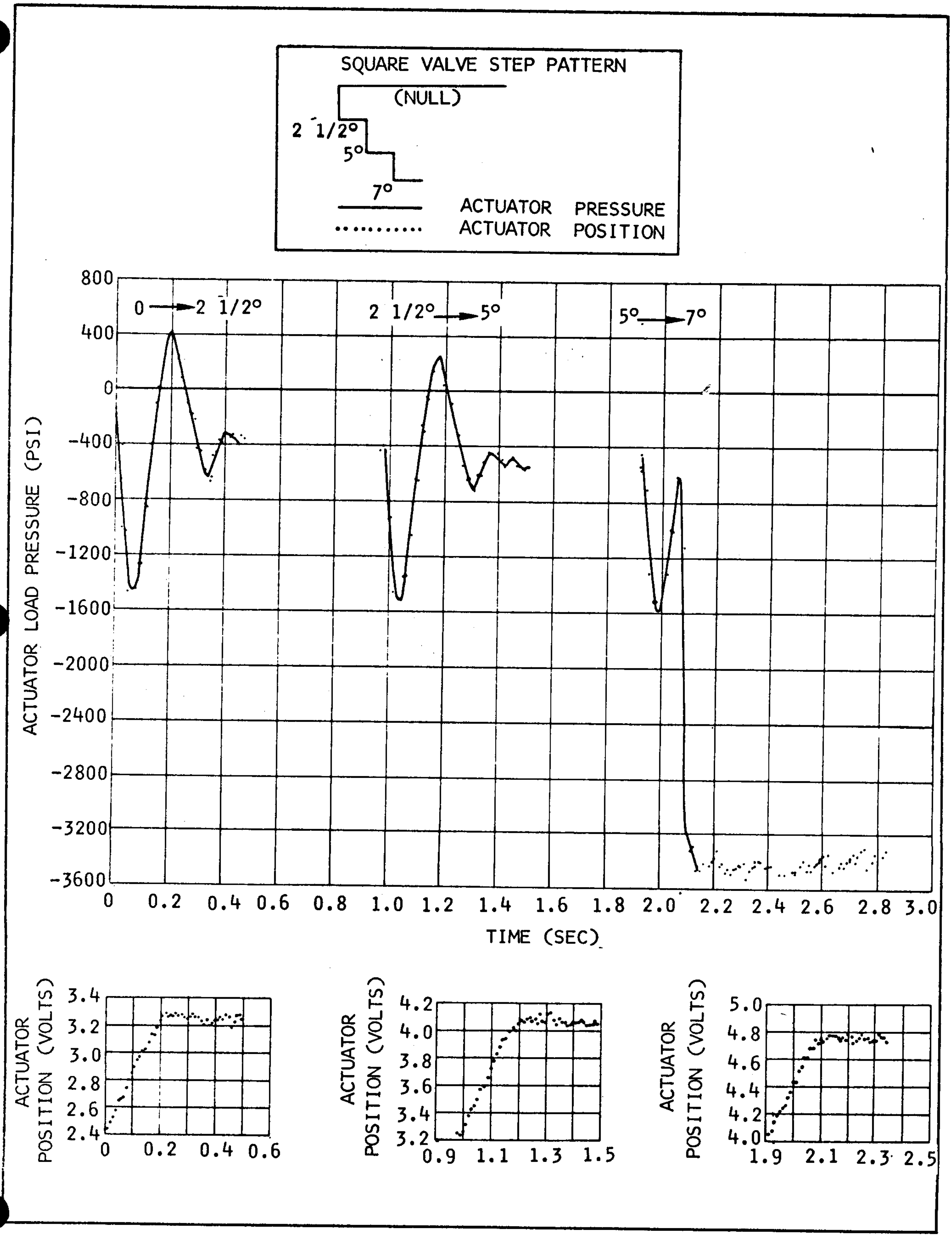

Figure 15-4 Transient Response Results

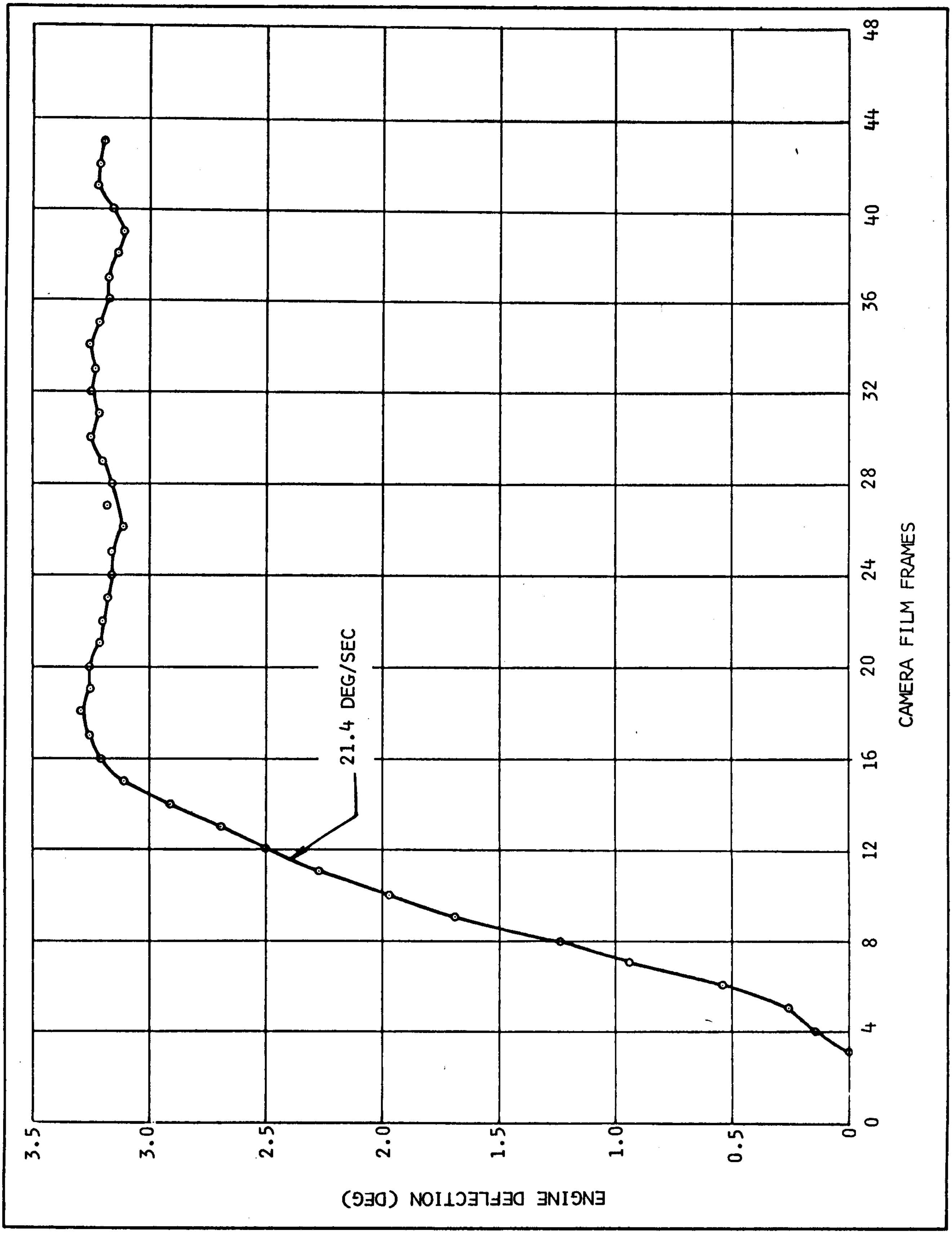

Figure 15-5 Transient Response for Engine Position

21 February 1966

SECTION 16

ACOUSTIC AND VIBRATION ANALYSES

16. ACOUSTIC AND VIBRATION ANALYSES

A total of fifty-nine acoustic and vibration parameters were monitored during the S-IVB battleship program. Data from sixteen countdowns (eighteen firings) were reduced and are included in this report. The shortest firing from which data are reported was CD (countdown) 614007 with a duration of 10.67 sec. Firings of shorter duration are not reported as stable mainstage data of sufficient duration for analysis were not obtained.

No distinction is made in this report between the S-IVB/IB and S-IVB/V phases of the program as no differences affecting the acoustic or vibration environment were present.

In general, data obtained over several firings from a particular parameter were very repeatable. The majority of the parameters monitored, both acoustic and vibration, exhibited high levels at ESC (Engine Start Command) and ECO (engine cutoff). These levels ranged from 2 db to 7 db higher than the steady-state levels during mainstage. At engine start, the transients lasted from two to seven seconds. The engine cutoff transients lasted from 0.5 to 1.5 sec after command cutoff.

The vibration measurements were generally restricted to locations on the engine because of the difference in the battleship structure (steel) and the flight type stage structure (aluminum). The measured vibration levels were lower than expected below 800 cps.

The acoustic measurements were located both in the far field (150 ft from the stage) and in the near field (immediate vicinity of the stage). The measured acoustic levels were as expected in the vicinity of the thrust structure but were lower than expected in the forward areas of the stage.

16.1 Data Acquisition

Thirty-five vibration and twenty-four acoustic parameters were monitored during the program. A list of the parameters including measurement number, composite levels, and data quality is presented in table 16-1. Composite levels are given during two time periods. The levels under "start transient" represent the high levels monitored during ignition, while the "mainstage" levels show the steady-state levels existing from approximately ESC +7 sec to engine cutoff. The location of the acoustic and vibration parameters are shown in figures 16-1 and 16-2.

16.1.1 Sequence of Acquisition

The acoustic parameters were divided into three groups. Two in the aft skirt region were monitored from CD 614020 to the end of the program (14 firings). Eleven far field parameters were monitored from CD 614024 to CD 614030 (4 firings), and eleven near field parameters were monitored from CD 614033 to CD 614044 (7 firings). The vibration parameters were also divided, with one group monitored from CD 614007 to CD 614030 (11 firings) and a second group monitored from CD 614033 to CD 614044 (7 firings). Eleven vibration parameters were monitored throughout the program (18 firings). The maximum number of parameters monitored on any one firing was thirty-three.

16.1.2 Data Recording

Three separate instrumentation systems were used to obtain the data. First was a "flight" type system using components designed to the flight stage environment, power and weight restrictions, and automatic checkout requirements. It consisted of a piezoelectric accelerometer or microphone, coaxial cable and a transistorized charge amplifier with relay controlled voltage insertion capabilities for calibration purposes. The second system was typical of those used during the S-IV static test program and consisted of a piezoelectric accelerometer, coaxial cable and a high input impedance ac voltage amplifier. The output from two of these channels (thrust chamber dome) was split to provide signals for the Rocketdyne vibration safety cutoffs in addition to the data signals. The vibration safety cutoffs monitored the vibration on the engine and provided an automatic engine cutoff if the vibration trend indicated impending destruction of the engine. The third system was used for the far field and near field acoustic surveys, and consisted of a microphone, coaxial cable, and a laboratory type charge amplifier.

All signals were FM tape recorded at 30 ips using a 54 kcps carrier. The available frequency response was 5 cps to 10 kcps on vibration parameters and 10 cps to 10 kcps on acoustic parameters. Six tape recorders were available throughout the program, of which four were used during a countdown. All data channels were calibrated prior to each countdown by the "voltage insert" method per 1B49437 using test set model DSV-4B-717.

16.2 Data Reduction

In anticipation of the use of the single sideband telemetry system for acoustic and vibration data acquisition on the S-IVB stages (frequency response 50 to 3,000 cps), all vibration data were reduced from 10 to 3,000 cps. This will permit a direct comparison of the hardwire and telemetry data. The acoustic parameters were reduced to the limits of the system, i.e., 10 cps to 10K cps.

Data reduction consisted of producing oscillograms of all channels after each firing. These records were produced by Data Processing at Huntington Beach using 5 Kcps Galvanometers with a paper speed of 0.4 ips during mainstage and 4.0 ips during the transients at engine start and cutoff. These oscillograms were used as the basis for preliminary data qualification. An oscilloscope was also used for very high frequency (10,000 cps) data qualification. All parameters considered valid were analyzed with one-third octave band filters. The one-third octave RMS time histories for the acoustic parameters were read during start transient and mainstage portions and plotted as decibels (db) vs frequency.

The vibration data were digitized at 8,000 samples per sec and analyzed using the IBM 7094 computer and computer program DA05. This program produced SC4020 plots of the auto correlation function and PSD (power spectral density) spectrum. A tabulation of the PSD values was also stored on digital magnetic tape. A bandwidth of 20 cps was used for all PSD analyses.

After all firings were reduced, the stored vibration PSD's from the digital magnetic tape were input to computer program DA07 which provided SC4020 plots of maximum, minimum, and mean values from a particular parameter or group of parameters. The acoustic data were enveloped and plotted by hand.

16.3 Discussion of Parameters

Thirty-two vibration parameters and all 24 of the acoustic parameters produced valid data during at least one countdown and firing. Three vibration parameters (E-0564, E-0575 and E-0578) did not produce valid data during the program. Considering a parameter monitored on one countdown as a measurement, a total of 535 measurements were attempted of which 289 were successful for a recovery rate of 54 percent.

Three basic test objectives were to be met during the program. These are discussed separately in the following paragraphs.

16.3.1 VB501 - Determination of the Acoustic Field Generated by the J-2 Engine

During countdowns 614025, 614028, and 614030, eleven microphones were placed on an arc 150 ft from the stage centerline, as shown in figure 16-1. Each microphone was placed at the top of a six foot stand with the diaphragm facing the stage. Spectra are shown for each measurement in figure 16-3, plotted in octave bands, and the overall levels are shown on a polar plot in figure 16-4. All levels presented are the maximum envelope of data from three firings. The polar plot shows that a maximum level of 141 db occurred 48 deg from the direction of the deflected exhaust gases (bucket centerline) which is close to the expected angle of 55 deg. The plot also shows a drop in level between 75 and 105 deg which is attributed to masking of the sound source by the test stand structure.

In the second phase of acoustic measurements, the microphones were relocated. Six were placed on a vertical line 12 ft from the stage centerline (6 to 12 in. from the tank skin) with the diaphragms pointed away from the stage, and four were placed on a radial line at distances of 25, 75, 300, and 600 ft from the stage with the diaphragms pointed toward the stage. All were located 55 deg from the bucket centerline. The eleventh microphone (B-0713) was placed on the helium fairing at position II. These locations are shown in figure 16-1.

Spectra from these microphones are shown in figure 16-5 and a profile of the overall levels is shown in figure 16-6. These spectra are the maximum envelope from five firings (CD 614042, CD 614043, and CD 614044). Data from CD 614033 and CD 614034 were considered invalid due to calibration errors.

The spectra in figure 16-5, from B-0706 and B-0707 show high overall levels dominated by high frequency components. This was due to the proximity of these microphones to the high frequency sources generated at the J-2 engine nozzle exit plane. Moving up the stage, the high frequency levels decreased more rapidly than the low frequency levels and the spectra tended to flatten. The data in figures 16-3 and 16-5 (B-0702, B-0706, B-0712, B-0714, B-0715 and B-0716), show that the overall levels decreased approximately 5.5 db each time the distance from the stage centerline doubled. This compares well with a theoretical decay of 6.0 db/double distance and experimentally measured free field decays of 5.5 db/double distance.

The near field acoustic measurements (6 to 12 in. from tank skin) were compared with similar data obtained by Rocketdyne during J-2 engine development firings. The Douglas measurements in the vicinity of the thrust structure show good agreement with the Rocketdyne data. The levels forward of the aft skirt however, were 5 to 8 db lower than the Rocketdyne data. These lower levels are attributed to masking of the sound source by the test stand structure.

16.3.2 VB 502 - To Monitor the Environment at the Gimbal Point, Thrust Chamber Dome, Turbopumps, Primary Instrumentation Package, and Ambient Panels No. 1 and 17

Three accelerometers were mounted on the gimbal block and oriented to measure vibration on the thrust (E-0511), pitch (E-0512), and yaw (E-0513) directions. Two accelerometers were mounted on the thrust structure at the attach points of the pitch (E-0561) and yaw (E-0562) actuators, oriented in the thrust direction. These locations are shown in figure 16-2. The data from these parameters are shown in figure 16-7*. Each parameter exhibited a relatively narrow amplitude band indicating very repeatable data. Also, the spectra of E-0512 and E-0513 were essentially identical, as were the spectra from E-0561 and E-0562. This was expected, as the stage is symmetrical in the pitch and yaw planes. All three gimbal point measurements exhibited a narrow peak at approximately 920 cps; the yaw measurement also showed a peak at 460 cps. These frequencies are the first and second harmonics of the LH2 turbopump rotational frequencies. These five parameters show the vibration input to the thrust structure from the engine.

During the first thirteen firings in the program, the primary instrumentation package was instrumented with three accelerometers. The accelerometers were oriented to monitor the vibration input to the package in the thrust (E-0505) radial (E-0506) and tangential (E-0507) axis. However, because of mounting

*Each plot in figures 16-7 through 16-12 presents a maximum, minimum, and mean spectrum computed using all valid data from that parameter difficulties, the accelerometers were located on the cover of the package and provided response instead of the required input vibration data (figure 16-7).

Two accelerometers on the combustion chamber dome (Rocketdyne vibration safety cutoffs No. 1 and 2) and one accelerometer on each of the propellant turbopumps were used to monitor vibration throughout the battleship program. The locations of these parameters are shown in figure 16-2 and the enveloped spectra are presented in figure 16-8. The spectra from the safety cutoffs, E-0706 and E-0707, showed good agreement from firing to firing and between the two parameters indicating uniform engine vibration. The data below 200 cps should not be used however, due to the presence of 60 cps noise and its harmonics at 30 cps and 180 cps.

The turbopump accelerometers were each mounted at the flange between the pump housing and the respective Rocketdyne low pressure duct feedline and were oriented radial to the housing. The data from these measurements (figure 16-8) are highly questionable. Very high amplitudes at approximately 6 Kcps overdrove the instrumentation recording system. The effect on the data in the frequency range of interest (5 to 3 Kcps) is not known but consistent data were not obtained from either parameter during the program. The data presented for the LH2 pump show agreement, but only two countdowns are shown and the levels are very low. Due to these problems, no attempts were made to determine if bearing degradation in the pumps could be determined.

Six vibration measurements and two acoustic measurements were mounted on ambient panels in the aft skirt. Vibration transducers were mounted in the thrust, radial, and tangential directions on both panel No. 1 and panel No. 17. E-0500, E-0501, and E-0502 were mounted on the sequencer panel (No. 1) near module A-10. E-0574, E-0575, and E-0576 were mounted on the 56 vdc power distribution panel near module A-1. These locations are shown in figure 16-2. Also shown in the figure are acoustic measurements B-0501 and B-0502. B-0501 was mounted at the upper left corner of the sequencer panel (No. 1) with its sensitive axis through the stage centerline on a 45 deg downward slope. B-0502 was mounted directly below panel No. 17 with its sensitive axis normal to the stage centerline.

Spectra from five of the vibration measurements and the two acoustic measurements are shown in figure 16-9. No valid data were obtained from E-0575. The vibration measurements exhibited similar spectra dominated by one broad peak, which shifted in frequency from parameter to parameter. It was expected that the highest vibration levels would be monitored in the radial direction due to acoustical excitation of the panels. This is not supported by the data. The vibration response on panel No. 1 was highest in the tangential direction. The data from B-0501 and B-0502 are shown in the same figure plotted in one-third octave bands. Two curves are presented on each plot. The higher spectrum on each plot is the maximum envelope of the steady-state data from countdowns 614020 through 614034. The lower spectrum is the maximum envelope of the steady-state data from countdowns 614042 through 614044. The drop in level during the later firings was due to the installation of a cover in the aft skirt area. Both sets of data are considered valid. The attenuation attributed to the cover is the difference between the two curves.

16.3.3 VB504 - Determine the Vibration Response of Selected Components

Measurements were mounted on the actuator servo-valves, propellant feedlines, PU valve, gas generator and the main hydraulic pump. The locations of these measurements are shown in figure 16-2.

Three accelerometers were mounted on each actuator (pitch and yaw) servo valve and oriented in directions radial (normal), axial, and tangential to the valve. Enveloped spectra from these measurements are shown in figure 16-10. E-0503 and E-0504 are highly contaminated with 60 cps noise. The levels at 20 cps, 60 cps, 180 cps, 300 cps, and 420 cps are subharmonics and harmonics of 60 cps and are not data. The spectra are included in this report to show the data above 500 cps which are considered valid. In this region, the measurements exhibited a broad peak between 400 cps and 900 cps. The data also exhibited a very narrow band of amplitude scatter. This was meaningful in the case of E-0503, E-0504, and E-0573 as data from five or more firings were included. The plots may be biased however, for E-0570, E-0571, and E-0572, as data from only one firing were available.

Three accelerometers were located on the PU valve, oriented to sense vibration in directions axial (E-0508), radial (E-0509), and tangential (E-0510) to the valve. The location of the measurements is shown in figure 16-2 and the spectra are presented in figure 16-11. The spectra all exhibit peaks in the region of 2 Kcps. In addition, the radial measurement shows a peak at approximately 150 cps. The tangential measurement shows peaks at 150, 300, and 450 cps, and a narrow peak at 900 cps. These frequencies were caused by energy from the LH2 turbopump, on which the valve was mounted.

Two accelerometers were mounted on the gas generator as shown in figure 16-2. The measurements were oriented in the thrust (E-0577) and radial (E-0578) directions. The lateral measurement provided no usable data. The envelope of data from the thrust measurement is presented in figure 16-11. Below 100 cps the data are invalid due to 60 cps noise.

The main hydraulic pump was instrumented with two accelerometers oriented in the thrust (E-0563) and lateral (E-0564) directions. The lateral measurement provided no usable data. An envelope of the thrust data is presented in figure 16-11. The spectrum is dominated by a broad peak at 150 cps and narrow peaks at 1,300 cps, 2,200 cps, and 2,400 cps.

Two accelerometers were mounted on each propellant feedline at the attachment points to the Rocketdyne low pressure ducts. Each pair were oriented in the thrust and lateral directions (parallel and normal to flow). The measurement locations are shown in figure 16-2 and the enveloped spectra are presented in figure 16-12. Both thrust measurements, E-0557 and E-0559, are considered questionable due to a cantilever design for the accelerometer mounting block. The lateral measurements exhibit good agreement and repeatability, although the spectrum of E-0558 is invalid below 60 cps due to instrumentation system noise. The LH2 feedline measurement (E-0560) does show very narrow peaks at 900 cps and 2,500 cps, which are not present in the LOX feedline measurement. These are localized vibrations generated by the LH2 turbopump.

TABLE 16-1
SUMMARY OF ACOUSTIC AND VIBRATION MEASUREMENTS

COUNTDOWN NO.	614007	614008	614009	614010	614020	614021	614023	614024	614025	614028	614030	614033	614034	614042	614043	614043	614044	614044
WIND SPEED (MPH)	7 TO 8	5	CALM	5	2 TO 5	4 TO 6	0 TO 3	18 TO 20	10 TO 11	3	8 TO 10	NOT RECORDED	NOT RECORDED	NOT RECORDED	4		6	
WIND DIRECTION	SOUTHWEST	WEST		SOUTHEAST	W NORTHWEST	S SOUTHEAST	E SOUTHEAST	SOUTH	S SOUTHWEST	SOUTH	SOUTH				SOUTH		SOUTHWEST	
BAROMETRIC PRESSURE	29.84 mmHg	29.94 mmHg	29.90 mmHg	29.90 mmHg	30.66 mmHg	30.10 mmHg	29.73 mmHg	29.91 mmHg	29.98 mmHg	29.84 mmHg	29.87 mmHg				29.70 mmHg		29.85 mmHg	
AMBIENT TEMPERATURE	62°F	60°F	50°F	64°F	59°F	60°F	59°F	56°F	60°F	70°F	66°F				81°F		80°F	
RELATIVE HUMIDITY	70%	59%	53%	79%	67%	78%	89%	65%	73%	63%	43%				39%		41%	
TEST DATE	12-1-64	12-9-64	12-15-64	12-23-64	3-13-65	3-19-65	3-31-65	4-7-65	4-15-65	4-27-65	5-4-65	6-19-65	6-25-65	8-13-65	8-17-65	8-17-65	8-20-65	8-20-65
TIME OF DAY	1457:10	1307:15	1519:50	1608:55	1508:15	1804:50	1711:05	1524:35	1747:25	2214:20	1327:30	1541:25	1222:37	1055:45	1141:04	1325:25	1305:20	1349:15
TEST DURATION	10.7 SEC	54.1 SEC	150.4 SEC	414.7 SEC	11.0 SEC	29.1 SEC	471.6 SEC	44.2 SEC	508 SEC	375.8 SEC	495.9 SEC	15.7 SEC	167.2 SEC	11.3 SEC	166.6 SEC	314.4 SEC	166.2 SEC	354.6 SEC

MSFC NO.	PARAMETERS	DIRECTION	614007 QUALITY	614007 START TRANSIENT	614007 MAIN STAGE	614008 QUALITY	614008 START TRANSIENT	614008 MAIN STAGE	614009 QUALITY	614009 START TRANSIENT	614009 MAIN STAGE	614010 QUALITY	614010 START TRANSIENT	614010 MAIN STAGE	614020 QUALITY	614020 START TRANSIENT	614020 MAIN STAGE	614021 QUALITY	614021 START TRANSIENT	614021 MAIN STAGE	614023 QUALITY	614023 START TRANSIENT	614023 MAIN STAGE
	VIBRATION — COMPOSITE LEVEL (G rms), FREQUENCY RANGE 10 - 3,000 cps																						
E0500	Sequencer at Module A10	Thr	V	-	4.4	I	-	-	V	-	4.0	V	-	3.9	I	-	-	I	-	-	I	-	-
E0501	Sequencer at Module A10	Rad	V	-	1.8	V	-	2.2	V	-	1.9	V	-	1.9	I	-	-	I	-	-	I	-	-
E0502	Sequencer at Module A10	Tan	V	-	8.6	V	-	9.8	V	-	7.8	V	-	7.8	I	-	-	V	-	8.0	V	-	8.0
E0503	Pitch Actuator Servo Valve	Rad																					
E0504	Yaw Actuator Servo Valve	Rad																					
E0505	Primary Instr Package	Thr	V	-	9.5	I	-	-	I	-	-	V	6.24	-	V	-	2.6	V	2.02	1.2	V	2.32	-
E0506	Primary Instr Package	Rad	V	-	9.1	V	-	8.1	V	-	9.7	I	-	-	I	-	-	V	-	5.8	V	-	9.8
E0507	Primary Instr Package	Tan	I	-	-	I	-	-	V	-	4.7	I	-	-	I	-	-	V	-	2.7	V	-	4.1
E0508	Propellant Utilization Valve	Ax	V	-	30.2	I	-	-	I	-	-	I	-	-	V	39.4	-	V	-	46.4	V	39.6	38.7
E0509	Propellant Utilization Valve	Rad	I	-	-	I	-	-	I	-	-	V	-	26.6	V	-	26.1	V	-	30.9	V	31.0	32.6
E0510	Propellant Utilization Valve	Tan	V	-	37.6	I	-	-	I	-	-	V	-	26.3	V	-	29.6	V	-	35.6	V	33.5	-
E0511	J-2 Engine Gimbal Point	Thr	V	-	2.4	V	-	2.5	V	-	2.0	I	-	-	V	-	2.1	V	-	2.1	V	-	2.2
E0512	J-2 Engine Gimbal Point	P	V	-	3.4	V	-	3.3	V	-	3.4	I	-	-	V	-	3.5	I	-	-	V	-	3.4
E0513	J-2 Engine Gimbal Point	Y	V	-	2.8	V	-	3.4	V	-	2.5	I	-	-	V	-	2.6	V	-	2.8	V	-	2.5
E0555	LOX Turbopump	Lat	V	-	16.9	V	-	14.9	I	-	-	V	7.5	-	I	-	-	I	-	-	I	-	-
E0556	LH2 Turbopump	Lat	V	-	5.2	V	-	5.0	I	-	-	I	-	-	I	-	-	I	-	-	I	-	-
E0557	LOX Feedline at Engine	Thr	V	-	6.4	I	-	-	I	-	-	I	-	-	I	-	-	V	5.23	-	V	-	6.2
E0558	LOX Feedline at Engine	Lat	I	-	-	I	-	-	I	-	-	I	-	-	I	-	-	V	-	3.9	V	-	3.9
E0559	LH2 Feedline at Engine	Thr	I	-	-	V	-	4.4	V	-	3.0	V	-	2.3	V	-	7.0	V	-	6.5	V	-	6.2
E0560	LH2 Feedline at Engine	Lat	I	-	-	V	-	9.2	I	-	-	I	-	-	I	-	-	V	-	9.7	I	-	-
E0561	Thrust Struc/Pitch Actuator Attach Pt.	Ax																					
E0562	Thrust Struc/Yaw Actuator Attach Point	Ax																					
E0563	Hydraulic Pump, Main	Thr																					
E0564	Hydraulic Pump, Main	Lat																					
E0570	Pitch Actuator Servovalve	Ax																					
E0571	Pitch Actuator Servovalve	Tan																					
E0572	Yaw Actuator Servovalve	Ax																					
E0573	Yaw Actuator Servovalve	Tan																					
E0574	Mod A1-56V Pwr Dist-Aft-Panel 17	Rad	V	-	8.8	V	-	6.0	V	-	5.3												
E0575	Mod A1-56V Pwr Dist-Aft-Panel 17	Tan	I	-	-	I	-	-	I	-	-												
E0576	Mod A1-56V Pwr Dist-Aft-Panel 17	Ax	V	-	4.1	I	-	-	V	-	3.2												
E0577	Gas Generator	Thr													I	-	-	V	-	9.2	I	-	-
E0578	Gas Generator	Rad													I	-	-	I	-	-	I	-	-
E0706	Vibration Safety Cutoff No. 2	Thr	V	-	4.7	V	-	3.8	V	-	2.5	V	-	1.9	I	-	-	I	-	-	I	-	-
E0707	Vibration Safety Cutoff No. 1	Thr	V	-	5.3	I	-	-	I	-	-	V	-	2.1	V	-	3.3	V	-	3.6	I	-	-
	ACOUSTICS — OVERALL SOUND PRESSURE LEVEL (db re 0.0002 MICROBAR), FREQUENCY RANGE 10 - 3,000 cps																						
B0501	Aft Skirt, Panel No. 1, Internal														V	-	152	V	-	152.5	V	156.5	152.5
B0502	Aft Skirt, Panel No. 17, Internal														V	-	152	V	-	153	V	156.5	153
B0700	0 Ft Height at 150 Ft Radius 30°																						
B0701	0 Ft Height at 150 Ft Radius 40°																						
B0702	0 Ft Height at 150 Ft Radius 50°																						
B0703	0 Ft Height at 150 Ft Radius 60°																						
B0704	0 Ft Height at 150 Ft Radius 70°																						
B0705	0 Ft Height at 150 Ft Radius 80°																						
B0706	0 Ft Height at 12 Ft Radius 55°																						
B0707	10 Ft Height at 12 Ft Radius 55°																						
B0708	20 Ft Height at 12 Ft Radius 55°																						
B0709	30 Ft Height at 12 Ft Radius 55°																						
B0710	45 Ft Height at 12 Ft Radius 55°																						
B0711	60 Ft Height at 12 Ft Radius 55°																						
B0712	0 Ft Height at 25 Ft Radius 55°																						
B0713	Helium Fairing, Sta 415, Pos II																						
B0714	0 Ft Height at 75 Ft Radius 55°																						
B0715	0 Ft Height at 300 Ft Radius 55°																						
B0716	0 Ft Height at 600 Ft Radius 55°																						
B0717	0 Ft Height at 150 Ft Radius 95°																						
B0718	0 Ft Height at 150 Ft Radius 110°																						
B0719	0 Ft Height at 150 Ft Radius 135°																						
B0720	0 Ft Height at 150 Ft Radius 160°																						
B0721	0 Ft Height at 150 Ft Radius 180°																						

MSFC NO.	PARAMETERS	DIRECTION	614024 QUALITY	614024 START TRANSIENT	614024 MAIN STAGE	614025 QUALITY	614025 START TRANSIENT	614025 MAIN STAGE	614028 QUALITY	614028 START TRANSIENT	614028 MAIN STAGE	614030 QUALITY	614030 START TRANSIENT	614030 MAIN STAGE	614033 QUALITY	614033 START TRANSIENT	614033 MAIN STAGE	614034 QUALITY	614034 START TRANSIENT	614034 MAIN STAGE
	VIBRATION — COMPOSITE LEVEL (G rms), FREQUENCY RANGE 10 - 3,000 cps																			
E0500	Sequencer at Module A10	Thr	I	-	-	V	-	4.3	V	-	4.2	V	-	4.5	V	7.3	5.5	V	8.5	7.3
E0501	Sequencer at Module A10	Rad	V	-	1.6	I	-	-	V	-	1.9	V	-	1.9						
E0502	Sequencer at Module A10	Tan	V	-	8.2	V	-	8.0	I	-	-	V	-	9.4						
E0503	Pitch Actuator Servo Valve	Rad																I		
E0504	Yaw Actuator Servo Valve	Rad													V	4.5	5.1	V	4.9	5.5
E0505	Primary Instr Package	Thr	I	-	-	V	-	5.0	V	-	4.5	V	-	4.3						
E0506	Primary Instr Package	Rad	V	-	8.8	V	-	8.4	V	-	8.6	I	-	-						
E0507	Primary Instr Package	Tan	V	-	3.8	V	-	2.6	V	-	4.6	I	-	-	V	13.5	10.8	V	BAD	9.4
E0508	Propellant Utilization Valve	Ax	V	-	36.5	V	32.6	-	I	-	-	I	-	-	V	-	69.7	V	70.2	77.3
E0509	Propellant Utilization Valve	Rad	V	-	36.8	V	-	35.4	V	33.6	39.7	V	-	31.5						
E0510	Propellant Utilization Valve	Tan	V	-	28.3	V	-	32.9	I	-	-	I	-	-						
E0511	J-2 Engine Gimbal Point	Thr	V	-	2.2	V	-	2.2	V	-	2.2	I	-	-	I	-	-	I	-	-
E0512	J-2 Engine Gimbal Point	P	I	-	-	V	-	3.3	V	-	4.1	V	-	3.6	V	3.3	3.4	V	3.4	2.7
E0513	J-2 Engine Gimbal Point	Y	V	-	2.6	V	-	2.9	V	-	3.0	V	-	2.7	I	-	-	I	-	-
E0555	LOX Turbopump	Lat	I	-	-	I	-	-	V	-	20.2	V	-	22.3	V	60.4	43.6	V	35.2	46.2
E0556	LH2 Turbopump	Lat	I	-	-	I	-	-	I	-	-	I	-	-	I	-	-	I	-	-
E0557	LOX Feedline at Engine	Thr	I	-	-	V	-	6.3	I	-	-	I	-	-	V	6.1	7.6	V	7.8	7.1
E0558	LOX Feedline at Engine	Lat	V	-	3.9	V	-	3.4	V	-	3.8	I	-	-	V	3.9	3.4	V	3.5	3.9
E0559	LH2 Feedline at Engine	Thr	V	-	5.8	V	-	5.4	V	-	4.6	V	6.51	4.9	V	7.2	4.8	V	7.6	4.5
E0560	LH2 Feedline at Engine	Lat	I	-	-	I	-	-	I	-	-	V	8.93	6.5	V	10.0	7.7	V	9.2	7.0
E0561	Thrust Struc/Pitch Actuator Attach Pt.	Ax													V	2.8	1.8	I	-	-
E0562	Thrust Struc/Yaw Actuator Attach Point	Ax													V	2.5	2.4	V	2.4	3.2
E0563	Hydraulic Pump, Main	Thr													V	11.9	10.1	V	12.0	11.3
E0564	Hydraulic Pump, Main	Lat																I	-	-
E0570	Pitch Actuator Servovalve	Ax													V	5.4	4.4	I	-	-
E0571	Pitch Actuator Servovalve	Tan													V	2.6	2.2	I	-	-
E0572	Yaw Actuator Servovalve	Ax													V	6.4	6.5	V	6.9	7.8
E0573	Yaw Actuator Servovalve	Tan													V	3.9	4.3	I	-	-
E0574	Mod A1-56V Pwr Dist-Aft-Panel 17	Rad																		
E0575	Mod A1-56V Pwr Dist-Aft-Panel 17	Tan																		
E0576	Mod A1-56V Pwr Dist-Aft-Panel 17	Ax																		
E0577	Gas Generator	Thr	V	-	8.7	V	-	11.5	I	-	-	I	-	-	I	-	-	I	-	-
E0578	Gas Generator	Rad	I	-	-	I	-	-	I	-	-	I	-	-	I	-	-	I	-	-
E0706	Vibration Safety Cutoff No. 2	Thr	I	-	-	I	-	-	V	-	2.6	V	-	2.8	I	-	-	I	-	-
E0707	Vibration Safety Cutoff No. 1	Thr	I	-	-	I	-	-	V	3.35	-	V	3.59	-	I	-	-	I	-	-
	ACOUSTICS — OVERALL SOUND PRESSURE LEVEL (db re 0.0002 MICROBAR), FREQUENCY RANGE 10 - 3,000 cps																			
B0501	Aft Skirt, Panel No. 1, Internal		V	-	153	I	-	-	V	158	153	V	160	154	V	158	152	V	157	151
B0502	Aft Skirt, Panel No. 17, Internal		V	-	153	I	-	-	V	157	153	V	156.5	153.5	V	156	152	V	156	153
B0700	0 Ft Height at 150 Ft Radius 30°		I	-	-	V	143	139	V	141	139	V	140.5	138						
B0701	0 Ft Height at 150 Ft Radius 40°		I	-	-	V	144	139	V	141	140	V	143	139						
B0702	0 Ft Height at 150 Ft Radius 50°		I	-	-	I	-	-	V	143	140	V	143	139						
B0703	0 Ft Height at 150 Ft Radius 60°		I	-	-	V	143	137	V	142	138	V	141	138						
B0704	0 Ft Height at 150 Ft Radius 70°		I	-	-	V	144	139	V	142	137	V	141	136						
B0705	0 Ft Height at 150 Ft Radius 80°		I	-	-	I	-	-	V	140	134	V	141	134						
B0706	0 Ft Height at 12 Ft Radius 55°														I	-	-	I	-	-
B0707	10 Ft Height at 12 Ft Radius 55°														I	-	-	I	-	-
B0708	20 Ft Height at 12 Ft Radius 55°														I	-	-	I	-	-
B0709	30 Ft Height at 12 Ft Radius 55°														I	-	-	I	-	-
B0710	45 Ft Height at 12 Ft Radius 55°														I	-	-	I	-	-
B0711	60 Ft Height at 12 Ft Radius 55°														I	-	-	I	-	-
B0712	0 Ft Height at 25 Ft Radius 55°														I	-	-	I	-	-
B0713	Helium Fairing, Sta 415, Pos II														I	-	-	I	-	-
B0714	0 Ft Height at 75 Ft Radius 55°														I	-	-	I	-	-
B0715	0 Ft Height at 300 Ft Radius 55°														I	-	-	I	-	-
B0716	0 Ft Height at 600 Ft Radius 55°														I	-	-	I	-	-
B0717	0 Ft Height at 150 Ft Radius 95°		I	-	-	V	138	129	V	138	133	V	138	133						
B0718	0 Ft Height at 150 Ft Radius 110°		I	-	-	V	BAD	133	V	139	134									
B0719	0 Ft Height at 150 Ft Radius 135°		I	-	-	V	139	133	V	142	135	V	142	135						
B0720	0 Ft Height at 150 Ft Radius 160°		I	-	-	I	-	-	V	131	127	V	131	127						
B0721	0 Ft Height at 150 Ft Radius 180°		I	-	-	I	-	-	V	133	128	V	BAD	128						

MSFC NO.	PARAMETERS	DIRECTION	614042 QUALITY	614042 START TRANSIENT	614042 MAIN STAGE	614043 QUALITY	614043 START TRANSIENT	614043 MAIN STAGE	614043 QUALITY	614043 START TRANSIENT	614043 MAIN STAGE	614044 QUALITY	614044 START TRANSIENT	614044 MAIN STAGE	614044 QUALITY	614044 START TRANSIENT	614044 MAIN STAGE
	VIBRATION — COMPOSITE LEVEL (G rms), FREQUENCY RANGE 10 - 3,000 cps																
E0500	Sequencer at Module A10	Thr															
E0501	Sequencer at Module A10	Rad															
E0502	Sequencer at Module A10	Tan															
E0503	Pitch Actuator Servo Valve	Rad				V	4.8	5.7	V	4.0	4.8	V	4.5	4.6	V	3.5	3.2
E0504	Yaw Actuator Servo Valve	Rad				V	4.1	5.4	V	3.8	5.4	V	4.1	6.2	V	4.1	4.5
E0505	Primary Instr Package	Thr															
E0506	Primary Instr Package	Rad															
E0507	Primary Instr Package	Tan															
E0508	Propellant Utilization Valve	Ax															
E0509	Propellant Utilization Valve	Rad															
E0510	Propellant Utilization Valve	Tan															
E0511	J-2 Engine Gimbal Point	Thr				I	-	-	I	-	-	I	-	-	I	-	-
E0512	J-2 Engine Gimbal Point	P				I	-	-	I	-	-	I	-	-	I	-	-
E0513	J-2 Engine Gimbal Point	Y				I	-	-	I	-	-	I	-	-	I	-	-
E0555	LOX Turbopump	Lat				I	-	-	I	-	-	I	-	-	I	-	-
E0556	LH2 Turbopump	Lat				I	-	-	I	-	-	I	-	-	I	-	-
E0557	LOX Feedline at Engine	Thr				V	15.9	18.0	I	-	-	V	10.2	11.3	V	12.3	10.7
E0558	LOX Feedline at Engine	Lat				I	-	-	I	-	-	I	-	-	I	-	-
E0559	LH2 Feedline at Engine	Thr															
E0560	LH2 Feedline at Engine	Lat				I	-	-	I	-	-	I	-	-	I	-	-
E0561	Thrust Struc/Pitch Actuator Attach Pt.	Ax				I	-	-	I	-	-	V	2.6	2.3	V	2.4	1.9
E0562	Thrust Struc/Yaw Actuator Attach Point	Ax				V	BAD	3.3	I	-	-	V	2.3	3.2	V	2.7	2.9
E0563	Hydraulic Pump, Main	Thr				I	-	-	I	-	-	I	-	-	V	10.8	9.9
E0564	Hydraulic Pump, Main	Lat															
E0570	Pitch Actuator Servovalve	Ax				I	-	-	I	-	-	I	-	-	I	-	-
E0571	Pitch Actuator Servovalve	Tan				I	-	-	I	-	-	I	-	-	I	-	-
E0572	Yaw Actuator Servovalve	Ax				V	9.5	10.7	V	7.9	10.9	I	-	-	V	8.5	8.9
E0573	Yaw Actuator Servovalve	Tan				I	-	-	I	-	-	I	-	-	I	-	-
E0574	Mod A1-56V Pwr Dist-Aft-Panel 17	Rad															
E0575	Mod A1-56V Pwr Dist-Aft-Panel 17	Tan															
E0576	Mod A1-56V Pwr Dist-Aft-Panel 17	Ax															
E0577	Gas Generator	Thr				I	-	-	I	-	-	I	-	-	I	-	-
E0578	Gas Generator	Rad				I	-	-	I	-	-	I	-	-	I	-	-
E0706	Vibration Safety Cutoff No. 2	Thr				I	-	-	I	-	-	I	-	-	I	-	-
E0707	Vibration Safety Cutoff No. 1	Thr				I	-	-	I	-	-	I	-	-	I	-	-
	ACOUSTICS — OVERALL SOUND PRESSURE LEVEL (db re 0.0002 MICROBAR), FREQUENCY RANGE 10 - 3,000 cps																
B0501	Aft Skirt, Panel No. 1, Internal		V	150	144	V	148	143	V	149	143	V	151	144	V	151	145
B0502	Aft Skirt, Panel No. 17, Internal		V	149	145	V	147	144	V	149	144	V	150	145	V	151	146
B0700	0 Ft Height at 150 Ft Radius 30°																
B0701	0 Ft Height at 150 Ft Radius 40°																
B0702	0 Ft Height at 150 Ft Radius 50°																
B0703	0 Ft Height at 150 Ft Radius 60°																
B0704	0 Ft Height at 150 Ft Radius 70°																
B0705	0 Ft Height at 150 Ft Radius 80°																
B0706	0 Ft Height at 12 Ft Radius 55°		V	162	158	V	159	157	V	159	156	V	BAD	158	V	160	158
B0707	10 Ft Height at 12 Ft Radius 55°		V	156	152	V	154	150	V	154	151	V	154	152	V	154	152
B0708	20 Ft Height at 12 Ft Radius 55°		V	148	146	V	148	143	V	147	143	I	-	-	I	-	-
B0709	30 Ft Height at 12 Ft Radius 55°		I	-	-	V	146	141	V	146	142	I	-	-	I	-	-
B0710	45 Ft Height at 12 Ft Radius 55°		I	-	-	V	143	138	V	142	138	V	144	140	V	143	139
B0711	60 Ft Height at 12 Ft Radius 55°		V	139	135	V	138	134	V	139	135	V	140	135	V	139	135
B0712	0 Ft Height at 25 Ft Radius 55°		V	154	152	V	153	150	V	153	150	V	154	151	V	153	151
B0713	Helium Fairing, Sta 415, Pos II		V	145	141	V	144	140	V	144	140	I	-	-	I	-	-
B0714	0 Ft Height at 75 Ft Radius 55°		V	145	146	V	145	145	V	145	BAD	V	146	145	V	146	143
B0715	0 Ft Height at 300 Ft Radius 55°		V	134	134	V	135	133	V	134	BAD	V	137	135	V	136	133
B0716	0 Ft Height at 600 Ft Radius 55°		I	-	-	I	-	-	I	-	-	V	131	129	V	130	128
B0717	0 Ft Height at 150 Ft Radius 95°																
B0718	0 Ft Height at 150 Ft Radius 110°																
B0719	0 Ft Height at 150 Ft Radius 135°																
B0720	0 Ft Height at 150 Ft Radius 160°																
B0721	0 Ft Height at 150 Ft Radius 180°																

V = Valid Data BAD = Not Valid During this Interval
I = Invalid Data RMS = Root Mean Square
NOTE: Blank Space Indicates Parameter Not Monitored.

START TRANSIENT = ESC +1 to ESC +5 Sec
MAIN STAGE = From ECO -5 Sec to ECO -1 Sec

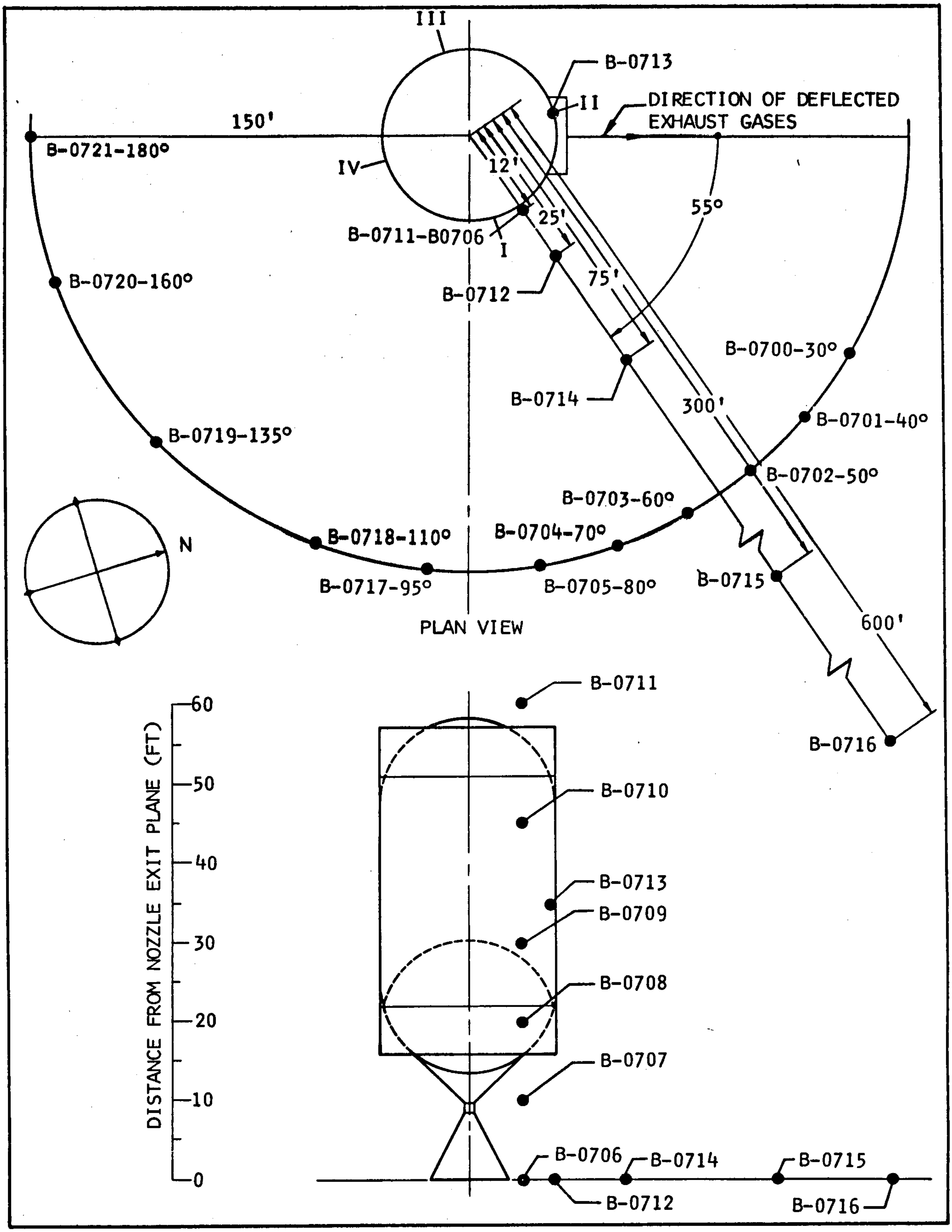

Figure 16-1 Acoustic Measurement Locations

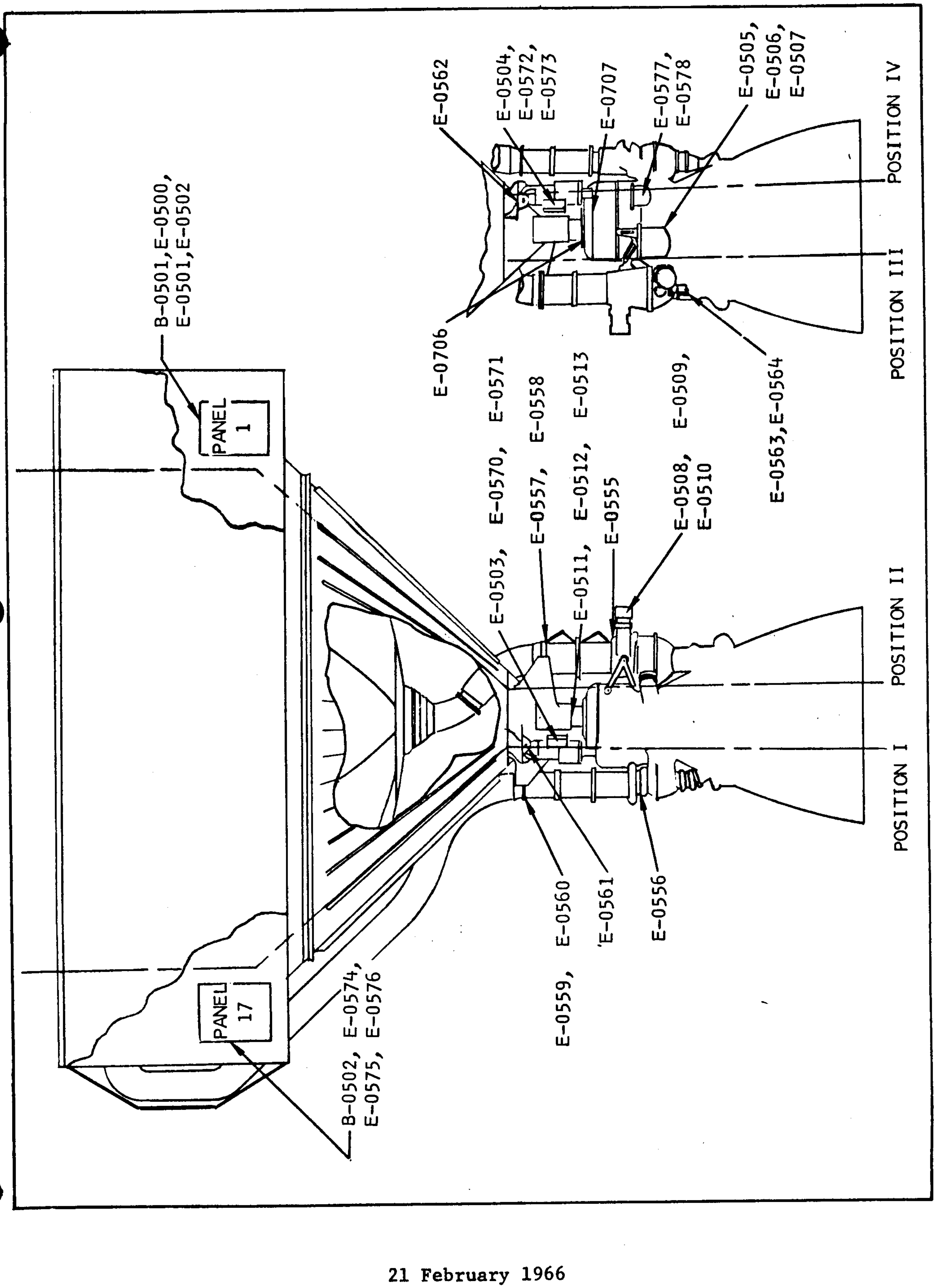

Figure 16-2 Vibration and Acoustic Measurement Locations

21 February 1966

SECTION 17

AERO/THERMODYNAMIC ANALYSIS

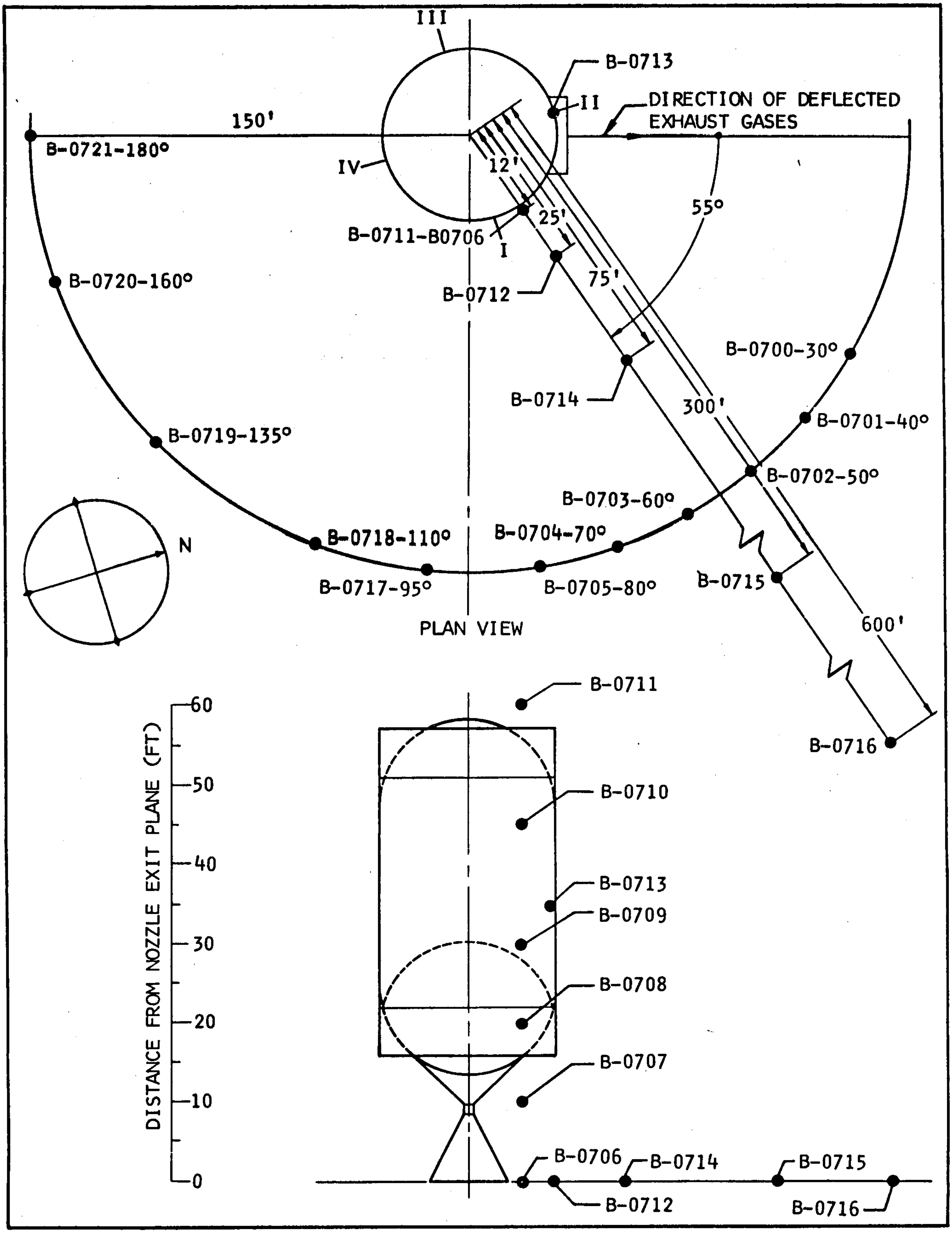

Figure 16-1 Acoustic Measurement Locations

21 February 1966

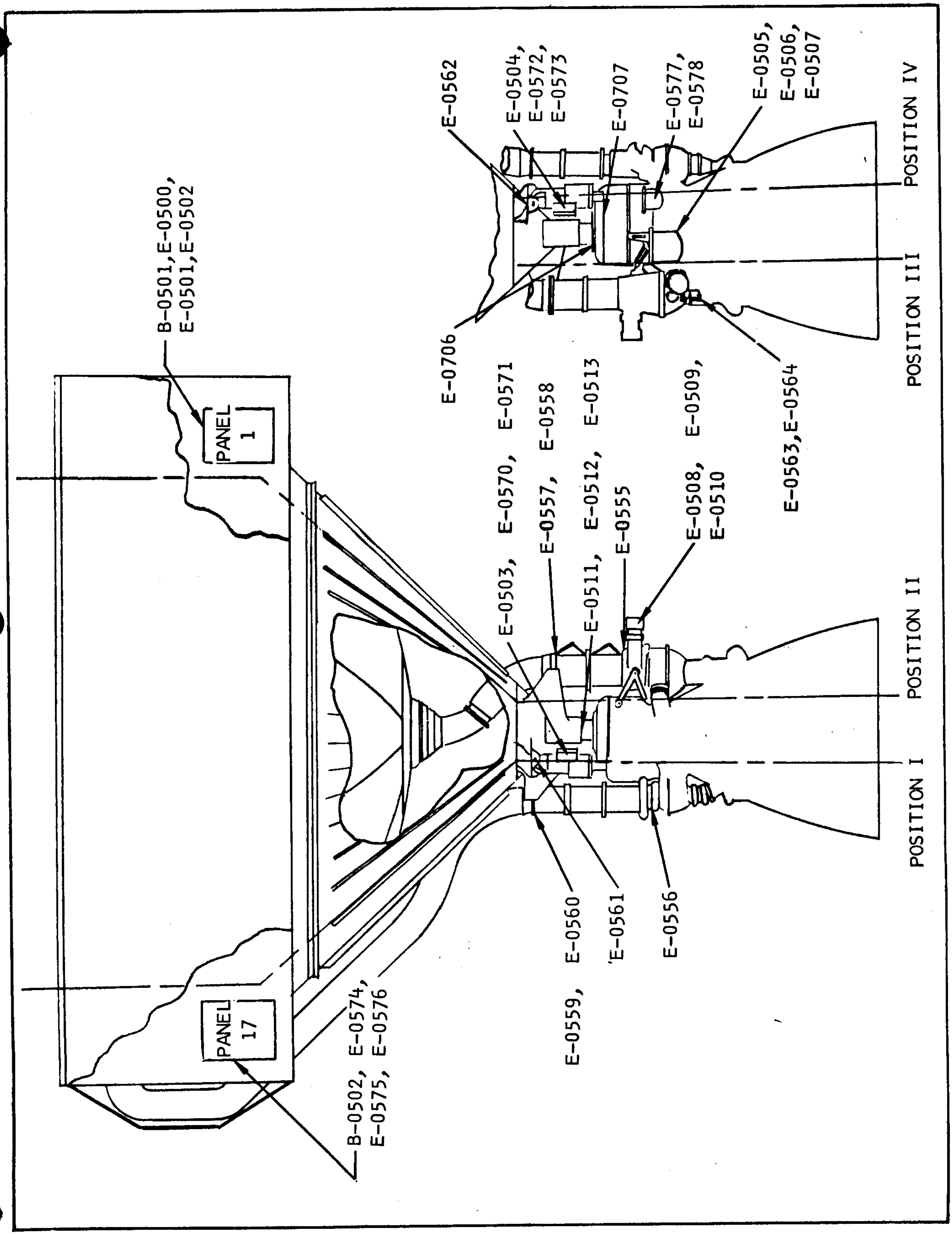

Figure 16-2 Vibration and Acoustic Measurement Locations

SECTION 17

AERO/THERMODYNAMIC ANALYSIS

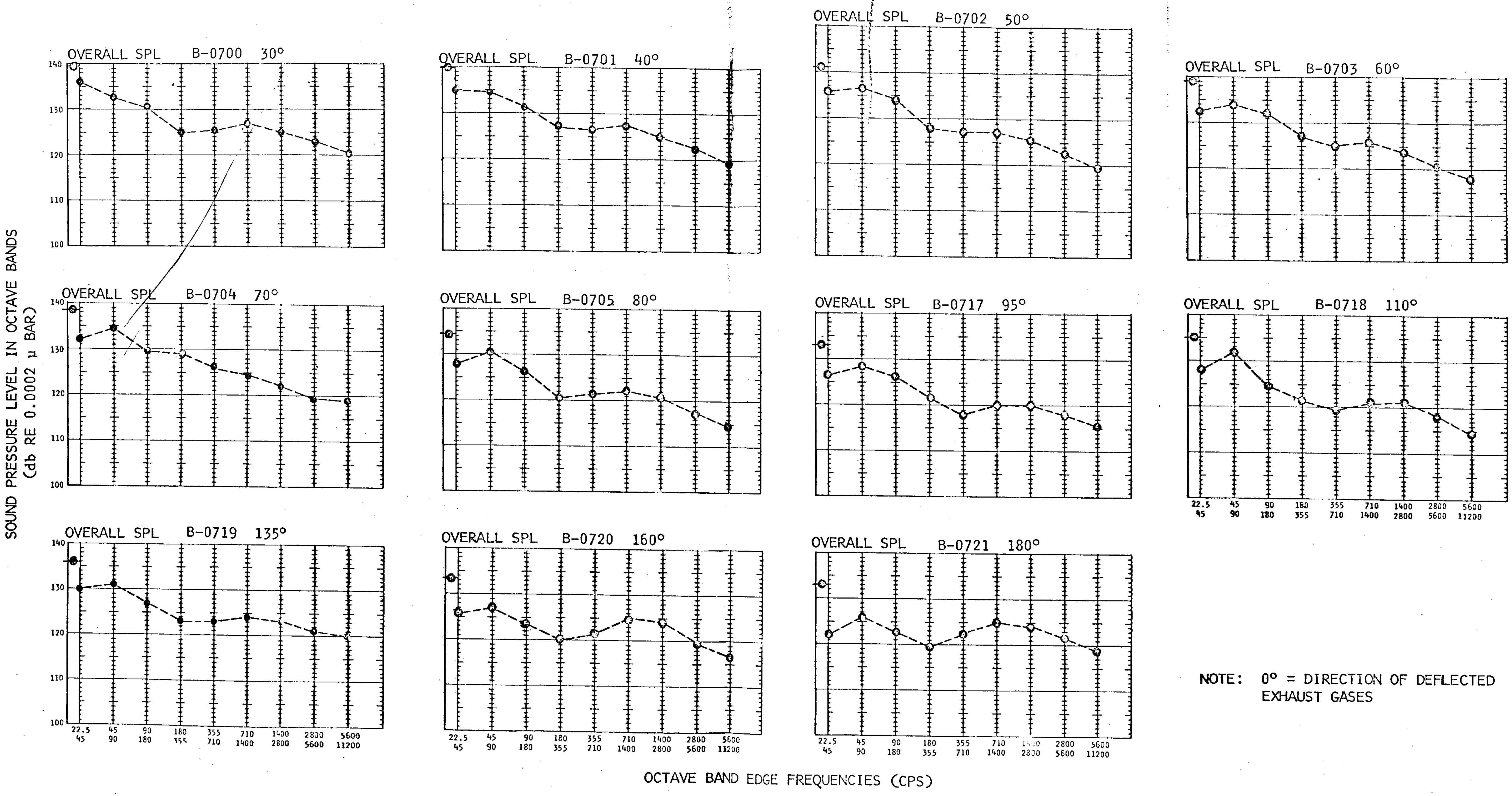

Figure 16-3 Acoustic Levels Measured 150 Feet from Stage Centerline

21 February 1966

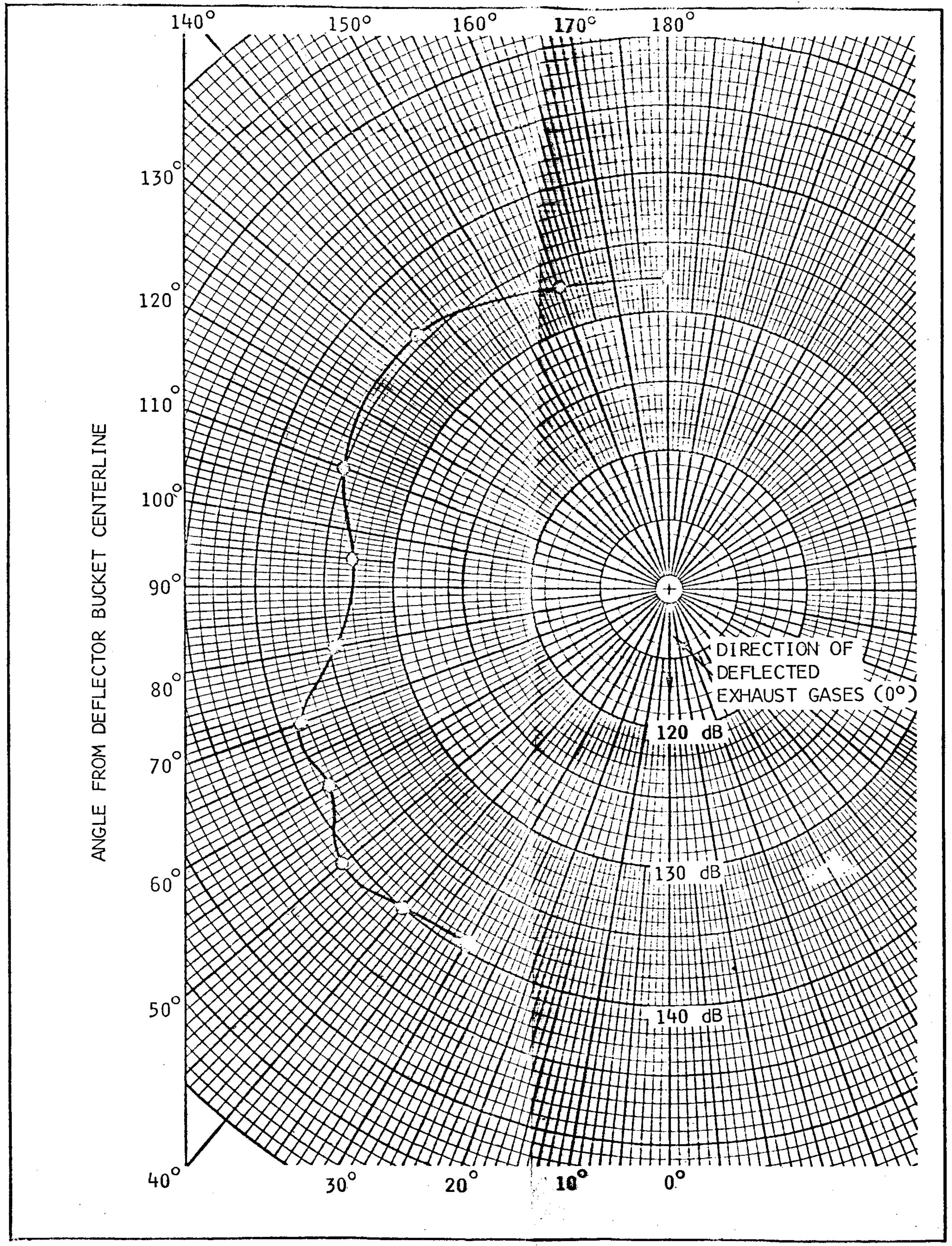

Figure 16-4 Directivity Pattern of Overall Sound Field Measured 150 Feet From Stage Centerline

21 February 1966

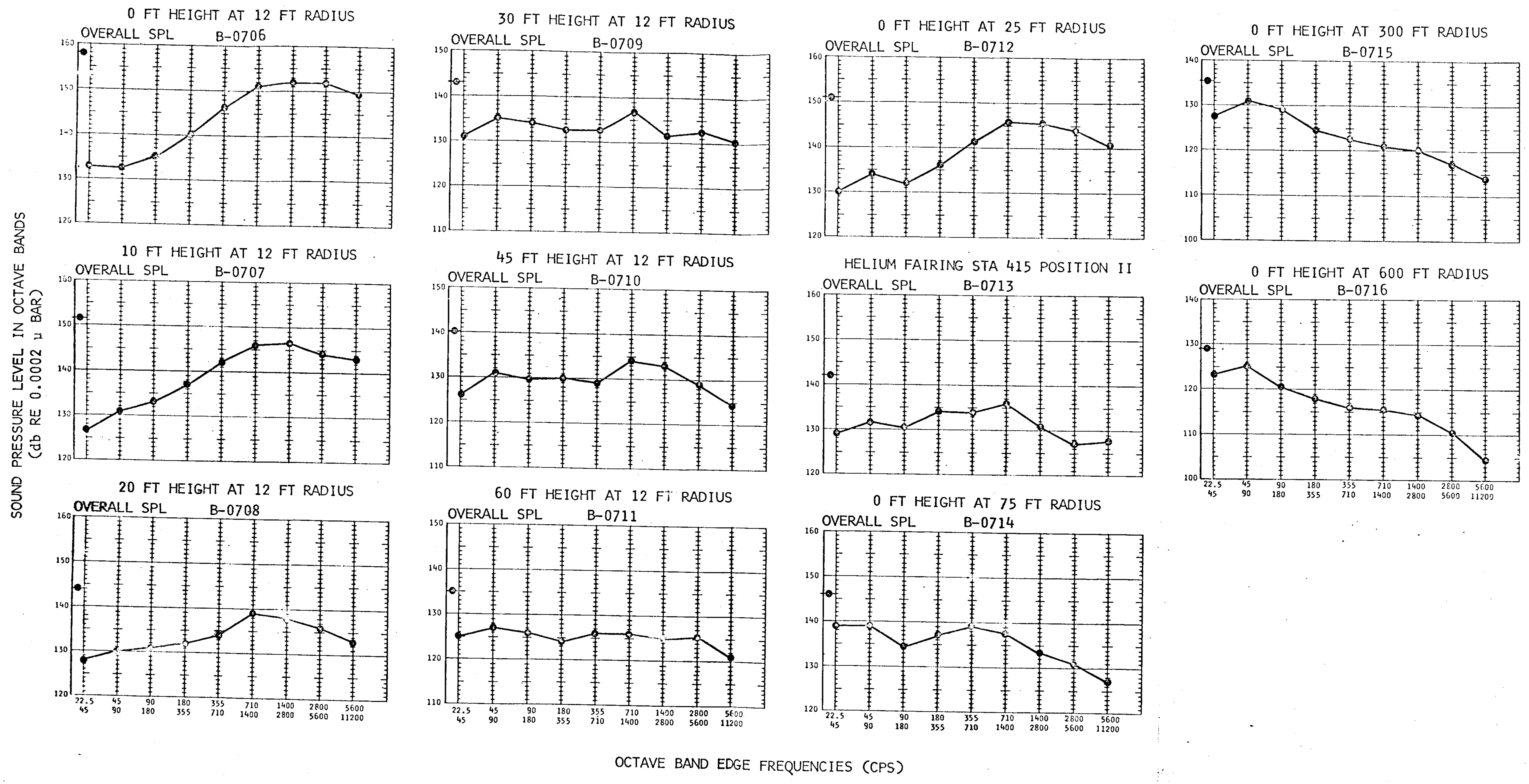

Figure 16-5 Sound Pressure Levels Measured in the Near Field (55° From Deflector Bucket)

21 February 1966

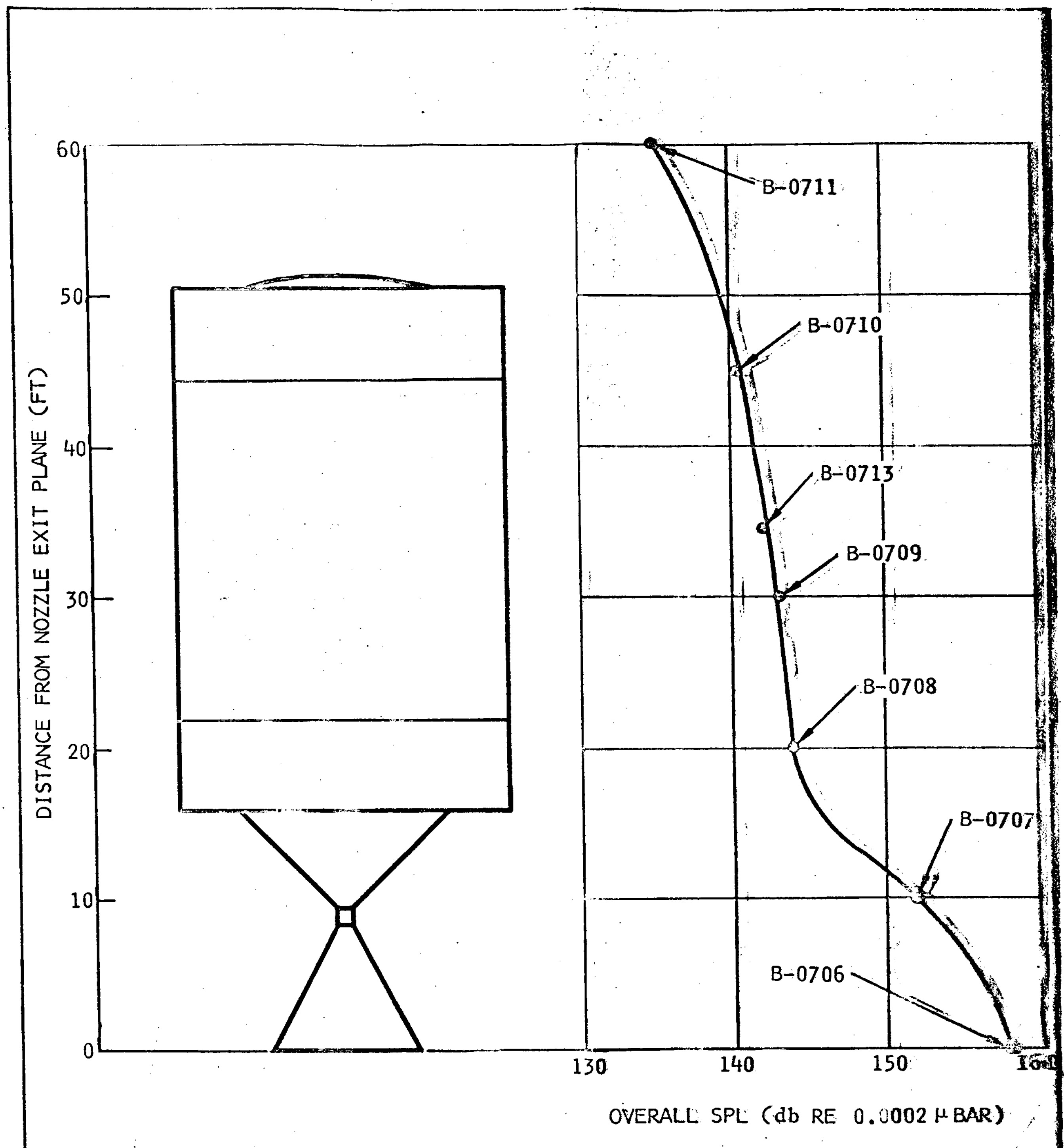

NOTE: MEASURED 55° FROM EXHAUST DEFLECTOR CENTERLINE

Figure 16-6 Profile of Sound Field Measured 12 feet from Stage Centerline

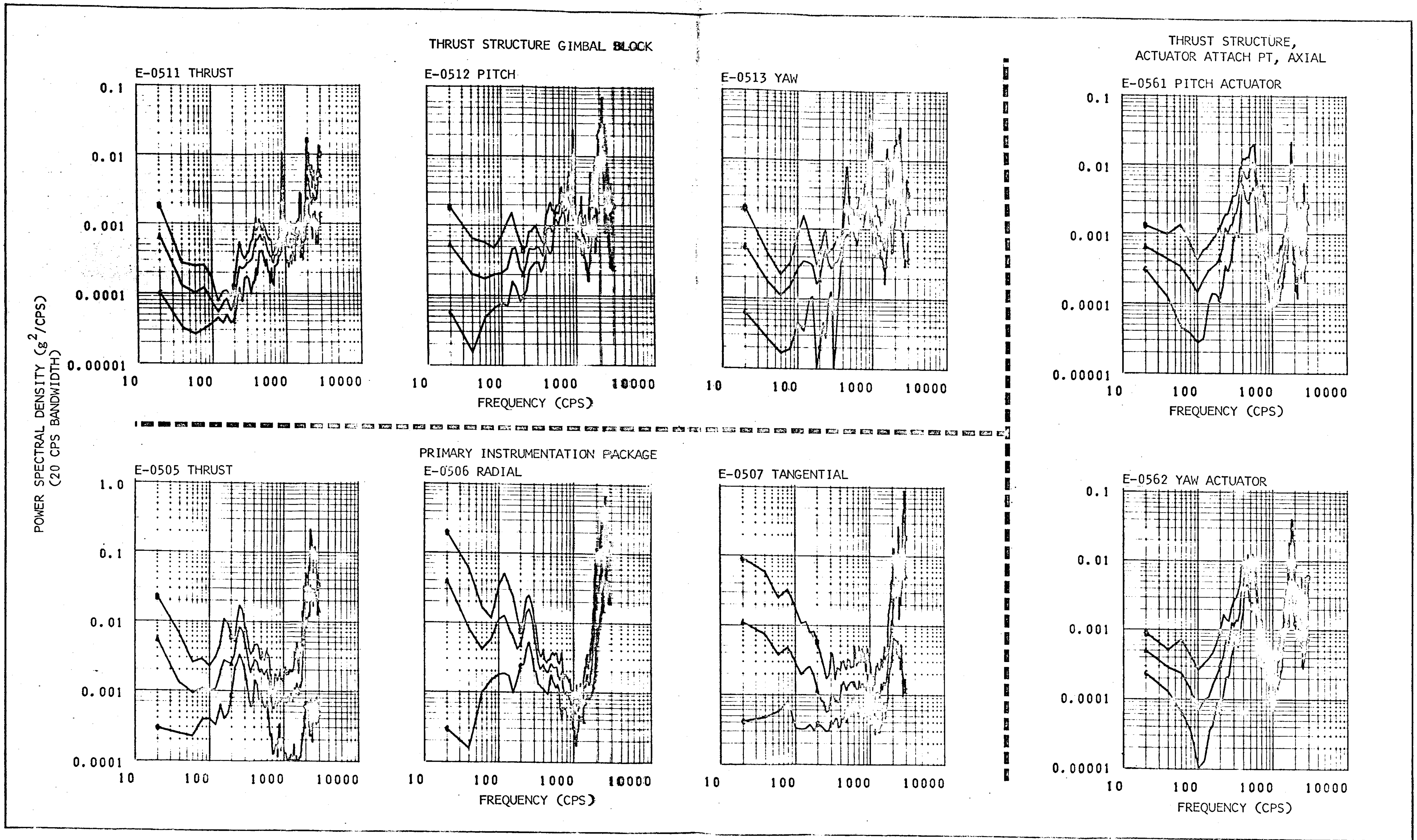

Figure 16-7 Vibration Input to Thrust Structure and Primary Instrumentation Package

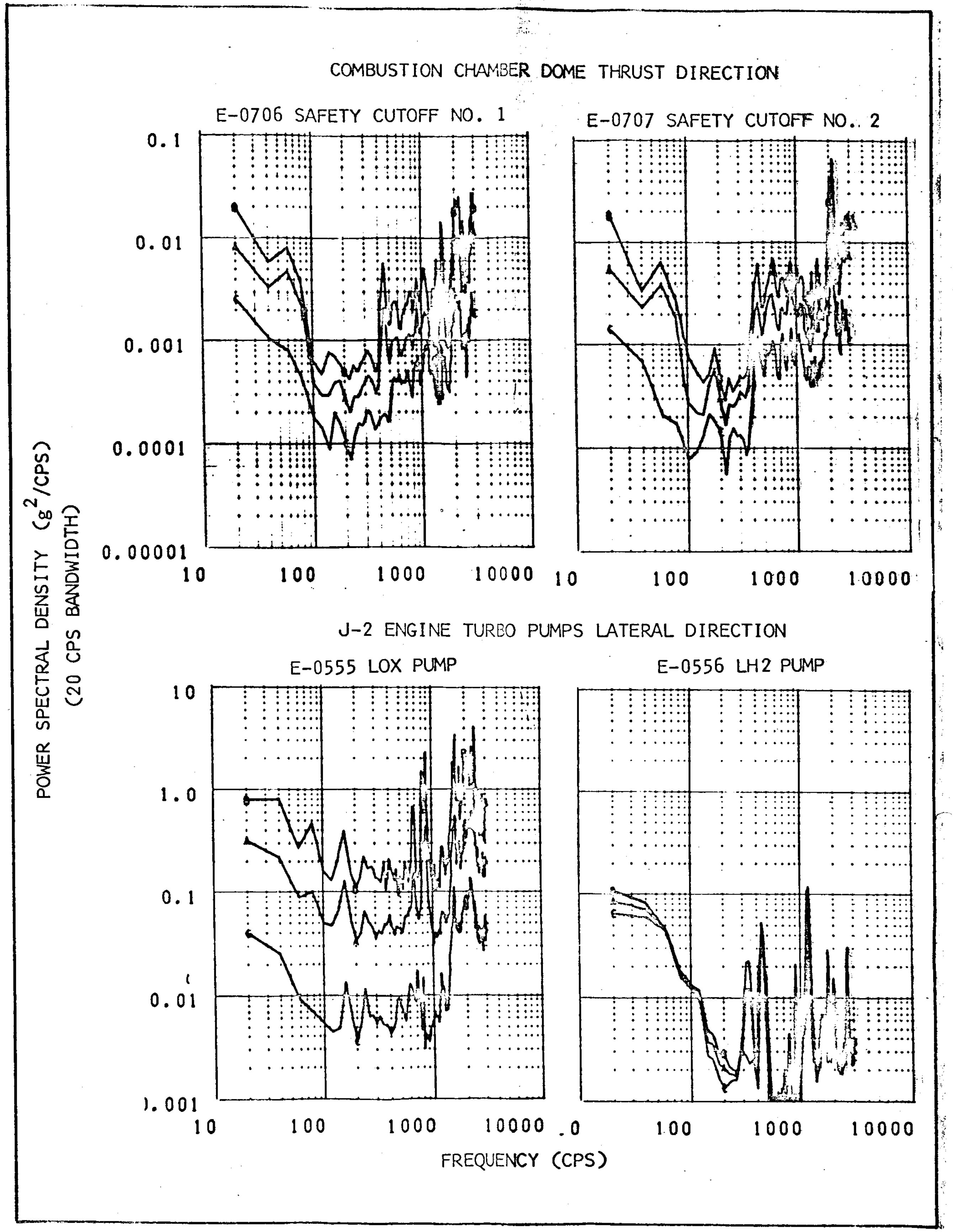

Figure 16-8 Vibration Measured on Combustion Chamber Dome and Propellant Turbo Pumps

21 February 1966

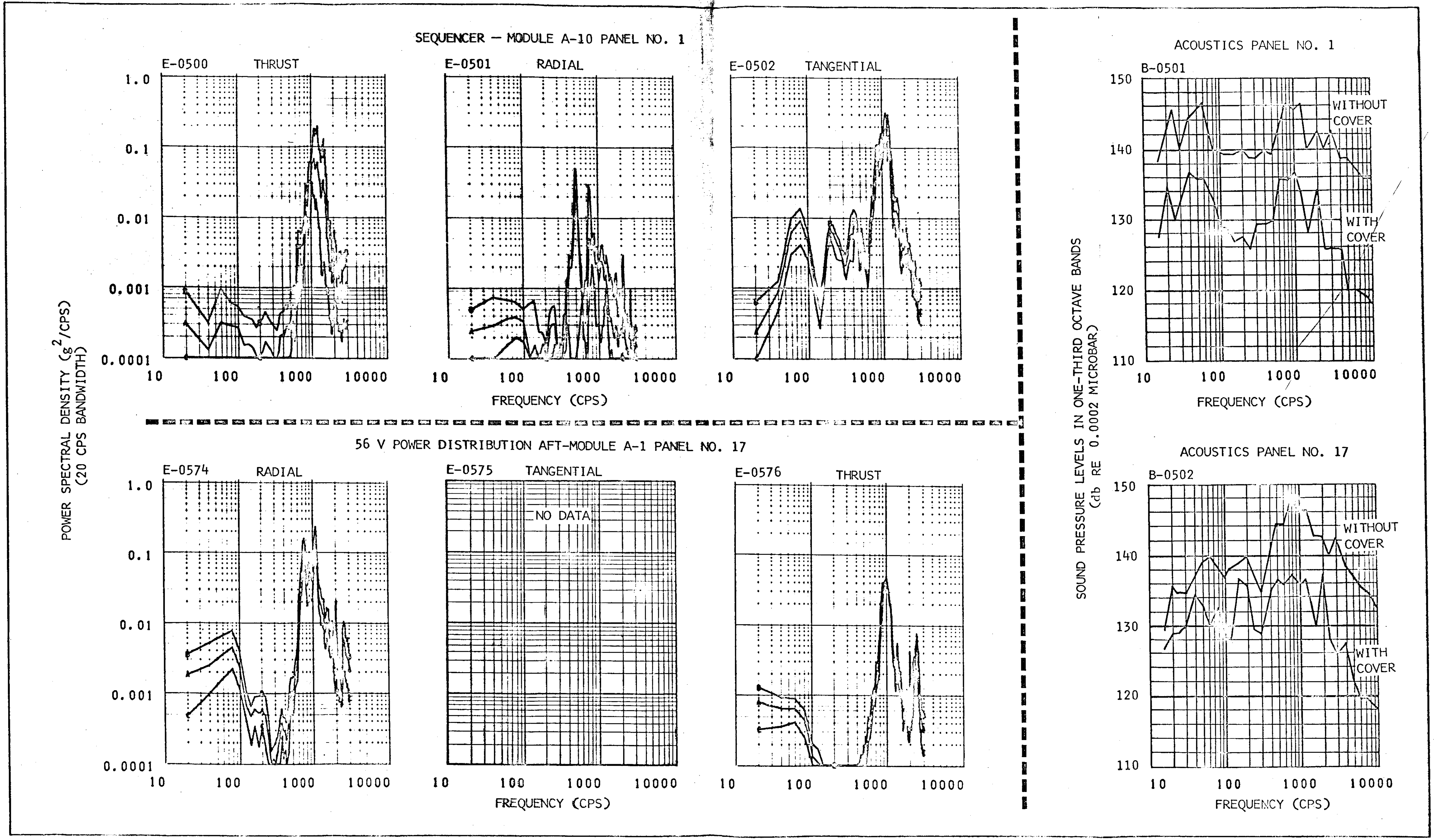

Figure 16-9 Environment of Ambient Panels (Aft Skirt)

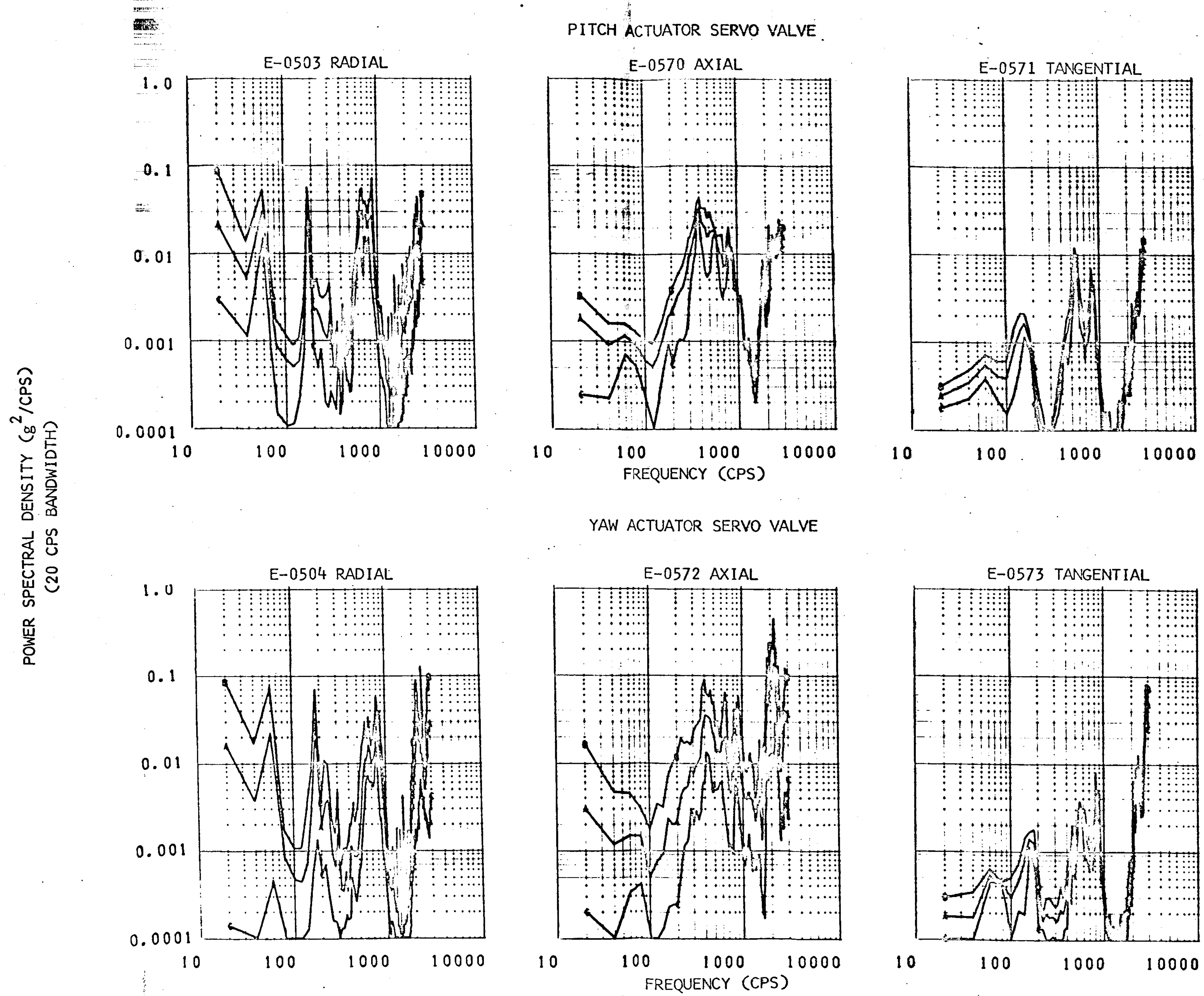

Figure 16-10 Vibration Measured on Actuator Servo Valves

21 February 1966

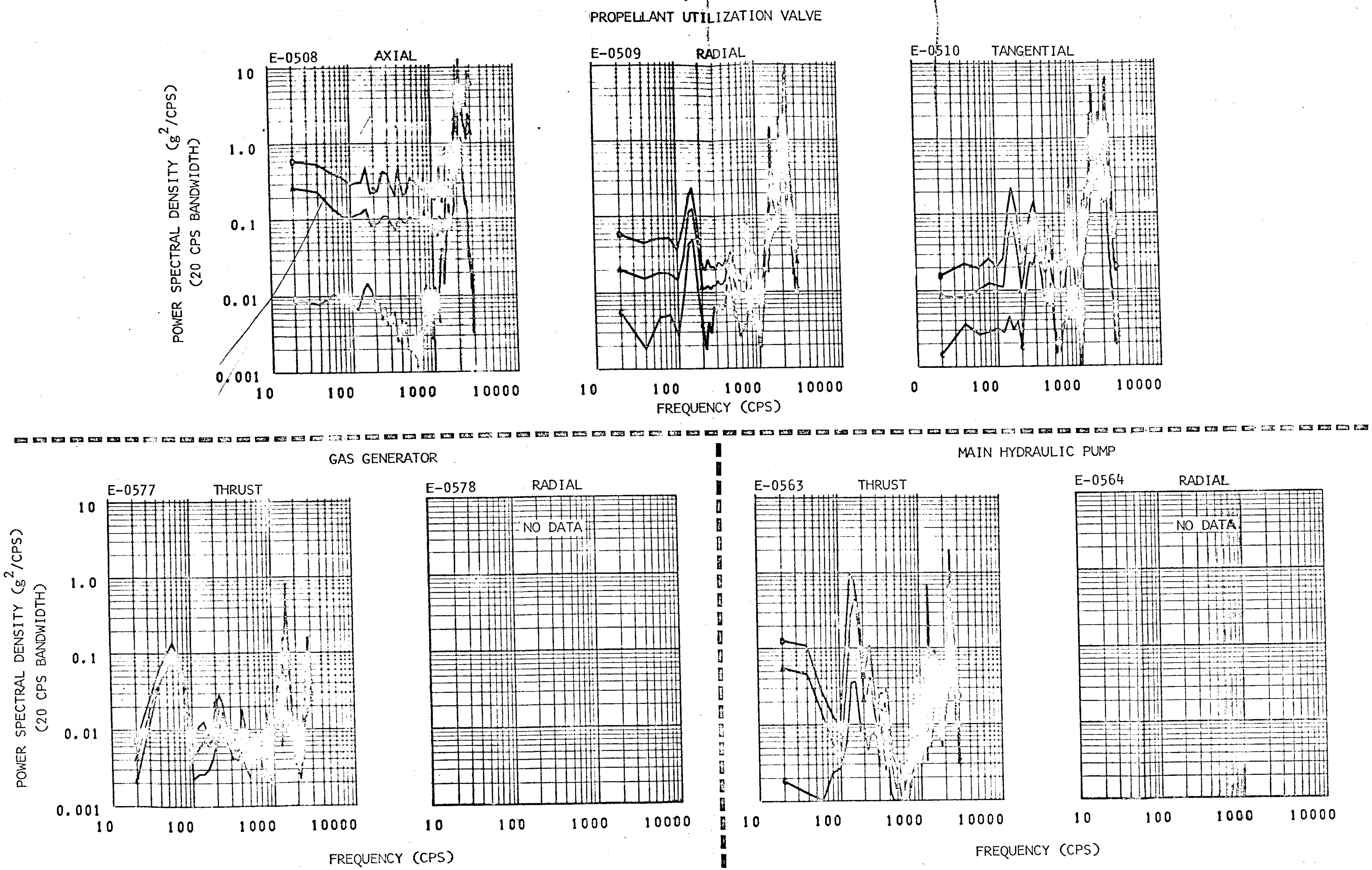

Figure 16-11 Vibration Measured on Engine Mounted Components

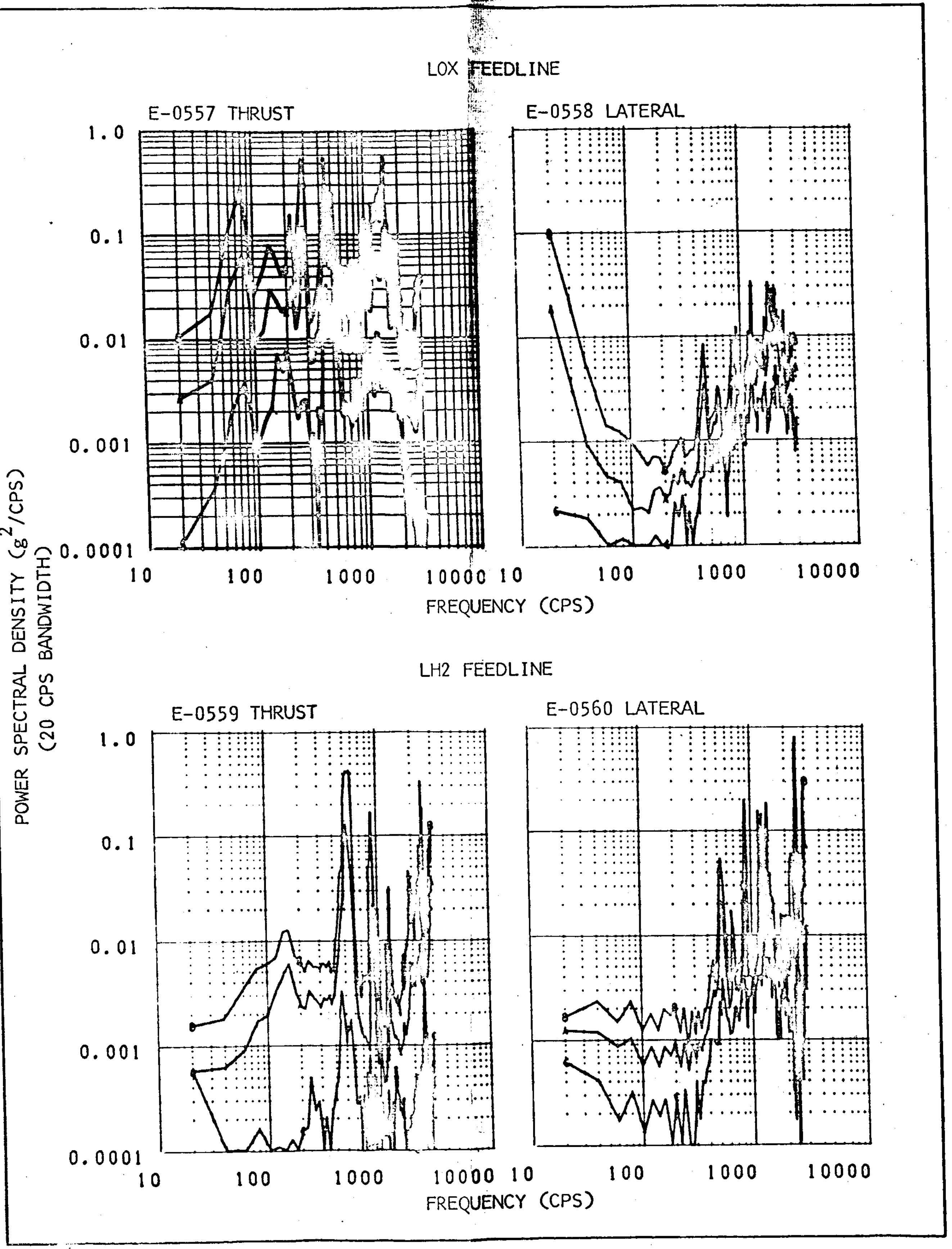

Figure 16-12 Vibration Input to the Propellant Feedlines

21 February 1966

17. AERO/THERMODYNAMIC ANALYSIS

17.1 J-2 Engine Thrust Chamber Temperature

Temperatures measured during the S-IVB/IB battleship aft interstage environmental tests (CD 614031 and 614032) by sensors located on the J-2 engine thrust chamber were used to verify analytical predictions made for the flight stages.

The purpose of the analysis, which was conducted prior to the test, was to determine whether the temperature of the engine thrust chamber tubes will exceed the maximum allowable starting temperature prior to first ignition. To aid in this investigation an analytical model was constructed to simulate the engine chilldown and thus, determine the thrust chamber temperature profile at liftoff. This model yielded results which indicate that the thrust chamber temperature at liftoff will be approximately 210 deg R forward of the manifolds, and 170 deg R aft of the manifolds. These results were in good agreement with the test data.

17.2 LOX Tank Ullage Gas Temperature

Shown in figure 17-1 are the LOX tank ullage gas temperatures measured during the full duration firing (CD 614010) which were used for the prediction of the flight stage common bulkhead temperatures during the LOX loading. Due to the difference in the battleship and flight stage common bulkhead configuration (the battleship utilized an insulated steel plate; the flight stages a honeycomb panel) the common bulkhead temperature measured during the test could not be used.

The purpose of the analysis was to determine the transient cooling characteristics of the flight stage bulkhead during LOX loading which in turn would be used to determine the stress in the bulkhead.

Temperature gradients across the honeycomb and along the weld seams during the LOX loading phase were generated analytically on the basis of the measured ullage gas temperatures and are shown in figures 17-2, 17-3, and 17-4.

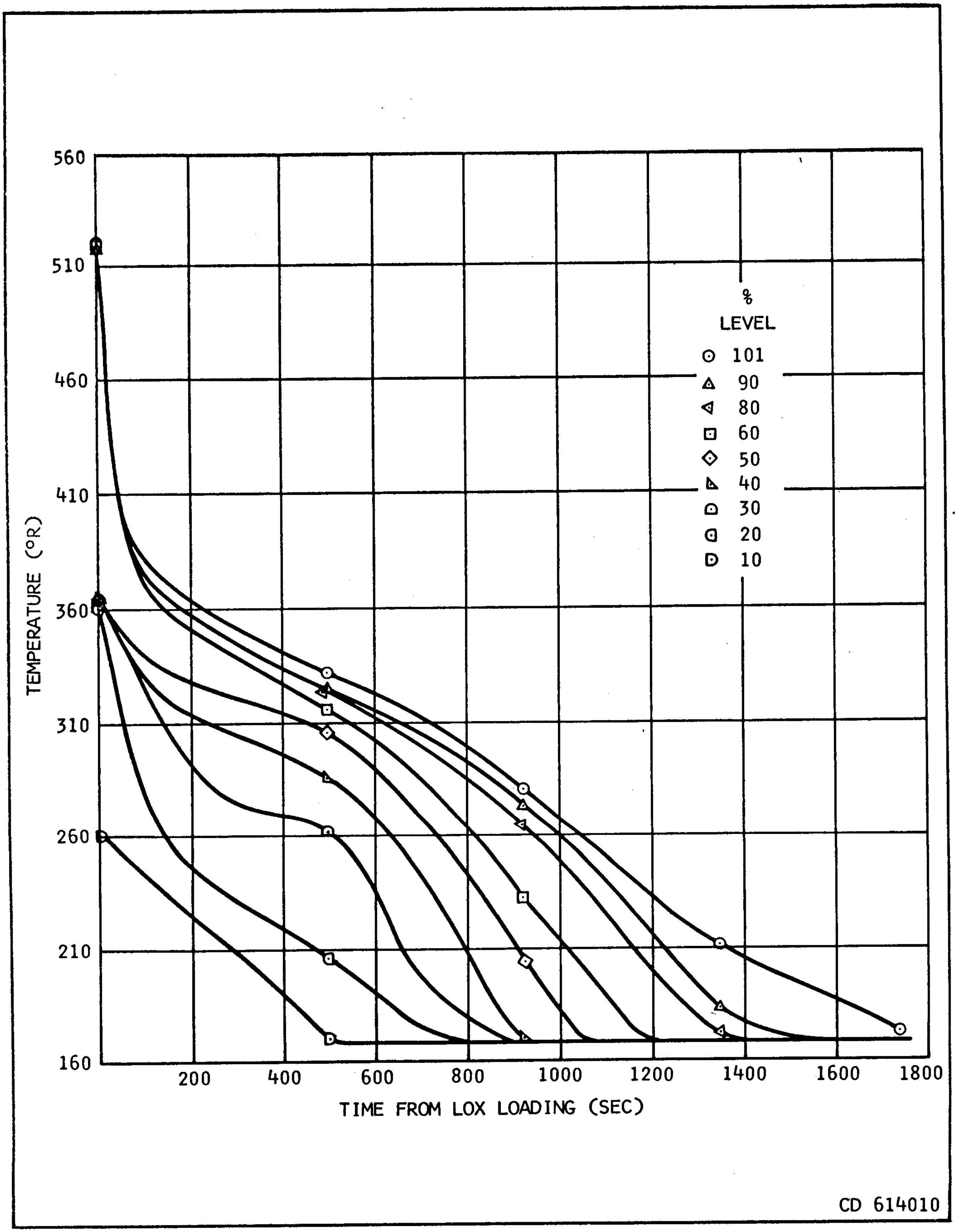

Figure 17-1 LOX Tank Ullage Gas Temperature History

21 February 1966

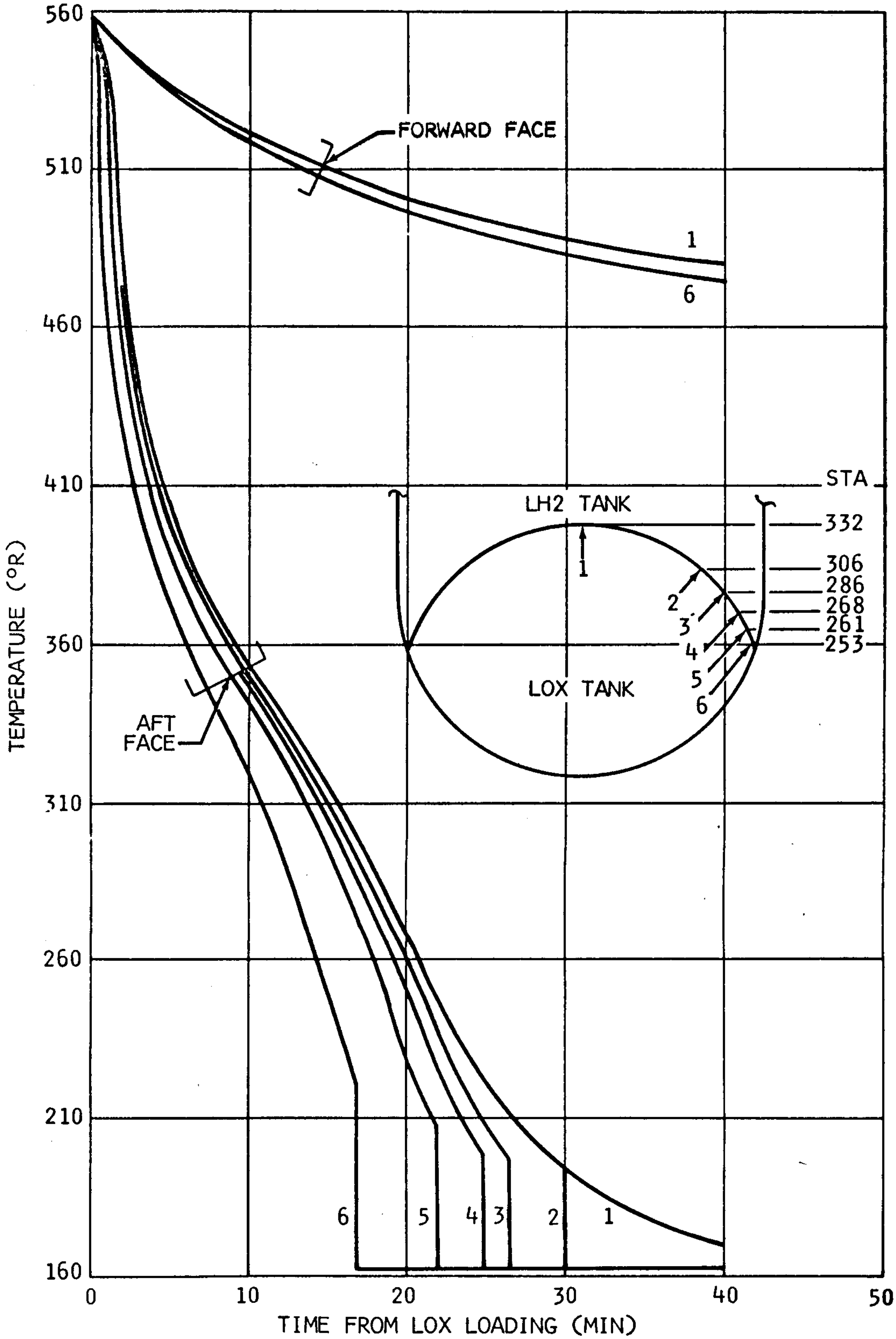

NOTES: 1. TUFT IS 520 DEG R
2. PROPELLANT LOADING SCHEDULE FROM CD 614010

Figure 17-2 Common Bulkhead Temperature History

21 February 1966

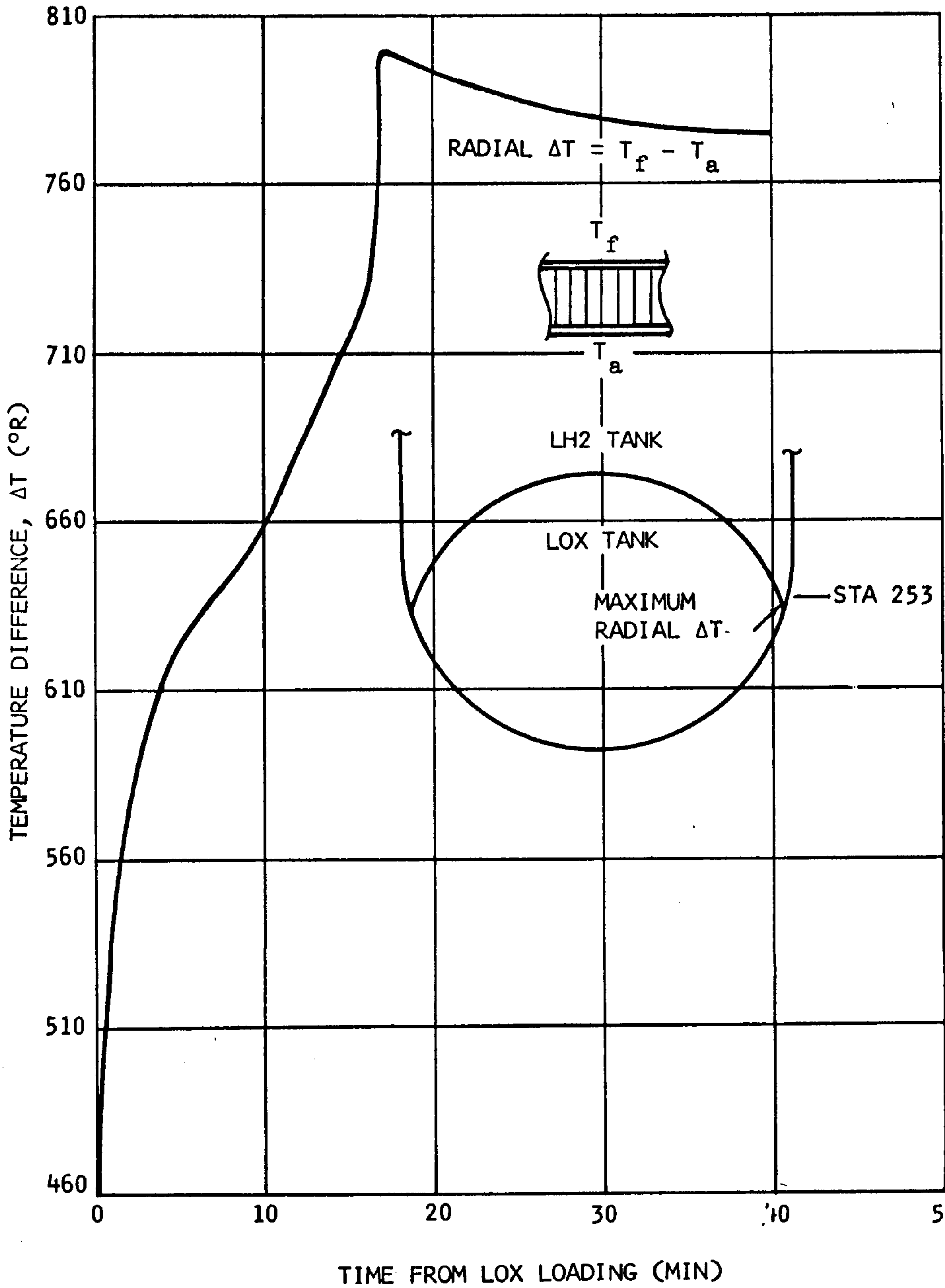

NOTES: 1. TUFT IS 520 DEG R
2. PROPELLANT LOADING SCHEDULE FROM CD 614010

Figure 17-3 Common Bulkhead Maximum Radial Temperature Difference

21 February 1966

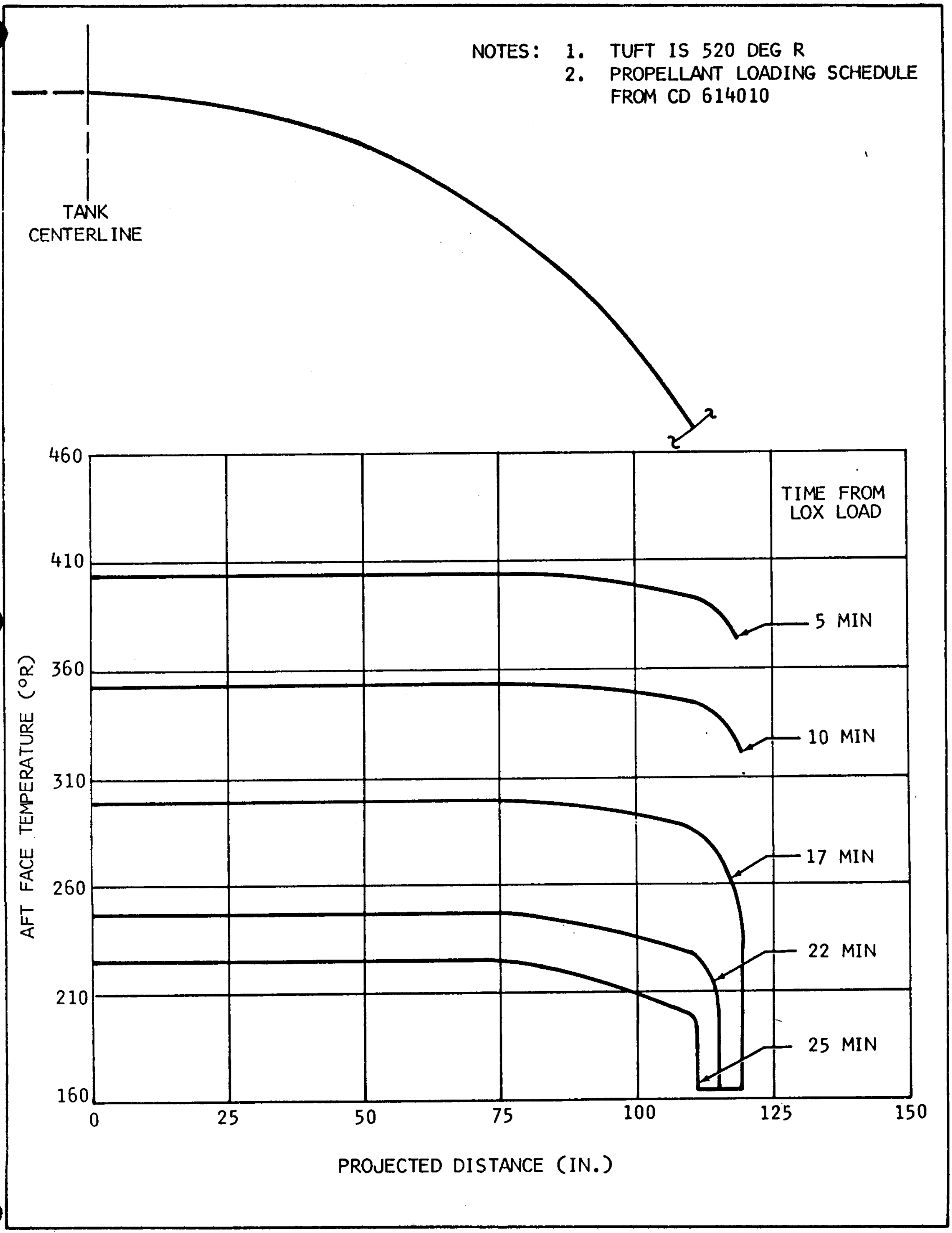

Figure 17-4 Common Bulkhead Meridional Temperature Distribution

SECTION 18

RELIABILITY AND HUMAN ENGINEERING

18. RELIABILITY AND HUMAN ENGINEERING

18.1 Reliability Engineering

The hardware failure summary of all functional flight critical items was prepared by reliability engineering. This summary is presented in Appendix 1 of this report.

18.2 Human Engineering

A human engineering evaluation of Complex Beta (Sacramento Test Center) was conducted and the following recommendations have been adopted or are being considered.

18.2.1 Recommendations Accepted

a. A desiccant system was installed in the test stand television cameras to prevent the accumulation of moisture which obscures the television monitor picture in the Test Control Center.

b. A system of warning lights was installed in the Test Control Center to indicate when personnel are present in hazardous areas of the vehicle or the facility.

c. Binocular mounts were placed in the up and down range observation stations to permit steady viewing of the vehicle and test stand during propellant loading and engine firing at Complex Beta.

d. A sound suppressant microphone was secured for the use of the test stand talker to reduce noise interference on the intercom system during test preparations.

e. A system analysis of the battleship GSE control panels in the Test Control Center was performed resulting in control and display nomenclature modifications to eliminate potential sources of human error.

f. Inputs were submitted to the Space Propulsion Branch for the layout of the vehicle monitor panel for battleship testing on test stand No. 1 at Complex Beta.

g. The following modifications to the overhead crane controls on test stand No. 1 at Complex Beta were accomplished:

   (1) A center "off" position for the boom control was provided.

   (2) The foot pedals were relocated to provide better access for the crane operator.

   (3) An auditory warning device was installed to indicate when the crane platform is in motion.

   (4) The rate of movement of the jib hoist was reduced to 75 fpm for more precise control.

   (5) Windshield wipers were added for use during inclement weather.

   (6) An electric heater was added for use of the crane operator during winter months.

h. Modifications were made to the interim LH2 tank vertical access kit to improve operator use and reduce the probability of human error.

i. Appropriate critical control indications were added to battleship GSE facility consoles containing emergency controls.

j. Human engineering requirements for the countdown and hold timers in the Test Control Center to be employed during battleship testing were specified and incorporated.

k. Display and control nomenclature was modified on test stand No. 1 facility at Complex Beta prior to battleship testing to correct situations contributing to human error.

l. Human engineering specifications were proved for the identification of test stand levels preparatory to battleship testing.

m. The format and nomenclature employed in battleship countdown manuals were reviewed to eliminate all potential sources of human error.

n. Human engineering coordinated with the safety department in establishing the breathing air requirements for the life support of personnel in the LH2 and LOX tanks.

o. Instructions were added to the GSE control consoles in the Test Control Center instructing operating personnel to log all cycles of time/cycle critical components.

p. A warning placard was placed on the door in the TCC adjacent to the steep stairs leading to the test stand No. 1 instrumentation tunnel.

q. Ear protection was obtained for personnel in the Complex Beta pumphouse during battleship testing to attenuate the high noise levels produced by the electric pumps. A sound suppressent microphone was also obtained for use by the pumphouse engineer to attenuate the background noise in the pumphouse and eliminate the attendant communication interference during voice transmissions.

r. Data was provided to Saturn Electronics regarding the optimum pulse density on oscillograph recordings for rapid and accurate counting of signals during the battleship testing program.

s. Specifications were provided for the selection of console chairs to be used in the Test Control Center during battleship testing.

t. Data was supplied to the Facilities Branch to correct the water contamination problem at Complex Beta that was causing a reduced deflector plate water flow during battleship testing.

u. The size of the numerals on the vehicle monitor panel gages on test stand No. 1 were increased to permit accurate determination of gage values on the TV monitors in the Test Control Center.

APPENDIX 1

FLIGHT TYPE HARDWARE FAILURE SUMMARY

TABLE AP 1-1 (Sheet 1 of 2)
S-IVB/IB HARDWARE FAILURE SUMMARY

PART NAME P/N & S/N	FAILURE DATE & TEST	FAILURE INDICATION	CAUSE	CORRECTIVE ACTION
LH2 Tank Vent Valve P/N 1A97040-1, S/N 001		Main seal leakage	Defective seal	Acceptable pending qualification and availability of P/N 1A97040-1A
Cold Helium Fill Module P/N 1A96810-1 -001, S/N 001		Failed close after 10 min of operation	Failure analysis disclosed inadequate valve pin and guide clearance	Engineering order issued to maintain clearance dimensions
Ambient Helium Fill Module, P/N 1A96810-1 -002, S/N 003		Vent leakage in both open and closed position.	Unknown	Stage replacement of unit. Subsequent bench tests did not duplicate failure. Unit returned to vendor for complete rework
LOX Bridge Module, P/N 1A59370-1, No S/N		Failure to provide an output signal	Undetermined	Delivered to M.R.C.C. for failure analysis and disposition
LOX Tank Shutoff Valve, P/N 1A97034 -501 S/N 001		Failure to open upon termination of close command	Cause considered to be design deficiences under severe cryogenic temperature	Presently undergoing redesign
LH2 Turbopump First Stage Seal, P/N 456158, S/N E-4681		Seal damage with 40% of honeycomb liner missing	Failure attributed by Rocketdyne as normal service wearout	Seal replaced
LOX Tank Vent Valve, P/N 1A97042-1 S/N 002		Talkback signal irregularities during tank venting and pressurization functions	Abnormal environmental factors considered responsible	No action taken. Bench test indicated normal operation. Switch improvements and/or redesign being considered

TABLE AP 1-1 (eet 2 of 2)
S-IVB/IB HARDWARE FAILURE SUMMARY

PART NAME P/N & S/N	FAILURE DATE & TEST	FAILURE INDICATION	CAUSE	CORRECTIVE ACTION
LH2 Fill and Drain Valve P/N 1A97034-501 S/N 003		Talkback signal irregularities during LH2 loading and unloading	Severe environmental conditions considered responsible	Action pending failure repetition. Bench test was satisfactory
LOX Tank Shut-off Valve, P/N 1A97034-501 S/N 001		Failed closed prior to sequence start, causing scrubbing of test (2nd occurrence).	Extreme gate closing velocity damaged lip seal	Reworked for interim pending availability of improved configuration
LH2 Tank Shut-off Valve, P/N 1A97034-1 S/N 001		Exhibited erratic response to commands, slow transittimes, and irregular	Severe galling of valve gate	Reworked for interim pending availability of improved configuration

TABLE AP 1-2 (Sheet 1 of 3)
S-IVB/V HARDWARE FAILURE SUMMARY

PART NAME P/N & S/N	FAILURE DATE & TEST	FAILURE INDICATION	CAUSE	CORRECTIVE ACTION
LOX Valve, Shutoff Chill System, P/N 1A49965-505, S/N 002	6-21-65 CD 614033 Simulated 3-Orbit Test	Valve failed to give an open talkback on command and was cycled 7 times before a normal talkback signal was received.	Moisture was suspected but not confirmed. Marginal adjustment was contributing factor.	Microswitch cover was removed and switch was adjusted and wires repositioned.
LOX Mass Probe, P/N 1A48430-503, S/N E-1	7-13-65 CD 614035 Post Fire Checkout	The pins in the J-98 connector were found shorted together internally. Further checks indicated none of the pins were shorted to ground.	To be determined.	New probe installed. Corrective action to be determined upon completion of failure analysis by manufacturer.
Gas Generator Temperature Probe, P/N 702990, S/N 210	6-28-65 CD 614034 Run No. 2	Probe transmitted an erroneous over-temperature signal causing premature engine cutoff.	Probe was checked and found to have no continuity between connector pins A and B.	New probe installed. Corrective action to be determined upon completion of investigation by manufacturer.
Accumulator Reservoir, P/N 1A78155-1-008-009, S/N 3	5-17-65 Hydraulic System Checkout	Leakage at the reservoir vent valve was noted to be approximately 12 milliliters during three actuator cycles. Acceptable leakage should not exceed two drops per 15 cycles.	Failure analysis disclosed that O-ring (P/N MS 28775-220) had apparently spiralled and chipped in two places.	New accumulator reservoir was installed. SEO 1A78155-010 authorized the replacement of the non-production backup rings with a production (Turcon) type.
Cold Helium Fill Module, P/N 1A49398-1, S/N 0018	8-14-65 CD 614041 Runs No. 2, 3, and 4, Simulated Three Orbit Test	The cold helium dump valve failed to open on command.	To be determined through subsequent investigation.	The valve will be shipped with the vehicle to Tullahoma, Tennessee for further disposition.

TABLE AP 1-2 (Sheet 2 of 3)
S-IVB/V HARDWARE FAILURE SUMMARY

PART NAME P/N & S/N	FAILURE DATE & TEST	FAILURE INDICATION	CAUSE	CORRECTIVE ACTION
Response Signal Conditioner, P/N 1A59947-1, S/N 0004	5-10-65 Electrical Checkout Phase No. 1	A logic 1, -6V, input to circuit No. 10 of the double inverter circuit board (P/N 1A49768-1), rack A-12, position AC6, resulted in continuous logic output at TP-9.	First stage transistor Q18, (P/N 1A74527-501) was inoperative and would not conduct with proper signal bias applied.	New circuit board installed. No further action required.
Check Valve, P/N 3864057-3, S/N 1003	6-7-65 Leak Check of GHE System	Bubble leak was noted between the two flanges when 500 psig was applied.	Not determined.	Valve was removed and the poppet and seat seal were replaced. Reinstalled after satisfactorily leak checked to 700 psig. No further action required.
Seven Relay Circuit Board, P/N 1A66881-1, S/N 00927	6-8-65 Electrical Checkout Phase No. 1	The computer stop light came on indicating shorting of the CR 15 polarity sensing diode. The SIM interrupt in progress light should have been on at this point in the checkout.	Shorted diode CR 15.	Board was removed and diode CR 15 and K5 relay replaced. The circuit board was recoated, tested per 1A66881, and reinstalled. No further action required.
LOX Tank Valve Shutoff, P/N 526941, S/N 002	8-14-65 CD 614041 Run No. 2 Simulated Three Orbit Test	Liquid was detected at the pump inlet with the LOX tank shutoff valve closed. This discrepancy was also noted during runs No. 3 and 4, but of a lesser degree.	Probable butterfly valve seal leakage.	The valve will be shipped with the vehicle to Tullahoma, Tennessee for further disposition.
LH2 Tank Pressurization Control Module, P/N 1B55200-1, S/N 1003	6-19-65 CD 614033	LH2 tank ullage pressure started to rise 5 sec after mainstage and stabilized at relief pressure. The flow rate increased to 4 times the amount observed during pre-test flow check.	Orifice dropped out of module and lodged against poppet in downstream check valve.	Downstream check valve was replaced and method of retaining orifice was modified to incorporate a threaded hub with a lock nut.

TABLE AP 1-2 (Sheet 3 of 3)
S-IVB/V HARDWARE FAILURE SUMMARY

PART NAME P/N & S/N	FAILURE DATE & TEST	FAILURE INDICATION	CAUSE	CORRECTIVE ACTION
LOX Recirculation Valve, P/N 1A49965-505 S/N 0022	8-14-65 CD 614041 Runs No. 2, 3, and 4, Simulated Three Orbit Test	The talkback switch of the valve was erratic. The switch indicated the valve was open at T +15 sec during Run No. 2, and the open talkback signal was lost during Runs No. 2 and 3.	Microswitches were out of adjustment.	The microswitches were adjusted.

APPENDIX 2

BATTLESHIP TEST HISTORY

1. BATTLESHIP TEST HISTORY

This appendix summarizes the S-IVB battleship test program at the Sacramento Test Center.

1.1 Coldflow and Childown Tests

1.1.1 CD 614000, LN2 and LH2 Propellant Loading, 18 September 1964

The initial battleship cryogenic loading was accomplished using LN2 and LH2. The test demonstrated safe propellant transfer, proper purge, tank pressurization and venting procedures, and proper functioning of control and instrumentation systems.

1.1.2 CD 614002, LOX and LH2 Propellant Loading, 25 September 1964

This test consisted of a successful initial LOX and LH2 loading, followed by two engine chilldown tests, an attempted thrust chamber chilldown, and a fill test of the engine helium control sphere and engine start tank.

LOX turbopump chilldown was achieved by utilizing the LOX recirculation system; for LH2 turbopump chilldown the LH2 overboard bleed system was used.

The thrust chamber, engine start tank and helium control sphere chilldown tests were unsuccessful because of an inadequate gas supply from pneumatic console "C," attributed to undersized orifices in the console.

1.1.3 CD 614003, Engine Chilldown Tests, 2 October 1964

Good turbopump chilldown was achieved in two successive tests utilizing onboard LH2 and LOX recirculation systems.

An attempt to chilldown the engine start tank by GH2 flow from the evaporator was unsuccessful; however, a second test was successful by using cold GH2 from the gas heat exchanger.

Two attempts to chilldown the thrust chamber jacket failed; however, a third test, conducted on 9 October, was successful.

Problems experienced with the thrust chamber and the engine start tank chilldown were caused by a restricted flow from the console. Restrictions in the cold helium system lines were caused by frozen contaminants.

1.1.4 CD 614004, Start Tank Blowdown Test, 24 October 1964

Following successful propellant loading and chilldown verification tests, the propellant prevalves were functionally checked. The prevalves did not properly respond to commands. The test sequence was then altered and the test proceeded through all chilldown cycles and start sphere fill operations. The test was terminated prior to the originally intended DAC automatic sequence which was to proceed through engine ignition.

1.2 Propulsion Development Firings

1.2.1 CD 614005, 10 Second Firing, 7 November 1964

The countdown resulted in three aborted runs.

Run 1 was terminated prior to initiation of DAC automatic start sequence for lack of deflector plate water pressure indication.

Run 2 was terminated at expiration of the DAC sequence monitor timer for lack of diffuser water pressure indication. Frozen water in the pressure sense line was suspected and the line was rerouted.

Run 3 was terminated 2.5 seconds after engine sequence start because of gas generator overtemperature indication. Just prior to cutoff, fire was noted in the gas generator area. Post-test investigation revealed damaged gas generator components and damaged LH2 pump and turbine.

Steps were taken to preclude recurrence, including installation of a heater blanket for the gas generator body.

During run 3, engine start conditions were achieved and maintained throughout the simulated boost phase.

1.2.2 CD 614006, Gas Generator Ignition Firing, 24 November 1964

The performance of the replacement gas generator was verified. Engine start conditions were successfully maintained throughout the simulated boost phase.

Cutoff occurred automatically after 1.325 seconds of engine sequence at the expiration of a special timer.

The new gas generator heater blanket maintained proper combustor body temperature prior to ignition.

All stage, GSE, and facility systems functioned satisfactorily.

1.2.3 CD 614007, 10-Sec Mainstage Shakedown Firing, 1 December 1964

The test was highly successful. Engine start conditions, ignition, and mainstage were achieved. Manual cutoff occurred after 10.67 sec of mainstage operation.

Engine sideloads experienced during start transients were normal and damped out in less than 7 sec.

LH2 pump stall was indicated just prior to LOX valve OPEN.

Overall stage, GSE, and facility performance was satisfactory; therefore, a decision was made to bypass the planned 20-sec mainstage firing and proceed with a 50-sec mainstage firing. The turbopump chilldown procedure was revised for subsequent tests in order to preclude possible LH2 pump stalls in the future.

1.2.4 CD 614008, 50-Sec Mainstage Shakedown Firing, 9 December 1964

The test was very successful. Mainstage duration was 50.7 sec. Propellants were loaded using point level sensors as reference.

The thrust chamber chilldown was extended to approximately 51 min and turbopump chilldown was extended to 10 min. A normal engine start was accomplished with no turbopump stall indicated. Engine performance data indicated normal operation through all phases, except that the side loads during start transients were higher than previously experienced and subsided approximately 8 sec after mainstage OK.

1.2.5 CD 614009, 150-Sec Mainstage Shakedown Firing, 15 December 1964

This test concluded the shakedown firing series in preparation for a full duration firing. Mainstage duration was 150.4 sec. Extended thrust chamber and turbopump chilldown sequences were again used. LH2 tank pressure was established and maintained during the test for the first time by a flight configuration LH2 pressurization module. LOX pressurization was maintained by the auxiliary pressurization system. The pneumatic power control module failed during pre-test setup and the stage pneumatic system was supplied from a ground source during the test.

Engine performance during start, steady-state, and shutdown, was very satisfactory.

1.2.6 CD 614010, Full Duration Firing, 23 December 1964

Run 1 on 22 December was aborted when thrust chamber chilldown could not be achieved because of adverse weather condition.

The initial full duration firing was very successful. Again extended chilldown was used for the thrust chamber jacket and turbopump. On-board LOX tank pressurization system was used with the cold helium spheres pressurized to 3,000 psig. LOX tank was prepressurized using the auxiliary pressurization system, tank pressure was controlled thereon by the on-board system. LH2 tank pressure was maintained during mainstage by the LH2 pressurization control module.

The PU system was used in this test. The system performed satisfactorily, indicating very close correlation between PU and point level sensor indicated mass values.

The engine operation was very satisfactory through start, mainstage, and cutoff. No pump stalls were indicated. The test duration was 414.6 sec or shorter than a full duration firing. This was to ensure that propellant depletion would not occur. Approximately 10,000 lb of propellants remained in the tanks after cutoff.

1.3 J-2 Engine Temperature Conditioning Tests

1.3.1 CD 614011, Run 1, 8 January 1965

Following propellant loading, three chilldown attempts were aborted because of component failures. In the first attempt the LH2 chilldown inverter failed. The chilldown pump was subsequently operated from a facility backup power. In the second attempt the engine start sequence was not attained because of a LOX chilldown valve malfunction. Warm air flow to the valve was increased for the third attempt. The third attempt was terminated when the LOX chilldown pump failed to attain the operating speed, and excessive current drain was indicated at the pump motor. The pump was replaced after the test.

1.3.2 CD 614012, Run 2, 14 January 1965

The test was terminated when the LOX chilldown pump failed in a special test. The pump was found contaminated with alcohol, the cleaning agent used by the vendor.

Prior to termination special tests were conducted on LOX and LH2 prevalves, chilldown valves, and LH2 tank vent and relief valves with satisfactory results.

1.3.3 CD 614013, Run 3, 16 January 1965

The test was terminated after the LH2 tank vent and relief valve failed in a special test. Also, the LOX chilldown pump seized after an apparently normal start transient during a special test prior to LH2 loading.

During post-test investigation, insufficient clearance was found between LOX chilldown pump impeller and wear ring. The pump was returned to vendor for corrective action.

J-2 engine S/N 2003 was replaced with S/N 2013 on 28 January.

1.3.4 CD 614014, Run 4, 9 February 1965

After completion of LOX loading and a special LOX chilldown pump test, LH2 loading was accomplished for the first time at the design transfer rate of 3,000 gpm. Special LH2 tank vent relief cycle and LH2 chilldown pump tests were conducted. The test proceeded through a successful chilldown sequence and was cut off after 1.14 sec of engine sequence. (The sequence includes full opening of main LH2 valve. The LH2 dumped through the thrust chamber is then ignited by special burner near thrust chamber exit.)

A fire was indicated approximately 2 sec after cutoff in the LH2 prevalve area. Minor damage was inflicted on components located in LH2 prevalve area and in Console "C". Also, engine instrumentation wiring was scorched and the dummy aft interstage protective wrapping was burned and charred. Subsequent tests used deflector plate water spray to assist in removing combustibles from the engine and thrust cone areas.

1.3.5 CD 614015, Run 5, 17 February 1965

LOX was loaded by utilizing the automatic propellant loading system (APLS) for the first time. The test was terminated after completion of LOX loading because of an inoperative engine LOX bleed valve. The valve was replaced after the test.

1.3.6 CD 614016, Run 6, 18 February 1965

Proper operation of LOX and LH2 chilldown systems and engine LOX bleed valve were verified. LOX loading was stopped at the 150,000 lbm level because of leakage noted at the "H" section of the LOX sled. LH2 loading was successfully accomplished utilizing the APLS system in the open-loop mode.

The countdown was terminated because of leakage at the gas heat exchanger fill valve after the completion of LH2 loading. Leaks were also disclosed at stem of LH2 sled main fill valve and stage LH2 prevalve.

Subsequent to this test, the J-2 engine temperature conditioning program was revised to expedite the main program objective: the achievement of a chilldown procedure which is compatible with S-IVB flight sequence.

1.3.7 CD 614017, Run 7, 25 February 1965

The countdown consisted of five chilldown tests. The tests were considered to be highly successful with only minor problems experienced. Prior to testing, a major effort was directed to the repair of all leakage noted in the propellant and pneumatic systems during the previous tests.

LOX chilldown inverter instrumentation problems were resolved and the inverter was used during the countdown.

A LOX storage tank vent line ruptured during venting following completion of LOX loading. The line was temporarily repaired for the next test.

1.3.8 CD 614018, Run 8, 2 March 1965

This countdown consisted of two successful chilldown tests prior to depletion of helium supply. During LOX storage tank venting, at completion of LOX loading, the LOX storage tank vent line ruptured. The first test consisted of three attempts. The first attempt was recycled to the start of terminal count when overpressure was indicated in the thrust chamber interface at SLO -2:45 min. The engine sequence was not completed during the second attempt because of lack of talkback from the hydrogen torch igniters. The third attempt proceeded through a very satisfactory chilldown and start sequence.

The second test followed after a thrust chamber warmup period. The chilldown and start sequence were again satisfactory and no LH2 pump stall was noted.

1.3.9 CD 614019, Run 9, 6 March 1965

This countdown concluded the J-2 engine temperature conditioning test series. Four out of five chilldown tests initiated were successfully accomplished. The engine environmental enclosure was removed for the last two tests to determine its effects on the thrust chamber chilldown.

During propellant unloading, a minor fire was noted in the LH2 prevalve area. No damage resulted; however, the LH2 prevalve adapter was removed after the test to prevent recurrence of hydrogen leaks in this area.

1.4 System Development Firings

1.4.1 CD 614020, 10-Sec Shakedown Firing, J-2 Engine S/N 2013, 13 March 1965

A special cold helium sphere blowdown test was conducted following propellant loading to gather data on thermal characteristics of the cold helium line to the LOX pressurization module. Thrust chamber chilldown was initiated at SLO -8:30 min; turbopump chilldown was started at SLO -5 min.

The first run was aborted at SLO -2:40 min when no LH2 fill and drain valve CLOSED talkback signal was received. The talkback signal was simulated in the sequence logic during the next run, and the position of the valve was verified by pressurizing the tank and observing off-loading conditions. The LH2 fill and drain valve was replaced after the test.

A successful shakedown firing was accomplished during the second run. The mainstage duration was 11.8 sec. No LH2 pump stall was indicated at engine start. Engine side loads during start transients were lower than observed on engine S/N 2003.

The PU system was activated at SLO +10 sec and was operating during the last 1.6 sec of the test. The PU valve properly responded to the excess of LH2 in the tank. The LH2 chilldown pump was operated from the backup power source; LOX chilldown pump received power from the LOX chilldown inverter.

1.4.2 CD 614021, Full Duration Systems Verification Firing, 19 March 1965

The test was manually cut off after 29.2 sec of firing due to instrumentation failure on a cutoff parameter (gas generator combustor body temperature).

The test proceeded through a successful chilldown and engine start sequence. The PU system was activated 10 sec after initiation of engine start sequence. The system operated in closed-loop mode and the PU valve properly responded to the indicated tank masses. Difficulties were experienced during shutdown sequence when the firing logic proceeded to restart the engine while attempting to reset. Open-fused circuit in the engine cutoff circuitry was discovered and post-firing modifications were made to avoid such recurrence. Also, the gas generator was provided with a redundant temperature measurement.

An interim GH2 supply with tube trailers was utilized during the test because of LH2 pump-vaporizer failure prior to countdown initiation which resulted in GH2 line contamination with oil.

1.4.3 CD 614022, High EMR, PU Excursion, 25 March 1965

Run 1 resulted in three aborted attempts. After completion of propellant loading a special test was conducted to verify turbopump chilldown characteristics under simulated S-IVB/V restart conditions. This attempt to chill the engine with warm ducts was unsuccessful due to erratic LH2 chilldown pump operation which was apparently caused by back pressure from boiling liquid in the duct. A check valve was subsequently installed in the low pressure duct.

The first attempt was aborted due to false ASI ignition indication. The second attempt was aborted due to an apparently high LH2 pump inlet temperature at engine start.

The third attempt was aborted because of lack of LH2 prevalve OPEN talkback signal. Both chilldown pumps were operated from the GSE backup power source during the test.

1.4.4 CD 614023, High EMR PU Excursion, 31 March 1965

A successful full duration firing was accomplished. The mainstage duration was 470 sec. Propellant loading, chilldown, and engine start sequence were accomplished without incident. The propellant loading was monitored by the Automatic Propellant Loading System (APLS). Normal engine side loads were noted during engine start transients. The PU system was activated at mainstage +13 sec. The overall PU system performance was excellent during the firing. The PU valve moved to the planned 5.5 to 1 mixture ratio and remained there for 82 sec. The test was cut off by a strip chart observer when the LH2 pump inlet conditions indicated imminent LH2 depletion. Simultaneously with cutoff, LH2 depletion sensors indicated depletion. The primary shut-off valve in the LOX tank pressurization control module malfunctioned causing the LOX tank to remain at relief pressure during the firing.

1.4.5 CD 614024, Low EMR, PU Excursion, 7 April 1965

The test was terminated approximately 42 sec after attaining mainstage because of instrumentation malfunction which resulted in an erroneous indication of excessive LH2 pump inlet pressure rise.

The J-2 engine control assembly malfunctioned during pre-test checkout and was replaced. Propellant tanks were loaded utilizing the APLS system. The engine performance was satisfactory in all phases of operation. At PU system activation (mainstage +13 sec) the PU valve immediately responded to compensate for the LH2 overload and remained in LH2-rich position until cutoff. No increase in engine side loads was noted as a result of the low engine mixture ratio (4.5 to 1).

1.4.6 CD 614025, Low EMR, PU Excursion, 15 April 1965

A low EMR firing of 506.75 sec mainstage duration was successfully accomplished. A special thrust chamber chilldown test was conducted to determine if chilldown could be achieved under the existing adverse weather conditions. As a result, a larger size orifice was installed in the chilldown line.

Propellant loading was accomplished using the APLS. The thrust chamber chilldown was started at SLO -12 min; the turbopump chilldown was started at SLO -5 min. The engine performance was satisfactory throughout the test. The PU valve moved to LH2-rich stop at PU system activation and remained there for 212 sec. Propellant residual of 2,000 lb LOX and 800 lb LH2 were in the tanks at cutoff.

The performance of all stage, GSE, and facility systems was satisfactory, including the hydraulic system which was installed prior to test.

1.4.7 CD 614026, Spring Rate Simulator Verification and Ambient Gimbal Test, 22 April 1965

The spring rate simulator adjustment verification and the ambient gimbal test were conducted under the control of an automatic program executed through the hydraulic control panel.

Prior to test, the hydraulic system was checked out and the clearance for a two-inch movement of the stage in any direction verified.

The tests indicated no significant stage clearance problems. Stage motion during the ambient gimbal test, which proceeded through maximum engine deflection at various frequency ranges, was minimal.

Post-test checkout revealed a spring rate simulator attachment bolt failure. All attachment bolts were replaced prior to next test.

1.4.8 CD 614028, High EMR Firing, 27 April 1965

This long duration high EMR firing was cut off manually after 374 sec of engine operation. Cutoff was initiated because the hydraulic reservoir oil temperature reached the cutoff valve.

The LH2 chilldown inverter was used to operate the LH2 chilldown pump for the first time. Also, retractable engine side load restrainer links were used for the first time.

The gimbal control system maintained the engine in the null position during the firing. A malfunctioning hydraulic system high-pressure relief valve prevented the programmed gimbal checkout and caused the oil temperature rise which resulted in early cutoff.

Following propellant loading, the thrust chamber chilldown was initiated at SLO -12 min. Turbopump chilldown was started at SLO -5 min and both chilldown pumps were operated by the chilldown inverters. A normal engine start sequence was experienced. After PU system activation the PU valve properly responded to LOX overload conditions, remaining at the LOX-rich stop for 115 sec. The engine side load restrainer links were retracted approximately 10 sec after PU system activation.

1.4.9 CD 614030, Hot Gimbal, Full Duration Firing, 4 May 1965

The highly successful full duration firing was manually terminated after 493.5 sec of mainstage.

Propellant loading was accomplished automatically using the APLS. A special LH2 recirculation system test was performed to verify performance of the check valve recently installed in the low-pressure chilldown duct. The valve performed as designed. The chilldown pump was operated from a facility backup source during the special test.

Thrust chamber and turbopump chilldown and engine start sequence were satisfactory. The PU system was activated 14 sec after engine start. The PU valve maintained a generally LH2-rich propellant mixture as expected.

Engine side load restrainer links were retracted 16 sec after engine start; 26 sec after engine start the hot gimbal program was initiated. The program proceeded through a gimbal sequence of varying frequencies and amplitudes up to the maximum allowable deflection in pitch and yaw planes. The hydraulic system performance was very satisfactory and stage deflection during gimbaling was minimal.

After the test, the LOX residual was quickly dumped through the emergency drain and good data were obtained of mass probe dry capacitance values under simulated flight conditions after cutoff.

This was the last hot firing test of the S-IVB/IB battleship program.

1.4.10 CD 614031 and CD 614032, Aft Interstage Environmental Tests, 13 and 14 May 1965

A verification test of the new facility GN2 forward and aft interstage purge system was performed on 11 May.

Run 1 was conducted on 13 May. Propellant loading was accomplished using the APLS. A temporary GN2 purge system shutdown was experienced during LOX loading and air was substituted for GN2 during this time. Approximately 3/16-in. layer of ice and frost accumulated on the LOX tank aft dome while air was used as the purging agent.

The first test proceeded through a successful thrust chamber and turbopump childown and a simulated engine start. The newly installed LOX pressurization module operated as designed.

The second test was conducted after system warmup, and proceeded through childown and simulated engine start sequence.

During LH2 detanking a hold was initiated at the 70 percent level and 15 psig ullage pressure to determine the extent of tank ullage gas saturation. Data indicated that ullage gas did not reach saturation level.

Data from run 1 tests were inconclusive because of the frost formation on the aft dome during GN2 purge system shutdown.

Run 2 was successfully accomplished on 14 May. Propellant loading again was accomplished by using the APLS. Thrust chamber chilldown was started at SLO -20 min, chilldown pumps were started at SLO -10 min. Post-test inspection revealed no significant accumulation of ice or frost on the LOX tank aft dome.

In essence, these tests demonstrated that the aft skirt and interstage purge and environmental systems are capable of maintaining the temperature of all electronics equipment in this area within proper operating range, and that the oxygen content can be reduced to and maintained at less than 4 percent by volume.

1.5 S-IVB/V Development Firings

1.5.1 CD 614033, Simulated Three-Orbit First Burn, Coast and Restart, 19 June 1965

The initial S-IVB/V battleship static firing was partially successful. The stage, J-2 engine S/N 2020, and facility shakedown was successfully accomplished and the special S-IVB/V configuration chilldown techniques verified.

The test was automatically terminated after 8.92 sec of first burn mainstage due to a momentary Facility Activate signal dropout. The momentary condition existed in the firing logic sequence where the engine start tank pressure switch generated simultaneously "pressurized" and "depressurized" signals, caused by a relay race and energizing a Test Enable signal.

This situation had existed since the S-IVB/IB battleship turbine spin tests and was thought to be compatible with the S-IVB/V configuration. The firing logic was corrected after the test to prevent similar incidents in the future.

Propellant loading was accomplished manually to over the top of the PU probe active elements, to obtain capacitance readings with probes totally submerged.

Turbopump chilldown was successfully accomplished starting with warm pump inlets. Thrust chamber chilldown was accomplished with LH2 lead just prior to engine start. Engine performance was satisfactory for the duration of the firing.

1.5.2 CD 614034, Simulated Three-Orbit Test with Second Burn, 26 June 1965

The test was partially successful. After a good first burn and simulated three-orbit coast, the second burn was terminated after 3.84 sec mainstage. Cutoff was caused by excessive instrumentation noise from the gas generator temperature probe. The duration of the first burn mainstage was 167 sec. Simulated orbital coast lasted for 94 min.

Propellant loading was accomplished manually to over the top of the PU probe active elements, to obtain capacitance readings with probes totally submerged.

Terminal count for the first attempt was terminated prior to engine start due to slow opening of the LOX prevalve which left insufficient time to complete the sequence.

All engine start conditions were successfully accomplished for the second attempt and the firing test proceeded through a smooth engine start and first burn mainstage. The PU system was operated in closed-loop mode. The hydraulic system was operating at design pressure although no gimbaling was performed. The first burn was manually cut off 171.5 sec after engine start.

The simulated orbital coast with vented propellant tanks lasted approximately 94 min during which time an LH2 mass boiloff similar to that experienced in a S-IVB/V flight stage coast in orbit was accomplished.

The terminal count for the second burn was satisfactory and the engine start sequence was normal. The engine firing was automatically terminated 3.84 sec in mainstage by R/NAA automatic monitoring system.

Although the test did not proceed through a full duration second burn, the J-2 engine restart capabilities were successfully demonstrated after the simulated coast. Also, repressurization of stage propellant tanks was successfully achieved.

1.5.3 CD 614035, Simulated Three-Orbit, Full Duration First and Second Burn and Hot Gimbal Test, 1 July 1965

The first attempt was terminated automatically 5.45 sec after engine start by the firing control logic when the "Restrainer Arms Up" signal dropped out momentarily.

The second attempt was cut off manually 6.37 sec after engine sequence start because of a visual evidence of fire in the thrust cone area. The fire was brought under control and extinguished by the test stand water deluge system.

In preparation for the hot gimbal test, ambient gimbal checkout was successfully accomplished on 30 June.

During propellant loading, the LOX and LH2 overfill sensors activated when the tank levels were near the top of the PU probes. Prevalves were closed during the loading.

Thrust chamber and turbopump chilldown was successfully achieved for both attempts. The "Engine Restrainer Arms Up" signal was simulated during the second attempt. The LH2 discharge duct purge was initated and continued until the second attempt.

After a normal start sequence and 1.72 sec of mainstage, the firing was manually terminated because of visual indication of fire. Post-test investigation revealed that the fire and accompanying explosion originated in the area of the thrust structure. The LH2 low-pressure duct and control and instrumentation wiring sustained severe damage. All fire damage was repaired and the stage completely checked out by the end of July.

1.5.4 CD 614041, Simulated Three-Orbit, Full Duration First and Second Burn and Hot Gimbal Test, 12 August 1965

The test proceeded through LOX loading and 60 percent LH2 loading. At this time excessive leakage was noted around the LH2 prevalve as indicated by the GH2 detector. Propellants were unloaded without incident. Loose caps of the LH2 tank anti-vortex screen pressure instrumentation ports were retorqued and a satisfactory leak check accomplished.

1.5.5 CD 614042, Simulated Three-Orbit, Full Duration First and Second Burn and Hot Gimbal Test, 13 August 1965

The test was manually terminated approximately 16 sec after engine sequence start by the uprange observer because of visual fire indications.

Propellants were loaded to the overfill sensor activate point. Thrust chamber and turbopump chilldown was achieved. Thrust chamber chilldown was continued until SLO +6 min because of wind conditions.

Engine start sequence was normal and PU system was activated 10 sec after mainstage OK. The fire was observed near the LH2 repressurization module and it went out prior to test stand deluge activation. Post-test inspection revealed no damage sustained, except that light scorching was noted on the control cable to the module. A loose B-nut was disclosed on the module solenoid bleed line.

1.5.6 CD 614043, Simulated Three-Orbit, Full Duration First and Second Burn and Hot Gimbal Test, 17 August 1965

A highly successful full duration hot gimbal firing was accomplished. The test consisted of approximately 170 sec of first burn, 92 min of orbital coast, and 319 sec of second burn. A tape-controlled hot gimbal program was accomplished during the second burn.

Propellant loading was completed at the activation of overfill sensors. Turbopump and thrust chamber chilldown sequence was normal. Engine start sequence was normal. The PU system was activated 10 sec after mainstage OK.

The LH2 tank was vented at first burn cutoff; LOX tank was vented at ECO +10 min. The LH2 low-pressure duct was purged continuously during the coast period. A total of 3,295 lb of LH2 were boiled off during the 92-min simulated orbital coast.

Engine start sequence of the second burn was satisfactory. The LH2 lead childown was accomplished in 4.12 sec. Engine side loads dampened out within 3 sec. PU system was activated at SLO +10 sec. After release of the engine restrainer arms, a tape-controlled gimbal program was initiated. The gimbal program was completed without difficulty. Cutoff was manually initiated by a strip chart observer due to imminent LH2 depletion.

The zero mass capacitance values were obtained on both LOX and LH2 probes after quick draining of propellant residuals.

1.5.7 CD 614044, Simulated One-Orbit Coast, Full Duration, Hot Gimbal Firing, 20 August 1965

This firing successfully concluded the S-IVB battleship program. The duration of the first burn was 170.9 sec. The simulated coast period lasted for 41 min, and the duration of the second burn was 360.2 sec. A gimbal program was performed during the second burn.

Propellants were loaded to the nominal S-IVB/V levels, through pre-chilled propellant transfer lines. Loadings were accomplished with the main fill and topping valves open from the start to determine the high initial fill rate effects on tank pressure transients. No abnormal ullage transients were observed.

Performance of all systems during the chilldown and first burn was satisfactory. The LH2 tank was vented at ECO; the LOX tank was vented at ECO +10 min. The one-orbit simulated boiloff period for 1,000 lb LH2 was completed in 16.5 min. The hold was continued for a total of 41 min and the propellants were then replenished.

The repressurization system performance was satisfactory. After a good engine start and achievement of mainstage, a tape-controlled gimbal program was performed between SLO +35 and SLO +270 sec with good results. The LOX tank pressurization system operated in the backup mode for both runs. Second burn cutoff was initiated when LOX mass had decreased to 1,650 lb.

Residual propellants were quickly drained and good zero mass probe capacitance values were obtained. An ambient gimbal program, using the same command tape, was performed during tank purge to obtain comparison data.

APPENDIX 3

ABBREVIATIONS

Table AP 3-1
ABBREVIATIONS

ITEM	TERM	ITEM	TERM
ac	Alternating current	gpm	Gallons per minute
Act	Actuator	GSE	Ground support equipment
APS	Auxiliary Propulsion System	Pt	Point
Attch	Attach	PU	Propellant utilization
Btu	British thermal units	Pwr	Power
Cfm	Cubic feet per minute	R	Rankine
Contr	Control	RAD	Radial
cps	Cycles per second	Refl	Reflected
DAC	Douglas Aircraft Company, Inc.	Reg	Regulator
db	Decibel	RF	Radio frequency
dc	Direct current	RMR	Reference mixture ratio
DDAS	Digital Data Acquisition System	RSS	Root sum square
Disch	Discharge	scim	Standard cubic inch per minute
DPF	Differential pressure feedback	scfm	Standard cubic foot per minute
EBW	Exploding bridgewire	sec	Second
ECO	Engine cutoff	SIM	Safety Item Monitor
E/I	External/Internal	STC	Sacramento Test Center
EMI	Electromagnetic interference	sw	Switch
EMR	Engine mixture ratio	Syst	System
ESC	Engine start command	T-0	Simulated S-IB Booster Liftoff
FLT	Flight	TAN	Tangential
ft	Feet	Temp	Temperature
FM	Frequency modulation	T/M	Telemetry
FTC	Florida Test Center	TP&E	Test Planning and Evaluation
Fwd	Forward	v	Volts
Gas gen	Gas generator	Vib	Vibration
GH2	Gaseous hydrogen	vdc	Volts direct current
GN2	Gaseous nitrogen	w	Watts

DISTRIBUTION LIST

DISTRIBUTION LIST

HUNTINGTON BEACH (A3)

A3-860	Director - Saturn Development Engineering
A3-860	Deputy Director - Saturn Development Engineering
KNOO	Chief - Design Engineer
KNOO	Deputy Chief - Design Engineer
KKOO	Chief - Project Engineer
KAOO	Chief Engineer - Mechanics and Reliability
KBOO	Chief Engineer - Structural Mechanical
KCOO	Chief Engineer - Propulsion
KDOO	Chief Engineer - Electronics
K910	Manager - Saturn System Development
KOSO	Manager - Saturn Program Control
K960	Program Engineer - S-IVB Series
K920	Branch Chief - System Engineering
A3-198	Branch Chief - System Testing
KKBO	Branch Chief - S-IVB Test Branch
KAFO	Branch Chief - S-IVB Mechanical and Reliability
KBFO	Branch Chief - S-IVB Structural Mechanical
KCGO	Branch Chief - S-IVB Propulsion
KKBO	Branch Chief - Test Council Chairman
KCBO	Branch Chief - Propulsion (R & VB)
KCDO	Branch Chief - Propulsion Test
KDCO	Branch Chief - GSE Design
KKBA	Section Chief - S-IVB TP&E
KABC	Section Chief - A&SD
KADA	Section Chief - Reliability
KCDB	Section Chief - Propulsion TP&E
KDFA	Section Chief - Data Processing
KDFB	Section Chief - Stage Instrumentation
KABA	TP&E - Strength Section
KABB	TP&E - Weight Control
KABC	TP&E - A&CD
KACA	TP&E - FD&C
KACB	TP&E - Aero/Thermo
KADA	TP&E - Reliability
KCDB	TP&E - Propulsion
KDBC	TP&E - Structural/Mechanical
KDBC	TP&E - Electronics

DISTRIBUTION LIST (Continued)

KKBA	TP&E - PU Chairman
KKBA	TP&E - Group Eng. Static
KKBA	TP&E - Group Eng. Flight
KEBG	Engineering Records (Reproducible)
A3-332	Library

DAC/FTC (A41)

M. F. Cooper
H. T. Gardner (2)
H. H. Nichols

DAC/STC (A45)

W. L. Duval
J. P. Monigal (5)
R. J. Mohr
E. E. Morris

DAC/MSFC (A61)

W. F. Shaver
J. A. Tobias
W. E. Naymola

DAC/MSC (A57)

R. E. Holmen

NASA/MSFC

H. S. Garrett (20) (1 vellum)
J. P. Lindberg